POD 3-D PARTICLE TRACKING MODELING STUDY

San Francisco Bay-Delta UnTRIM Model Calibration Report

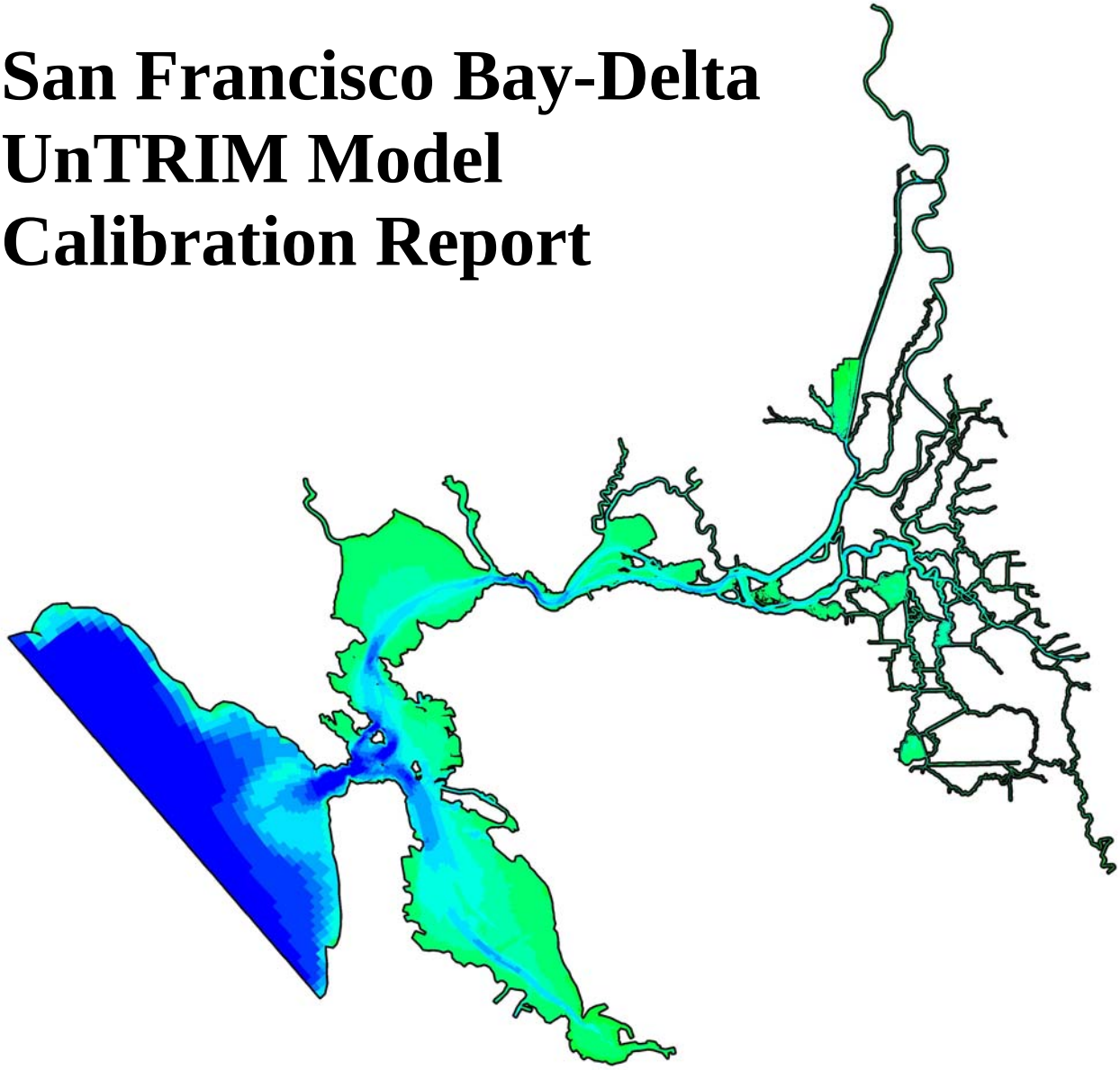

Prepared For:

California Department of Water Resources

Prepared By:

Michael L. MacWilliams, Ph.D.

Francis G. Salcedo

Edward S. Gross, Ph.D.

December 19, 2008

[This page intentionally left blank.]

Executive Summary

The motivation for this study is the observed decline of delta smelt and other pelagic organisms of the upper San Francisco Estuary. Three general factors identified to explain lower pelagic productivity are 1) toxic effects; 2) exotic species effects; and 3) water project effects (Resources Agency, 2007). For each of these factors the location and movement of delta smelt are likely to be critical for understanding the reasons for the pelagic organism decline (POD) and the efficacy of any actions taken to sustain pelagic fish populations.

In order to investigate the location movement of delta smelt within the Delta, a three-dimensional hydrodynamic model was applied to simulate hydrodynamics in the Sacramento-San Joaquin Delta, and the hydrodynamic results were used with a particle tracking model to investigate delta smelt distribution and behavior. The Bay-Delta UnTRIM model developed for this project builds on previous applications (e.g., MacWilliams et al., 2007), and is the first three-dimensional hydrodynamic model extending from the Pacific Ocean through the entire Sacramento-San Joaquin Delta.

This report presents the results of a detailed model calibration of the Bay-Delta UnTRIM model. The report includes a discussion of the governing equations, model implementation and boundary conditions, as well as a detailed presentation of model calibration and validation comparisons. Since it is expected that the model will continue to be improved and expanded for future applications, the report includes suggestions for future model refinements.

The Bay-Delta UnTRIM model is suitable for detailed studies of Delta hydrodynamics, including but not limited to:

- Investigating potential impacts of sea level rise on salinity intrusion into the Delta;
- Predicting salt entrainment into the Delta resulting from Delta levee failure(s);
- Assessing the suitability alternative conveyance strategies for Delta water supply;
- Quantifying potential impacts of alternative conveyance strategies on Delta hydrodynamics and water quality;
- Evaluating fish behavior hypotheses and fish entrainment through coupling of UnTRIM hydrodynamics with the FISH-PTM (Gross et al., in prep.).

Questions, comments, or suggestions for future improvements to the Bay-Delta UnTRIM model should be addressed to Michael MacWilliams at: michael@rivermodeling.com.

Table of Contents

Executive Summary i

List of Tables v

List of Figures v

Abbreviations xxii

1. Introduction 1

2. UnTRIM Model Description 3

2.1 Governing Equations 3

2.2 Turbulence Model 5

2.3 Previous Applications 5

2.4 Model Uncertainty 5

3. San Francisco Bay-Delta UnTRIM Model 8

3.1 Model Domain and Grid 8

3.2 Model Bathymetry 13

3.2.1 Pacific Ocean and Golden Gate 13

3.2.2 Central and South San Francisco Bay and San Pablo Bay 13

3.2.3 Suisun Bay and Sacramento-San Joaquin Delta 13

3.2.4 Projection and Datum Conversion 15

3.3 Simulation Periods 15

3.4 Salinity Boundary and Initial Conditions 15

3.5 Tidal Boundary 16

3.6 River Inflows 18

3.7 Delta Exports 20

3.8 Evaporation and Precipitation 21

3.9 Delta Island Consumptive Use 21

3.10 Wind 25

3.11 Bottom Friction 25

3.12 Delta Control Structures 25

3.12.1 Delta Cross Channel 26

3.12.2 Head of Old River 26

3.12.3 Old River near Tracy (DMC) 26

3.12.4 Middle River 27

3.12.5 Grant Line Canal 27

3.12.6 Suisun Marsh Salinity Control Gates 27

4. Model Calibration 29

4.1 Model Assessment Method 29

4.2 Description of 2007 Simulation Period ____ *30*

4.3 Water Level Calibration ____ *31*
4.3.1 San Francisco Bay ____ 32
4.3.2 Northern Sacramento-San Joaquin Delta ____ 32
4.3.3 Central Sacramento-San Joaquin Delta ____ 33
4.3.4 Southern Sacramento-San Joaquin Delta ____ 34

4.4 Flow Calibration ____ *92*
4.4.1 Northern Sacramento-San Joaquin Delta ____ 92
4.4.2 Central Sacramento-San Joaquin Delta ____ 93
4.4.3 Southern Sacramento-San Joaquin Delta ____ 95

5. Model Validation ____ 134

5.1 Description of 2002 Simulation Period ____ *134*

5.2 Water Level Validation ____ *134*
5.2.1 San Francisco Bay ____ 135
5.2.2 Northern Sacramento-San Joaquin Delta ____ 136
5.2.3 Central Sacramento-San Joaquin Delta ____ 137
5.2.4 Southern Sacramento-San Joaquin Delta ____ 138

5.3 Flow Validation ____ *194*
5.3.1 Northern Sacramento-San Joaquin Delta ____ 194
5.3.2 Central Sacramento-San Joaquin Delta ____ 195
5.3.3 Southern Sacramento-San Joaquin Delta ____ 197

6. Discussion and Future Improvements ____ 225

6.1 UnTRIM Bay-Delta Model Accuracy Relative to RMA2 and DSM2 ____ *225*

6.2 Vertical Datum and Additional Bathymetry ____ *229*

6.3 Spatially-variable Roughness ____ *229*

6.4 Improved Barrier Operations ____ *233*
6.4.1 Delta Cross Channel Gate Operations ____ 233
6.4.2 Head of Old River Temporary Barrier Operations ____ 236

6.5 Improved Delta Island Consumptive Use Estimation ____ *244*

6.6 Improved Salinity Calibration ____ *244*

6.7 Future Model Development ____ *244*

7. Summary and Conclusions ____ 245

Acknowledgments ____ 246

References ____ 247

Appendix A. Model Validation Figures for 1999 Simulation Period ____ 252

A.1 Description of 1999 Simulation Period ____ *252*

A.2 Water Level Comparison Figures ____ *253*
A.2.1 San Francisco Bay ____ 253
A.2.2 Northern Sacramento-San Joaquin Delta ____ 253
A.2.3 Central Sacramento-San Joaquin Delta ____ 253
A.2.4 Southern Sacramento-San Joaquin Delta ____ 253

A.3 Delta Flow Comparison Figures _____ *293*
A.3.1 Northern Sacramento-San Joaquin Delta _____ 293
A.3.2 Central Sacramento-San Joaquin Delta _____ 293
A.3.3 Southern Sacramento-San Joaquin Delta _____ 293

v1.0

List of Tables

Table 4-1 Predicted and observed stage and cross-correlation statistics for stage monitoring stations in San Francisco Bay and the Sacramento-San Joaquin Delta during the 2007 simulation period. 36
Table 4-2 Predicted and observed stage and cross-correlation statistics for flow monitoring stations in the Sacramento-San Joaquin Delta during the 2007 simulation period. 97
Table 5-1 Predicted and observed stage and cross-correlation statistics for stage monitoring stations in San Francisco Bay and the Sacramento-San Joaquin Delta during the 2002 simulation period. 140
Table 5-2 Predicted and observed stage and cross-correlation statistics for flow monitoring stations in the Sacramento-San Joaquin Delta during the 2002 simulation period. 198
Table A-1 Predicted and observed stage and cross-correlation statistics for stage monitoring stations in San Francisco Bay and the Sacramento-San Joaquin Delta during the 1999 simulation period. 254
Table A-2 Predicted and observed stage and cross-correlation statistics for flow monitoring stations in the Sacramento-San Joaquin Delta during the 1999 simulation period. 294

List of Figures

Figure 3.1-1 Model domain for the UnTRIM-Bay Delta model. 9

Figure 3.1-2 UnTRIM model grid in San Francisco Bay. 10

Figure 3.1-3 UnTRIM model grid in western portion of the Sacramento-San Joaquin Delta. 11

Figure 3.1-4 UnTRIM model grid in southern portion of the Sacramento-San Joaquin Delta. 12

Figure 3.4-1 Location of USGS synoptic monitoring stations and Delta salinity stations used for salinity initial conditions. 17

Figure 3.6-1 Locations of Delta river inflows, exports, and barriers applied to the Bay-Delta UnTRIM model. 19

Figure 3.8-1 Location of CIMIS evaporation and precipitation data collection stations used in the San Francisco Bay-Delta UnTRIM model. Evaporation and precipitation stations in the Delta are not used because evaporation and precipitation in the Delta is included as part of DICU. 22

Figure 3.9-1 Location of DICU nodes (red) applied to Bay-Delta UnTRIM model grid.23

Figure 3.10-1 Location of wind measurement stations used to specify wind in the Bay-Delta UnTRIM model. 24

Figure 3.12-1 Photograph of Head of Old River Barrier (top) from DWR TBP (2008); photograph showing location and numbering of six culverts through the 2002 Head of Old River Barrier (bottom) from DWR (2003)..... 28

Figure 4.2-1 Historical barrier operations schedule during the 2007 simulation period. . 31

Figure 4.3-1 Location of NOAA water level monitoring stations in San Francisco Bay used for 2007 stage calibration. 38

Figure 4.3-2 Observed and predicted stage at San Francisco Fort Point NOAA station (9414290) during the 2007 simulation period. 39

Figure 4.3-3 Observed and predicted stage at Alameda NOAA station (9414750) during the 2007 simulation period..... 40

Figure 4.3-4 Observed and predicted stage at Redwood City NOAA station (9414523) during the 2007 simulation period. 41

Figure 4.3-5 Observed and predicted stage at Richmond NOAA station (9414863) during the 2007 simulation period..... 42

Figure 4.3-6 Observed and predicted stage at Port Chicago NOAA station (9415144) during the 2007 simulation period. 43

Figure 4.3-7 Location of water level monitoring stations in the northern portion of the Sacramento-San Joaquin Delta used for 2007 stage calibration. 44

Figure 4.3-8 Observed and predicted stage at Cache Slough at Ryer Island USGS station (CCH) during the 2007 simulation period. 45

Figure 4.3-9 Observed and predicted stage at Sacramento River South of Georgiana Slough USGS station (WGB) during the 2007 simulation period. 46

Figure 4.3-10 Observed and predicted stage at Georgiana Slough near Sacramento River USGS station (GEO) during the 2007 simulation period. 47

Figure 4.3-11 Observed and predicted stage at Delta Cross Channel USGS station (DCC) during the 2007 simulation period. 48

Figure 4.3-12 Observed and predicted stage at Sacramento River North of Delta Cross Channel USGS station (WGA) during the 2007 simulation period..... 49

Figure 4.3-13 Observed and predicted stage at Mokelumne River near Thornton (Benson's Ferry) DWR station (RMKL027) during the 2007 simulation period..... 50

Figure 4.3-14 Observed and predicted stage at Miner Slough at Highway 84 Bridge USGS station (MIN) during the 2007 simulation period. 51

Figure 4.3-15 Observed and predicted stage at Steamboat Slough between Sacramento River and Sutter Slough USGS station (STM) during the 2007 simulation period. 52

Figure 4.3-16 Observed and predicted stage at Sutter Slough at Courtland USGS station (SUT) during the 2007 simulation period. 53

Figure 4.3-17 Observed and predicted stage at Sacramento River at Freeport USGS station (FPT) during the 2007 simulation period. 54

Figure 4.3-18 Location of water level monitoring stations in the central portion of the Sacramento-San Joaquin Delta used for 2007 stage calibration. 55

Figure 4.3-19 Observed and predicted stage at Antioch DWR station (RSAN007) during the 2007 simulation period. 56

Figure 4.3-20 Observed and predicted stage at Sacramento River at Rio Vista USGS station (RIO) during the 2007 simulation period. 57

Figure 4.3-21 Observed and predicted stage at Threemile Slough North at San Joaquin River USGS station (TMN) during the 2007 simulation period. 58

Figure 4.3-22 Observed and predicted stage at San Joaquin River at Jersey Point USGS station (JPT) during the 2007 simulation period. 59

Figure 4.3-23 Observed and predicted stage at False River USGS station (FAL) during the 2007 simulation period. 60

Figure 4.3-24 Observed and predicted stage at Dutch Slough at Jersey Island USGS station (DCH) during the 2007 simulation period. 61

Figure 4.3-25 Observed and predicted stage at Old River at San Joaquin River USGS station (OSJ) during the 2007 simulation period. 62

Figure 4.3-26 Observed and predicted stage at Mokelumne River near San Joaquin River USGS station (MOK) during the 2007 simulation period. 63

Figure 4.3-27 Observed and predicted stage at Old River at Quimby Island near Bethel Island USGS station (ORQ) during the 2007 simulation period. 64

Figure 4.3-28 Observed and predicted stage at Holland Cut USGS station (HOL) during the 2007 simulation period. 65

Figure 4.3-29 Observed and predicted stage at Rock Slough at Contra Costa Canal DWR station (SLRCK005) during the 2007 simulation period. 66

Figure 4.3-30 Observed and predicted stage at San Joaquin River at Prisoners Point USGS station (PRI) during the 2007 simulation period. 67

Figure 4.3-31 Observed and predicted stage at San Joaquin River at Venice Island DWR station (RSAN043) during the 2007 simulation period. 68

Figure 4.3-32 Observed and predicted stage at Little Potato Slough at Terminous USGS station (LPS) during the 2007 simulation period. 69

Figure 4.3-33 Observed and predicted stage at Middle River south of Columbia Cut USGS station (MRC) during the 2007 simulation period. 70

Figure 4.3-34 Observed and predicted stage at Turner Cut near Holt USGS station (TRN) during the 2007 simulation period. 71

Figure 4.3-35 Location of water level monitoring stations in the southern portion of the Sacramento-San Joaquin Delta used for 2007 stage calibration. 72

Figure 4.3-36 Observed and predicted stage at Middle River at Middle River USGS station (MID) during the 2007 simulation period. 73

Figure 4.3-37 Observed and predicted stage at Middle River at Tracy Boulevard DWR station (RMID027) during the 2007 simulation period. 74

Figure 4.3-38 Observed and predicted stage at Middle River at Howard Road Bridge DWR station (CDEC MHR) during the 2007 simulation period. 75

Figure 4.3-39 Observed and predicted stage at Old River at Bacon Island USGS station (OLD) during the 2007 simulation period. 76

Figure 4.3-40 Observed and predicted stage at Discovery Bay at Indian Slough DWR station (CDEC DBI) during the 2007 simulation period. 77

Figure 4.3-41 Observed and predicted stage at Old River near Byron USGS station (ORF) during the 2007 simulation period. 78

Figure 4.3-42 Observed and predicted stage at Victoria Canal near Byron USGS station (VIC) during the 2007 simulation period. 79

Figure 4.3-43 Observed and predicted stage at Italian Slough Headwater near Byron DWR station (CDEC ISH) during the 2007 simulation period. 80

Figure 4.3-44 Observed and predicted stage at Old River at Coney Island DWR station (CDEC CIS) during the 2007 simulation period. 81

Figure 4.3-45 Observed and predicted stage at Clifton Court Forebay Radial Gates DWR station (CHWST000) during the 2007 simulation period. 82

Figure 4.3-46 Observed and predicted stage at Grant Line Canal near Clifton Court Ferry USGS station (GLW) during the 2007 simulation period. 83

Figure 4.3-47 Observed and predicted stage at Grant Line Canal at Tracy Boulevard DWR station (CHGRL009) during the 2007 simulation period. 84

Figure 4.3-48 Observed and predicted stage at Old River near Delta Mendota Canal Downstream of Barrier DWR station (ROLD046) during the 2007 simulation period. .. 85

Figure 4.3-49 Observed and predicted stage at Delta Mendota Canal Upstream of Barrier USGS station (DMC) during the 2007 simulation period. 86

Figure 4.3-50 Observed and predicted stage at San Joaquin River at Stockton USGS station (STK) during the 2007 simulation period. 87

Figure 4.3-51 Observed and predicted stage at San Joaquin River at Brandt Bridge DWR station (RSAN072) during the 2007 simulation period. 88

Figure 4.3-52 Observed and predicted stage at San Joaquin River below Old River near Lathrop DWR station (CDEC SJL) during the 2007 simulation period. 89

Figure 4.3-53 Observed and predicted stage at Old River at Head DWR station (ROLD074) during the 2007 simulation period..... 90

Figure 4.3-54 Observed and predicted stage at San Joaquin River at Mossdale DWR station (RSAN087) during the 2007 simulation period. 91

Figure 4.4-1 Location of flow monitoring stations in the northern portion of the Sacramento-San Joaquin Delta used for 2007 flow calibration. 99

Figure 4.4-2 Observed and predicted flow at Sacramento River South of Georgiana Slough USGS station (WGB) during the 2007 simulation period. 100

Figure 4.4-3 Observed and predicted flow at Georgiana Slough near Sacramento River USGS station (GEO) during the 2007 simulation period. 101

Figure 4.4-4 Observed and predicted flow at Delta Cross Channel USGS station (DCC) during the 2007 simulation period. 102

Figure 4.4-5 Observed and predicted flow at Sacramento River North of Delta Cross Channel USGS station (WGA) during the 2007 simulation period..... 103

Figure 4.4-6 Observed and predicted flow at Sacramento River at Freeport USGS station (FPT) during the 2007 simulation period..... 104

Figure 4.4-7 Observed and predicted flow at Cache Slough at Ryer Island USGS station (CCH) during the 2007 simulation period. 105

Figure 4.4-8 Observed and predicted flow at Miner Slough at Highway 84 Bridge USGS station (MIN) during the 2007 simulation period. 106

Figure 4.4-9 Observed and predicted flow at Steamboat Slough between Sacramento River and Sutter Slough USGS station (STM) during the 2007 simulation period..... 107

Figure 4.4-10 Observed and predicted flow at Sutter Slough at Courtland USGS station (SUT) during the 2007 simulation period. 108

Figure 4.4-11 Location of flow monitoring stations in the central portion of the Sacramento-San Joaquin Delta used for 2007 flow calibration. 109

Figure 4.4-12 Observed and predicted flow at Sacramento River at Rio Vista USGS station (RIO) during the 2007 simulation period. 110

Figure 4.4-13 Observed and predicted flow at Threemile Slough North at San Joaquin River USGS station (TMN) during the 2007 simulation period. 111

Figure 4.4-14 Observed and predicted flow at San Joaquin River at Jersey Point USGS station (JPT) during the 2007 simulation period..... 112

Figure 4.4-15 Observed and predicted flow at False River USGS station (FAL) during the 2007 simulation period..... 113

Figure 4.4-16 Observed and predicted flow at Dutch Slough at Jersey Island USGS station (DCH) during the 2007 simulation period. 114

Figure 4.4-17 Observed and predicted flow at Old River at San Joaquin USGS station (OSJ) during the 2007 simulation period. 115

Figure 4.4-18 Observed and predicted flow at Mokelumne River near San Joaquin River USGS station (MOK) during the 2007 simulation period. 116

Figure 4.4-19 Observed and predicted flow at Old River at Quimby Island near Bethel Island USGS station (ORQ) during the 2007 simulation period. 117

Figure 4.4-20 Observed and predicted flow at Holland Cut USGS station (HOL) during the 2007 simulation period..... 118

Figure 4.4-21 Observed and predicted flow at San Joaquin River at Prisoners Point USGS station (PRI) during the 2007 simulation period. 119

Figure 4.4-22 Observed and predicted flow at Little Potato Slough at Terminous USGS station (LPS) during the 2007 simulation period. 120

Figure 4.4-23 Observed and predicted flow at Middle River south of Columbia Cut USGS station (MRC) during the 2007 simulation period..... 121

Figure 4.4-24 Observed and predicted flow at Turner Cut near Holt USGS station (TRN) during the 2007 simulation period. 122

Figure 4.4-25 Location of flow monitoring stations in the southern portion of the Sacramento-San Joaquin Delta used for 2007 flow calibration. 123

Figure 4.4-26 Observed and predicted flow at Middle River at Middle River USGS station (MID) during the 2007 simulation period. 124

Figure 4.4-27 Observed and predicted flow at Old River at Bacon Island USGS station (OLD) during the 2007 simulation period. 125

Figure 4.4-28 Observed and predicted flow at Old River near Byron USGS station (ORF) during the 2007 simulation period. 126

Figure 4.4-29 Observed and predicted flow at Victoria Canal near Byron USGS station (VIC) during the 2007 simulation period. 127

Figure 4.4-30 Observed and predicted flow at Grant Line Canal near Clifton Court Ferry USGS station (GLW) during the 2007 simulation period. 128

Figure 4.4-31 Observed and predicted flow at Old River near Delta Mendota Canal Upstream of Barrier USGS station (DMC) during the 2007 simulation period. 129

Figure 4.4-32 Observed and predicted flow at San Joaquin River at Stockton USGS station (STK) during the 2007 simulation period. 130

Figure 4.4-33 Observed and predicted flow at San Joaquin River below Old River near Lathrop DWR station (CDEC SJL) during the 2007 simulation period. 131

Figure 4.4-34 Observed and predicted flow at Old River at Head DWR station (ROLD074) during the 2007 simulation period. 132

Figure 4.4-35 Observed and predicted flow at San Joaquin River at Mossdale DWR station (RSAN087) during the 2007 simulation period. 133

Figure 5.1-1 Historical barrier operations schedule during the 2002 simulation period. 135

Figure 5.2-1 Location of NOAA water level monitoring stations in San Francisco Bay used for 2002 stage calibration. 142

Figure 5.2-2 Observed and predicted stage at San Francisco Fort Point NOAA station (9414290) during the 2002 simulation period. 143

Figure 5.2-3 Observed and predicted stage at Alameda NOAA station (9414750) during the 2002 simulation period. 144

Figure 5.2-4 Observed and predicted stage at Redwood City NOAA station (9414523) during the 2002 simulation period. 145

Figure 5.2-5 Observed and predicted stage at Richmond NOAA station (9414863) during the 2002 simulation period..... 146

Figure 5.2-6 Observed and predicted stage at Port Chicago NOAA station (9415144) during the 2002 simulation period. 147

Figure 5.2-7 Location of water level monitoring stations in the northern portion of the Sacramento-San Joaquin Delta used for 2002 water level calibration. 148

Figure 5.2-8 Observed and predicted stage at Sacramento River South of Georgiana Slough USGS station (WGB) during the 2002 simulation period. 149

Figure 5.2-9 Observed and predicted stage at Georgiana Slough near Sacramento River USGS station (GEO) during the 2002 simulation period. 150

Figure 5.2-10 Observed and predicted stage at Delta Cross Channel USGS station (DCC) during the 2002 simulation period. 151

Figure 5.2-11 Observed and predicted stage at Sacramento River North of Delta Cross Channel USGS station (WGA) during the 2002 simulation period..... 152

Figure 5.2-12 Observed and predicted stage at Mokelumne River near Thornton (Benson's Ferry) DWR station (RMKL027) during the 2002 simulation period..... 153

Figure 5.2-13 Observed and predicted stage at South Fork Mokelumne River at New Hope Bridge DWR station (RSMKL024) during the 2002 simulation period. 154

Figure 5.2-14 Observed and predicted stage at Steamboat Slough between Sacramento River and Sutter Slough USGS station (STM) during the 2002 simulation period..... 155

Figure 5.2-15 Observed and predicted stage at Sacramento River at Freeport USGS station (FPT) during the 2002 simulation period. 156

Figure 5.2-16 Location of water level monitoring stations in the central portion of the Sacramento-San Joaquin Delta used for 2002 water level calibration. 157

Figure 5.2-17 Observed and predicted stage at Antioch DWR station (RSAN007) during the 2002 simulation period..... 158

Figure 5.2-18 Observed and predicted stage at Sacramento River at Rio Vista USGS station (RIO) during the 2002 simulation period. 159

Figure 5.2-19 Observed and predicted stage at Threemile Slough at San Joaquin River USGS station (TMS) during the 2002 simulation period. 160

Figure 5.2-20 Observed and predicted stage at San Joaquin River at Jersey Point USGS station (JPT) during the 2002 simulation period..... 161

Figure 5.2-21 Observed and predicted stage at False River USGS station (FAL) during the 2002 simulation period..... 162

Figure 5.2-22 Observed and predicted stage at Dutch Slough at Jersey Island USGS station (DCH) during the 2002 simulation period. 163

Figure 5.2-23 Observed and predicted stage at Taylor Slough USGS station (TYLR) during the 2002 simulation period. 164

Figure 5.2-24 Observed and predicted stage at Sand Mound Slough USGS station (SMS) during the 2002 simulation period. 165

Figure 5.2-25 Observed and predicted stage at San Joaquin River at San Andreas Landing DWR station (RSAN032) during the 2002 simulation period. 166

Figure 5.2-26 Observed and predicted stage at Old River at San Joaquin River USGS station (OSJ) during the 2002 simulation period. 167

Figure 5.2-27 Observed and predicted stage at Mokelumne River near San Joaquin River USGS station (MOK) during the 2002 simulation period. 168

Figure 5.2-28 Observed and predicted stage at North Fork Mokelumne River at Georgiana Slough DWR station (RMKL005) during the 2002 simulation period..... 169

Figure 5.2-29 Observed and predicted stage at Franks Tract East USGS station (FRE) during the 2002 simulation period. 170

Figure 5.2-30 Observed and predicted stage at Franks Tract West USGS station (FRW) during the 2002 simulation period. 171

Figure 5.2-31 Observed and predicted stage at Old River at Mandeville Island USGS station (MAN) during the 2002 simulation period. 172

Figure 5.2-32 Observed and predicted stage at Holland Cut USGS station (HOL) during the 2002 simulation period..... 173

Figure 5.2-33 Observed and predicted stage at San Joaquin River at Venice Island DWR station (RSAN043) during the 2002 simulation period. 174

Figure 5.2-34 Observed and predicted stage at San Joaquin River at Rindge Pump DWR station (RSAN052) during the 2002 simulation period. 175

Figure 5.2-35 Observed and predicted stage at Middle River South of Columbia Cut USGS station (MRC) during the 2002 simulation period..... 176

Figure 5.2-36 Location of water level monitoring stations in the southern portion of the Sacramento-San Joaquin Delta used for 2002 water level calibration. 177

Figure 5.2-37 Observed and predicted stage at Middle River at Middle River USGS station (MID) during the 2002 simulation period. 178

Figure 5.2-38 Observed and predicted stage at Middle River at Borden Highway DWR station (RMID023) during the 2002 simulation period. 179

Figure 5.2-39 Observed and predicted stage at Middle River at Tracy Boulevard DWR station (RMID027) during the 2002 simulation period. 180

Figure 5.2-40 Observed and predicted stage at Middle River at Howard Road Bridge DWR station (CDEC MHR) during the 2002 simulation period..... 181

Figure 5.2-41 Observed and predicted stage at Middle River at Mowry Bridge DWR station (RMID040) during the 2002 simulation period. 182

Figure 5.2-42 Observed and predicted stage at Old River at Bacon Island USGS station (OLD) during the 2002 simulation period. 183

Figure 5.2-43 Observed and predicted stage at Old River near Byron USGS station (ORF) during the 2002 simulation period..... 184

Figure 5.2-44 Observed and predicted stage at Old River at Clifton Court Ferry DWR station (ROLD040) during the 2002 simulation period..... 185

Figure 5.2-45 Observed and predicted stage at Clifton Court Forebay DWR station (CHWST000) during the 2002 simulation period. 186

Figure 5.2-46 Observed and predicted stage at Grant Line Canal at Tracy Boulevard USGS station (GLC) during the 2002 simulation period..... 187

Figure 5.2-47 Observed and predicted stage at Old River near Delta Mendota Canal Downstream of Barrier DWR station (ROLD046) during the 2002 simulation period. 188

Figure 5.2-48 Observed and predicted stage at Delta Mendota Canal Upstream of Barrier USGS station (DMC) during the 2002 simulation period. 189

Figure 5.2-49 Observed and predicted stage at Old River at Tracy Boulevard DWR station (ROLD059) during the 2002 simulation period..... 190

Figure 5.2-50 Observed and predicted stage at Stockton Ship Channel at Burns Cutoff DWR station (RSAN058) during the 2002 simulation period..... 191

Figure 5.2-51 Observed and predicted stage at San Joaquin River at Stockton USGS station (STK) during the 2002 simulation period. 192

Figure 5.2-52 Observed and predicted stage at San Joaquin River below Old River near Lathrop DWR station (CDEC SJL) during the 2002 simulation period. 193

Figure 5.3-1 Location of flow monitoring stations in the northern portion of the Sacramento-San Joaquin Delta used for 2002 flow calibration. 199

Figure 5.3-2 Observed and predicted flow at Sacramento River South of Georgiana Slough USGS station (WGB) during the 2002 simulation period. 200

Figure 5.3-3 Observed and predicted flow at Georgiana Slough near Sacramento River USGS station (GEO) during the 2002 simulation period. 201

Figure 5.3-4 Observed and predicted flow at Delta Cross Channel USGS station (DCC) during the 2002 simulation period. 202

Figure 5.3-5 Observed and predicted flow at Sacramento River North of Delta Cross Channel USGS station (WGA) during the 2002 simulation period. 203

Figure 5.3-6 Observed and predicted flow at Sacramento River at Freeport USGS station (FPT) during the 2002 simulation period. 204

Figure 5.3-7 Observed and predicted flow at Steamboat Slough between Sacramento River and Sutter Slough USGS station (STM) during the 2002 simulation period. 205

Figure 5.3-8 Location of flow monitoring stations in the central portion of the Sacramento-San Joaquin Delta used for 2002 flow calibration. 206

Figure 5.3-9 Observed and predicted flow at Sacramento River at Rio Vista USGS station (RIO) during the 2002 simulation period. 207

Figure 5.3-10 Observed and predicted flow at Threemile Slough at San Joaquin River USGS station (TMS) during the 2002 simulation period. 208

Figure 5.3-11 Observed and predicted flow at San Joaquin River at Jersey Point USGS station (JPT) during the 2002 simulation period. 209

Figure 5.3-12 Observed and predicted flow at False River USGS station (FAL) during the 2002 simulation period. 210

Figure 5.3-13 Observed and predicted flow at Dutch Slough at Jersey Island USGS station (DCH) during the 2002 simulation period. 211

Figure 5.3-14 Observed and predicted flow at Taylor Slough USGS station (TYLR) during the 2002 simulation period. 212

Figure 5.3-15 Observed and predicted flow at Fisherman's Cut USGS station (FISH) during the 2002 simulation period. 213

Figure 5.3-16 Observed and predicted flow at Old River at San Joaquin USGS station (OSJ) during the 2002 simulation period. 214

Figure 5.3-17 Observed and predicted flow at Mokelumne River near San Joaquin River USGS station (MOK) during the 2002 simulation period. 215

Figure 5.3-18 Observed and predicted flow at Old River at Mandeville Island USGS station (MAN) during the 2002 simulation period. 216

Figure 5.3-19 Observed and predicted flow at Holland Cut USGS station (HOL) during the 2002 simulation period..... 217

Figure 5.3-20 Observed and predicted flow at Middle River south of Columbia Cut USGS station (MRC) during the 2002 simulation period..... 218

Figure 5.3-21 Location of flow monitoring stations in the southern portion of the Sacramento-San Joaquin Delta used for 2002 flow calibration..... 219

Figure 5.3-22 Observed and predicted flow at Middle River at Middle River USGS station (MID) during the 2002 simulation period. 220

Figure 5.3-23 Observed and predicted flow at Old River at Bacon Island USGS station (OLD) during the 2002 simulation period. 221

Figure 5.3-24 Observed and predicted flow at Old River near Byron USGS station (ORF) during the 2002 simulation period..... 222

Figure 5.3-25 Observed and predicted flow at San Joaquin River at Stockton USGS station (STK) during the 2002 simulation period. 223

Figure 5.3-26 Observed and predicted flow at Old River at Head DWR station (ROLD074) during the 2002 simulation period..... 224

Figure 6.1-1 Comparison between observed flow and flow predicted by DSM2 on Old River at the San Joaquin River. Top figure shows tidal time-scale flow. Bottom figure shows tidally-averaged flow for observed (grey), predicted using current DSM2geometry (dashed grey), and modified DSM2 geometry (black). From Suits and Wilde (2004). 227

Figure 6.1-2 Comparison between observed flow and flow predicted by DSM2 on Fisherman's Cut. Top figure shows tidal time-scale flow. Bottom figure shows tidally-averaged flow for observed (grey), predicted using current DSM2geometry (dashed grey), and modified DSM2 geometry (black). From Suits and Wilde (2004)..... 228

Figure 6.2-2 Location of several islands along the San Joaquin River which flood on high tides or are permanently flooded, but are not included in available Delta bathymetry or the current model grid..... 231

Figure 6.2-3 Location of several islands south of Franks Tract, including Little Mandeville Island (center) and Rhode Island (lower left), which flood on high tides or are permanently flooded, but are not included in available Delta bathymetry or the current model grid. 232

Figure 6.4-1 Location of four USGS flow monitoring stations near the Delta Cross Channel used in net flow comparison for 2007 simulation period. 234

Figure 6.4-2 Observed (black arrows) and Predicted (green arrows) average net flow at four USGS flow monitoring stations near the Delta Cross Channel during 2007 simulation period spanning from April 4, 2007 through September 1, 2007. 235

Figure 6.4-3 Location of four USGS and DWR flow monitoring stations near the Head of Old River used in net flow and inter-model comparisons for 2007 simulation period. 238

Figure 6.4-4 Comparison between observed flows and flows predicted by DSM2 and UnTRIM on the San Joaquin River at Mossdale (RSAN087). The top figure shows tidal-timescale flows over a 15-day period. The bottom figure shows tidally-averaged flows over the full simulation period between April 5, 2007 and September 1, 2007. 239

Figure 6.4-5 Comparison between observed flows and flows predicted by DSM2 and UnTRIM on Old River just downstream from the Head of Old River Barrier (ROLD074). The top figure shows tidal-timescale flows over a 55-day period spanning the period between April 20 and May 22 when the Head of Old River barrier was in operation. The bottom figure shows tidally-averaged flows over the full simulation period between April 5, 2007 and September 1, 2007. 240

Figure 6.4-6 Comparison between observed flows and flows predicted by UnTRIM on the San Joaquin River below Old River near Lathrop (SJL). Predicted DSM2 flows were not available at this station. The top figure shows tidal-timescale flows over a 15-day period. The bottom figure shows tidally-averaged flows over the full simulation period between April 5, 2007 and September 1, 2007. 241

Figure 6.4-7 Comparison between observed flows and flows predicted by DSM2 and UnTRIM on the San Joaquin River at Stockton (STK). The top figure shows tidal-timescale flows over a 15-day period. The bottom figure shows tidally-averaged flows over the full simulation period between April 5, 2007 and September 1, 2007. 242

Figure 6.4-8 Observed average net flows (black arrows) and average net flows predicted by UnTRIM (green arrows) and DSM2 (blue arrows) at four USGS and DWR flow monitoring stations on the San Joaquin River and Old River for the time period spanning from April 20 to May 22, 2007 when the spring Head of Old River barrier was in operation during the 2007 simulation period. 243

Figure A.1-1 Historical barrier operations schedule during the 1999 simulation period. 252

Figure A.2-1 Location of NOAA water level monitoring stations in San Francisco Bay used for 1999 stage calibration. 256

Figure A.2-2 Observed and predicted stage at San Francisco Fort Point NOAA station (9414290) during the 1999 simulation period. 257

Figure A.2-3 Observed and predicted stage at Alameda NOAA station (9414750) during the 1999 simulation period..... 258

Figure A.2-4 Observed and predicted stage at Redwood City NOAA station (9414523) during the 1999 simulation period. 259

Figure A.2-5 Observed and predicted stage at Richmond NOAA station (9414863) during the 1999 simulation period. 260

Figure A.2-6 Observed and predicted stage at Port Chicago NOAA station (9415144) during the 1999 simulation period. 261

Figure A.2-7 Location of water level monitoring stations in the northern portion of the Sacramento-San Joaquin Delta used for 1999 water level calibration. 262

Figure A.2-8 Observed and predicted stage at Sacramento River South of Georgiana Slough USGS station (WGB) during the 1999 simulation period. 263

Figure A.2-9 Observed and predicted stage at Sacramento River North of Delta Cross Channel USGS station (WGA) during the 1999 simulation period..... 264

Figure A.2-10 Observed and predicted stage at Mokelumne River near Thornton (Benson's Ferry) DWR station (RMKL027) during the 1999 simulation period..... 265

Figure A.2-11 Observed and predicted stage at South Fork Mokelumne River at New Hope Bridge DWR station (RSMKL024) during the 1999 simulation period. 266

Figure A.2-12 Location of water level monitoring stations in the central portion of the Sacramento-San Joaquin Delta used for 1999 water level calibration. 267

Figure A.2-13 Observed and predicted stage at Antioch DWR station (RSAN007) during the 1999 simulation period..... 268

Figure A.2-14 Observed and predicted stage at Sacramento River at Rio Vista USGS station (RIO) during the 1999 simulation period. 269

Figure A.2-15 Observed and predicted stage at Threemile Slough at San Joaquin River USGS station (TMS) during the 1999 simulation period. 270

Figure A.2-16 Observed and predicted stage at San Joaquin River at Jersey Point USGS station (JPT) during the 1999 simulation period..... 271

Figure A.2-17 Observed and predicted stage at Dutch Slough at Jersey Island USGS station (DCH) during the 1999 simulation period. 272

Figure A.2-18 Observed and predicted stage at San Joaquin River at San Andreas Landing DWR station (RSAN032) during the 1999 simulation period. 273

Figure A.2-19 Observed and predicted stage at North Fork Mokelumne River at Georgiana Slough DWR station (RMKL005) during the 1999 simulation period. 274

Figure A.2-20 Observed and predicted stage at San Joaquin River at Venice Island DWR station (RSAN043) during the 1999 simulation period. 275

Figure A.2-21 Observed and predicted stage at San Joaquin River at Rindge Pump DWR station (RSAN052) during the 1999 simulation period. 276

Figure A.2-22 Observed and predicted stage at Middle River south of Columbia Cut USGS station (MRC) during the 1999 simulation period. 277

Figure A.2-23 Location of water level monitoring stations in the southern portion of the Sacramento-San Joaquin Delta used for 1999 water level calibration. 278

Figure A.2-24 Observed and predicted stage at Middle River at Middle River USGS station (MID) during the 1999 simulation period. 279

Figure A.2-25 Observed and predicted stage at Middle River at Borden Highway DWR station (RMID023) during the 1999 simulation period. 280

Figure A.2-26 Observed and predicted stage at Middle River at Tracy Boulevard DWR station (RMID027) during the 1999 simulation period. 281

Figure A.2-27 Observed and predicted stage at Middle River at Mowry Bridge DWR station (RMID040) during the 1999 simulation period. 282

Figure A.2-28 Observed and predicted stage at Old River at Bacon Island USGS station (OLD) during the 1999 simulation period. 283

Figure A.2-29 Observed and predicted stage at Old River near Byron DWR station (ROLD034) during the 1999 simulation period. 284

Figure A.2-30 Observed and predicted stage at Old River at Clifton Court Ferry DWR station (ROLD040) during the 1999 simulation period. 285

Figure A.2-31 Observed and predicted stage at Grant Line Canal at Tracy Boulevard DWR station (CDEC GCT) during the 1999 simulation period. 286

Figure A.2-32 Observed and predicted stage at Grant Line Canal at Head DWR station (CHGRL012) during the 1999 simulation period. 287

Figure A.2-33 Observed and predicted stage at Old River near Delta Mendota Canal Downstream of Barrier DWR station (ROLD046) during the 1999 simulation period. 288

Figure A.2-34 Observed and predicted stage at Old River near Delta Mendota Canal Upstream of Barrier DWR station (ROLD047) during the 1999 simulation period. 289

Figure A.2-35 Observed and predicted stage at Old River at Tracy Boulevard DWR station (ROLD059) during the 1999 simulation period. 290

Figure A.2-36 Observed and predicted stage at San Joaquin River at Stockton USGS station (STK) during the 1999 simulation period. 291

Figure A.2-37 Observed and predicted stage at San Joaquin River at Mossdale DWR station (RSAN087) during the 1999 simulation period. 292

Figure A.3-1 Location of flow monitoring stations in the northern portion of the Sacramento-San Joaquin Delta used for 1999 flow calibration. 295

Figure A.3-2 Observed and predicted flow at Sacramento River South of Georgiana Slough USGS station (WGB) during the 1999 simulation period. 296

Figure A.3-3 Observed and predicted flow at Sacramento River North of Delta Cross Channel USGS station (WGA) during the 1999 simulation period. 297

Figure A.3-4 Observed and predicted flow at Sacramento River at Freeport USGS station (FPT) during the 1999 simulation period. 298

Figure A.3-5 Location of flow monitoring stations in the central portion of the Sacramento-San Joaquin Delta used for 1999 flow calibration. 299

Figure A.3-6 Observed and predicted flow at Sacramento River at Rio Vista USGS station (RIO) during the 1999 simulation period. 300

Figure A.3-7 Observed and predicted flow at Threemile Slough at San Joaquin River USGS station (TMS) during the 1999 simulation period. 301

Figure A.3-8 Observed and predicted flow at San Joaquin River at Jersey Point USGS station (JPT) during the 1999 simulation period. 302

Figure A.3-9 Observed and predicted flow at Dutch Slough at Jersey Island USGS station (DCH) during the 1999 simulation period. 303

Figure A.3-10 Observed and predicted flow at Middle River south of Columbia Cut USGS station (MRC) during the 1999 simulation period. 304

Figure A.3-11 Location of flow monitoring stations in the southern portion of the Sacramento-San Joaquin Delta used for 1999 flow calibration. 305

Figure A.3-12 Observed and predicted flow at Middle River at Middle River USGS station (MID) during the 1999 simulation period. 306

Figure A.3-13 Observed and predicted flow at Old River at Bacon Island USGS station (OLD) during the 1999 simulation period. 307

Figure A.3-14 Observed and predicted flow at Grant Line Canal at Tracy Boulevard USGS station (GLC) during the 1999 simulation period..... 308

Figure A.3-15 Observed and predicted flow at San Joaquin River at Stockton USGS station (STK) during the 1999 simulation period. 309

Abbreviations

1D	One-Dimensional
2D	Two-Dimensional
3D	Three-Dimensional
ADCP	Acoustic Doppler Current Profiler
BAAQCD	Bay Area Air Quality Control District
BBID	Byron Bethany Irrigation District
CCWD	Contra Costa Water District
CDEC	California Data Exchange Center
CIMIS	California Irrigation Management Information System
CSUMB	California State University Monterey Bay
CVP	Central Valley Project
DCC	Delta Cross Channel
DICU	Delta Island Consumptive Use
DEM	Digital Elevation Model
DFG	Department of Fish and Game
DMC	Delta Mendota Canal
DRMS	Delta Risk Management Strategy
DSS	Data Storage System
DWR	Department of Water Resources
EC	Electrical Conductivity
GLC	Grant Line Canal
GLS	Generic Length Scale
HOR	Head of Old River
IEP	Interagency Ecological Program
MLLW	Mean Lower Low Water
MR	Middle River
NAD27	North American Datum of 1927
NBA	North Bay Aqueduct
NGVD 29	National Geodetic Vertical Datum of 1929
NOAA	National Oceanic & Atmospheric Administration
NOS	National Ocean Service (NOAA)
OMR	Old and Middle River
ORT	Old River near Tracy
POD	Pelagic Organism Decline
PTM	Particle Tracking Model
SCWA	Solano County Water Agency
SFML	Seafloor Mapping Lab
SFPORTS	San Francisco Physical Oceanographic Real-Time System
SMSCG	Suisun Marsh Salinity Control Gates
SWP	State Water Project
TBP	Temporary Barriers Project
TRIM	Tidal, Residual, Intertidal & Mudflat Model
UnTRIM	Unstructured Tidal, Residual, Intertidal & Mudflat Model

USACE	United States Army Corps of Engineers
USBR	United States Bureau of Reclamation
USGS	United States Geological Survey
UTM	Universal Transverse Mercator

1. Introduction

The motivation for this study is the observed decline of delta smelt and other pelagic organisms of the upper San Francisco Estuary. Three general factors identified to explain lower pelagic productivity are 1) toxic effects; 2) exotic species effects; and 3) water project effects (Resources Agency, 2007). For each of these factors the location and movement of delta smelt are likely to be critical for understanding the reasons for the pelagic organism decline (POD) and the efficacy of any actions taken to sustain pelagic fish populations.

In order to investigate the location movement of delta smelt within the Delta, a three-dimensional hydrodynamic model was applied to simulate hydrodynamics in the Sacramento-San Joaquin Delta, and the hydrodynamic results were used with a particle tracking model to investigate delta smelt distribution and behavior. The Bay-Delta UnTRIM model developed for the Delta Risk Management Strategy (DRMS) project (MacWilliams et al., 2007) was extended to include the entire Sacramento-San Joaquin Delta. This report presents the results of the hydrodynamic modeling component of the project.

The results from the 3-D UnTRIM model of the San Francisco Bay-Delta are being used with a Particle Tracking Model (PTM) developed by Dr. Edward Gross. The particle tracking simulations are being compared to observed delta smelt distributions to test hypothesis regarding delta smelt hatching rates, distribution, and behavior. The results from the particle tracking applications will be presented in a separate report.

This report is divided into eight major sections:

- **Section 1. Introduction.** This section presents the project approach and objectives, as well as a summary of the scope and organization of the report.

- **Section 2. UnTRIM Model Description.** This section provides a description of the UnTRIM hydrodynamic model, with a discussion of the governing equations and model uncertainty.

- **Section 3. San Francisco Bay-Delta UnTRIM Model.** This section presents the model domain, and boundary conditions, and initial conditions used in the Bay-Delta UnTRIM model.

- **Section 4. Hydrodynamic Calibration.** This section presents the water level and flow calibration results for the Bay-Delta UnTRIM model during the 2007 calibration period.

- **Section 5. Hydrodynamic Validation.** This section presents the water level and flow validation results for the Bay-Delta UnTRIM model during the 2002 validation period.

- **Section 6. Discussion and Future Improvements.** This section provides a discussion of the model results and identifies potential improvements that can be incorporated into future Bay-Delta UnTRIM model applications.

- **Section 7. Summary and Conclusions.** This section presents a brief summary of the hydrodynamic modeling results and the conclusions drawn from the model implementation and calibration.

- **Appendix A. Model Validation Figures for 1999 Simulation Period.** An additional period during April through July 1999 was simulated to provide hydrodynamic output to be used with the particle tracking model. This section presents an additional set of hydrodynamic validation figures for the 1999 simulation period.

2. UnTRIM Model Description

The primary tool used in this technical study was the three-dimensional hydrodynamic model UnTRIM (Casulli and Zanolli, 2002). A complete description of the governing equations, numerical discretization, and numerical properties of UnTRIM are described in Casulli and Zanolli (2002, 2005), Casulli (1999), and Casulli and Walters (2000).

The UnTRIM model solves the three-dimensional Navier-Stokes equations (3.1-3.3) on an unstructured grid in the horizontal plane. The boundaries between vertical layers are at fixed elevations, and cell heights can be varied vertically to provide increased resolution near the surface or other vertical locations. Volume conservation is satisfied by a volume integration of the incompressible continuity equation (3.4), and the free-surface is calculated by integrating the continuity equation over the depth (3.5), and using a kinematic condition at the free-surface as described in Casulli (1990). The numerical method allows full wetting and drying of cells in the vertical and horizontal directions. The governing equations are discretized using a finite difference – finite volume algorithm. Discretization of the governing equations and model boundary conditions are presented in detail by Casulli and Zanolli (2002) and is not reproduced here. All details and numerical properties of this state-of-the-art three-dimensional model are well-documented in peer reviewed literature (Casulli and Zanolli, 2002; 2005).

2.1 Governing Equations

Three-dimensional simulations were made using the three-dimensional non-hydrostatic hydrodynamic model for free-surface flows on unstructured grids, UnTRIM, described in Casulli and Zanolli (2002). The UnTRIM model solves the full three-dimensional momentum equations for an incompressible fluid under a free-surface given by

$$\frac{\partial u}{\partial t}+u\frac{\partial u}{\partial x}+v\frac{\partial u}{\partial y}+w\frac{\partial u}{\partial z}-fv=-\frac{\partial p}{\partial x}+\nu^h\left(\frac{\partial^2 u}{\partial x^2}+\frac{\partial^2 u}{\partial y^2}\right)+\frac{\partial}{\partial z}\left(\nu^v\frac{\partial u}{\partial z}\right) \tag{3.1}$$

$$\frac{\partial v}{\partial t}+u\frac{\partial v}{\partial x}+v\frac{\partial v}{\partial y}+w\frac{\partial v}{\partial z}+fu=-\frac{\partial p}{\partial y}+\nu^h\left(\frac{\partial^2 v}{\partial x^2}+\frac{\partial^2 v}{\partial y^2}\right)+\frac{\partial}{\partial z}\left(\nu^v\frac{\partial v}{\partial z}\right) \tag{3.2}$$

$$\frac{\partial w}{\partial t}+u\frac{\partial w}{\partial x}+v\frac{\partial w}{\partial y}+w\frac{\partial w}{\partial z}=-\frac{\partial p}{\partial z}+\nu^h\left(\frac{\partial^2 w}{\partial x^2}+\frac{\partial^2 w}{\partial y^2}\right)+\frac{\partial}{\partial z}\left(\nu^v\frac{\partial w}{\partial z}\right)-g \tag{3.3}$$

where $u(x,y,z,t)$ and $v(x,y,z,t)$ are the velocity components in the horizontal x - and y - directions, respectively; $w(x,y,z,t)$ is the velocity component in the vertical z - direction; t is the time; $p(x,y,z,t)$ is the normalized pressure defined as the pressure divided by a constant reference density; f is the Coriolis parameter; g is the gravitational acceleration; and ν^h and ν^v are the coefficients of horizontal and vertical eddy viscosity, respectively (Casulli and Zanolli, 2002). Conservation of volume is expressed by the continuity equation for incompressible fluids

$$\frac{\partial u}{\partial x}+\frac{\partial v}{\partial y}+\frac{\partial w}{\partial z}=0. \tag{3.4}$$

The free-surface equation is obtained by integrating the continuity equation over depth and using a kinematic condition at the free-surface (Casulli and Zanolli, 2002)

$$\frac{\partial \eta}{\partial t}+\frac{\partial}{\partial x}\left[\int_{-h}^{\eta} u dz\right]+\frac{\partial}{\partial y}\left[\int_{-h}^{\eta} v dz\right]=0, \tag{3.5}$$

where $h(x,y)$ is the prescribed bathymetry measured downward from the reference elevation and $\eta(x,y,t)$ is the free-surface elevation measured upward from the reference elevation. Thus, the total water depth is given by $H(x,y,t)=h(x,y)+\eta(x,y,t)$.

The boundary conditions at the free-surface are specified by the prescribed wind stresses as (Casulli and Zanolli, 2002)

$$\nu^{v}\frac{\partial u}{\partial z}=\tau_x{}^{w}, \quad \nu^{v}\frac{\partial v}{\partial z}=\tau_y{}^{w}, \quad \text{at } z=\eta \tag{3.6}$$

where τ_x^w and τ_y^w are the wind stress components in the x and y direction, respectively. Similarly, at the sediment-water interface the bottom friction is specified by

$$\nu^{v}\frac{\partial u}{\partial z}=\tau_x, \quad \nu^{v}\frac{\partial v}{\partial z}=\tau_y, \quad \text{at } z=-h \tag{3.7}$$

where τ_x and τ_y are the bottom stress components in the x and y direction, respectively. A quadratic stress formula is applied at each boundary. At the free-surface the coefficient of drag is specified as a function of wind speed using the formulation of Large and Pond (1981). At the bottom boundary the coefficient of drag is estimated using a specified roughness coefficient (z_0).

The governing equation for salt transport (Casulli and Zanolli, 2002) is

$$\frac{\partial s}{\partial t}+\frac{\partial(us)}{\partial x}+\frac{\partial(vs)}{\partial y}+\frac{\partial(ws)}{\partial z}=\frac{\partial}{\partial x}\left(\varepsilon_h\frac{\partial s}{\partial x}\right)+\frac{\partial}{\partial y}\left(\varepsilon_h\frac{\partial s}{\partial y}\right)+\frac{\partial}{\partial z}\left(\varepsilon_v\frac{\partial s}{\partial z}\right) \tag{3.8}$$

where s is the scalar concentration; ε_h is the horizontal diffusion coefficient; and ε_v is the vertical diffusion coefficient. A linear equation of state was used to relate salinity to density. This approximation allows a substantial reduction in computational time relative to the use of the nonlinear relationships. The estimation of eddy viscosity and eddy diffusivity is discussed below.

2.2 Turbulence Model

The turbulence closure model used in the present study is a two-equation model comprised of a turbulent kinetic energy equation and a generic length-scale equation. The parameters of the generic length-scale (GLS) equation are chosen to yield the "gen" closure proposed by Umlauf and Burchard (2003). The Kantha and Clayson quasi-equilibrium stability functions (Kantha and Clayson, 1994) are used. This closure has been shown by Warner et al. (2005) to have several advantages relative to the commonly used Mellor-Yamada level 2.5 closure and to generally perform similarly to the GLS versions of k-ε and k-ω. All parameter values used in the "gen" closure are identical to those used by Warner et al. (2005), except for the minimum eddy diffusivity and eddy viscosity values which were $5x10^{-5}$ m^2/s. The numerical method used to solve the equations of the turbulence closure is a semi-implicit method that results in tridiagonal positive-definite matrices in each water column and ensures that the turbulent variables remain positive (Deleersnijder et al., 1997).

2.3 Previous Applications

The TRIM3D model (Casulli and Cheng, 1992) and UnTRIM model have been applied previously to San Francisco Bay (Cheng and Casulli, 2002; MacWilliams and Cheng, 2007; MacWilliams et. al, 2007). The TRIM3D model (Casulli and Cattani 1994) which follows a similar numerical approach on structured horizontal grids has been widely applied in San Francisco Bay (e.g., Cheng et al. 1993; Cheng and Casulli, 1996; Gross et al., 1999; Gross et al., 2006), and a 2D version, TRIM2D, is used in San Francisco Bay Physical Oceanographic Real-Time System, SFPORTS (URL: http://sfports.wr.usgs.gov/sfports) (Cheng and Smith, 1998). Thus, the UnTRIM numerical approach has been well-tested in San Francisco Bay, and is very well suited to perform the types of analysis used in this study.

2.4 Model Uncertainty

As discussed above, the TRIM and UnTRIM models have been widely used in San Francisco Bay, and numerous detailed model calibrations have been performed (e.g., Cheng et al., 1993; Gross and Schaaf & Wheeler, 2003; Gross et al., 2006; MacWilliams and Cheng, 2007; MacWilliams and Gross, 2007). Due to this extensive history of application, these models are the best established three-dimensional models of San Francisco Bay.

The equations governing fluid motion and salt transport, representing conservation of water volume, momentum and salt mass, are well established, but cannot be solved analytically for complex geometry and boundary conditions. Therefore numerical models are used to give approximate solutions to these governing equations. Many decisions are made in constructing and applying numerical models. The governing equations are first chosen to represent the appropriate physical processes in one, two or three-dimensions and at the appropriate time scale. Then these governing equations that describe fluid motion and salt transport in a continuum are discretized giving rise to a set of algebraic equations. The resulting discretized algebraic equations must be solved, often requiring the use of an iterative matrix solver. The discretization

and matrix solution must be developed carefully to yield a numerical scheme that is consistent with the governing equations, stable and efficient. To apply the models, the bathymetric grid, boundary conditions, initial conditions and several model parameters must be chosen. The accuracy of the model application depends on the appropriate choice of these inputs, including site-specific parameters, the numerical scheme for solving the governing equations, and the associated choice of time step and grid size.

The three-dimensional model applied in this project provides a more detailed description of fluid motion in San Francisco Bay than depth-averaged or one-dimensional models. The UnTRIM model, like almost all large scale hydrodynamic models, averages over the turbulent time scale to describe tidal time scale motions. The resulting three-dimensional hydrodynamic models represent the effect of turbulent motions as small scale mixing of momentum and salt, parameterized by eddy viscosity and eddy diffusivity coefficients, respectively. These turbulent mixing coefficients are estimated from the tidal flow properties (velocity and density) by "turbulence closure" models embedded within the three-dimensional models. Three-dimensional models estimate the variability in velocity and salinity in all dimensions and through the tidal cycle, therefore provide a detailed description of hydrodynamics and salinity. However, several sources of uncertainty are inherent in the application of these three-dimensional models:

- Spatial resolution/computational cost – the spatial resolution of the bathymetry of the model domain, and velocity and salinity distributions, is limited by the large computational expense associated with high-resolution models. The description of the Bay-Delta bathymetry is improved by the use of a flexible unstructured grid, with coarser grid resolution used in the bay portions of the grid and increasing grid resolution in the Delta to optimize computational efficiency.
- Bathymetry data – limited spatial coverage and accuracy of bathymetry data can be a substantial source of uncertainty. Converting all data to a uniform vertical datum and horizontal datum can lead to some error. In particular, LiDAR data may have substantial errors in vertical datum and removing vegetation from the dataset can be difficult. In the present application, bathymetric data from multiple sources were merged to develop the model bathymetry.
- Site-specific parameters – the UnTRIM model requires bottom friction coefficients to parameterize the resistance to flow at solid boundaries. These parameters are specified and adjusted in model calibration. The values used in the present application have been applied in several recent applications (e.g., MacWilliams et al., 2007).
- Turbulence closure – the effect of turbulent motions on the tidal time scale motions is parameterized by a turbulence closure. While many turbulence closures are available (e.g., Warner et al., 2005), this is an ongoing area of research and, particularly in stratified settings, the effect of turbulence on tidal flows and salinity is not easy to estimate accurately. Different turbulence closures may give significantly different results in stratified settings (e.g., Stacey, 1996).
- Numerical errors – a numerical method approximates the governing equations to some level of accuracy. The mathematical properties of the numerical method of the TRIM and UnTRIM models are well understood due to detailed mathematical analysis presented in several peer reviewed publications. While the stability and conservation properties of the

method are ideal, a remaining source of error in the numerical method is some limited numerical diffusion of momentum, which may cause some damping of tidal propagation.

- Boundary conditions and initial conditions – The salinity in San Francisco Bay varies laterally (e.g., Huzzey et al., 1990) but this lateral variability can not be described by existing observations. In addition, only limited observations are available to describe the vertical distribution of salinity. Therefore, lateral and vertical salinity distributions must be achieved by interpolation and extrapolation from the limited observations to obtain initial salinity fields. Inflows to the estuary are also quite uncertain in several regions due to un-gauged portions of watersheds and uncertainty in estimates of outflows and diversions in the Sacramento-San Joaquin Delta.

Though additional potential sources of uncertainty can be identified, the largest sources of uncertainty for hydrodynamic predictions are the accuracy and resolution of available bathymetry and the grid resolution used to represent this bathymetry in the model. This study made use of the best available high resolution bathymetric data, and the highest computationally practical grid resolution throughout the Delta. However, many of the available bathymetry data sets in other portions of the San Francisco Bay are fairly old and they required vertical and or horizontal coordinate transformations for the grid used in this project. Additionally, the most recent bathymetry for the Delta does not include many in-channel islands and other subtidal areas that are subject to flooding at high water, particularly during spring tide.

The uncertainty in Delta outflows can also be a substantial uncertainty in summer conditions, particularly when consumptive use within the Delta (which is only known approximately) is typically the same order of magnitude as Delta tributary flows. The current application makes use of monthly Delta Island Consumptive Use (DICU) estimates from DWR. However, because these estimates of diversions and return flows and salinities are approximate, they may not be representative of actual consumptive use in a particular year. This uncertainty would impact the accuracy of net Delta outflows predicted at the flow monitoring stations in the western Delta, when compared to observed flows. In addition, uncertainty in net Delta outflows and agricultural return flow salinities also has a significant impact on salinity predictions throughout the Delta.

3. San Francisco Bay-Delta UnTRIM Model

This project builds on an existing model of San Francisco Bay and the Sacramento-San Joaquin Delta developed for the Department of Water Resources (DWR) as part of the Delta Risk Management Strategy (DRMS) project by MacWilliams and Gross (2007). As part of the current project, the model domain was extended west to Point Reyes in order to include a larger portion of the coastal Pacific Ocean, and the Sacramento-San Joaquin Delta portion of the model domain was expanded to encompass the entire Delta.

This section provides the details of the UnTRIM model application to the San Francisco Bay-Delta, and includes a discussion of the model domain and grid, bathymetric data sources, simulation periods, boundary conditions, and the model implementation of Delta agricultural diversions and operations. Calibration of the resulting hydrodynamic model for a period during summer 2007 is presented in Section 4, and validation for summer 2002 conditions is presented in Section 5. An additional validation period during summer 1999 is presented in Appendix A.

3.1 Model Domain and Grid

The model grid developed for this project expands on the UnTRIM model grid originally developed for the DRMS project as described by MacWilliams and Gross (2007). Several significant improvements were made to the model grid. The Pacific Ocean portion of the grid, which had previously used a simplified geometry, was replaced with an accurate representation of the coastal Pacific Ocean geometry and bathymetry outside of the Golden Gate, extending to Point Reyes. The “False Delta” boxes used to represent prism in unresolved portions of the Delta were removed, and the Delta portion of the model grid was refined and expanded to encompass the entire Sacramento-San Joaquin Delta. The resulting model domain extends from the coastal Pacific Ocean at Point Reyes through the entire Sacramento-San Joaquin Delta, and includes South Bay, Central Bay, San Pablo Bay, and Suisun Bay, as shown in Figure 3.1-1.

The unstructured grid for the model domain was developed using the grid generator JANET (Lippert and Sellerhoff, 2007). The grid was developed such that the main channels of the estuary are discretized using “orthogonal curvilinear” quadrilaterals which are aligned with the principal flow directions, while the remainder of the mesh is constructed using a mix of triangles and quadrilaterals. The grid resolution along the axis of the estuary varies as necessary to resolve bathymetric variability. Grid cell side lengths are approximately 1 km at the Ocean Boundary, 400 m at the Golden Gate and in the Central Bay (Figure 3.1-2) and become gradually smaller eastward, with resolution of 50 to 75 m in the western Delta (Figure 3.1-3), and resolution of 10 to 50 m in the central and southern Delta (Figure 3.1-4). This approach takes advantage of the full flexibility of unstructured grids, and offers significant advantages both in terms of numerical efficiency and accuracy. The vertical grid resolution is specified to be 1 m in all portions of the model domain. The resulting model domain contains 126,498 horizontal grid cells, more than 1.2 million 3-D grid cells, and more than 2.6 million active cell faces in three dimensions where the face normal velocity is computed at each time step.

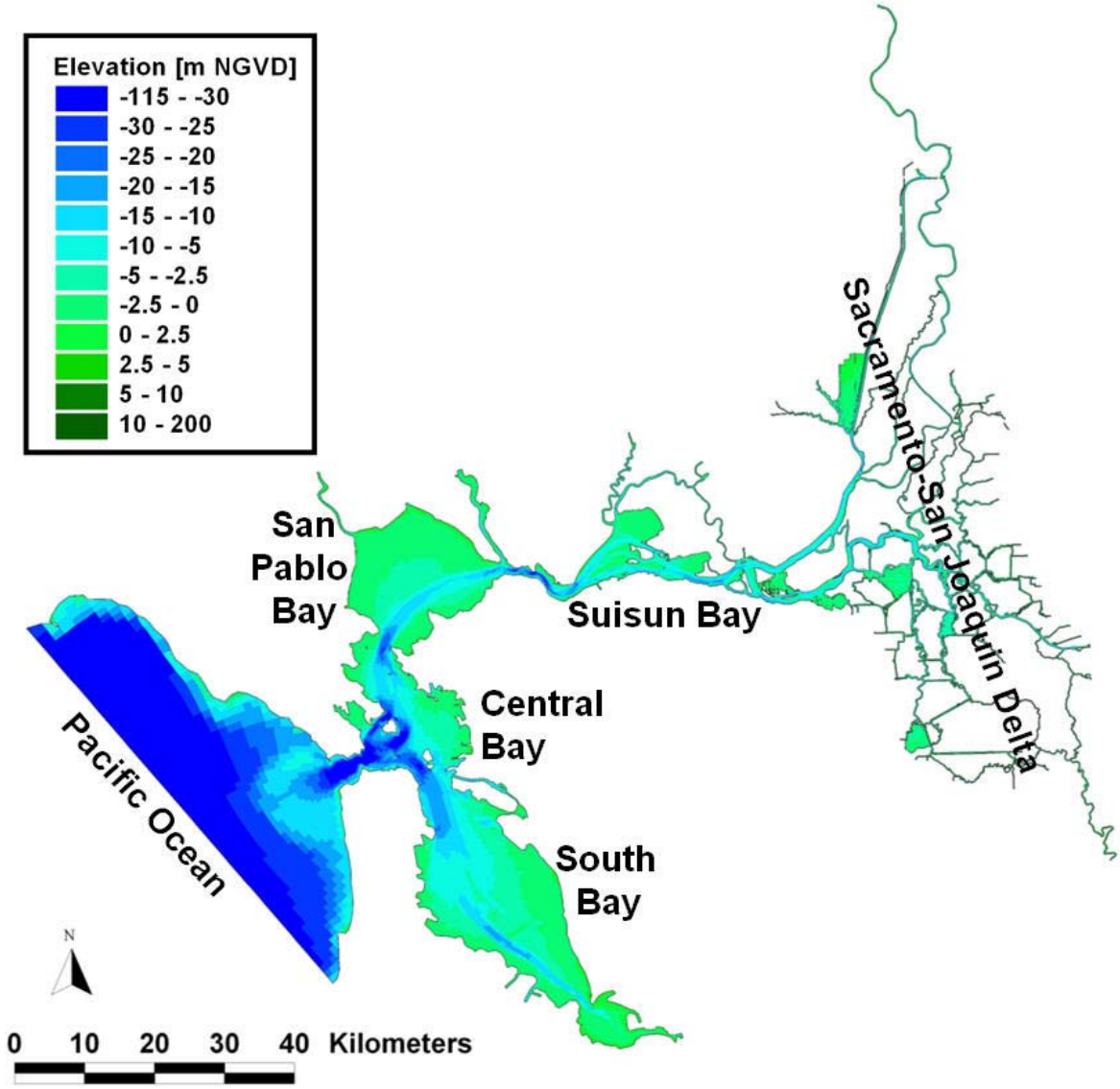

Figure 3.1-1 Model domain for the UnTRIM-Bay Delta model.

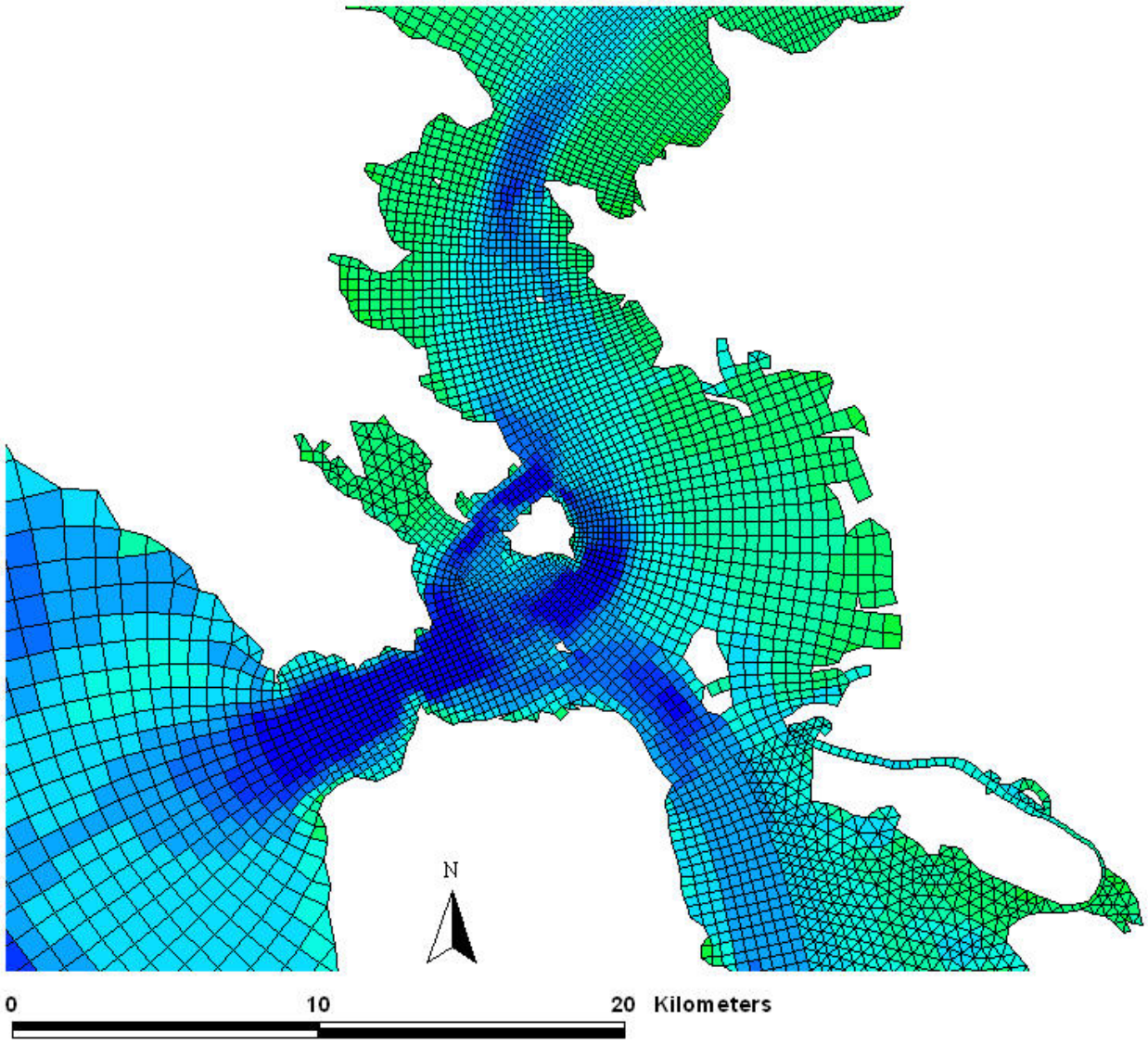

Figure 3.1-2 UnTRIM model grid in San Francisco Bay.

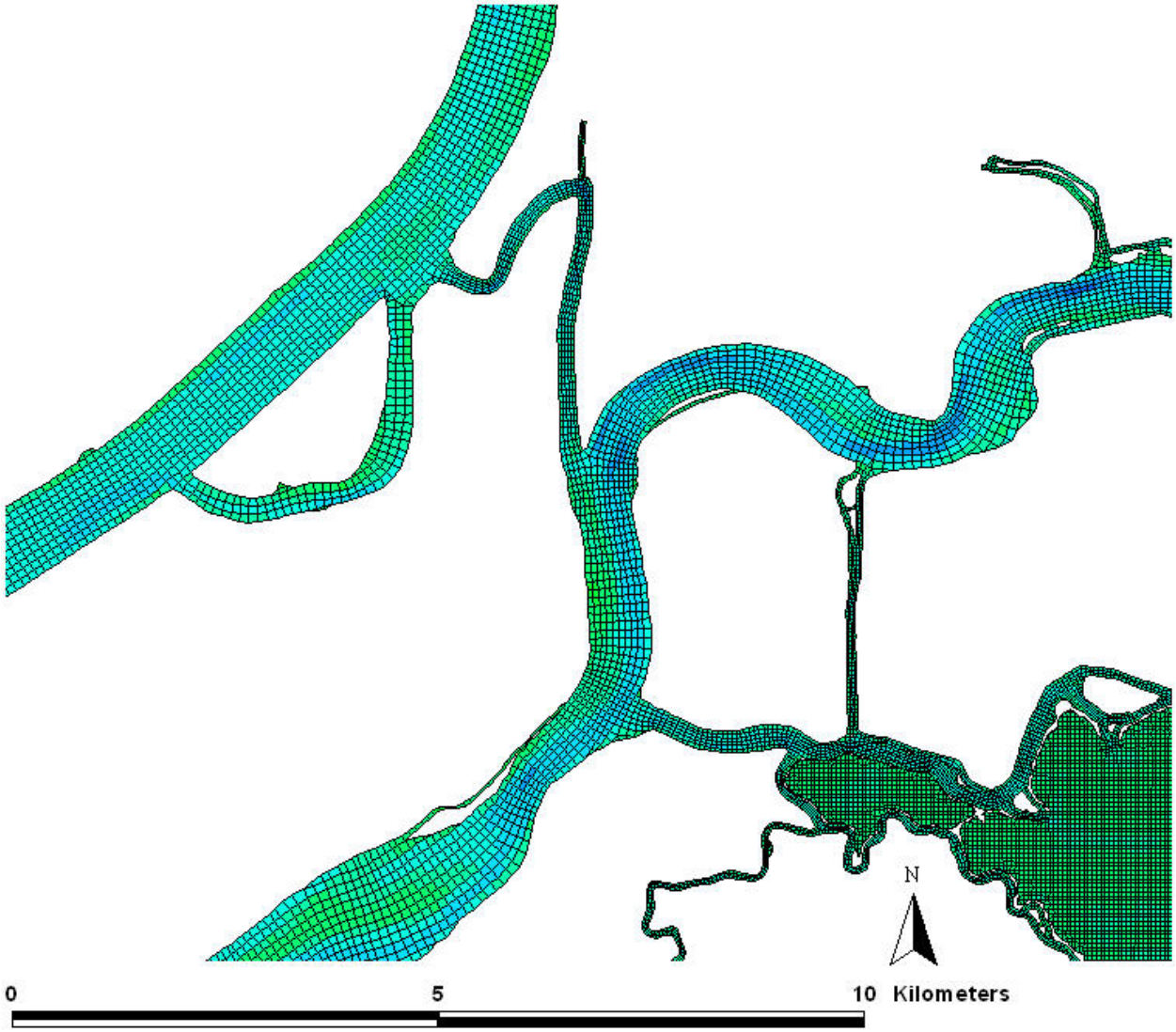

Figure 3.1-3 UnTRIM model grid in western portion of the Sacramento-San Joaquin Delta.

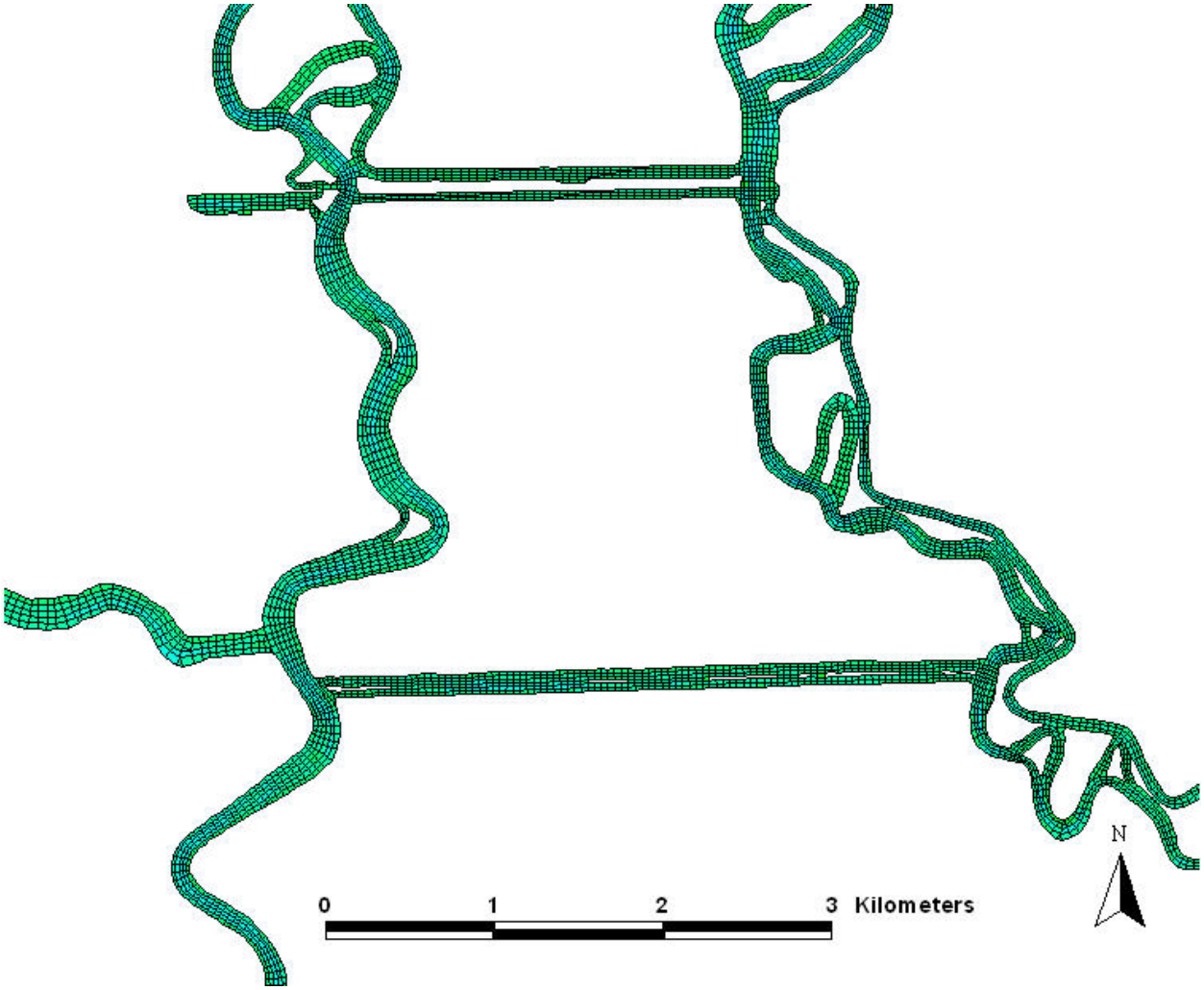

Figure 3.1-4 UnTRIM model grid in southern portion of the Sacramento-San Joaquin Delta.

3.2 Model Bathymetry

In order to provide the most accurate representation of San Francisco Bay and Sacramento-San Joaquin Delta bathymetry on the Bay-Delta UnTRIM model grid, high resolution bathymetric data from several sources were incorporated into the model bathymetry.

3.2.1 Pacific Ocean and Golden Gate

In 2004 and 2005, the Seafloor Mapping Lab (SFML) at CSUMB conducted the first bathymetric survey of the entrance region to the Golden Gate since the 1950s. This survey, done in conjunction with the USGS, was carried out to assist a USGS study of the wave regime and sediment movement at Ocean Beach, San Francisco. Bathymetric and backscatter (sidescan) data were collected aboard the R/V VenTresca using a Reson 8101 multibeam echosounder. The multibeam bathymetry data were post processed using Caris Hips and Sips hydrographic software, and were made available at 2 m horizontal resolution.

Bathymetry for the remaining portions of the coastal Pacific Ocean included in the model grid were derived from a California-vicinity bathymetric and terrestrial digital elevation model (DEM) at 90 meter resolution, distributed by the California Department of Fish and Game (DFG). This data set was produced largely from the NOAA NGDC Coastal Relief Model product (version 4.1). Data sources include NOAA NOS Hydrographic Surveys and U.S. Geological Survey 3-arc-second terrestrial DEM's. In addition to the Coastal Relief Model data, some far offshore areas were supplemented with other USGS bathymetric data processed by DFG.

3.2.2 Central and South San Francisco Bay and San Pablo Bay

In 1996 and 1997 the USGS in coordination with the National Oceanographic and Atmospheric Administration (NOAA) collected high resolution multibeam data from the Golden Gate into Central San Francisco Bay. This mapping of Central San Francisco Bay was done in three different surveys, using a Kongsberg Simrad EM-1000 Multibeam System hull mounted to the C&C Technologies' RV Coastal Surveyor. The Bathymetry was processed using the approach described by Gardner et al. (1998), and was made available at 4 m resolution (USGS, 2007).

The primary data source for the bathymetric grid of South San Francisco Bay, the remaining portions of Central Bay not covered by the 1996-1997 USGS survey, and San Pablo Bay was from NOAA DEM (Digital Elevation Model) data. The DEM data specifies depth on a 30 meter grid in San Francisco Bay. The DEM data were generated by NOAA using NOS soundings and other bathymetry data collected in San Francisco Bay from 1979 to 1985.

3.2.3 Suisun Bay and Sacramento-San Joaquin Delta

In Suisun Bay and the Sacramento-San Joaquin Delta, the bathymetry was developed using the USGS 10 m horizontal resolution bathymetric grid based on nearly one million depth soundings augmented by contours and recent aerial photography (Smith et al., 2003). The USGS

bathymetry was augmented by additional bathymetric data in portions of the Delta not included in the USGS data set, including Liberty Island, Mildred Island, Barker Slough, and upstream portions of the Sacramento River and San Joaquin River.

Bathymetry data for Liberty Island were obtained from the 2005 LiDAR flight of the Yolo Bypass, commissioned by DWR. Due to technological limitations and issues with the flight path, the 2005 data did not fit within the predetermined specifications set by DWR and readings from water surfaces were not properly removed from the data set (Lower Yolo Bypass Planning Forum, 2008). As a result the bathymetry for this portion of the model grid (as well as other in-channel islands and marshes) should be updated when the 2007 Delta LiDAR data collected by DWR are available.

Bathymetric data for Barker Slough and Lindsey Slough were from a survey conducted by Philip Williams & Associates in 2006 as part of a study for the Solano County Water Agency (SCWA). The SCWA Barker Slough survey was conducted by boat using a survey grade fathometer and survey grade RTK GPS system. The coordinates of the original data were California State Plane Zone 2, NAD 83, NGVD 29, and converted to UTM10 NAVD 88 using the Corpscon program (USACE, 2008).

To the authors' knowledge detailed bathymetric data for Mildred Island are not currently available. The model bathymetry used in this study was derived by digitizing a rough contour map developed for Mildred Island by the USGS based on a limited number of depth measurements collected using an ADCP (Pete Smith, 2008, personal communication). Shorelines and the size and locations of breaches in the levee surrounding Mildred Island were determined from aerial photography. It is expected that significant uncertainty exists in this data, resulting in significant uncertainty in the hydrodynamics inside Mildred Island. More accurate bathymetry for Mildred Island is needed to improve the model representation of Mildred Island hydrodynamics. However, since the breaches and flooded area were determined using available aerial photography, the current approach should represent the tidal prism of Mildred Island with reasonable accuracy.

No bathymetry data are currently available for Little Mandeville Island, which is also currently flooded. Additionally, topography data are not available for a large number of in-channel islands and marshes which appear to be flooded on high tides. These data gaps likely result in an under estimation of tidal prism in some portions of the Delta, particularly in the region south of Franks Tract. This is discussed in more detail in Section 6.2. When the 2007 DWR LiDAR data are available, additional in-channel islands and marshes should be added to the model grid, provided that the effects of vegetation and water surface are removed from the data. Additional bathymetric surveying of Little Mandeville Island is likely to be required since the island is already flooded.

The bathymetric data for the Sacramento Deep Water Ship Channel ends approximately 4 km from the Port of Sacramento. Bathymetry for the upstream reach of the Sacramento Deep Water Ship Channel was approximated using a representative cross-section from the upstream extent of the available data. Bathymetry in the Port of Sacramento and the marsh north of the port was also approximated using approximate estimates of depth and marsh elevation. It is expected that

this approach gives a reasonable estimate of the total prism of the Sacramento Deep Water Ship Channel and the Port of Sacramento but that additional bathymetry should be collected in the Port of Sacramento if a more detailed study of the area is conducted.

Some approximations to the model bathymetry were used in the upstream portions of the Sacramento River and San Joaquin River portions of the grid. On the Sacramento River upstream of the junction with the American River, detailed bathymetric data were not available. The levees and shoreline between the American River and Verona, CA was digitized based on available aerial photography, and the channel slope and shape was approximated based on average land surface slope in the reach. A similar approach was applied on the San Joaquin River between Mossdale Bridge and Vernalis, CA. These portions of the model grid were necessary to obtain a reasonable representation of tidal prism in the upstream portions of the Sacramento River and San Joaquin River.

3.2.4 Projection and Datum Conversion

Each of the bathymetric data sets was projected to the UTM NAD83 coordinate system and the vertical datum was adjusted to NGVD29. Some minor smoothing was done along the shorelines where bathymetry was not available and at locations where bathymetric data sources overlapped to minimize any artifacts resulting from combining multiple bathymetric data sources. The bathymetric data were then sampled over each grid cell and the specified water depth was determined as the mean of the bathymetric data points falling within each grid cell. The resulting model bathymetry can be seen in Figures 3.1-1 through 3.1-4.

3.3 Simulation Periods

Three separate periods were simulated as part of this project. The period spanning from April 2, 2007 through September 1, 2007 was used for the model calibration period. This period was selected due to the large number of flow and stage monitoring data available in the Delta during this period. The results of the 2007 calibration period are presented in Section 4. The model validation period spans from May 6, 2002 through September 1, 2002. This period was selected for model validation due to the available monitoring data around Franks Tract collected by the USGS in 2002. This period was also used for model calibration of RMA2 for the Flooded Islands Pre-Feasibility Study (RMA, 2005) and in the DRMS Project (MacWilliams and Gross, 2007). The results of the 2002 model validation period are presented in Section 5. An additional period spanning from April 13, 1999 through August 1, 1999 was simulated in order to provide hydrodynamic model output for use with the Particle Tracking Model (PTM). This period was also used as an additional validation period for flow and stage. The results for this simulation period are presented in Appendix A.

3.4 Salinity Boundary and Initial Conditions

The salinity at the ocean boundary is assumed to be 33.5 psu, which is a typical of observed salinity in the coastal ocean near San Francisco Bay (Dever and Lentz, 1994). The initial salinity

field is specified based on synoptic salinity data collected by the USGS in the main channel of San Francisco Bay (USGS, 2008), and assuming that salinity is laterally uniform in the Estuary and equal to 33.5 psu in the coastal ocean. Therefore the initial salinity field varies longitudinally and vertically but is laterally uniform. The synoptic salinity data are typically collected over a period of 10 to 12 hours, as the USGS research vessel travels along the channel of San Francisco Bay from the South Bay to the western Delta. The location of the synoptic monitoring stations are shown on Figure 3.4-1. For each simulation period, the simulation start date is approximately one to two days prior to a USGS synoptic salinity collection period to allow for hydrodynamic spin-up.

The observed salinity field was specified at the beginning of the simulation as an initial condition and then reset to the observed values again at approximately the mid-point of the cruise, when realistic tidal velocities were present in the simulation. Applying the initial condition in the entire domain simultaneously and assuming laterally uniform salinity, results in some error in initial salinity predictions.

For the 2007 simulation period, the salinity initial condition was specified using the synoptic salinity data collected by the USGS on April 3, 2007. For the 2002 simulation period the salinity initial condition was specified using the synoptic salinity data collected by the USGS on May 7, 2002. The synoptic salinity data collected by the USGS on April 14, 1999 was used to specify the salinity initial condition for the 1999 simulation period.

Initial salinity conditions for the Delta were specified along the axis of the Sacramento River, San Joaquin River, and Middle River by interpolating linearly between available observed salinity data at the DWR continuous salinity monitoring stations (Figure 3.4-1) at the time of the salinity reset for each simulation. It is expected that this approach introduces significant uncertainty, particularly for the Delta salinity initial conditions, and that several months of model "spin-up" would be needed before the salinity predictions are suitable for comparison with salinity observations. Since the longest simulation considered in this study is 5 months, a detailed salinity calibration was not completed for this study. Preliminary salinity comparisons indicate fairly good agreement between observed and predicted salinity. It is expected that a thorough salinity calibration of the Bay-Delta UnTRIM model will be conducted as part of a future study, following the approach used by MacWilliams and Gross (2007).

3.5 Tidal Boundary

Observations of water surface elevation at the NOAA San Francisco station, located at Fort Point (see Figure 4.3-1), near the southern end of the Golden Gate, were used to drive the tidal (ocean) boundary of the model domain. For all three simulation periods, 6-minute observed stage data from Fort Point were filtered using a fourth order Butterworth filter with a cutoff frequency of 1/3 $hours^{-1}$ to remove high frequency noise in the observed water levels. The filtered observations were multiplied by an amplification factor of 0.99 to account for the difference in tidal range between observed Fort Point tides and tides along the model ocean boundary, and a phase lead of 44 minutes was applied to account for the phase difference between Fort Point and the model boundary, following the approach of Gross et al. (2006). The amplification factor and

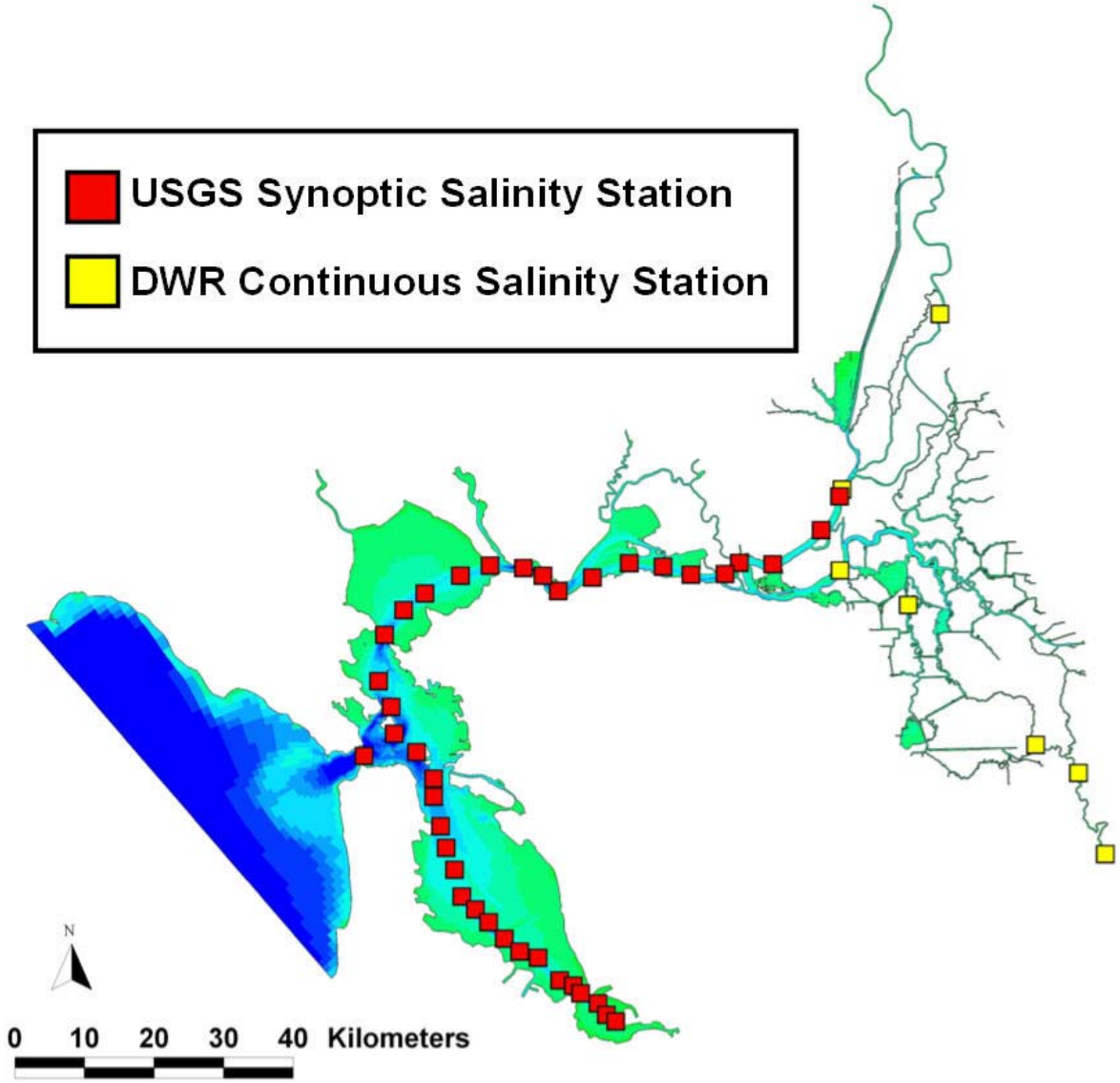

Figure 3.4-1 Location of USGS synoptic monitoring stations and Delta salinity stations used for salinity initial conditions.

phase lag were selected to minimize the phase and amplitude error between observed and predicted water levels at Fort Point for the 2007 calibration period. Since the Pacific Ocean boundary was moved farther from the Golden Gate relative to the previous UnTRIM application for the DRMS project (MacWilliams et al., 2007), the amplification factor and phase lag were updated during the model calibration to account for the updated coastal Pacific Ocean representation in the Bay-Delta UnTRIM model grid.

3.6 River Inflows

The river inflows to the model domain include both tributary inflows to the Delta, discharges from water pollution control plants, and other San Francisco Bay tributary inflows, shown on Figure 3.6-1. At the landward boundaries of the Delta in the UnTRIM model, flow boundary conditions were applied to account for the primary freshwater inflows to San Francisco Bay from the Delta. Delta inflow values were obtained from daily averaged flows estimated at several locations in the Delta by the DAYFLOW program, made available by the California Department of Water Resources (CDWR, 1986). The flows are estimated using a volume balance approach incorporating the principal Delta stream inflows, Delta precipitation, Delta exports, and Delta net channel depletions (CDWR, 1986). Delta freshwater inflows from DAYFLOW are used for inflow boundary conditions for the Sacramento River (QSAC), Yolo Bypass (QYOLO), Cosumnes River (QCSMR), Mokelumne River (QMOKE), San Joaquin River (QSJR), Eastern Delta Inflow (QEAST), and Miscellaneous Stream Flow (QMISC), are used to represent Delta freshwater inflows to the Bay-Delta UnTRIM model, as shown on Figure 3.6-1. Additional DAYFLOW components are used to represent Delta exports, as discussed in Section 3.7.

Delta outflow estimates of flows produced by the DAYFLOW program contain substantial uncertainty, particularly during low Delta flow conditions, because several terms in the volume balance are quite uncertain. Flow monitoring data collected since 1997 (Oltmann, 1998) suggests that the actual daily-averaged Delta outflows can be very different from the "DAYFLOW" values. In particular, consumptive use in the Delta can only be estimated (either by QGCD in DAYFLOW or through the DICU estimates), and this can result in significant uncertainty in net Delta outflows. For the present study, QGCD values are not used, and Delta channel depletion is represented through the DICU estimates as discussed in Section 3.9. Comparisons of river inflow values from DAYFLOW and computed net flow from the Delta flow monitoring stations near the inflow boundaries suggest that the DAYFLOW estimates of tributary inflows are generally consistent with the net flows computed from the flow monitoring data.

In addition to the Delta freshwater inflows, freshwater inflow from several rivers, creeks and water pollution control plants (WPCPs) are included in the simulations. The additional inflows considered in the simulations are Napa River, Petaluma River, Alameda Creek, Guadalupe River, Coyote Creek, and flows from the San Jose/Santa Clara WPCP. Santa Clara WPCP flows were available from the City of San Jose for the 1999 and 2002 simulation periods; for the 2007 simulation period a typical value was used and assumed to be constant throughout the 2007 period. The remaining tributary inflow data were obtained from USGS stream gauging stations.

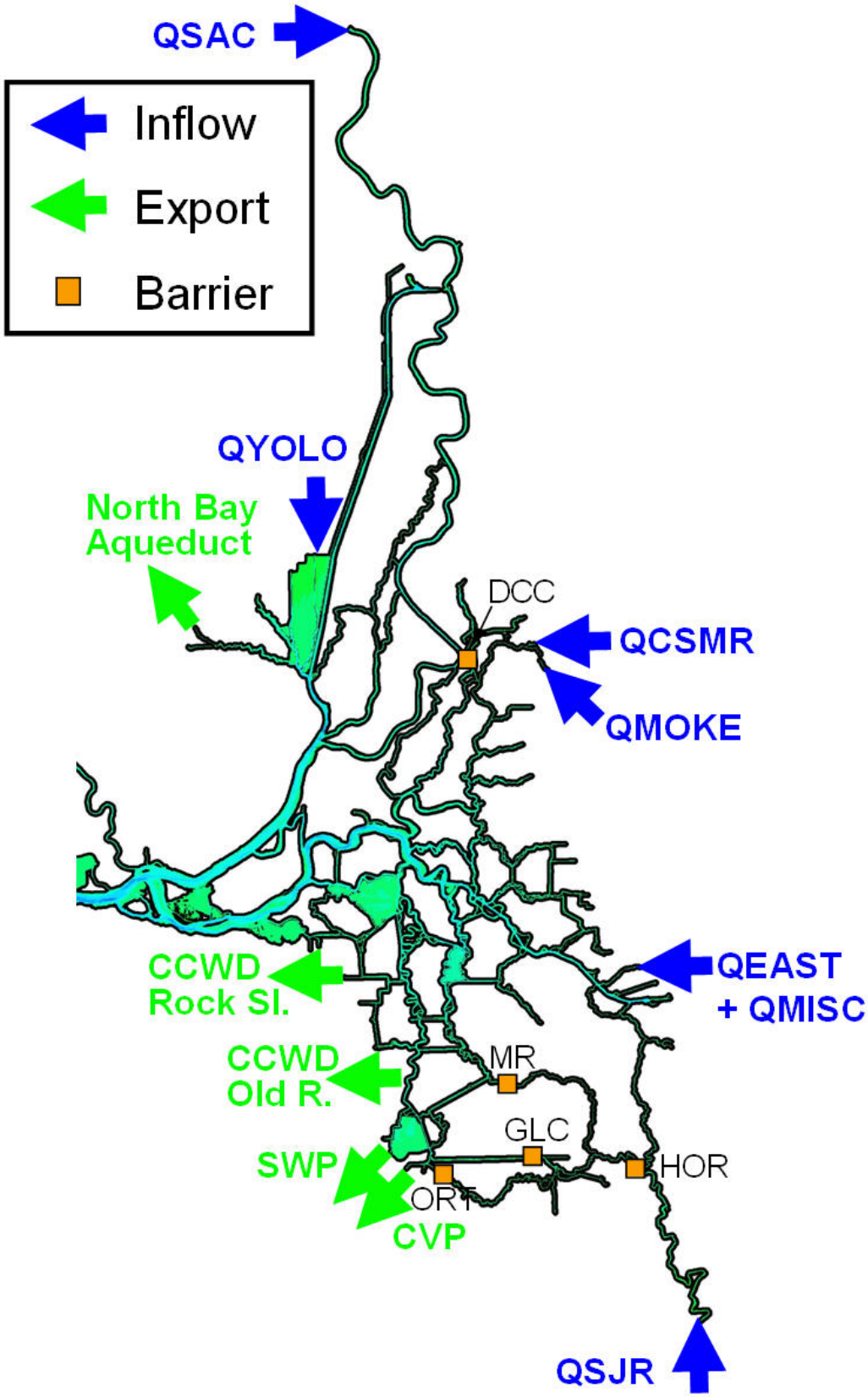

Figure 3.6-1 Locations of Delta river inflows, exports, and barriers applied to the Bay-Delta UnTRIM model.

Daily-averaged inflow salinity for the Sacramento River and Yolo Bypass was calculated by daily averaging the observed salinity at the Sacramento River at Hood DWR station (see Figure 3.4-1). For the San Joaquin River, daily-averaged inflow salinity was calculated by daily averaging the observed salinity at the San Joaquin River at Vernalis DWR station (see Figure 3.4-1). A constant inflow salinity of 0.056 psu (EC 120 umhos/cm) was used for the Mokelumne and Cosumnes River inflows. A constant inflow salinity of 0.24 psu (EC 500 umhos/cm) was used for the Eastern Delta (QEAST) and Miscellaneous (QMISC) stream inflows. These values are consistent with EC values used by in RMA2 simulations of the Delta (e.g., RMA 2005) for tributary inflow salinity (Richard Rachiele, personal communication). The salinity of all other non-Delta tributary inflows was considered to be 0 psu.

3.7 Delta Exports

The San Francisco Bay-Delta UnTRIM model includes water exports from the State Water Project (SWP), Central Valley Project (CVP), the North Bay Aqueduct (NBA), Contra Costa Water District (CCWD) exports at Rock Slough and Old River, and Byron Bethany Irrigation District (BBID) exports from Clifton Court Forebay. The location of the primary diversion locations are shown in Figure 3.6-1. Additionally, agricultural diversions and returns within the Delta are implemented as discussed in Section 3.9.

Daily-averaged flows from DAYFLOW are used for the Central Valley Project (QCVP) and North Bay Aqueduct (QNBA) exports. Daily-averaged CCWD exports at Old River (ROLD034) are obtained from the IEP DSS database (IEP, 2008). Following the approach used by RMA (2005), CCWD exports at Rock Slough are calculated as the difference between the DAYFLOW value for QCCC and the IEP values for ROLD34. Through this approach, the total daily-averaged value of CCWD exports equals the reported daily QCCC value, with constant daily flow rates divided between the two separate CCWD export locations at Rock Slough and Old River.

Hourly SWP exports are applied for the Clifton Court Forebay (CCF) Radial Gates, and hourly exports from CCF are applied at the Banks Pumping Plant. Additionally, daily BBID diversions from CCF as reported by USBR (2008) are also applied. Hourly flows through the radial gates are computed from the hourly water surface elevations inside and outside of CCF and the gate opening heights each of the five CCF radial gates using the Hills (1998) equations given by

$$Q_1 = H_1 \left\{ 0.44 + 215.224 \left(Elev_{outside} - Elev_{inside} \right)^{1/2} \right\} \quad (3.1)$$

$$Q_2 = H_2 \left\{ 4.46 + 181.804 \left(Elev_{outside} - Elev_{inside} \right)^{1/2} \right\} \quad (3.2)$$

$$Q_3 = H_3 \left\{ 4.76 + 173.378 \left(Elev_{outside} - Elev_{inside} \right)^{1/2} \right\} \quad (3.2)$$

$$Q_4 = H_4 \left\{ 3.38 + 173.378 \left(Elev_{outside} - Elev_{inside} \right)^{1/2} \right\} \quad (3.4)$$

$$Q_5 = H_5 \left\{ 2.38 + 168.790 \left(Elev_{outside} - Elev_{inside} \right)^{1/2} \right\} \quad (3.5)$$

$$Q_{total} = Q_1 + Q_2 + Q_3 + Q_4 + Q_5 \quad (3.6)$$

where, Q_i is the flow through gate i (cfs), H_i is the gate opening height of gate i (ft), $Elev_{outside}$ is

the stage outside of CCF (ft), $Elev_{inside}$ is the stage inside CCF (ft), and Q_{total} is the total CCF inflow through the radial gates (cfs).

In order to obtain accurate mass conservation inside CCF, the hourly gate flows into CCF are corrected to match the reported SWP DAYFLOW value for each day, by multiplying each hourly value by the ratio of total daily reported volume to total reported hourly inflow volume. Similarly, hourly pumping rates reported by DWR for Banks are corrected to match the total daily reported value in the IEP DSS database (IEP, 2008). These two corrections are necessary in order to meet the multiple goals of predicting observed water levels inside CCF, applying hourly operations, and maintaining daily flow rates consistent with the DAYFLOW values. A more detailed discussion of the flow corrections applied to the CCF inflow and outflow values is presented in a separate report on flow, circulation, and particle transport patterns inside CCF (Gross and MacWilliams, in preparation).

3.8 Evaporation and Precipitation

Hourly evaporation and precipitation data collected by the California Irrigation Management Information System (CIMIS) at stations bordering San Francisco Bay were used to specify spatially variable evaporation and precipitation at the water surface of the estuary. Due to limited data availability, the same stations could not be used for all simulation periods. For each period, the closest available CIMIS station was used to specify uniform evaporation and precipitation within each embayment of San Francisco Bay. South Bay evaporation and precipitation was specified using data from the Fremont station for 1999, and the Union City station for 2002 and 2007. Evaporation and precipitation in the Central Bay was specified using the Oakland Hills data for all three simulation periods. Evaporation and precipitation in San Pablo and Suisun Bay were specified using data collected at Novato in 1999, Carneros in 2002, and Suisun Valley in 2007. The location of the CIMIS stations used for evaporation and precipitation within the San Francisco Bay portion of the model domain are shown on Figure 3.8-1. Evaporation and precipitation were not specified in the Delta because evaporation and precipitation are accounted for in the Delta Island Consumptive Use model components as discussed in Section 3.9.

3.9 Delta Island Consumptive Use

Irrigation diversions and agricultural returns in the Delta significantly impact Delta hydrodynamics and water quality (DWR, 1995). The Delta Island Consumptive Use (DICU) model (DWR, 1995; DWR 2000) flow estimates incorporate channel depletions, infiltration, evaporation, precipitation, and agricultural use in the Delta. These flows are grouped into monthly estimates of net diversions, seepage, and agricultural return discharge and salinity for a total of 142 Delta sub-areas. In DSM2 (DWR, 2008a), the DICU values for each of these sub-areas are distributed onto a total of 258 nodes on the model grid. Following the approach used by RMA (2005), each node in DSM2 was mapped to the nearest UnTRIM cell (Figure 3.9-1) and the corresponding DICU values for that location were was applied to the UnTRIM model. The seepage and flow components were applied as outflows, while the return flow was applied as an inflow with salinity corresponding to the EC value reported in the DICU model.

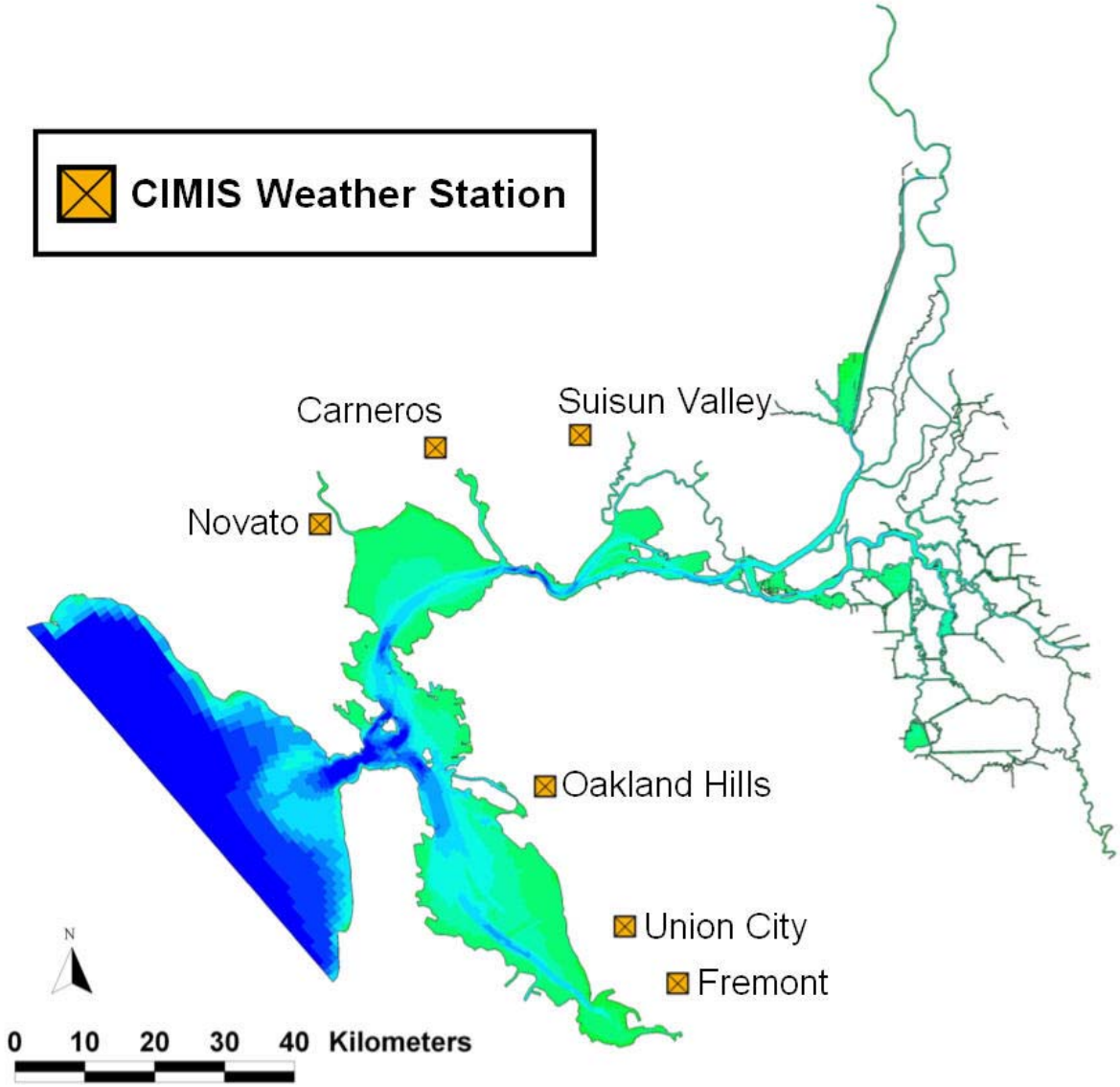

Figure 3.8-1 Location of CIMIS evaporation and precipitation data collection stations used in the San Francisco Bay-Delta UnTRIM model. Evaporation and precipitation stations in the Delta are not used because evaporation and precipitation in the Delta is included as part of DICU.

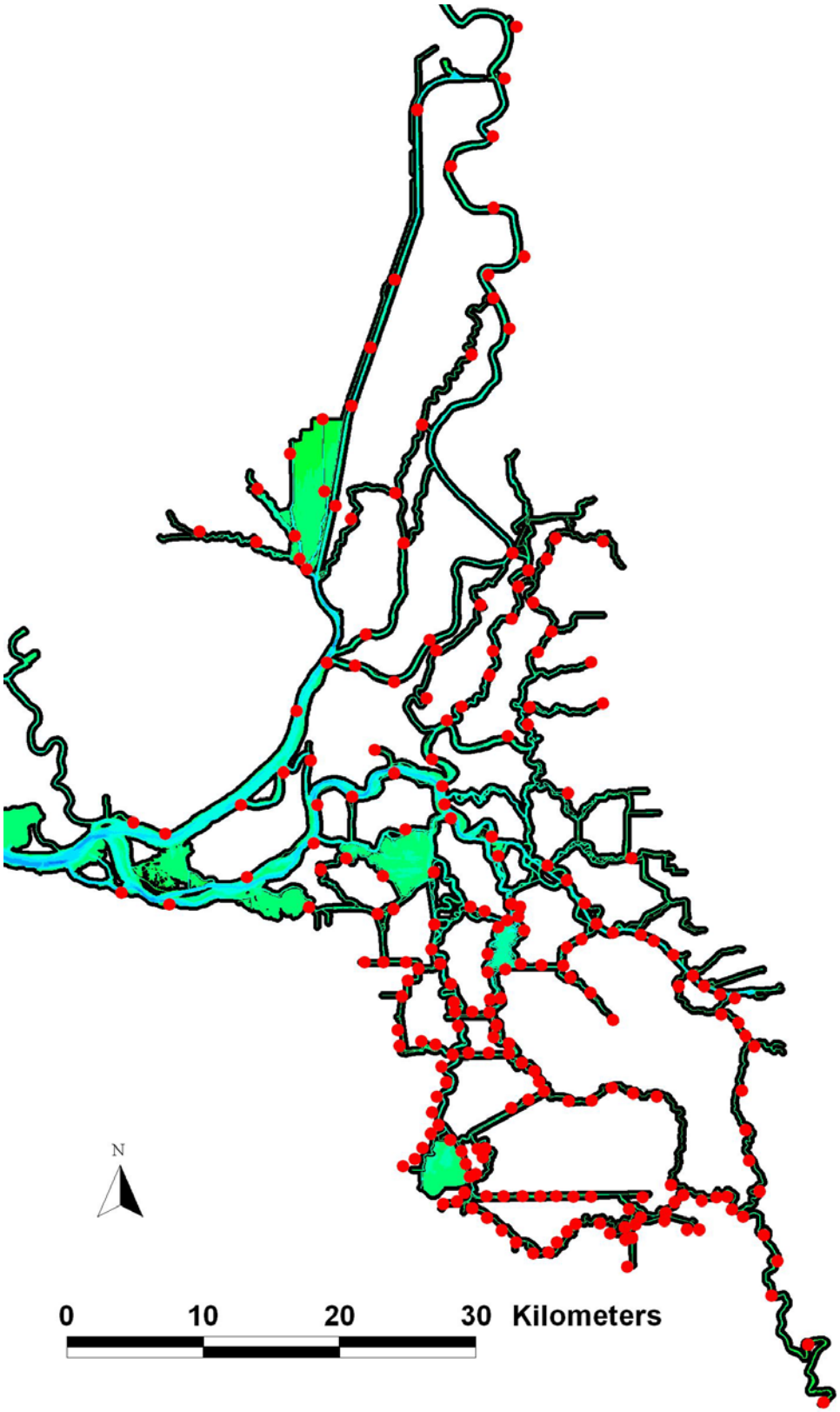

Figure 3.9-1 Location of DICU nodes (red) applied to Bay-Delta UnTRIM model grid.

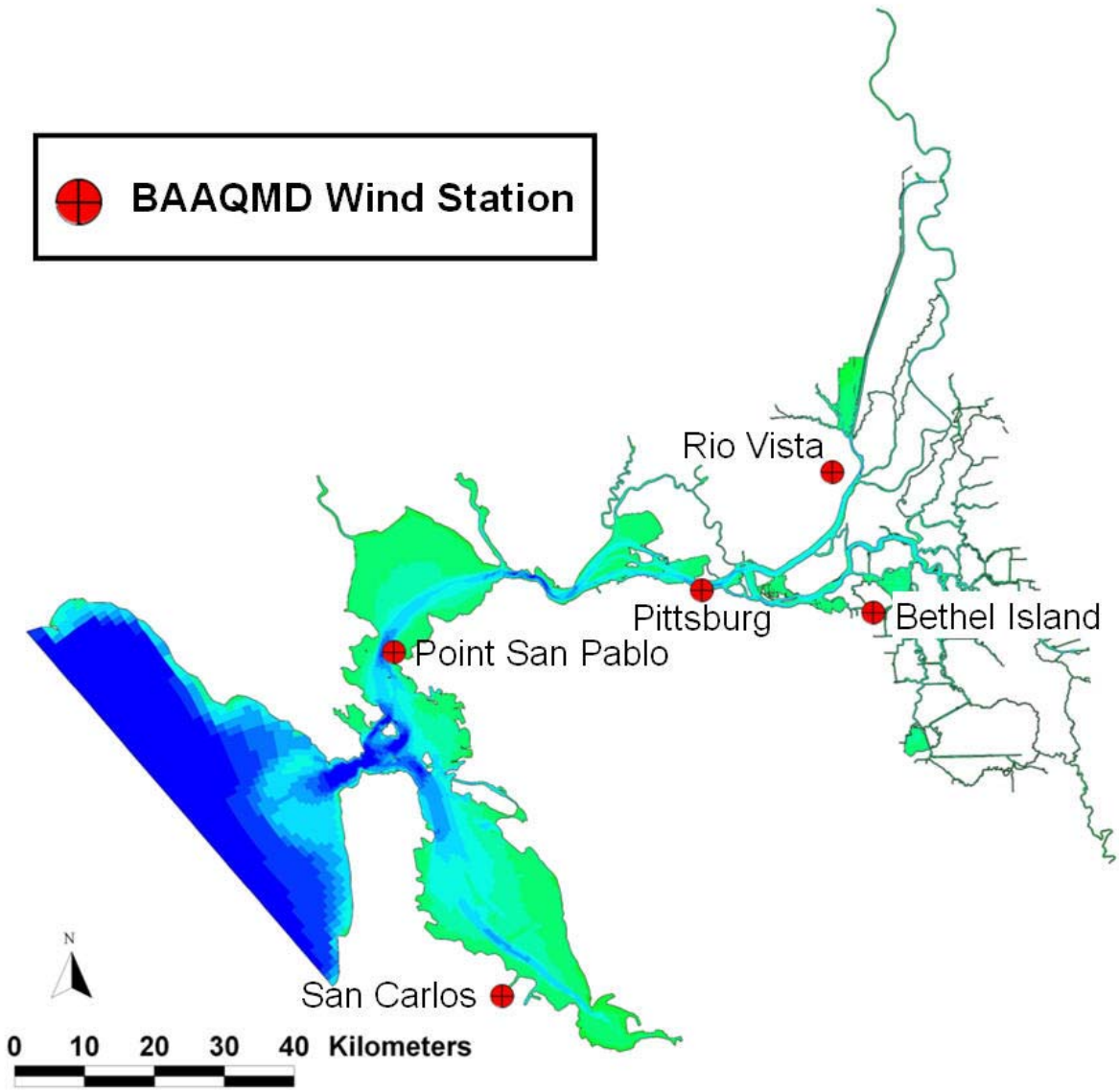

Figure 3.10-1 Location of wind measurement stations used to specify wind in the Bay-Delta UnTRIM model.

3.10 Wind

Wind forcing was applied at the water surface as a wind stress. The wind drag coefficient is varied based on local wind speed according to the formulation of Large and Pond (1981). Observed hourly wind speed and direction from the Bay Area Air Quality Control District (BAAQCD) from five locations were used to account for spatial variability in wind velocities. Observed hourly wind data from San Carlos was used in South San Francisco Bay, observed hourly wind data collected at Point San Pablo was used in Central San Francisco Bay and San Pablo Bay, and observed hourly wind data at Pittsburg was used in Carquinez Strait and Suisun Bay. These stations were selected because they are considered to be the stations which provide measurements most representative of wind speeds over water, and because they provide a geographic distribution of wind speed and direction over the Bay. Observed hourly Wind data at Rio Vista was used in the northern portion of the Delta, and observed hourly data at Bethel Island was used in the central and southern portions of the Delta. The locations of the BAAQCD wind monitoring stations used in this study are shown in Figure 3.10-1.

3.11 Bottom Friction

The bottom roughness coefficient, z_o, is used to characterize the bottom friction. In San Francisco Bay, the values of z_o used varied as a function of water column depth and ranged from 0.01 mm to 1 cm, with the highest values in intertidal regions and the lowest values in the deep channel following the approach used by Gross et al. (2006). These roughness values were determined through previous calibration studies (e.g., MacWilliams et al., 2007). Identical bottom friction was applied in all simulation periods, using the same roughness values applied by MacWilliams et al. (2007).

In the Delta portion of the model grid, a uniform bottom roughness coefficient of 0.01 mm was used. This value is equal to the value typically applied to channels in the San Francisco Bay portion of the model domain. No channel-specific "tuning" of roughness was used to calibrate net flows. This approach is consistent with field observations by Jon Burau, who has suggested that "the bed is very similar throughout the Delta, and except for variations in bed forms, the friction coefficients used in the models should be very similar throughout the Delta" (Jon Burau, personal communication).

3.12 Delta Control Structures

Permanent control gates and temporary barriers are used in the Delta to manage water quality, protect fish migrating through the Delta, and ensure an adequate water supply for agricultural diversions in the south Delta. Six Delta control structures are currently included in the Bay-Delta UnTRIM model. The implementation is flexible and allows for the inclusion of additional control structures, barriers, or alternative operations scenarios to be considered.

The Delta control structures currently implemented in the Bay-Delta UnTRIM model include the Delta Cross Channel gates, and the temporary barriers at Head of Old River, Old River near Tracy, Middle River, and Grant Line Canal, and the Suisun Marsh Salinity Control Gates. The locations of the Delta barriers are shown on Figure 6.1-1. A description of the model representation of each of these barriers and the typical timing for barrier construction and removal for each barrier is described below. The specific timing of barrier operations during each of the simulation years is presented in the description of the simulation period in for 2007 in Section 4.2, for 2002 in Section 5.1, and for 1999 in Appendix A.

3.12.1 Delta Cross Channel

The Delta Cross Channel (DCC) was constructed in 1951 by the U.S. Bureau of Reclamation to aid in transferring water from the Sacramento River across the Delta. The facility consists of two radial gates with a total width of approximately 36.6 m (120 ft). In the Bay-Delta UnTRIM model, the Delta Cross Channel is implemented as a single gate 36.6 m wide, which can either be open or closed. Opening of closing of the gate is implemented following the Delta Cross Channel Gates Historical Log (USBR, 2008).

3.12.2 Head of Old River

The Head of Old River (HOR) temporary barrier serves as a "fish barrier" because it is intended primarily to benefit migrating San Joaquin River Chinook salmon (DWR TBP, 2008). This barrier has been in place most years since 1963 between September and November 30, and has also been installed in the spring between April 15 and May 30 during some years since 1992. The spring Head of Old River barrier was installed in spring 2002 and 2007, but was not installed during spring 1999.

The Head of Old River barrier consists of six operable circular culverts and a single weir. The culverts are 4 feet in diameter, and are modeled using a Manning's n value of 0.02, a length of 17 m (56 ft), and an invert elevation of -1.2 m NGVD. The weir is 61 m (200 ft) wide and has a crest elevation of 3.04 m (10 ft) NGVD. Figure 3.12-1 shows two photographs of the Head of Old River Barrier. This barrier configuration consisting of a weir and a number of culverts is also used for the Old River at Tracy, Middle River, and Grant Line Canal temporary barriers.

The model implementation allows for each of the culverts in the Head of Old River Barrier to be operated individually to allow for flow in only one, or in both directions. The UnTRIM model implementation uses the information from the historical operations log used by DSM2 (DWR, 2008b) to specify the number of culverts in place, the weir length and height, the timing of the barrier placement and removal, and the timing of changes to culvert operations during each simulation period.

3.12.3 Old River near Tracy (DMC)

The Old River near Tracy (ORT) barrier is located near the Delta Mendota Canal (DMC) has been installed between April 15 and September 30 of each year since 1991. The Old River near Tracy barrier is implemented in the Bay-Delta UnTRIM model as a single weir with a width of

22.9 m (75 ft), and six operable culverts with tide gates. The information from the historical operations log (DWR, 2008b) is used to specify the number of culverts in place, the weir length and height, the timing of the barrier placement and removal, and the timing of changes to culvert operations during each simulation period.

3.12.4 Middle River

The primary purpose of the Middle River (MR) temporary barrier is to increase water levels, circulation patterns, and water quality in the southern Delta area for local agricultural diversions (DWR TBP, 2008). It has been installed since 1987. The Middle River barrier is implemented in the Bay-Delta UnTRIM model as a single weir with a width of 42.7 m (140 ft), and six operable culverts with tide gates. The information from the historical operations log (DWR, 2008b) is used to specify the number of culverts in place, the weir length and height, the timing of the barrier placement and removal, and the timing of changes to culvert operations during each simulation period.

3.12.5 Grant Line Canal

A rock barrier in Grant Line Canal (GLC) was first installed in spring 1996, and has been installed every year since, except for 1998. The primary purpose of the GLC temporary barrier is to increase water levels, circulation patterns, and water quality in the southern Delta area for local agricultural diversions (DWR TBP, 2008). The Grant Line Canal barrier is implemented in the Bay-Delta UnTRIM model as a single weir with a width of 38.1 m (125 ft), and six operable culverts with tide gates. The information from the historical operations log (DWR, 2008b) is used to specify the number of culverts in place, the weir length and height, the timing of the barrier placement and removal, and the timing of changes to culvert operations during each simulation period.

3.12.6 Suisun Marsh Salinity Control Gates

The Suisun Marsh Salinity Control Gates (SMSCG) are located on the eastern side of Montezuma Slough, and consist of a series of three radial gates, flashboards, and a boat lock (IEP, 2008a). The three radial gates are each 36 feet wide, and the flashboard width is 66 feet (Harrison, 2002). The SMSCG usually begin operating in early October and, depending on salinity conditions, may continue operating through the end of the control season in May (Harrison, 2002). Current model implementation for the SMSCG allows for the gates to be open or closed. A more accurate representation could be incorporated following the approach used on the temporary barriers could be used when simulating conditions when the gates are operating. For each of the three periods simulated in this study, the three gates were considered to be open and the flashboards were out, corresponding with normal summer operating conditions (IEP, 2008b).

Figure 3.12-1 Photograph of Head of Old River Barrier (top) from DWR TBP (2008); photograph showing location and numbering of six culverts through the 2002 Head of Old River Barrier (bottom) from DWR (2003).

4. Model Calibration

The hydrodynamic calibration indicates the ability of the Bay-Delta UnTRIM model to accurately predict water levels (stage) and flows in the San Francisco Bay and the Sacramento-San Joaquin Delta. Accurate prediction of water levels in San Francisco Bay demonstrates that tides are accurately propagating through the Bay and into the Delta. Comparison of predicted flows to observations in the Delta demonstrate the degree that the model captures the instantaneous, tidally-averaged, and net flows in specific channels within the Delta.

This section presents the method used to assess the model calibration, and provides an extensive set of comparisons between observed and predicted water levels and flows at observation stations in San Francisco Bay and in the Delta for the model calibration period in 2007.

4.1 Model Assessment Method

Predicted stage, flow, and salinity were compared to observation data at stations where data were collected by NOAA, USGS, and DWR. Data from NOAA were downloaded from the Tides and Currents webpage (NOAA, 2008) and are identified using the seven digit NOAA station identification number. USGS data were provided by Cathy Ruhl and Nick Leach from the USGS Sacramento office and are identified using the three letter USGS identifier. The DWR data were obtained both from the IEP DSS database (IEP, 2008) and from the California Data Exchange Center (CDEC) online database. Data extracted from the IEP DSS database are identified using the DSS B value field which consists of a string of letters and numbers, while data downloaded from CDEC are identified by the three letter CDEC identifier, which in some cases differs from the USGS three letter identifier for the same station.

The quality of fit between predicted model results and observed stage, flow, and salinity time series data are assessed following a cross-correlation procedure similar to that used by RMA (2005). This approach has also been used by MacWilliams and Gross (2007), and provides a thorough description of the differences between time series records through a quantitative measure of differences in terms of phase, mean, amplitude, and constant offsets. Statistics are derived to quantify the differences between predicted and observed time series data. Four types of statistics are presented in this report, following the approach used by RMA (2005):

- Mean – Comparison of simple mean values of the predicted and observed time series.
- Phase Shift – The average shift in time between the predicted and observed time series.
- Amplitude Ratio – Comparison of the time series range, which ideally would equal 1. This value is estimated after removing the phase shift between predicted and observed time series.
- Scatter – The remaining difference between predicted and observed time series after phase and amplitude errors are removed. One measure of the scatter is the goodness of

fit parameter, R^2, from a linear regression performed on the observed and predicted time series with phase error removed. Note that this R^2 is a measure of the scatter around a best-fit line, not a 1:1 line, on the scatter plots.

For each stage and velocity time series comparison, a total of three different types of figures are shown. The top figure shows the tidal time scale variability for a period of approximately fifteen days. On the lower left, a tidally-averaged plot is shown for the full analysis period to evaluate spring-neap and longer time scale variability, as well as non-tidal forcing such as storm surge. Tidal averages are computed by filtering twice using a 24.75 hour running average filter. On the lower right, the scatter plot shows a comparison between the observed and predicted data over the analysis period. The scatter plot is produced by first running a cross-correlation between the observed data and model predictions to find the average phase lag over the entire record. The cross-correlation was performed following the procedure outlined by RMA (2005). The process entails repeatedly shifting the predicted time series record at one minute increments relative to the observed time series and computing the correlation coefficient at each time shift. The correlation has a maximum value when the shifted model time series best matches the observed time series. The time shift when the maximum correlation occurs represents the phase difference in minutes between the predicted and observed data, with positive values indicating that the predicted time series lags the observed time series. The linear regression is then performed between the time shifted model results and observed data record to yield the amplitude ratio, best-fit line, and correlation coefficient. In summary, the statistics reported on each scatter plot include the following:

- Mean Obs – Average value of observed time series for analysis period
- Mean Pred – Average value of predicted time series for analysis period
- Lag – Phase difference in minutes between observed and predicted; a positive value indicates that the predicted time series lags behind the observed time series.
- Y = slope*X + offset – Best linear fit, where Y is predicted, X is observed. The slope value is used as the amplitude ratio.
- R^2 – Linear regression goodness of fit parameter.

The observed and predicted means, phase lag, amplitude ratio, and R^2 value are also summarized in tables for each simulation period.

4.2 Description of 2007 Simulation Period

The 2007 simulation period that spans from April 2, 2007 through September 1, 2007 was used as the model calibration period in this study. This period was selected due to the large number of flow and stage monitoring data available in the Delta during this time span.

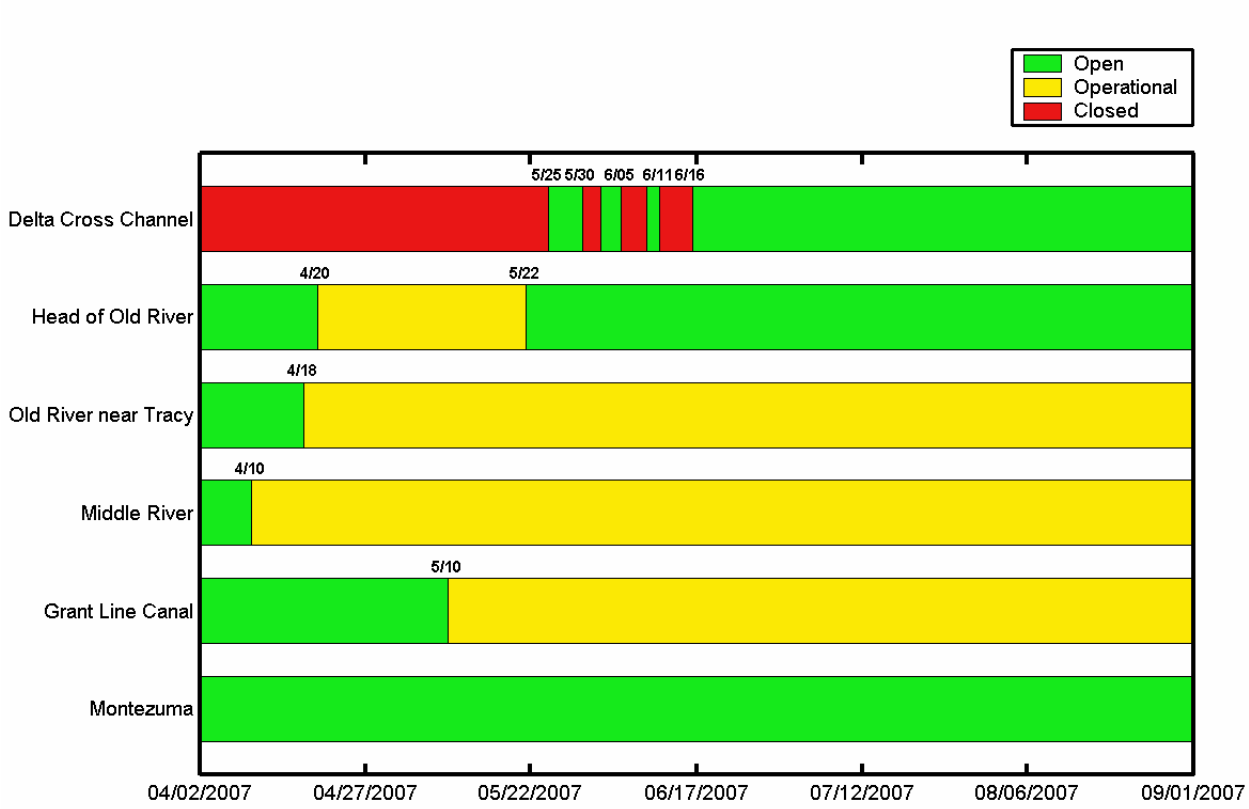

Figure 4.2-1 Historical barrier operations schedule during the 2007 simulation period.

Figure 4.2-1 shows the historical barrier operations schedule during the 2007 simulation period. During periods when the barriers are closed, no flow is allowed through the barrier. When the barrier is open, no barrier controls are specified and the channel operates normally. During periods when the barrier is operational, the weir and culvert configurations are implemented as discussed in Section 3.12 and described in the historical operations log (DWR, 2008b).

4.3 Water Level Calibration

The calibration of stage in the UnTRIM Bay-Delta Model entails comparing observed and predicted water levels over the analysis period following the approach outlined in Section 4.1. The water level calibration period spans from April 4, 2007 through September 1, 2007. Observed and predicted water levels were compared at five NOAA stations in San Francisco Bay and at forty-five stations in the Delta. At each station, observed and predicted water levels were plotted over a fifteen day period to show the water level agreement over tidal time scales. In addition, the observed and predicted stage are tidally-averaged, to assess the accuracy of the model in predicting water level variability on spring-neap time scales, as well as non-tidal forcing such as storms. Lastly, the cross-correlation procedure (as described in Section 4.1) was used to determine the mean observed and predicted water level, the amplitude ratio, the phase lag, and the correlation coefficient squared (R^2). For each of the water level stations, these values are compiled in Table 4-1.

In San Francisco Bay, the datum of each water level observation station is well-defined and variations between observed and predicted mean water levels are typically small. However, in the Delta, water levels at some stations are measured relative to an arbitrary datum. Where station datum information was available, the observed water levels were converted to NGVD29 as described in Section 3.2. At stations where it was not possible to definitively reference the observed stage to NGVD, an arbitrary vertical datum correction was applied such that the observed mean water level was identical to the predicted mean water level in NGVD. Stations where an arbitrary vertical correction was made to the observed data are indicated with a "*" where the observed mean water level is given in Table 4-1. At these stations, comparison of absolute stage is not possible, however, the cross-correlation analysis is not affected by the vertical datum and the amplitude ratio, phase lag, and R^2 values all provide useful measures of model performance even for stations where the vertical datum of the observed stage is arbitrary.

4.3.1 San Francisco Bay

Water level calibration comparisons were performed at five NOAA continuous observation stations in the San Francisco Estuary at the locations shown in Figure 4.3-1. At Fort Point (NOAA station 9414290), the observed and predicted water levels are nearly identical, indicating that the applied offset and amplification at the simplified ocean boundary is accurately propagating tides into the estuary (Figure 4.3-2). The cross-correlation analysis shows a phase lag of 0 minutes indicating the model is exactly in phase with observed tides, an amplitude ratio of 1.001 indicating that observed and predicted tidal ranges are nearly identical, and an R^2 of 0.999. The observed and predicted water levels show identical mean water level, and the tidally-averaged stage demonstrates that the model is accurately capturing spring-neap and longer time scale filling and draining of the Bay. The agreement between observed and predicted stage at Fort Point demonstrates that the ocean boundary condition described in Section 3.5 is accurately propagating tides into the estuary. At Alameda (NOAA station 9414750), the observed and predicted water levels show a similar level of agreement (Figure 4.3-3), with a phase lag of 8 minutes, an amplitude ratio of 1.007 and an R^2 of 0.998. The observed and predicted water levels show a slight difference of 0.01 m in the mean water level, and the model accurately predicts trends in the tidally-averaged stage. A similar level of agreement is achieved at Redwood City (NOAA station 9414523) and at Richmond (NOAA station 9414863), as seen in Figure 4.3-4 and 4.3-5, respectively. At Port Chicago (NOAA station 9415144), the observed and predicted water levels show good agreement (Figure 4.3-6), with a phase lag of 5 minutes, an amplitude ratio of 0.934 indicating slightly lower predicted tidal amplitude than the observed tidal amplitude, and an R^2 of 0.997.

4.3.2 Northern Sacramento-San Joaquin Delta

Water level calibration comparisons were performed at ten continuous water level observation stations in the northern portion of the Delta, at the locations shown in Figure 4.3-7. Water level comparisons at these stations are shown in Figures 4.3-8 through 4.3-17.

At Cache Slough (Figure 4.3-8) the observed and predicted water levels show good agreement, with a phase lead of 3 minutes, an amplitude ratio of 1.025 and an R^2 of 0.995. Predicted and observed water levels in the Sacramento River South of Georgiana Slough (Figure 4.3-9), in

Georgiana Slough near the Sacramento River (Figure 4.3-10), in the Delta Cross Channel (Figure 4.3-11), and in the Sacramento River North of the Delta Cross Channel (Figure 4.3-12) all show similar correlation with amplitude ratios between 1.07 and 1.10, a phase lead of 7 to 12 minutes, and R^2 values ranging from 0.985 to 0.989. At these four stations near the Delta Cross Channel, the predicted tidal amplitude is about 7 to 10% greater than the observed tidal amplitude. This amplification may be party caused by not accurately representing the full extent of the marsh areas in Snodgrass Slough east of the Delta Cross Channel or by reflection off of the upstream boundaries. Further east in the Mokelumne River near Thornton (Figure 4.3-13), the amplitude ratio is 1.17, suggesting that additional amplification is occurring near the model boundary on the upstream portion of the Mokelumne River. Since the observed tidal range in the Mokelumne River at Thornton is more than 1 m, this suggests that the Mokelumne River may need to be extended further upstream to eliminate tidal reflection at the upstream extent of the model grid.

In Miner Slough (Figure 4.3-14), Steamboat Slough (Figure 4.3-15) and Sutter Slough at Cortland (Figure 4.3-16), predicted water levels agree well with observed water levels, with slightly higher predicted than observed tidal range. At these three stations, the amplitude ratio is between 1.08 and 1.14, with a phase lead of 12 to 28 minutes, and R^2 values ranging from 0.974 to 0.990. Further upstream on the Sacramento River at Freeport (Figure 4.3-17), the observed and predicted water levels show good agreement, with a phase lead of 22 minutes, an amplitude ratio of 1.015 and an R^2 of 0.980. During the model calibration, the Sacramento River portion of the model grid was extended upstream from the mouth of the American River to Verona in order to reduce reflection at the upstream portion of the Sacramento River. This approach was successful, since the predicted tidal amplitude is only about 1.5% greater than the observed tidal amplitude in the Sacramento River at Freeport.

4.3.3 Central Sacramento-San Joaquin Delta

Water level calibration comparisons were performed at sixteen continuous water level observation stations in the central portion of the Delta, at the locations shown in Figure 4.3-18. Water level comparisons at these stations are shown in Figures 4.3-19 through 4.3-34.

On the San Joaquin River at Antioch (Figure 4.3-19), the observed and predicted water levels show good agreement, with a phase lag of 9 minutes, an amplitude ratio of 0.911 and an R^2 of 0.995. The observed and predicted tidally-averaged stage show good correlation, with a slight vertical offset of about 0.06 m which is likely due to uncertainty in the vertical datum. Since Antioch is near the seaward boundary of the Delta, this indicates that the model accurately predicts spring-neap filling and draining of the Delta.

At Rio Vista (Figure 4.3-20), predicted water levels show good agreement with observed water levels, with a phase lag of 0 minutes, an amplitude ratio of 1.013 and an R^2 of 0.995. The predicted tidally-averaged stage shows nearly-identical trends to the observed tidally-averaged stage indicating accurate predictions of spring-neap filling and draining of the northern regions of the Delta, which include Liberty Island, the Sacramento Deep Water Ship Channel, Steamboat Slough, and the Sacramento River. In Threemile Slough (Figure 4.3-21), Jersey Point (Figure 4.3-22), and False River (Figure 4.3-23), predicted and observed water levels are nearly identical with an amplitude ratio between 0.988 and 0.994, and a phase difference of less than 3 minutes.

Overall, the predicted stage shows very good agreement with observed stage at these four stations in the western Delta, in terms of amplitude, phase, and spring-neap variations in tidally-averaged stage. At Dutch Slough (Figure 4.3-24), observed and predicted water levels show good agreement, with a phase lead of 10 minutes, an amplitude ratio of 0.960 and an R^2 of 0.982.

At the remaining ten central Delta stations—Old River at the San Joaquin River (Figure 4.3-25), the Mokelumne River near the San Joaquin River (Figure 4.3-26), Old River at Quimby Island (Figure 4.3-27), Holland Cut (Figure 4.3-28), Rock Slough at Contra Costa Canal (Figure 4.3-29), San Joaquin River at Prisoners Point (Figure 4.3-30), the San Joaquin River at Venice Island (Figure 4.3-31), Little Potato Sough (Figure 4.3-32), Middle River south of Columbia Cut (Figure 4.3-33), and Turner Cut near Holt (Figure 4.3-34)—the cross-correlation demonstrates that the predicted and observed water levels agree extremely well with amplitude ratios between 1.006 and 1.028 indicating that the predicted and observed tidal range is within 2.8 %, with phase differences of less than 6 minutes at all 10 stations, and R^2 values between 0.992 and 0.995. These results demonstrate that the model is accurately predicting water levels in the Central Delta, in terms of amplitude, phase, and spring-neap variations in tidally-averaged stage.

4.3.4 Southern Sacramento-San Joaquin Delta

Water level calibration comparisons were performed at sixteen continuous water level observation stations in the southern portion of the Delta, at the locations shown in Figure 4.3-35. Water level comparisons at these stations are shown in Figures 4.3-36 through 4.3-54.

In Middle River at Middle River (Figure 4.3-36), predicted water levels show good agreement with observed water levels, with a phase lead of 4 minutes, an amplitude ratio of 1.018 and an R^2 of 0.994. The mean predicted stage is 0.12 m less than the mean observed stage, which is likely the result of uncertainty in the observed vertical datum; this results in a vertical offset on the stage and tidally-averaged stage plots. The stage in the Middle River at Tracy Boulevard (Figure 4.3-37) and at the Howard Road Bridge (Figure 4.3-38) is strongly influenced by the installation of the Middle River barrier on April 10. Both stations are upstream of the barrier. At the Howard Road Bridge, the predicted tidal range is significantly less than the observed tidal range, with the predicted low water elevations significantly higher than the observed water elevations. This suggests that this reach of Middle River is not fully draining at low water, and that better grid resolution or bathymetry of the channel thalweg may be needed to ensure proper draining in the model. Since low water levels in this reach of Middle River are in part controlled by the height of the weir on the temporary barrier, any differences between reported (and modeled) weir height and actual weir height may also account for some of these differences during the period the Middle River barrier is in place.

At the stations along or near Old River between Bacon Island and Clifton Court Forebay—Old River at Bacon Island (Figure 4.3-39), Discovery Bay at Indian Slough (Figure 4.3-40), Old River near Byron (Figure 4.3-41), Victoria Canal near Byron (Figure 4.3-42), Italian Slough Headwater near Byron (Figure 4.3-43), and Old River at Coney Island (Figure 4.3-44)—the cross-correlation statistics show that the model is accurately predicting water levels, with amplitude ratios between 1.011 and 1.034, phase differences of less than 12 minutes, and R^2 values between 0.990 and 0.994.

The comparison of observed and predicted water levels inside Clifton Court Forebay near the radial gates (Figure 4.3-45) demonstrates that the model is capturing the daily timescale changes in water level in response to the opening and closing of the radial gates and the time-variable exports from the Banks Pumping Plant. Predicted water levels agree well with observed water levels, with no phase error, an amplitude ratio of 1.015, and an R^2 of 0.977. This comparison confirms that the hourly inflows obtained through the gate equations of Hills (1988) combined with the hourly observed exports are able to reproduce the short timescale changes in water level. Comparison of tidally-averaged water levels inside Clifton Court Forebay demonstrate that the daily volume corrections applied to the hourly flows (see Section 3.7) are meeting the objective of maintaining accurate volumes inside of Clifton Court Forebay over the full simulation period. These results demonstrate that the approach used to represent Clifton Court Forebay operations in the Bay-Delta UnTRIM model is meeting the multiple goals of predicting observed water levels inside CCF, applying hourly operations, maintaining daily flow rates consistent with the DAYFLOW values.

In Grant Line Canal near Clifton Court Ferry (Figure 4.4-46), predicted water levels show good agreement with observed water levels, with a phase lead of 14 minutes, an amplitude ratio of 1.041 and an R^2 of 0.990. Further east, in Grant Line Canal at Tracy Boulevard (Figure 4.4-47), predicted water levels show good agreement with observed water levels, with a phase lag of 15 minutes, an amplitude ratio of 0.967 and an R^2 of 0.979. In Old River downstream of the temporary barrier (Figure 4.3-48), predicted water levels show good agreement with observed water levels, with a phase lead of 6 minutes, an amplitude ratio of 1.043 and an R^2 of 0.986. Just upstream of the barrier in Old River (Figure 4.3-49), predicted water levels show good agreement with observed water levels, with a phase lead of 8 minutes, an amplitude ratio of 0.964 and an R^2 of 0.934. The overall good level of agreement between observed and predicted water levels in Grant Line Canal and Old River near the temporary barriers demonstrates that the influence of these barriers on water levels in the south Delta is being accurately represented in the UnTRIM model.

In the five stations along the San Joaquin River from Stockton to Mossdale—San Joaquin River at Stockton (Figure 4.3-50), San Joaquin River at Brandt Bridge (Figure 4.3-51), San Joaquin River below Old River near Lathrop (Figure 4.3-52), the Head of Old River at the Junction with the San Joaquin (Figure 4.3-53), and the San Joaquin River at Mossdale (Figure 4.3-54)— the cross-correlation statistics show that the model is accurately predicting water levels, with amplitude ratios between 0.960 and 1.019, phase differences of less than 18 minutes, and R^2 values between 0.971 and 0.994. On the San Joaquin River near Lathrop (Figure 4.3-52), the tidally-average stage demonstrates the influence of the Head of Old River barrier, which is in place between April 20 and May 22, on stage in the San Joaquin River. The predicted and observed tidally-averaged stage time series are nearly identical, demonstrating that the model is accurately representing the effect of the temporary barrier on stage in the San Joaquin River. A similar result can be seen at Mossdale (Figure 4.3-54).

Table 4-1 Predicted and observed stage and cross-correlation statistics for stage monitoring stations in San Francisco Bay and the Sacramento-San Joaquin Delta during the 2007 simulation period.

Location	Data Source	Figure Number	Mean Water Level		Cross Correlation		R^2
			Observed (m)	Predicted (m)	Amp Ratio	Lag (min)	
2007 San Francisco Bay Stage Stations (Figure 4.3-1)							
San Francisco	NOAA	4.3-2	0.08	0.08	1.001	0	0.999
Alameda	NOAA	4.3-3	0.10	0.11	1.007	8	0.998
Redwood City	NOAA	4.3-4	0.14	0.13	0.995	4	0.998
Richmond	NOAA	4.3-5	0.12	0.11	0.995	1	0.998
Port Chicago	NOAA	4.3-6	0.35	0.29	0.934	5	0.997
2007 North Delta Stage Stations (Figure 4.3-7)							
Cache Slough at Ryer Island	USGS	4.3-8	0.46	0.38	1.025	-3	0.995
Sacramento River South of Georgiana Slough	USGS	4.3-9	0.65	0.54	1.093	-7	0.989
Georgiana Slough near Sacramento River	USGS	4.3-10	0.62	0.54	1.083	-8	0.989
Delta Cross Channel	USGS	4.3-11	0.57	0.48	1.077	-8	0.985
Sacramento River North of Delta Cross Channel	USGS	4.3-12	0.67	0.55	1.106	-12	0.986
Mokelumne River near Thornton	DWR	4.3-13	0.51	0.48	1.144	-36	0.981
Miner Slough at Hwy 84 Bridge	USGS	4.3-14	0.59	0.49	1.083	-12	0.990
Steamboat Slough between Sacramento River and Sutter Sl.	USGS	4.3-15	0.62	0.54	1.102	-10	0.986
Sutter Slough at Courtland	USGS	4.3-16	0.80	0.59	1.143	-28	0.974
Sacramento River at Freeport	USGS	4.3-17	0.78*	0.78	1.015	-22	0.980
2007 Central Delta Stage Stations (Figure 4.3-18)							
San Joaquin River at Antioch	DWR	4.3-19	0.40	0.34	0.911	9	0.995
Sacramento River at Rio Vista	USGS	4.3-20	0.38*	0.38	1.013	0	0.995
Threemile Slough North at San Joaquin River	USGS	4.3-21	0.43	0.36	0.991	1	0.995
San Joaquin River at Jersey Point	USGS	4.3-22	0.41	0.36	0.988	3	0.995
False River	USGS	4.3-23	0.36*	0.36	0.994	-1	0.995
Dutch Slough at Jersey Island	USGS	4.3-24	0.43	0.36	0.960	-10	0.982
Old River at San Joaquin River	USGS	4.3-25	0.38*	0.38	1.014	1	0.995
Mokelumne River near San Joaquin River	USGS	4.3-26	0.38*	0.38	1.028	-6	0.994
Old River at Quimby Island near Bethel Island	USGS	4.3-27	0.37*	0.37	1.007	1	0.994
Holland Cut	USGS	4.3-28	0.37*	0.37	1.005	0	0.994
Rock Slough at Contra Costa Canal	DWR	4.3-29	0.45	0.35	1.024	-5	0.992
San Joaquin River at Prisoners Point	USGS	4.3-30	0.38*	0.38	1.014	1	0.994
San Joaquin River at Venice Isl.	DWR	4.3-31	0.39*	0.39	1.010	5	0.995

Little Potato Slough at Terminous	USGS	4.3-32	0.40*	0.40	1.021	1	0.994
Middle River south of Columbia Cut	USGS	4.3-33	0.38*	0.38	1.006	0	0.994
Turner Cut near Holt	USGS	4.3-34	0.39*	0.39	1.007	2	0.994
2007 South Delta Stage Stations (Figure 4.3-35)							
Middle River at Middle River	USGS	4.3-36	0.49	0.37	1.018	-4	0.994
Middle River at Tracy Blvd	DWR	4.3-37	0.44	0.41	0.868	-22	0.949
Middle River at Howard Road Bridge	DWR	4.3-38	0.40	0.45	0.748	22	0.944
Old River at Bacon Island	USGS	4.3-39	0.47	0.36	1.017	-2	0.994
Discovery Bay at Indian Slough	DWR	4.3-40	0.43	0.34	1.011	-7	0.994
Old River near Byron	USGS	4.3-41	0.40	0.31	1.023	-12	0.993
Victoria Canal near Byron	USGS	4.3-42	0.29*	0.29	1.029	-7	0.990
Italian Slough Headwater near Byron	DWR	4.3-43	0.31	0.29	1.025	-11	0.992
Old River at Coney Island	DWR	4.3-44	0.36	0.28	1.034	-5	0.992
Clifton Court Forebay	DWR	4.3-45	-0.20	-0.17	1.015	0	0.977
Grant Line Canal near Clifton Court Ferry	USGS	4.3-46	0.30	0.24	1.041	-14	0.990
Grant Line Canal at Tracy Blvd	DWR	4.3-47	0.35	0.30	0.967	15	0.979
Old River near Delta Mendota Canal (Downstream of Barrier)	DWR	4.3-48	0.28	0.23	1.043	-6	0.986
Old River near Delta Mendota Canal (Upstream of Barrier)	USGS	4.3-49	0.42	0.41	0.964	-8	0.934
San Joaquin River at Stockton	USGS	4.3-50	0.47	0.42	1.013	1	0.994
San Joaquin River at Brandt Bridge	DWR	4.3-51	0.58	0.49	1.019	7	0.991
San Joaquin River below Old River near Lathrop	DWR	4.3-52	0.66	0.65	0.987	13	0.987
Old River at Head	DWR	4.3-53	0.54	0.55	0.960	18	0.971
San Joaquin River at Mossdale	DWR	4.3-54	0.75	0.71	0.965	10	0.981

* Observed data are measured relative to arbitrary vertical datum. Observed data are offset to match predicted mean water level for comparison plots.

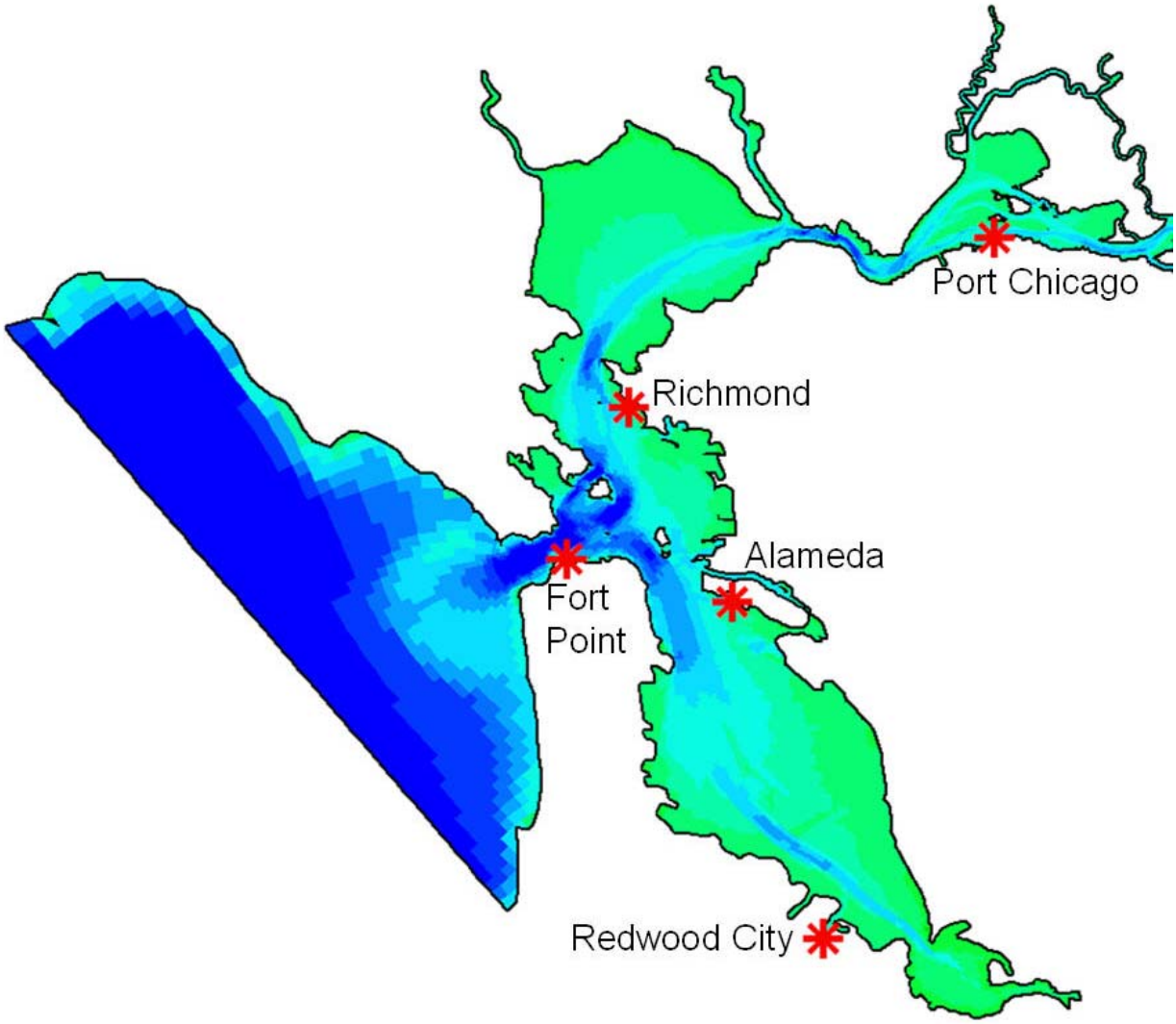

Figure 4.3-1 Location of NOAA water level monitoring stations in San Francisco Bay used for 2007 stage calibration.

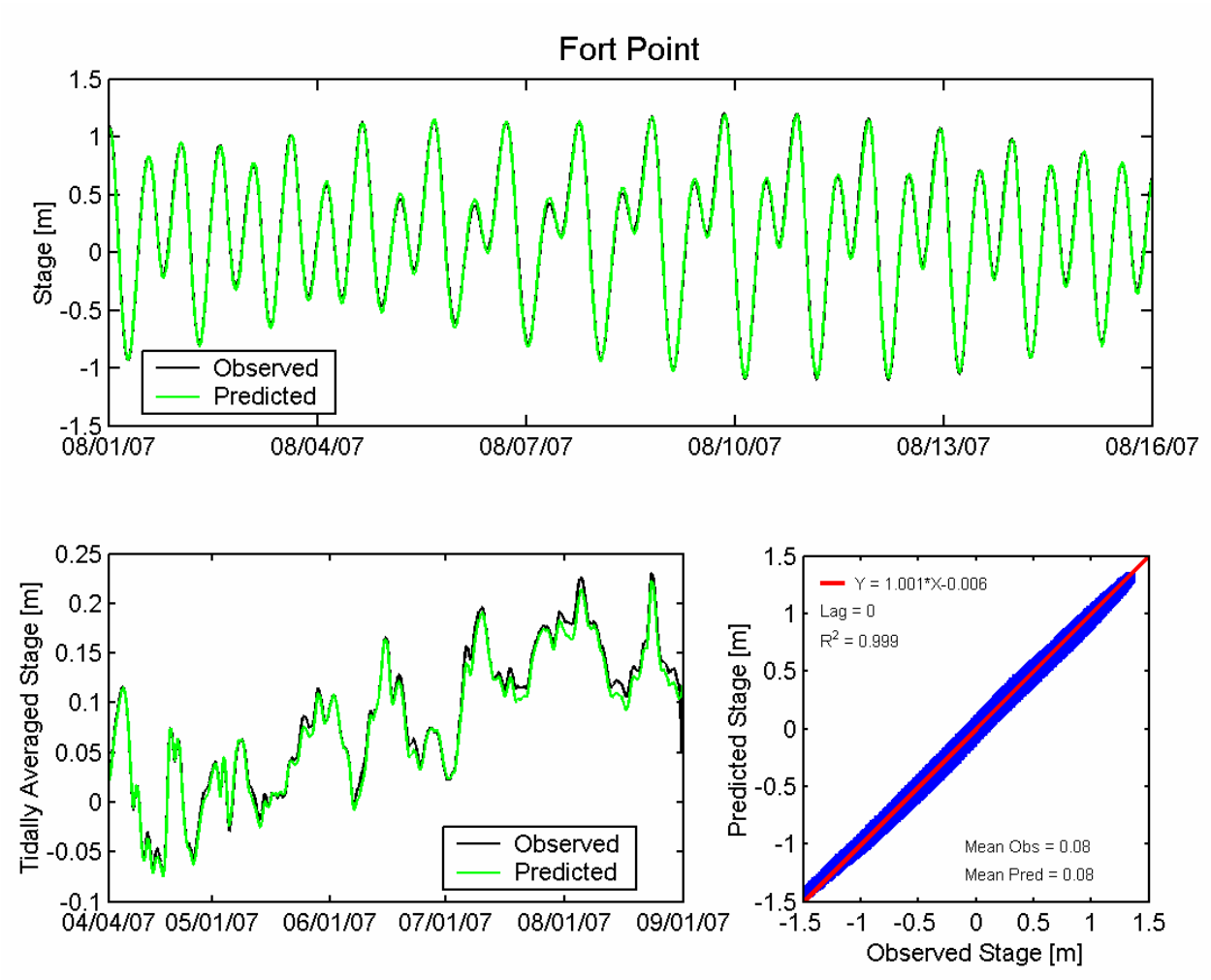

Figure 4.3-2 Observed and predicted stage at San Francisco Fort Point NOAA station (9414290) during the 2007 simulation period.

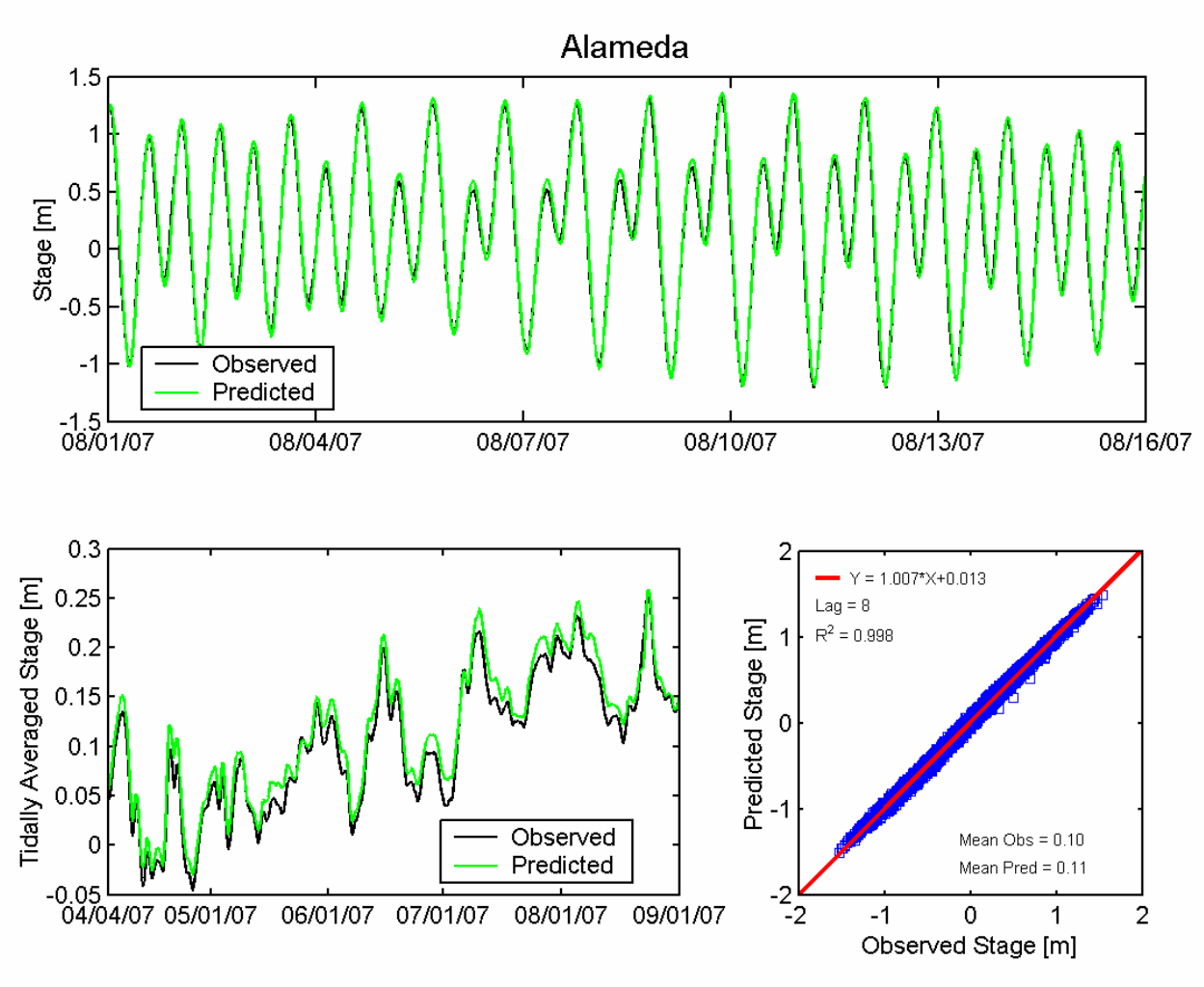

Figure 4.3-3 Observed and predicted stage at Alameda NOAA station (9414750) during the 2007 simulation period.

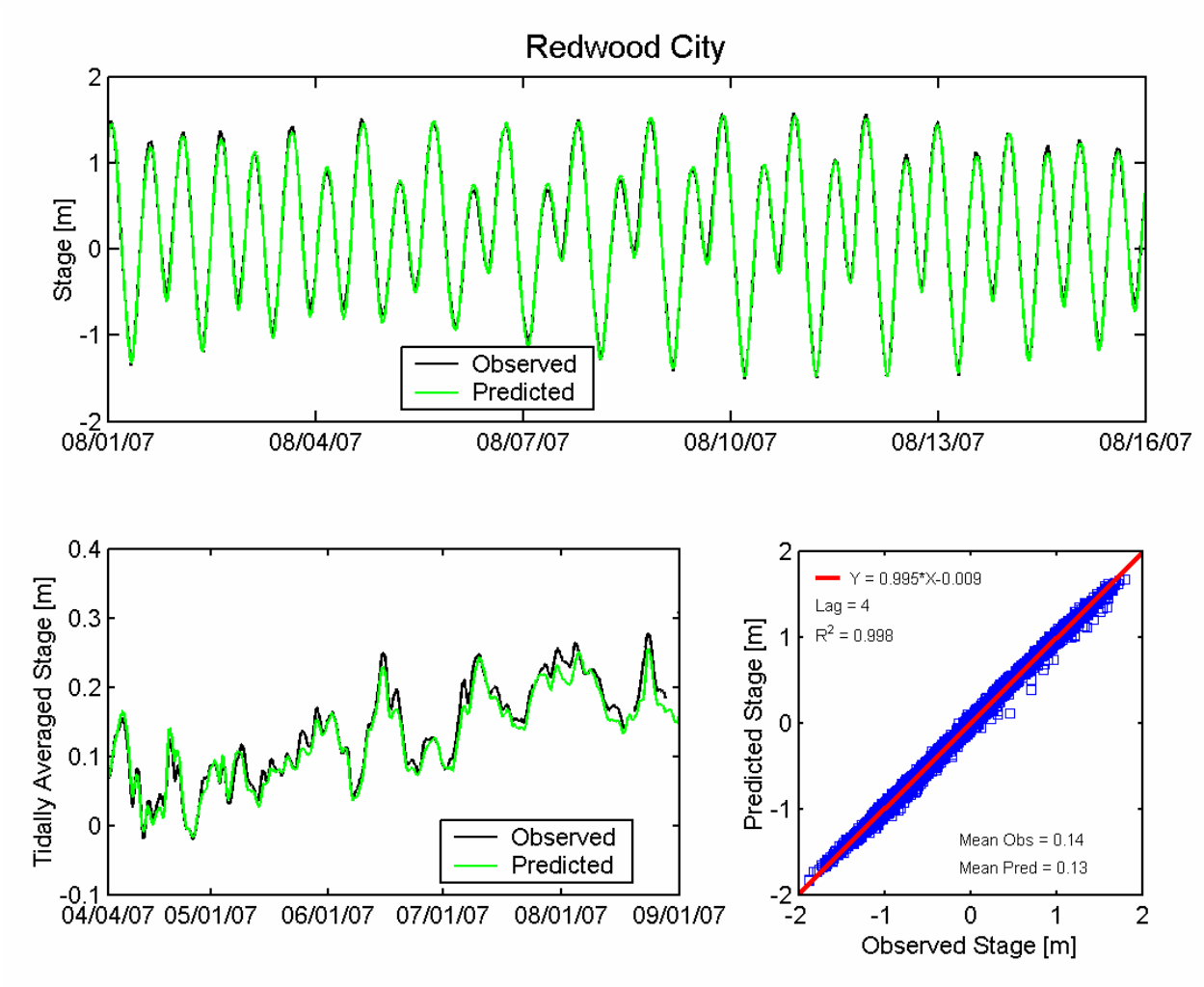

Figure 4.3-4 Observed and predicted stage at Redwood City NOAA station (9414523) during the 2007 simulation period.

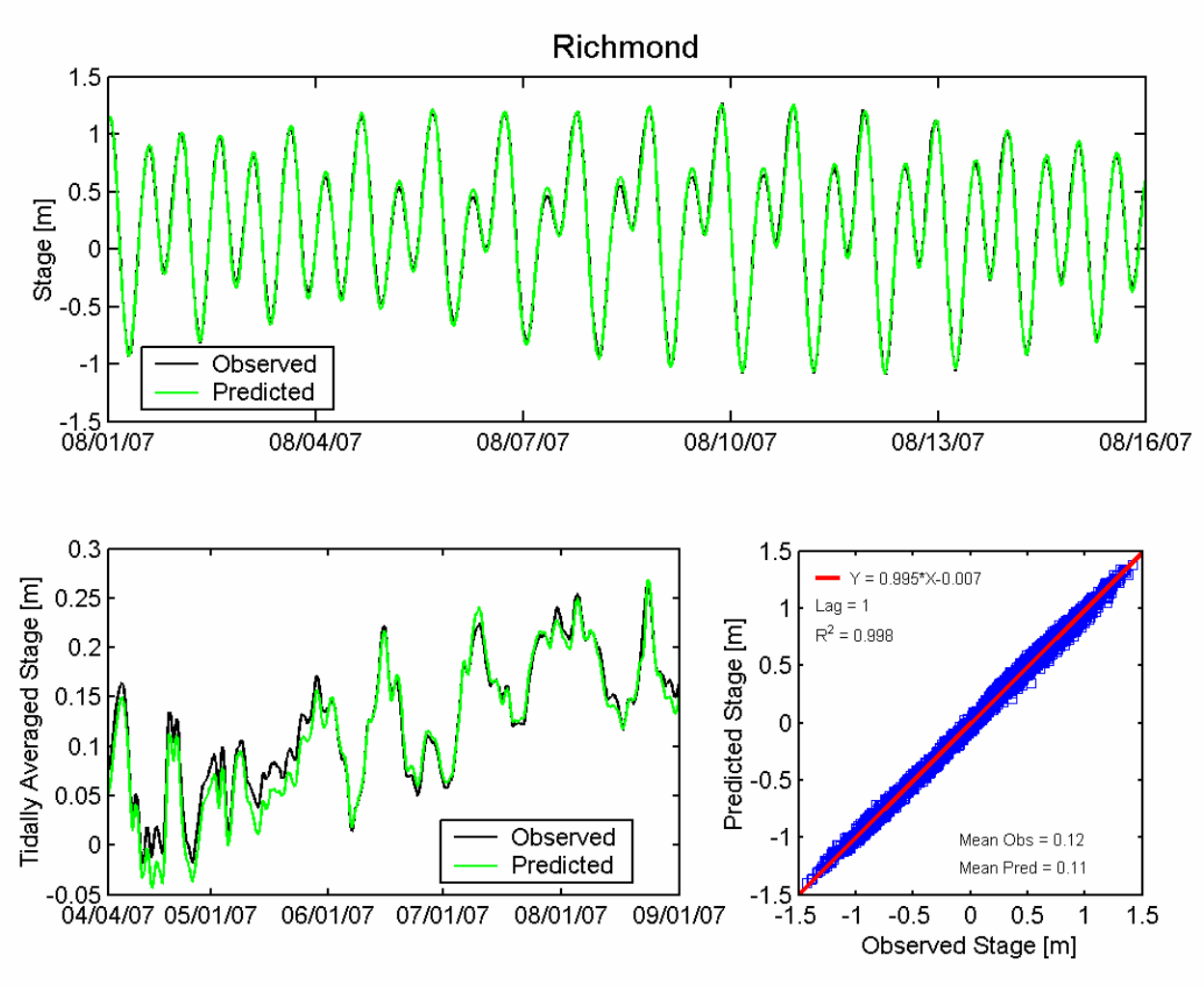

Figure 4.3-5 Observed and predicted stage at Richmond NOAA station (9414863) during the 2007 simulation period.

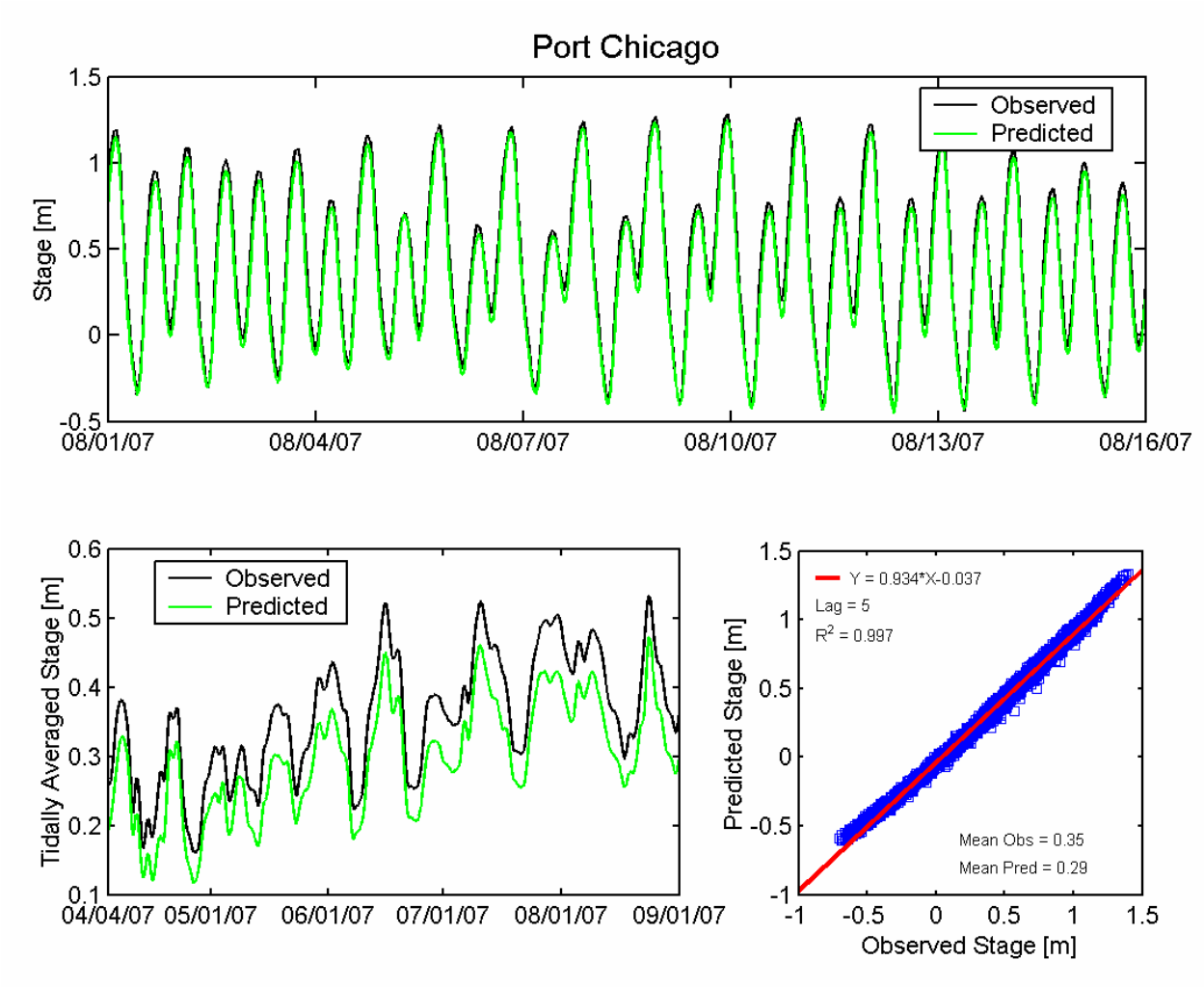

Figure 4.3-6 Observed and predicted stage at Port Chicago NOAA station (9415144) during the 2007 simulation period.

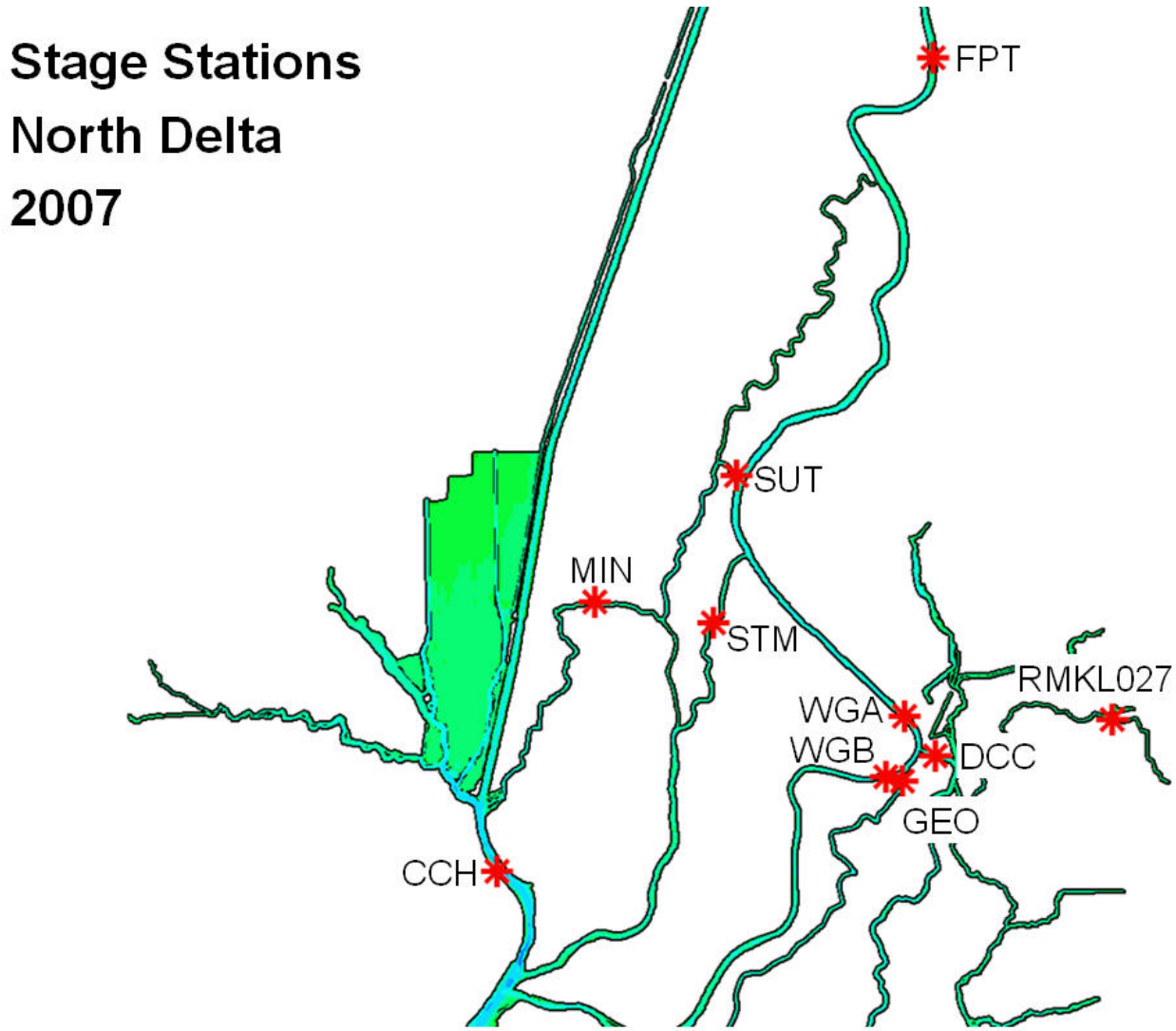

Station Names

CCH, Cache Slough at Ryer Island

WGB, Sacramento River South of Georgiana Slough

GEO, Georgiana Slough near Sacramento River

DCC, Delta Cross Channel

WGA, Sacramento River North of Delta Cross Channel

RMKL027, Mokelumne River near Thornton (Benson's Ferry)

MIN, Miner Slough at Hwy 84 Bridge

STM, Steamboat Slough between Sacramento River and Sutter Sl.

SUT, Sutter Slough at Courtland

FPT, Sacramento River at Freeport

Figure 4.3-7 Location of water level monitoring stations in the northern portion of the Sacramento-San Joaquin Delta used for 2007 stage calibration.

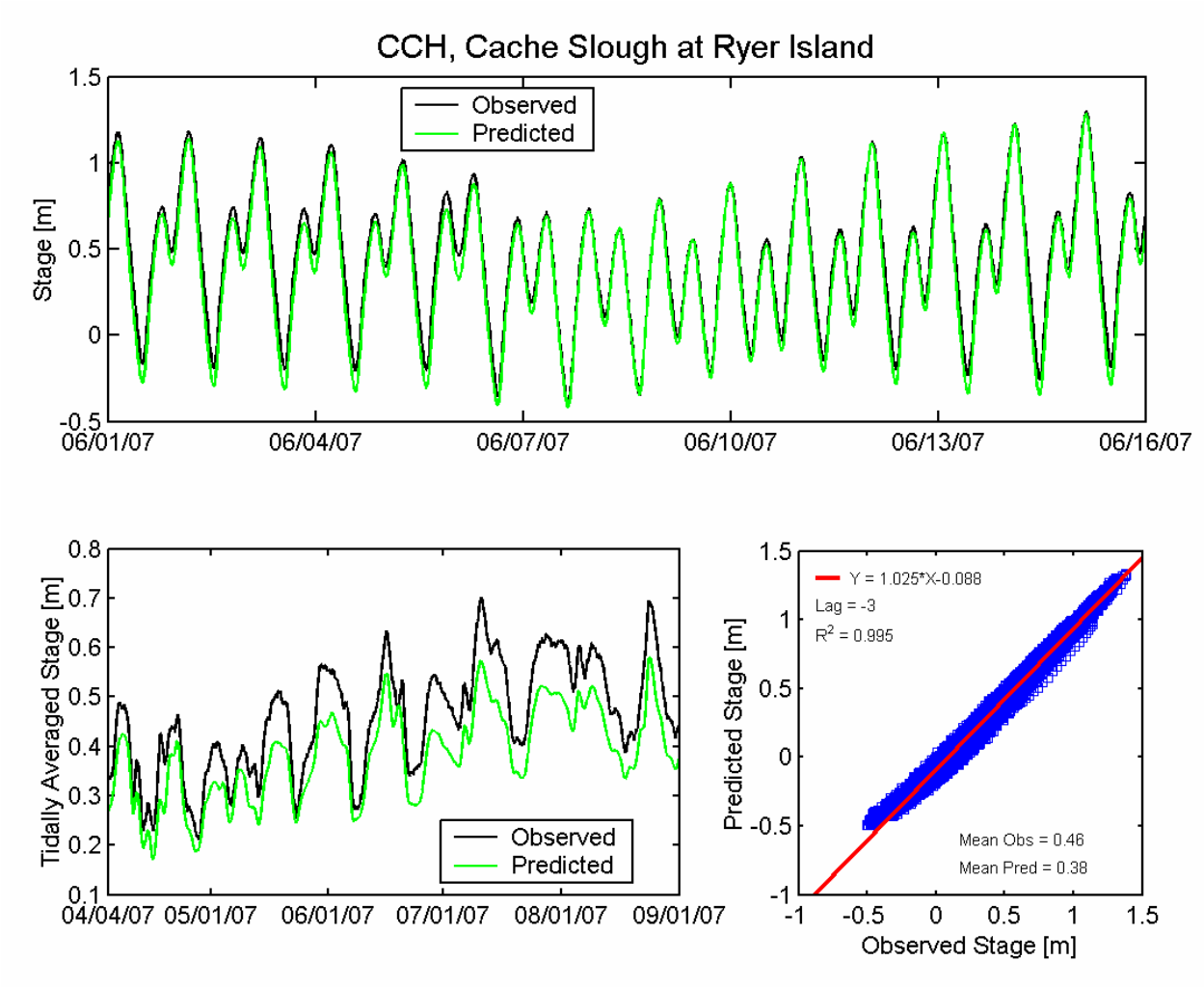

Figure 4.3-8 Observed and predicted stage at Cache Slough at Ryer Island USGS station (CCH) during the 2007 simulation period.

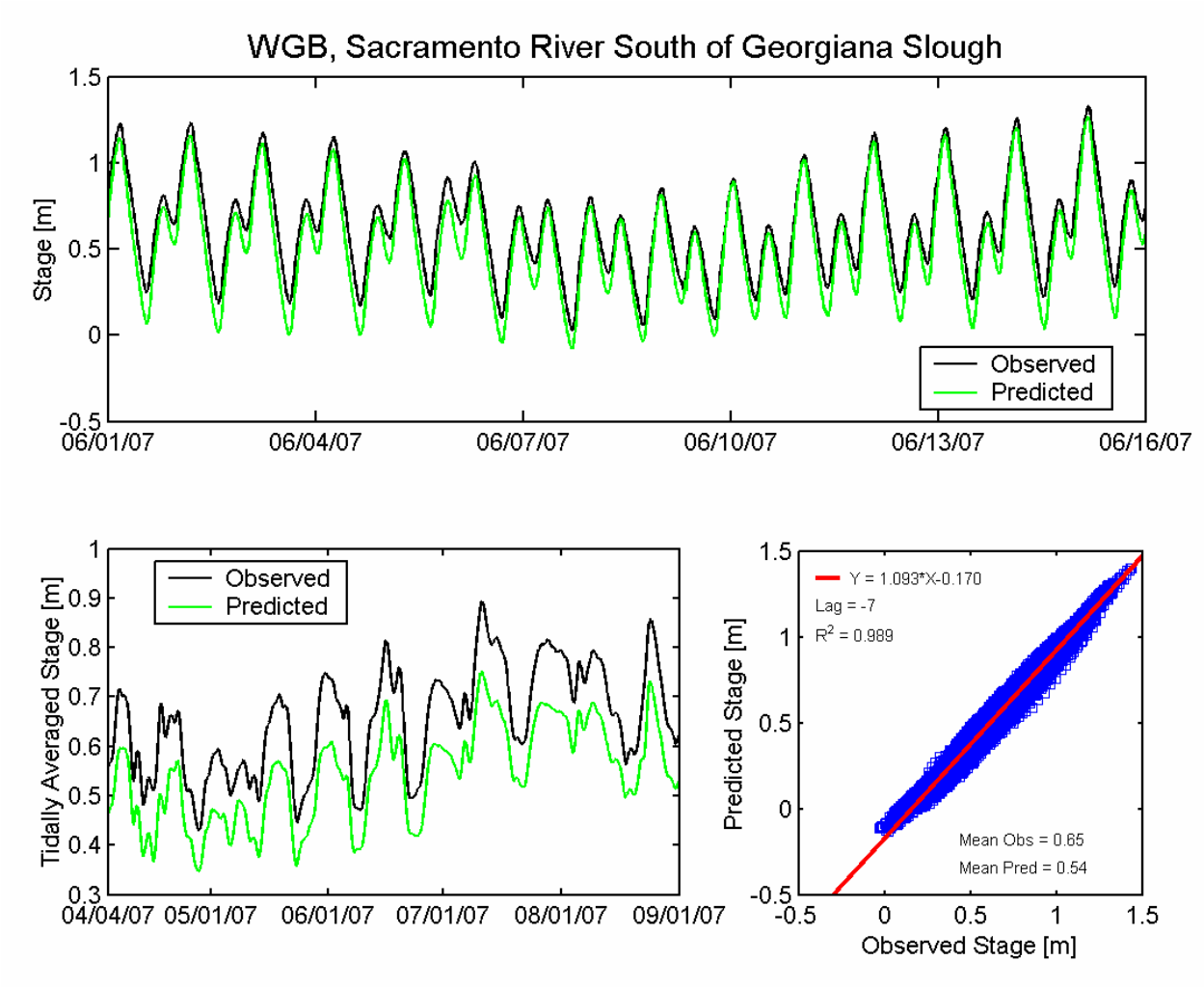

Figure 4.3-9 Observed and predicted stage at Sacramento River South of Georgiana Slough USGS station (WGB) during the 2007 simulation period.

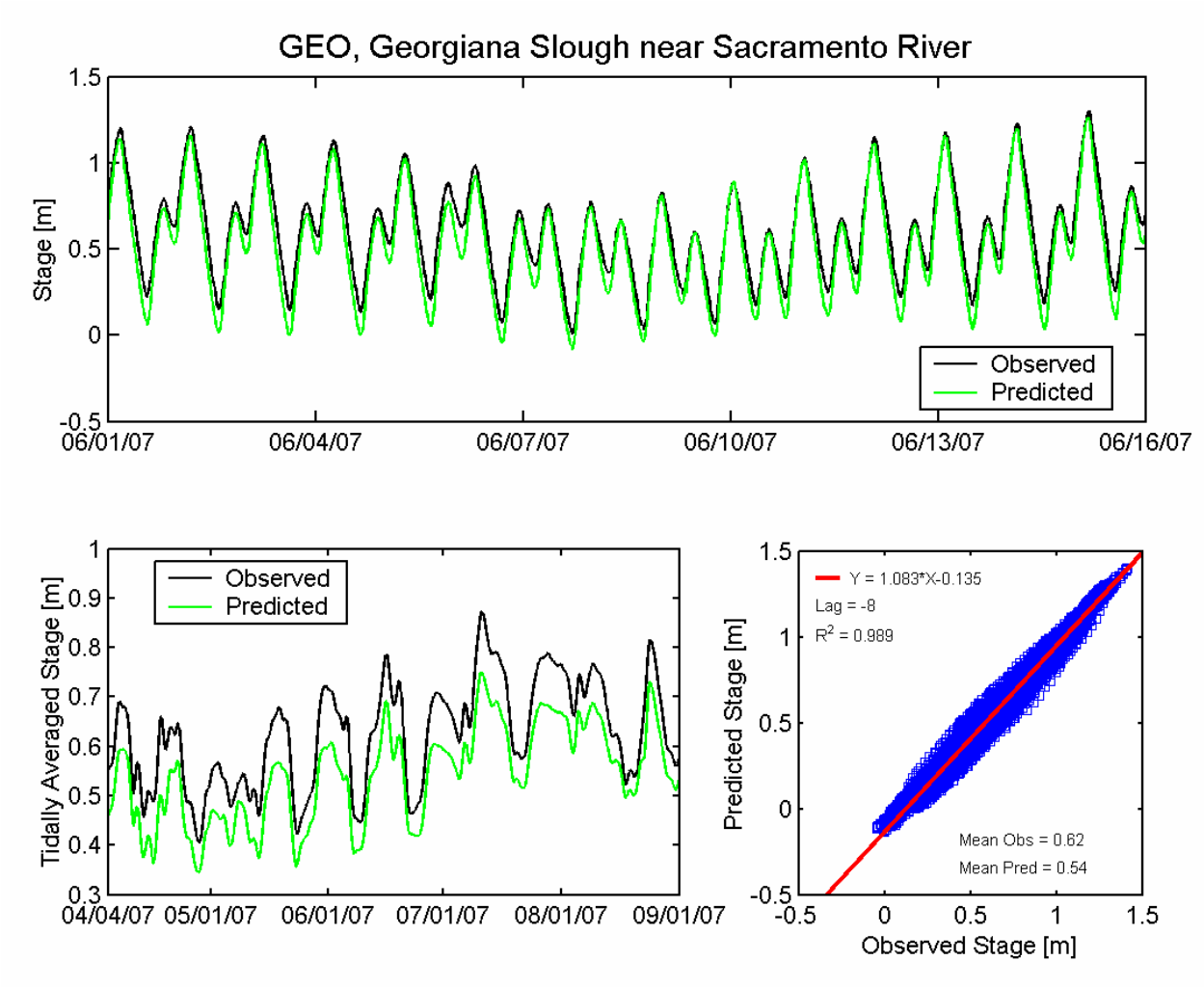

Figure 4.3-10 Observed and predicted stage at Georgiana Slough near Sacramento River USGS station (GEO) during the 2007 simulation period.

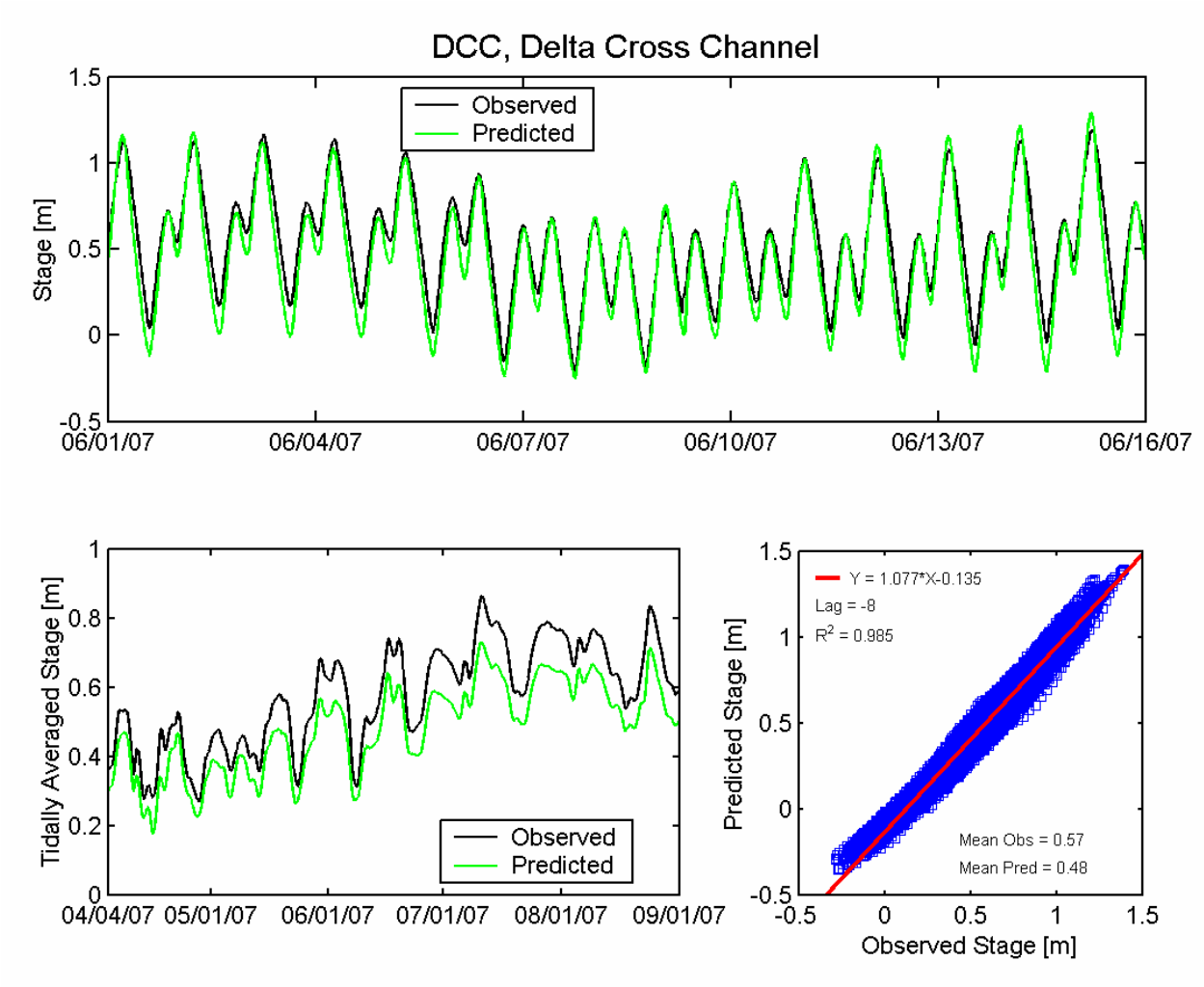

Figure 4.3-11 Observed and predicted stage at Delta Cross Channel USGS station (DCC) during the 2007 simulation period.

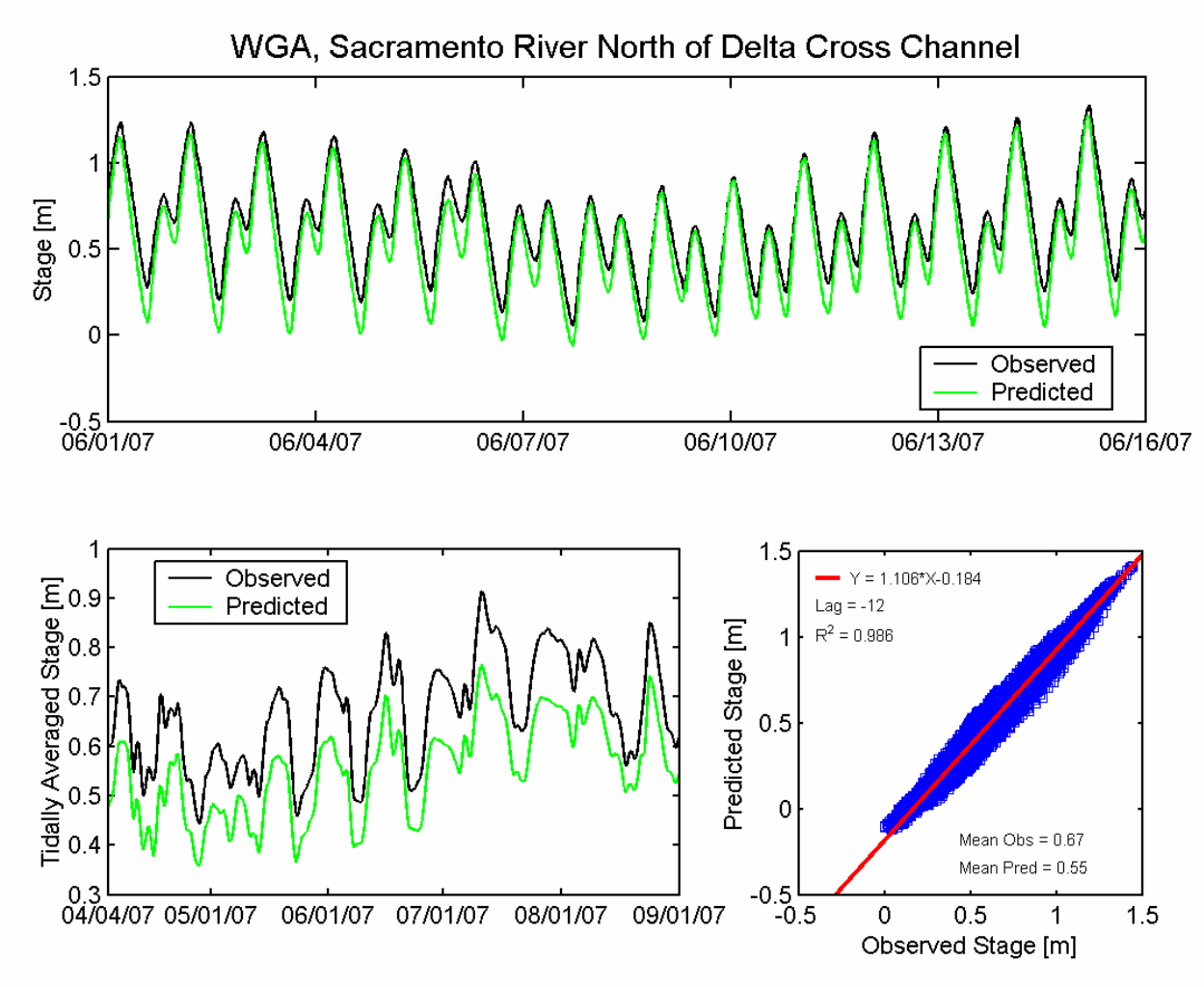

Figure 4.3-12 Observed and predicted stage at Sacramento River North of Delta Cross Channel USGS station (WGA) during the 2007 simulation period.

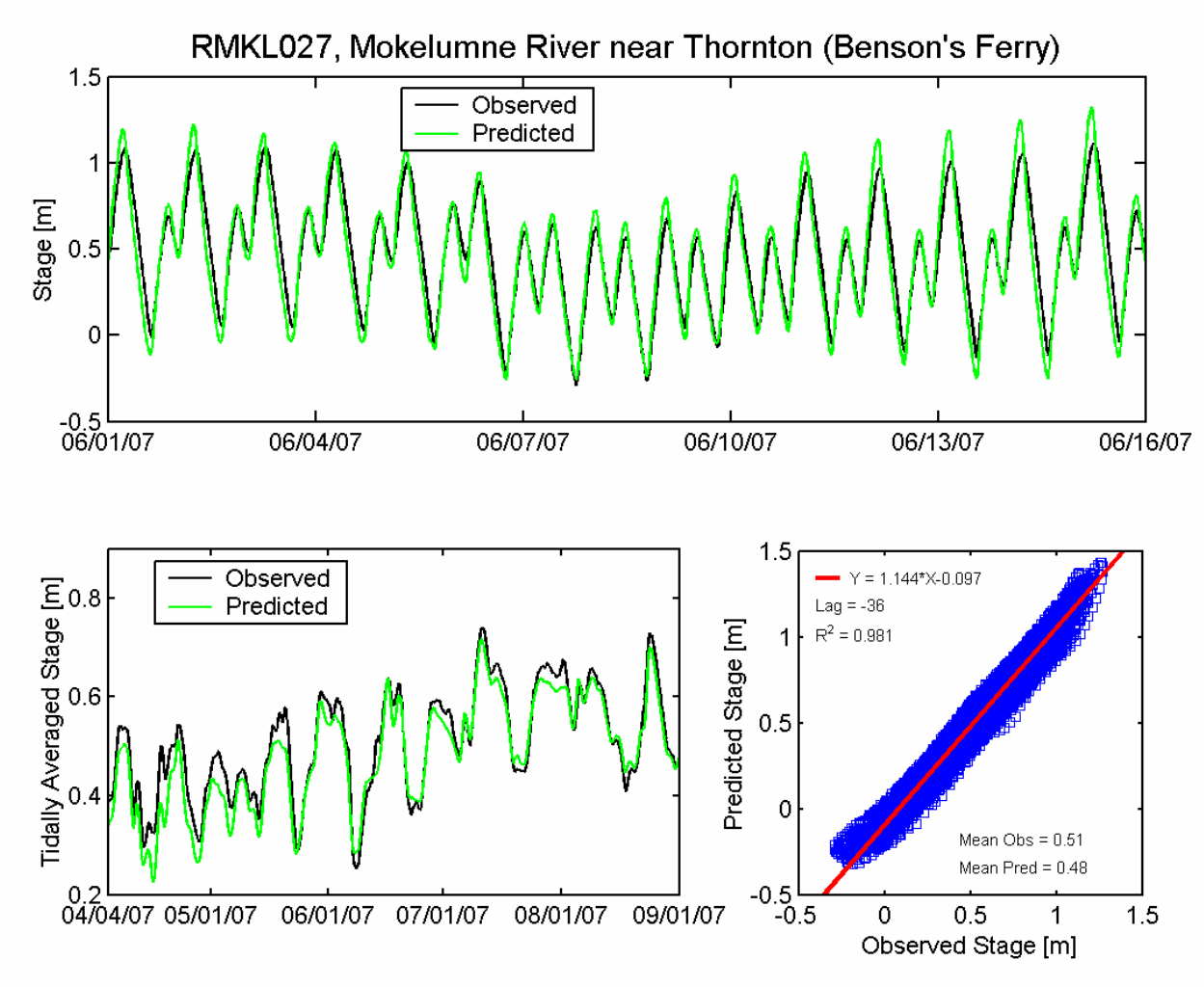

Figure 4.3-13 Observed and predicted stage at Mokelumne River near Thornton (Benson's Ferry) DWR station (RMKL027) during the 2007 simulation period.

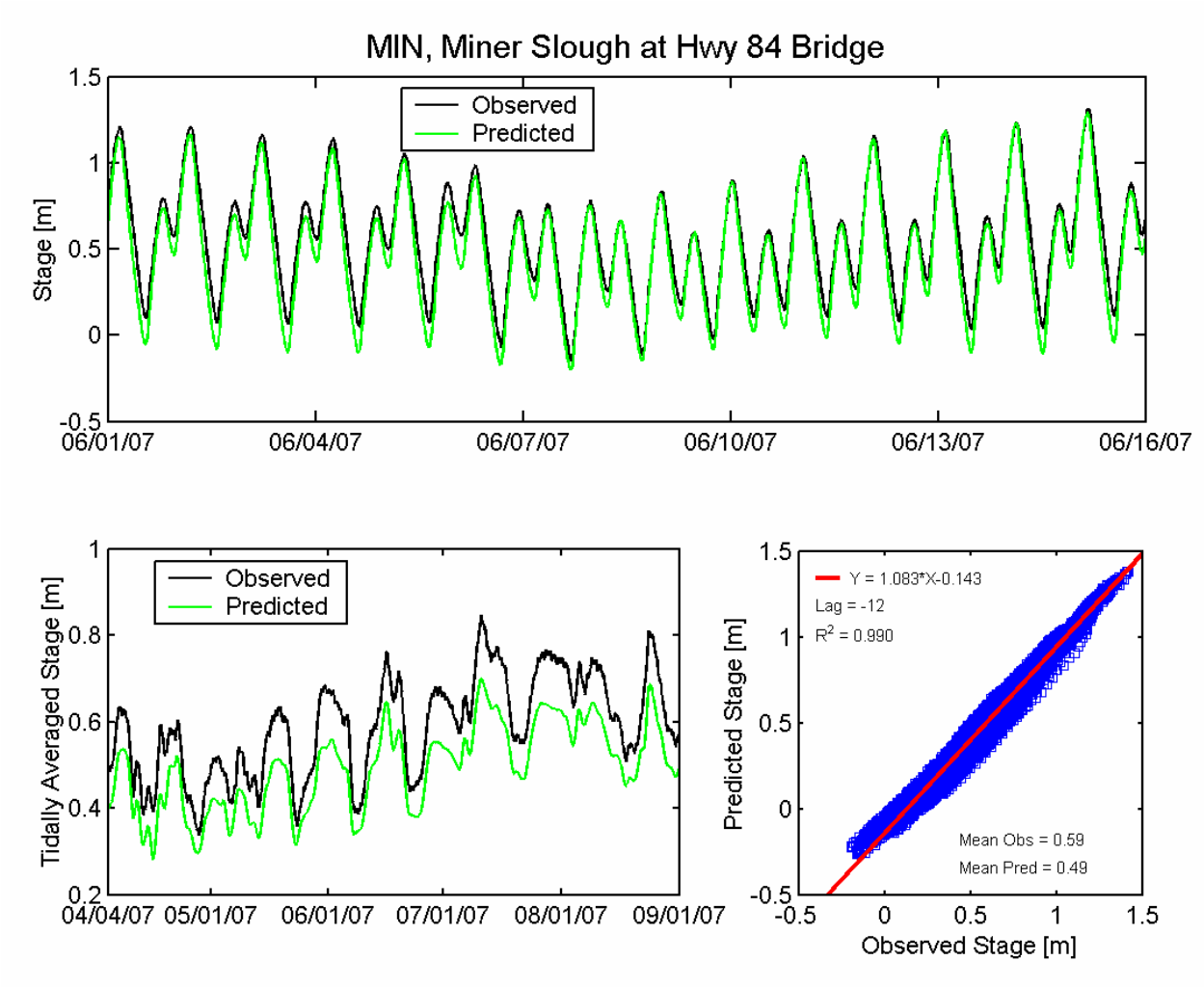

Figure 4.3-14 Observed and predicted stage at Miner Slough at Highway 84 Bridge USGS station (MIN) during the 2007 simulation period.

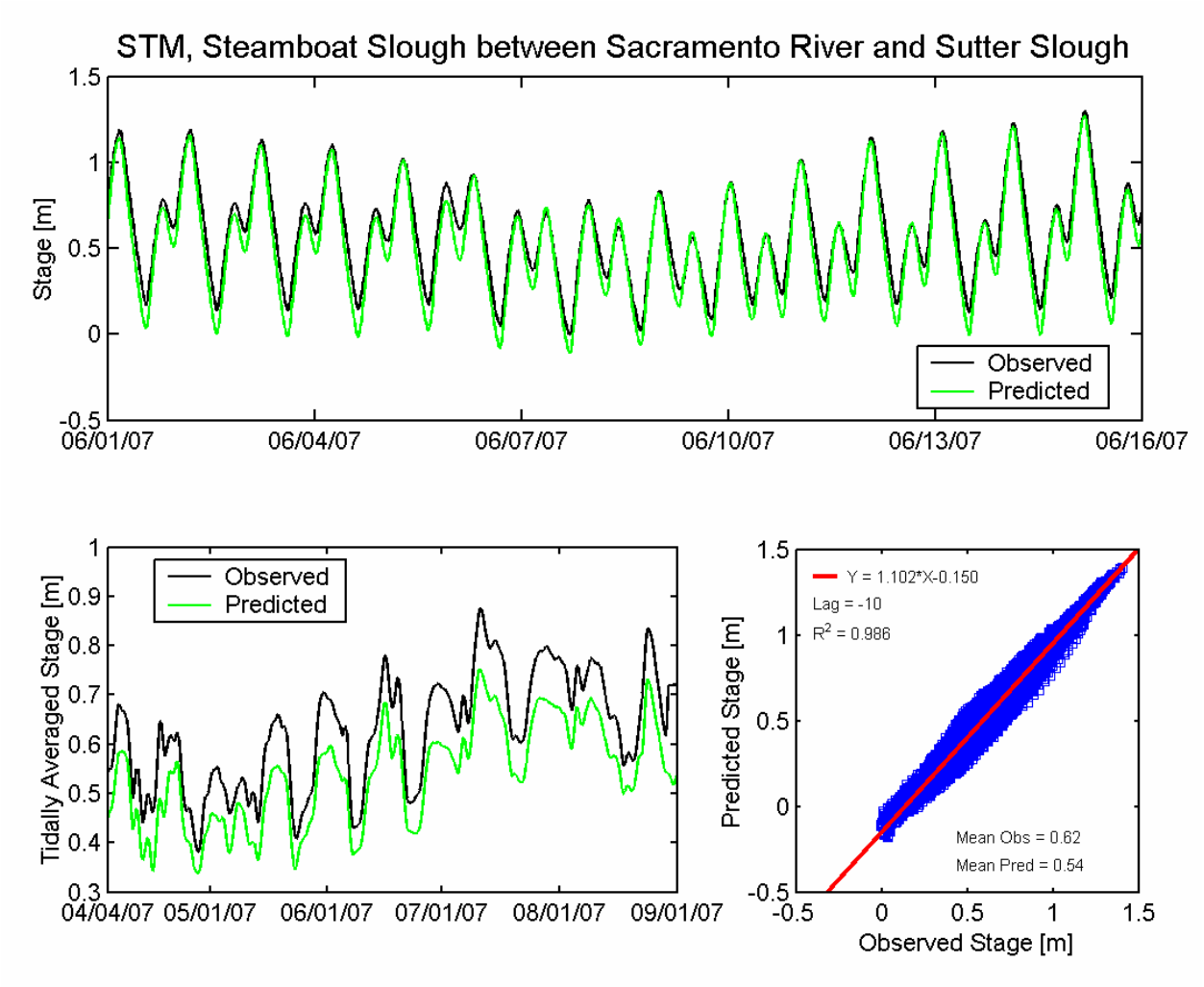

Figure 4.3-15 Observed and predicted stage at Steamboat Slough between Sacramento River and Sutter Slough USGS station (STM) during the 2007 simulation period.

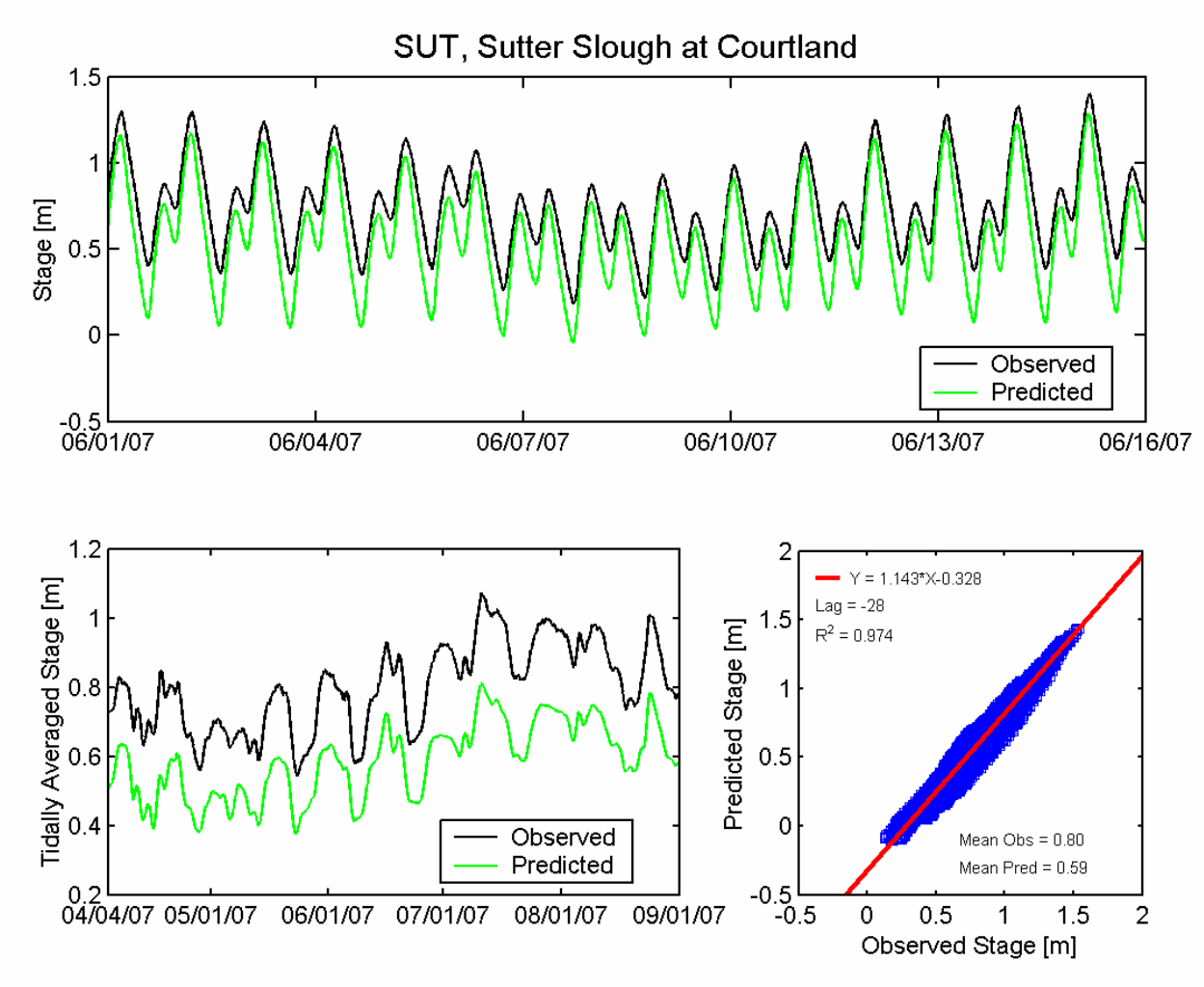

Figure 4.3-16 Observed and predicted stage at Sutter Slough at Courtland USGS station (SUT) during the 2007 simulation period.

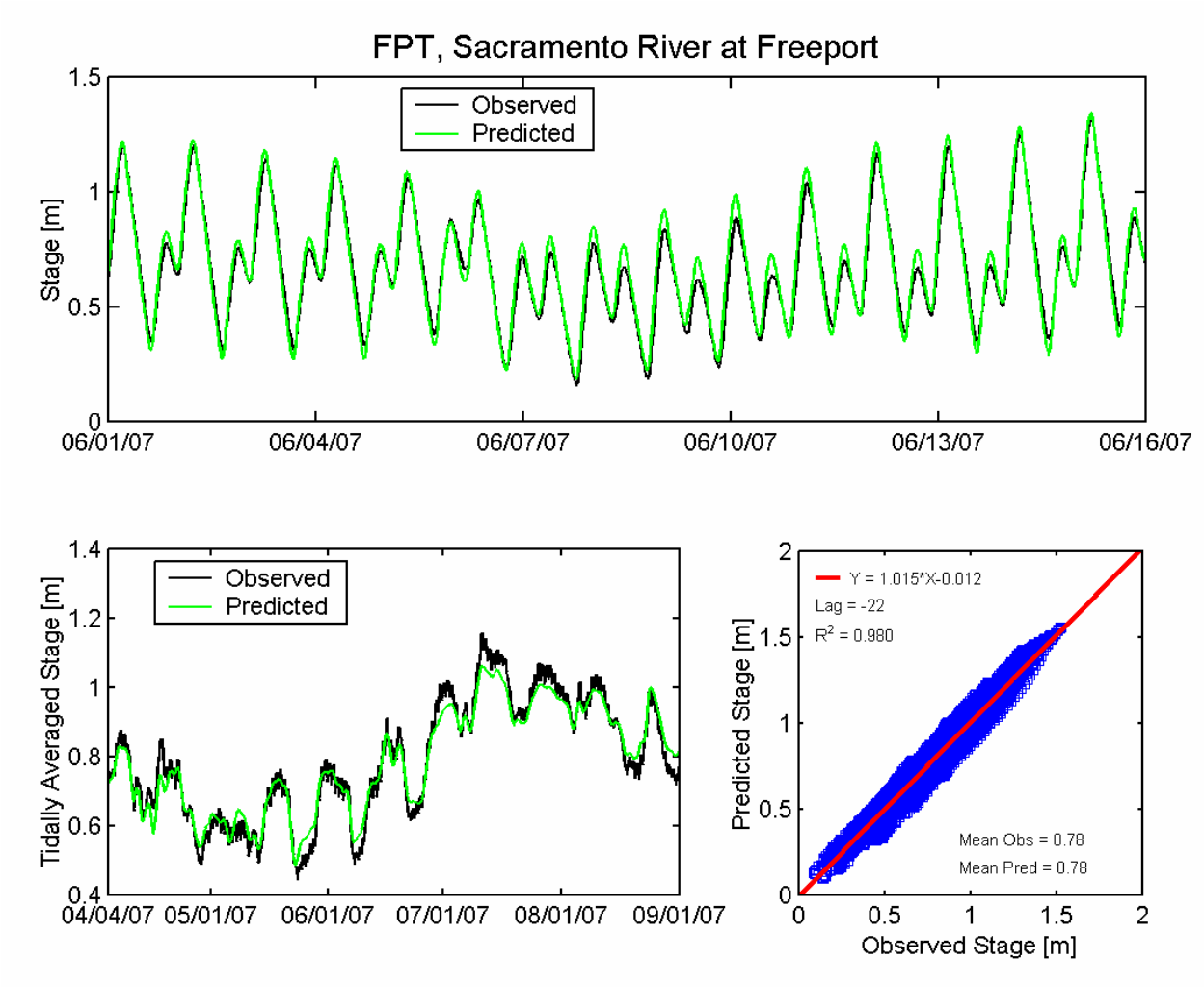

Figure 4.3-17 Observed and predicted stage at Sacramento River at Freeport USGS station (FPT) during the 2007 simulation period.

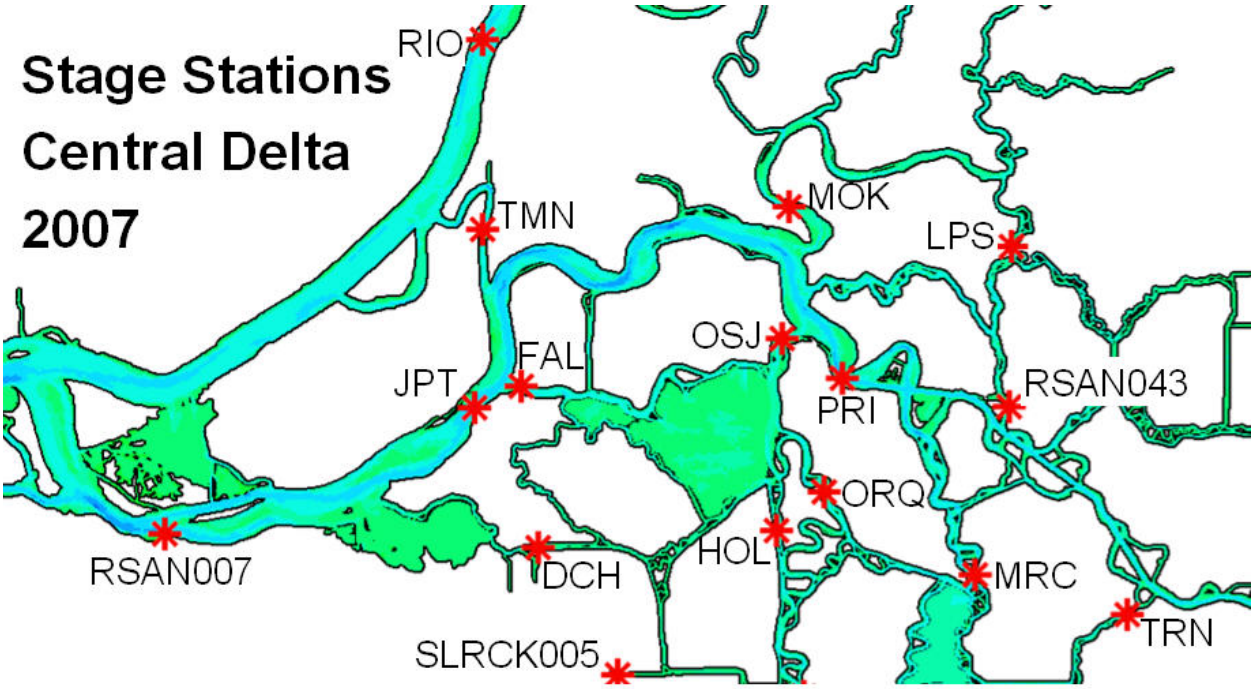

Station Names

RSAN007, San Joaquin River at Antioch

RIO, Sacramento River at Rio Vista

TMN, Threemile Slough North at San Joaquin River

JPT, San Joaquin River at Jersey Point

FAL, False River

DCH, Dutch Slough at Jersey Island

OSJ, Old River at San Joaquin River

MOK, Mokelumne River near San Joaquin River

ORQ, Old River at Quimby Island near Bethel Island

HOL, Holland Cut

SLRCK005, Rock Slough at Contra Costa Canal

PRI, San Joaquin River at Prisoners Point

RSAN043, San Joaquin River at Venice Island

LPS, Little Potato Slough at Terminous

MRC, Middle River South of Columbia Cut

TRN, Turner Cut near Holt

Figure 4.3-18 Location of water level monitoring stations in the central portion of the Sacramento-San Joaquin Delta used for 2007 stage calibration.

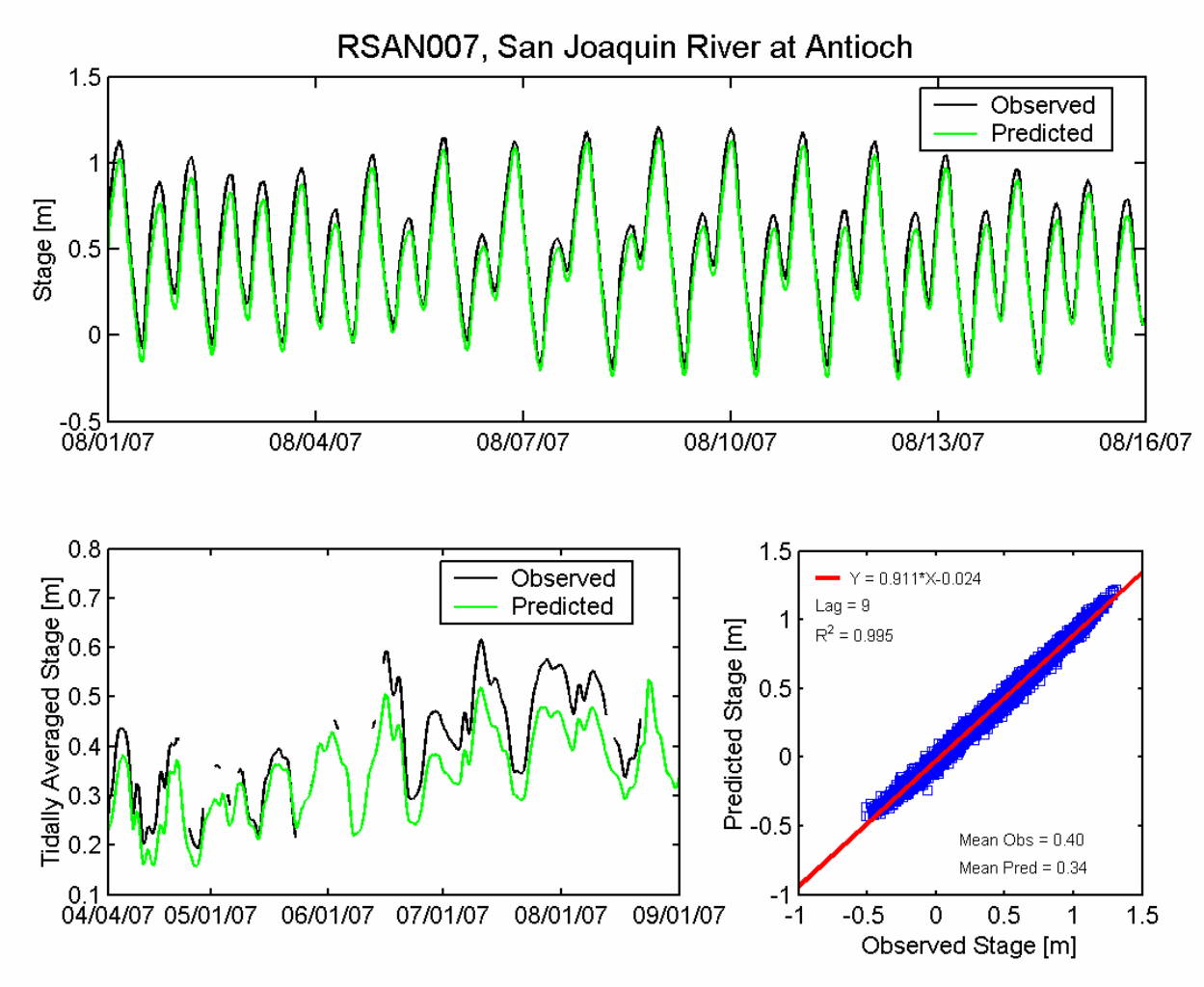

Figure 4.3-19 Observed and predicted stage at Antioch DWR station (RSAN007) during the 2007 simulation period.

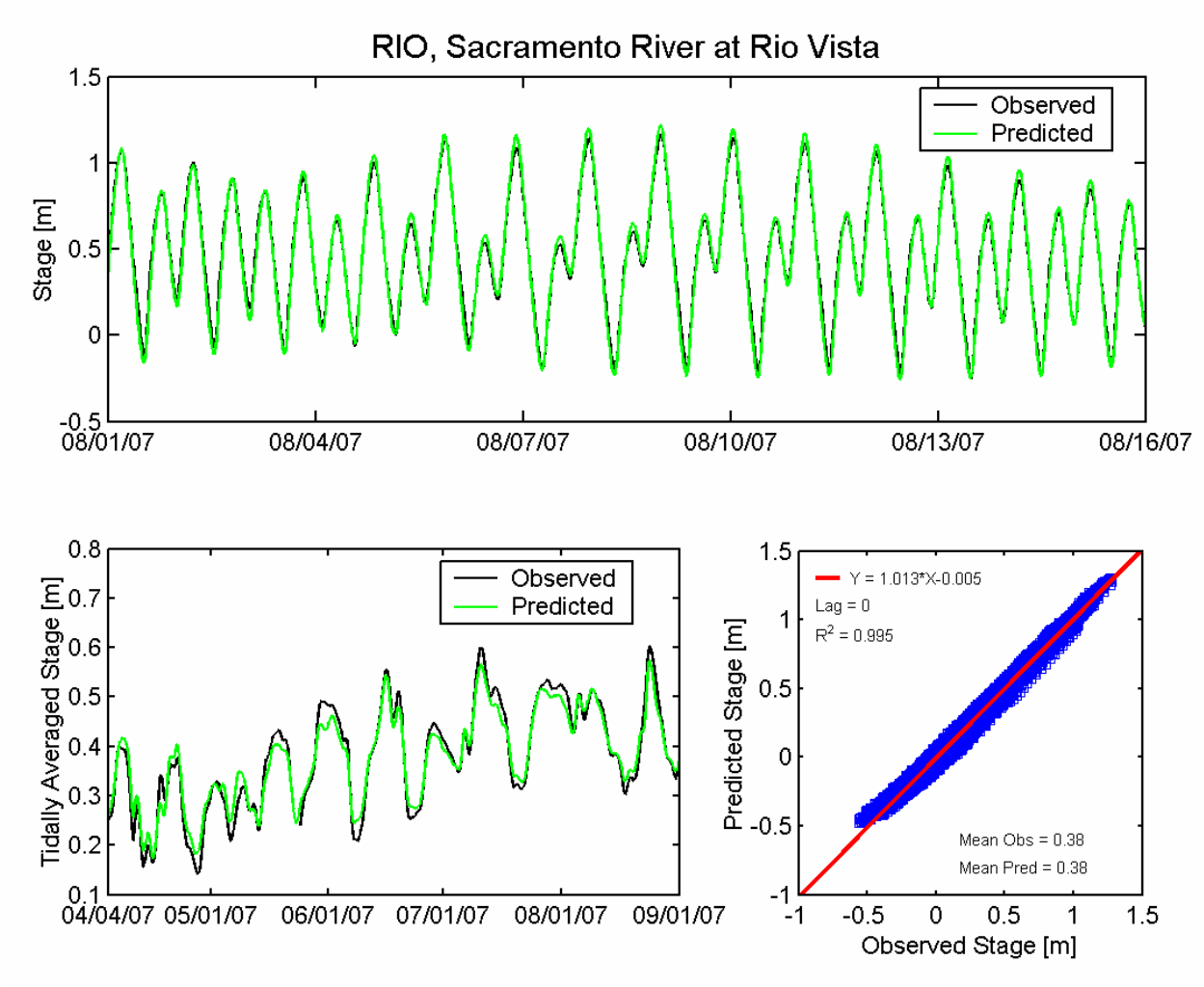

Figure 4.3-20 Observed and predicted stage at Sacramento River at Rio Vista USGS station (RIO) during the 2007 simulation period.

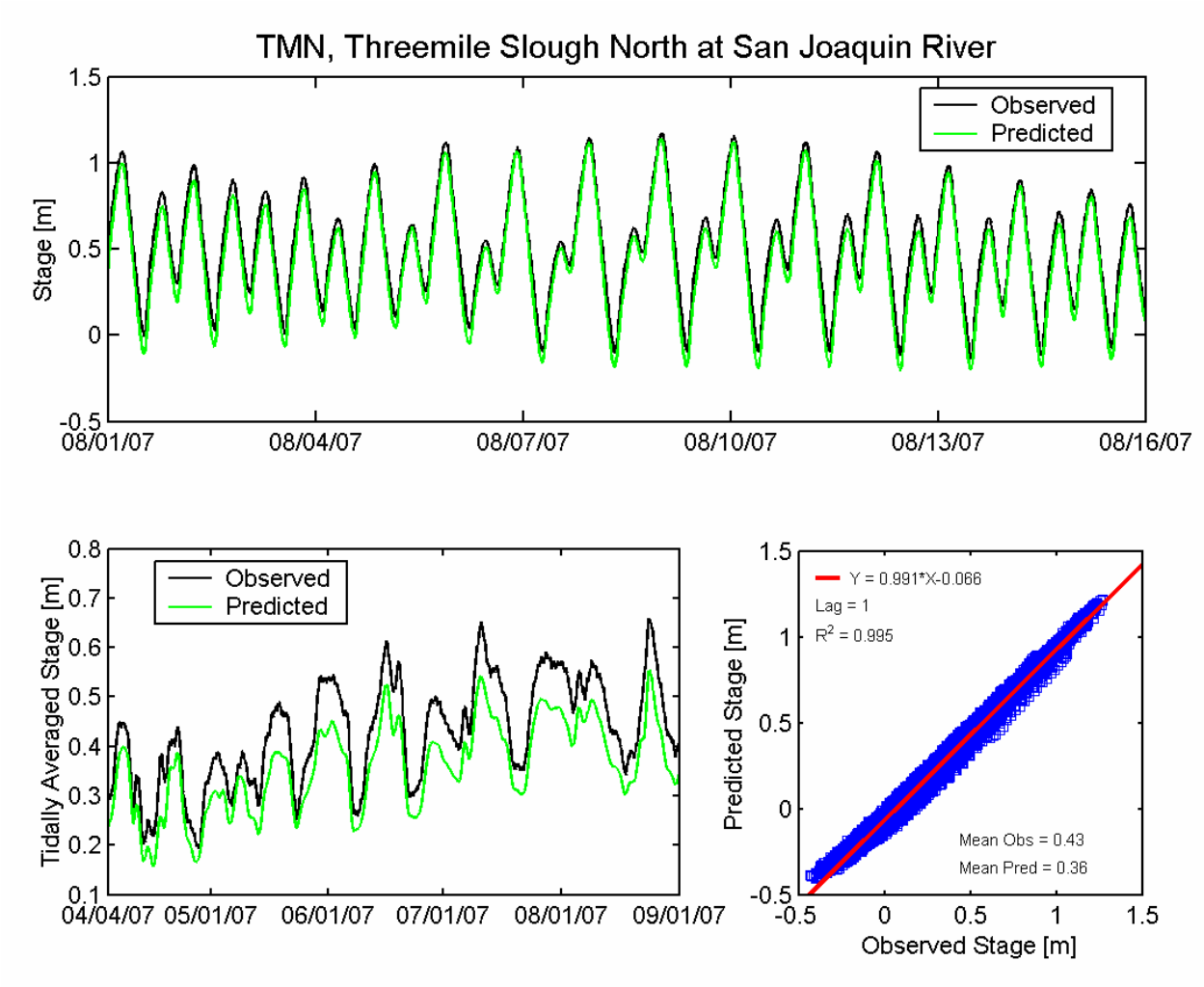

Figure 4.3-21 Observed and predicted stage at Threemile Slough North at San Joaquin River USGS station (TMN) during the 2007 simulation period.

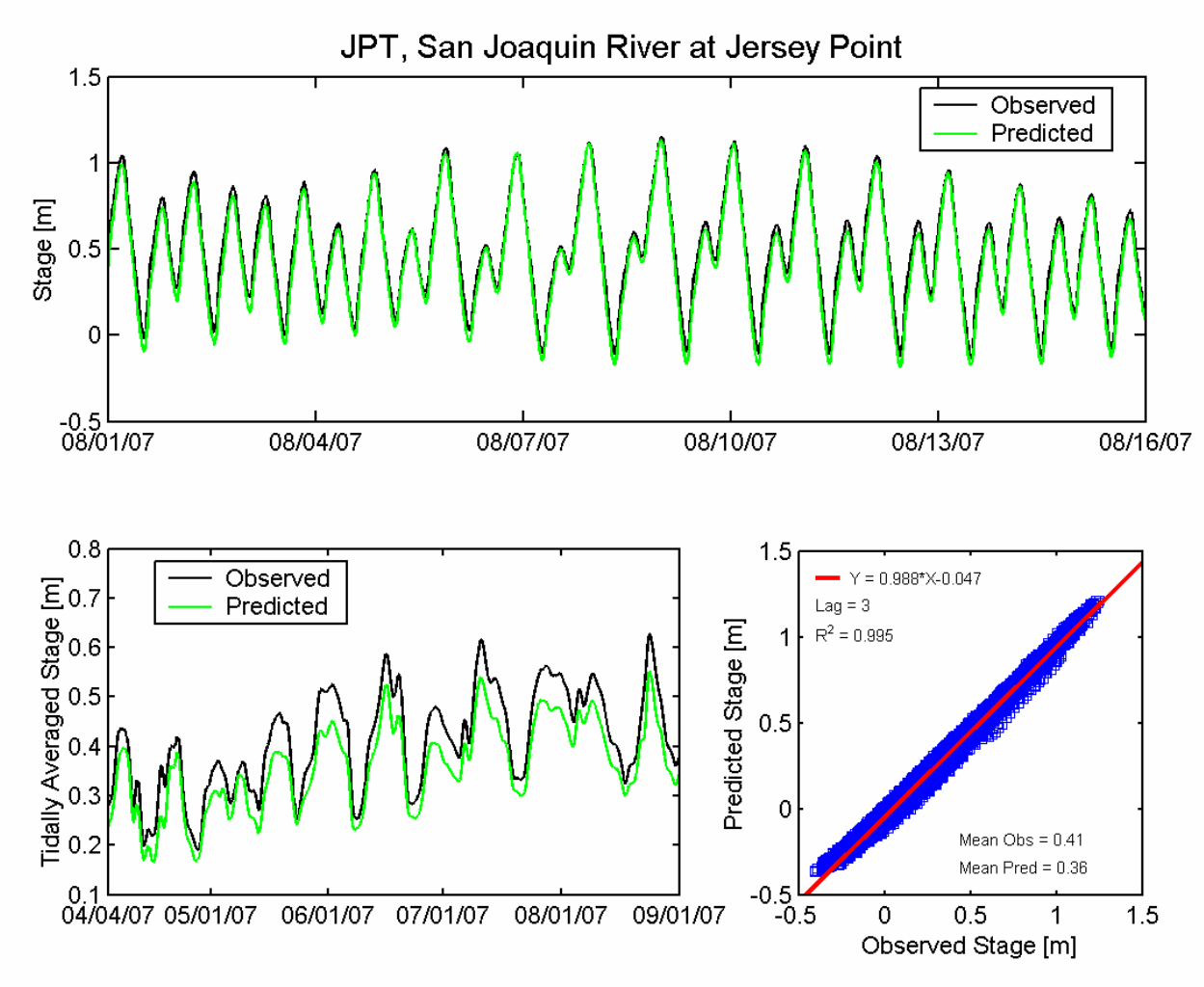

Figure 4.3-22 Observed and predicted stage at San Joaquin River at Jersey Point USGS station (JPT) during the 2007 simulation period.

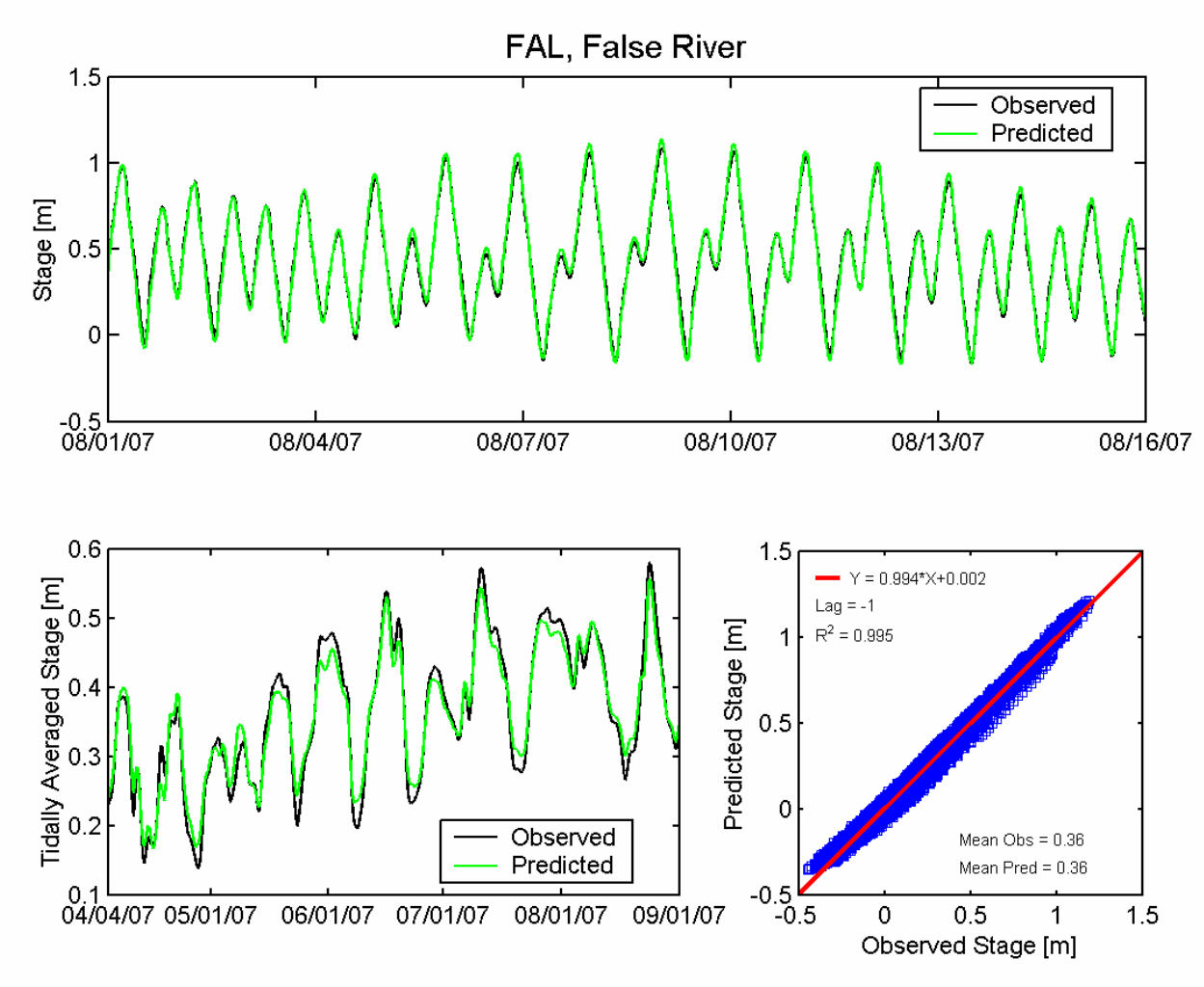

Figure 4.3-23 Observed and predicted stage at False River USGS station (FAL) during the 2007 simulation period.

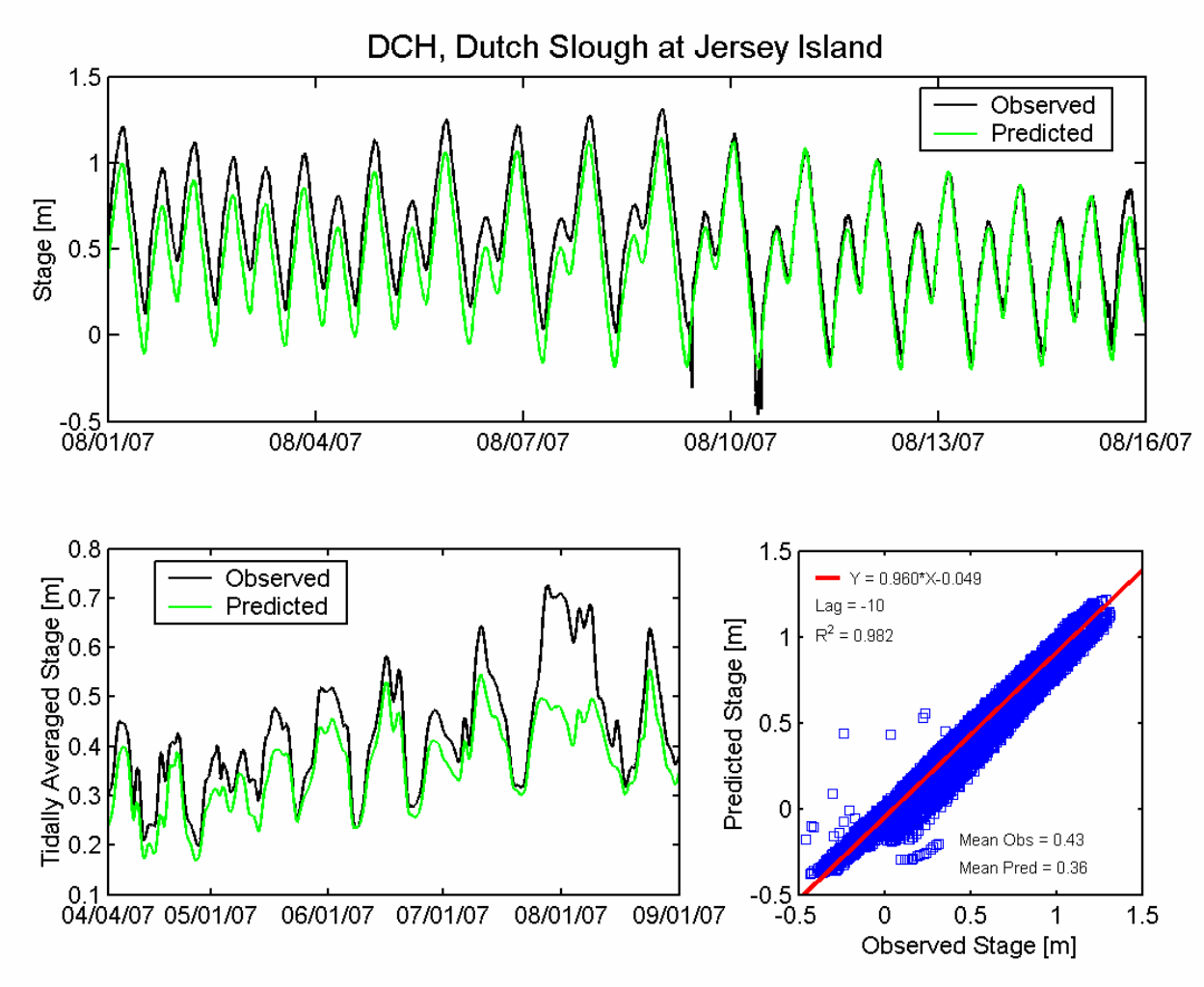

Figure 4.3-24 Observed and predicted stage at Dutch Slough at Jersey Island USGS station (DCH) during the 2007 simulation period.

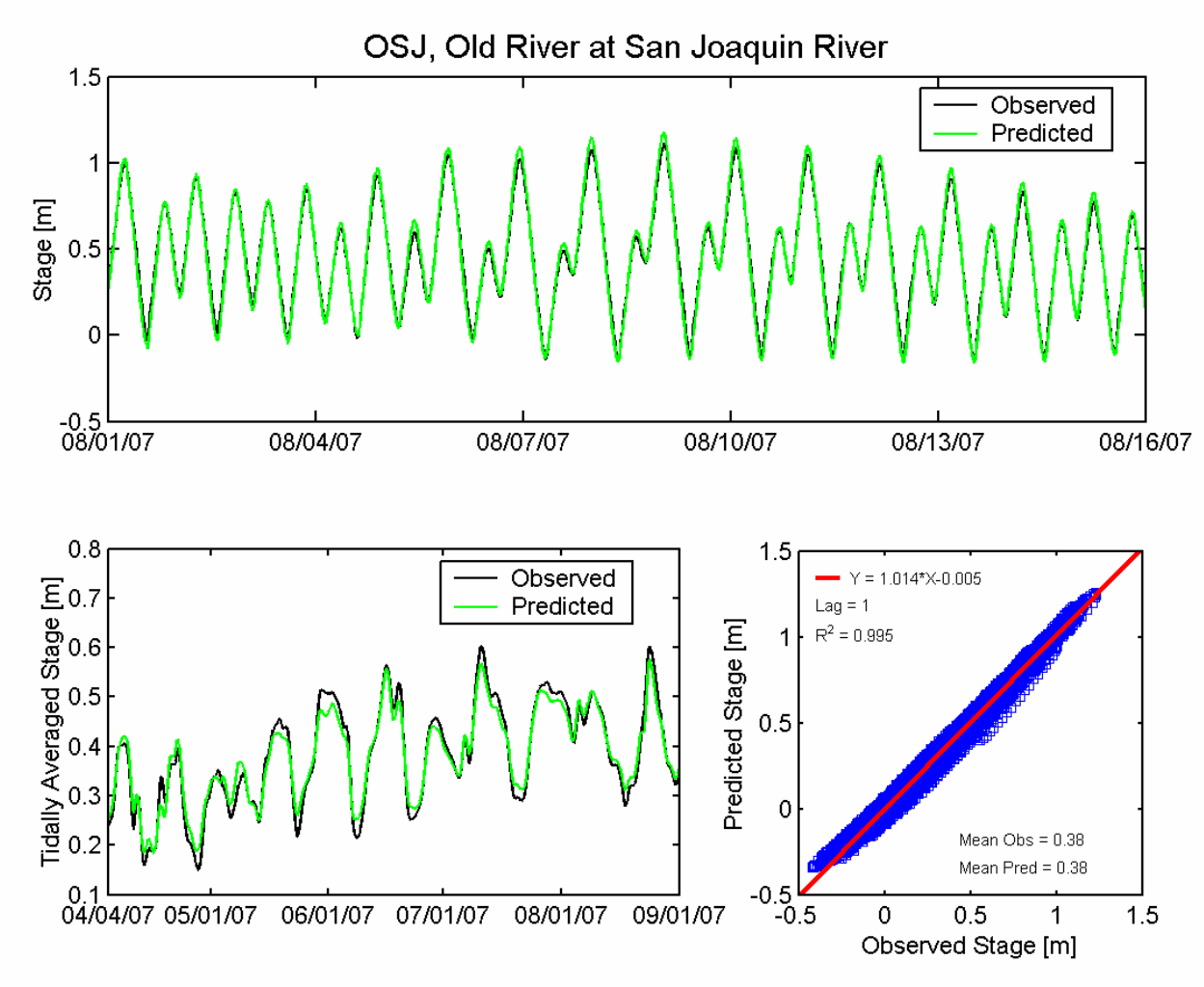

Figure 4.3-25 Observed and predicted stage at Old River at San Joaquin River USGS station (OSJ) during the 2007 simulation period.

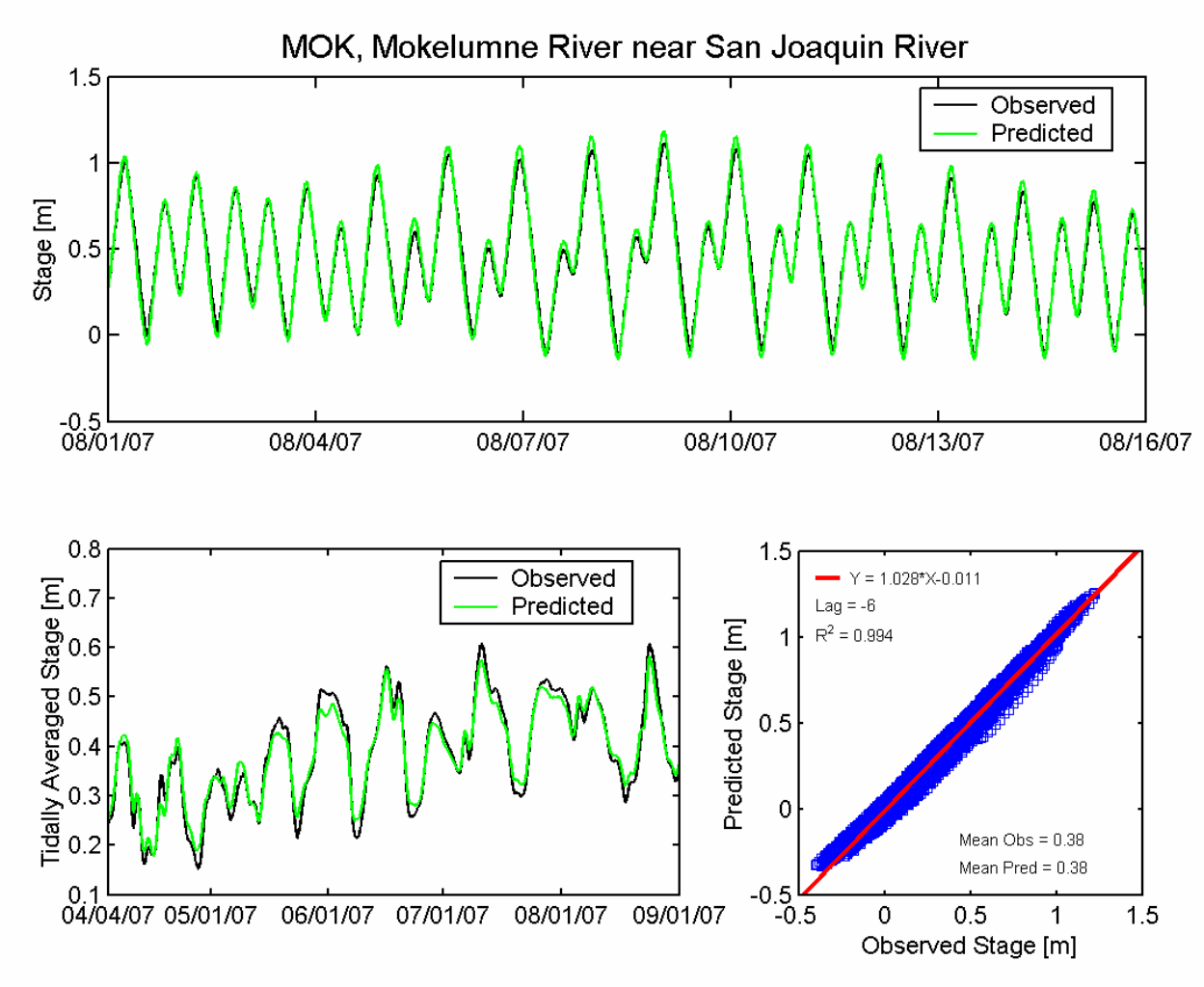

Figure 4.3-26 Observed and predicted stage at Mokelumne River near San Joaquin River USGS station (MOK) during the 2007 simulation period.

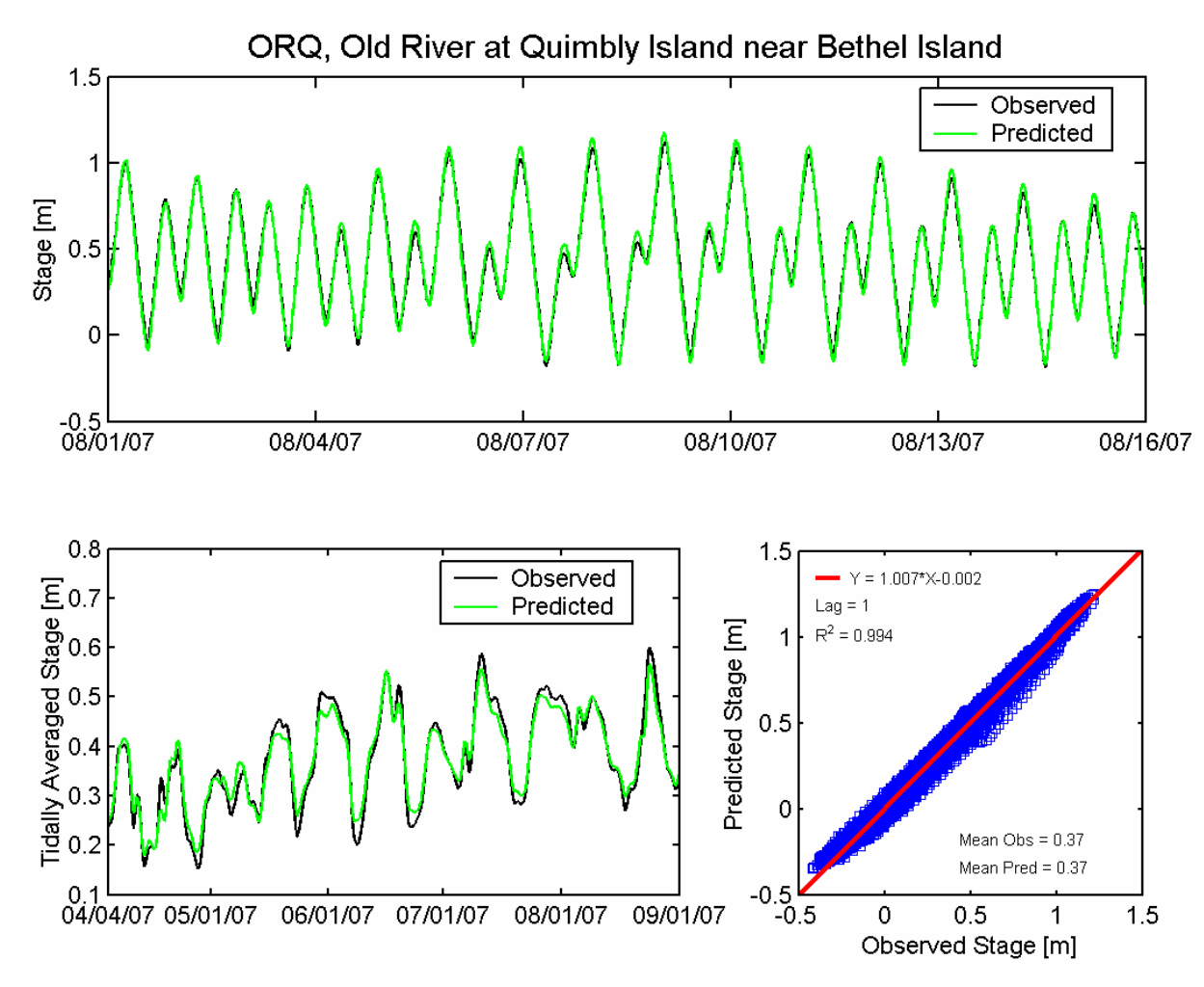

Figure 4.3-27 Observed and predicted stage at Old River at Quimby Island near Bethel Island USGS station (ORQ) during the 2007 simulation period.

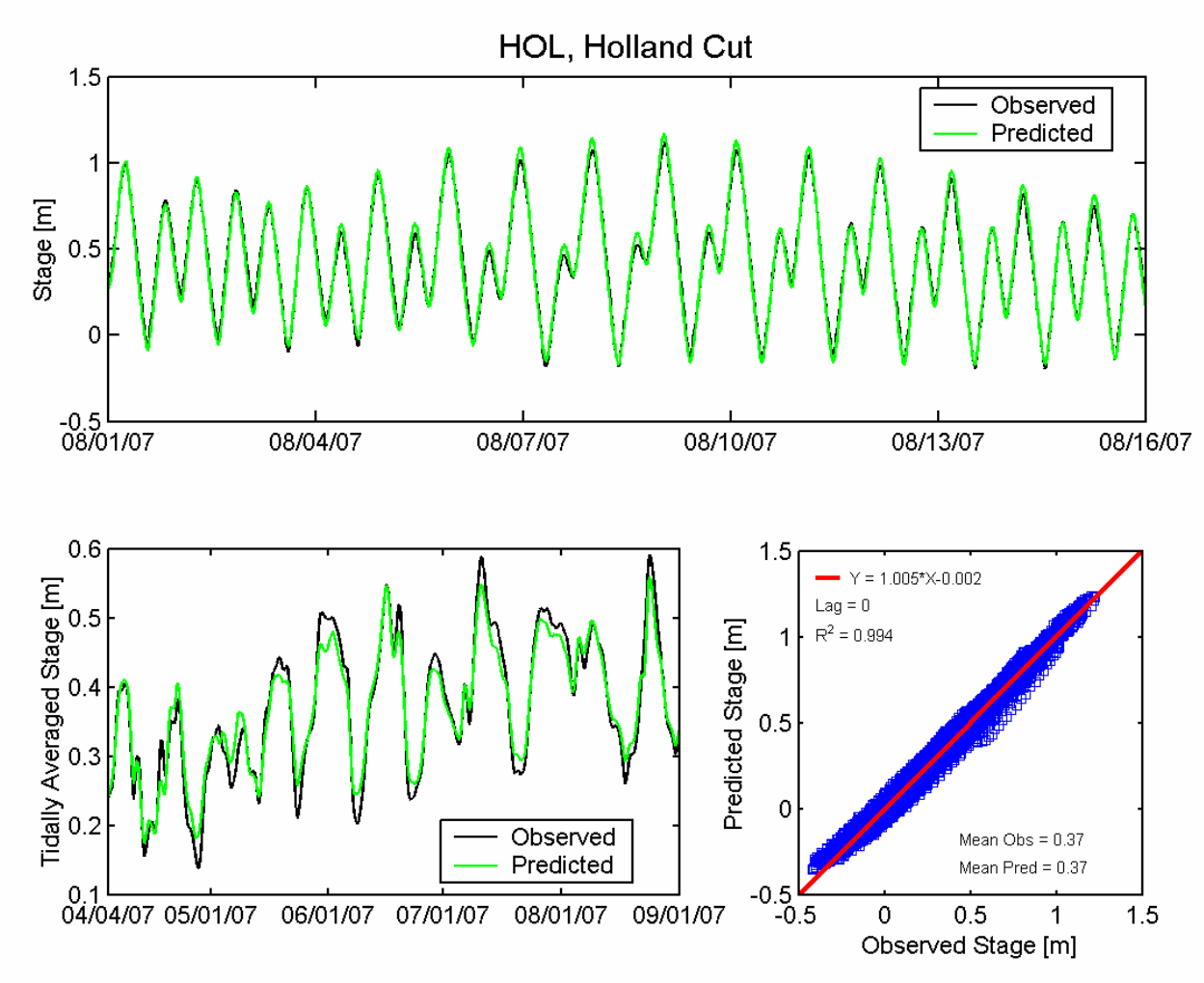

Figure 4.3-28 Observed and predicted stage at Holland Cut USGS station (HOL) during the 2007 simulation period.

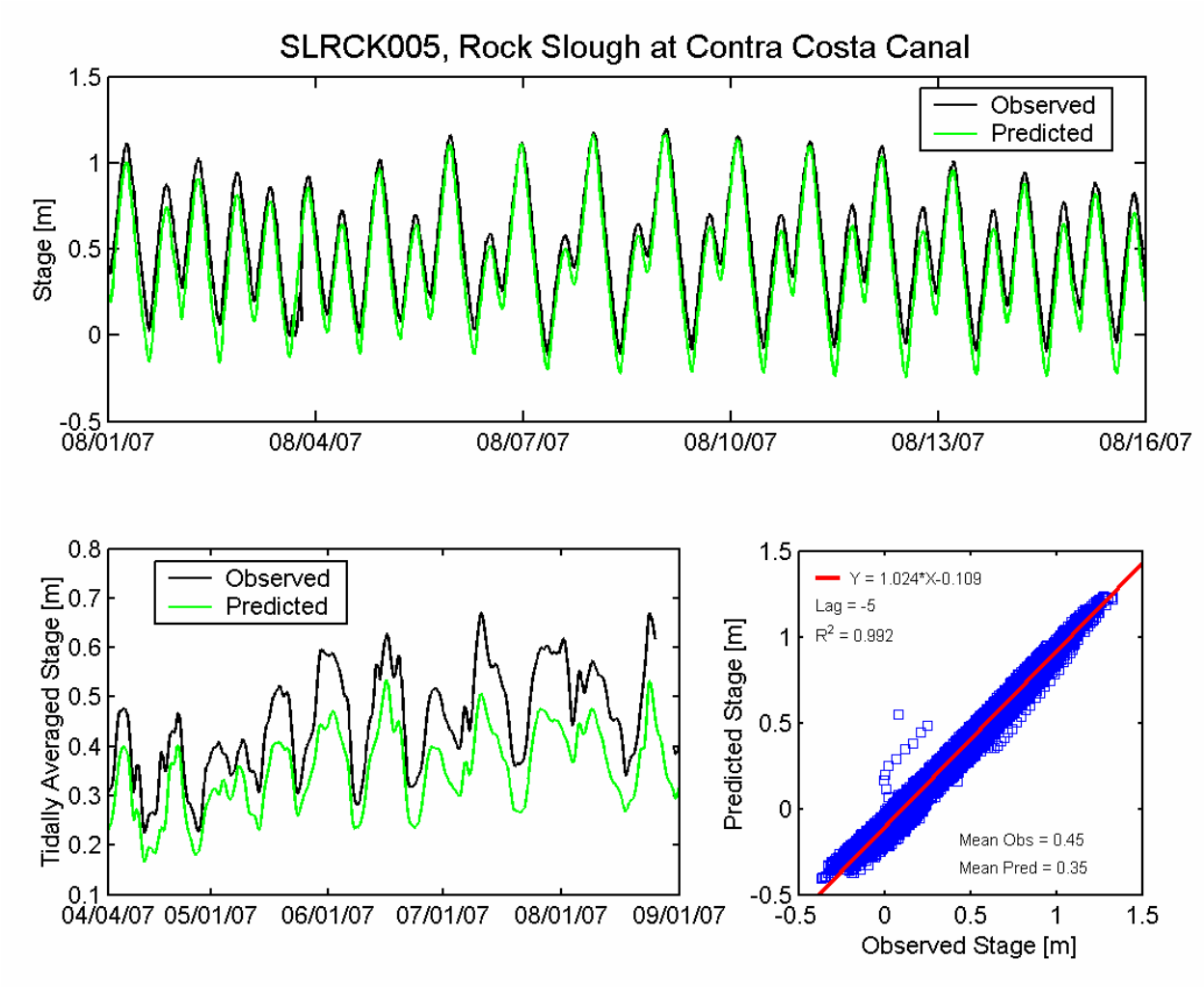

Figure 4.3-29 Observed and predicted stage at Rock Slough at Contra Costa Canal DWR station (SLRCK005) during the 2007 simulation period.

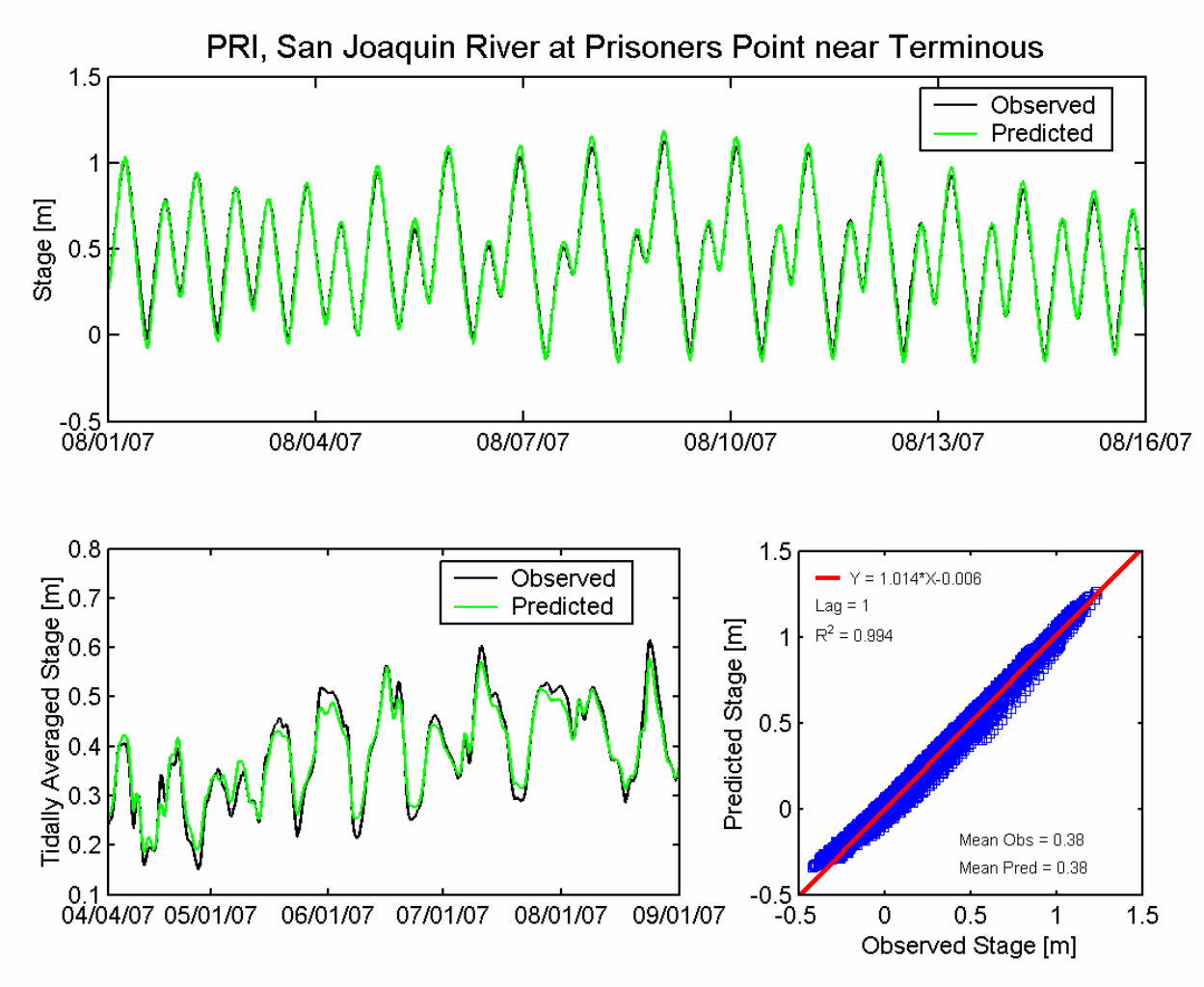

Figure 4.3-30 Observed and predicted stage at San Joaquin River at Prisoners Point USGS station (PRI) during the 2007 simulation period.

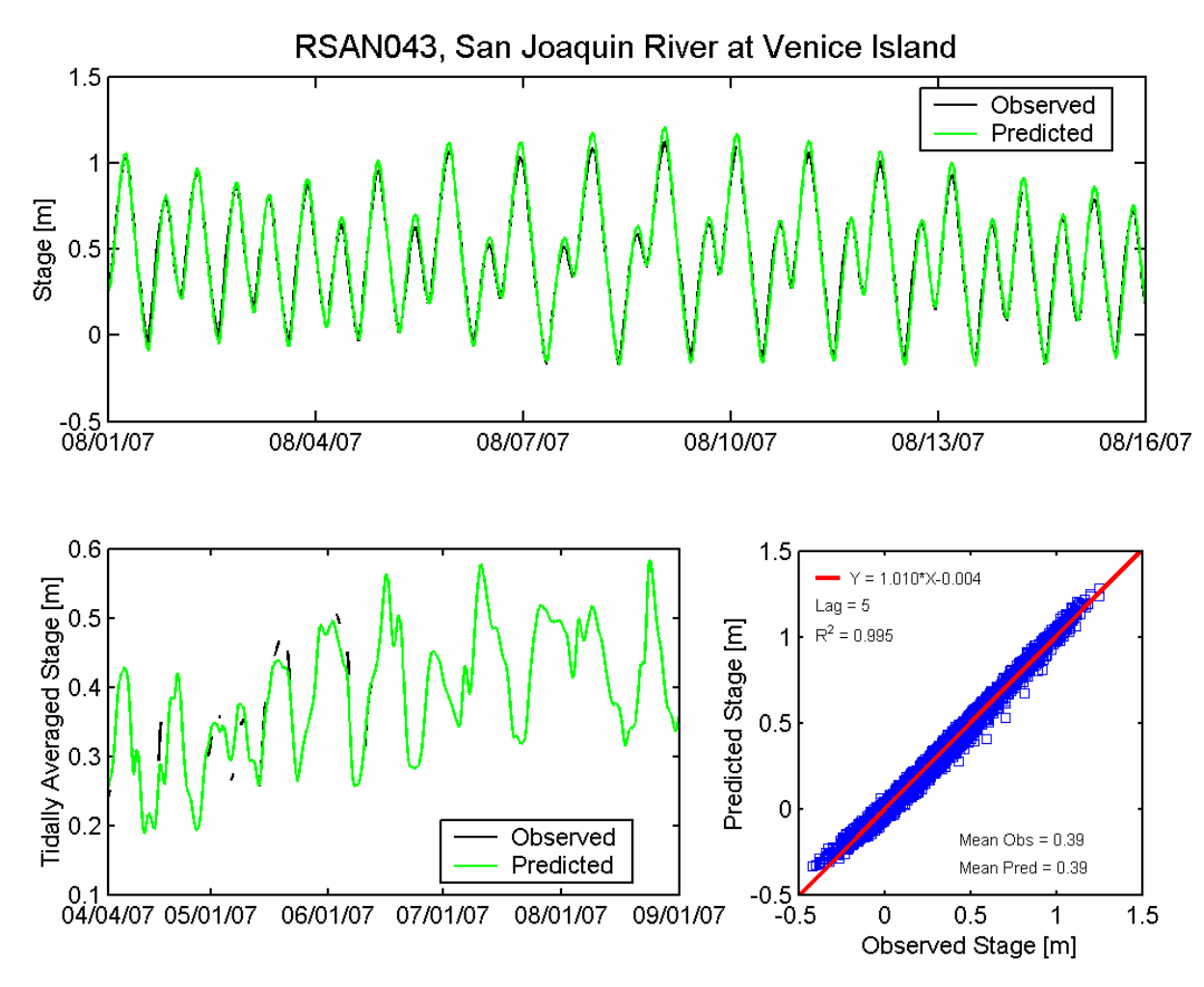

Figure 4.3-31 Observed and predicted stage at San Joaquin River at Venice Island DWR station (RSAN043) during the 2007 simulation period.

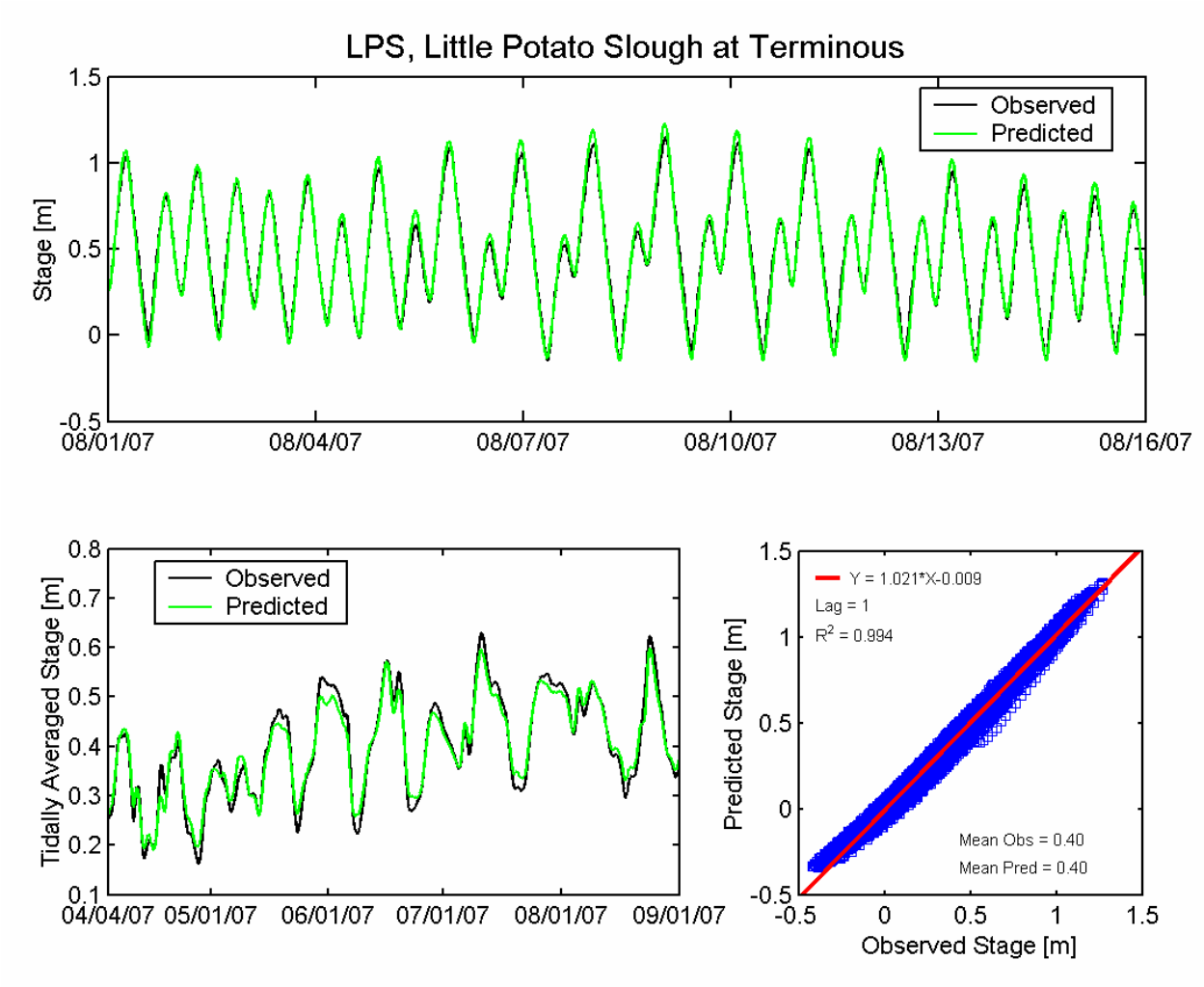

Figure 4.3-32 Observed and predicted stage at Little Potato Slough at Terminous USGS station (LPS) during the 2007 simulation period.

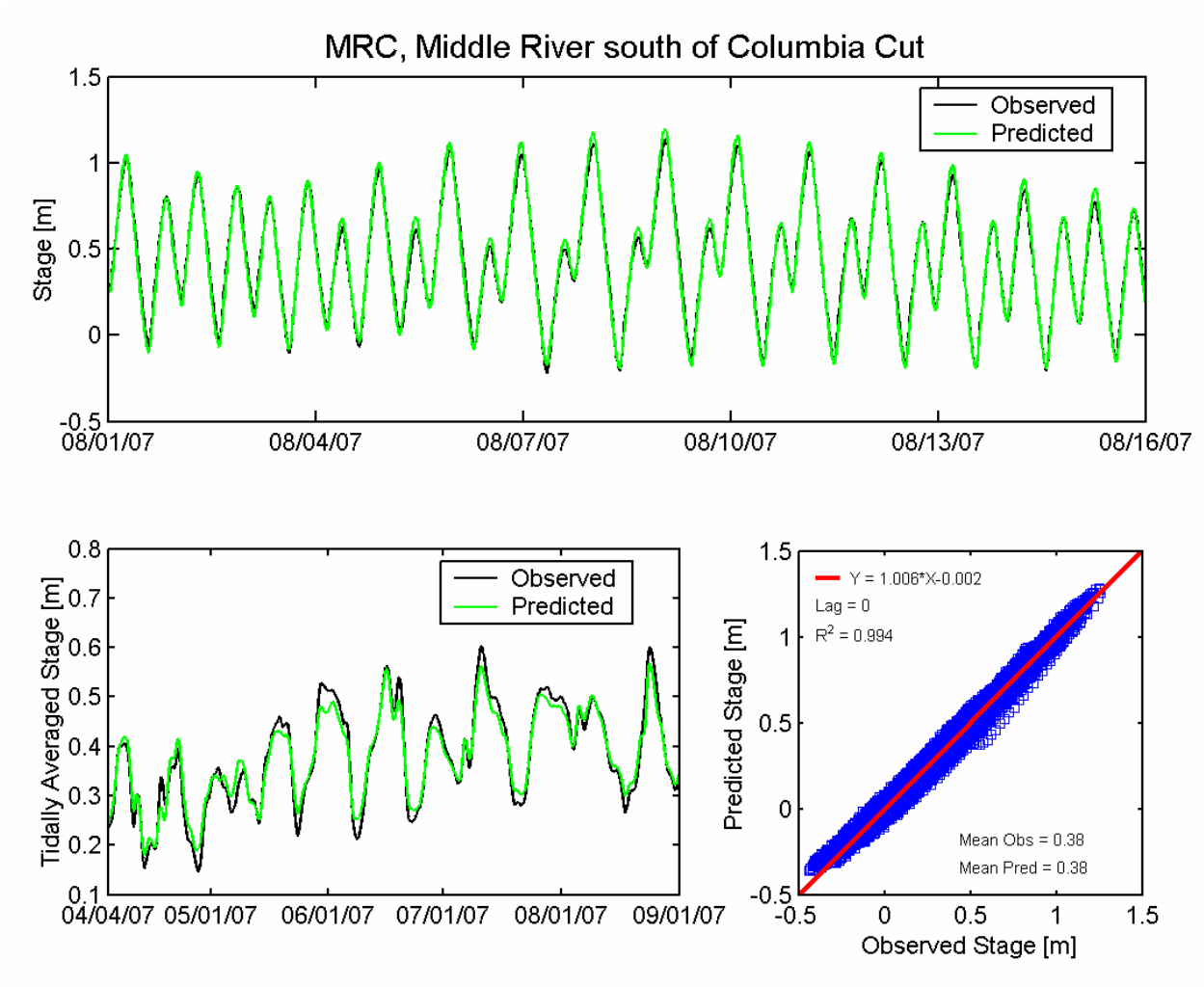

Figure 4.3-33 Observed and predicted stage at Middle River south of Columbia Cut USGS station (MRC) during the 2007 simulation period.

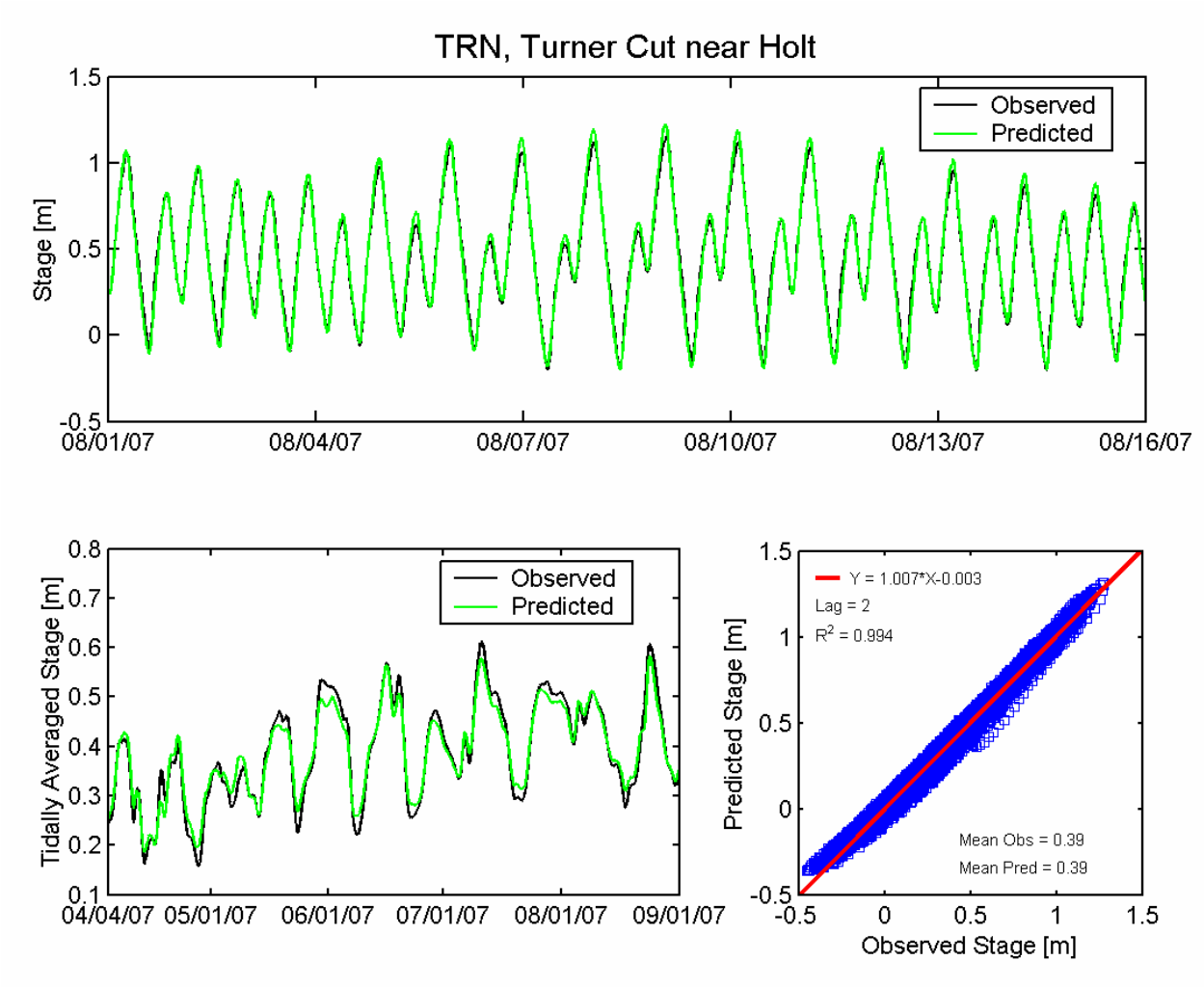

Figure 4.3-34 Observed and predicted stage at Turner Cut near Holt USGS station (TRN) during the 2007 simulation period.

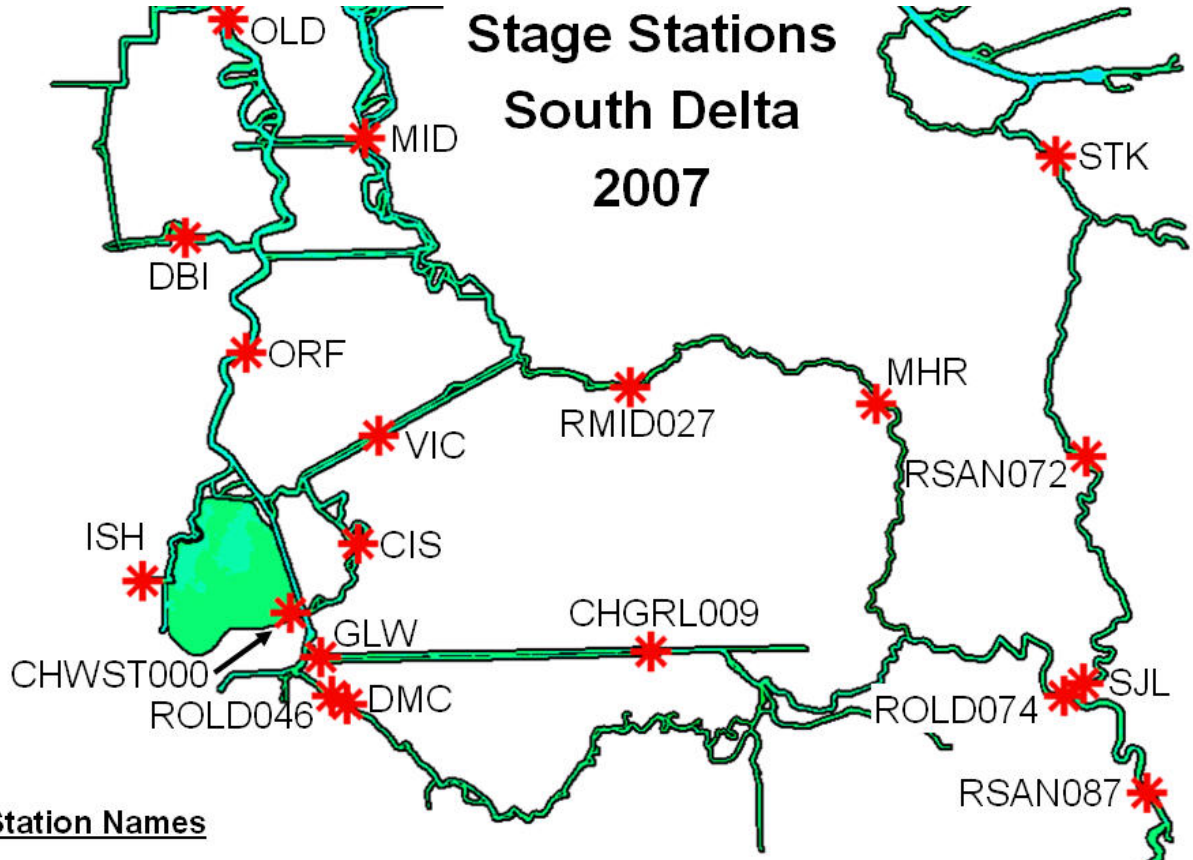

Station Names

MID, Middle River at Middle River

RMID027, Middle River at Tracy Blvd

MHR, Middle River at Howard Road Bridge

OLD, Old River at Bacon Island

DBI, Discovery Bay at Indian Slough

ORF, Old River near Byron

VIC, Victoria Canal near Byron

ISH, Italian Slough Headwater near Byron

CIS, Old River at Coney Island

CHWST000, Clifton Court Forebay

GLW, Grant Line Canal near Clifton Court Ferry

CHGRL009, Grant Line Canal at Tracy Blvd

ROLD046, Old River near Delta Mendota Canal (Downstream of Barrier)

DMC, Old River near Delta Mendota Canal (Upstream of Barrier)

STK, San Joaquin River at Stockton

RSAN072, San Joaquin River at Brandt Bridge

SJL, San Joaquin River below Old River near Lathrop

ROLD074, Old River at Head

RSAN087, San Joaquin River at Mossdale

Figure 4.3-35 Location of water level monitoring stations in the southern portion of the Sacramento-San Joaquin Delta used for 2007 stage calibration.

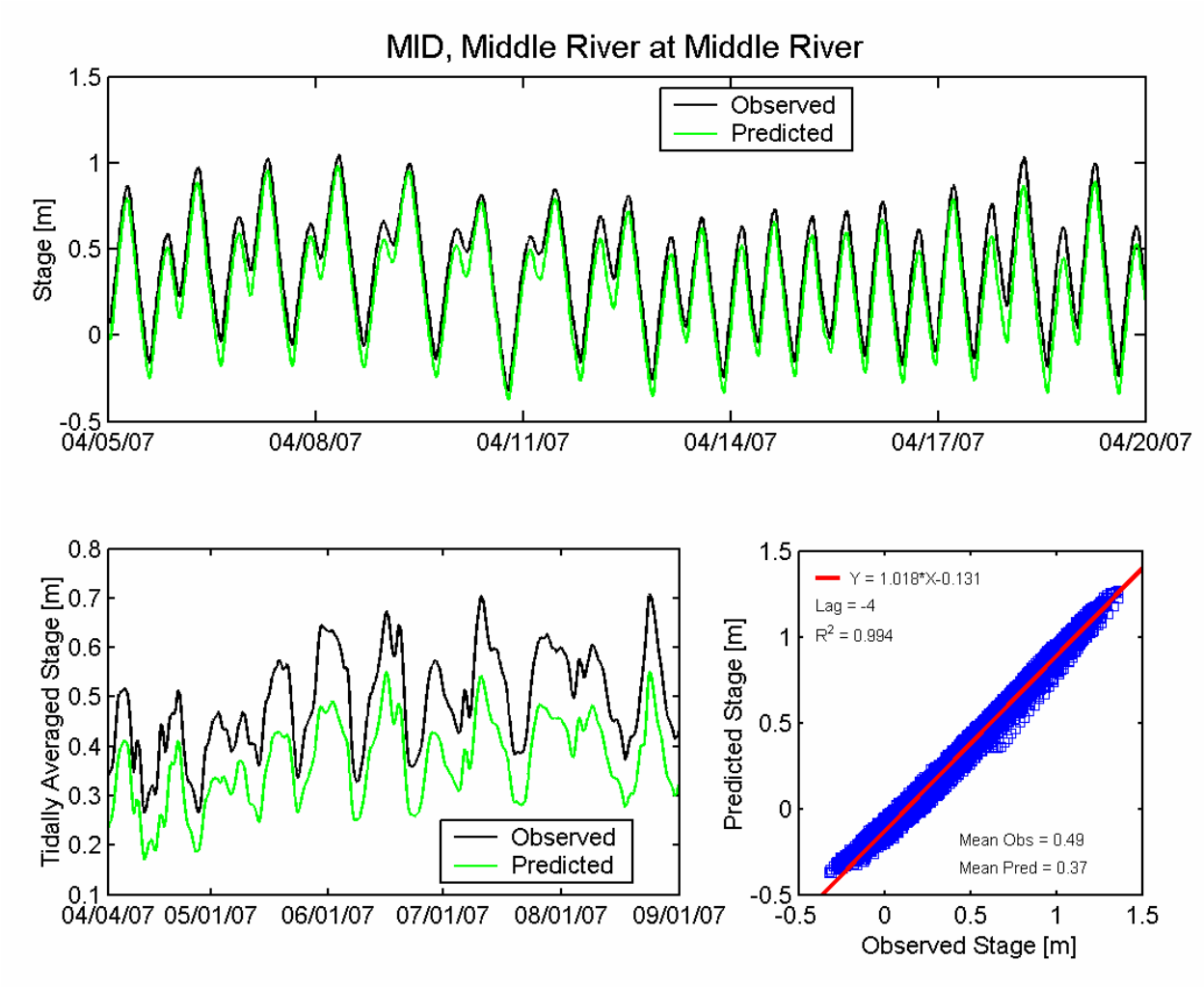

Figure 4.3-36 Observed and predicted stage at Middle River at Middle River USGS station (MID) during the 2007 simulation period.

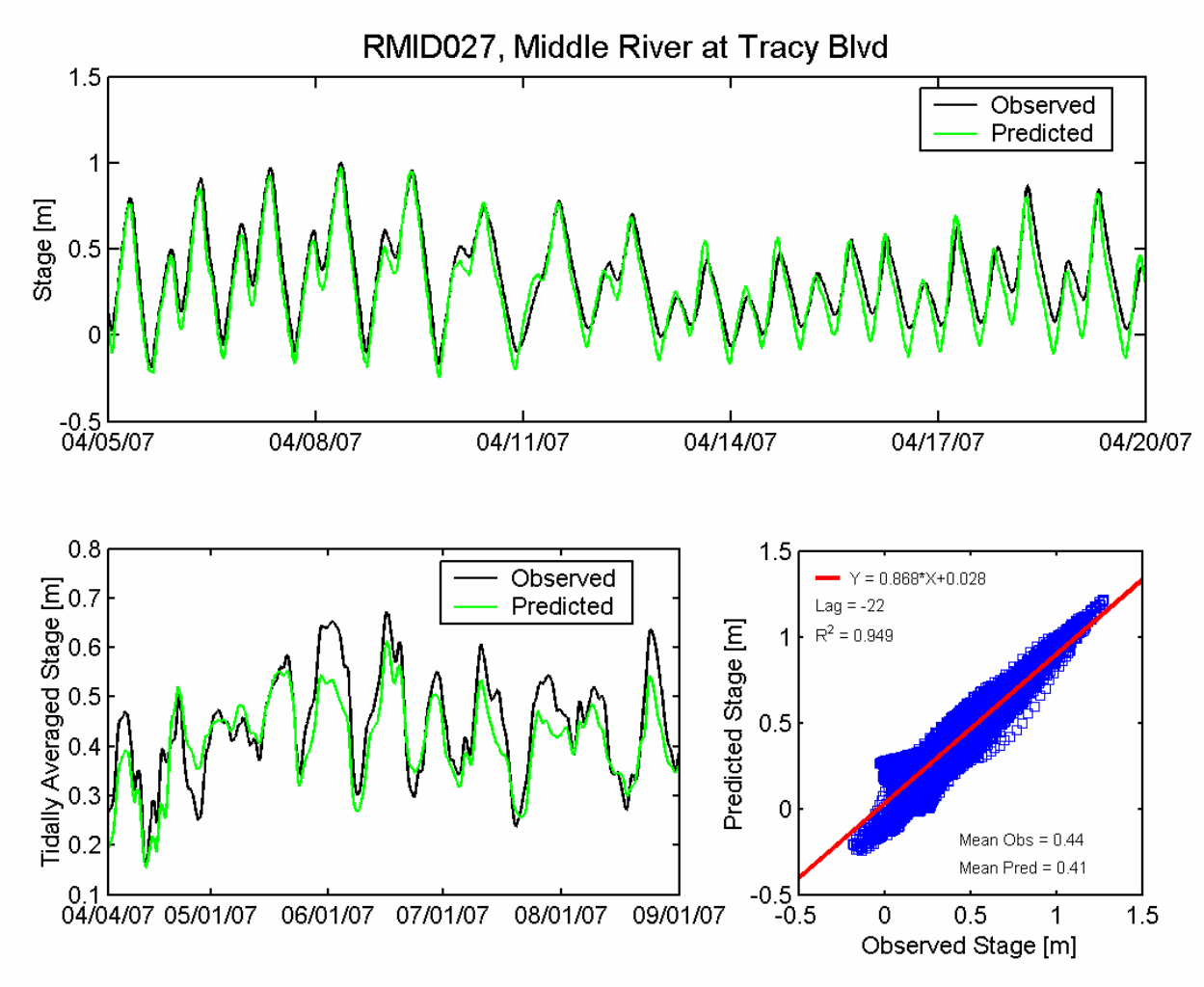

Figure 4.3-37 Observed and predicted stage at Middle River at Tracy Boulevard DWR station (RMID027) during the 2007 simulation period.

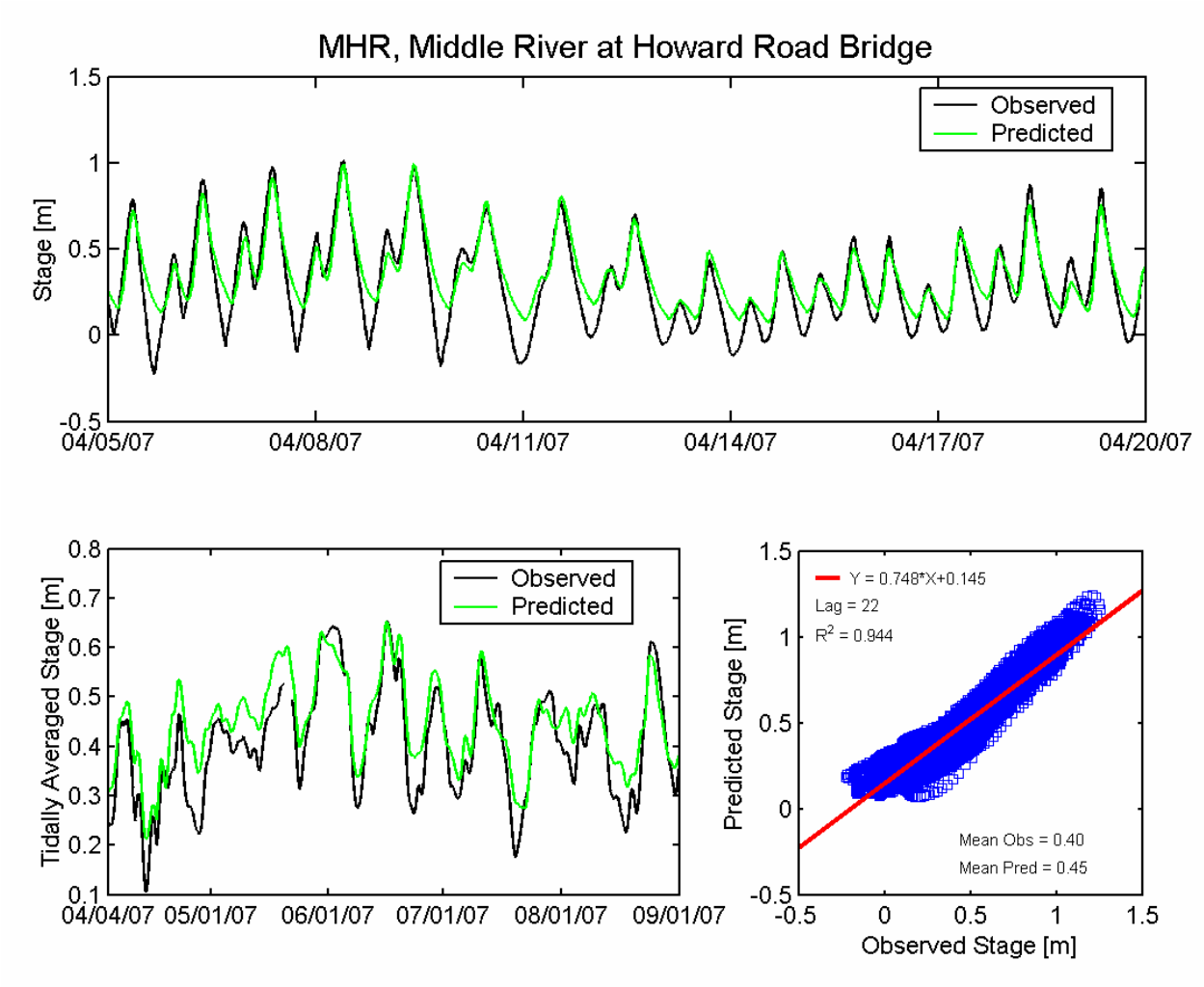

Figure 4.3-38 Observed and predicted stage at Middle River at Howard Road Bridge DWR station (CDEC MHR) during the 2007 simulation period.

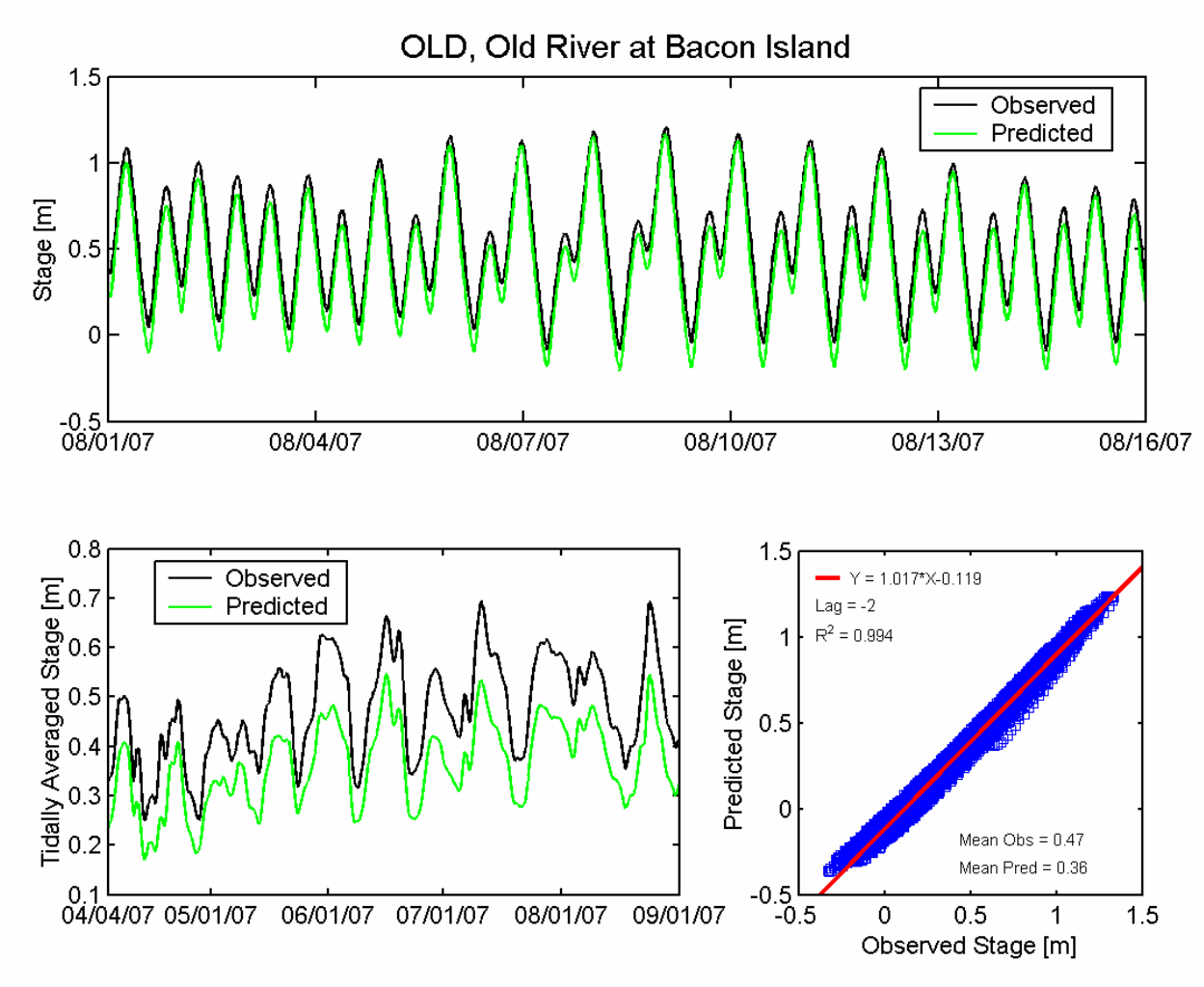

Figure 4.3-39 Observed and predicted stage at Old River at Bacon Island USGS station (OLD) during the 2007 simulation period.

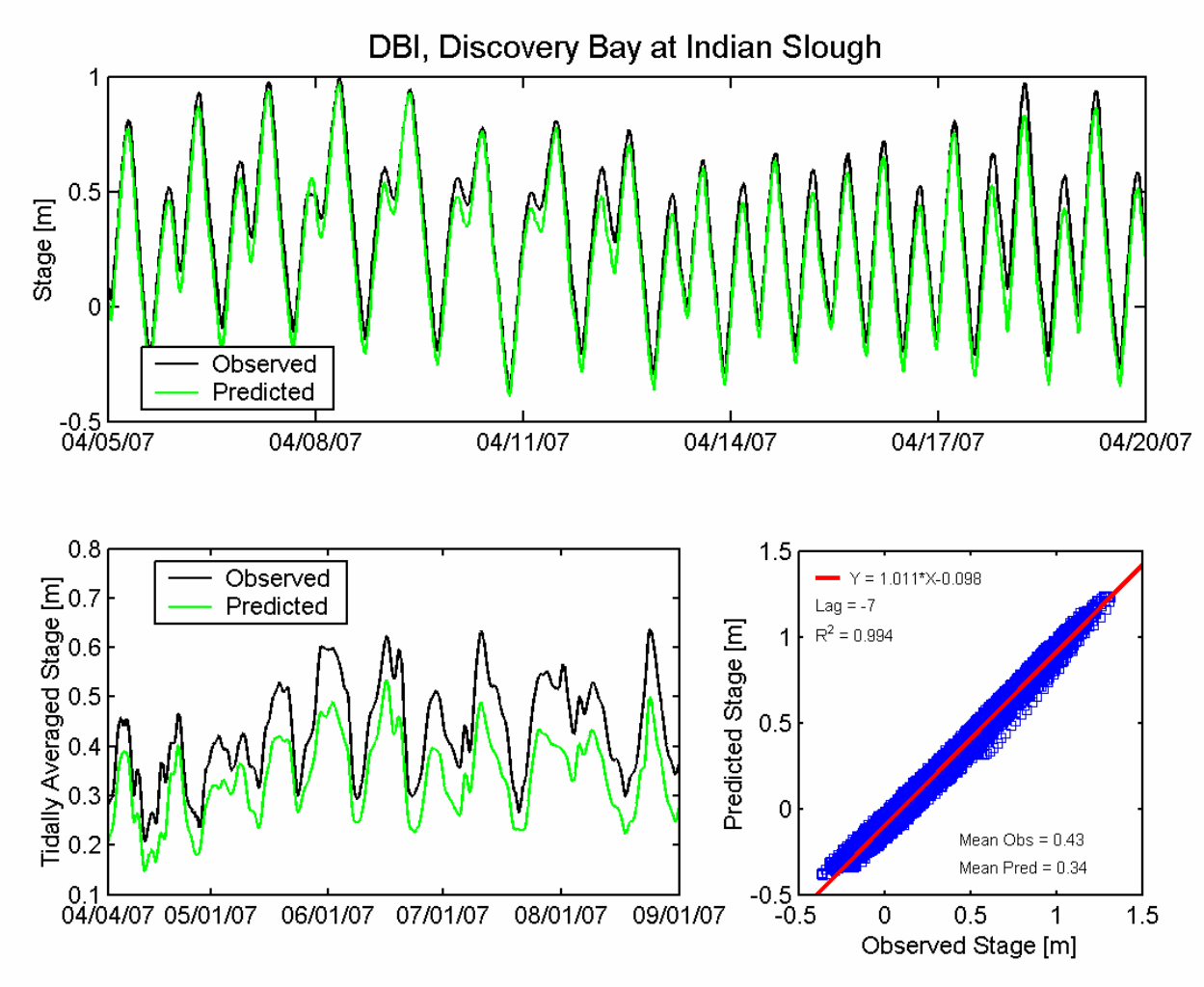

Figure 4.3-40 Observed and predicted stage at Discovery Bay at Indian Slough DWR station (CDEC DBI) during the 2007 simulation period.

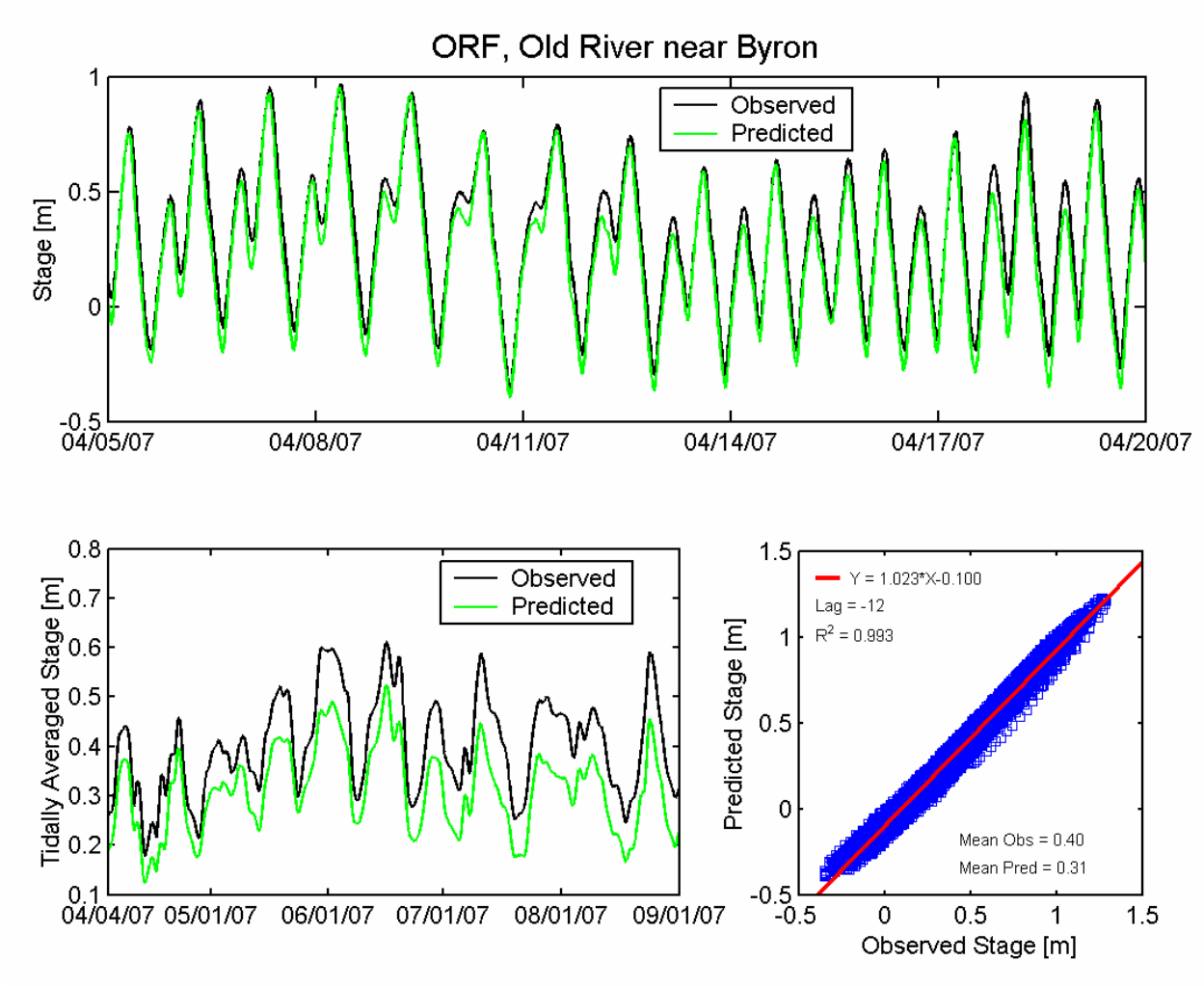

Figure 4.3-41 Observed and predicted stage at Old River near Byron USGS station (ORF) during the 2007 simulation period.

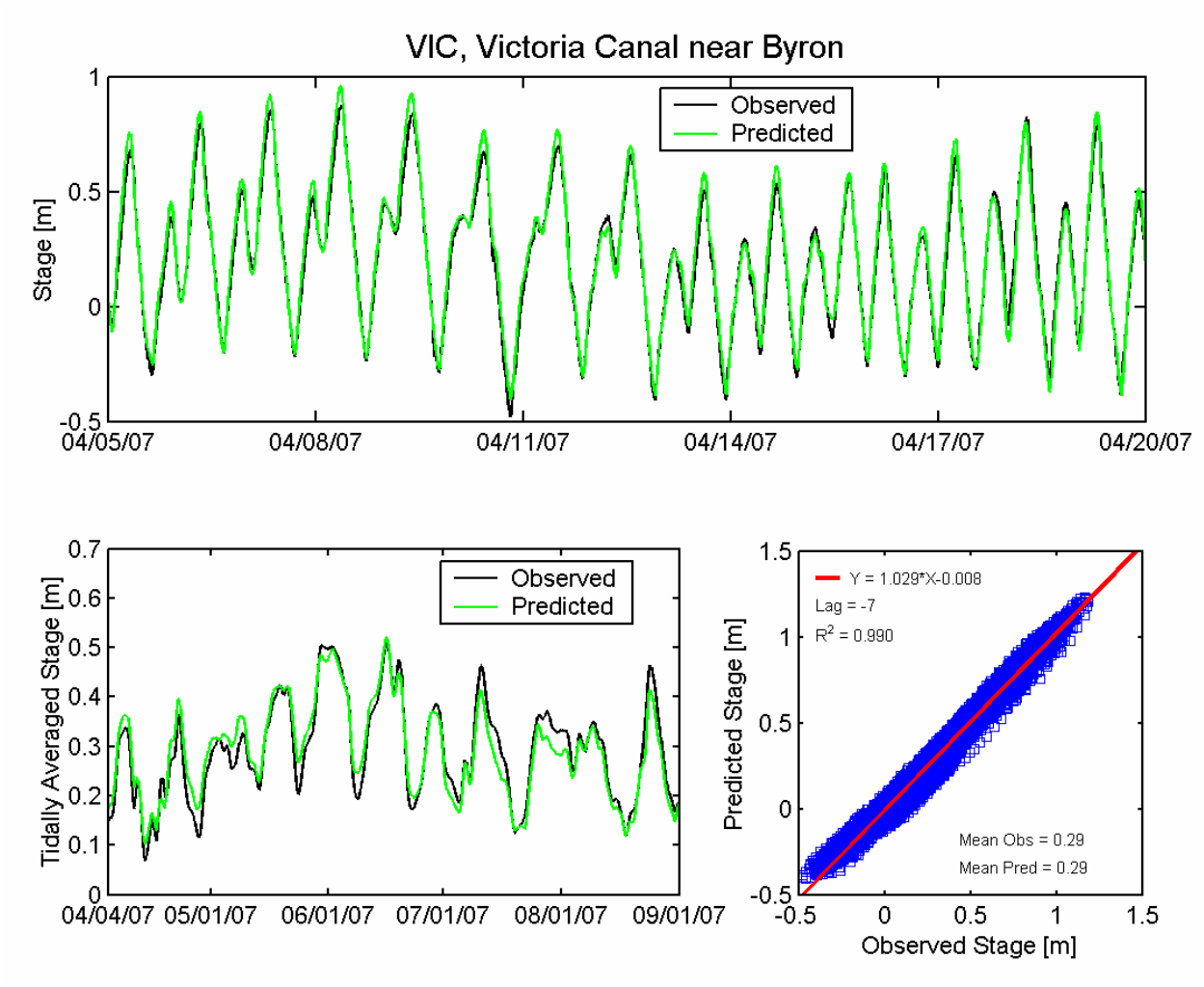

Figure 4.3-42 Observed and predicted stage at Victoria Canal near Byron USGS station (VIC) during the 2007 simulation period.

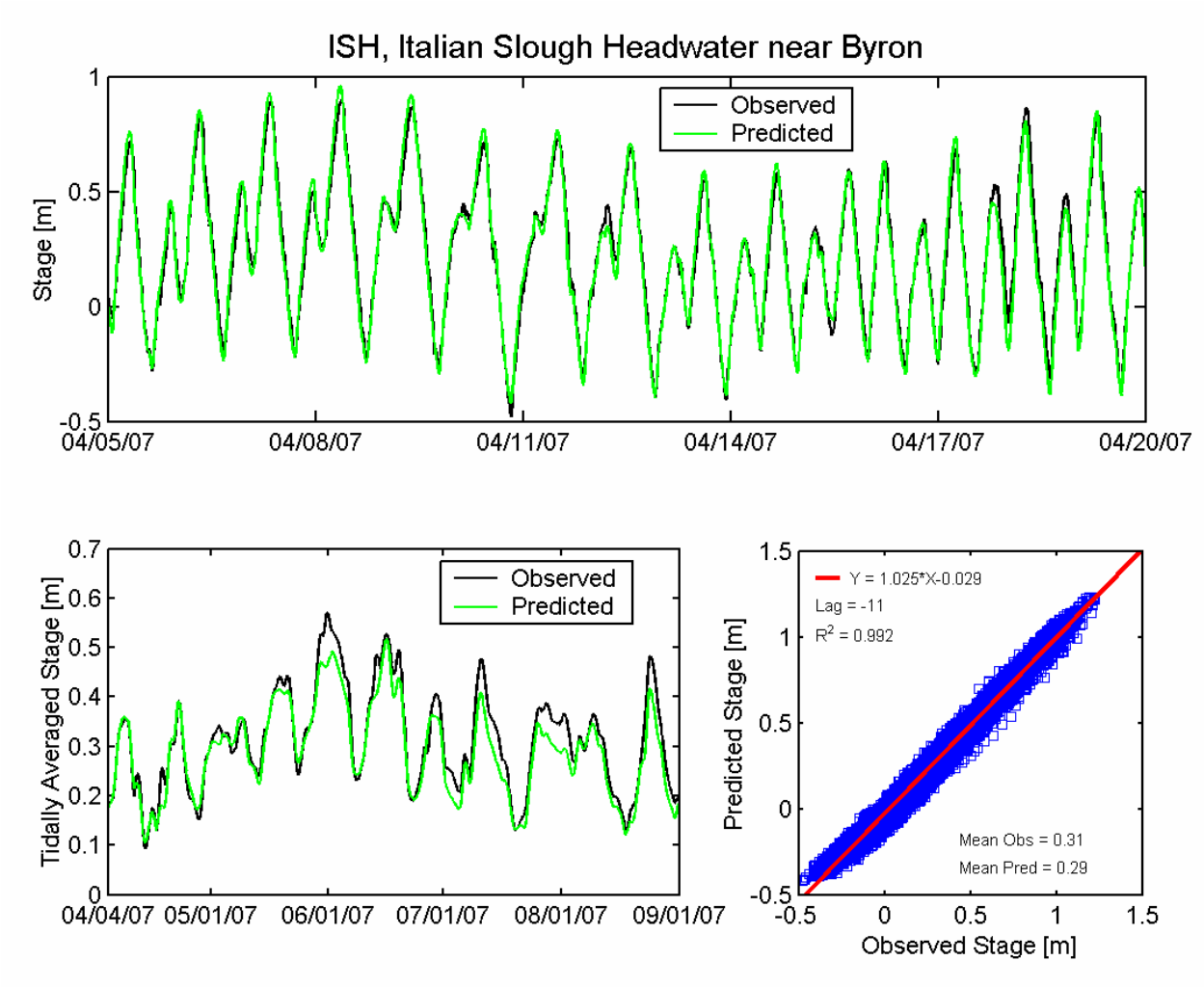

Figure 4.3-43 Observed and predicted stage at Italian Slough Headwater near Byron DWR station (CDEC ISH) during the 2007 simulation period.

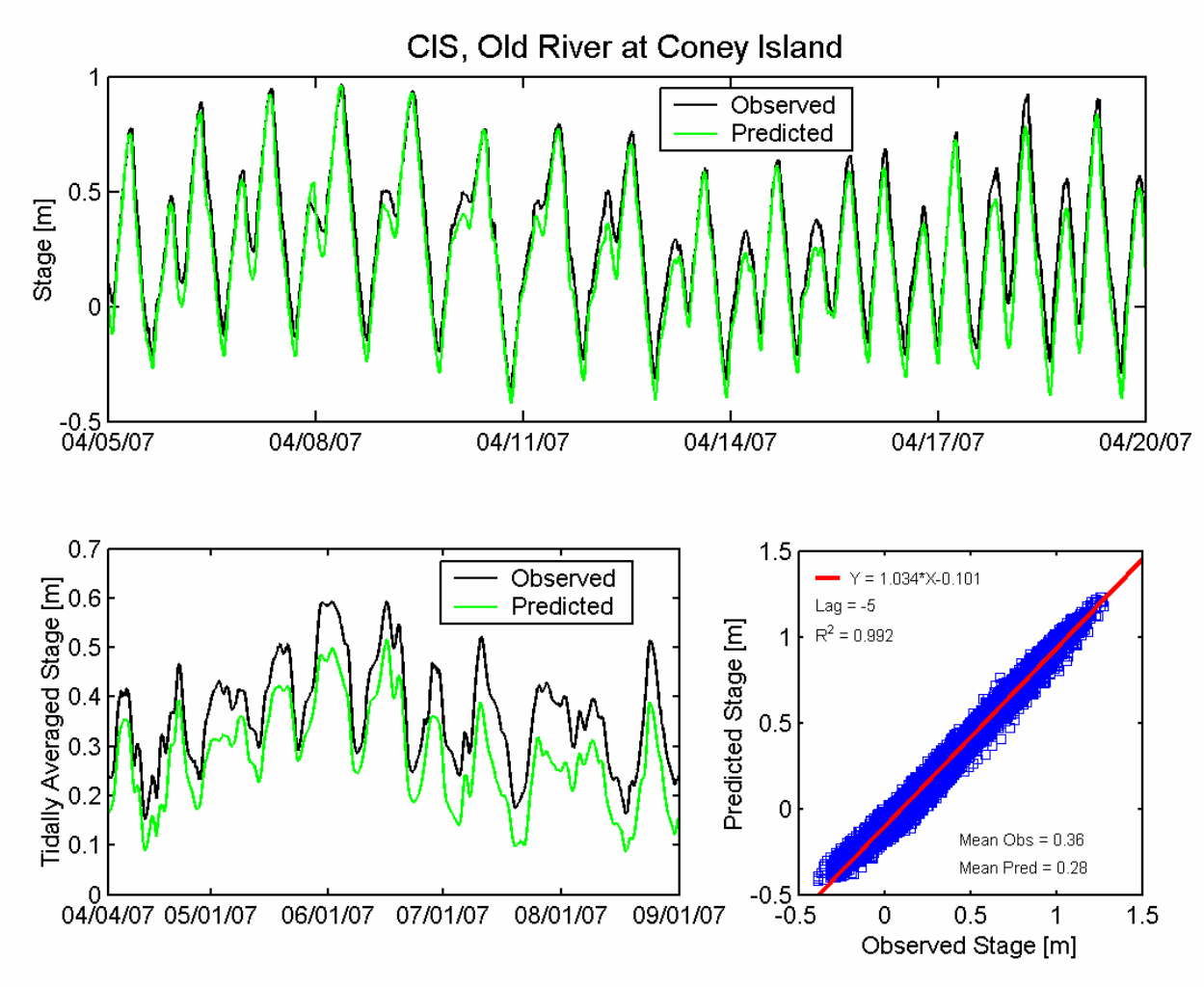

Figure 4.3-44 Observed and predicted stage at Old River at Coney Island DWR station (CDEC CIS) during the 2007 simulation period.

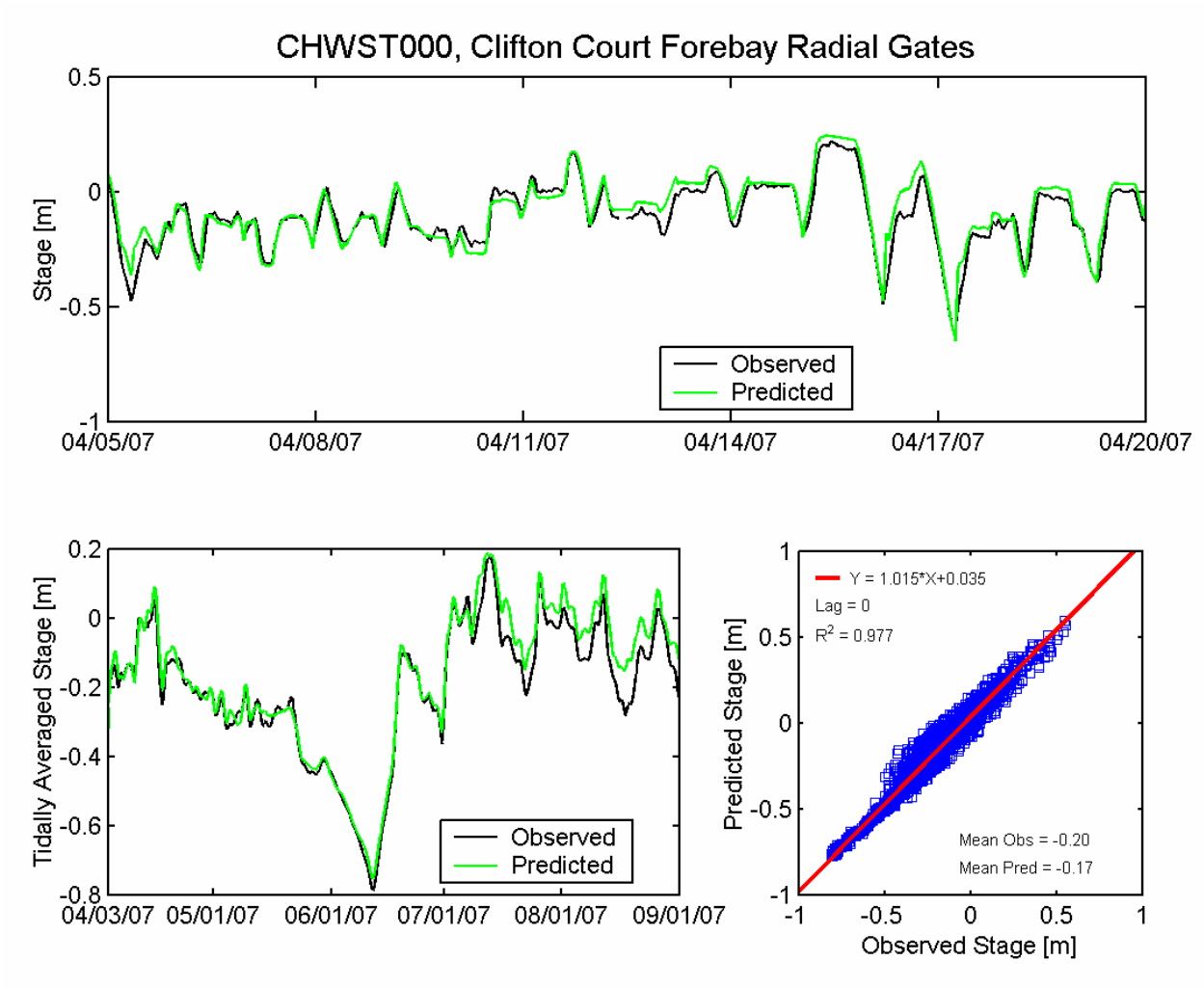

Figure 4.3-45 Observed and predicted stage at Clifton Court Forebay Radial Gates DWR station (CHWST000) during the 2007 simulation period.

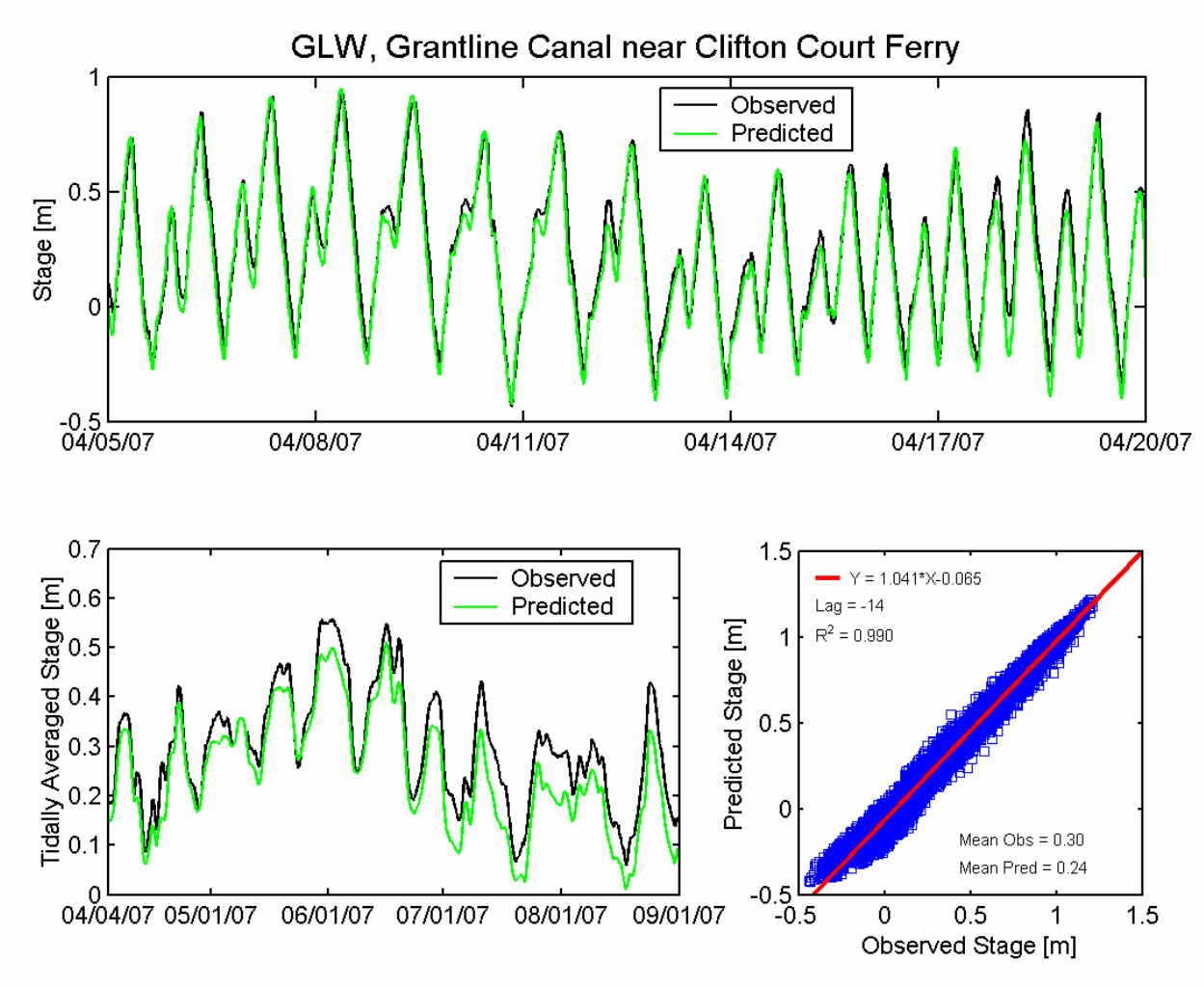

Figure 4.3-46 Observed and predicted stage at Grant Line Canal near Clifton Court Ferry USGS station (GLW) during the 2007 simulation period.

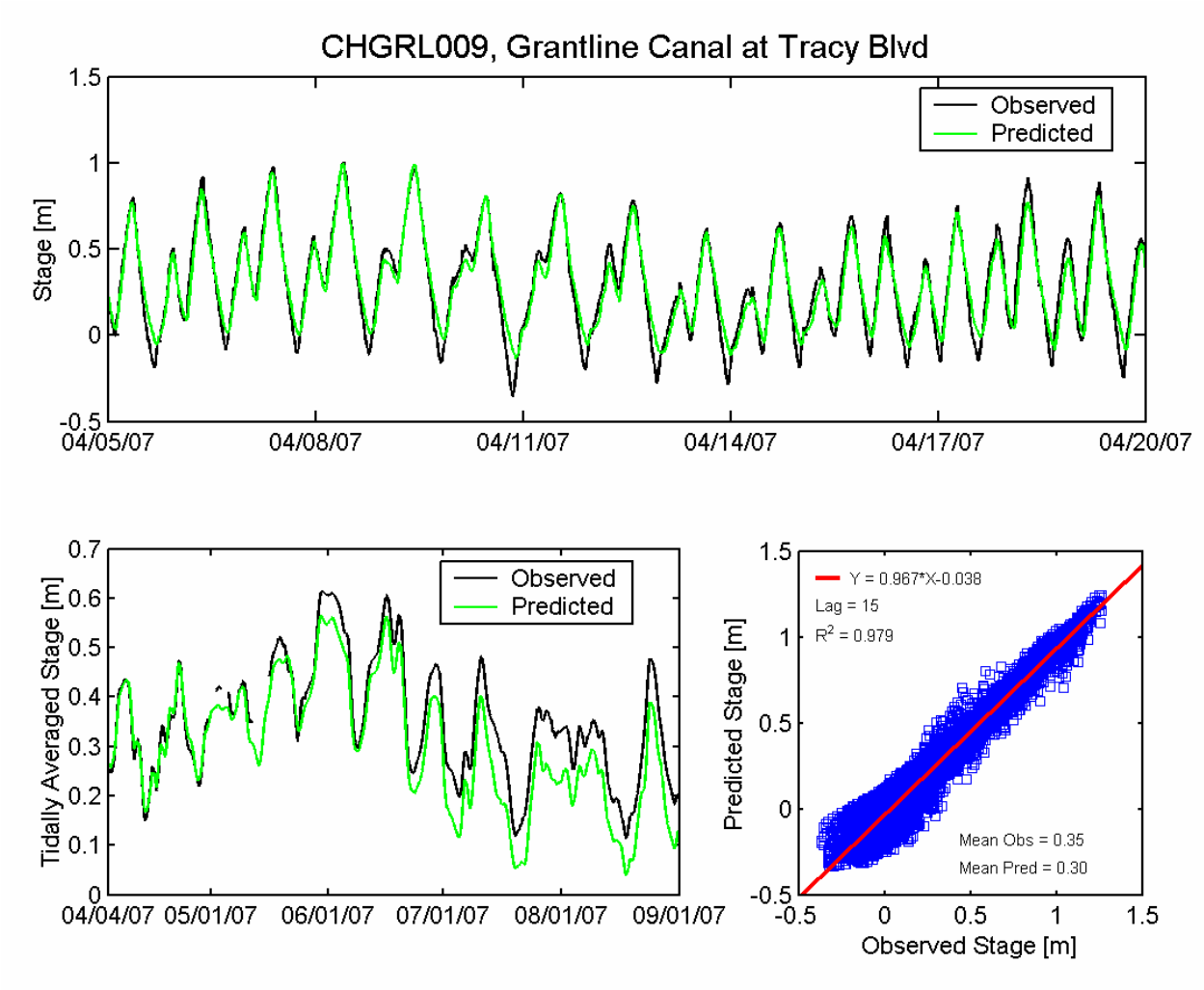

Figure 4.3-47 Observed and predicted stage at Grant Line Canal at Tracy Boulevard DWR station (CHGRL009) during the 2007 simulation period.

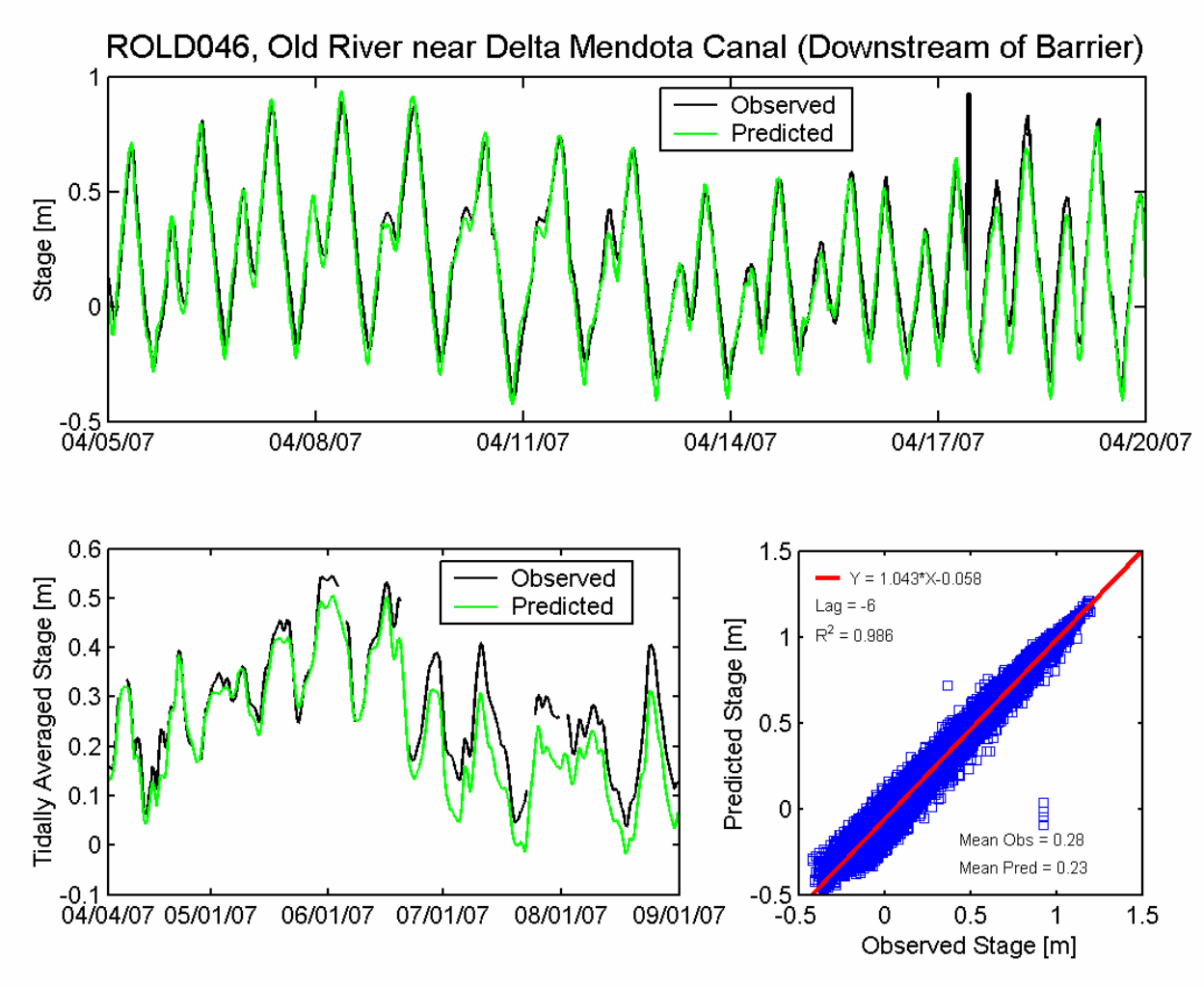

Figure 4.3-48 Observed and predicted stage at Old River near Delta Mendota Canal Downstream of Barrier DWR station (ROLD046) during the 2007 simulation period.

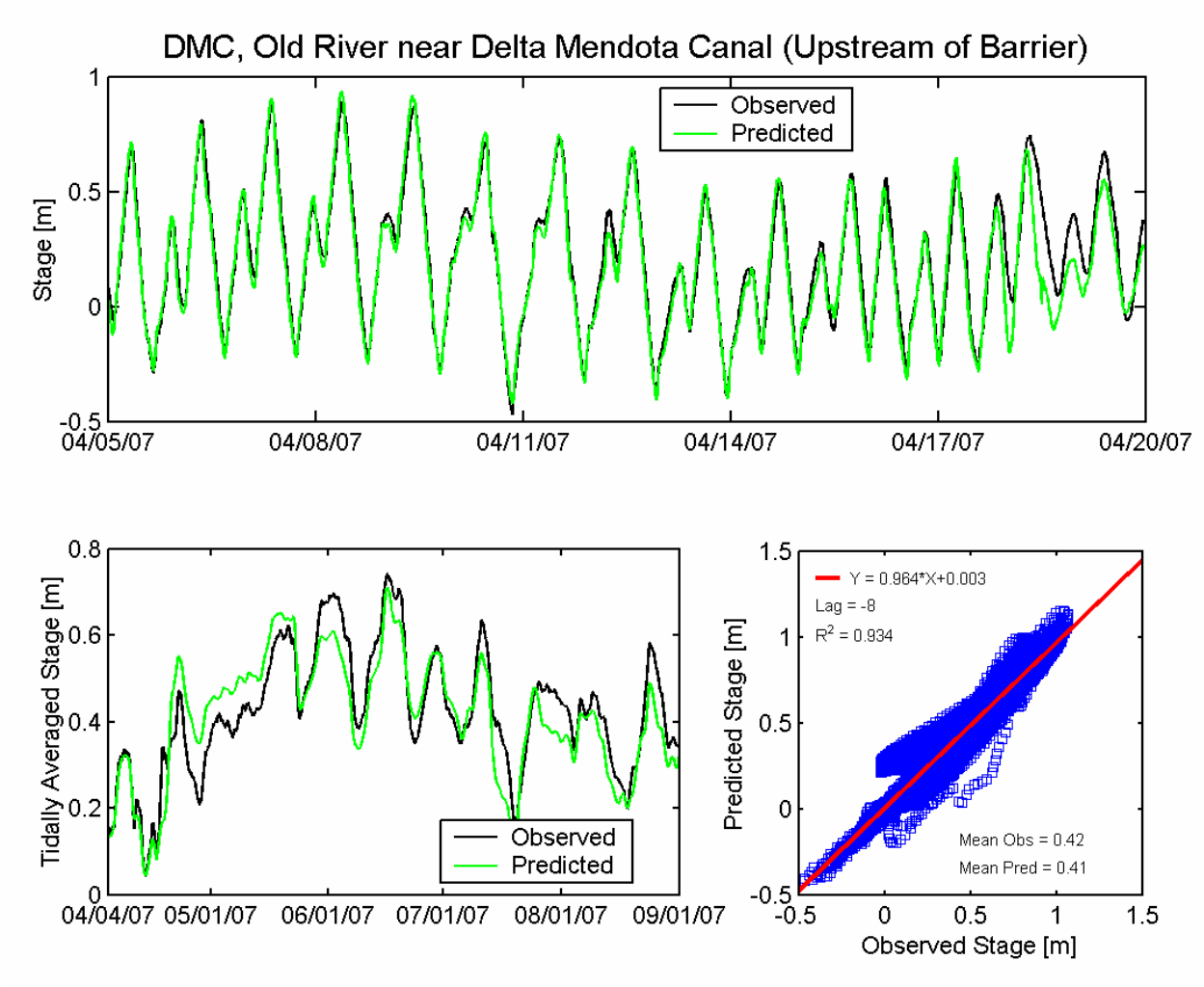

Figure 4.3-49 Observed and predicted stage at Delta Mendota Canal Upstream of Barrier USGS station (DMC) during the 2007 simulation period.

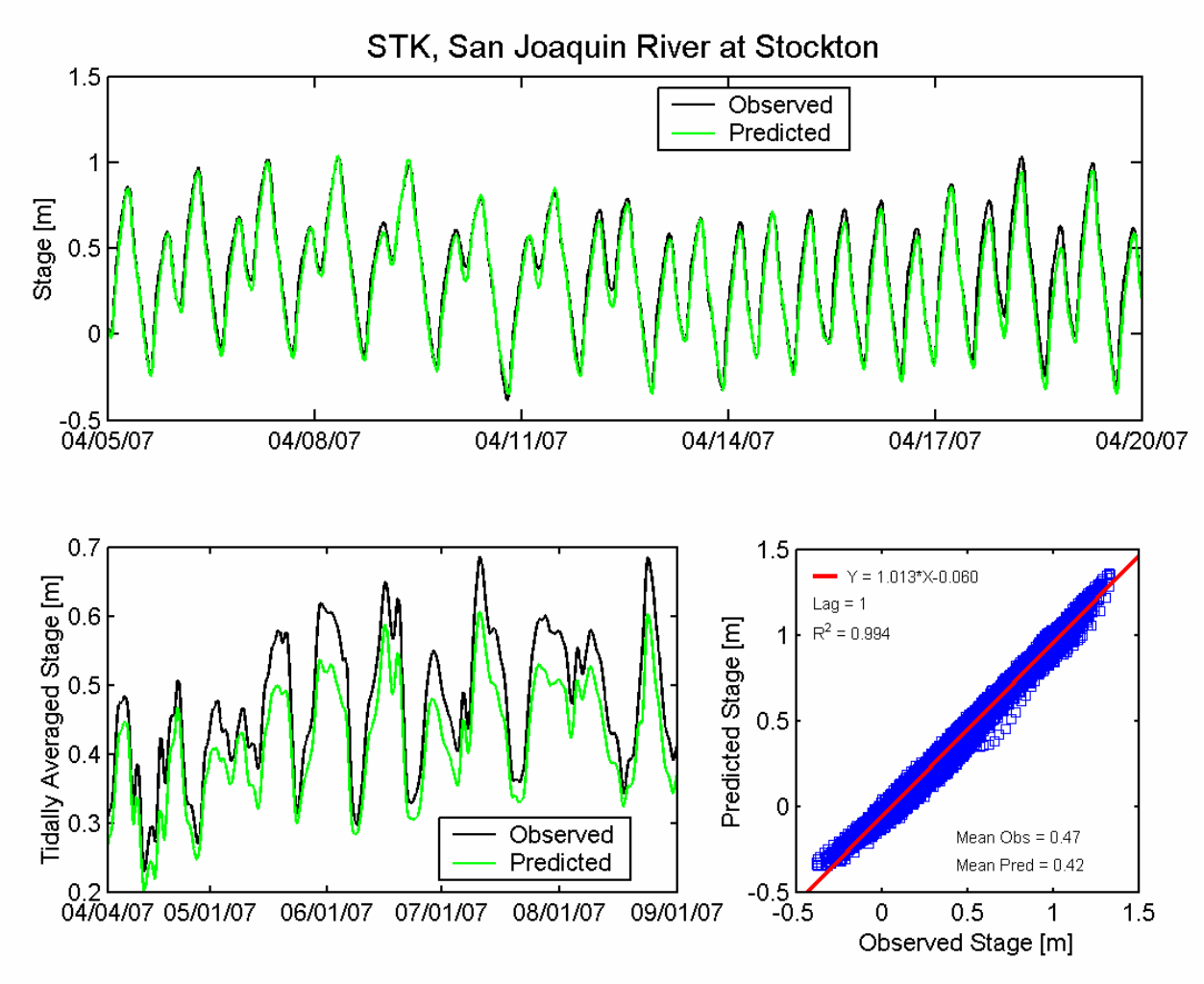

Figure 4.3-50 Observed and predicted stage at San Joaquin River at Stockton USGS station (STK) during the 2007 simulation period.

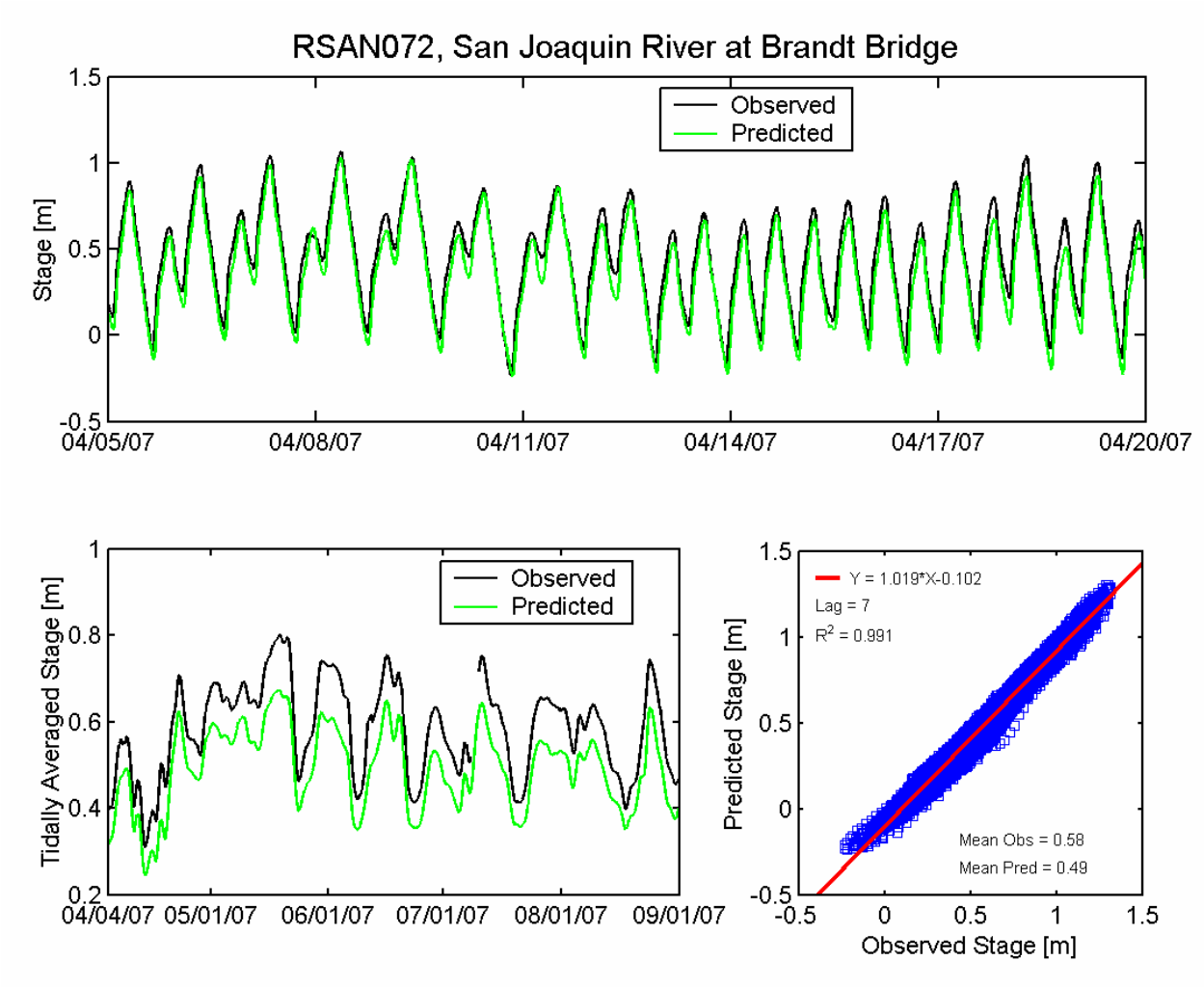

Figure 4.3-51 Observed and predicted stage at San Joaquin River at Brandt Bridge DWR station (RSAN072) during the 2007 simulation period.

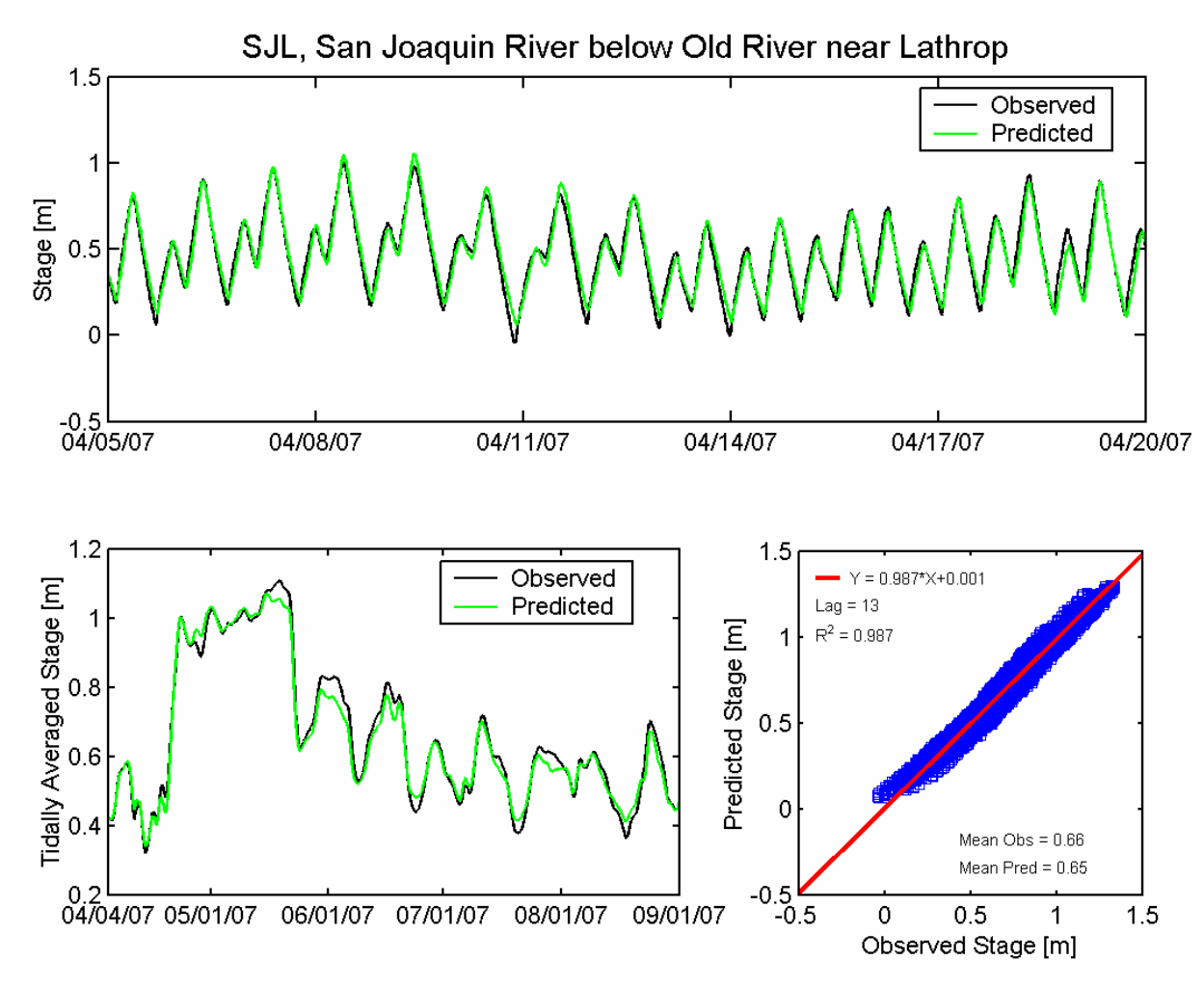

Figure 4.3-52 Observed and predicted stage at San Joaquin River below Old River near Lathrop DWR station (CDEC SJL) during the 2007 simulation period.

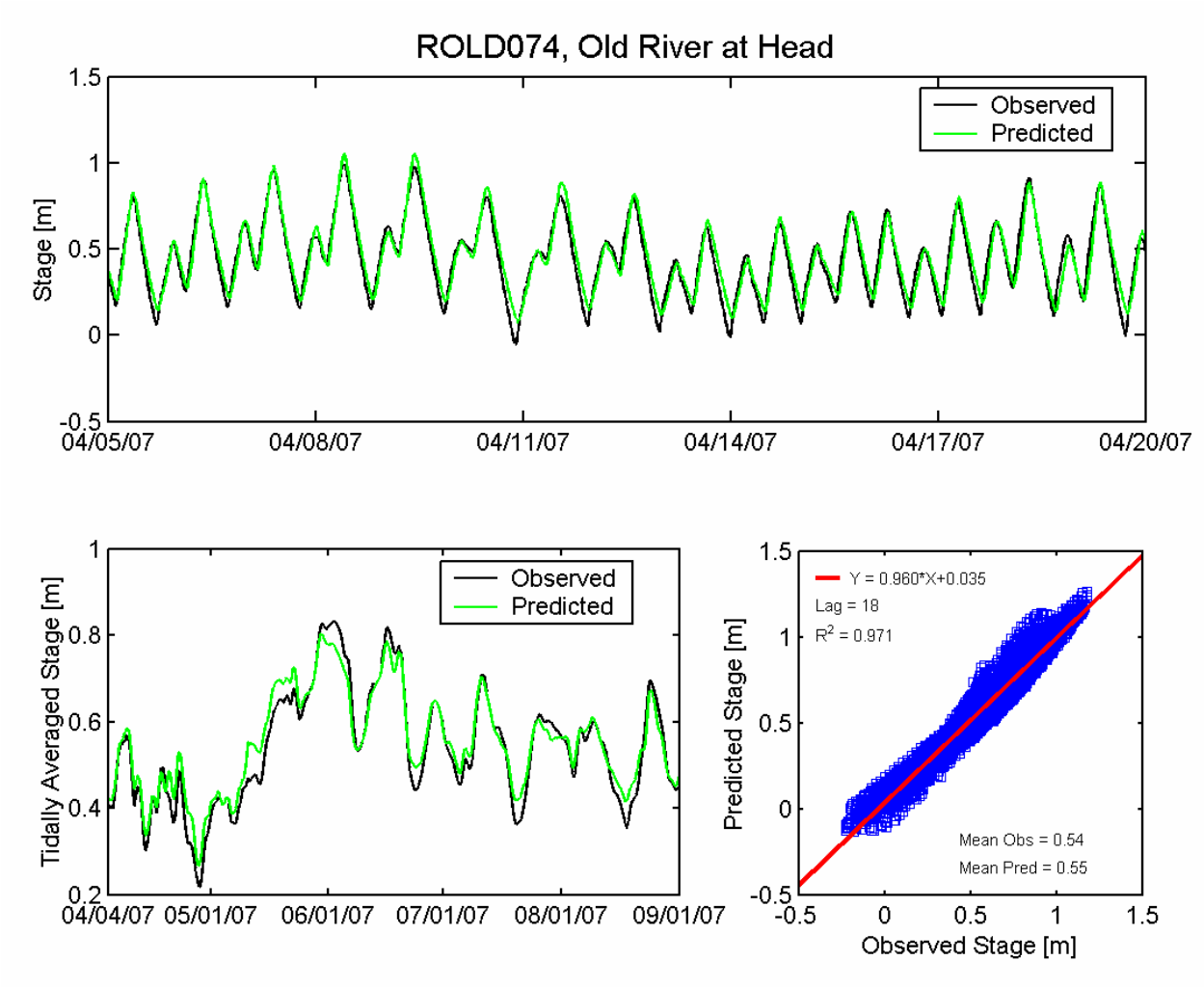

Figure 4.3-53 Observed and predicted stage at Old River at Head DWR station (ROLD074) during the 2007 simulation period.

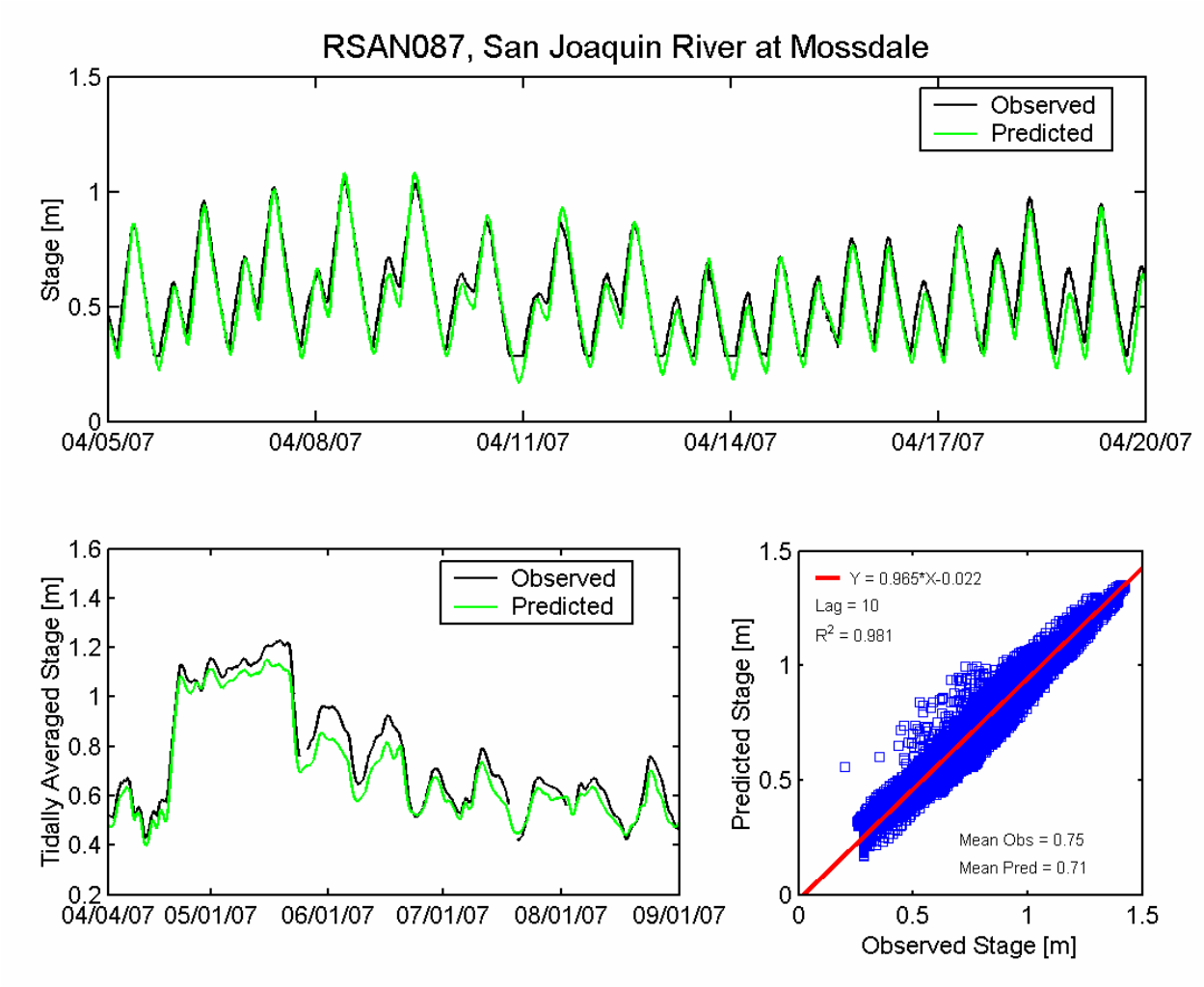

Figure 4.3-54 Observed and predicted stage at San Joaquin River at Mossdale DWR station (RSAN087) during the 2007 simulation period.

4.4 Flow Calibration

During the 2007 calibration period, flow measurements are available at a total of thirty-two flow monitoring stations in the Sacramento-San Joaquin Delta. The majority of the flow data were collected by the USGS, with some flow data available at a few DWR stations in the south Delta.

For each station, the mean observed and predicted net flow was calculated over the full simulation period, and the same cross-correlation procedure used in the water level analysis was applied to flow. Table 4-2 gives the predicted and observed mean flow at each station as well as the corresponding amplitude ratio, phase lag, and R^2 for each station.

4.4.1 Northern Sacramento-San Joaquin Delta

Flow calibration comparisons were performed at nine continuous flow monitoring stations in the northern portion of the Delta, at the locations shown in Figure 4.4-1. Flow comparisons at these stations are shown in Figures 4.4-2 through 4.4-10.

Observed and predicted flows on the Sacramento River south of Georgiana Slough (Figure 4.4-2), agree well, both in terms of tidal flow magnitudes with an amplitude ratio of 1.004, and in terms of tidally-averaged flow. Average observed net flow during the simulation period was 112 m^3/s, compared to 107 m^3/s predicted net flow. These results show that the model is accurately predicting flows in the Sacramento River, downstream of the Delta Cross Channel and Georgiana Slough. Predicted tidal and tidally-averaged flows in Georgina Sough (Figure 4.4-3) agree well with observed flows, with observed and predicted net flows of 79.5 m^3/s and 80.9 m^3/s, respectively. Predicted tidal time-scale flows in Georgina Slough show a similar pattern to observed flows, with noticeably higher flows in Georgina Slough during periods when the Delta Cross Channel is open (see Figure 4.4-4). In the Delta Cross Channel (Figure 4.4-4), observed and predicted flows agree well during periods when the Delta Cross Channel is open and closed (shown in top panel of Figure 4.4-4; operations schedule shown in Figure 4.2-1), and a similar pattern of tidally-averaged flows is evident. During periods when the Delta Cross Channel is open, predicted tidally-averaged flows are slightly less than observed flows, resulting in observed and predicted average net flows during the simulation period of 76 m^3/s and 69 m^3/s, respectively. In the Sacramento River upstream of the Delta Cross Channel (Figure 4.4-5), observed and predicted flows agree well, both in terms of tidal flow magnitudes with an amplitude ratio of 0.994, and in terms of tidally-averaged flow. Average observed and predicted net flows during the simulation period were identical, at 257 m^3/s. Further upstream on the Sacramento River at Freeport (Figure 4.4-6), predicted tidal flows are somewhat larger than observed tidal flows, with an amplitude ratio of 1.119, but observed and predicted tidally-averaged flows are nearly identical. Observed and predicted average net flows during the simulation period are 405 m^3/s and 400 m^3/s, respectively.

On Cache Slough at Ryer Island (Figure 4.4-7), predicted tidal flows agree well with observed tidal flows, with an amplitude ratio of 0.962 indicating a slightly smaller (~4%) predicted tidal prism in Cache Slough than observed. Predicted tidally-averaged flows are slightly higher than observed, resulting in observed and predicted average net flows during the simulation period of

25 m^3/s and 58.7 m^3/s, respectively. This result suggests that the net of the inflow of Yolo Bypass and the export of the North Bay Aqueduct (NBA) applied to the model from DAYFLOW are not accurately representing the observed net flows through Cache Slough and result in a higher predicted than observed net outflow from Cache Slough. At Miner Slough at the Highway 84 Bridge (Figure 4.4-8), Steamboat Slough between the Sacramento River and Sutter Slough (Figure 4.4-9), and at Sutter Slough at Courtland (Figure 4.4-10), predicted tidal prism is somewhat higher than observed, with amplitude ratios between 1.355 and 1.588. This result is consistent with the higher predicted than observed range in tidal elevation at these stations (see Figures 4.3-14 through 4.3-16). However, predicted tidally-averaged and average net flows show better agreement with observed tidally-averaged and observed net flows at these three stations.

4.4.2 Central Sacramento-San Joaquin Delta

Flow calibration comparisons were performed at thirteen continuous flow monitoring stations in the central portion of the Delta, at the locations shown in Figure 4.4-11. Flow comparisons at these stations are shown in Figures 4.4-12 through 4.4-24.

At Rio Vista on the Sacramento River (Figure 4.4-12), the observed and predicted flows show good agreement, with typical peak tidal flows of 3000 m^3/s. The cross-correlation analysis yields an amplitude ratio of 1.007, indicating that the model is accurately predicting the flow amplitude, and a phase lead of 12 minutes. Overall the model shows similar tidally-averaged flows over the analysis period, and the observed and predicted mean flows are 262 m^3/s and 257 m^3/s, respectively, indicating nearly identical observed and predicted net flows at Rio Vista. At Threemile Slough North at the San Joaquin River (Figure 4.4-13), observed and predicted peak flows are typically 700 to 1000 m^3/s, with the model predicting slightly larger negative (south) net flows. The predicted and observed flows have similar amplitude, with an amplitude ratio of 0.997 and a phase lag of 6 minutes. Observed and predicted net flows south through Threemile Slough during the simulation period are 46.1 m^3/s and 50.9 m^3/s, respectively, indicating slightly larger observed than predicted average net flow. At Jersey Point (Figure 4.4-14), peak flows are typically 4000 m^3/s; predicted flows show a slightly smaller amplitude than observed flows, with an amplitude ratio of 0.907, and a phase lead of 8 minutes. The predicted tidally-averaged flows show good agreement with observed tidally-averaged flows, with a somewhat larger predicted mean observed net flow than mean predicted net flow.

Observed and predicted flows at False River (Figure 4.4-15) show good agreement, with typical peak flows of 1200 m^3/s. Predicted flows have slightly smaller amplitude than observed flows, with an amplitude ratio of 0.890, and a phase lead of 2 minutes. The predicted tidally-averaged flow shows very good agreement with observed tidally-averaged flow, with slightly less negative (east) predicted than observed net flows, of -14.8 m^3/s and -36.7 m^3/s, respectively. At Dutch Slough (Figure 4.4-16), with typical peak tidal flows of 250 m^3/s, predicted tidal flows agree well with observed tidal flows during ebb, but predicted flows are somewhat smaller than observed flows during flood tide. This results in a net observed flow of 13.8 m^3/s (west) and a net predicted flow of -10.6 m^3/s (east) during the simulation period.

At Old River between Franks Tract and the San Joaquin River (Figure 4.4-17), the predicted and observed flows show better agreement with typical peak flows of 400 m^3/s. The predicted tidally-averaged and net flows into Franks Tract through Old River are slightly more negative than observed, resulting in observed and predicted average net flows south during the simulation period of 8.8 m^3/s and 30.9 m^3/s, respectively. At the Mokelumne River near the San Joaquin River (Figure 4.4-18), the predicted and observed flows show relatively good agreement with peak flows typically around 500 m^3/s during ebb and 250 m^3/s during flood tide, and an amplitude ratio of 1.072. Average observed net flow during the simulation period was 86.5 m^3/s, compared to 104 m^3/s predicted net flow, indicating slightly higher predicted net flow through the Mokelumne River than observed.

South of Franks Tract, on Old River at Quimby Island near Bethel Island (Figure 4.4-19) and at Holland Cut (Figure 4.4-20), predicted tidal flows are less than observed tidal flows, indicating a smaller predicted than observed tidal prism south of Franks Tract. It is believed that this occurs because some tidal areas south of Franks Tract, such as little Mandeville Island, which is currently flooded, and some additional in-channel islands which flood near high water, are not included in the available bathymetric data, and are therefore not included in the current model. It is believed that including some of these additional areas will improve the prediction of tidal prism at these stations (see discussion in Section 6.2). Predicted net flows at Old River near Quimby Island are slightly less negative (south) than observed, while they are slightly more negative (south) than observed at Holland Cut.

On the San Joaquin River at Prisoners Point (Figure 4.4-21), predicted tidal flows are less than observed tidal flows, indicating a smaller predicted than observed tidal prism upstream of Prisoners Point on the San Joaquin River. It is believed this may be the result of some in-channel islands which are not included the bathymetry data, but which are believed to flood near high water based on aerial photographs (see discussion in Section 6.2). Observed and predicted average net flows south at Prisoners Point during the simulation period are 80.1 m^3/s and 51.1 m^3/s, respectively. On Little Potato Slough at Terminous (Figure 4.4-22), the observed and predicted flows show relatively good agreement during flood tide with peak flows typically around 50 m^3/s, but the model predicted lower than observed peak flows during ebb tide. Observed and predicted average net flows south at Little Potato Slough during the simulation period are 56.4 m^3/s and 43.2 m^3/s, respectively.

On Middle River south of Columbia Cut (Figure 4.4-23), the observed and predicted flows show good agreement, with typical peak tidal flows of 500 m^3/s. Overall the model shows similar tidally-averaged net flows over the analysis period, and the observed and predicted mean net flows south are 74.3 m^3/s and 69.3 m^3/s, respectively. On Turner Cut near Holt (Figure 4.4-24), the predicted tidal flows tend to be significantly less than the observed tidal flows, particularly during ebb, however the tidally-averaged predicted and observed flows are more similar, with observed and predicted mean net flows south of 32.7 m^3/s and 37.8 m^3/s, respectively.

4.4.3 Southern Sacramento-San Joaquin Delta

Flow calibration comparisons were performed at ten continuous flow monitoring stations in the southern portion of the Delta, at the locations shown in Figure 4.4-25. Flow comparisons at these stations are shown in Figures 4.4-26 through 4.4-35.

On Middle River at Middle River (Figure 4.4-26), the predicted tidal flows tend to be somewhat less than the observed tidal flows, particularly during ebb, however the tidally-averaged predicted and observed flows are nearly identical, with observed and predicted mean net flows south of 100 m^3/s and 100 m^3/s, respectively. A similar result is evident at Old River at Bacon Island (Figure 4.4-27), with slightly lower predicted than observed tidal flows, but nearly identical tidally-averaged flows. Observed and predicted average net flows south at Old River at Bacon Island during the simulation period are 59.9 m^3/s and 63.5 m^3/s, respectively. The very good agreement of tidally-averaged and net flows at the Middle River at Middle River and Old River and Bacon Island stations is significant, since the net flow at these two stations collectively form the basis of the Old and Middle River (OMR) flow index.

On Old River near Byron (Figure 4.4-28), the observed and predicted flows show good agreement, with typical peak tidal flows of 100 m^3/s during ebb and 300 to 400 m^3/s during flood tide. The cross-correlation analysis yields an amplitude ratio of 1.017, indicating that the model is accurately predicting the flow amplitude, and a phase lead of 11 minutes. Overall the model shows similar tidally-averaged net flows over the analysis period, and the observed and predicted mean net flows south are 109 m^3/s and 120 m^3/s, respectively. In Victoria Canal near Byron (Figure 4.4-29), the predicted tidal flows tend to be somewhat less than the observed tidal flows, however the tidally-averaged predicted and observed flows are more similar, with observed and predicted mean net flows south of 52.6 m^3/s and 40.9 m^3/s, respectively. In Grant Line Canal near Clifton Court Ferry (Figure 4.4-30), the observed and predicted flows show good agreement, with typical peak tidal flows of 100 m^3/s. Observed and predicted average net flows in Grant Line Canal toward Clifton Court Forebay during the simulation period are 8.6 m^3/s and 13.4 m^3/s, respectively.

On Old River near the Delta Mendota Canal upstream of the temporary barrier (Figure 4.4-31), predicted and observed tidal flows are similar at the beginning of the simulation period at the commencement of barrier installation on April 2, and following the closing of the barrier on April 18 and the beginning of operations on April 23 (DWR TBP, 2008). In the model, the barrier is considered open until April 18, however in actuality, the barrier is being built during the period between April 2 and April 18. This is evident in the differences between observed and predicted tidal flows, particularly between April 8 and April 18, 2007. Observed and predicted average net flows in at the barrier during the simulation period are 7 m^3/s and 0.55 m^3/s, respectively. The flow comparisons at this station demonstrate that there are some significant differences between observed and predicted flows during barrier installation. However, incorporating the barrier construction as a gradual, rather than one-time event would require additional information about the barrier construction than is currently available and would be difficult to incorporate into the model. The comparison between tidal flows at the beginning and end of the period shown (top of Figure 4.4-31) demonstrate that the model is accurately

predicting flows when the temporary barrier is out or is beginning construction (near the beginning of the simulation period) or is fully installed (after April 18).

On the San Joaquin River near Stockton (Figure 4.4-32), the observed and predicted flows show good agreement, with typical peak tidal flows of 100 m^3/s. The cross-correlation analysis yields an amplitude ratio of 1.040, indicating that the model is accurately predicting the flow amplitude, a phase lead of 1 minute. Overall the model shows similar tidally-averaged net flows over the analysis period, and the observed and predicted mean flows are 21.6 m^3/s and 23.6 m^3/s, respectively. The largest differences between observed and predicted tidally-averaged flows occur between April 20 and May 22, corresponding to the period when the Head of Old River temporary barrier is installed. During this period, predicted tidally-averaged flows are typically 10 m^3/s greater than observed tidally-averaged flows. On the San Joaquin River below Old River near Lathrop (Figure 4.4-33), predicted tidal flows are significantly larger than observed tidal flows. Tidally-averaged flows show similar trends, but differ significantly in magnitude. The data at this station is collected by DWR, while the majority of the other flow data are from the USGS. Since the tidal prism is accurately predicted downstream at Stockton (Figure 4.4-32) and upstream at Mossdale (Figure 4.4-35), it is believed that the flow rating calculations for the observed flows at the San Joaquin River near Lathrop station are not accurate (see discussion in Section 6.4).

On Old River at Head (Figure 4.4-34), predicted and observed flows show a similar pattern prior to completion of the temporary barrier on April 20. During the period when the barrier is operating, between April 20 and May 22 (see Figure 4.2-1), predicted flows through the barrier tend to be less than observed flows. A similar trend is present in the DSM2 predicted flows (see discussion in Section 6.4). This result suggests some improvements can be made to the culvert rating curves for this barrier to better represent flows while the barrier is operating. The observed and predicted mean net flows at this station over the simulation period are 29.9 m^3/s and 22.3 m^3/s, respectively.

On the San Joaquin River at Mossdale (Figure 4.4-35), the observed and predicted flows show good agreement, with typical peak tidal flows of 70 m^3/s during ebb and near 0 m^3/s during flood tide. The cross-correlation analysis yields an amplitude ratio of 0.964, indicating that the model is accurately predicting the flow amplitude, and a phase lead of 18 minutes. Overall the model shows similar tidally-averaged net flows over the analysis period, and the observed and predicted mean flows are 44.8 m^3/s and 48.4 m^3/s, respectively. The largest differences between observed and predicted tidally-averaged flows occur during July and August.

Table 4-2 Predicted and observed stage and cross-correlation statistics for flow monitoring stations in the Sacramento-San Joaquin Delta during the 2007 simulation period.

Location	Data Source	Figure Number	Mean Flow		Cross Correlation		R^2
			Observed (m^3/s)	Predicted (m^3/s)	Amp Ratio	Lag (min)	
2007 North Delta Flow Stations (Figure 4.4-1)							
Sacramento River South of Georgiana Slough	USGS	4.4-2	112	107	1.004	-9	0.994
Georgiana Slough near Sacramento River	USGS	4.4-3	79.5	80.9	1.120	36	0.946
Delta Cross Channel	USGS	4.4-4	76.0	69.0	0.926	-26	0.984
Sacramento River North of Delta Cross Channel	USGS	4.4-5	257	257	0.994	-8	0.990
Sacramento River at Freeport	USGS	4.4-6	405	400	1.119	0	0.979
Cache Slough at Ryer Island	USGS	4.4-7	25.0	58.7	0.962	-11	0.995
Miner Slough at Hwy 84 Bridge	USGS	4.4-8	64.6	51.9	1.470	-24	0.966
Steamboat Slough between Sacramento River and Sutter Sl.	USGS	4.4-9	58.1	58.7	1.355	-12	0.979
Sutter Slough at Courtland	USGS	4.4-10	91.3	81.1	1.588	-22	0.949
2007 Central Delta Flow Stations (Figure 4.4-11)							
Sacramento River at Rio Vista	USGS	4.4-12	262	257	1.007	-12	0.996
Threemile Slough North at San Joaquin River	USGS	4.4-13	-46.1	-50.9	0.977	6	0.993
San Joaquin River at Jersey Point	USGS	4.4-14	93.9	49.4	0.907	-8	0.994
False River	USGS	4.4-15	-36.7	-14.8	0.890	-2	0.995
Dutch Slough at Jersey Island	USGS	4.4-16	13.8	-10.6	0.863	-11	0.992
Old River at San Joaquin River	USGS	4.4-17	-8.8	-30.9	1.097	-24	0.961
Mokelumne River near San Joaquin River	USGS	4.4-18	86.5	104.4	1.072	-8	0.991
Old River at Quimby Island near Bethel Island	USGS	4.4-19	-43.1	-33.8	0.753	-4	0.988
Holland Cut	USGS	4.4-20	-21.5	-41.5	0.784	-5	0.992
San Joaquin River at Prisoners Point	USGS	4.3-21	-80.1	-51.1	0.804	-17	0.987
Little Potato Slough at Terminous	USGS	4.4-22	56.4	43.2	0.738	-17	0.968
Middle River south of Columbia Cut	USGS	4.4-23	-74.3	-69.3	0.822	-12	0.985
Turner Cut near Holt	USGS	4.4-24	-32.7	-37.8	0.593	-15	0.957
2007 South Delta Flow Stations (Figure 4.4-25)							
Middle River at Middle River	USGS	4.4-26	-100	-100	0.697	-12	0.980
Old River at Bacon Island	USGS	4.4-27	-59.9	-63.5	0.788	-12	0.991
Old River near Byron	USGS	4.4-28	-109	-120	1.017	-11	0.989
Victoria Canal near Byron	USGS	4.4-29	-52.6	-40.9	0.613	-9	0.948
Grant Line Canal near Clifton Court Ferry	USGS	4.4-30	8.6	13.4	0.904	0	0.935

Old River near Delta Mendota Canal (Upstream of Barrier)	USGS	4.4-31	6.96	0.55	0.724	66	0.572
San Joaquin River at Stockton	USGS	4.4-32	21.6	23.6	1.040	-1	0.985
San Joaquin River below Old River near Lathrop	DWR	4.4-33	14.0	25.2	1.629	-6	0.973
Old River at Head	DWR	4.4-34	29.9	22.3	0.727	3	0.883
San Joaquin River at Mossdale	DWR	4.4-35	44.8	48.4	0.964	-18	0.964

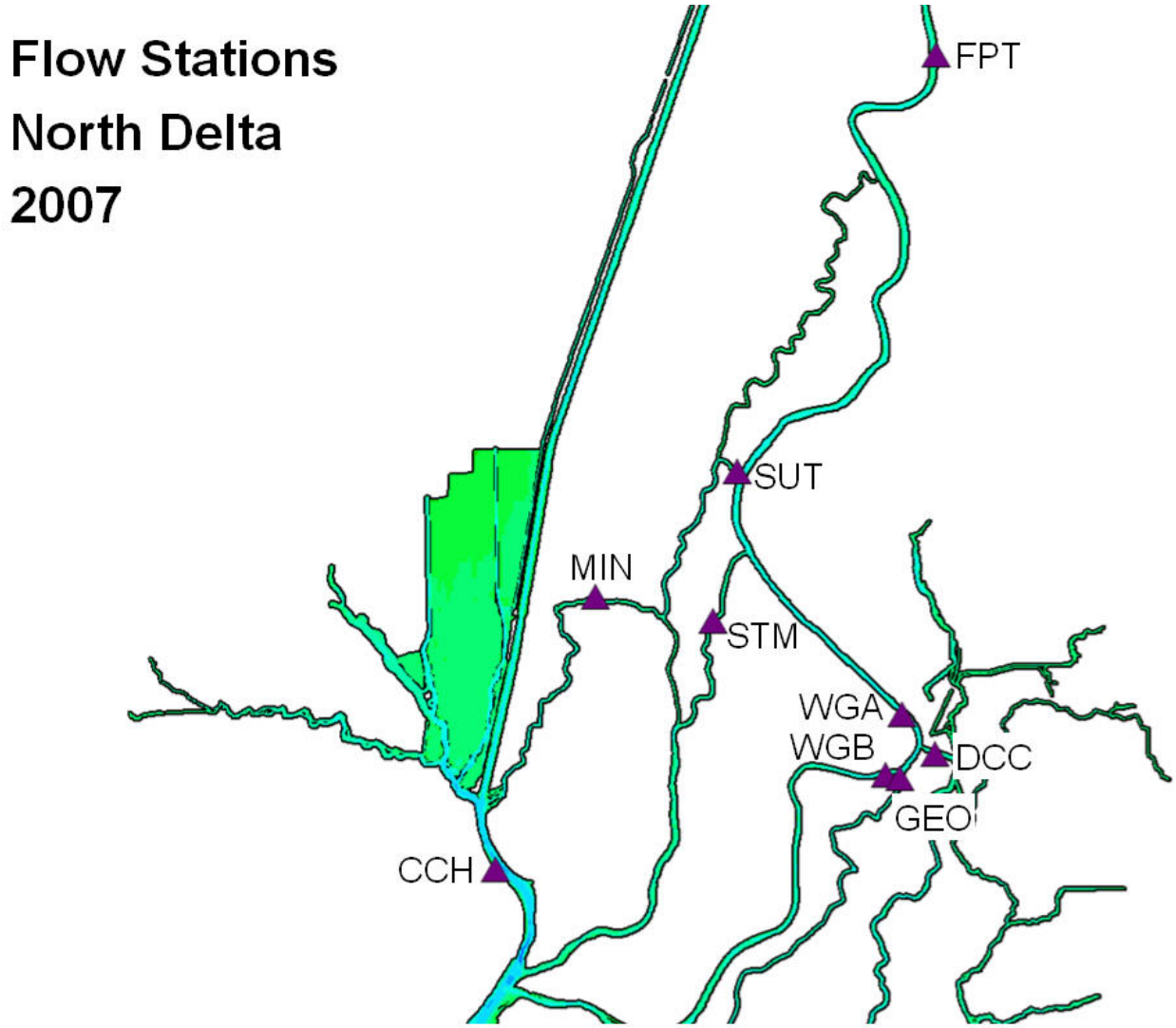

Station Names

WGB, Sacramento River South of Georgiana Slough

GEO, Georgiana Slough near Sacramento River

DCC, Delta Cross Channel

WGA, Sacramento River North of Delta Cross Channel

FPT, Sacramento River at Freeport

CCH, Cache Slough at Ryer Island

MIN, Miner Slough at Hwy 84 Bridge

STM, Steamboat Slough between Sacramento River and Sutter Sl.

SUT, Sutter Slough at Courtland

Figure 4.4-1 Location of flow monitoring stations in the northern portion of the Sacramento-San Joaquin Delta used for 2007 flow calibration.

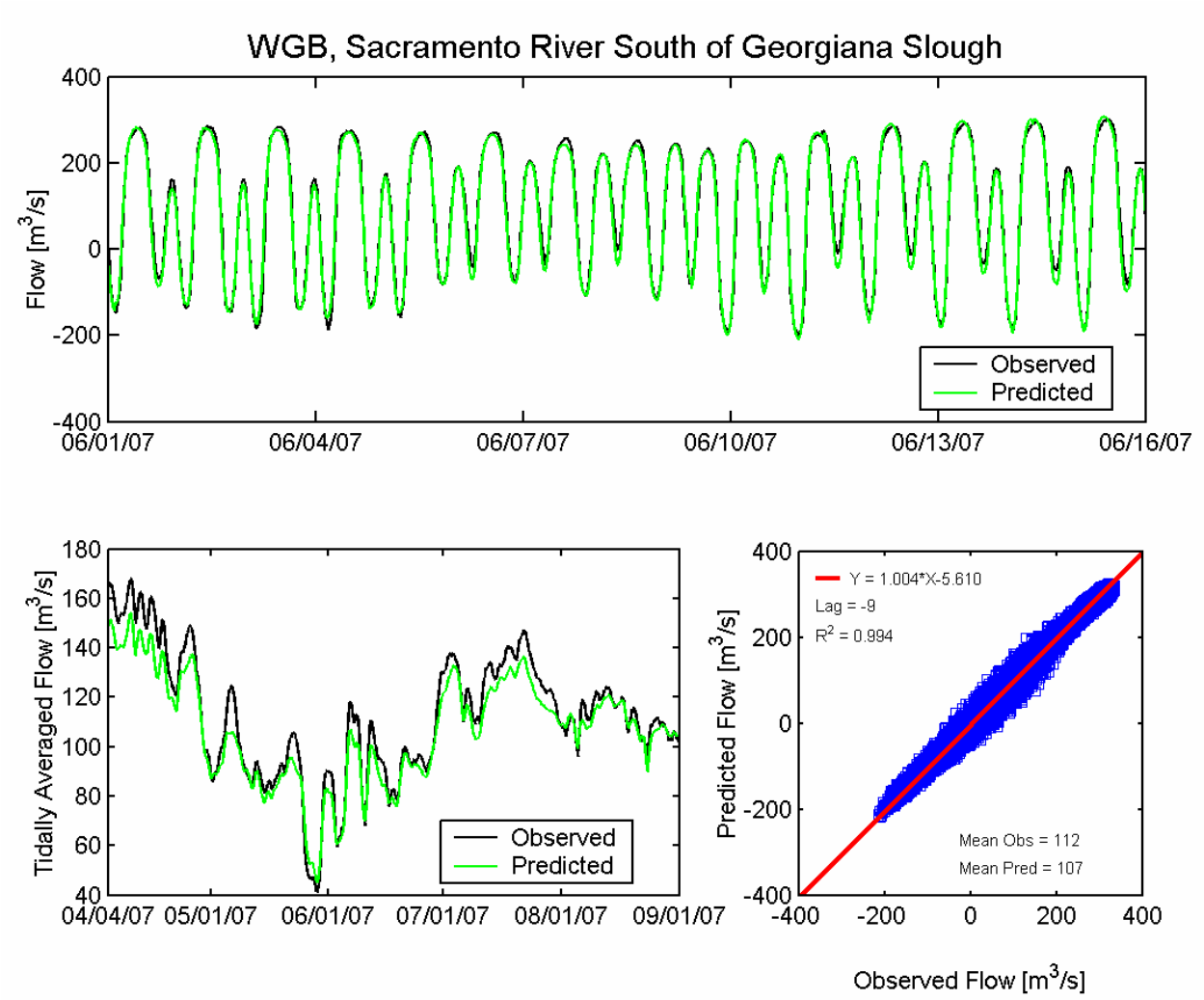

Figure 4.4-2 Observed and predicted flow at Sacramento River South of Georgiana Slough USGS station (WGB) during the 2007 simulation period.

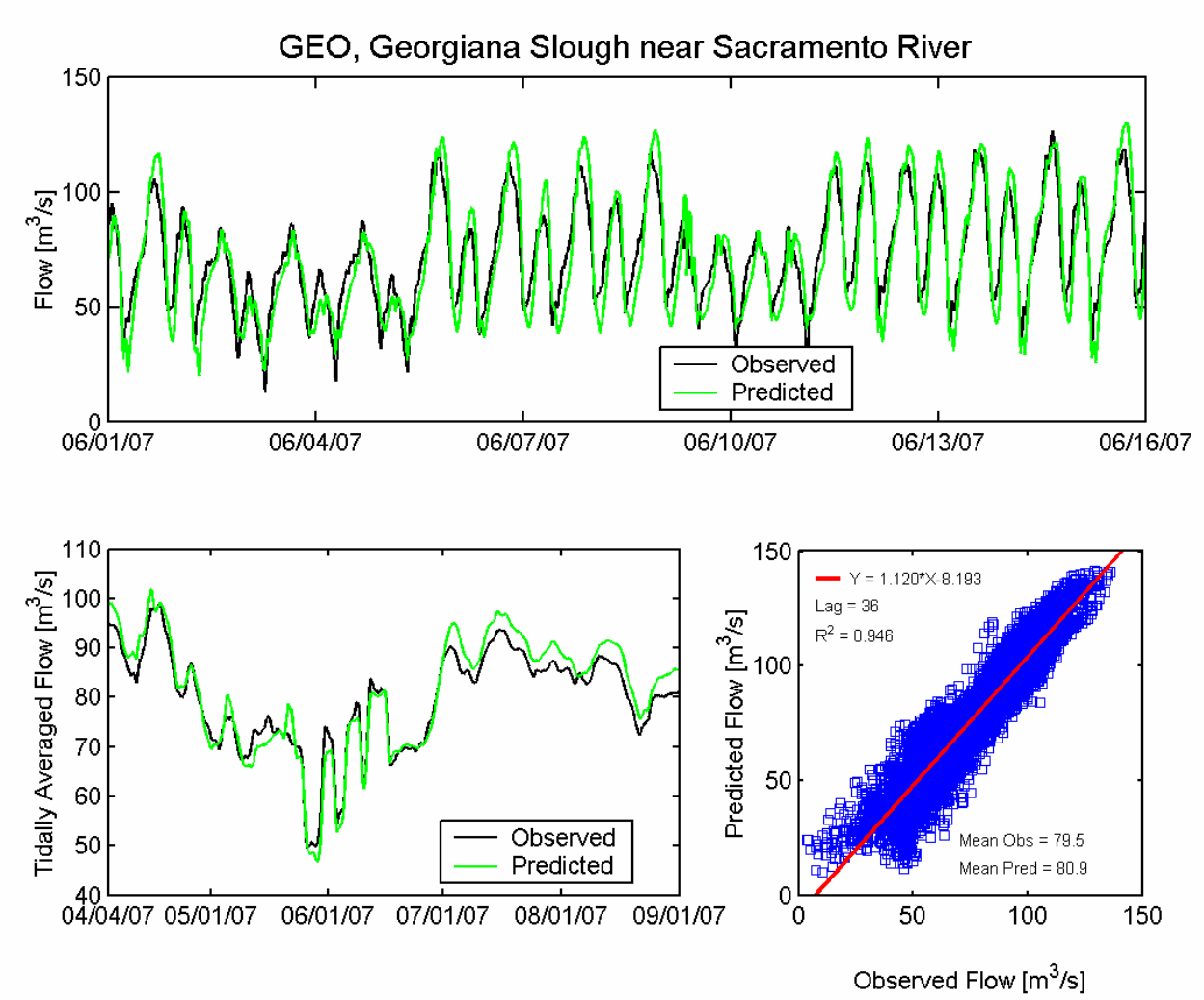

Figure 4.4-3 Observed and predicted flow at Georgiana Slough near Sacramento River USGS station (GEO) during the 2007 simulation period.

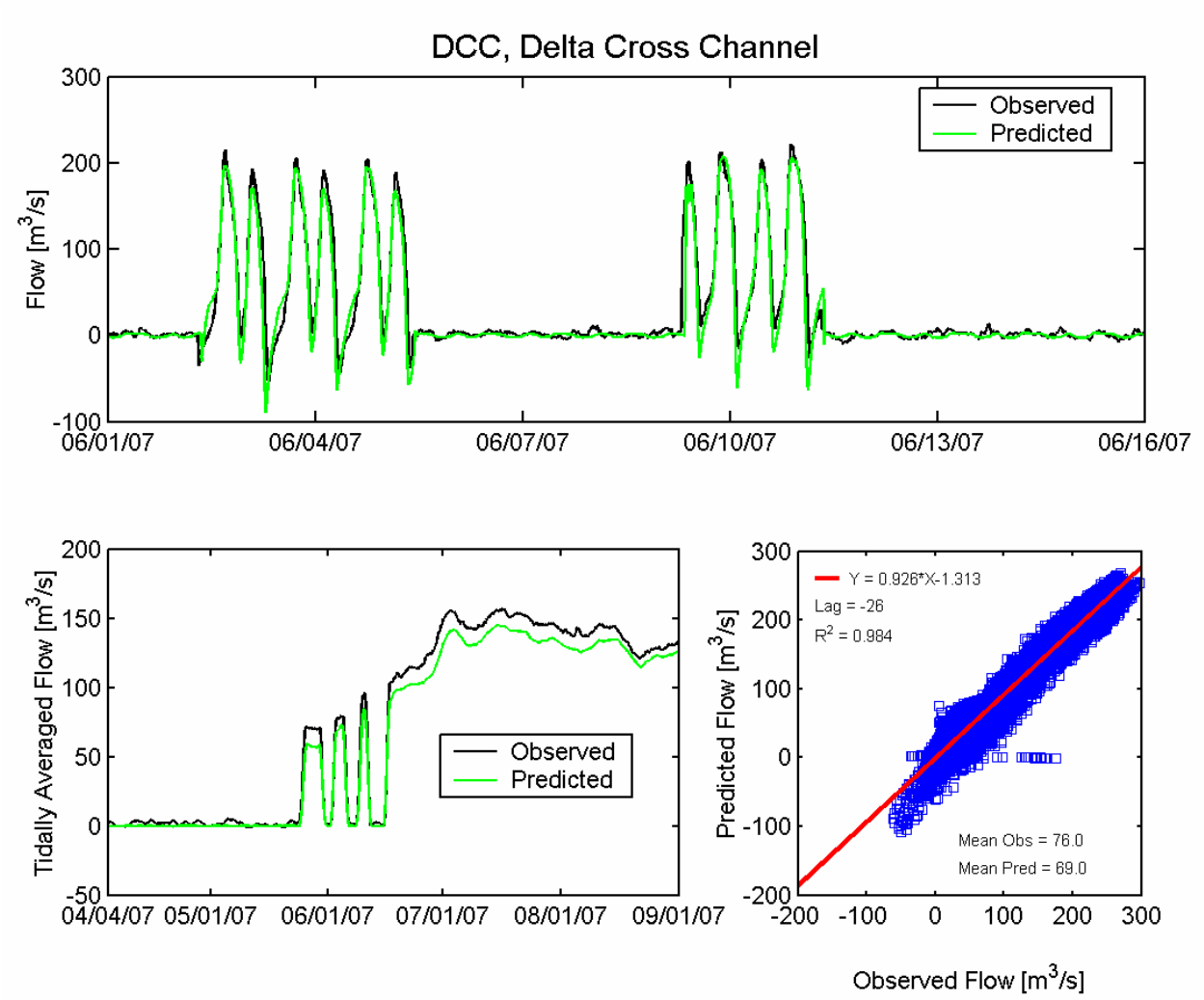

Figure 4.4-4 Observed and predicted flow at Delta Cross Channel USGS station (DCC) during the 2007 simulation period.

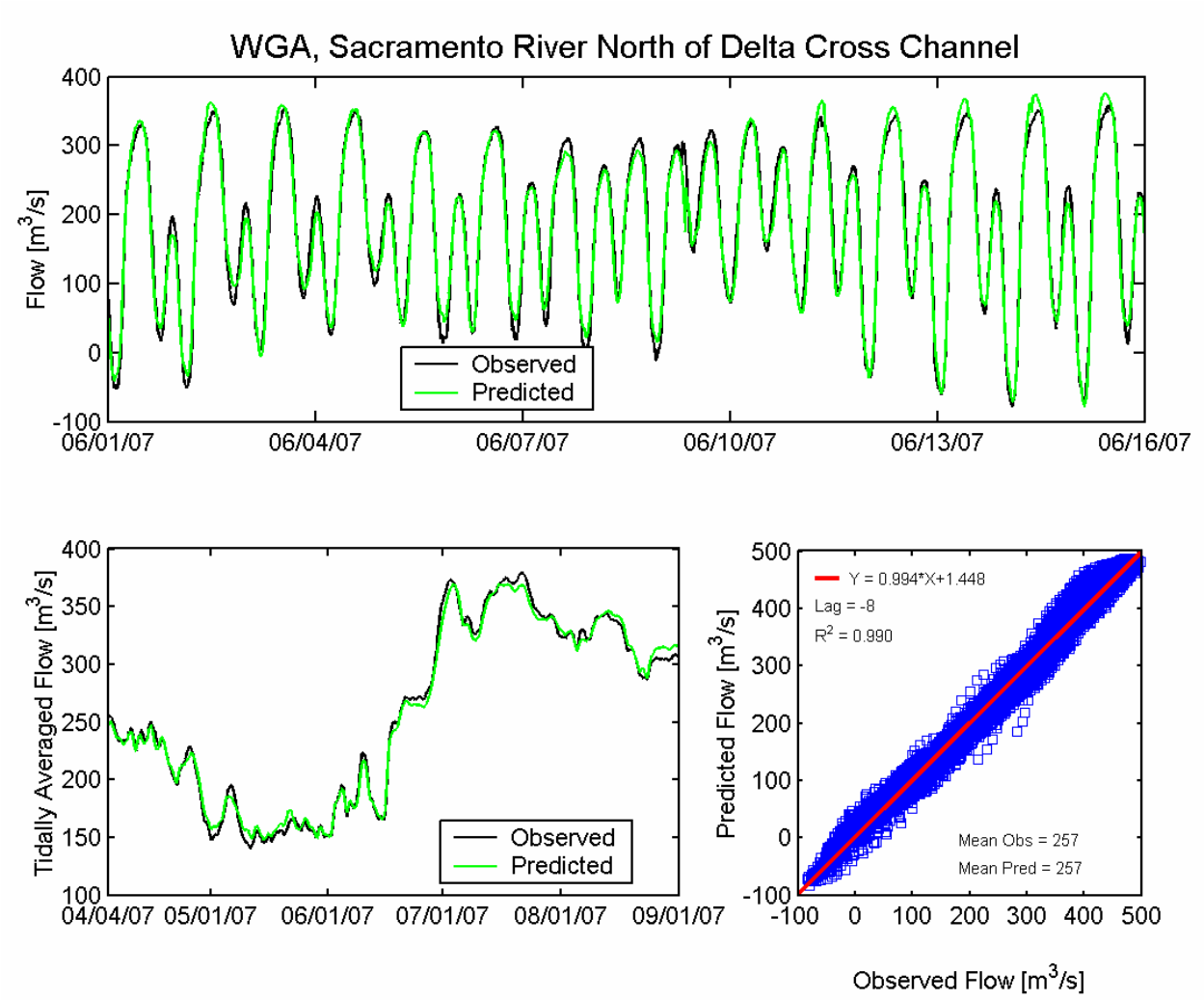

Figure 4.4-5 Observed and predicted flow at Sacramento River North of Delta Cross Channel USGS station (WGA) during the 2007 simulation period.

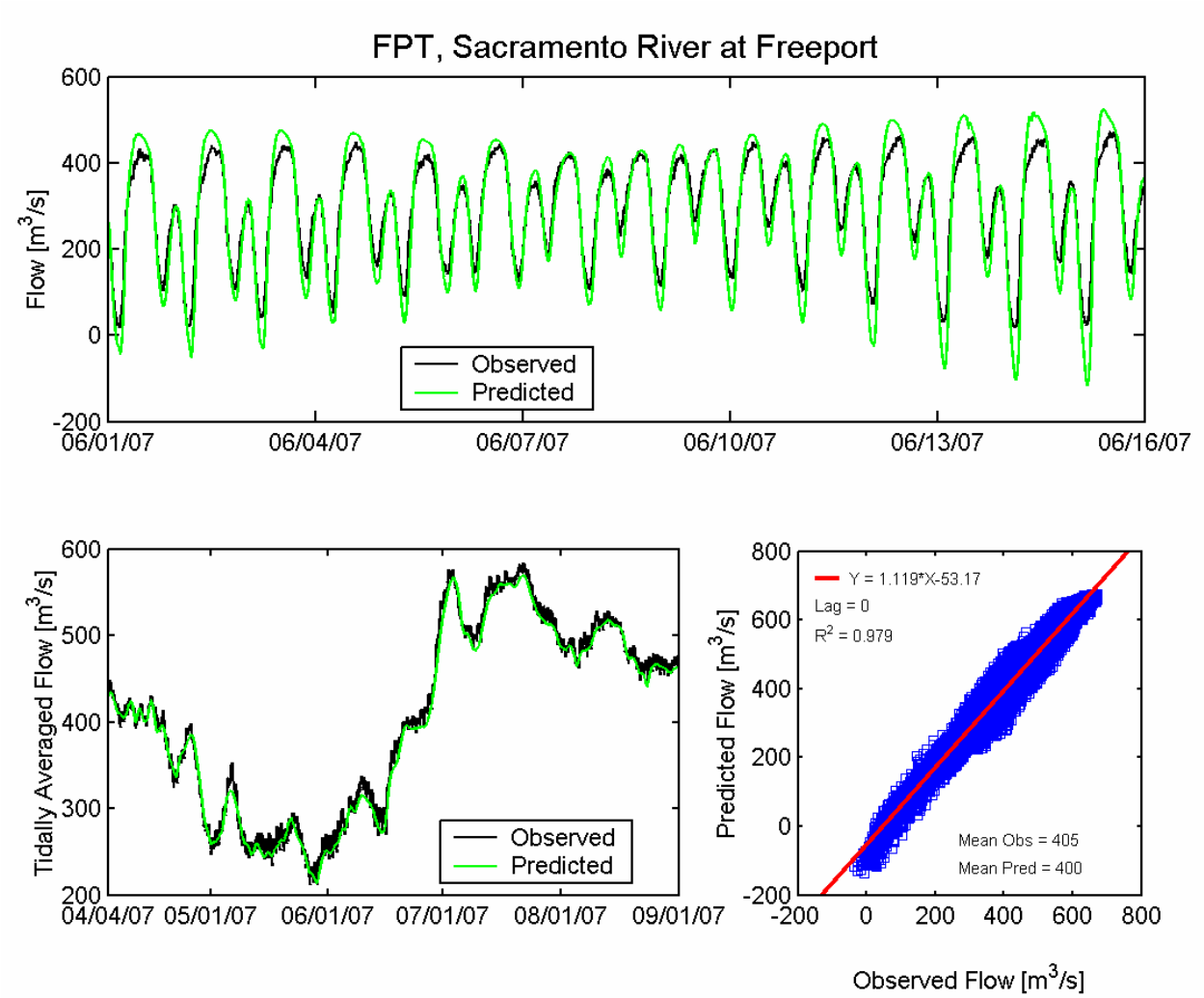

Figure 4.4-6 Observed and predicted flow at Sacramento River at Freeport USGS station (FPT) during the 2007 simulation period.

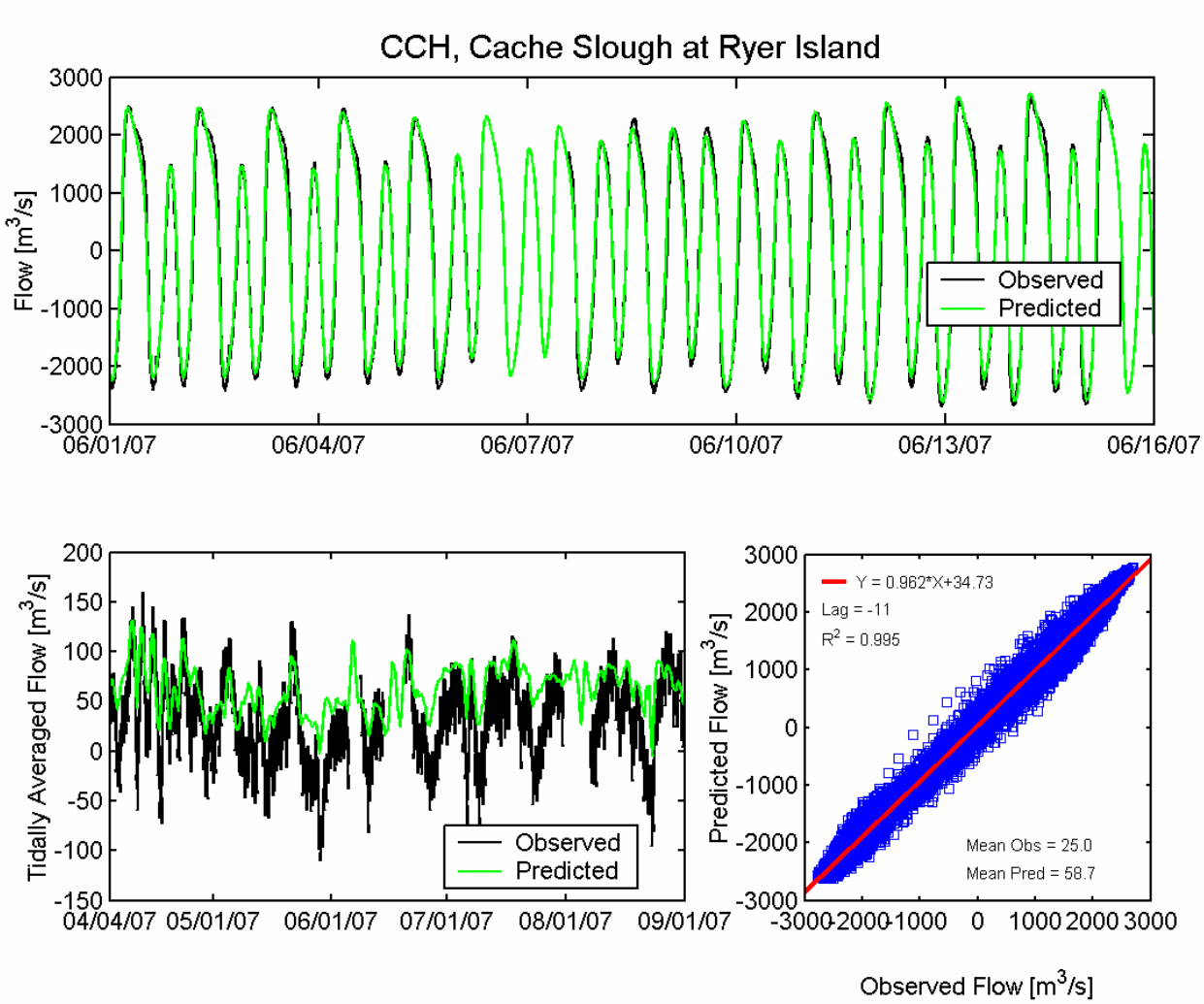

Figure 4.4-7 Observed and predicted flow at Cache Slough at Ryer Island USGS station (CCH) during the 2007 simulation period.

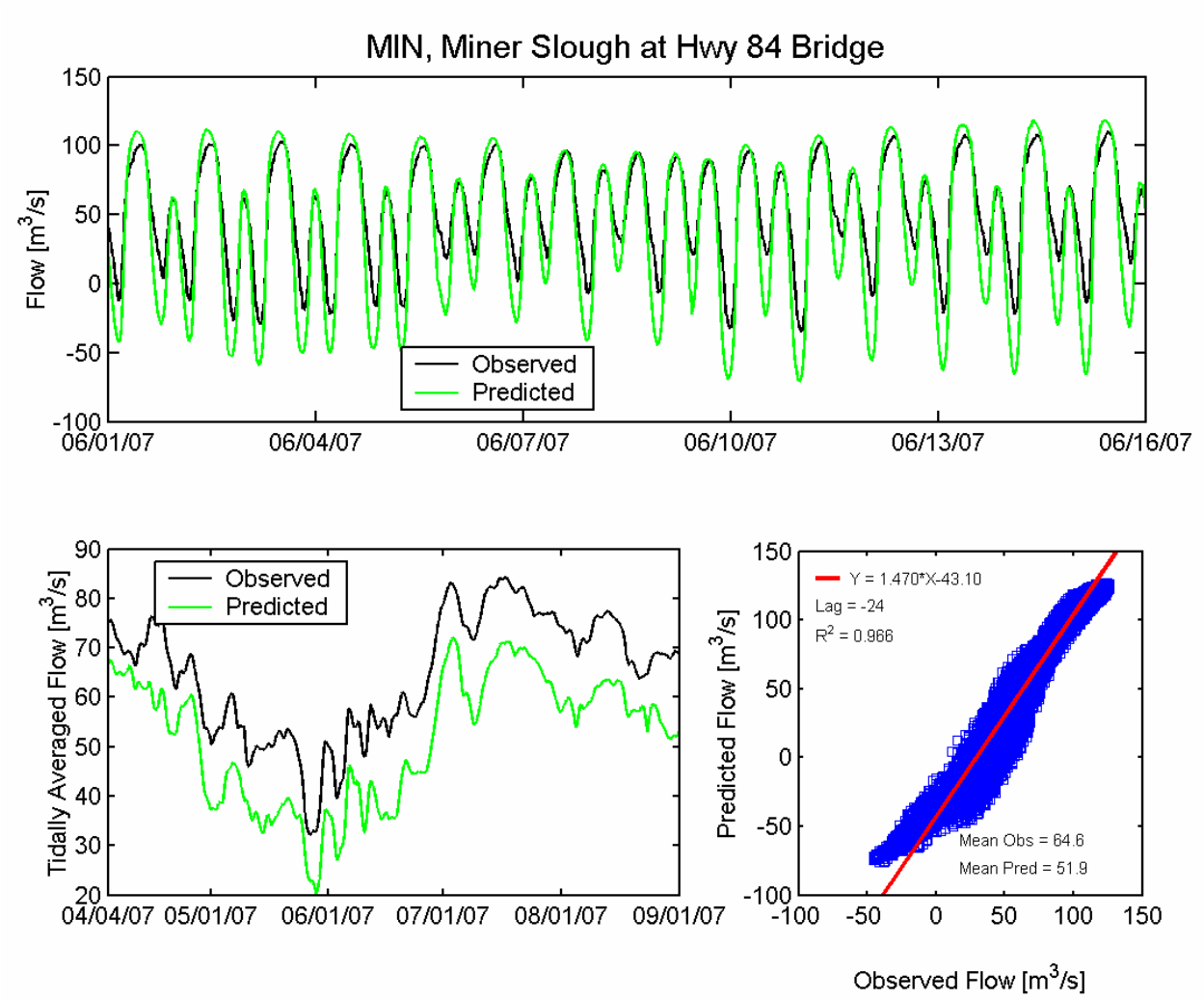

Figure 4.4-8 Observed and predicted flow at Miner Slough at Highway 84 Bridge USGS station (MIN) during the 2007 simulation period.

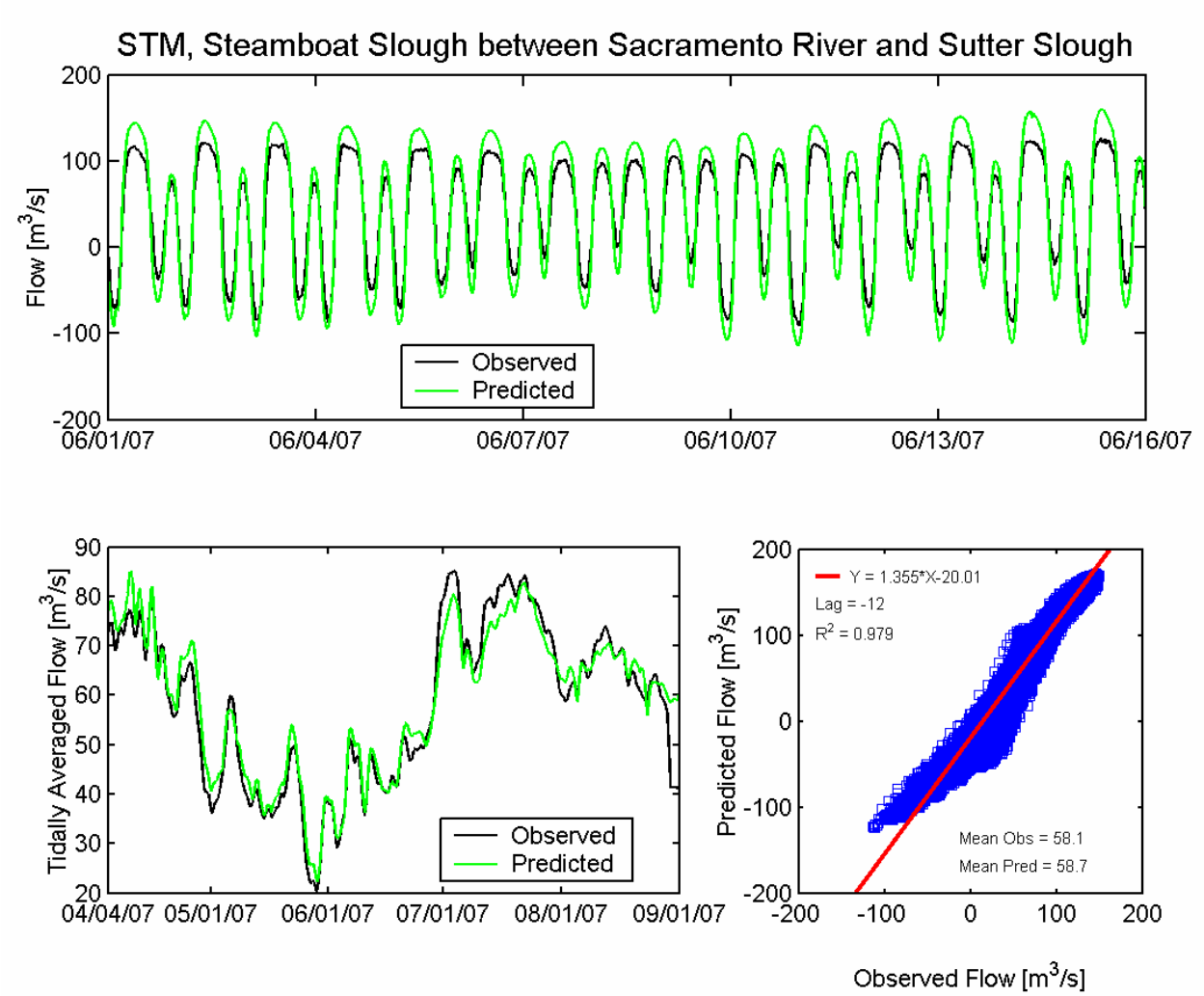

Figure 4.4-9 Observed and predicted flow at Steamboat Slough between Sacramento River and Sutter Slough USGS station (STM) during the 2007 simulation period.

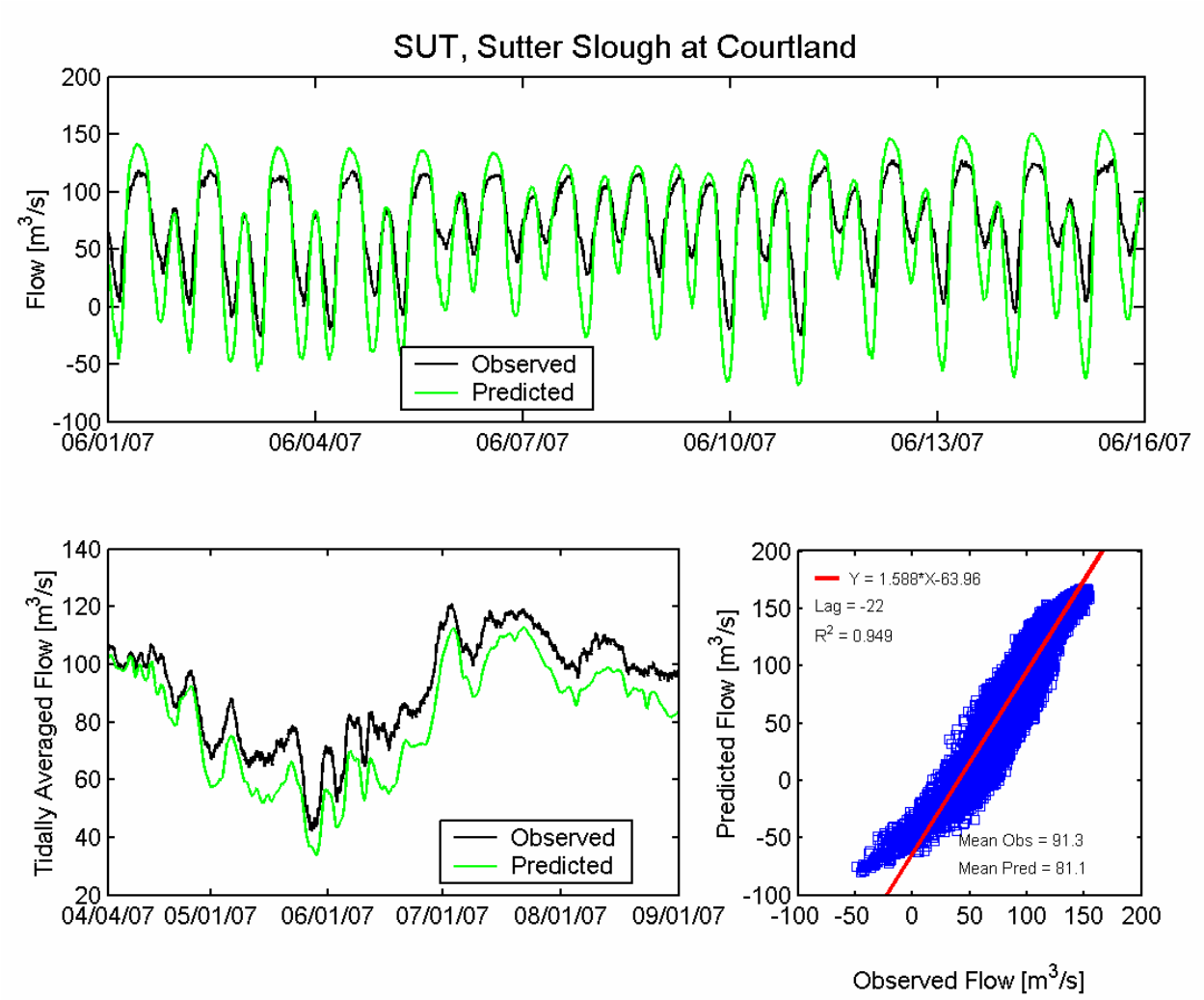

Figure 4.4-10 Observed and predicted flow at Sutter Slough at Courtland USGS station (SUT) during the 2007 simulation period.

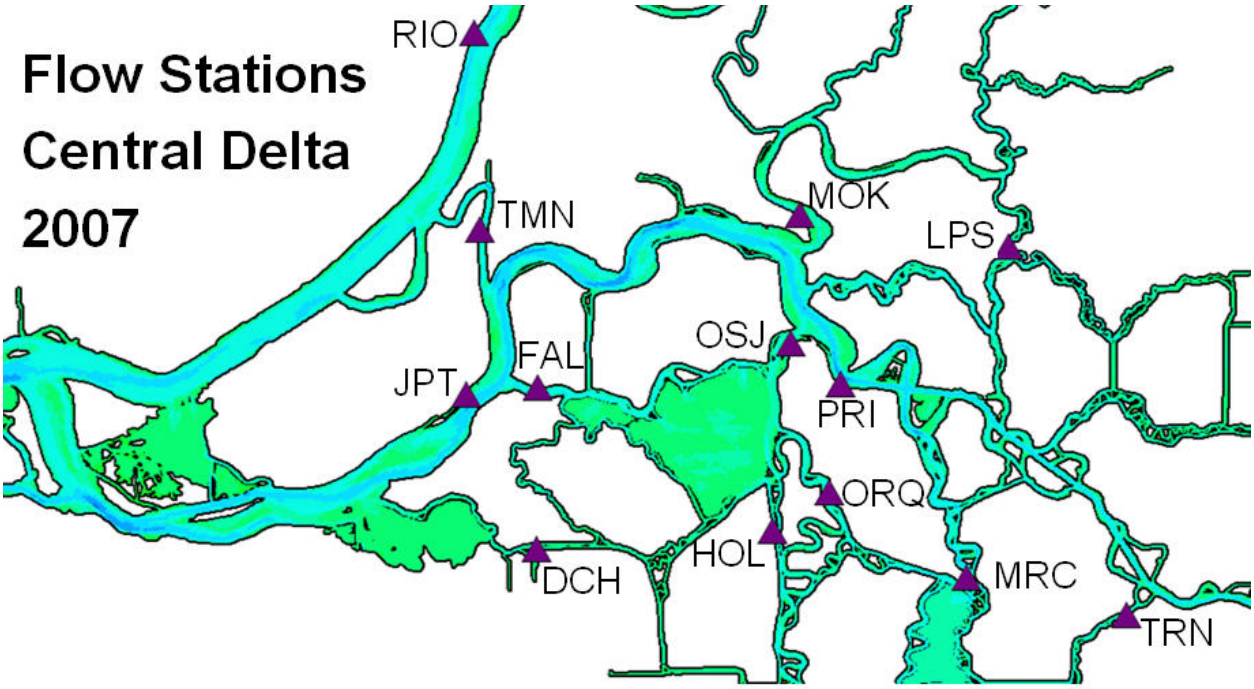

Station Names

RIO, Sacramento River at Rio Vista

TMN, Threemile Slough North at San Joaquin River

JPT, San Joaquin River at Jersey Point

FAL, False River

DCH, Dutch Slough at Jersey Island

OSJ, Old River at San Joaquin River

MOK, Mokelumne River near San Joaquin River

ORQ, Old River at Quimby Island near Bethel Island

HOL, Holland Cut

PRI, San Joaquin River at Prisoners Point

LPS, Little Potato Slough at Terminous

MRC, Middle River South of Columbia Cut

TRN, Turner Cut near Holt

Figure 4.4-11 Location of flow monitoring stations in the central portion of the Sacramento-San Joaquin Delta used for 2007 flow calibration.

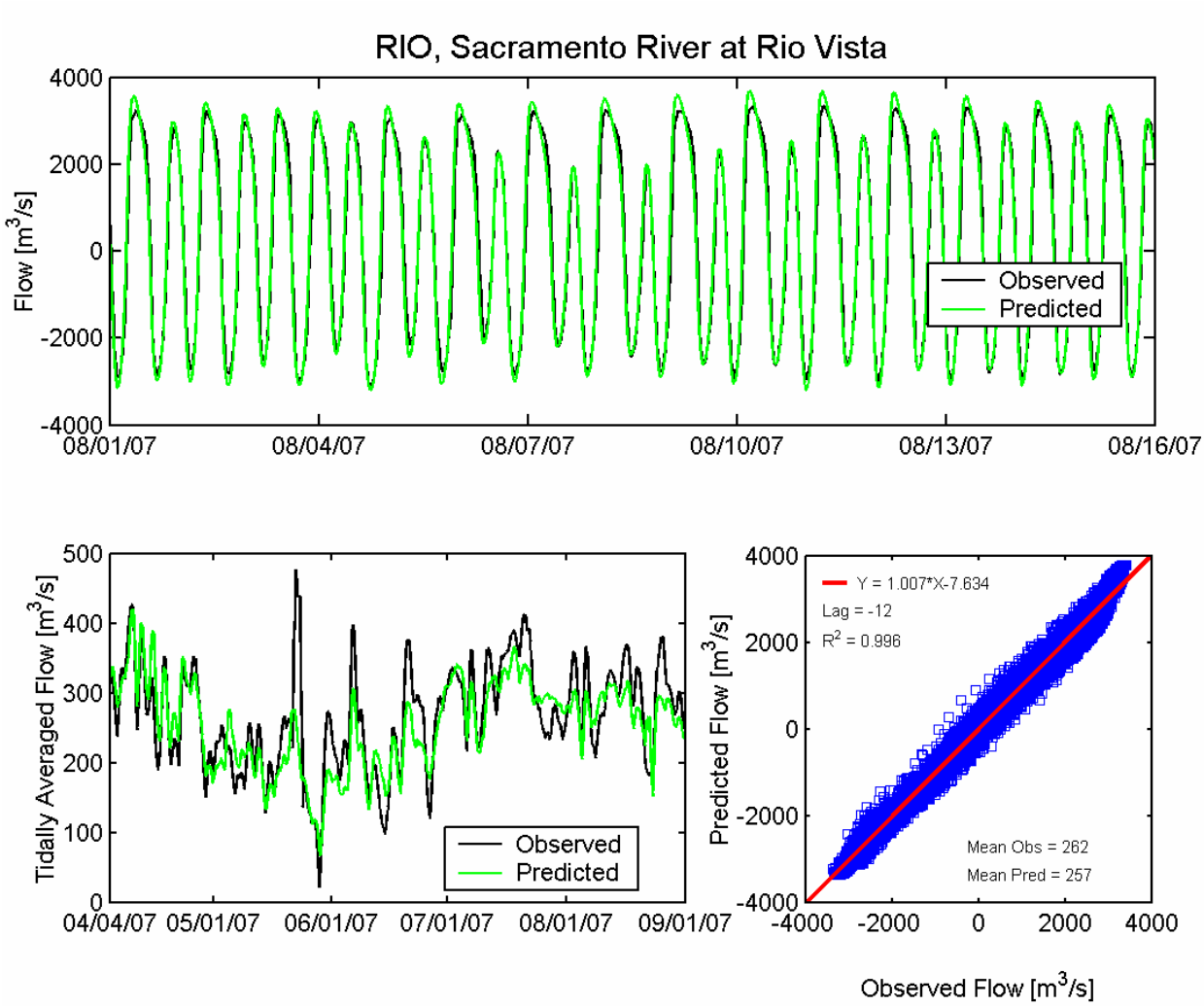

Figure 4.4-12 Observed and predicted flow at Sacramento River at Rio Vista USGS station (RIO) during the 2007 simulation period.

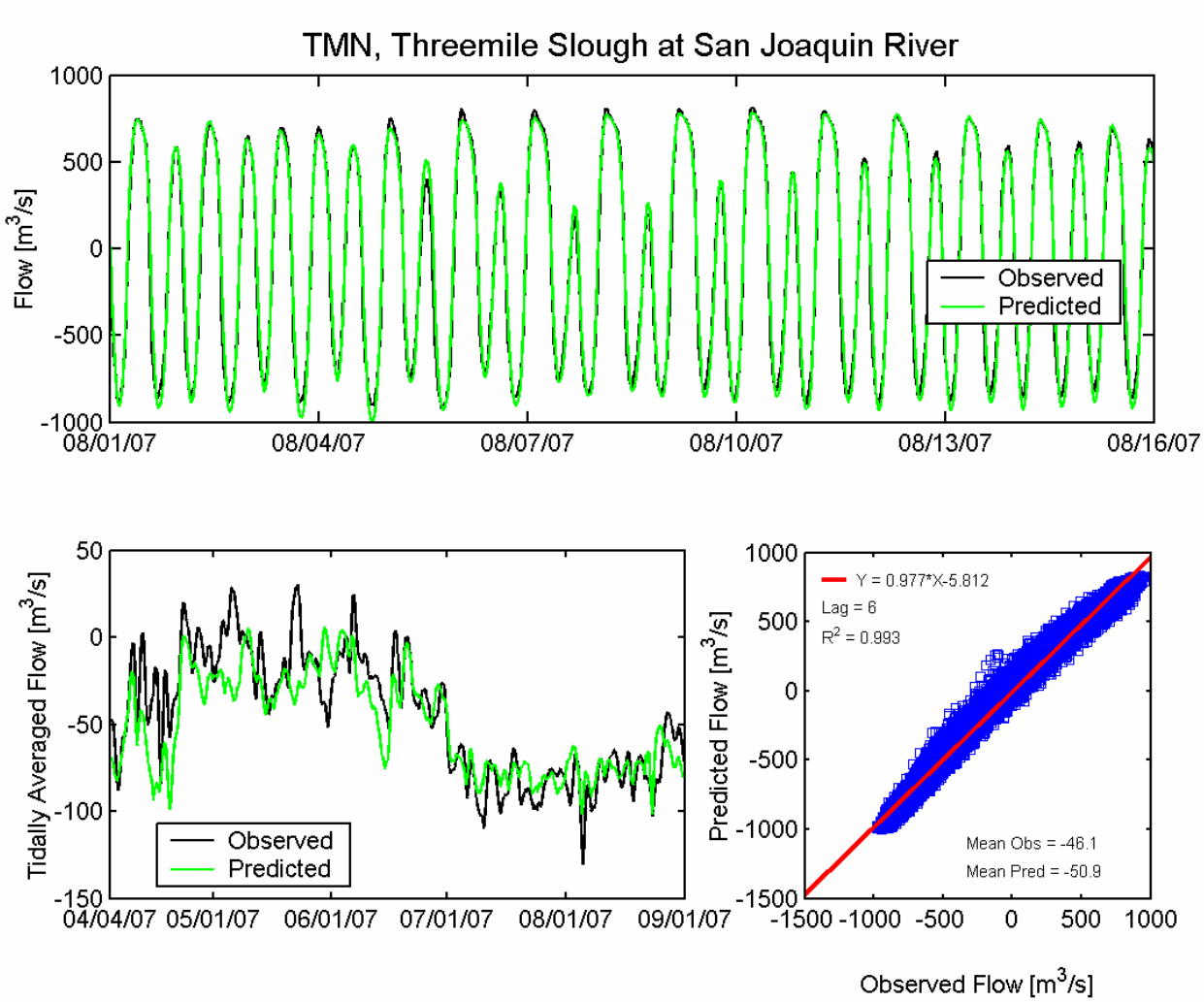

Figure 4.4-13 Observed and predicted flow at Threemile Slough North at San Joaquin River USGS station (TMN) during the 2007 simulation period.

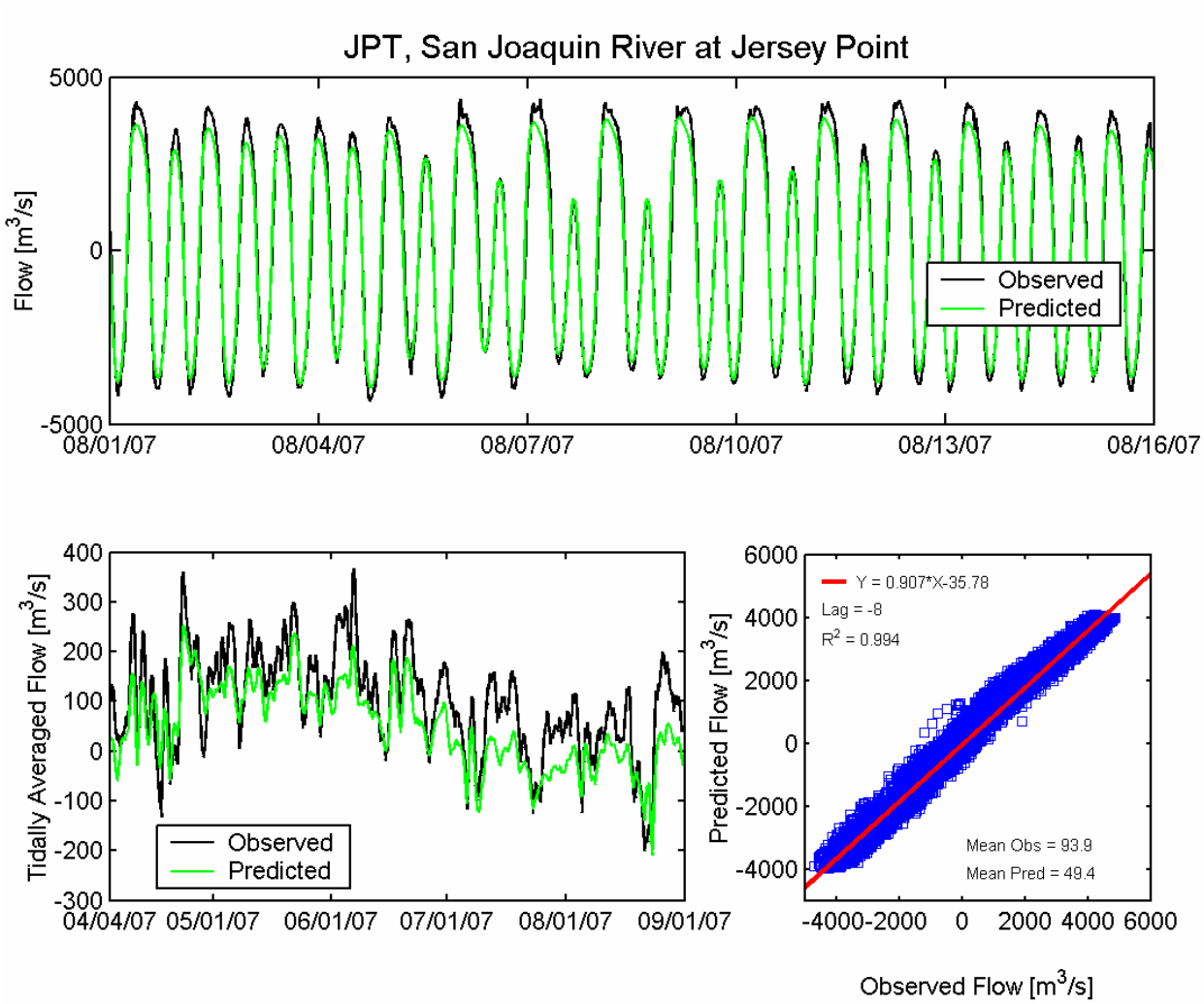

Figure 4.4-14 Observed and predicted flow at San Joaquin River at Jersey Point USGS station (JPT) during the 2007 simulation period.

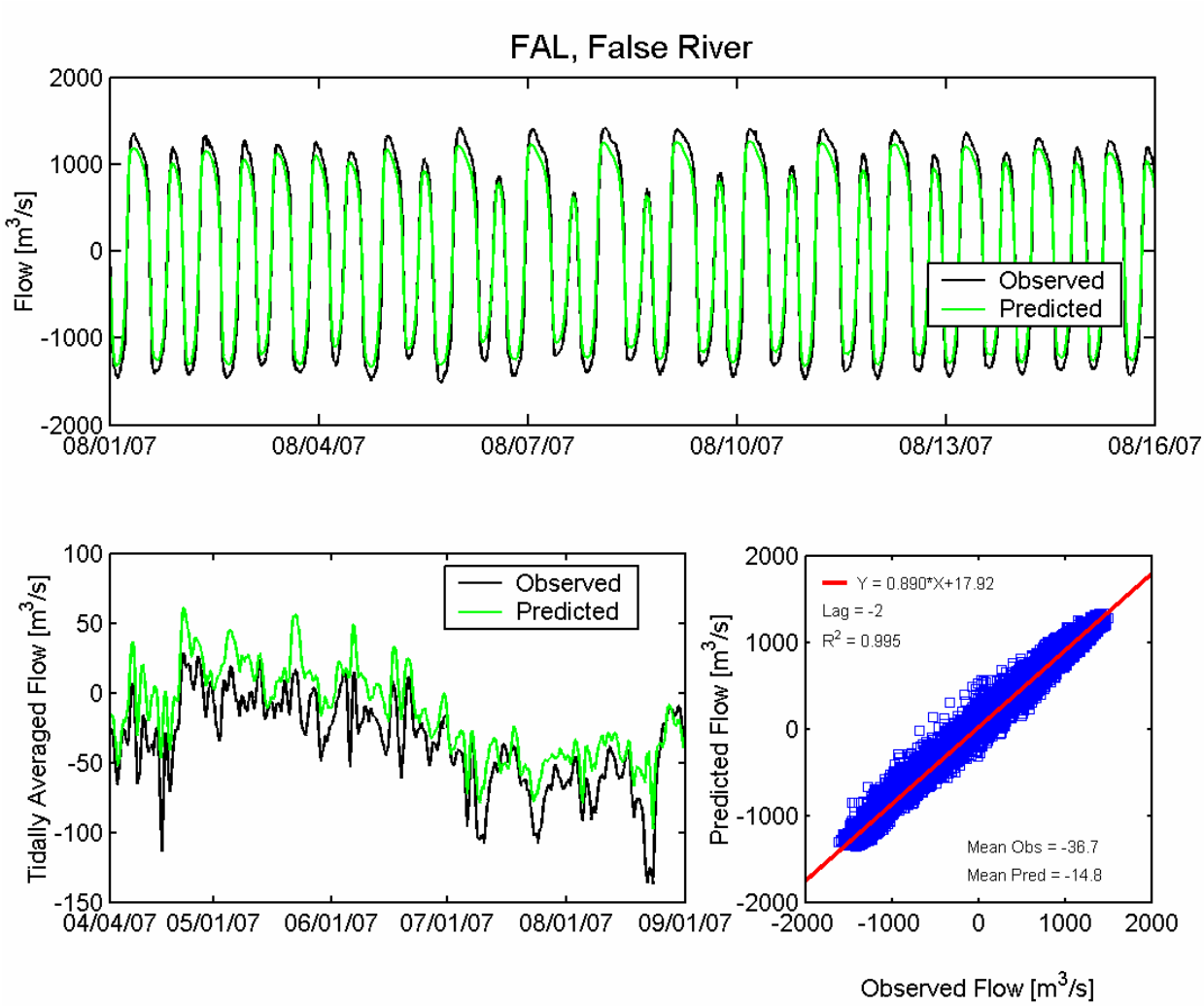

Figure 4.4-15 Observed and predicted flow at False River USGS station (FAL) during the 2007 simulation period.

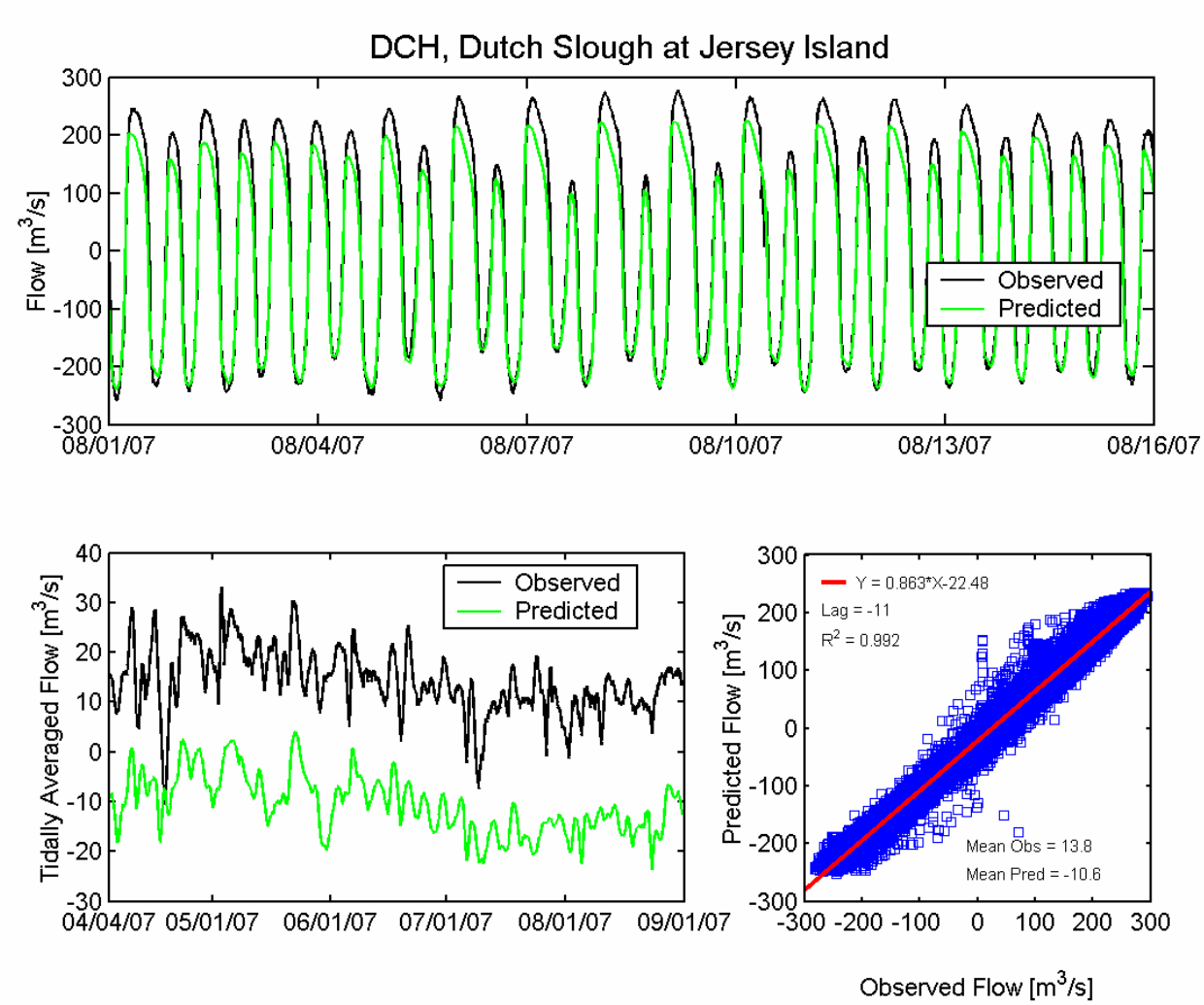

Figure 4.4-16 Observed and predicted flow at Dutch Slough at Jersey Island USGS station (DCH) during the 2007 simulation period.

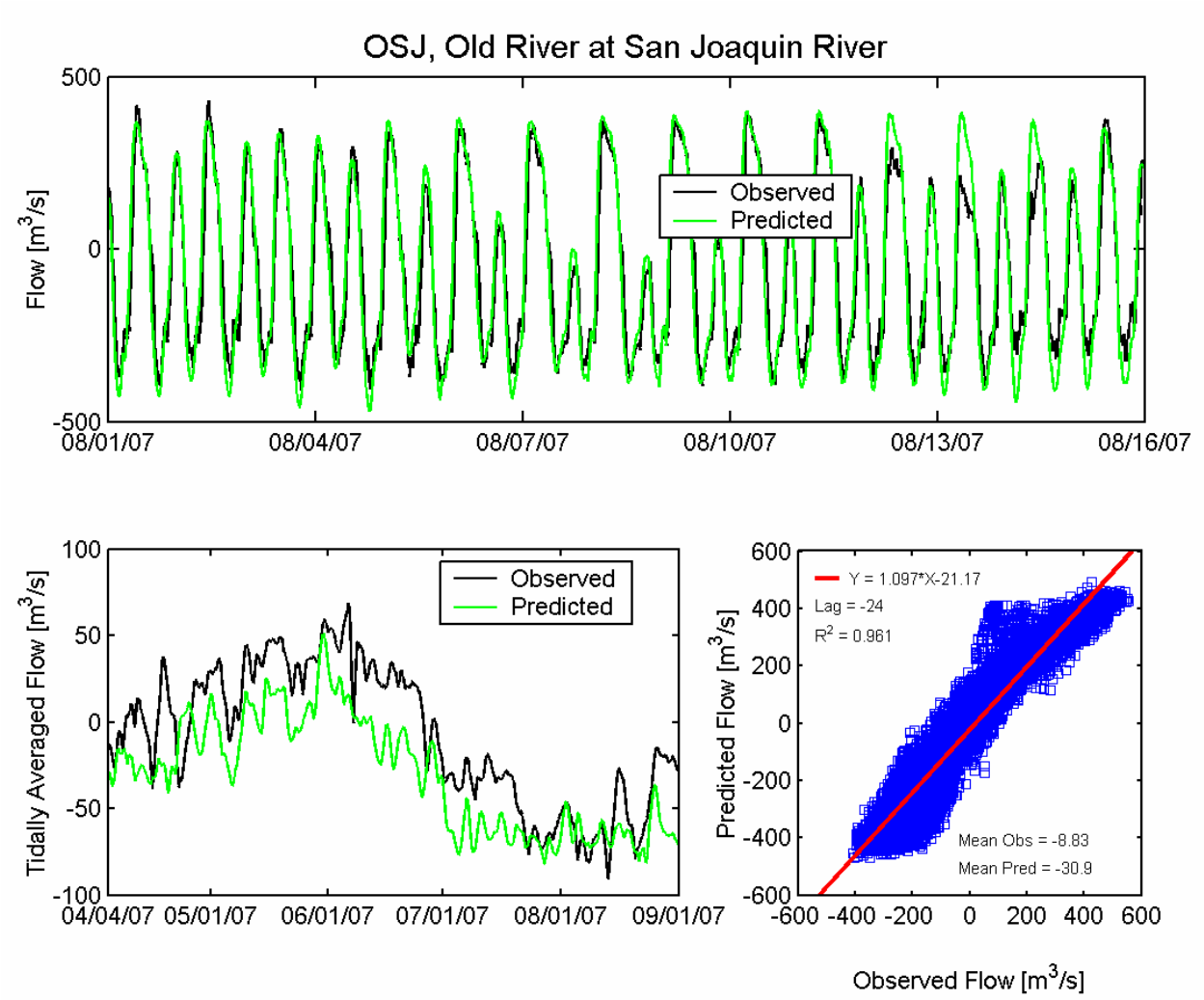

Figure 4.4-17 Observed and predicted flow at Old River at San Joaquin USGS station (OSJ) during the 2007 simulation period.

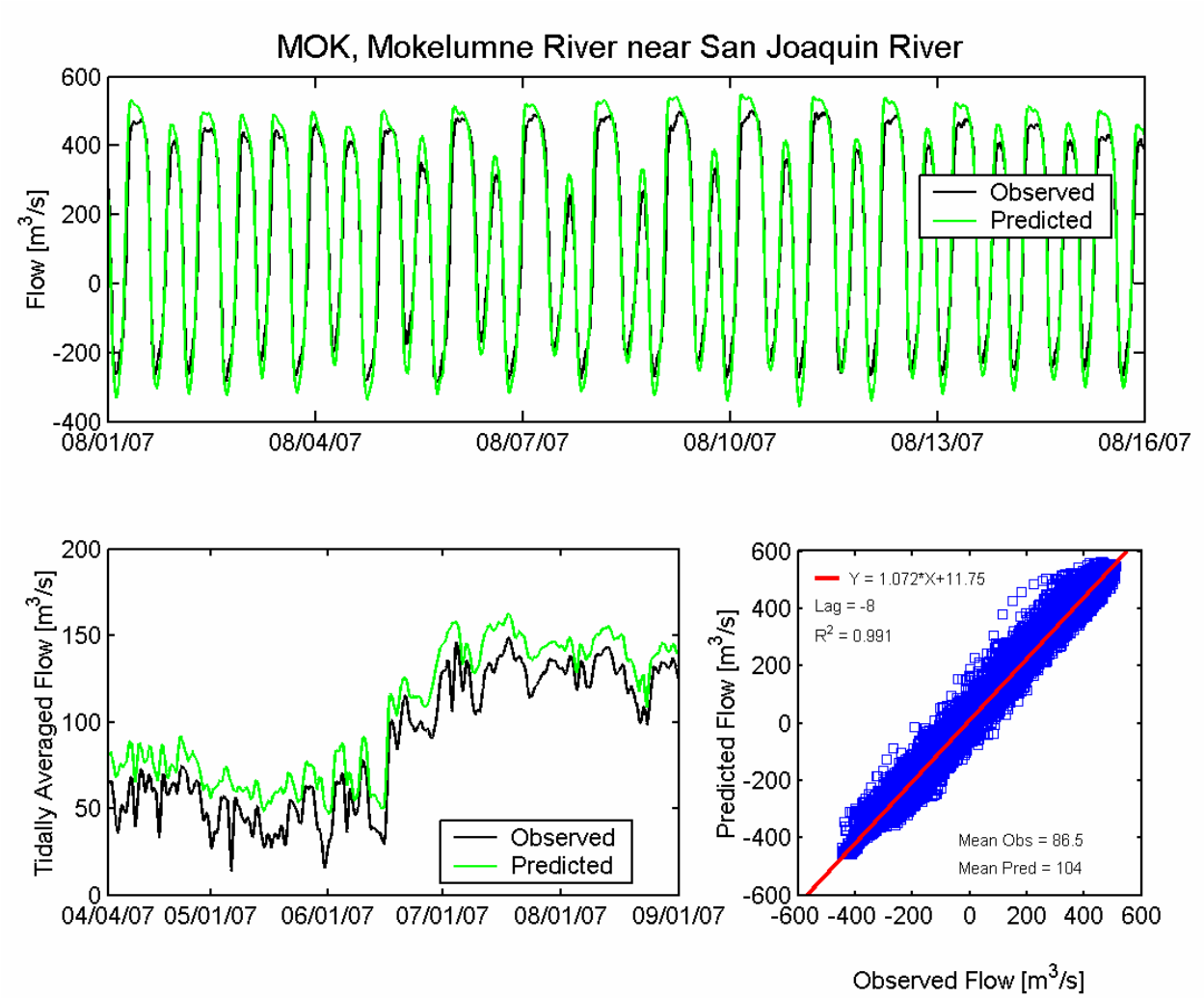

Figure 4.4-18 Observed and predicted flow at Mokelumne River near San Joaquin River USGS station (MOK) during the 2007 simulation period.

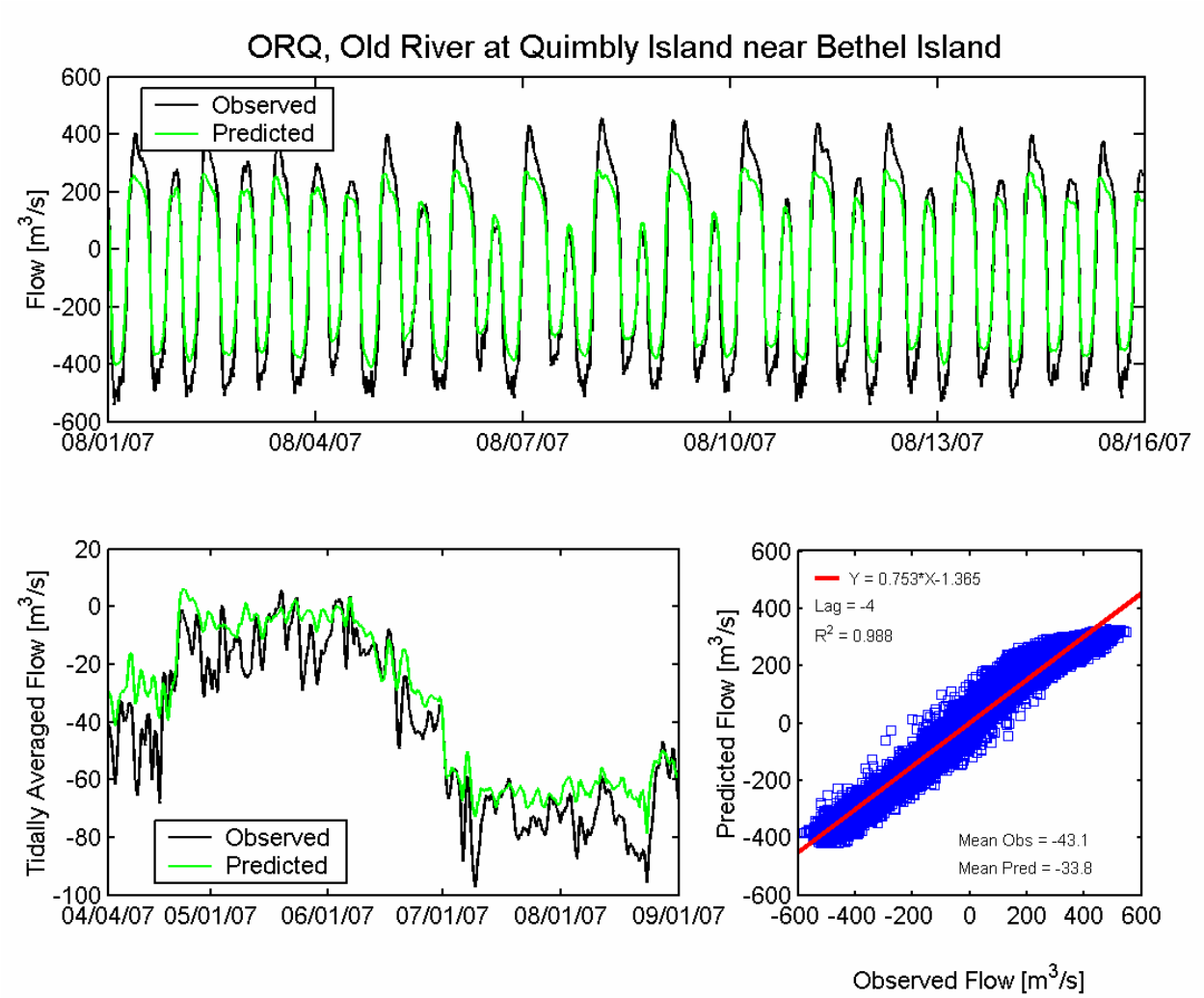

Figure 4.4-19 Observed and predicted flow at Old River at Quimby Island near Bethel Island USGS station (ORQ) during the 2007 simulation period.

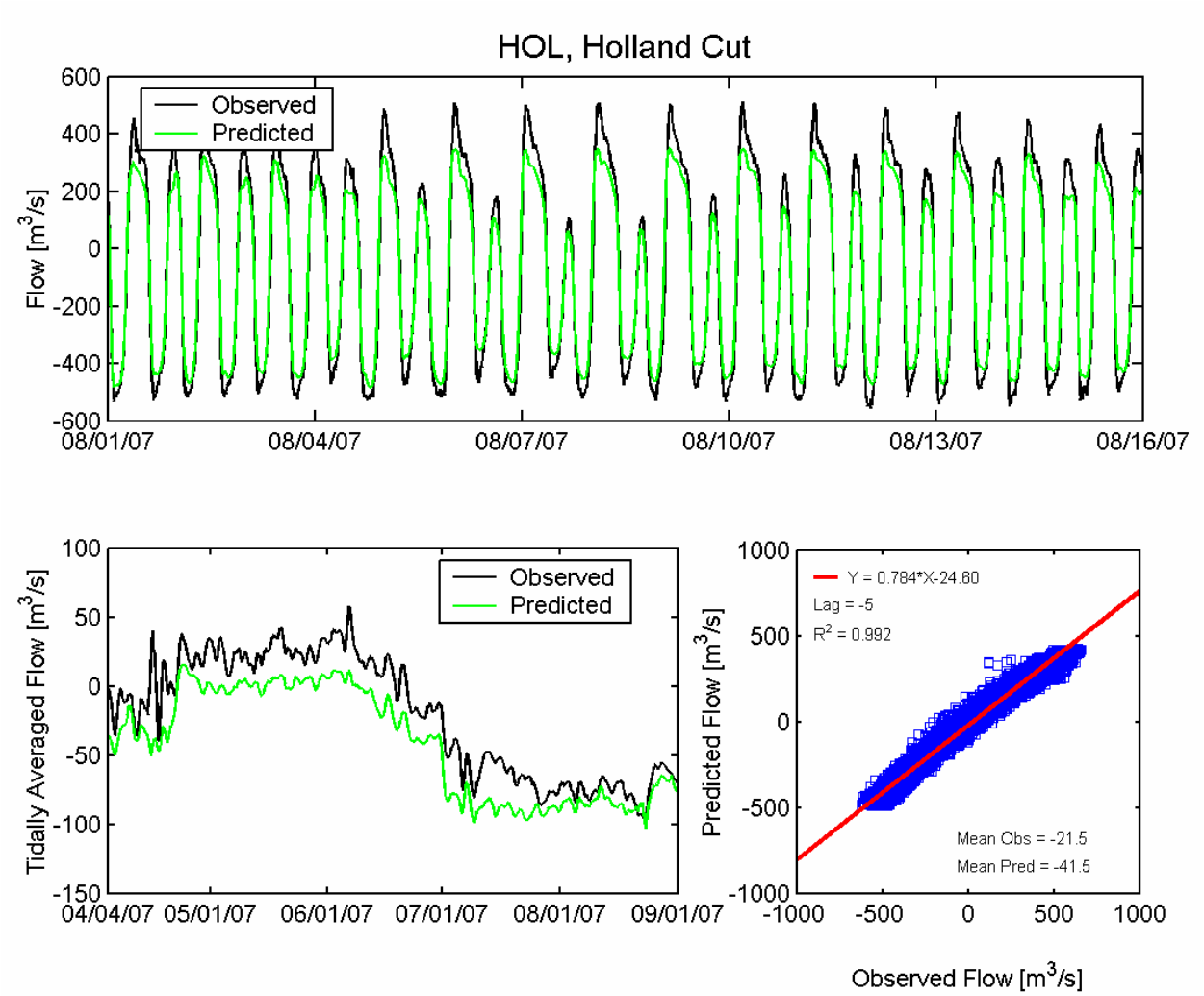

Figure 4.4-20 Observed and predicted flow at Holland Cut USGS station (HOL) during the 2007 simulation period.

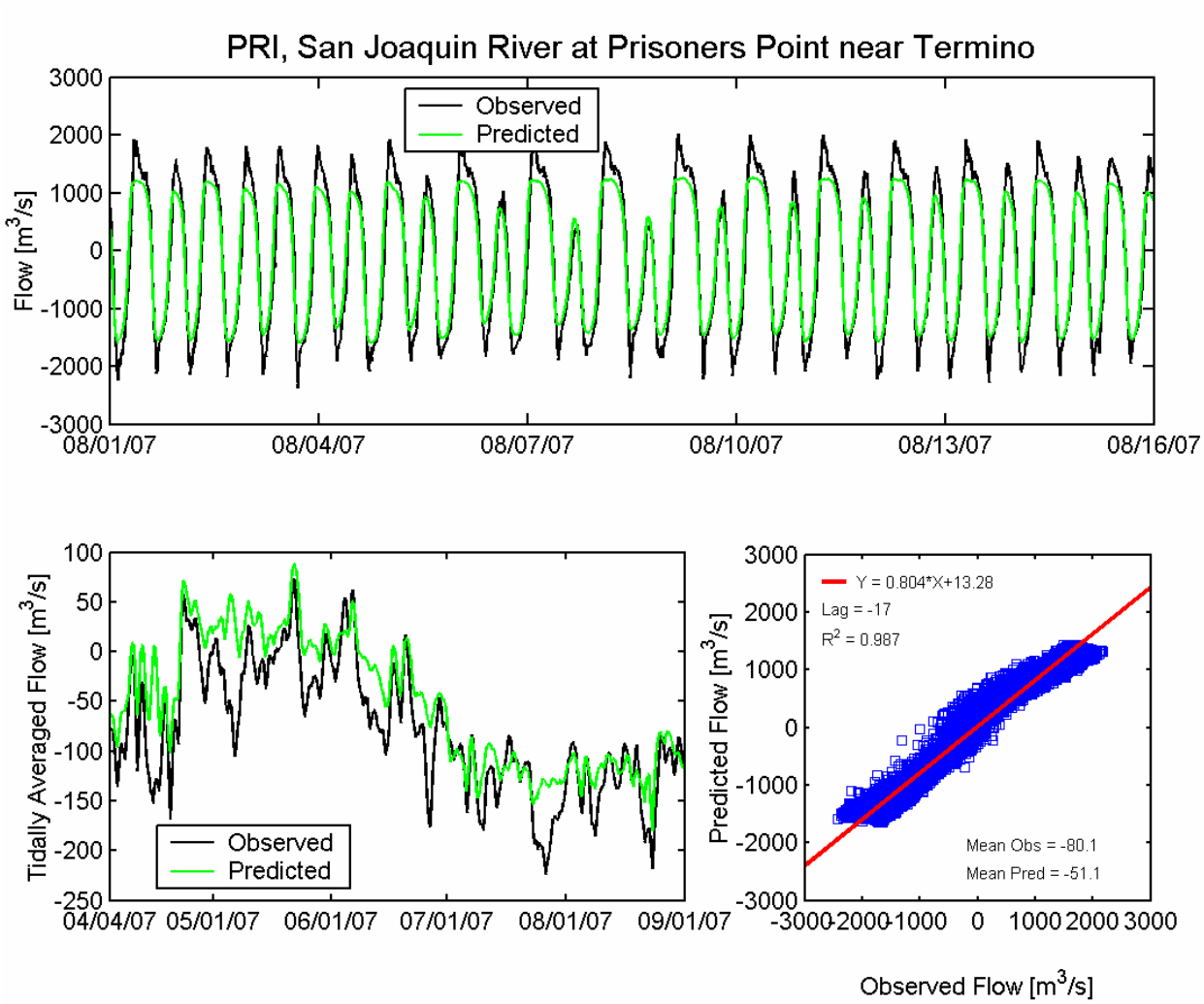

Figure 4.4-21 Observed and predicted flow at San Joaquin River at Prisoners Point USGS station (PRI) during the 2007 simulation period.

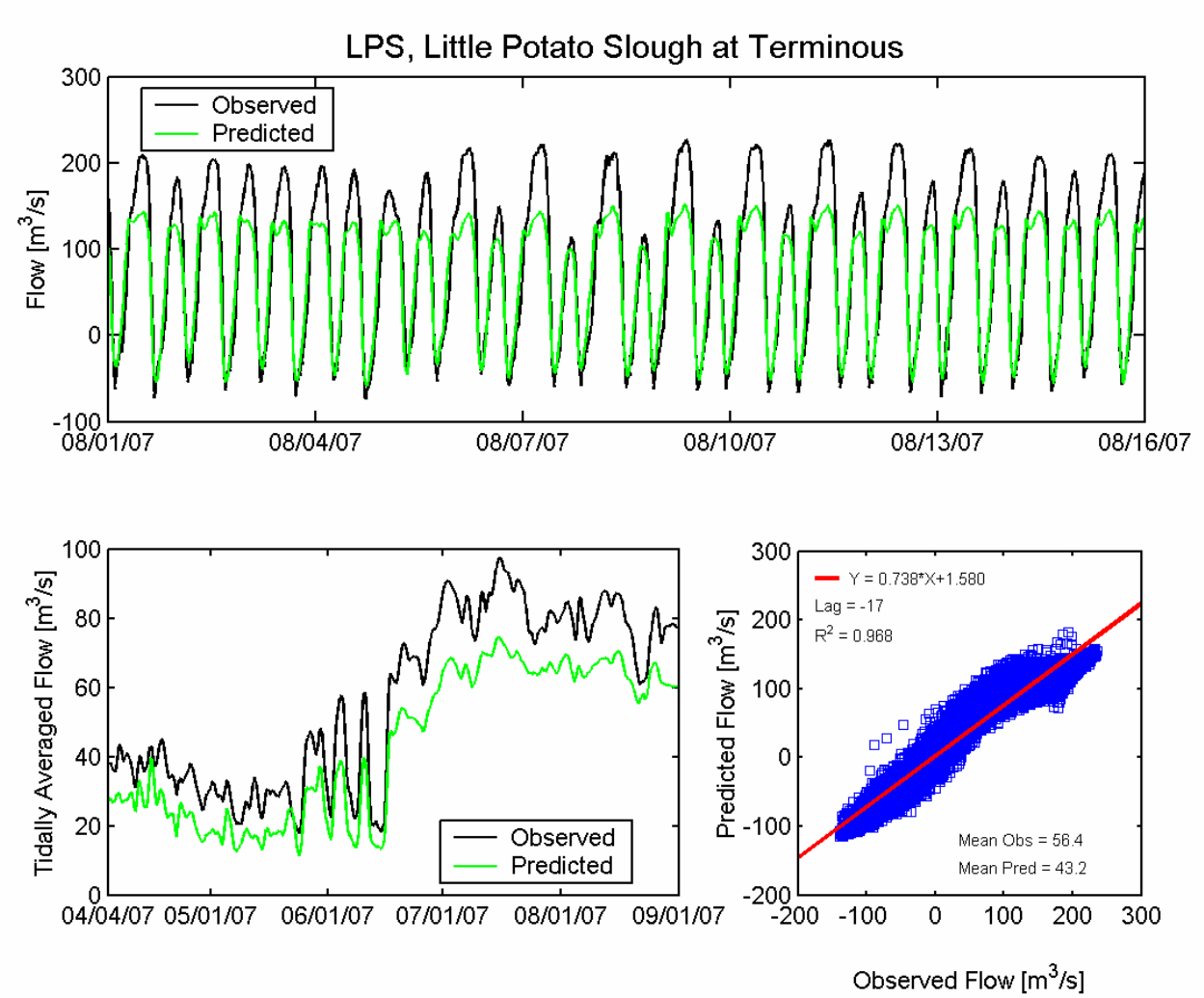

Figure 4.4-22 Observed and predicted flow at Little Potato Slough at Terminous USGS station (LPS) during the 2007 simulation period.

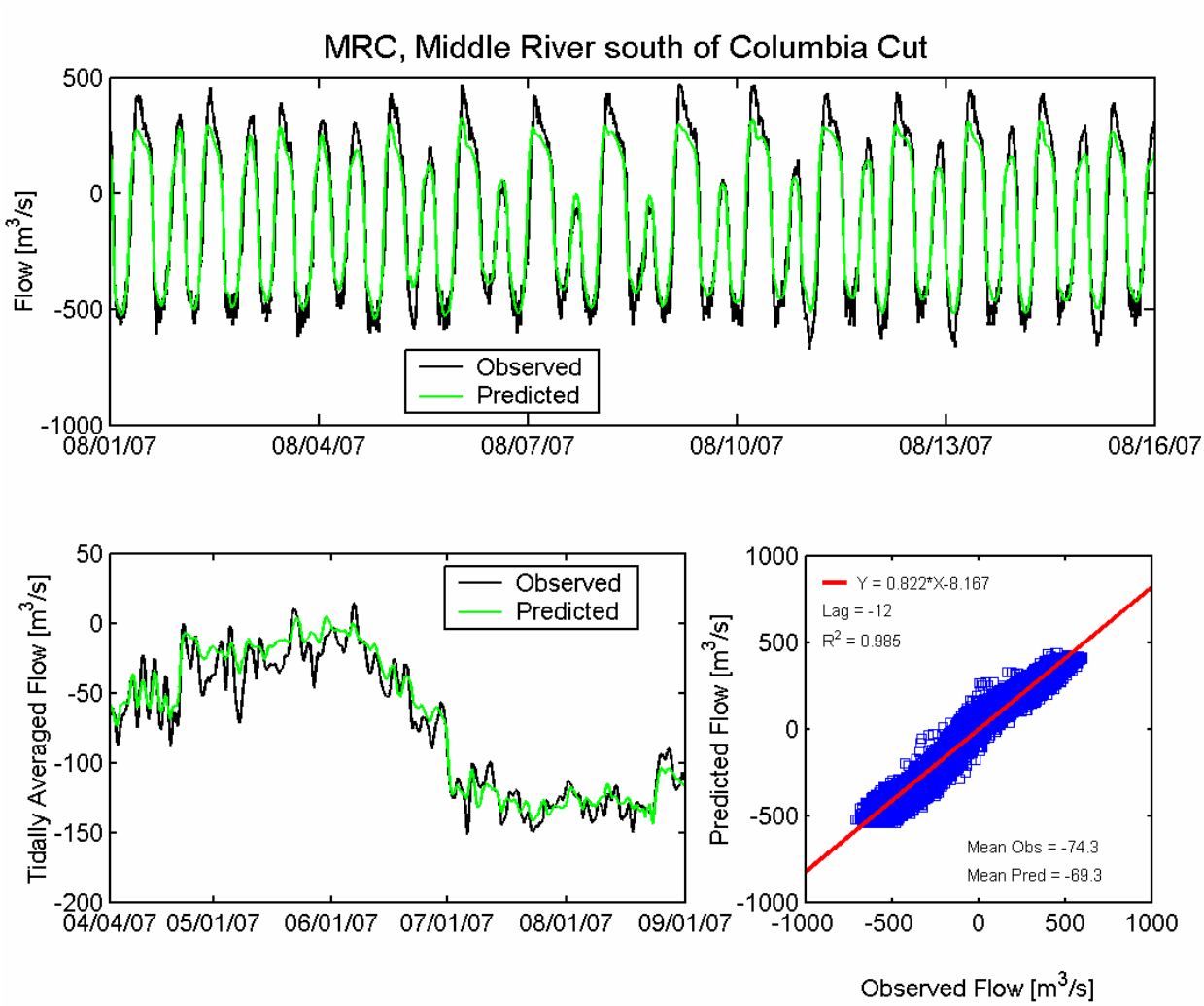

Figure 4.4-23 Observed and predicted flow at Middle River south of Columbia Cut USGS station (MRC) during the 2007 simulation period.

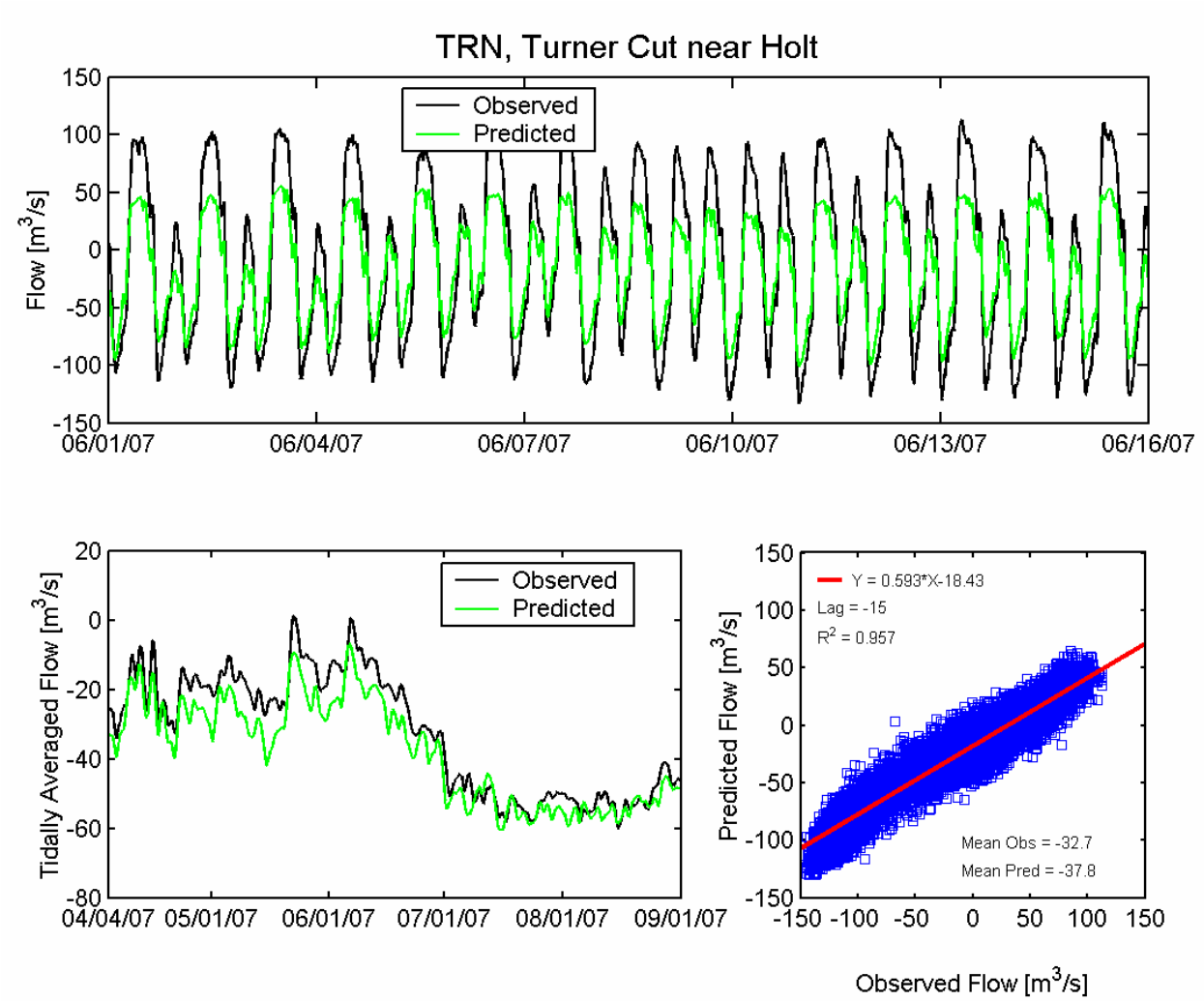

Figure 4.4-24 Observed and predicted flow at Turner Cut near Holt USGS station (TRN) during the 2007 simulation period.

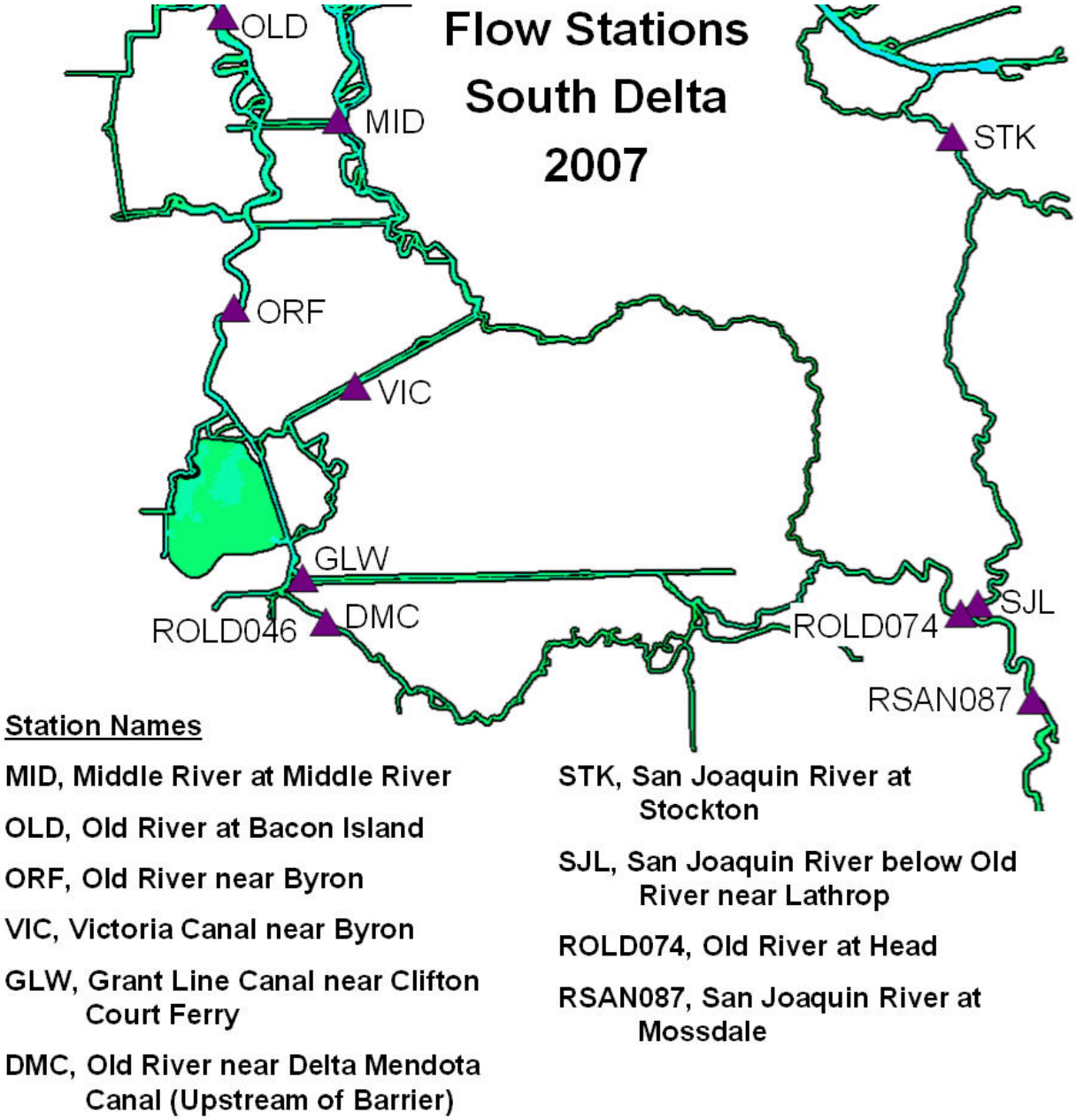

Figure 4.4-25 Location of flow monitoring stations in the southern portion of the Sacramento-San Joaquin Delta used for 2007 flow calibration.

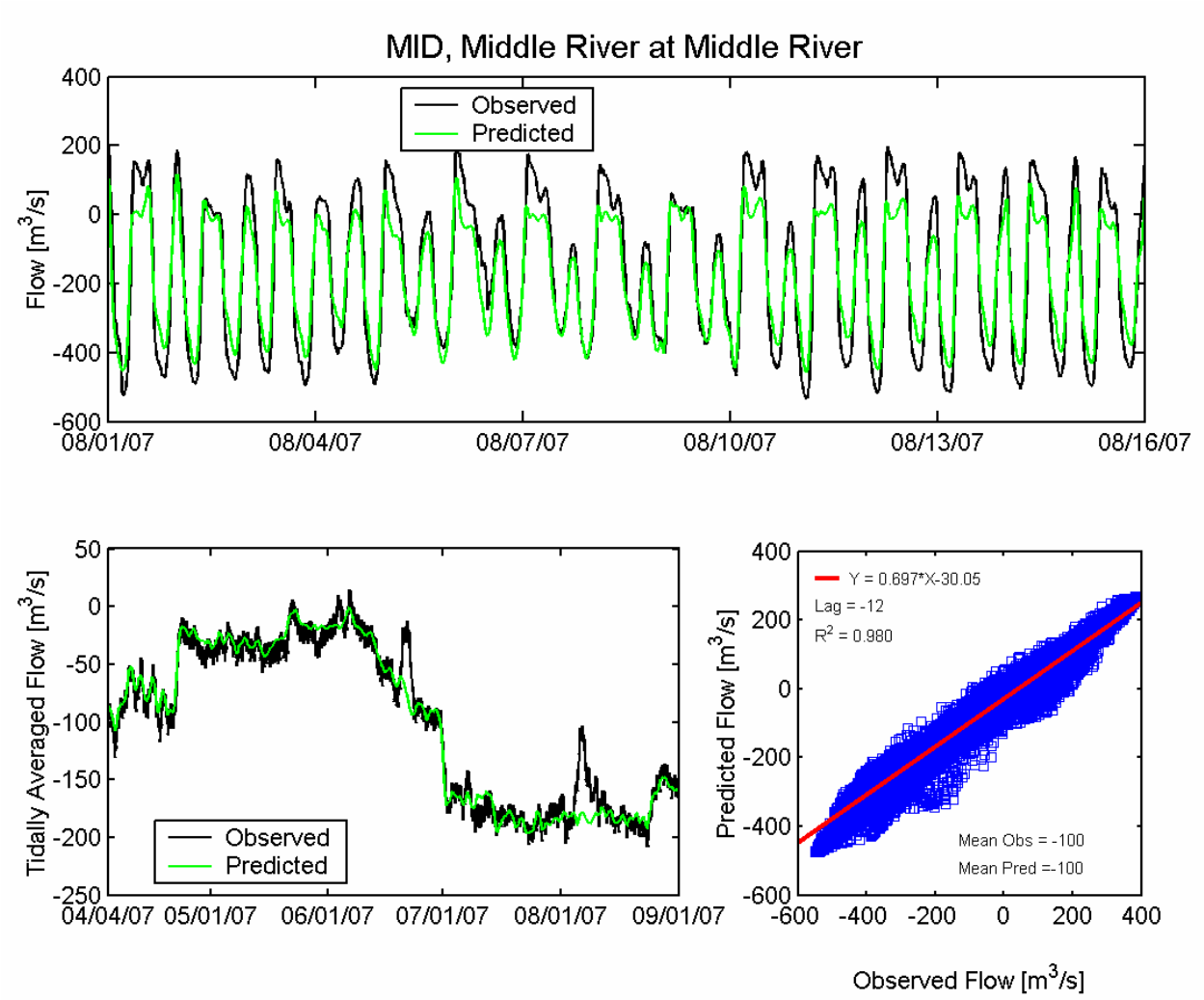

Figure 4.4-26 Observed and predicted flow at Middle River at Middle River USGS station (MID) during the 2007 simulation period.

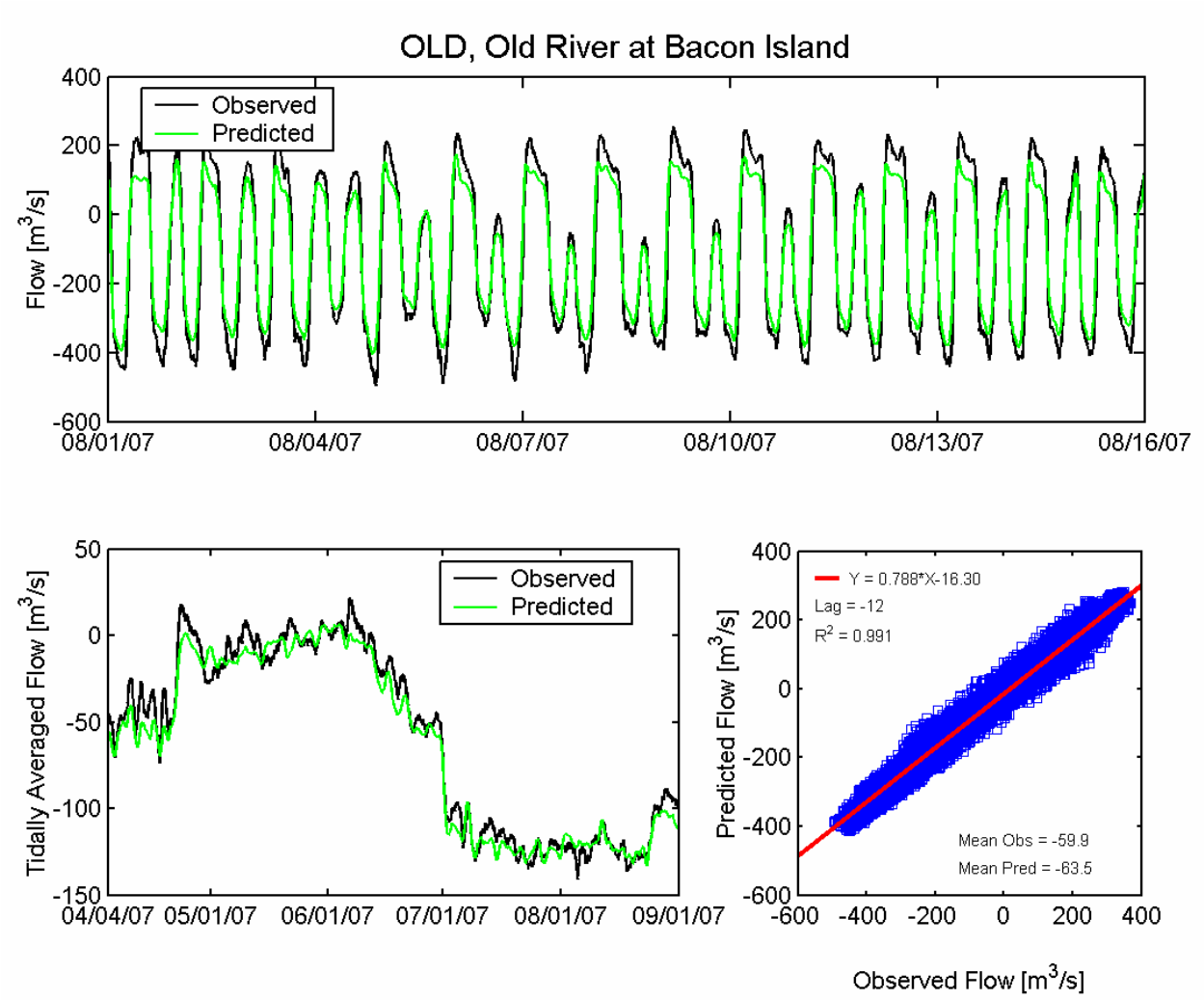

Figure 4.4-27 Observed and predicted flow at Old River at Bacon Island USGS station (OLD) during the 2007 simulation period.

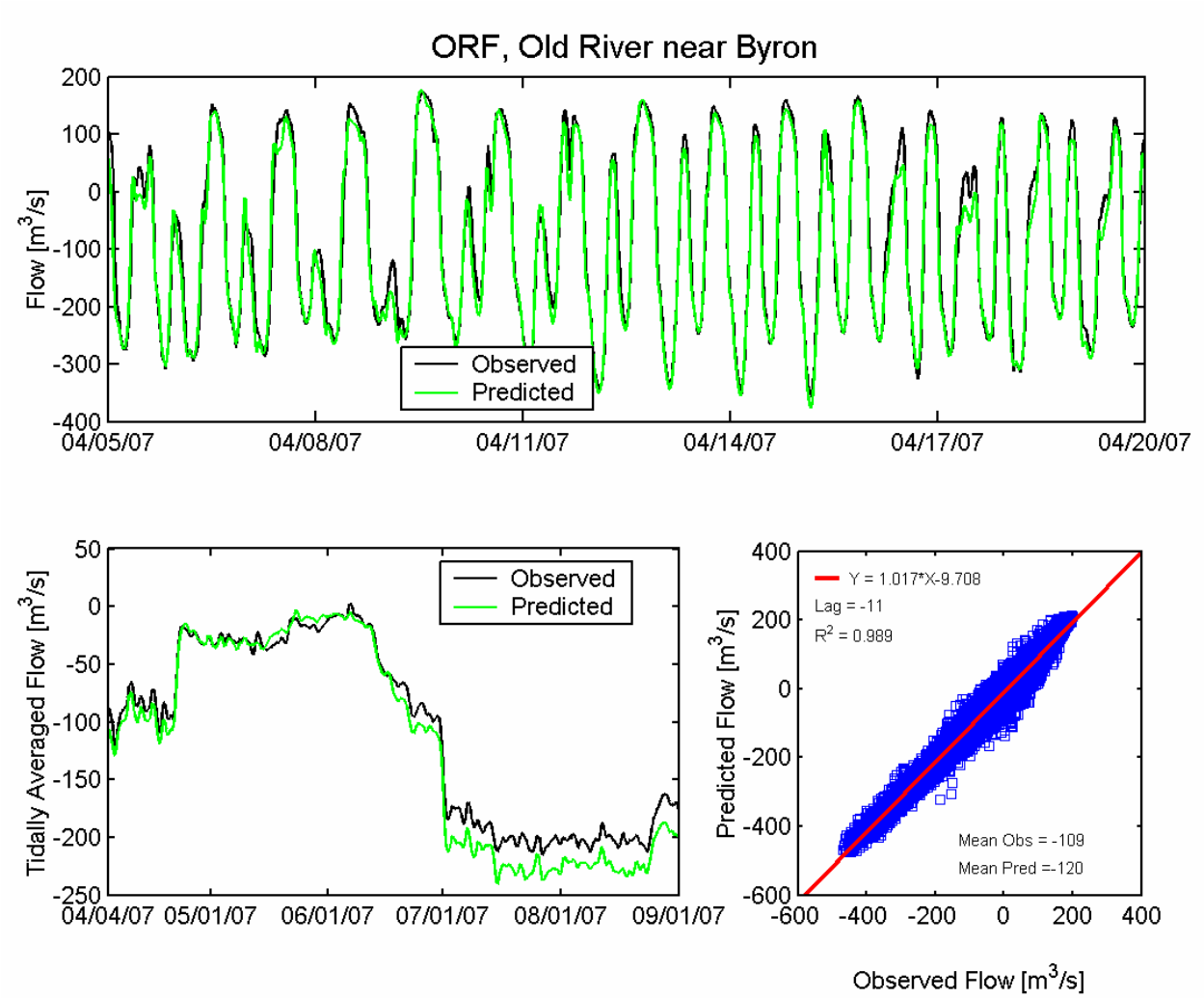

Figure 4.4-28 Observed and predicted flow at Old River near Byron USGS station (ORF) during the 2007 simulation period.

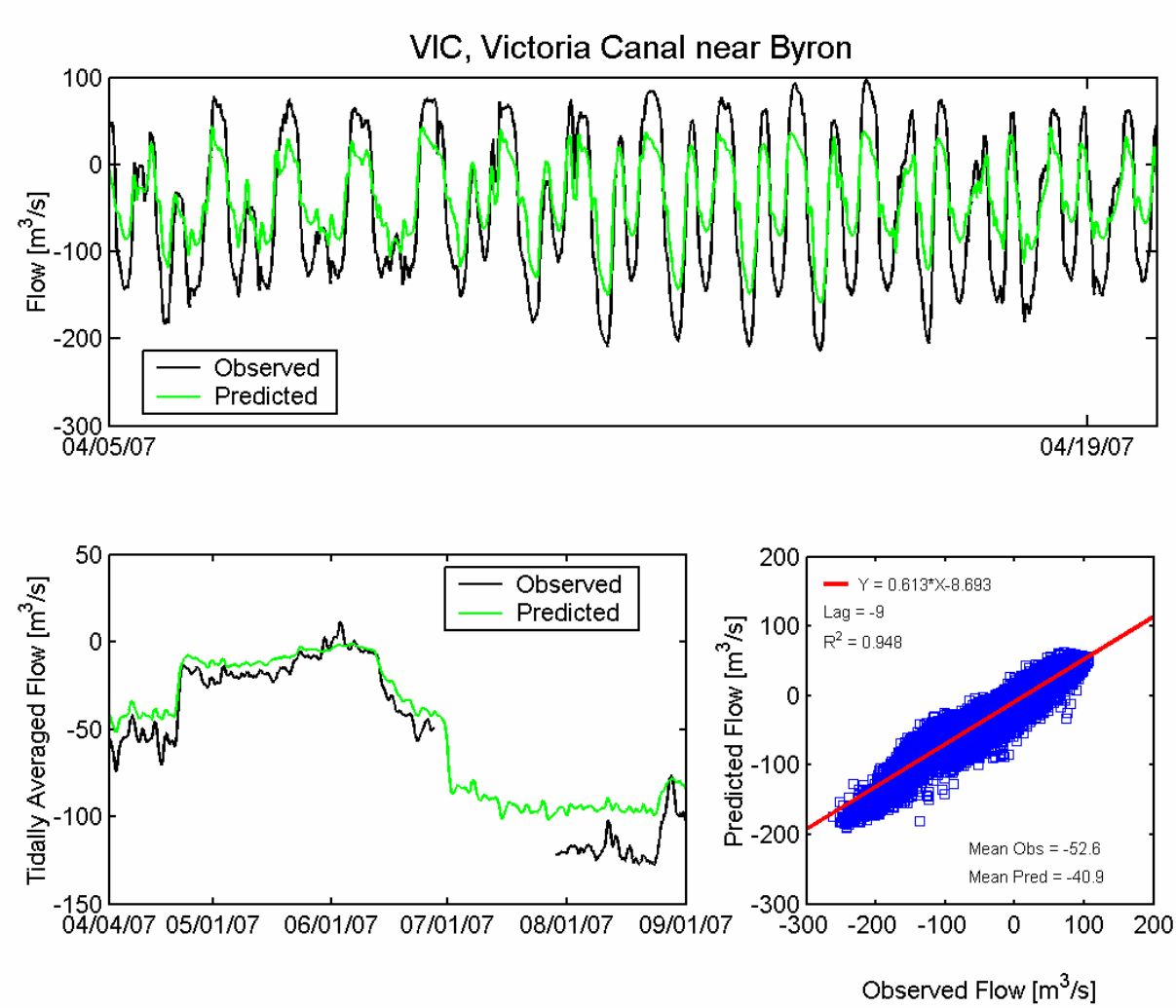

Figure 4.4-29 Observed and predicted flow at Victoria Canal near Byron USGS station (VIC) during the 2007 simulation period.

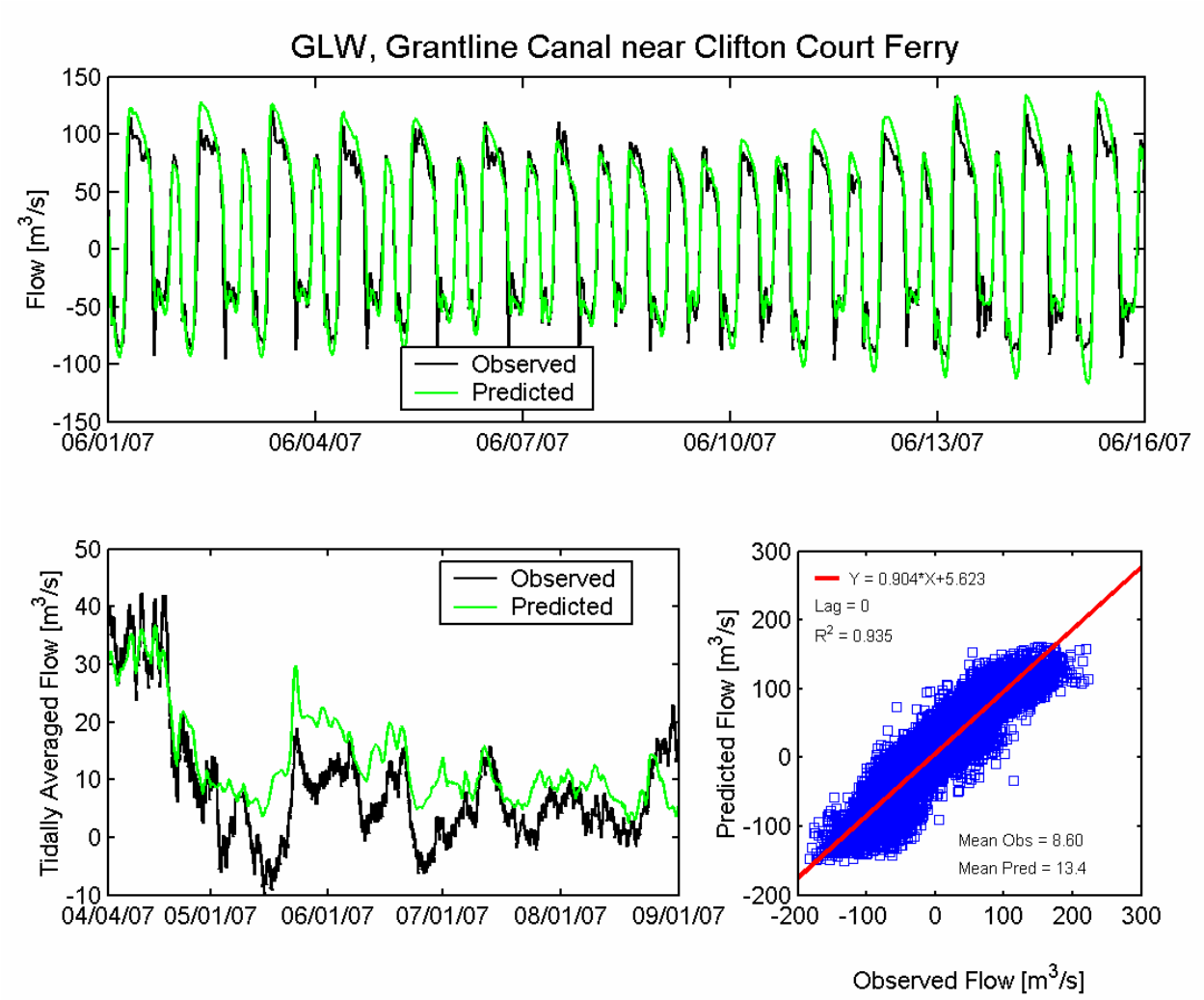

Figure 4.4-30 Observed and predicted flow at Grant Line Canal near Clifton Court Ferry USGS station (GLW) during the 2007 simulation period.

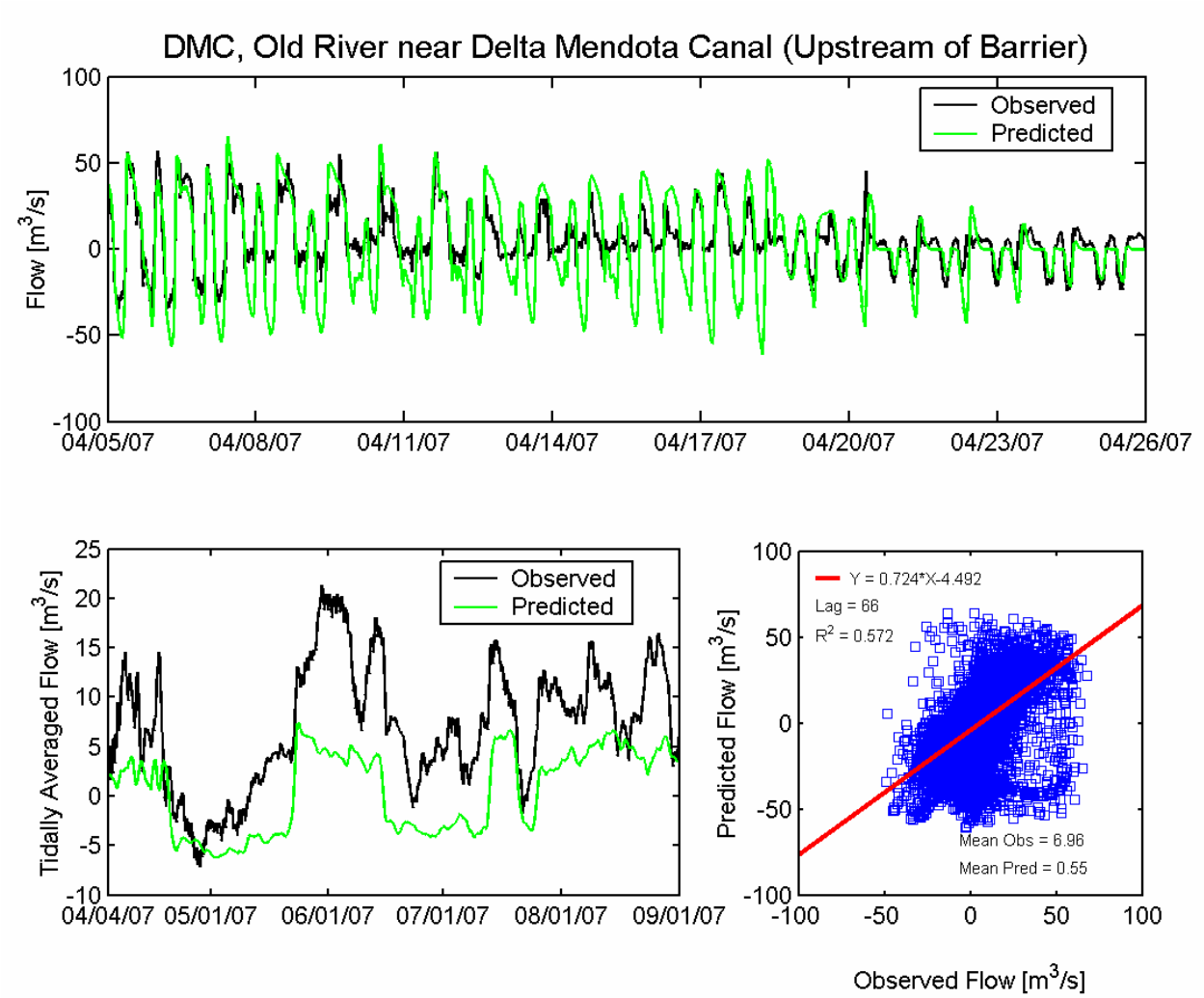

Figure 4.4-31 Observed and predicted flow at Old River near Delta Mendota Canal Upstream of Barrier USGS station (DMC) during the 2007 simulation period.

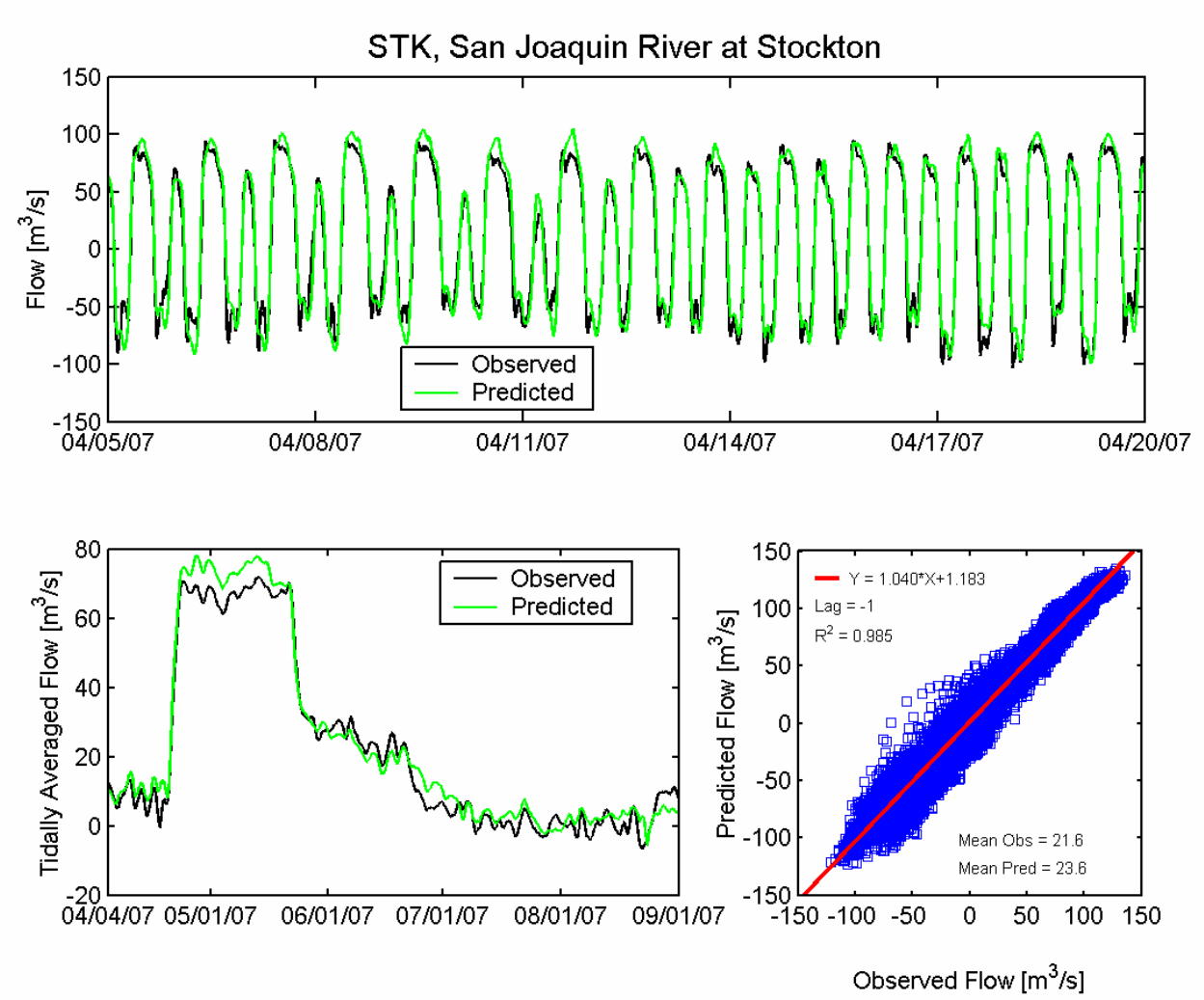

Figure 4.4-32 Observed and predicted flow at San Joaquin River at Stockton USGS station (STK) during the 2007 simulation period.

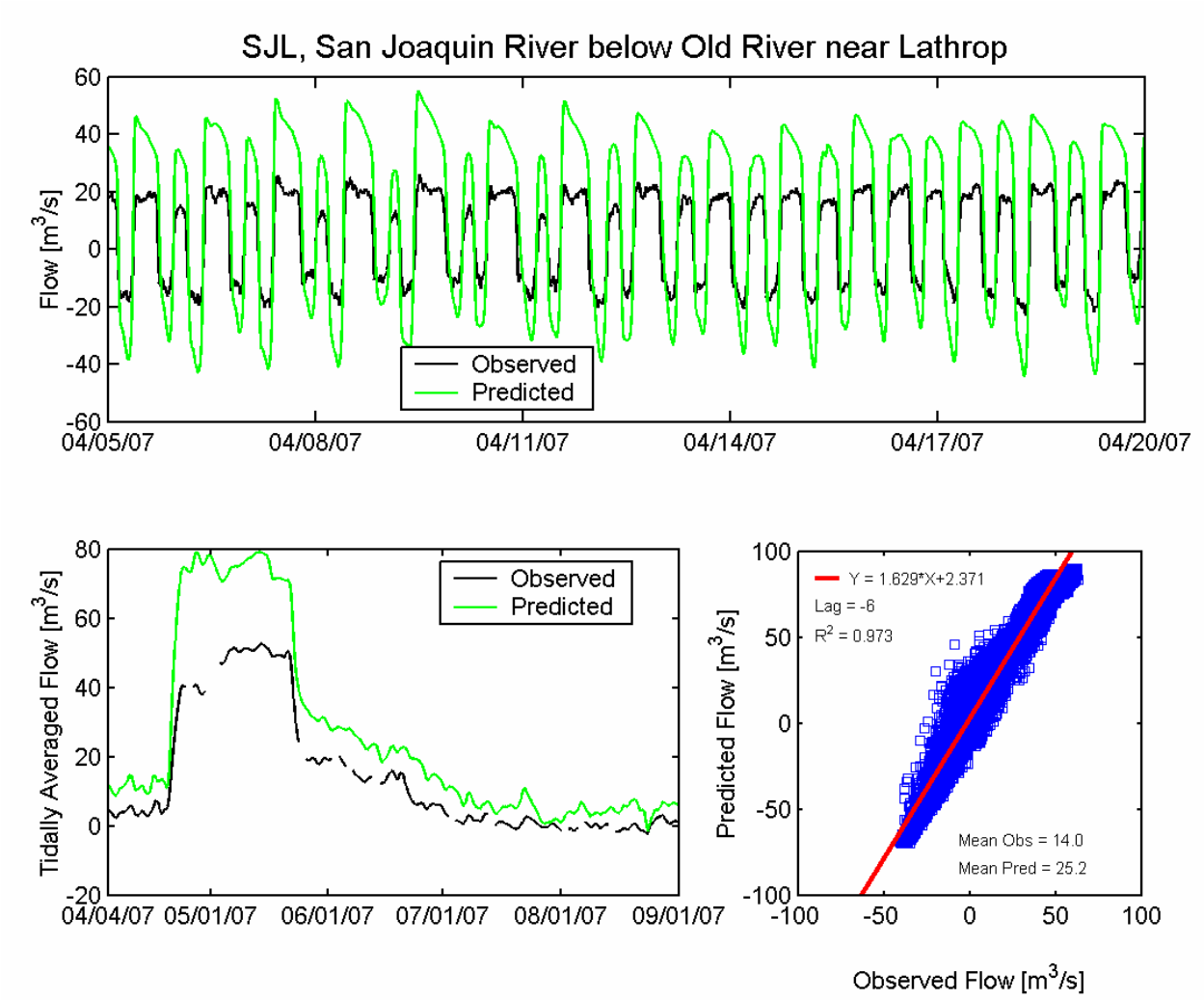

Figure 4.4-33 Observed and predicted flow at San Joaquin River below Old River near Lathrop DWR station (CDEC SJL) during the 2007 simulation period.

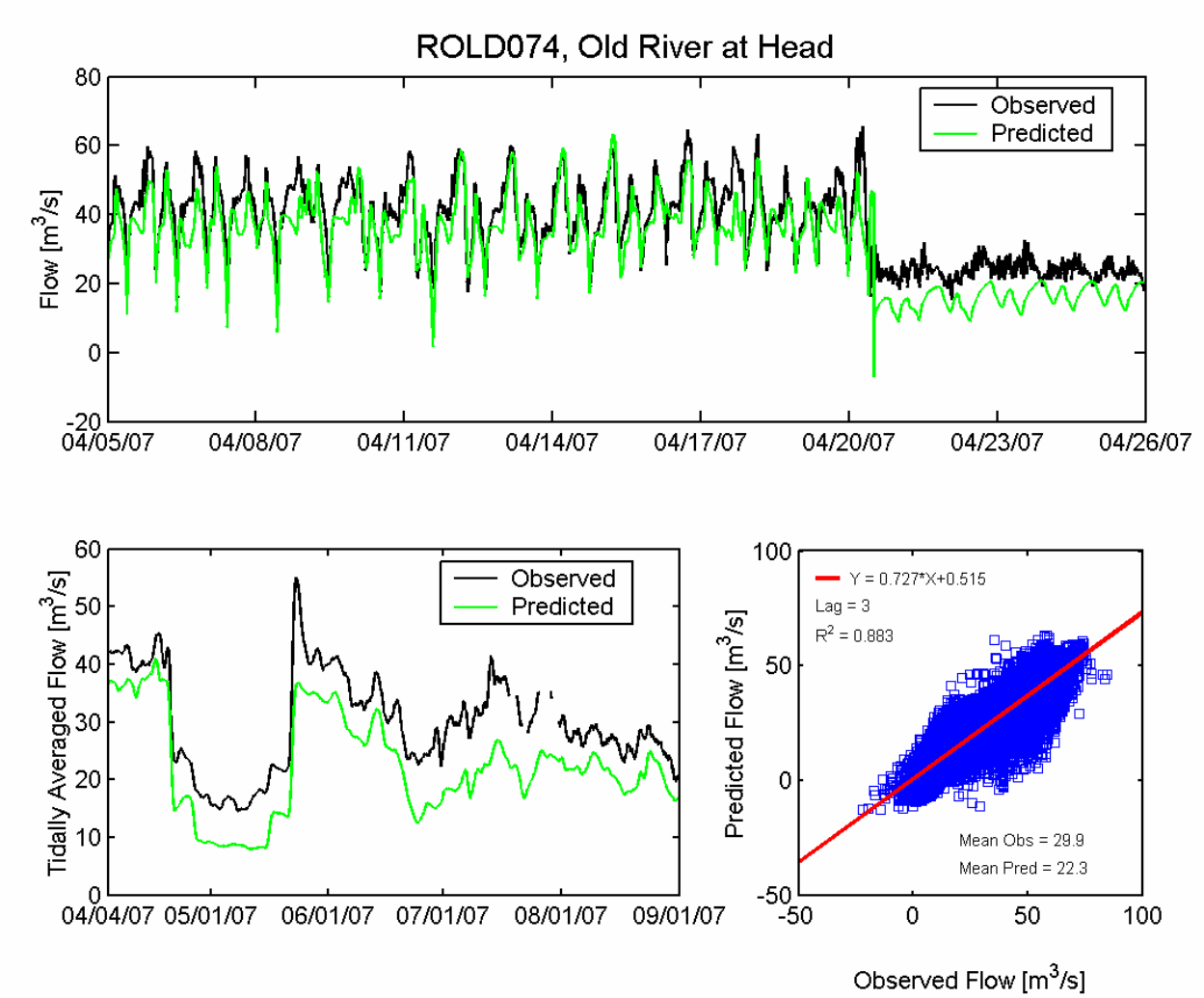

Figure 4.4-34 Observed and predicted flow at Old River at Head DWR station (ROLD074) during the 2007 simulation period.

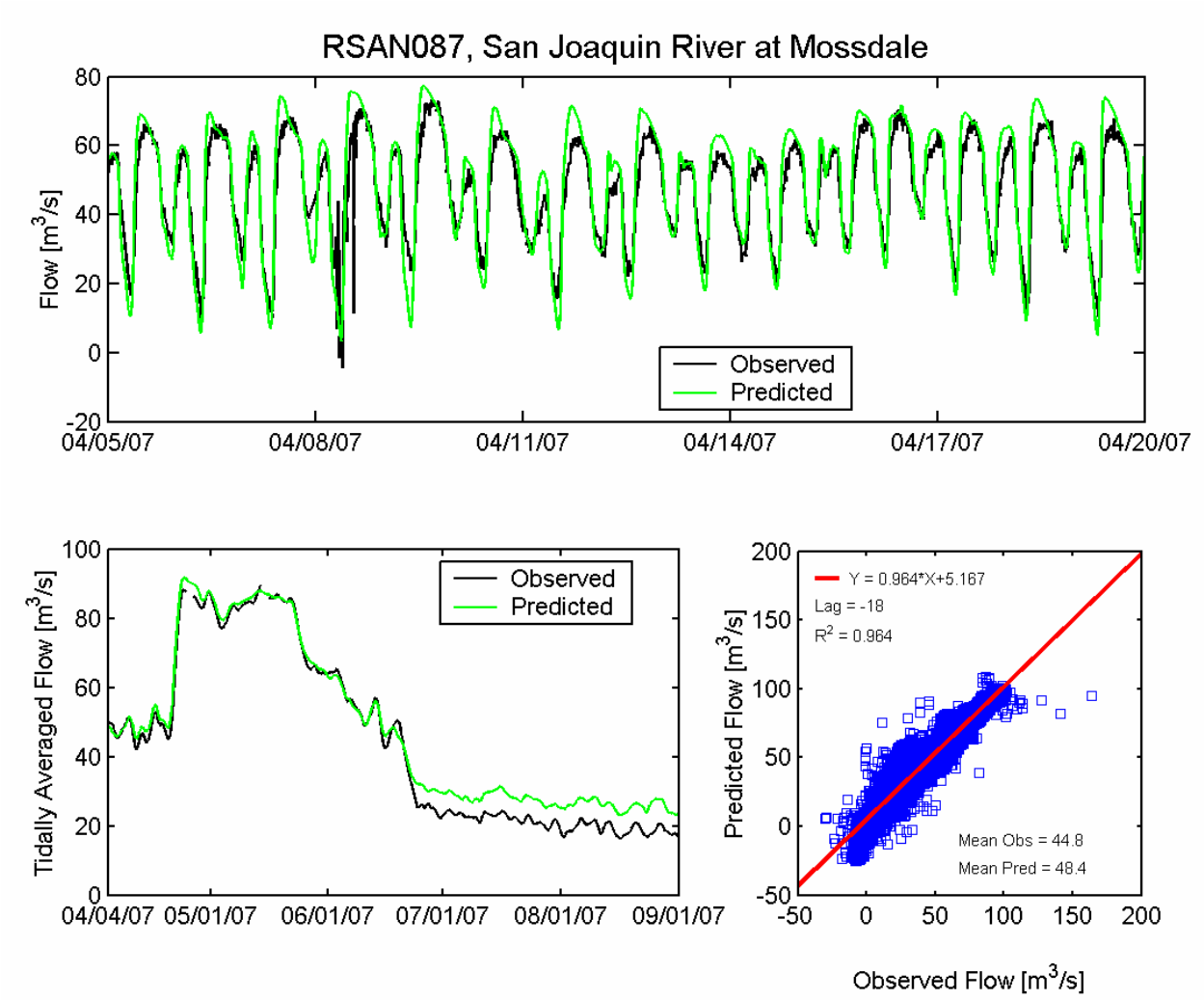

Figure 4.4-35 Observed and predicted flow at San Joaquin River at Mossdale DWR station (RSAN087) during the 2007 simulation period.

5. Model Validation

The hydrodynamic calibration indicates the ability of the Bay-Delta UnTRIM model to accurately predict water levels (stage) and flows in the San Francisco Bay and Sacramento-San Joaquin Delta. In order to validate these results, an additional period was simulated using the same approach and model parameters used during the calibration period, and the predicted water levels and flows were compared with observed water levels and flows. This section provides an extensive set of comparisons between observed and predicted water levels and flows at observation stations in San Francisco Bay and the Sacramento San Joaquin Delta for the model validation period in 2002.

5.1 Description of 2002 Simulation Period

The 2002 simulation period that spans from May 6, 2002 through September 1, 2002 was used as the model validation period in this study. This period was selected for model validation due to the available monitoring data around Franks Tract, collected by the USGS in 2002. This period was also used for model calibration of RMA2 for the Flooded Islands Pre-Feasibility Study (RMA, 2005) and for UnTRIM in the DRMS Project (MacWilliams and Gross, 2007).

Figure 5.1-1 shows the historical barrier operations schedule during the 2002 simulation period. During periods when the barriers are closed, no flow is allowed through the barrier. When the barrier is open, no barrier controls are specified and the channel operates normally. During periods when the barrier is operational, the weir and culvert configurations are implemented as discussed in Section 3.12 and described in the historical operations log (DWR, 2008b).

5.2 Water Level Validation

The validation of stage in the UnTRIM Bay-Delta Model entails comparing observed and predicted water levels over the analysis period following the approach outlined in Section 4.1. The water level validation period spans from May 8, 2002 through September 1, 2002. Observed and predicted water levels were compared at five NOAA stations in San Francisco Bay and at forty-three stations in the Sacramento-San Joaquin Delta.

The approach used for water level validation is identical to the approach used for water level calibration described in Section 4.3. At each station, observed and predicted water levels were plotted over a fifteen day period to show the water level agreement over tidal time scales. In addition, the observed and predicted stage are tidally-averaged, to assess the accuracy of the model in predicting water level variability on spring-neap time scales, as well as non-tidal forcing such as storms. Lastly, the cross-correlation procedure (as described in Section 4.1) was used to determine the mean observed and predicted water level, the amplitude ratio, the phase lag, and the correlation coefficient squared (R^2). For each of the water level stations, these values are compiled in Table 5-1.

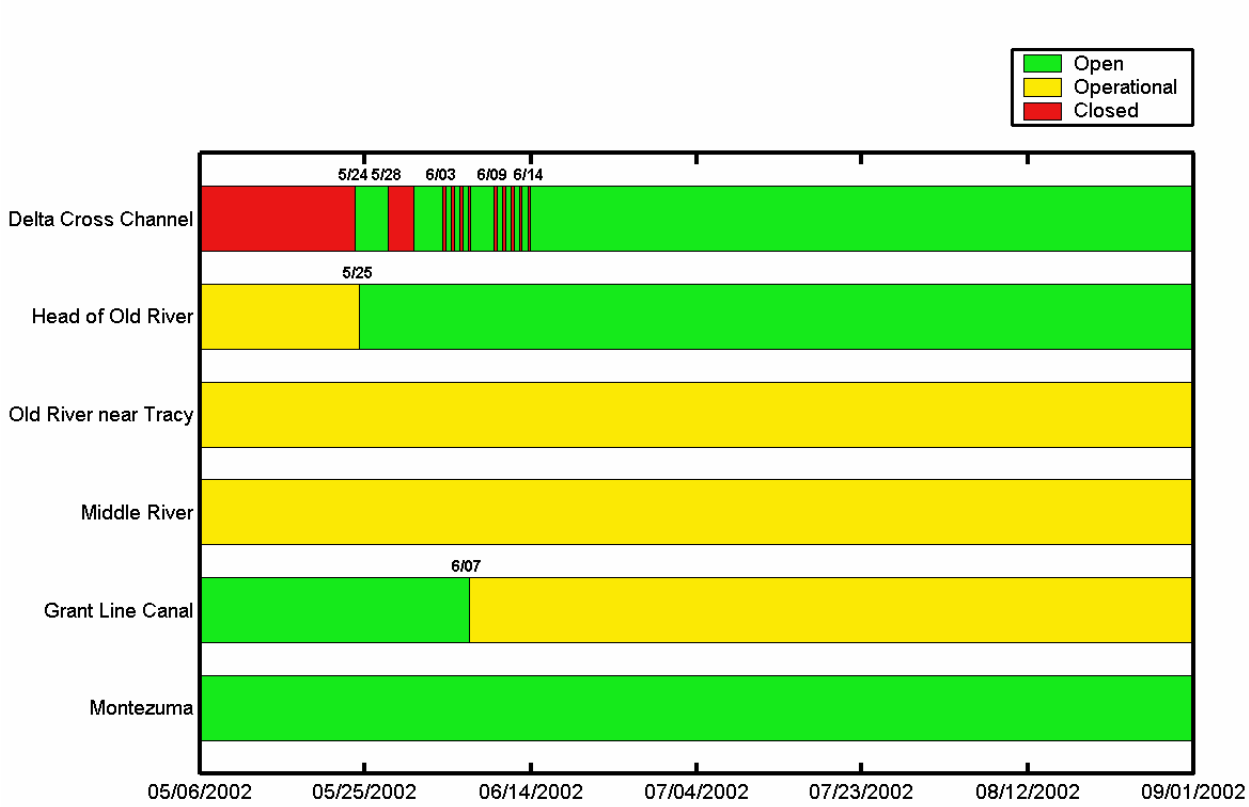

Figure 5.1-1 Historical barrier operations schedule during the 2002 simulation period.

In San Francisco Bay, the datum of each water level observation station is well-defined and variations between observed and predicted mean water levels are typically small. However, in the Delta, water levels at some stations are measured relative to an arbitrary datum. Where station datum information was available, the observed water levels were converted to NGVD29 as described in Section 3.2. At stations where it was not possible to definitively reference the observed stage to NGVD, an arbitrary vertical datum correction was applied such that the observed mean water level was identical to the predicted mean water level in NGVD. Stations where an arbitrary vertical correction was made to the observed data are indicated with a "*" where the observed mean water level is given in Table 5-1. At these stations, comparison of absolute stage is not possible, however, the cross-correlation analysis is not affected by the vertical datum and the amplitude ratio, phase lag, and R^2 values all provide useful measures of model performance even for stations where the vertical datum of the observed stage is arbitrary.

5.2.1 San Francisco Bay

Water level calibration comparisons were performed at five NOAA continuous observation stations in the San Francisco Estuary at the locations shown in Figure 5.2-1. At the Fort Point (NOAA station 9414290), the observed and predicted water levels are nearly identical, indicating that the applied offset and amplification at the simplified ocean boundary is accurately propagating tides into the estuary (Figure 5.2-2). The cross-correlation analysis shows a phase lag of 0 minutes indicating the model is exactly in phase with observed tides, an amplitude ratio

of 1.001 indicating that observed and predicted tidal range is nearly identical, and an R^2 of 0.999. These values are identical to the cross-correlation statistics at Fort Point during the 2007 calibration period, and demonstrate that the ocean boundary condition is accurately propagating tides into the estuary. At Alameda (NOAA station 9414750), the observed and predicted water levels show a similar level of agreement (Figure 5.2-3), with a phase lag of 19 minutes, an amplitude ratio of 1.016 and an R^2 of 0.998. The observed and predicted water levels show a slight difference of 0.02 m in the mean water level, and the model accurately predicts trends in the tidally-averaged stage. A similar level of agreement is achieved at Redwood City (NOAA station 9414523) and at Richmond (NOAA station 9414863), as seen in Figure 5.2-4 and 5.2-5, respectively. At Port Chicago (NOAA station 9415144), the observed and predicted water levels show good agreement (Figure 5.2-6), with a phase lag of 16 minutes, an amplitude ratio of 0.951 indicating slightly lower predicted tidal amplitude than the observed tidal amplitude, and an R^2 of 0.998. Overall, the comparison between observed and predicted water levels in San Francisco Bay for the validation are very similar to the results achieved for the calibration period presented in Section 4.3.1.

5.2.2 Northern Sacramento-San Joaquin Delta

Water level calibration comparisons were performed at ten continuous water level observation stations in the northern portion of the Delta, at the locations shown in Figure 5.2-7. Water level comparisons at these stations are shown in Figures 5.2-8 through 5.2-15.

Predicted and observed water levels in the Sacramento River South of Georgiana Slough (Figure 5.2-8), in Georgiana Slough near the Sacramento River (Figure 5.2-9), in the Delta Cross Channel (Figure 5.2-10), and in the Sacramento River North of the Delta Cross Channel (Figure 5.2-11) all show similar correlation with amplitude ratios between 1.03 and 1.10, a phase difference of 5 to 14 minutes, and R^2 values ranging from 0.959 to 0.991. At these four stations near the Delta Cross Channel, the predicted tidal amplitude is about 7 to 10% greater than the observed tidal amplitude, which is similar to the result for the 2007 period. It is believed that this amplification may be party caused by not accurately representing the full extent of the marsh areas in Snodgrass Slough east of the Delta Cross Channel or by reflection off of the upstream boundaries. Further east in the Mokelumne River near Thornton (Figure 5.2-12), the amplitude ratio is 1.14, suggesting that additional amplification is occurring near the model boundary on the upstream portion of the Mokelumne River, similar to that observed in the 2007 period. In the South Fork of the Mokelumne River at New Hope Bridge (Figure 5.2-13), predicted water levels show good agreement with observed water levels, with a phase lag of 14 minutes, an amplitude ratio of 1.078 and an R^2 of 0.991.

In Steamboat Slough (Figure 5.2-14) predicted water levels agree well with observed water levels, with slightly higher predicted than observed tidal range, with an amplitude ratio of 1.106, a phase lag of 7 minutes, and an R^2 of 0.984. On the Sacramento River at Freeport (Figure 5.2-15), the observed and predicted water levels show good agreement, with a phase lead of 34 minutes, an amplitude ratio of 1.034 and an R^2 of 0.982. These results are also similar to the water levels comparisons at these stations for the 2007 calibration period.

5.2.3 Central Sacramento-San Joaquin Delta

Water level calibration comparisons were performed at sixteen continuous water level observation stations in the central portion of the Delta, at the locations shown in Figure 5.2-16. Water level comparisons at these stations are shown in Figures 5.2-17 through 5.2-35.

On the San Joaquin River at Antioch (Figure 5.2-17), the observed and predicted water levels show good agreement, with a phase lag of 20 minutes, an amplitude ratio of 0.926 and an R^2 of 0.997. The observed and predicted tidally-averaged stage show nearly identical agreement. Since Antioch is near the seaward boundary of the Delta, this indicates that the model accurately predicts spring-neap filling and draining of the Delta. The vertical datum offset seen in the 2007comparison is not evident for this period.

At Rio Vista (Figure 5.2-18), predicted water levels show good agreement with observed water levels, with a phase lag of 16 minutes, an amplitude ratio of 0.982 and an R^2 of 0.995. The predicted tidally-averaged stage shows nearly-identical trends to the observed tidally-averaged stage indicating that the spring-neap filling and draining of the northern regions of the Delta, which include Liberty Island, the Sacramento Deep Water Ship Channel, and Steamboat Slough, and the Sacramento River. In Threemile Slough (Figure 5.2-19), Jersey Point (Figure 5.2-20), False River (Figure 4.3-21), and Dutch Slough (Figure 5.2-22), predicted and observed water levels are nearly identical with an amplitude ratio between 0.987 and 1.033, phase differences of between 6 and 27 minutes, and an R^2 of 0.994 to 0.996. Overall, the predicted stage shows very good agreement with observed stage at these four stations in the western Delta, in terms of amplitude, phase, and spring-neap variations in tidally-averaged stage, similar to the results achieved at these stations for the 2007 period.

Comparisons between observed and predicted water levels at two temporary USGS stations near Franks Tract in Taylor Slough (Figure 5.2-23) and Sand Mound Slough (Figure 5.2-24) show similar correlation, with amplitude ratios of 1.040 and 1.022, phase lags of 24 and 27 minutes, and R^2 values of 0.995 and 0.989, respectively.

At the remaining eleven central Delta stations at which observation data are available during the 2002 period—San Joaquin River at San Andreas Landing (Figure 5.2-25), Old River at the San Joaquin River (Figure 5.2-26), the Mokelumne River near the San Joaquin River (Figure 4.3-27), North Fork of Mokelumne River at Georgiana Slough (Figure 5.2-28), Franks Tract East (Figure 5.2-29), Franks Tract West (Figure 5.2-30), Old River at Mandeville Island (Figure 5.2-31), Holland Cut (Figure 5.2-32), San Joaquin River at Venice Island (Figure 5.2-33), San Joaquin River at Rindge Pump (Figure 5.2-34), and Middle River south of Columbia Cut (Figure 5.2-35)—the cross correlation demonstrates that the predicted and observed water levels agree extremely well with amplitude ratios between 1.001 and 1.046 indicating that the predicted and observed tidal range is within 4.8 % (and within 1% at most stations), with phase differences between 10 and 29 minutes, and R^2 values between 0.992 and 0.995. These are similar to the comparisons in this region for the 2007 period, with somewhat larger phase differences evident in the 2002 period, and demonstrate that the model is accurately predicting water levels in the central Delta, in terms of amplitude, phase, and spring-neap variations in tidally-averaged stage.

5.2.4 Southern Sacramento-San Joaquin Delta

Water level calibration comparisons were performed at sixteen continuous water level observation stations in the southern portion of the Delta, at the locations shown in Figure 5.2-36. Water level comparisons at these stations are shown in Figures 5.2-37 through 5.2-52.

Water level observations are available at five stations in Middle River during the 2002 simulation period. In Middle River at Middle River (Figure 5.2-37), predicted water levels show good agreement with observed water levels, with a phase lead of 8 minutes, an amplitude ratio of 1.016 and an R^2 of 0.995. The mean predicted stage is 0.10 m less than the mean observed stage, which is likely the result of uncertainty in the observed vertical datum, results in a vertical offset on the stage and tidally-averaged stage plots. These results are nearly identical to the comparison made at this station for the 2007 period. On Middle River at Borden Highway (Figure 5.2-38), predicted water levels show good agreement with observed water levels, with a phase lag of 8 minutes, an amplitude ratio of 1.005 and an R^2 of 0.994. The stage in the Middle River at Tracy Boulevard (Figure 5.2-39) and at the Howard Road Bridge (Figure 5.2-40) is strongly influenced by the Middle River temporary barrier, which is in place during the entire 2002 simulation period. Both stations are upstream of the barrier. At the Howard Road Bridge, the predicted water levels show better agreement with observed water levels than during the 2007 period. However, at the Middle River at Tracy Boulevard station the model is over predicting stage at low water. Since low water levels in this reach of Middle River are in part controlled by the height of the weir on the temporary barrier, any differences between reported (and modeled) weir height and actual weir height may also account for some of these differences during the period the Middle River barrier is in place. On the Middle River at Mowry Bridge (Figure 5.2-41) predicted and observed water levels still show some differences in tidal amplitude, with an amplitude ratio of 0.885, a phase lag of 26 minutes, and an R^2 of 0.966.

At the stations along or near Old River between Bacon Island and Clifton Court Forebay—Old River at Bacon Island (Figure 5.2-42), Old River near Byron (Figure 5.2-43), and Old River at Clifton Court Ferry (Figure 5.2-44)—the cross-correlation statistics show that the model is accurately predicting water levels, with amplitude ratios between 1.007 and 1.016, phase differences of less than 8 minutes, and R^2 values between 0.992 and 0.994. A similar level of agreement between observed and predicted water levels was achieved in this region during 2007 calibration period.

The comparison of observed and predicted water levels inside Clifton Court Forebay near the radial gates (Figure 5.2-45) demonstrates that the model is capturing the daily timescale changes in water level in response to the opening and closing of the radial gates and the time-variable exports from the Banks Pumping Plant. Predicted water levels agree well with observed water levels, with a phase lead of 23 minutes, an amplitude ratio of 0.973, and an R^2 of 0.965. Comparison of tidally-averaged water levels inside Clifton Court Forebay demonstrate that the daily volume corrections applied to the hourly flows (see Section 3.7) are meeting the objective of maintaining accurate volumes inside of Clifton Court Forebay over the full simulation period.

In Grant Line Canal at Tracy Boulevard (Figure 5.2-46), predicted water levels show good agreement with observed water levels, with a phase lag of 23 minutes, an amplitude ratio of

0.955 and an R^2 of 0.970. In Old River downstream of the temporary barrier (Figure 5.2-47), predicted water levels show good agreement with observed water levels, with a phase lead of 1 minutes, an amplitude ratio of 1.002 and an R^2 of 0.989. Just upstream of the barrier in Old River (Figure 5.2-48), predicted water levels show good agreement with observed water levels, with a phase lead of 13 minutes, an amplitude ratio of 0.876 and an R^2 of 0.901. Further upstream in Old River at Tracy Boulevard (Figure 5.2-49), predicted water levels show good overall agreement with observed water levels, with an amplitude ratio of 0.922, a phase lag of 3 minutes, and an R^2 of 0.945. The overall good level of agreement between observed and predicted water levels in Grant Line Canal and Old River near the temporary barriers demonstrates that the influence of these barriers on water levels in the south Delta is being accurately represented in the UnTRIM model.

In the Stockton Ship Channel at Burns Cutoff (Figure 5.2-50), predicted water levels show good overall agreement with observed water levels, with an amplitude ratio of 0.999, a phase lag of 21 minutes, and an R^2 of 0.994, demonstrating that the model is accurately propagating tides from the Pacific Ocean to the Stockton Ship Harbor. The water level comparison for the San Joaquin River at Stockton (Figure 5.2-51), shows a similar result with an amplitude ratio of 1.021, a phase lag of 12 minutes, and an R^2 of 0.993. Further upstream on the San Joaquin River below Old River near Lathrop (Figure 5.2-52), predicted tidal amplitude is slightly higher than observed tidal amplitude, with an amplitude ratio of 1.105, a phase lag of 19 minutes, and an R^2 of 0.970. Overall, comparisons between observed and predicted water levels in the south Delta show a similar level of agreement as similar comparisons made for the 2007 period.

Table 5-1 Predicted and observed stage and cross-correlation statistics for stage monitoring stations in San Francisco Bay and the Sacramento-San Joaquin Delta during the 2002 simulation period.

Location	Data Source	Figure Number	Mean Water Level		Cross Correlation		R^2
			Observed (m)	Predicted (m)	Amp Ratio	Lag (min)	
2002 San Francisco Bay Stage Stations (Figure 5.2-1)							
San Francisco	NOAA	5.2-2	0.11	0.10	1.001	0	0.999
Alameda	NOAA	5.2-3	0.12	0.14	1.016	19	0.998
Redwood City	NOAA	5.2-4	0.15	0.14	1.007	10	0.998
Richmond	NOAA	5.2-5	0.16	0.14	1.001	12	0.998
Port Chicago	NOAA	5.2-6	0.36	0.32	0.951	16	0.998
2002 North Delta Stage Stations (Figure 5.2-7)							
Sacramento River South of Georgiana Slough	USGS	5.2-8	0.56	0.59	1.076	-7	0.991
Georgiana Slough near Sacramento River	USGS	5.2-9	0.58*	0.59	1.075	8	0.988
Delta Cross Channel	USGS	5.2-10	0.56*	0.56	1.034	14	0.959
Sacramento River North of Delta Cross Channel	USGS	5.2-11	0.56	0.60	1.101	5	0.990
Mokelumne River near Thornton	DWR	5.2-12	0.55*	0.55	1.142	-18	0.984
South Fork Mokelumne River at New Hope Bridge	DWR	5.2-13	0.49	0.51	1.078	14	0.991
Steamboat Slough between Sacramento River and Sutter Sl.	USGS	5.2-14	0.58*	0.58	1.106	7	0.984
Sacramento River at Freeport	USGS	5.2-15	0.86*	0.86	1.037	-34	0.982
2002 Central Delta Stage Stations (Figure 5.2-16)							
San Joaquin River at Antioch	DWR	5.2-17	0.37	0.37	0.926	20	0.997
Sacramento River at Rio Vista	USGS	5.2-18	0.41*	0.41	0.982	16	0.996
Threemile Slough at San Joaquin River	USGS	5.2-19	0.38*	0.38	1.033	6	0.994
San Joaquin River at Jersey Point	USGS	5.2-20	0.58	0.38	0.992	14	0.994
False River	USGS	5.2-21	0.45	0.38	1.022	27	0.996
Dutch Slough at Jersey Island	USGS	5.2-22	0.42	0.39	0.987	12	0.994
Taylor Slough	USGS	5.2-23	0.46	0.39	1.040	24	0.995
Sand Mound Slough	USGS	5.2-24	0.47	0.40	1.033	27	0.989
San Joaquin River at San Andreas Landing	DWR	5.2-25	0.38	0.40	1.027	17	0.996
Old River at San Joaquin River	USGS	5.2-26	0.47	0.41	1.046	26	0.996
Mokelumne River near San Joaquin River	USGS	5.2-27	0.52	0.41	1.005	13	0.987
North Fork of Mokelumne River at Georgiana Slough	DWR	5.2-28	0.51	0.43	1.031	10	0.995
Franks Tract East	USGS	5.2-29	0.45	0.40	1.039	27	0.995
Franks Tract West	USGS	5.2-30	0.49	0.40	1.001	29	0.979
Old River at Mandeville Island	USGS	5.2-31	0.47	0.40	1.051	27	0.996

Holland Cut	USGS	5.2-32	0.50	0.39	1.003	26	0.979
San Joaquin River at Venice Island	DWR	5.2-33	0.42	0.42	1.015	18	0.996
San Joaquin River at Rindge Pump	DWR	5.2-34	0.42	0.42	1.006	20	0.995
Middle River south of Columbia Cut	USGS	5.2-35	0.28	0.41	1.018	-14	0.995
2002 South Delta Stage Stations (Figure 5.2-36)							
Middle River at Middle River	USGS	5.2-37	0.29	0.39	1.016	-8	0.995
Middle River at Borden Highway	DWR	5.2-38	0.33	0.34	1.005	8	0.994
Middle River at Tracy Blvd	DWR	5.2-39	0.38	0.45	0.888	-3	0.974
Middle River at Howard Road Bridge	DWR	5.2-40	0.46	0.46	0.825	16	0.944
Middle River at Mowry Bridge	DWR	5.2-41	0.47	0.50	0.885	26	0.966
Old River at Bacon Island	USGS	5.2-42	0.39	0.39	1.014	8	0.994
Old River near Byron	USGS	5.2-43	0.27	0.33	1.016	-5	0.992
Old River at Clifton Court Ferry	DWR	5.2-44	0.24	0.32	1.007	-7	0.992
Clifton Court Forebay	DWR	5.2-45	-0.23	-0.22	0.973	-23	0.965
Grant Line Canal at Tracy Blvd	USGS	5.2-46	0.26	0.30	0.955	23	0.970
Old River near Delta Mendota Canal (Downstream of Barrier)	DWR	5.2-47	0.22	0.31	1.002	-1	0.989
Old River near Delta Mendota Canal (Upstream of Barrier)	USGS	5.2-48	0.41	0.47	0.876	-13	0.901
Old River at Tracy Blvd	DWR	5.2-49	0.40	0.48	0.922	3	0.945
Stockton Ship Channel at Burns Cutoff	DWR	5.2-50	0.48	0.43	0.999	21	0.994
San Joaquin River at Stockton	USGS	5.2-51	0.40	0.44	1.021	12	0.993
San Joaquin River below Old River near Lathrop	DWR	5.2-52	0.62*	0.62	1.105	19	0.970

* Observed data are measured relative to arbitrary vertical datum. Observed data are offset to match predicted mean water level for comparison plots.

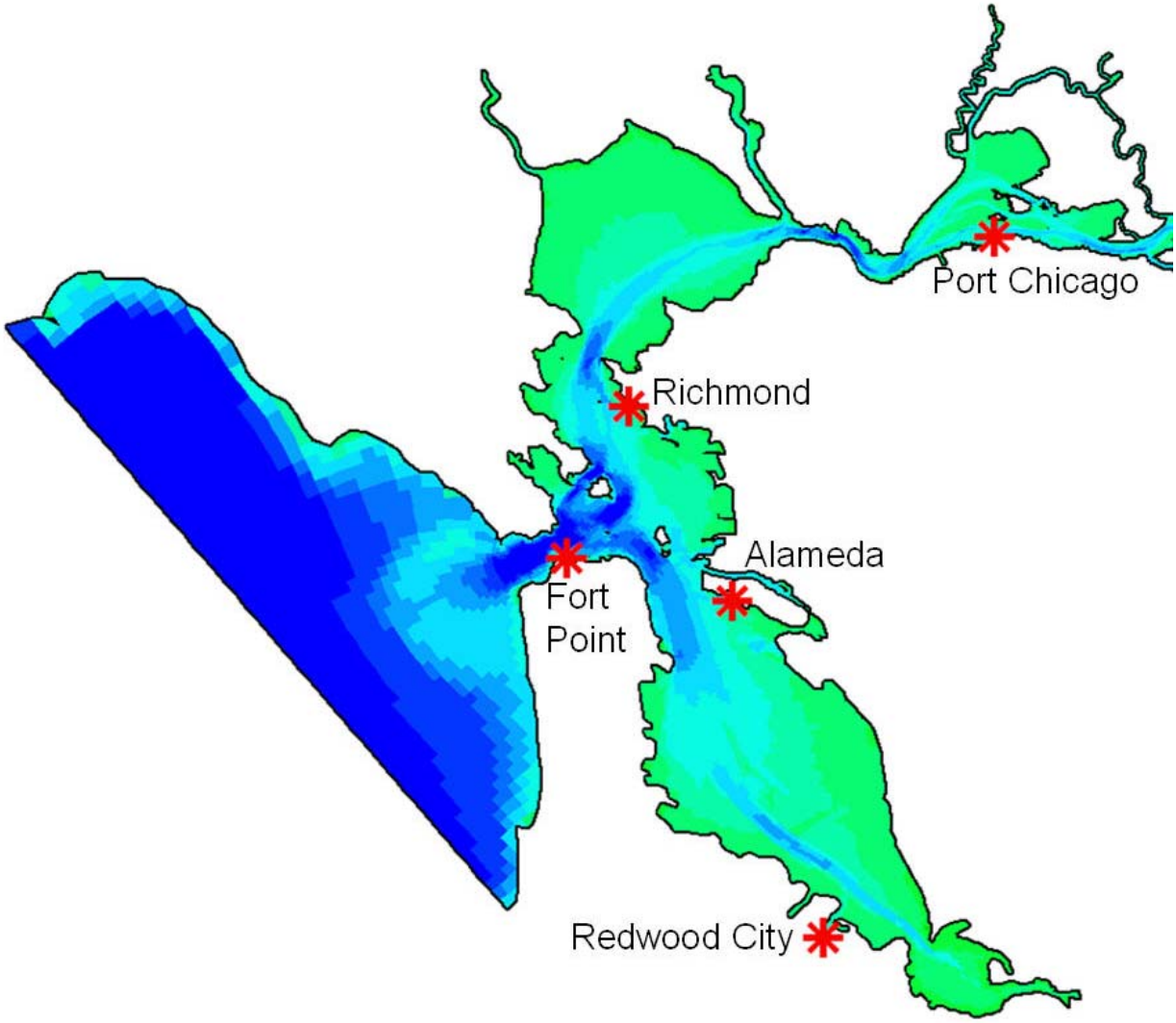

Figure 5.2-1 Location of NOAA water level monitoring stations in San Francisco Bay used for 2002 stage calibration.

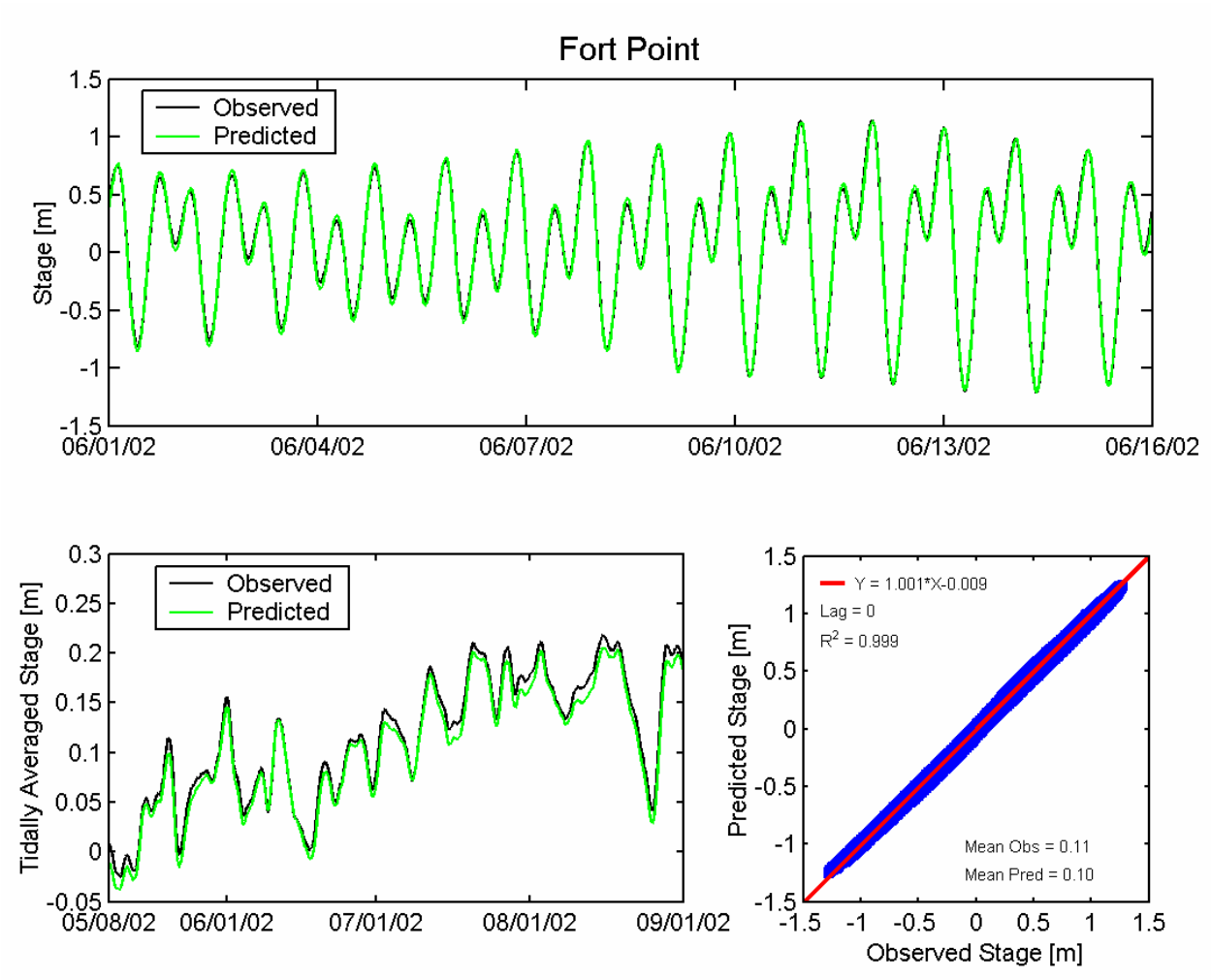

Figure 5.2-2 Observed and predicted stage at San Francisco Fort Point NOAA station (9414290) during the 2002 simulation period.

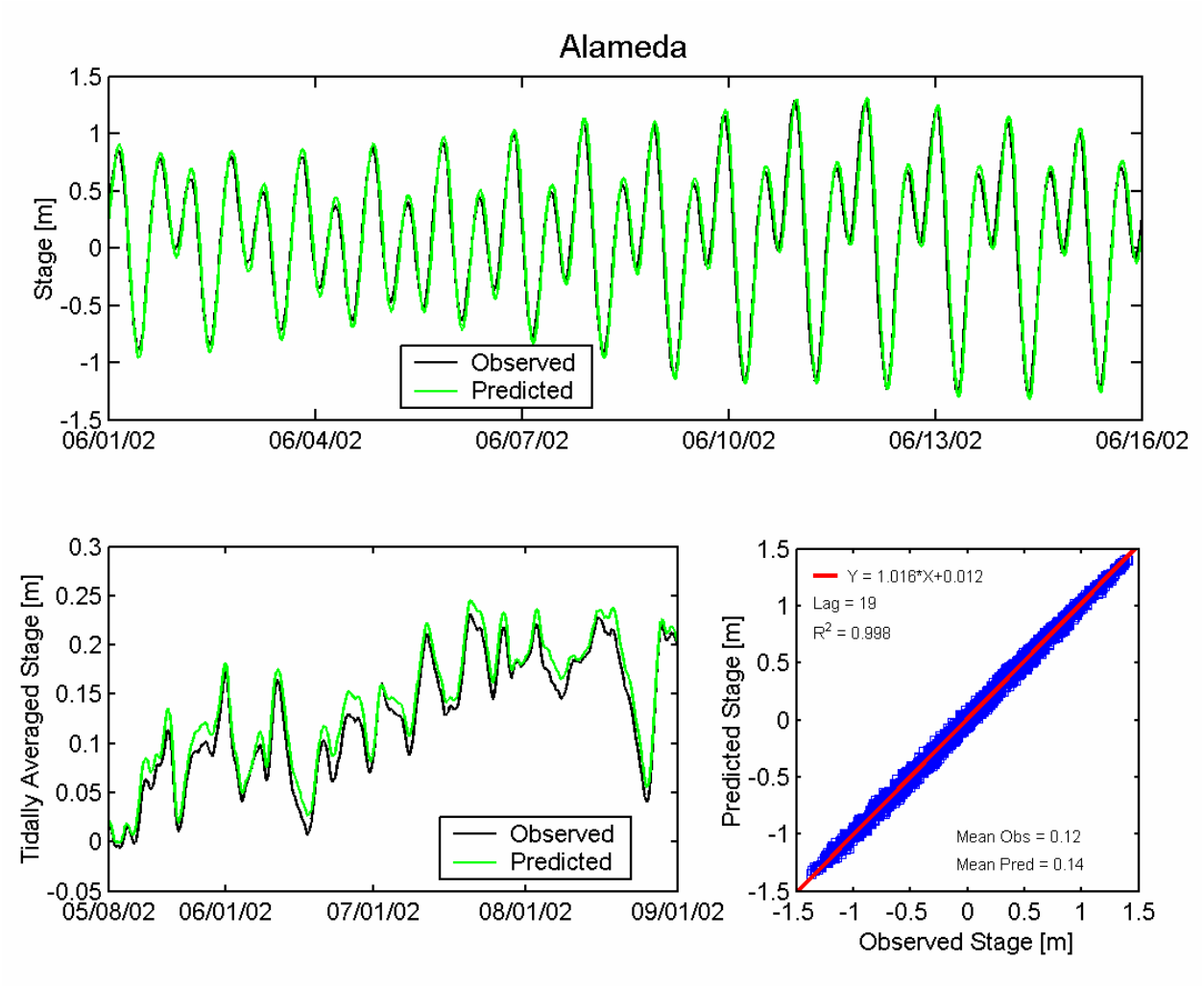

Figure 5.2-3 Observed and predicted stage at Alameda NOAA station (9414750) during the 2002 simulation period.

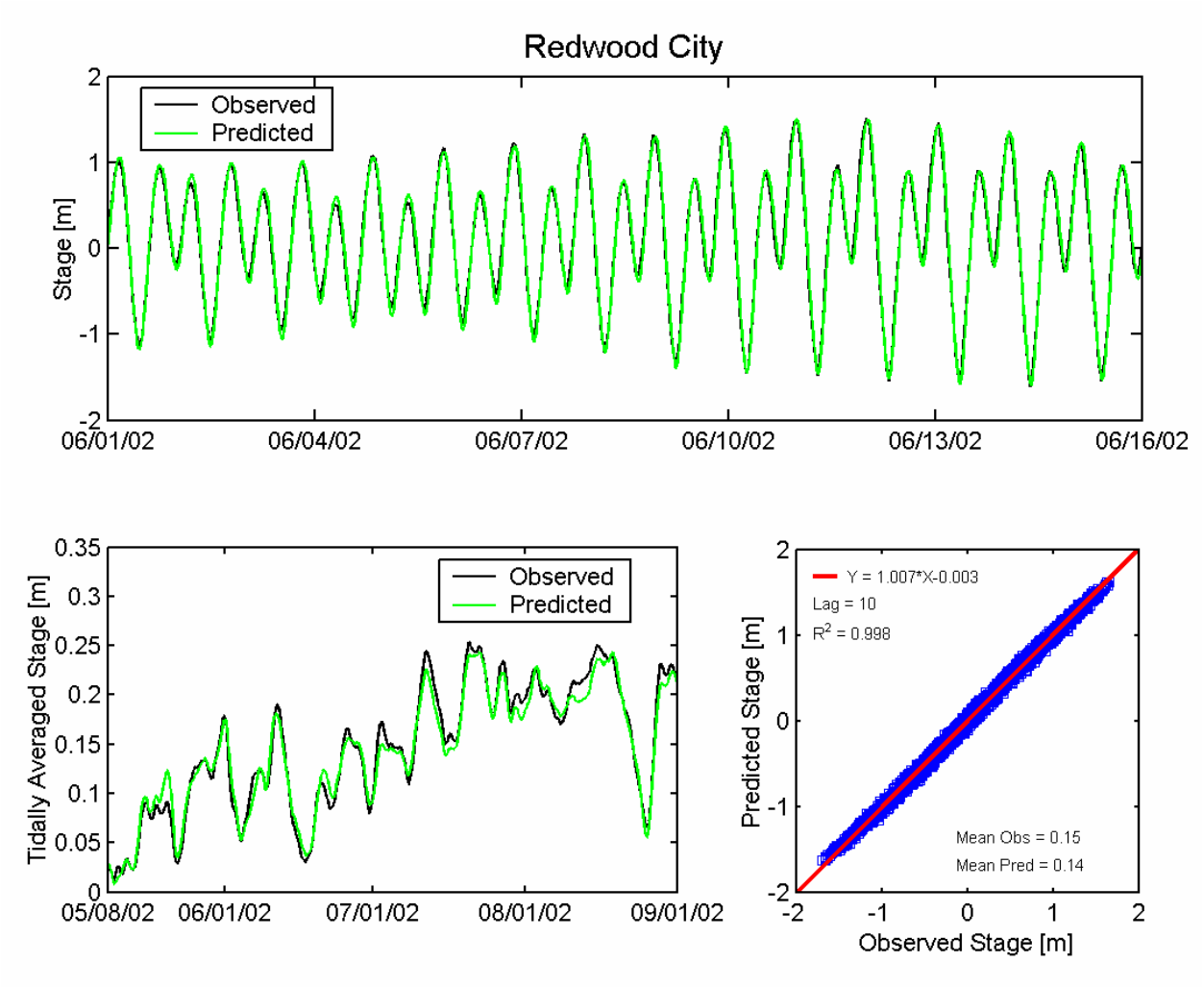

Figure 5.2-4 Observed and predicted stage at Redwood City NOAA station (9414523) during the 2002 simulation period.

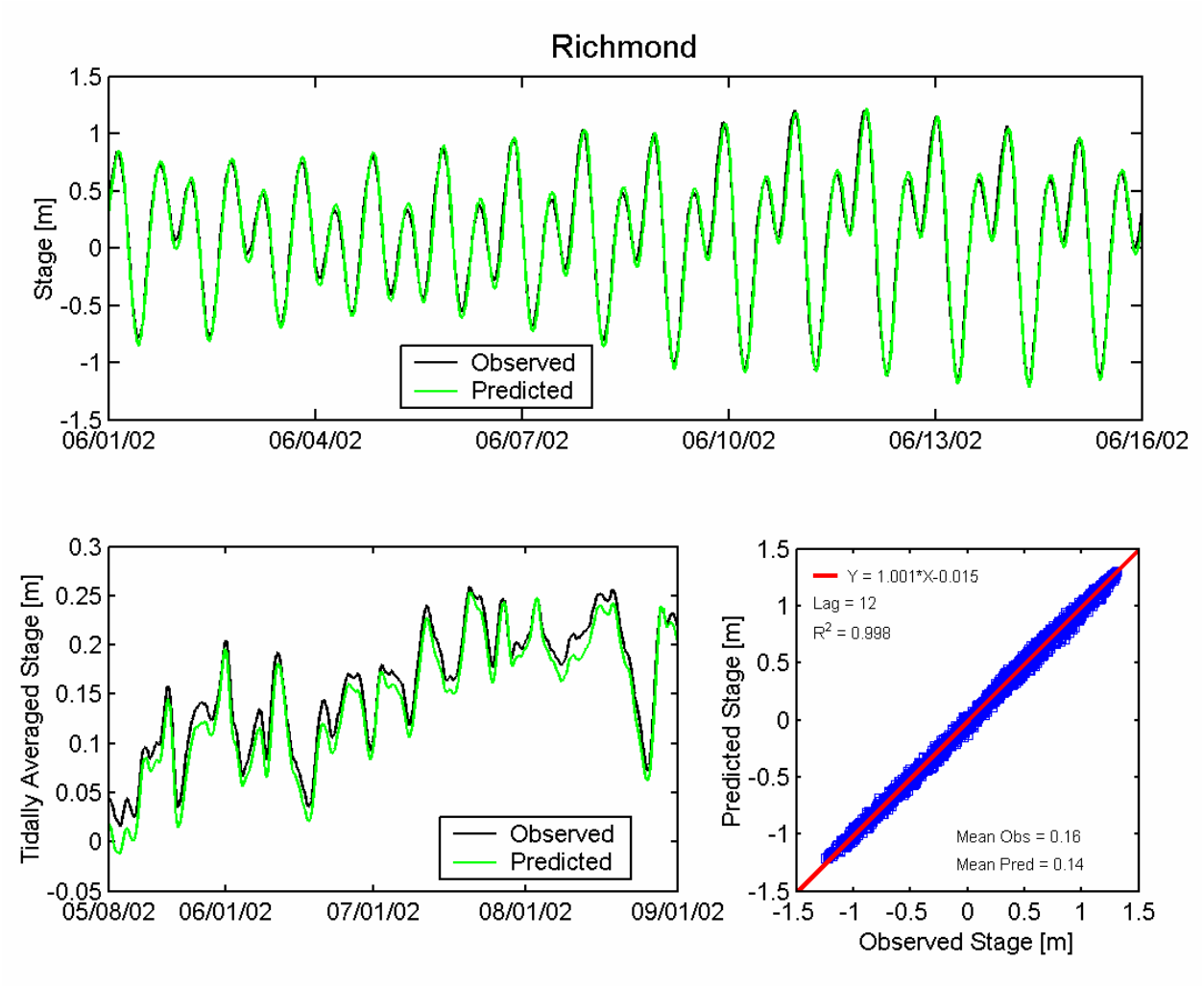

Figure 5.2-5 Observed and predicted stage at Richmond NOAA station (9414863) during the 2002 simulation period.

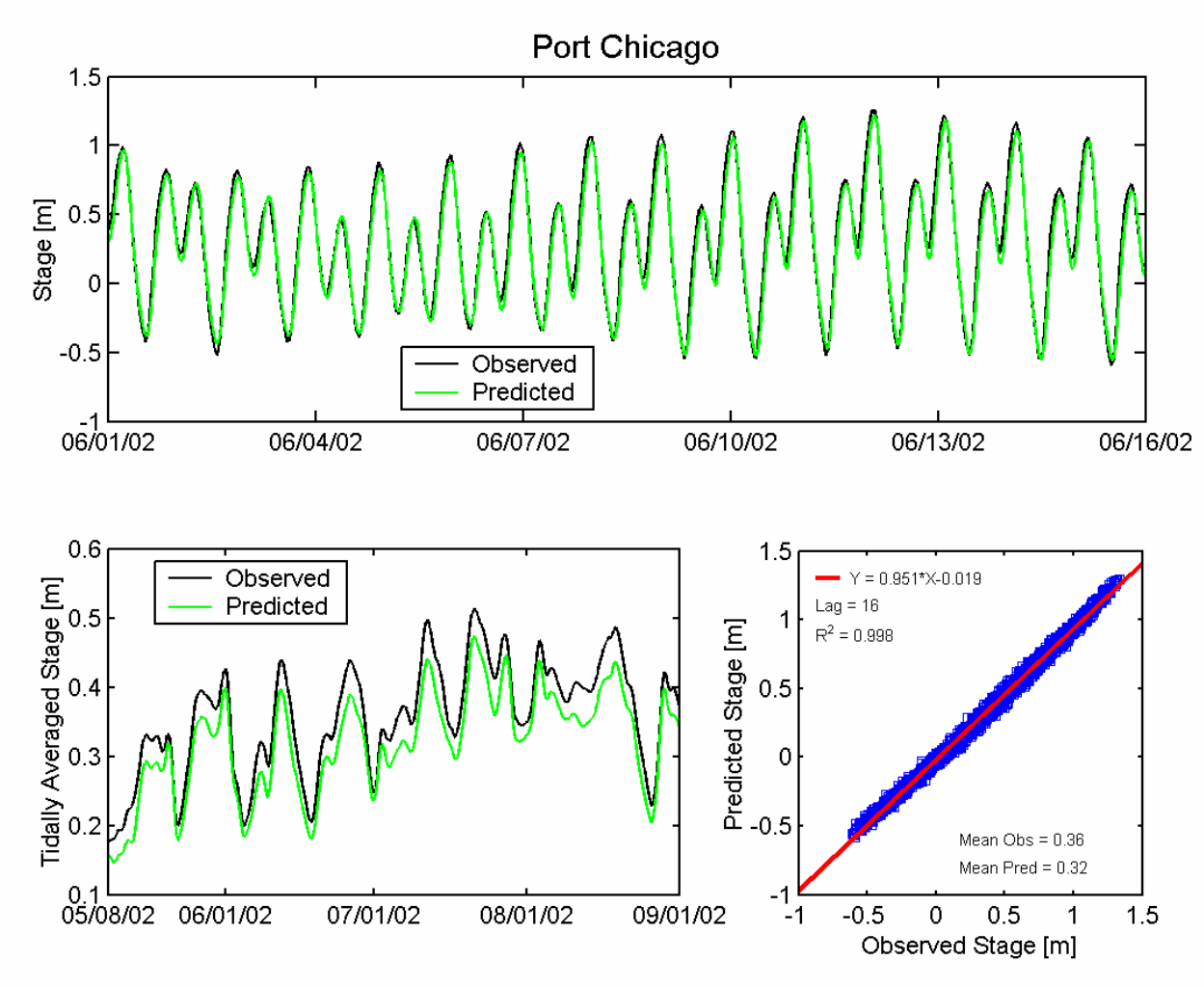

Figure 5.2-6 Observed and predicted stage at Port Chicago NOAA station (9415144) during the 2002 simulation period.

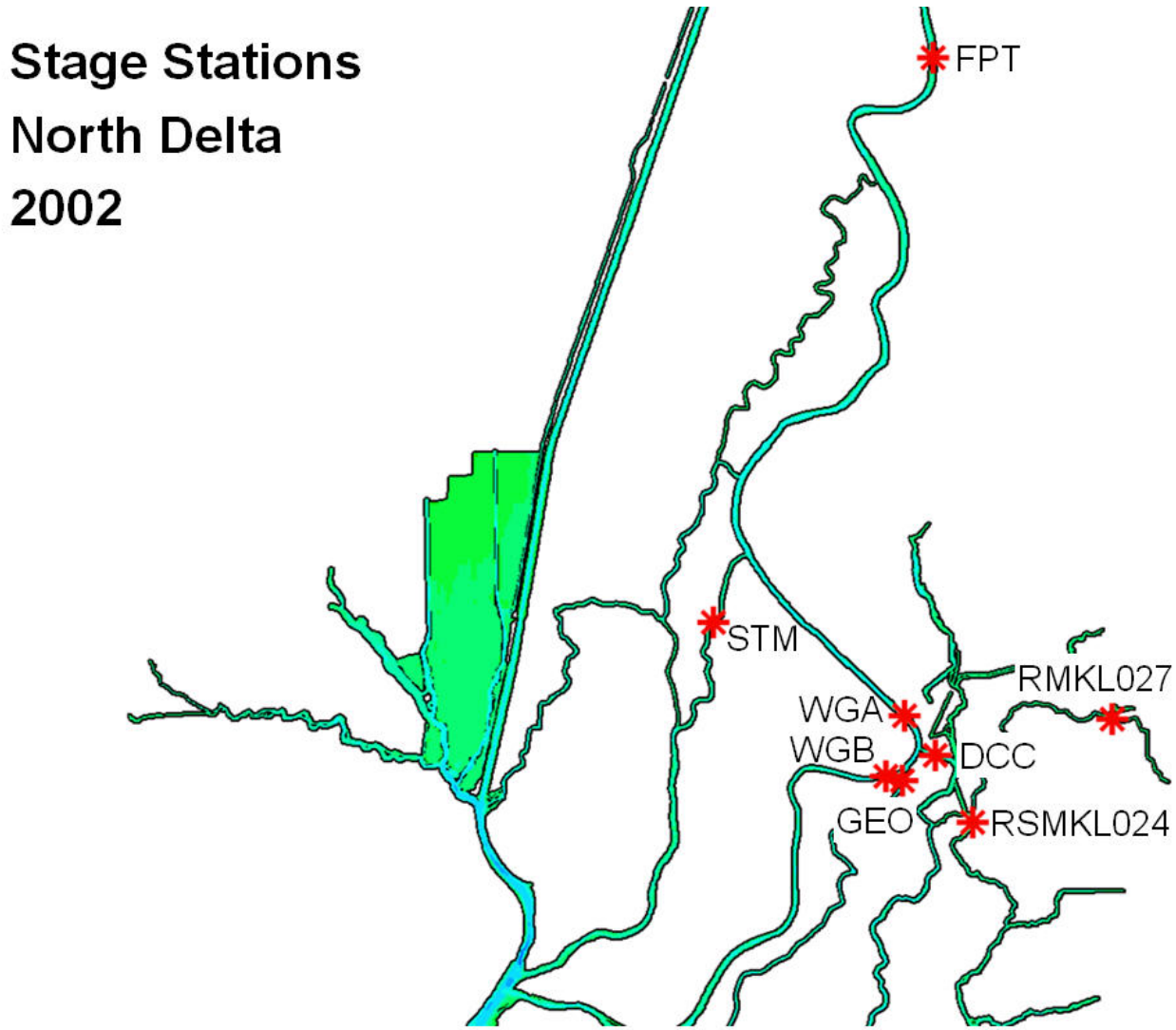

Station Names

WGB, Sacramento River South of Georgiana Slough

GEO, Georgiana Slough near Sacramento River

DCC, Delta Cross Channel

WGA, Sacramento River North of Delta Cross Channel

RMKL027, Mokelumne River near Thornton (Benson's Ferry)

RSMKL024, South Fork Mokelumne River at New Hope Bridge

STM, Steamboat Slough between Sacramento River and Sutter Sl.

FPT, Sacramento River at Freeport

Figure 5.2-7 Location of water level monitoring stations in the northern portion of the Sacramento-San Joaquin Delta used for 2002 water level calibration.

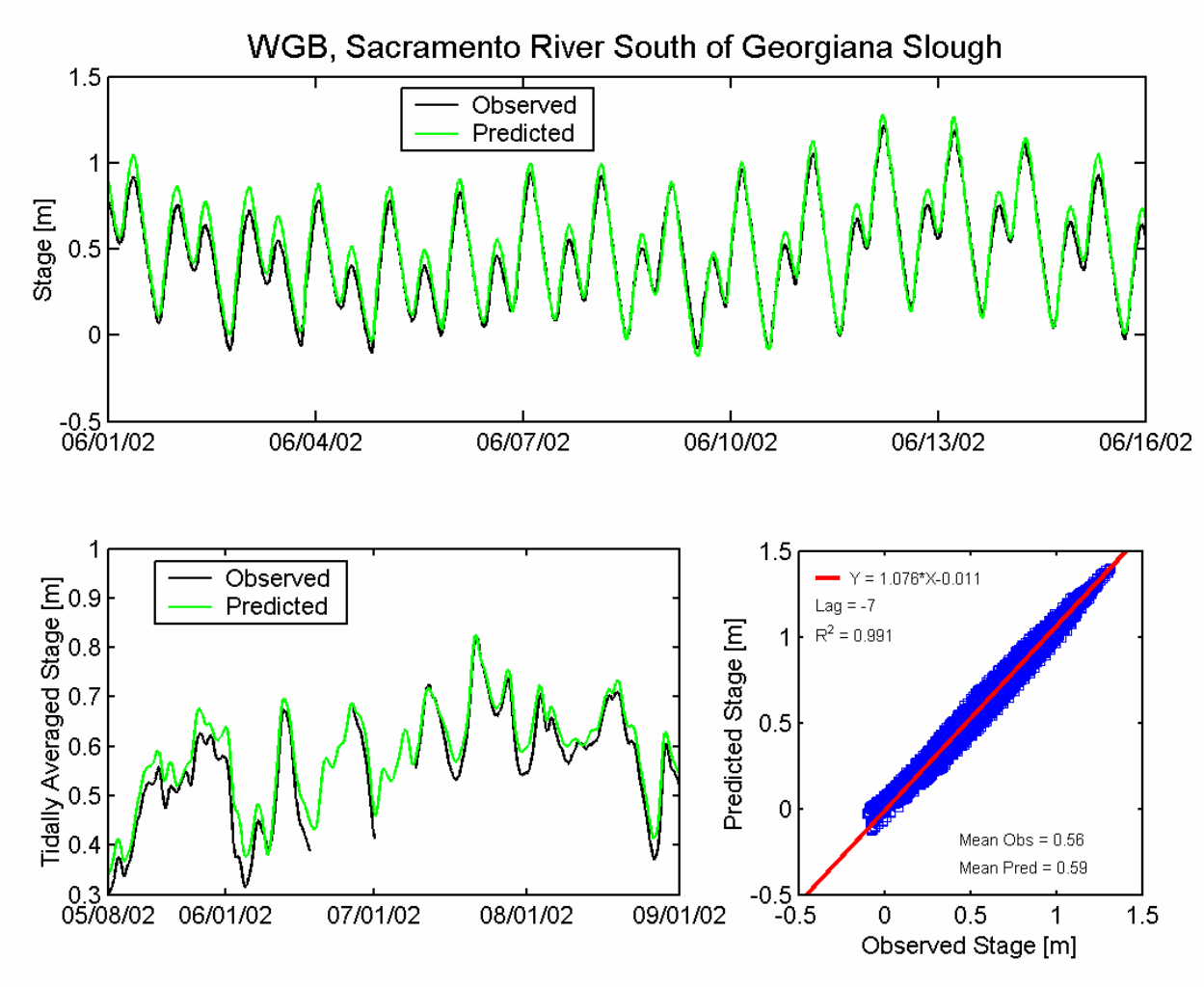

Figure 5.2-8 Observed and predicted stage at Sacramento River South of Georgiana Slough USGS station (WGB) during the 2002 simulation period.

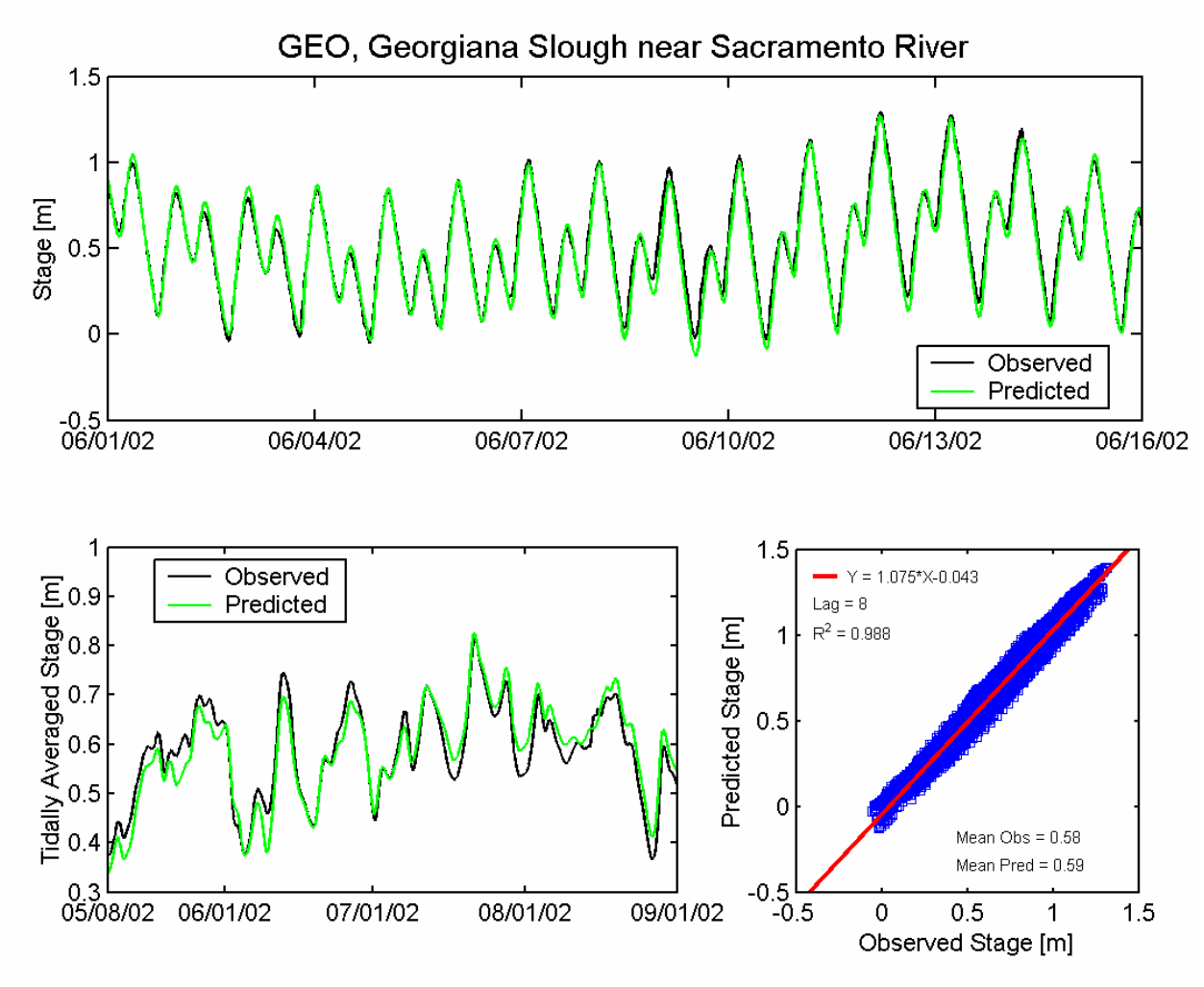

Figure 5.2-9 Observed and predicted stage at Georgiana Slough near Sacramento River USGS station (GEO) during the 2002 simulation period.

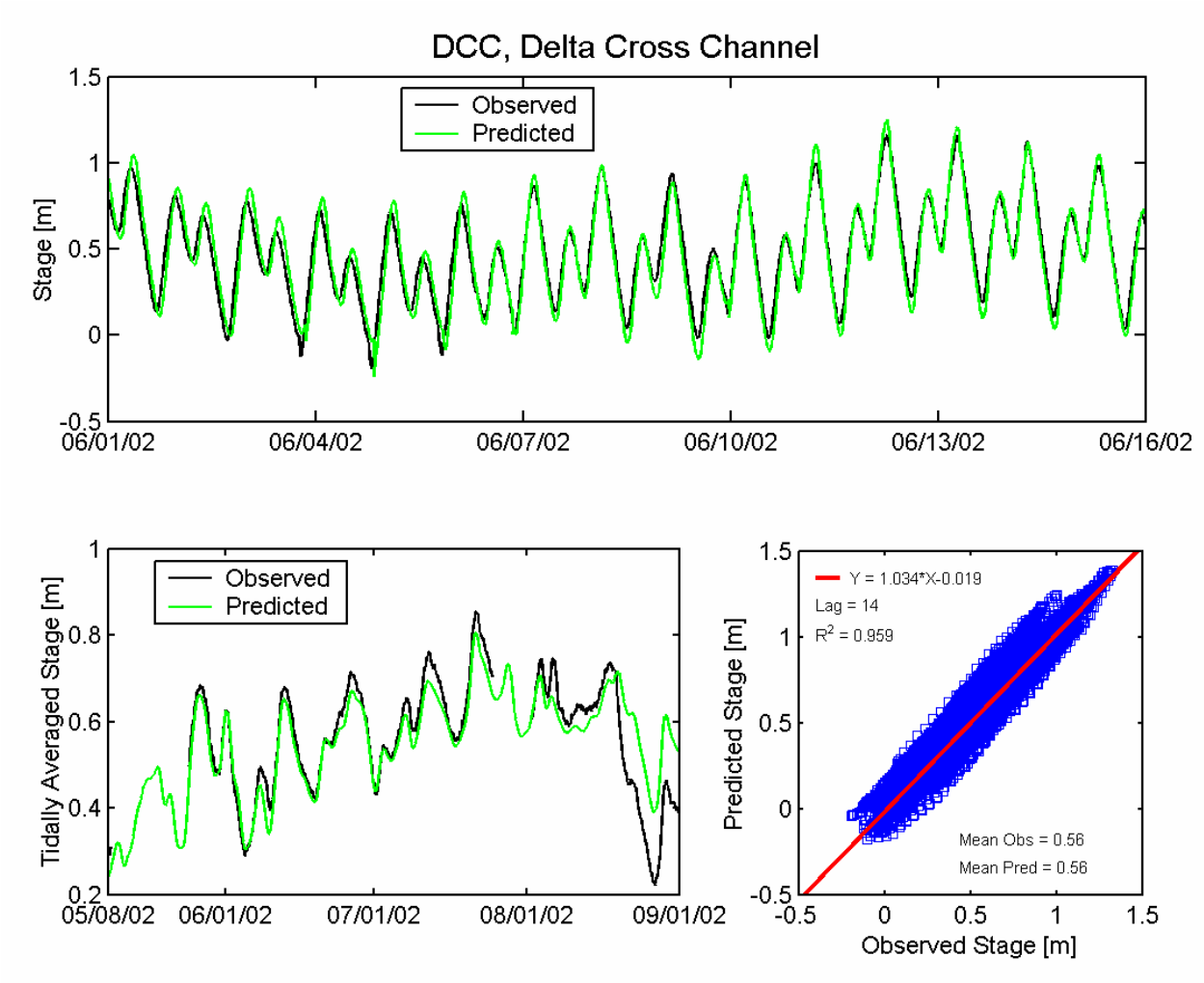

Figure 5.2-10 Observed and predicted stage at Delta Cross Channel USGS station (DCC) during the 2002 simulation period.

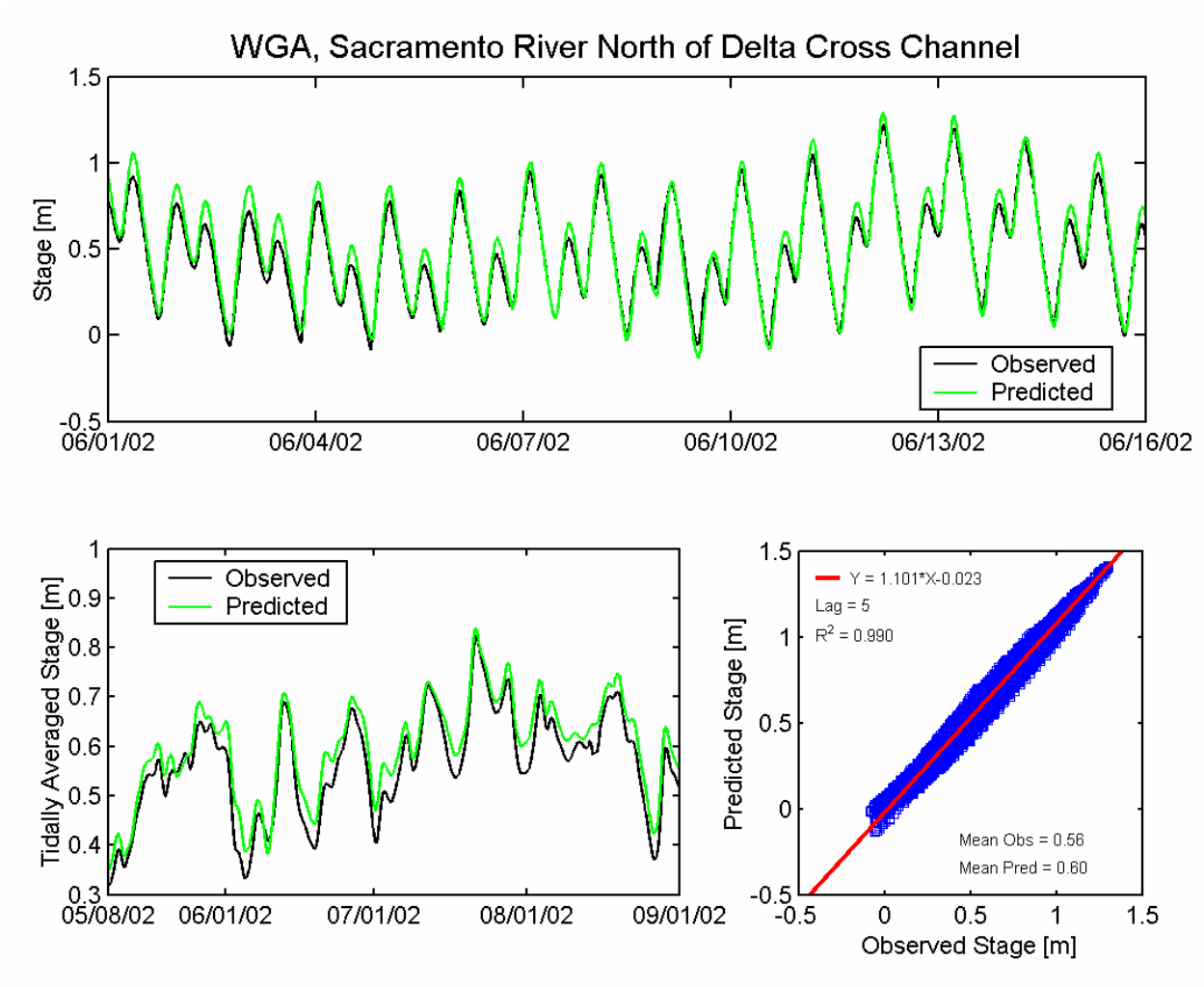

Figure 5.2-11 Observed and predicted stage at Sacramento River North of Delta Cross Channel USGS station (WGA) during the 2002 simulation period.

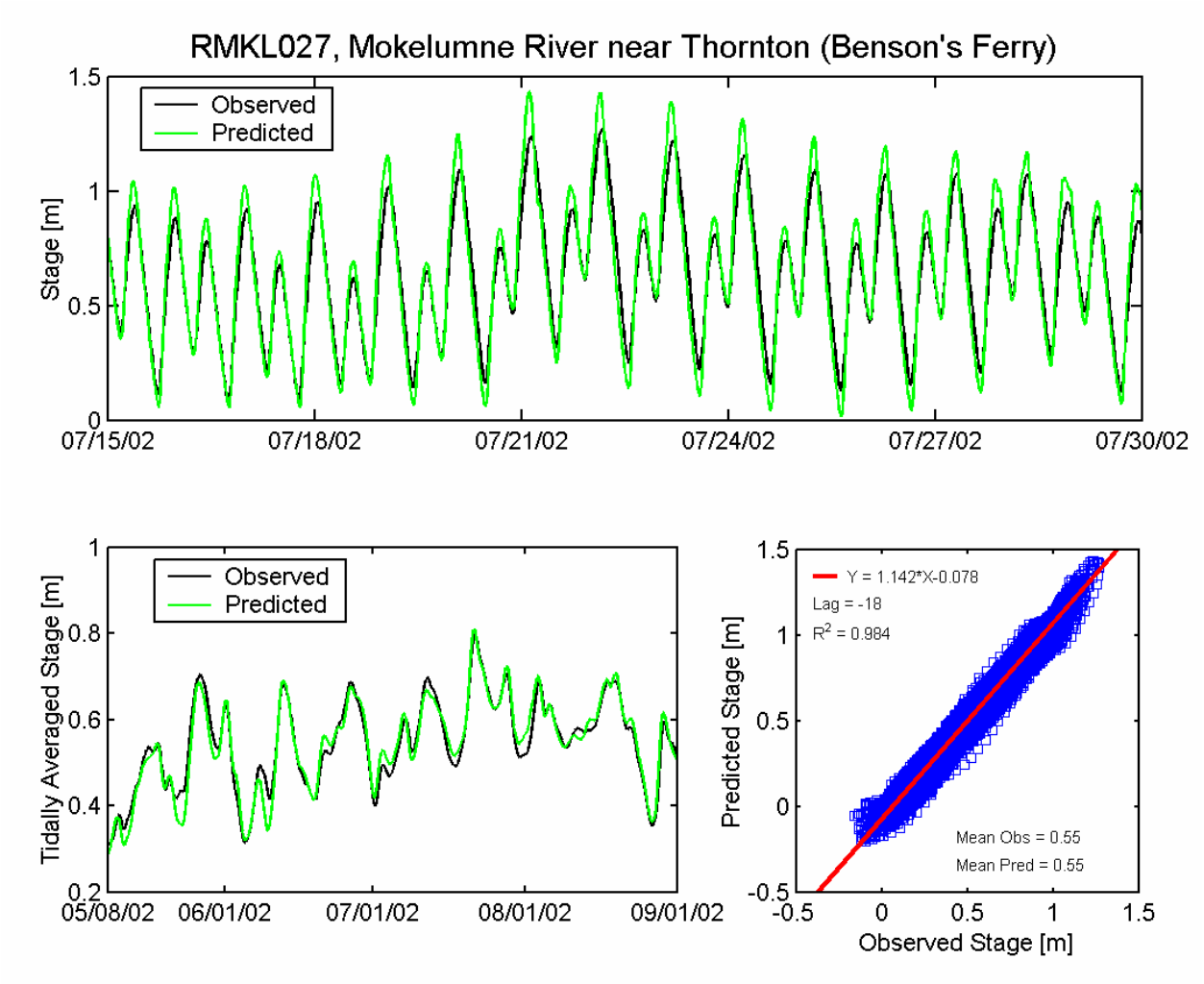

Figure 5.2-12 Observed and predicted stage at Mokelumne River near Thornton (Benson's Ferry) DWR station (RMKL027) during the 2002 simulation period.

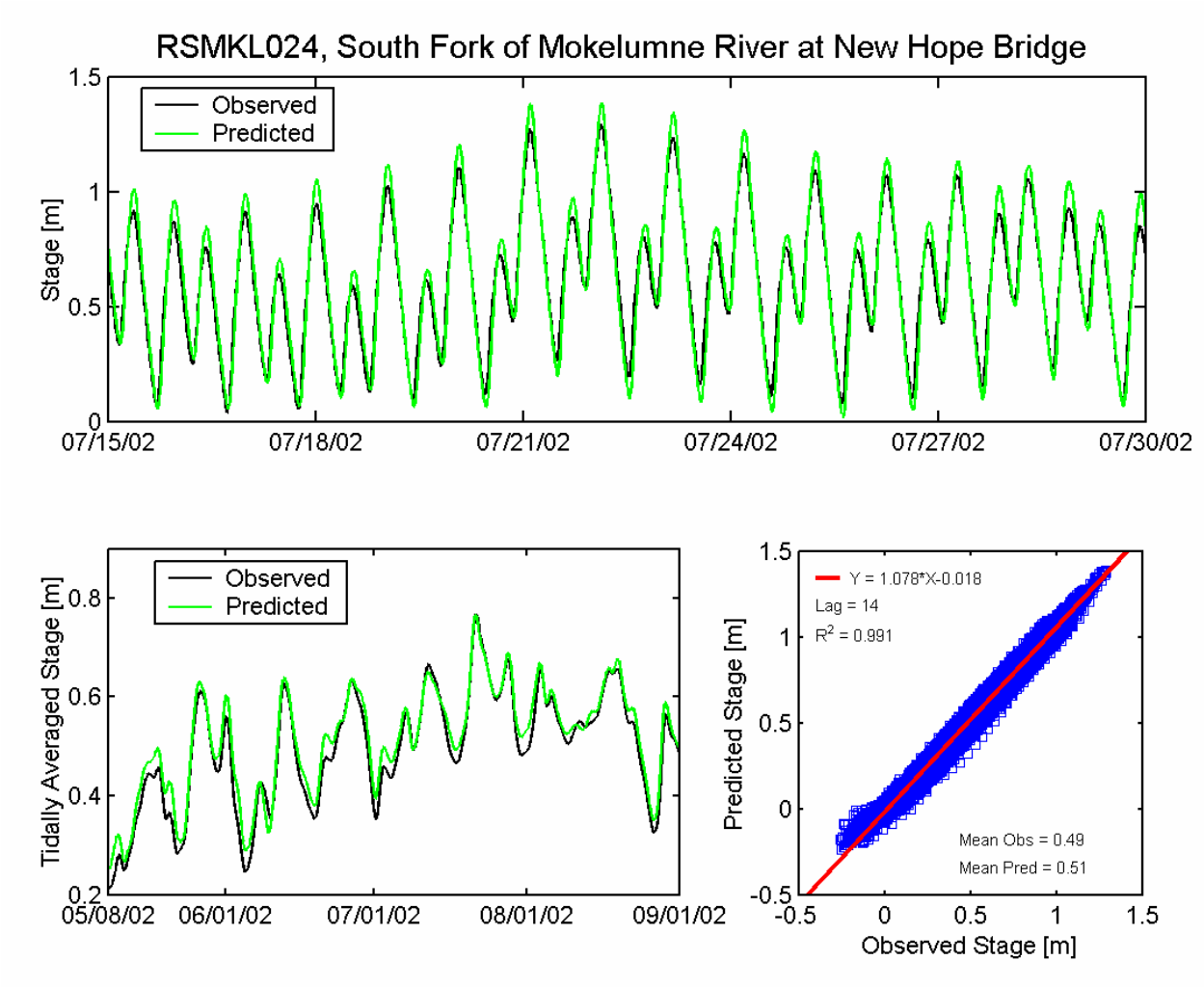

Figure 5.2-13 Observed and predicted stage at South Fork Mokelumne River at New Hope Bridge DWR station (RSMKL024) during the 2002 simulation period.

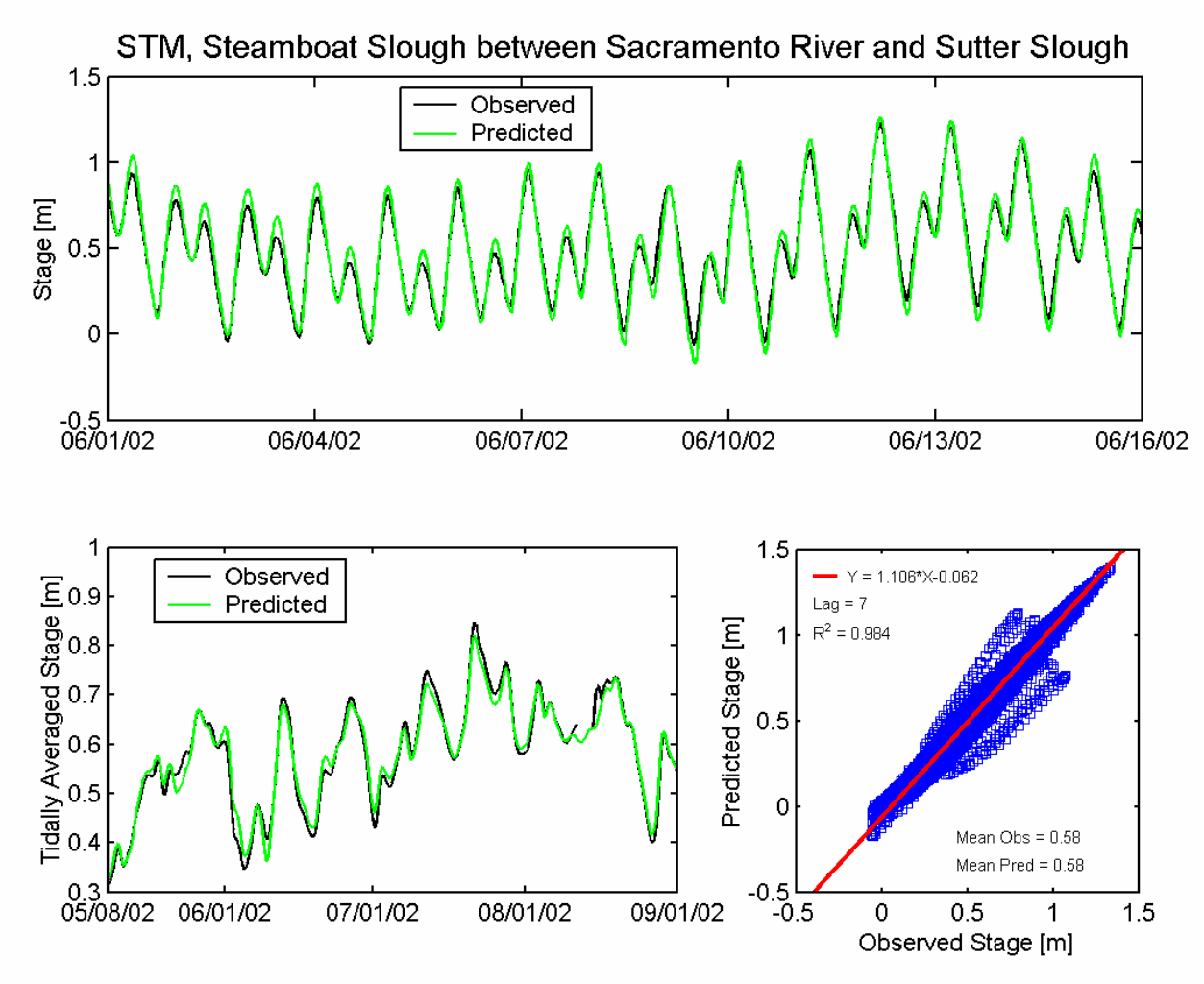

Figure 5.2-14 Observed and predicted stage at Steamboat Slough between Sacramento River and Sutter Slough USGS station (STM) during the 2002 simulation period.

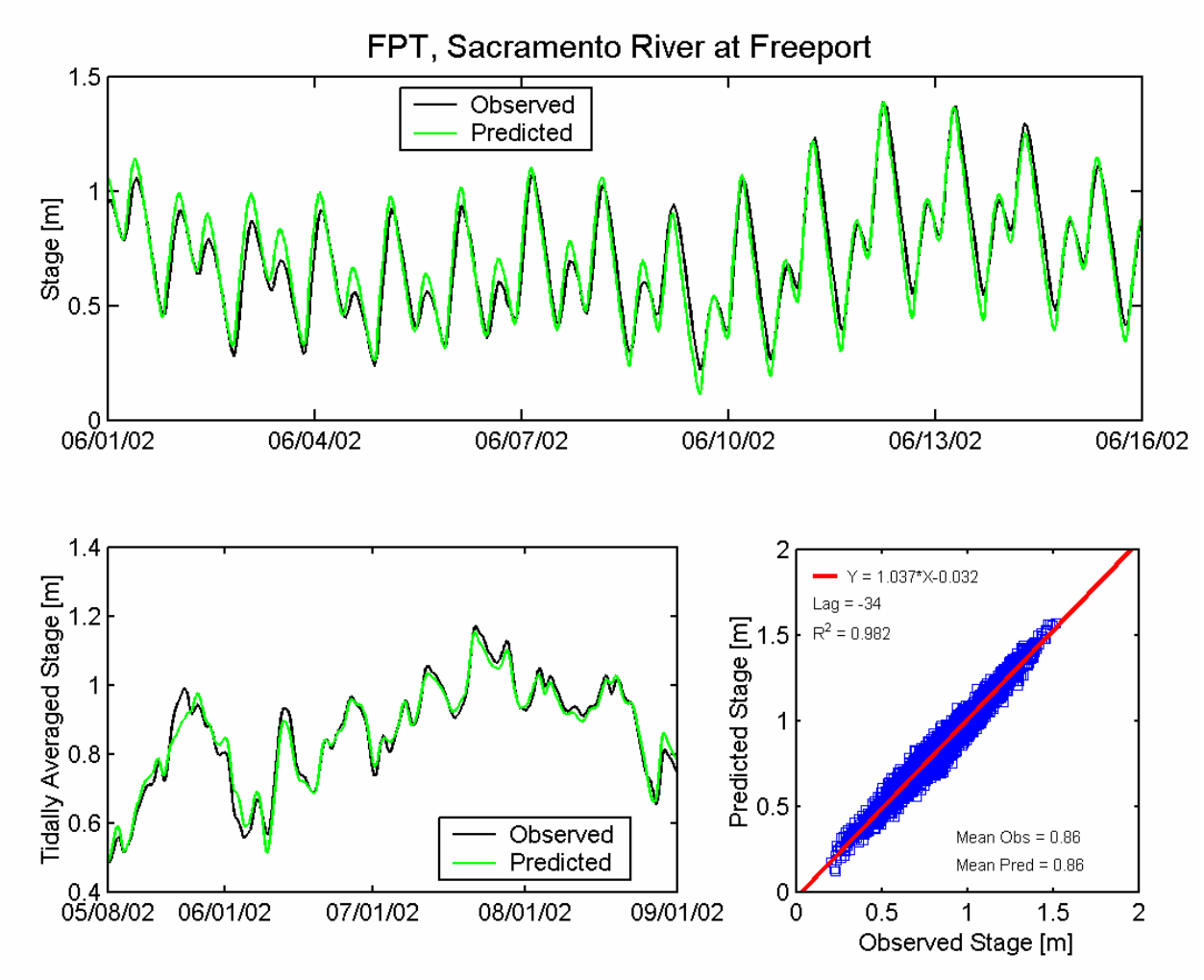

Figure 5.2-15 Observed and predicted stage at Sacramento River at Freeport USGS station (FPT) during the 2002 simulation period.

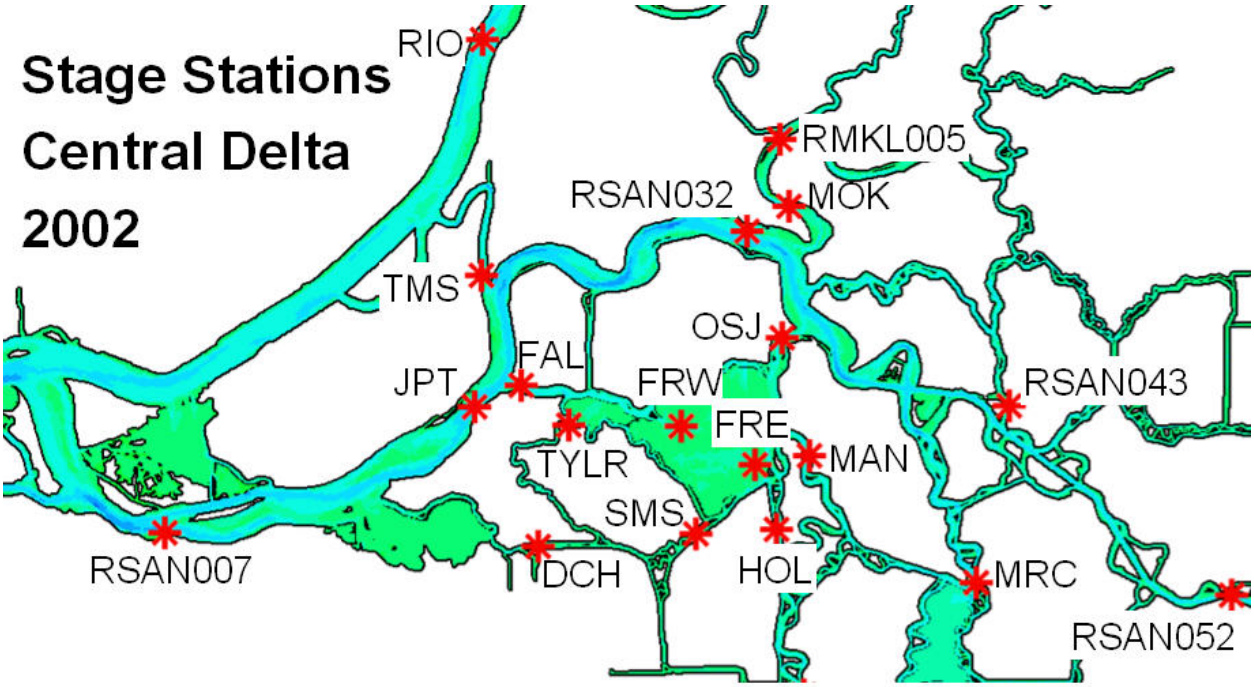

Station Names

RSAN007, San Joaquin River at Antioch

RIO, Sacramento River at Rio Vista

TMS, Threemile Slough at San Joaquin River

JPT, San Joaquin River at Jersey Point

FAL, False River

DCH, Dutch Slough at Jersey Island

TYLR, Taylor Slough

SMS, Sand Mound Slough

RSAN032, San Joaquin River at San Andreas Landing

OSJ, Old River at San Joaquin River

MOK, Mokelumne River near San Joaquin River

RMKL005, North Fork of Mokelumne River at Georgiana Slough

FRE, Franks Tract East

FRW, Franks Tract West

MAN, Old River at Mandeville Island

HOL, Holland Cut

RSAN043, San Joaquin River at Venice Island

RSAN052, San Joaquin River at Rindge Pump

MRC, Middle River South of Columbia Cut

Figure 5.2-16 Location of water level monitoring stations in the central portion of the Sacramento-San Joaquin Delta used for 2002 water level calibration.

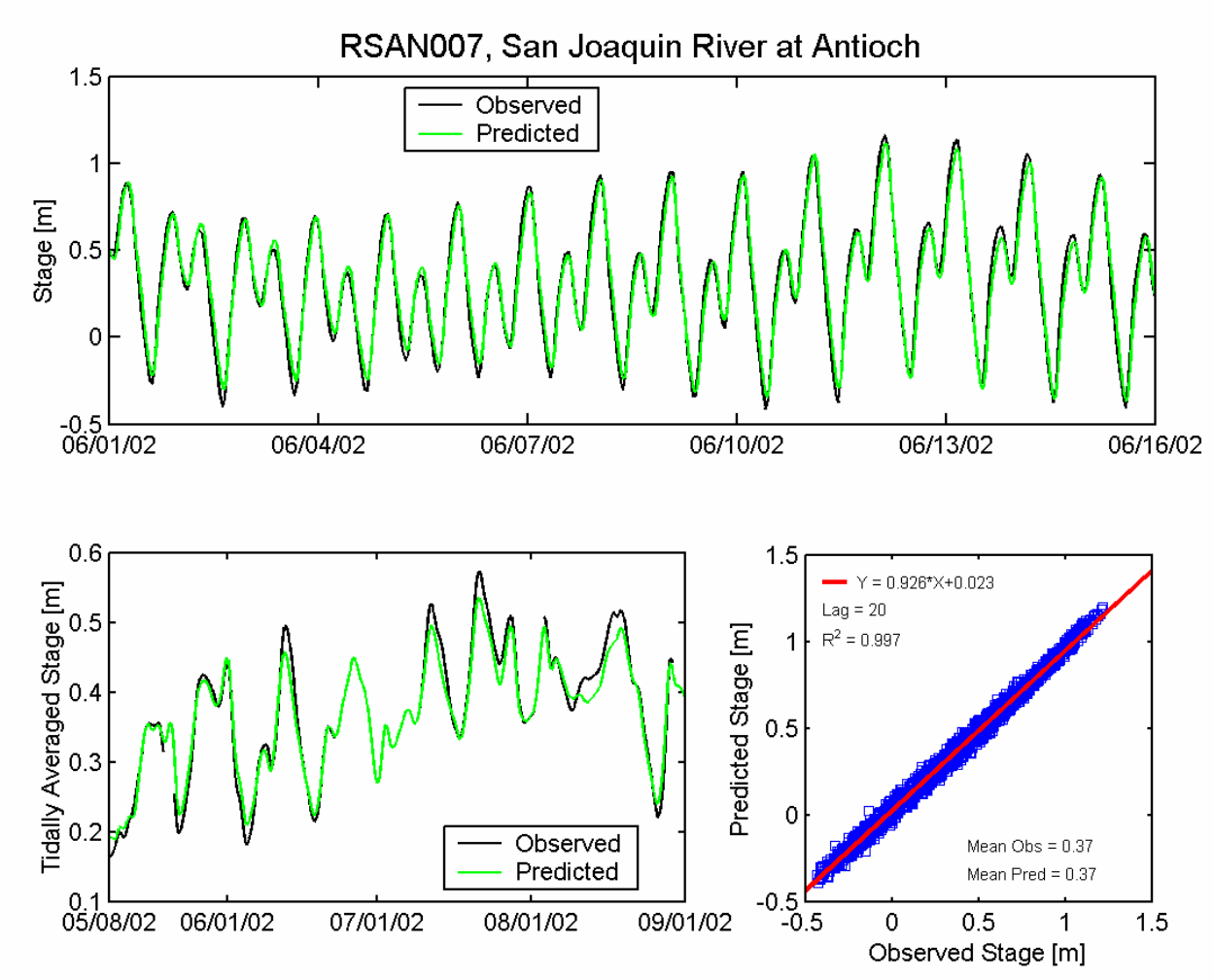

Figure 5.2-17 Observed and predicted stage at Antioch DWR station (RSAN007) during the 2002 simulation period.

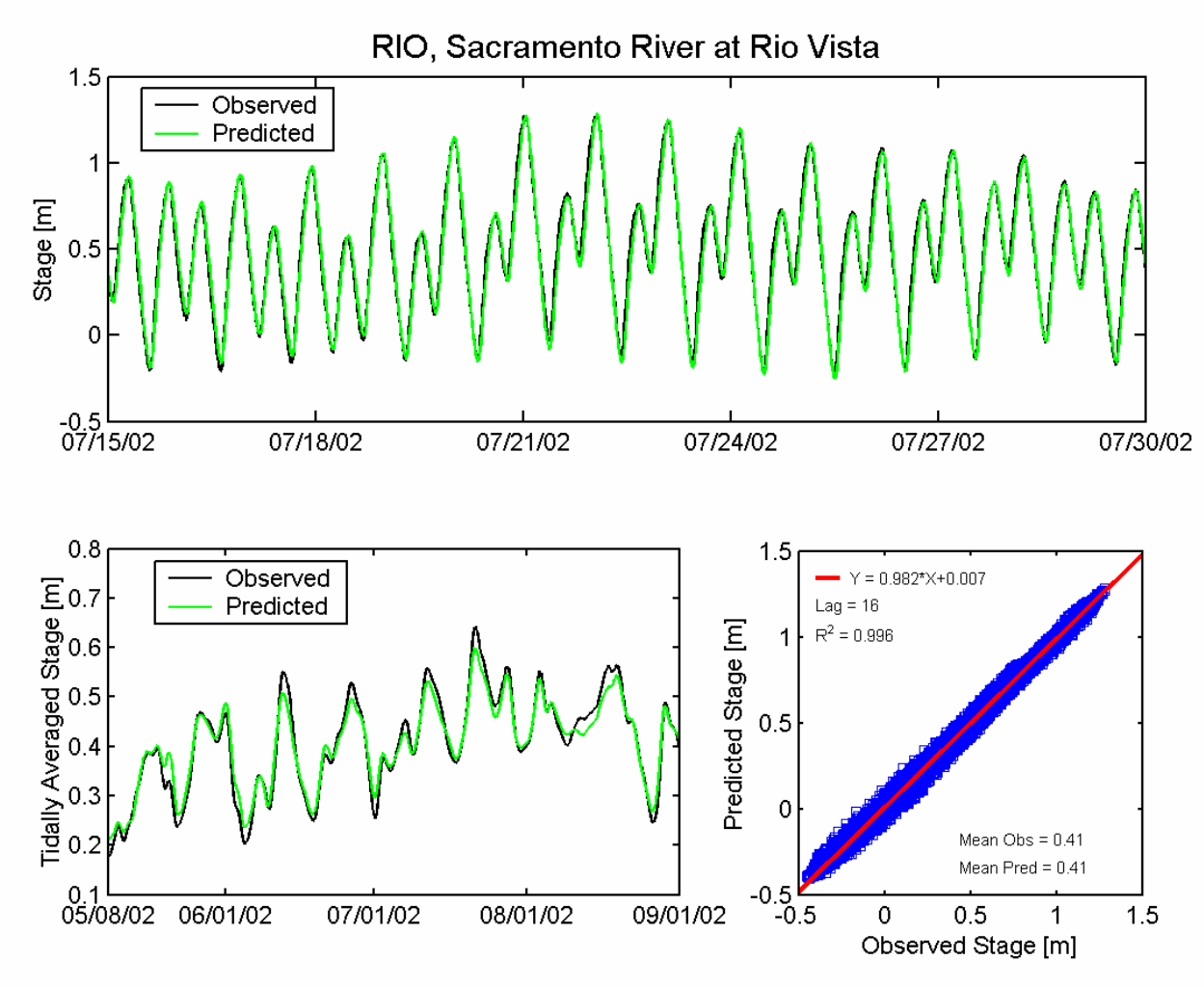

Figure 5.2-18 Observed and predicted stage at Sacramento River at Rio Vista USGS station (RIO) during the 2002 simulation period.

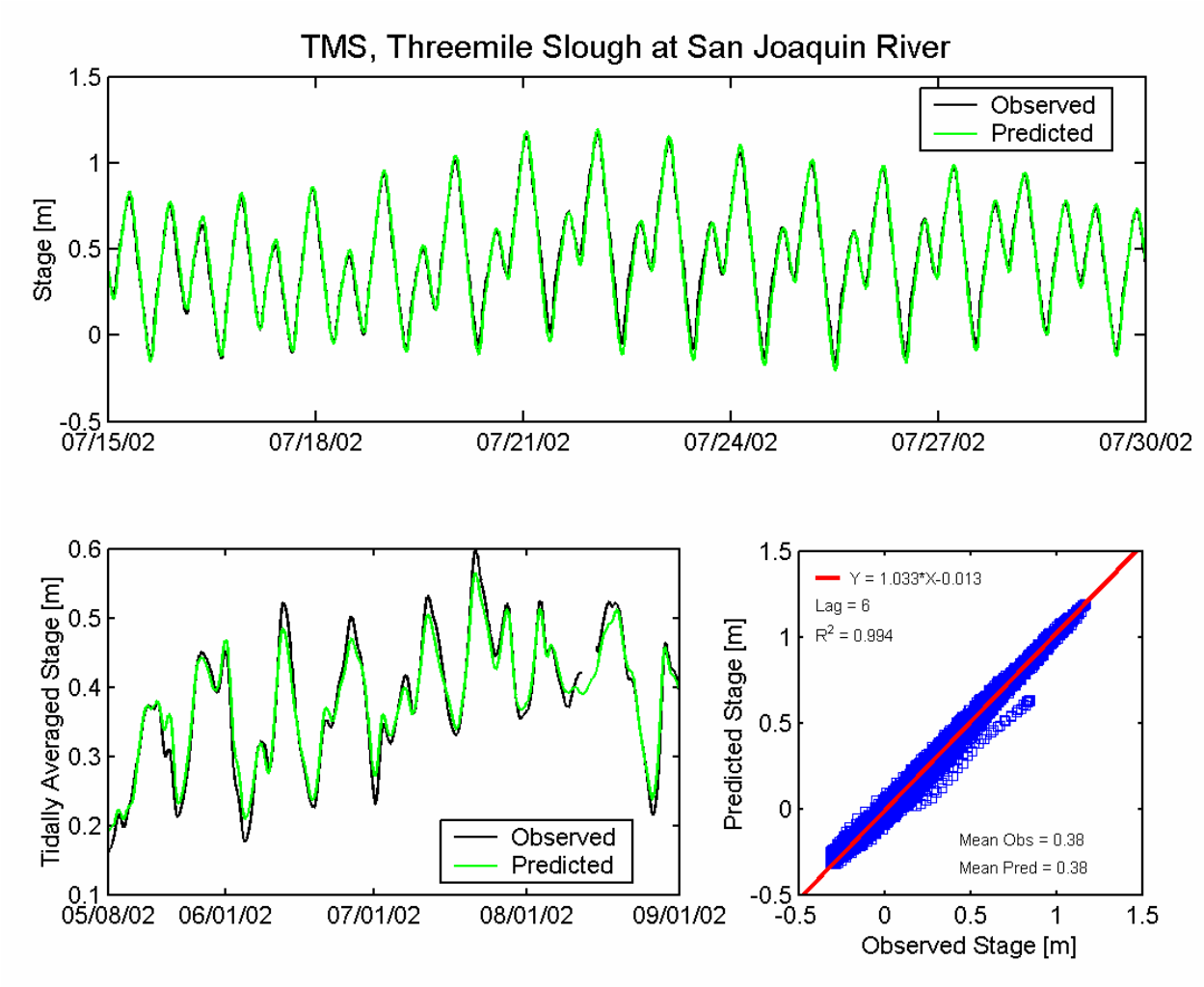

Figure 5.2-19 Observed and predicted stage at Threemile Slough at San Joaquin River USGS station (TMS) during the 2002 simulation period.

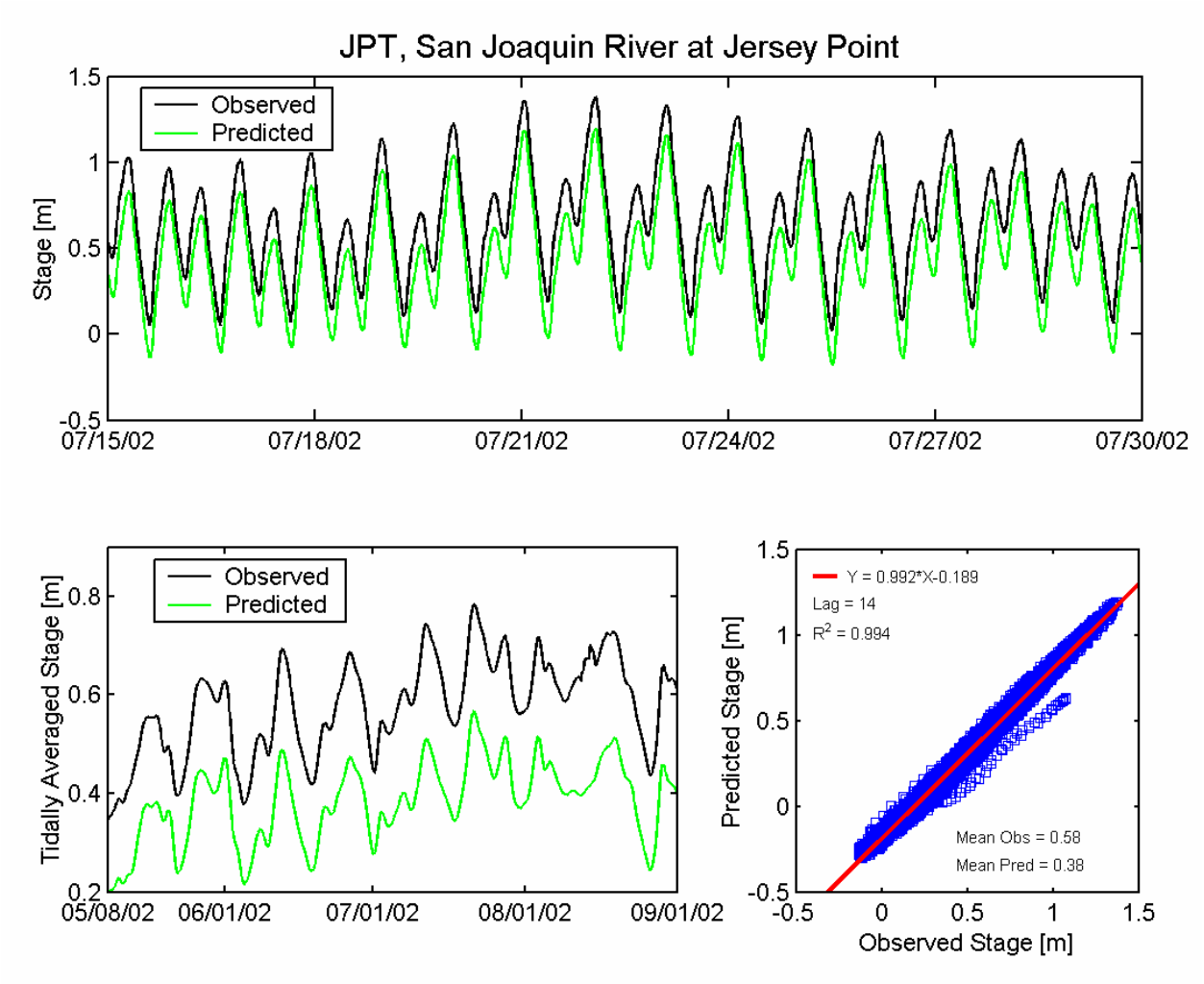

Figure 5.2-20 Observed and predicted stage at San Joaquin River at Jersey Point USGS station (JPT) during the 2002 simulation period.

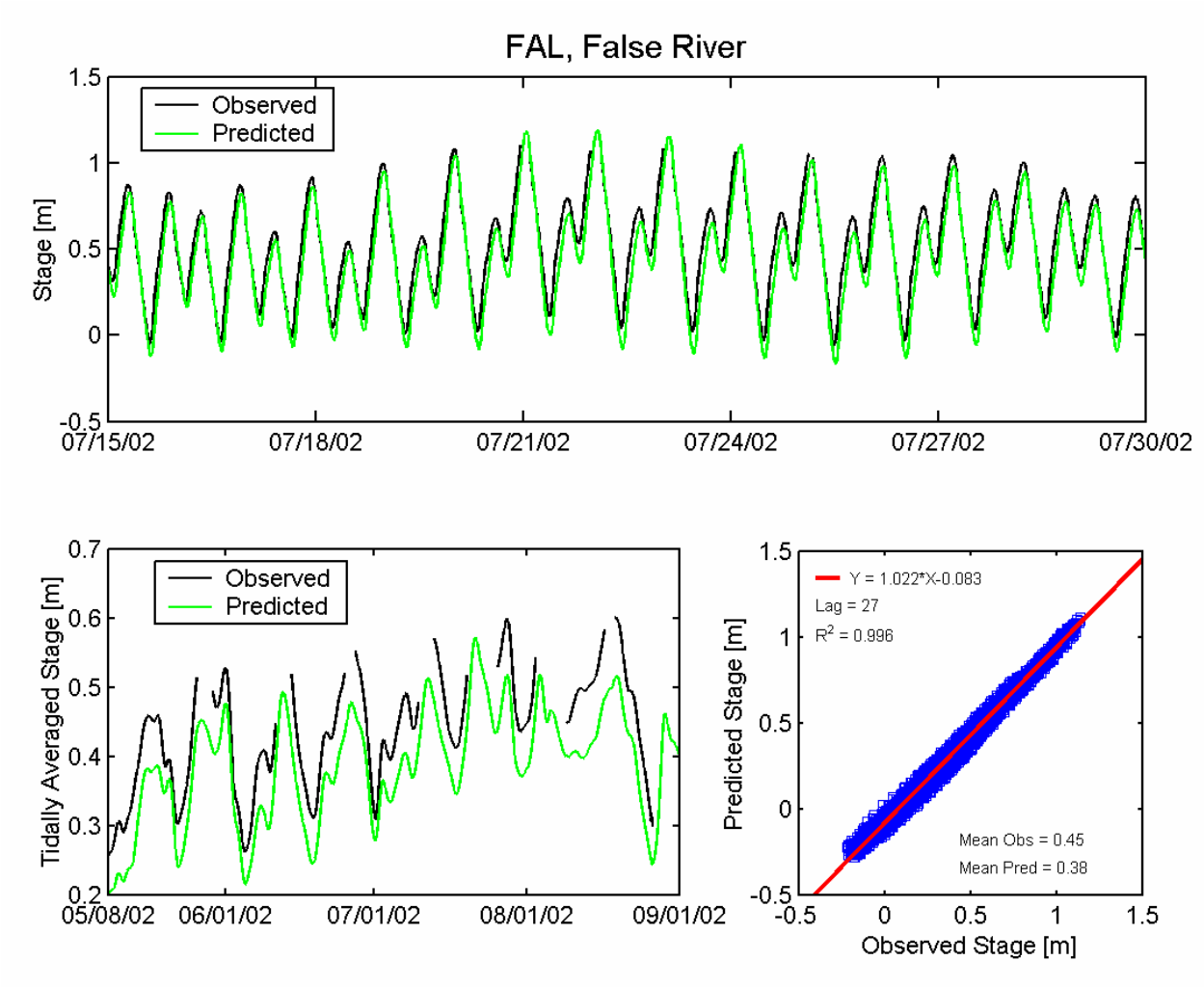

Figure 5.2-21 Observed and predicted stage at False River USGS station (FAL) during the 2002 simulation period.

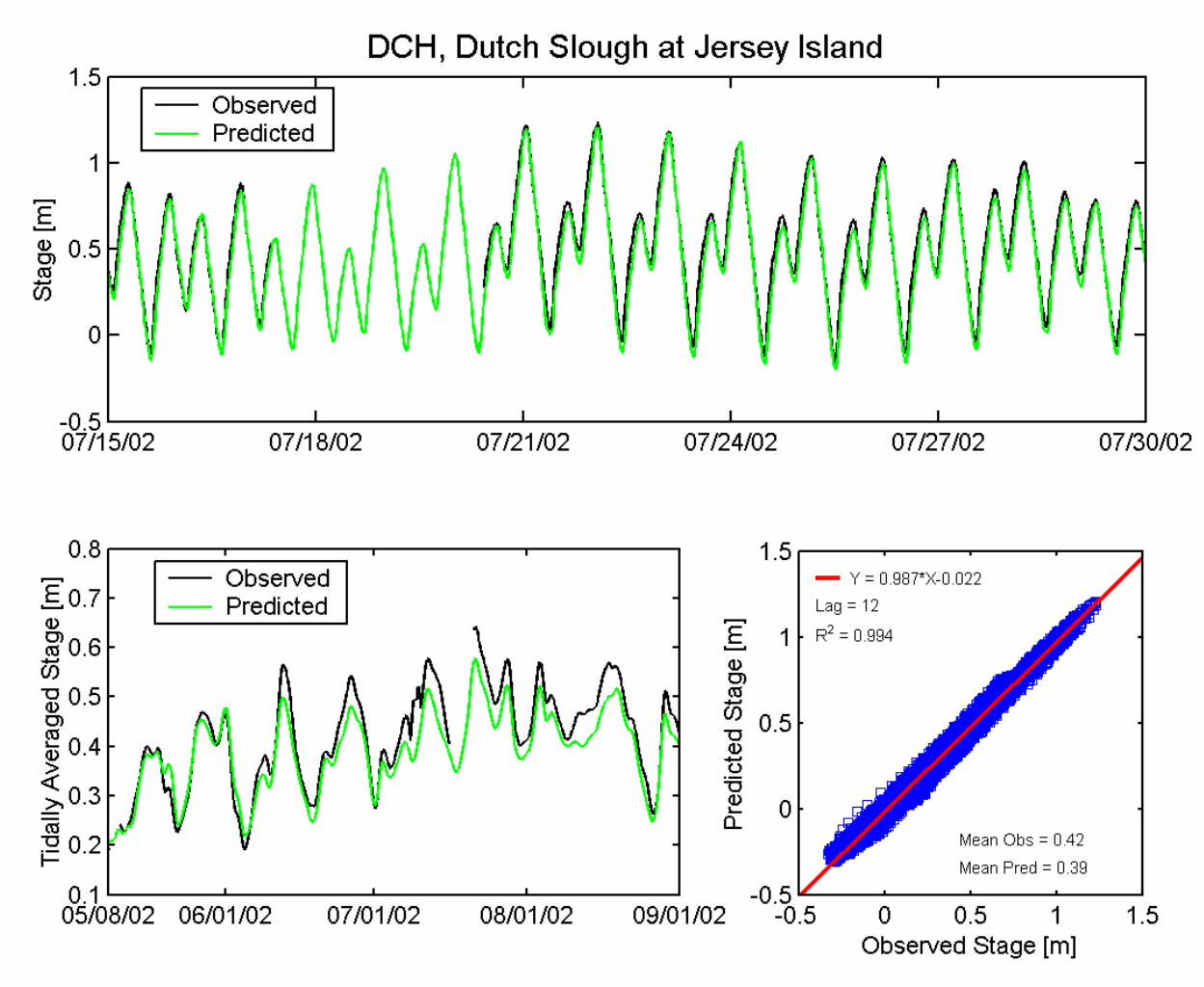

Figure 5.2-22 Observed and predicted stage at Dutch Slough at Jersey Island USGS station (DCH) during the 2002 simulation period.

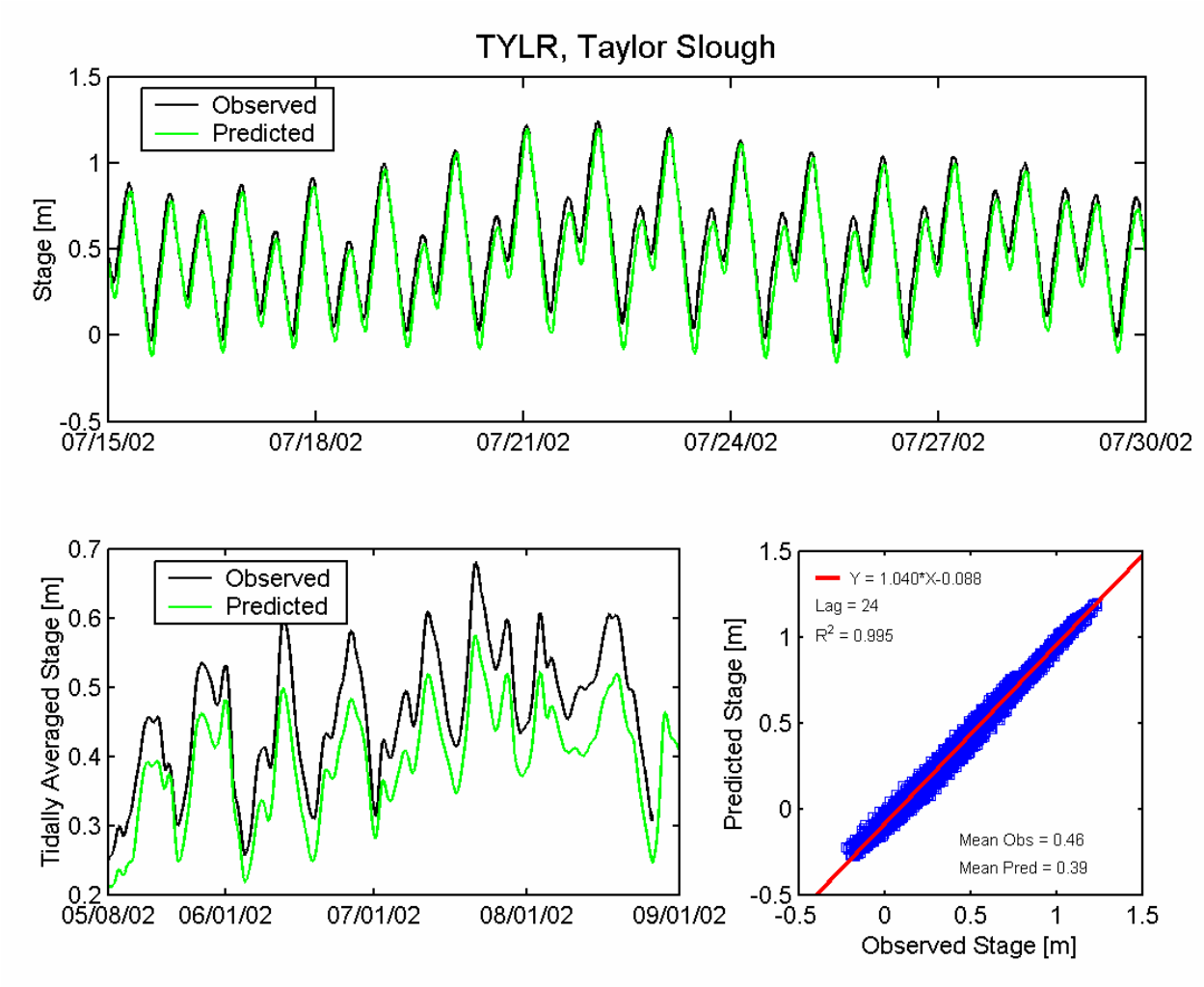

Figure 5.2-23 Observed and predicted stage at Taylor Slough USGS station (TYLR) during the 2002 simulation period.

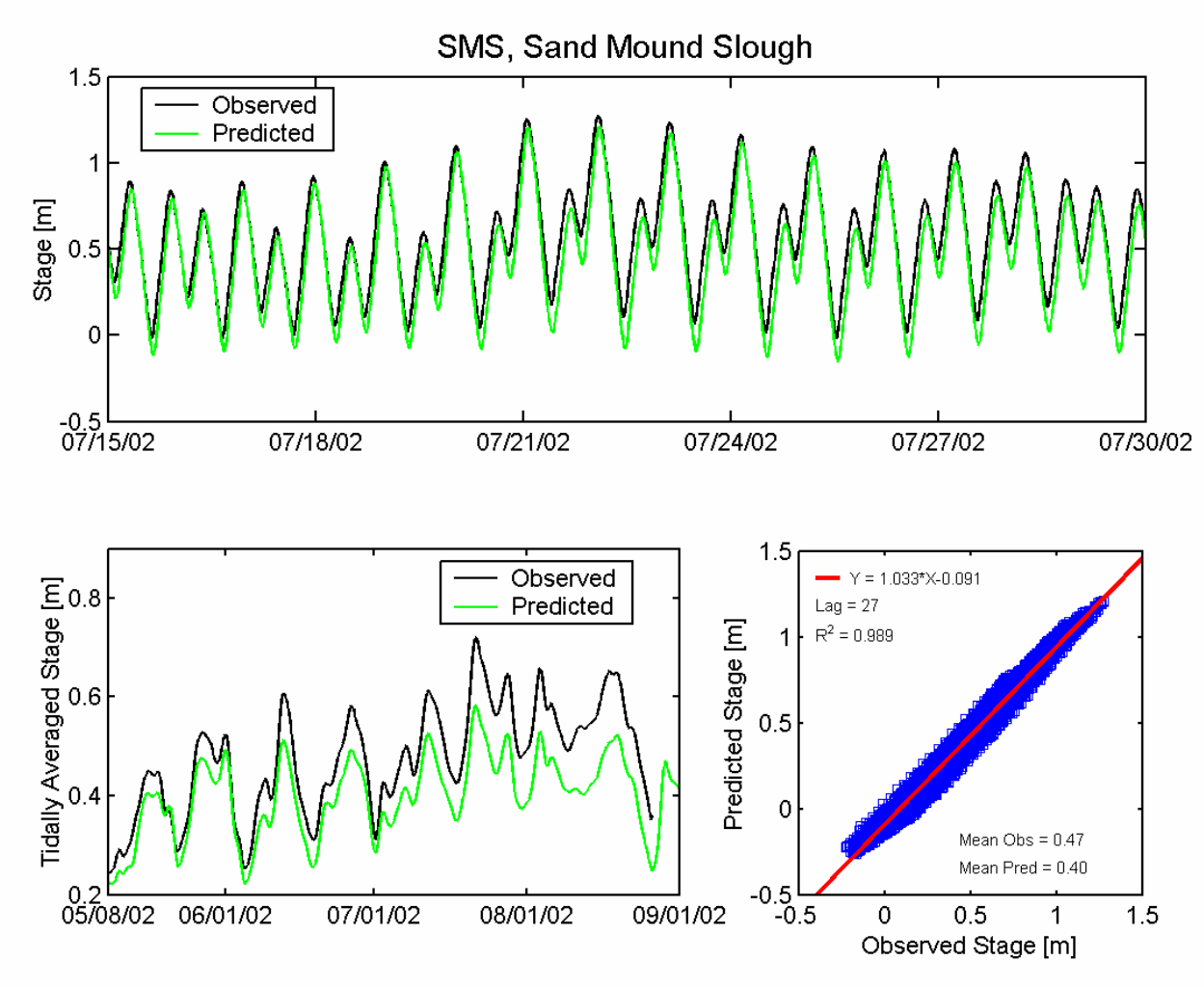

Figure 5.2-24 Observed and predicted stage at Sand Mound Slough USGS station (SMS) during the 2002 simulation period.

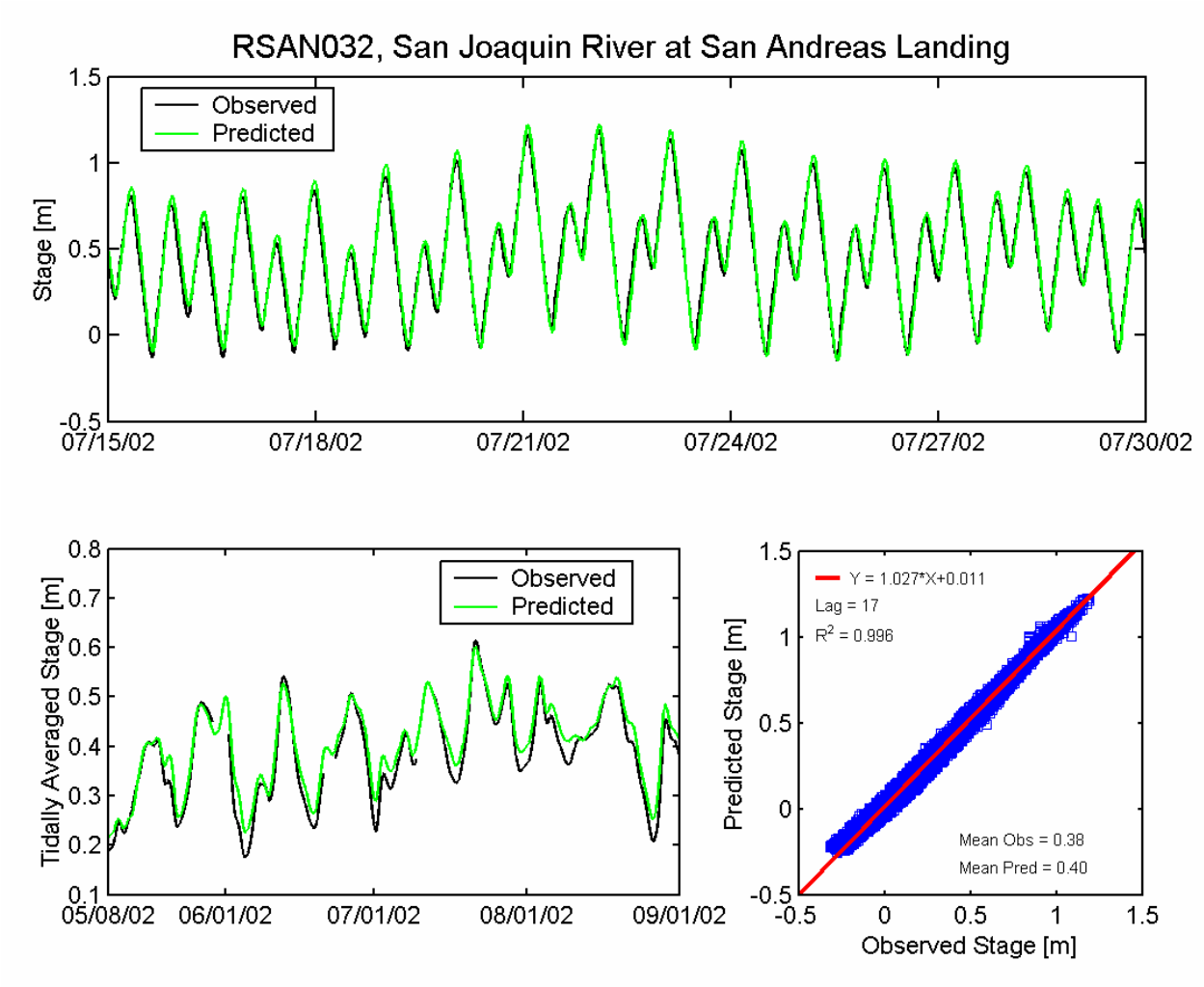

Figure 5.2-25 Observed and predicted stage at San Joaquin River at San Andreas Landing DWR station (RSAN032) during the 2002 simulation period.

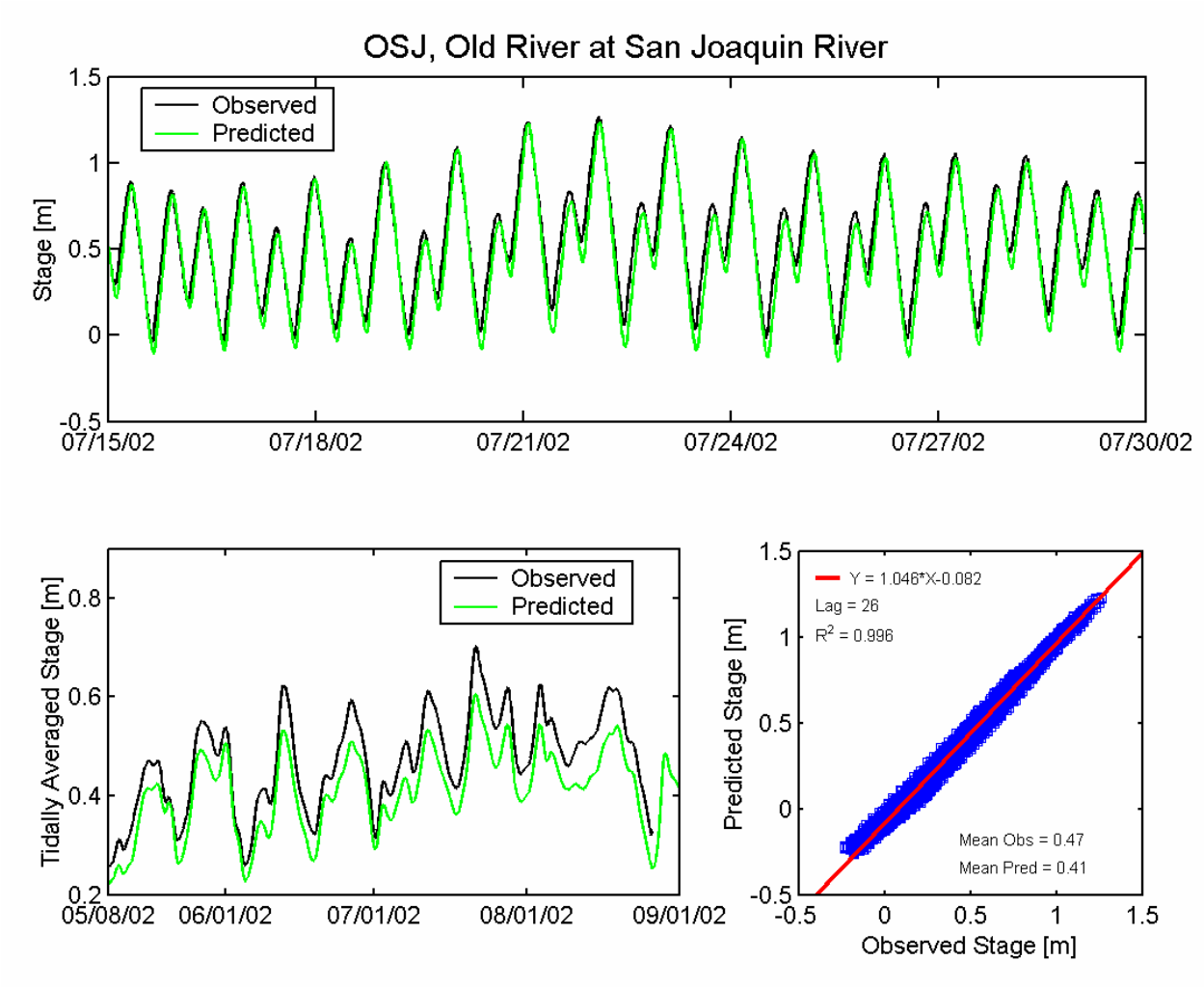

Figure 5.2-26 Observed and predicted stage at Old River at San Joaquin River USGS station (OSJ) during the 2002 simulation period.

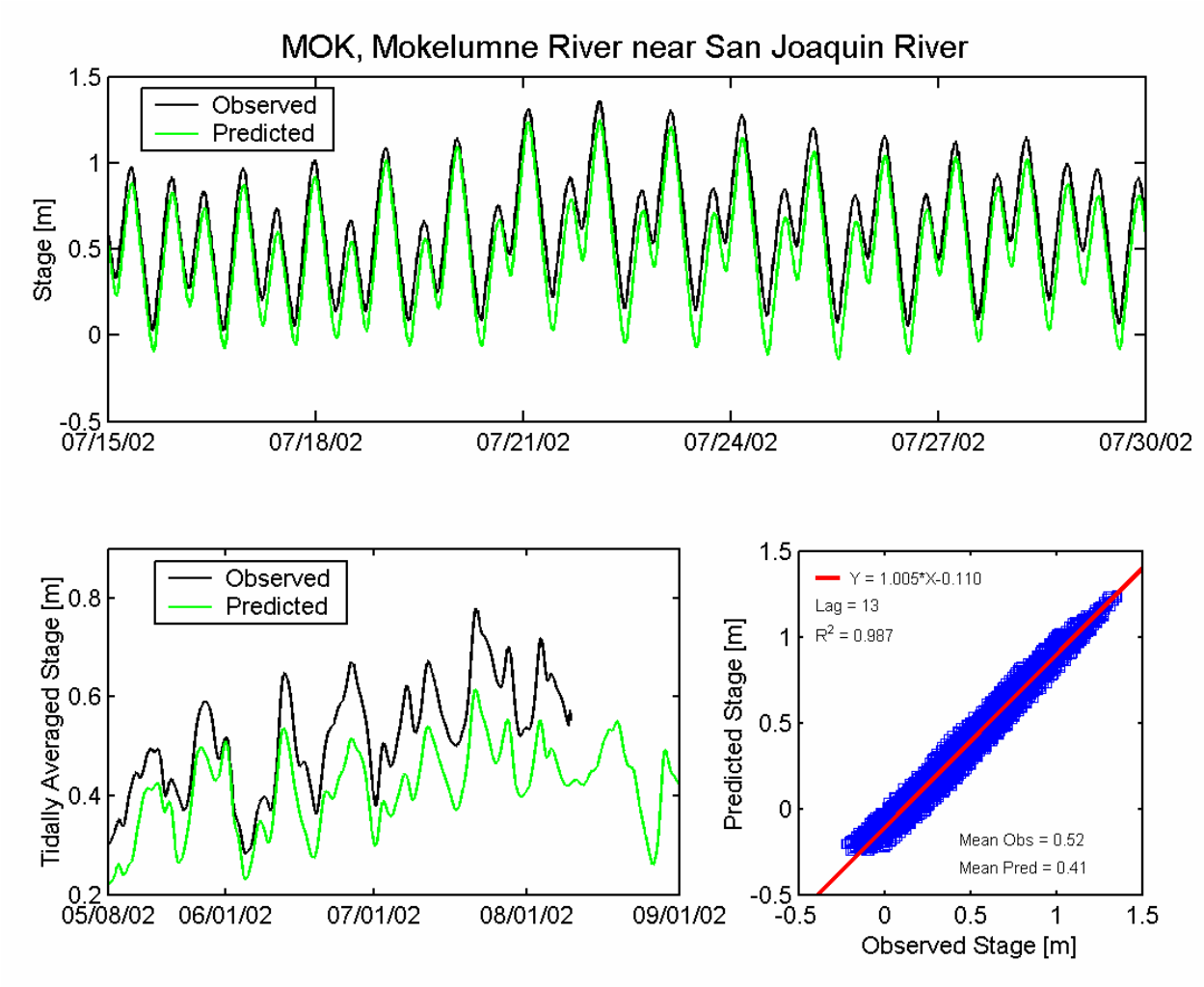

Figure 5.2-27 Observed and predicted stage at Mokelumne River near San Joaquin River USGS station (MOK) during the 2002 simulation period.

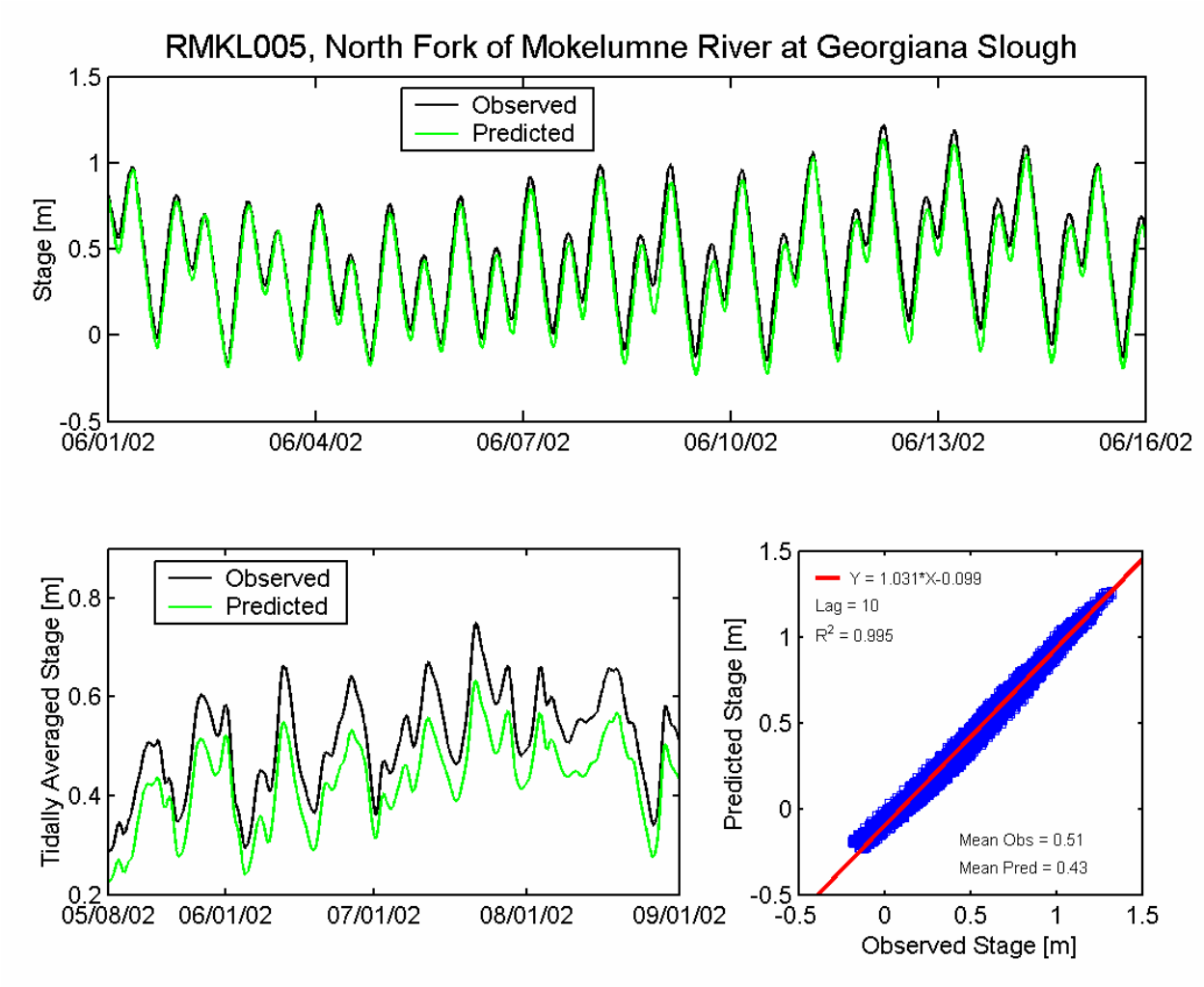

Figure 5.2-28 Observed and predicted stage at North Fork Mokelumne River at Georgiana Slough DWR station (RMKL005) during the 2002 simulation period.

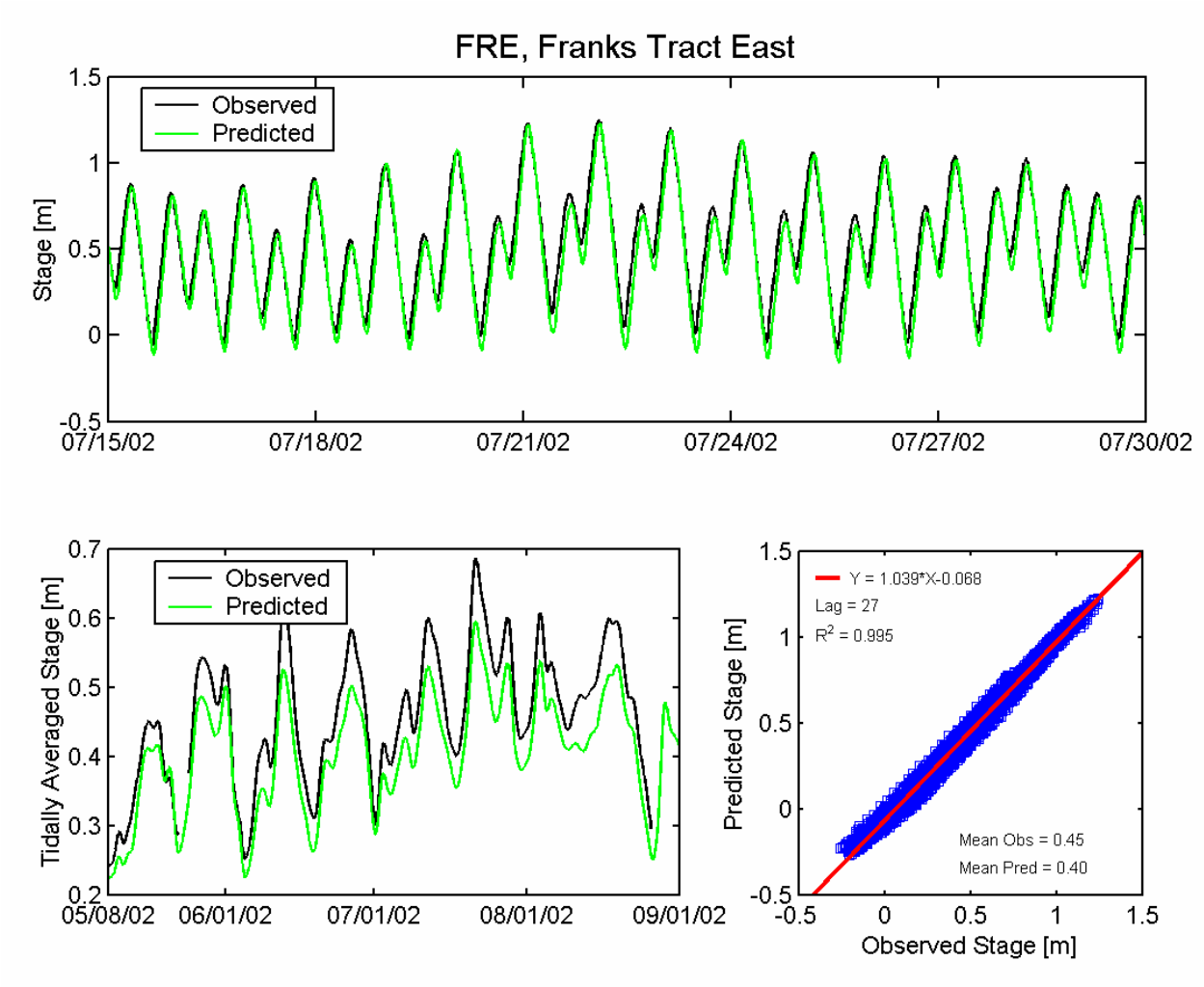

Figure 5.2-29 Observed and predicted stage at Franks Tract East USGS station (FRE) during the 2002 simulation period.

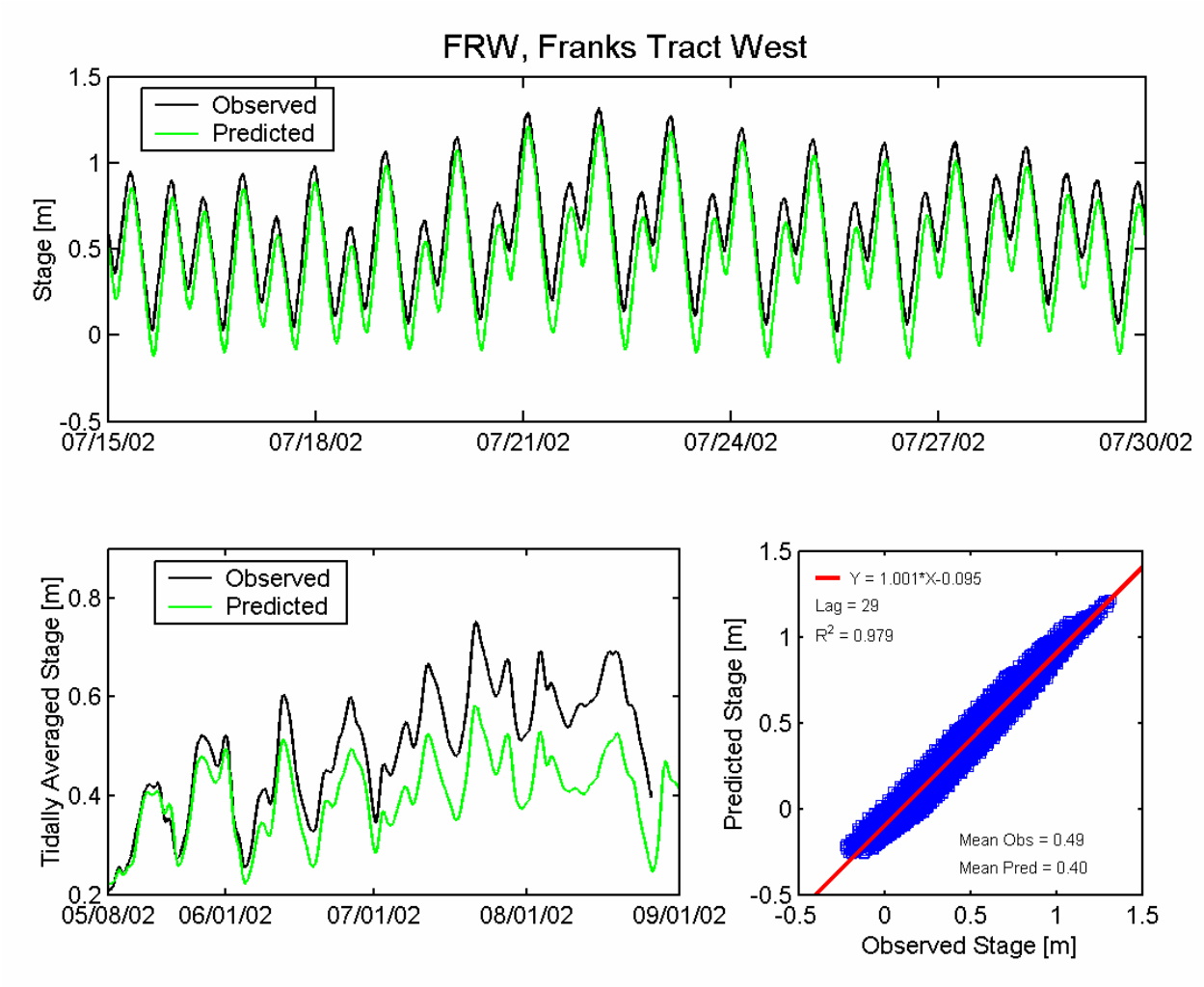

Figure 5.2-30 Observed and predicted stage at Franks Tract West USGS station (FRW) during the 2002 simulation period.

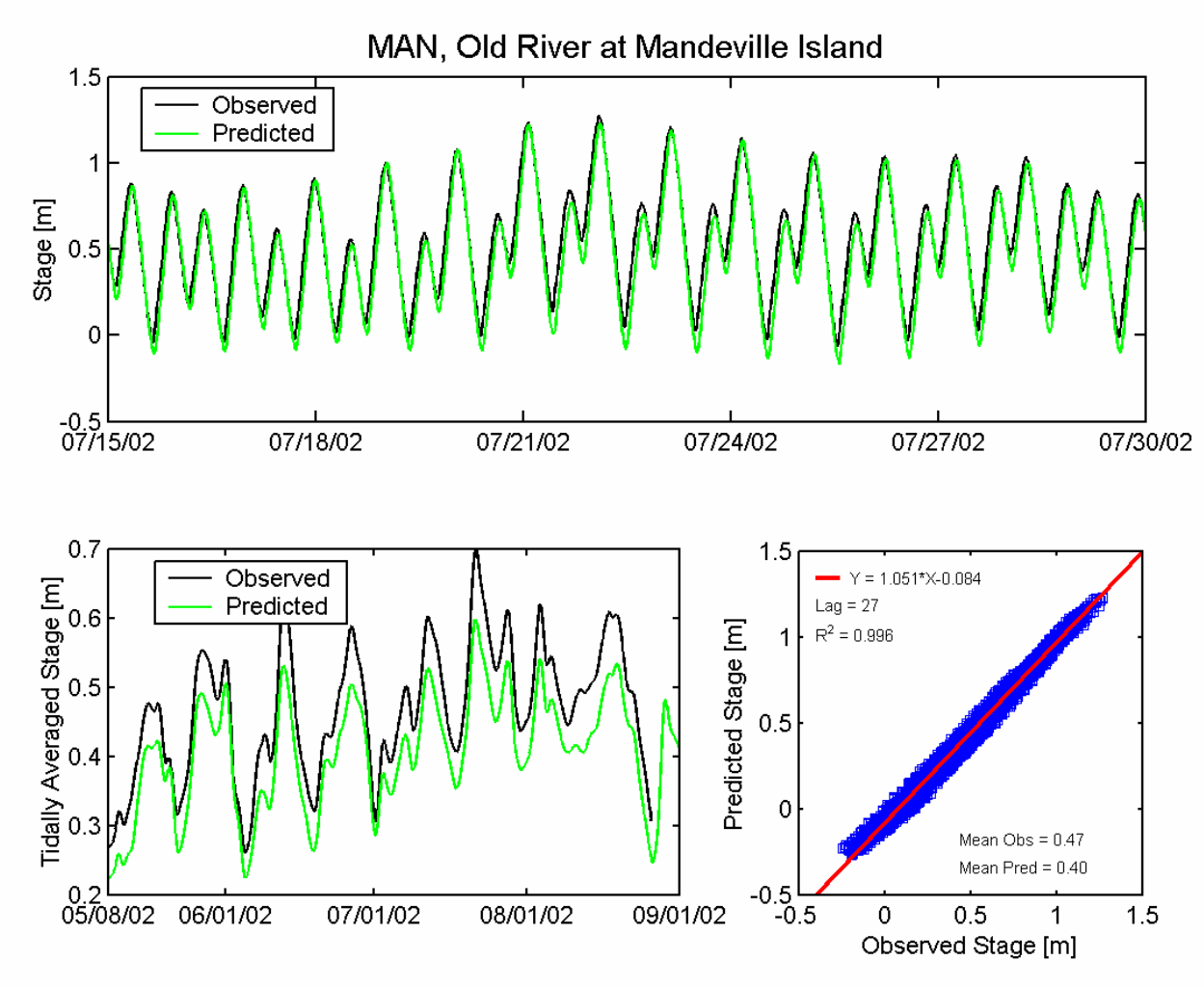

Figure 5.2-31 Observed and predicted stage at Old River at Mandeville Island USGS station (MAN) during the 2002 simulation period.

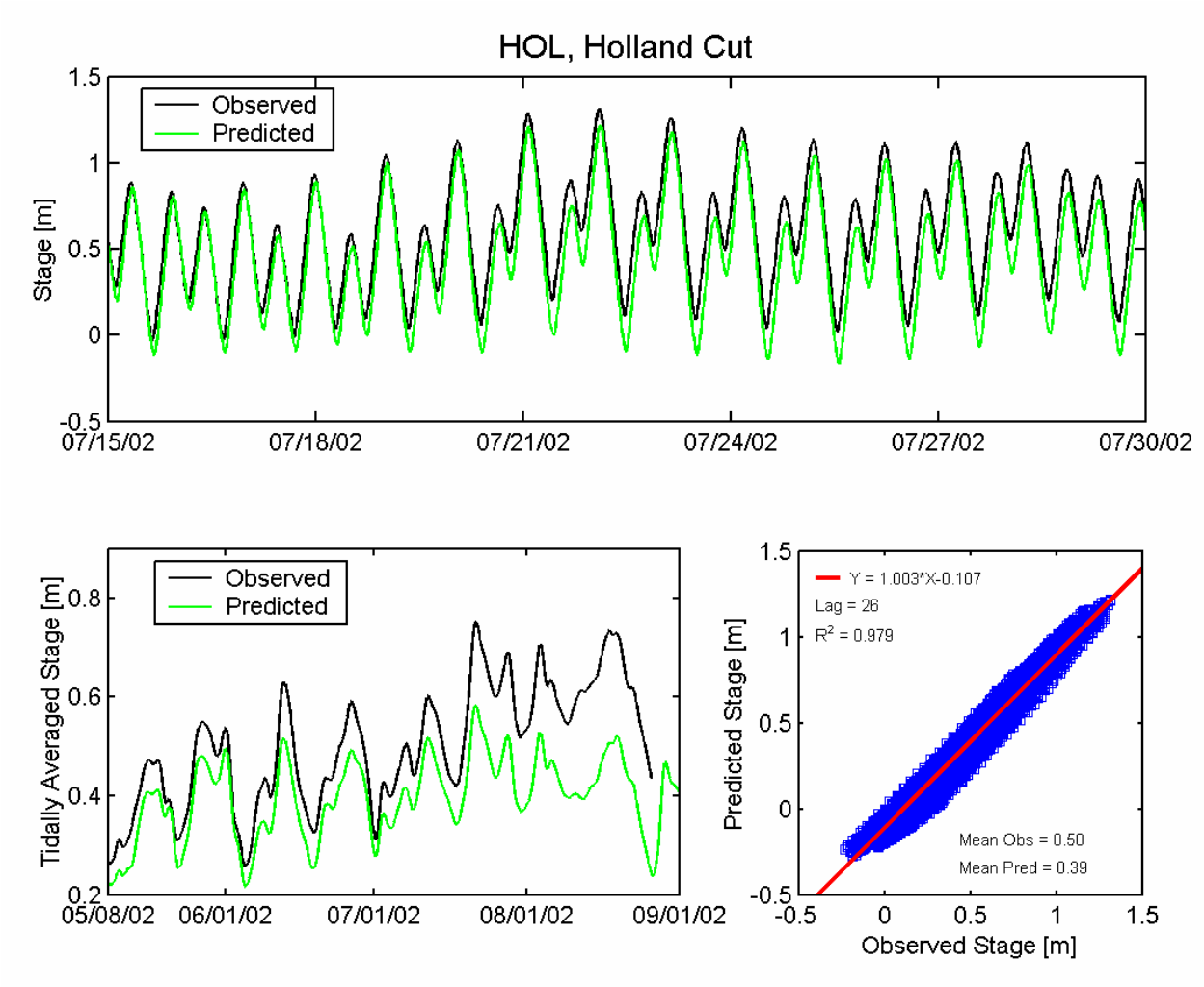

Figure 5.2-32 Observed and predicted stage at Holland Cut USGS station (HOL) during the 2002 simulation period.

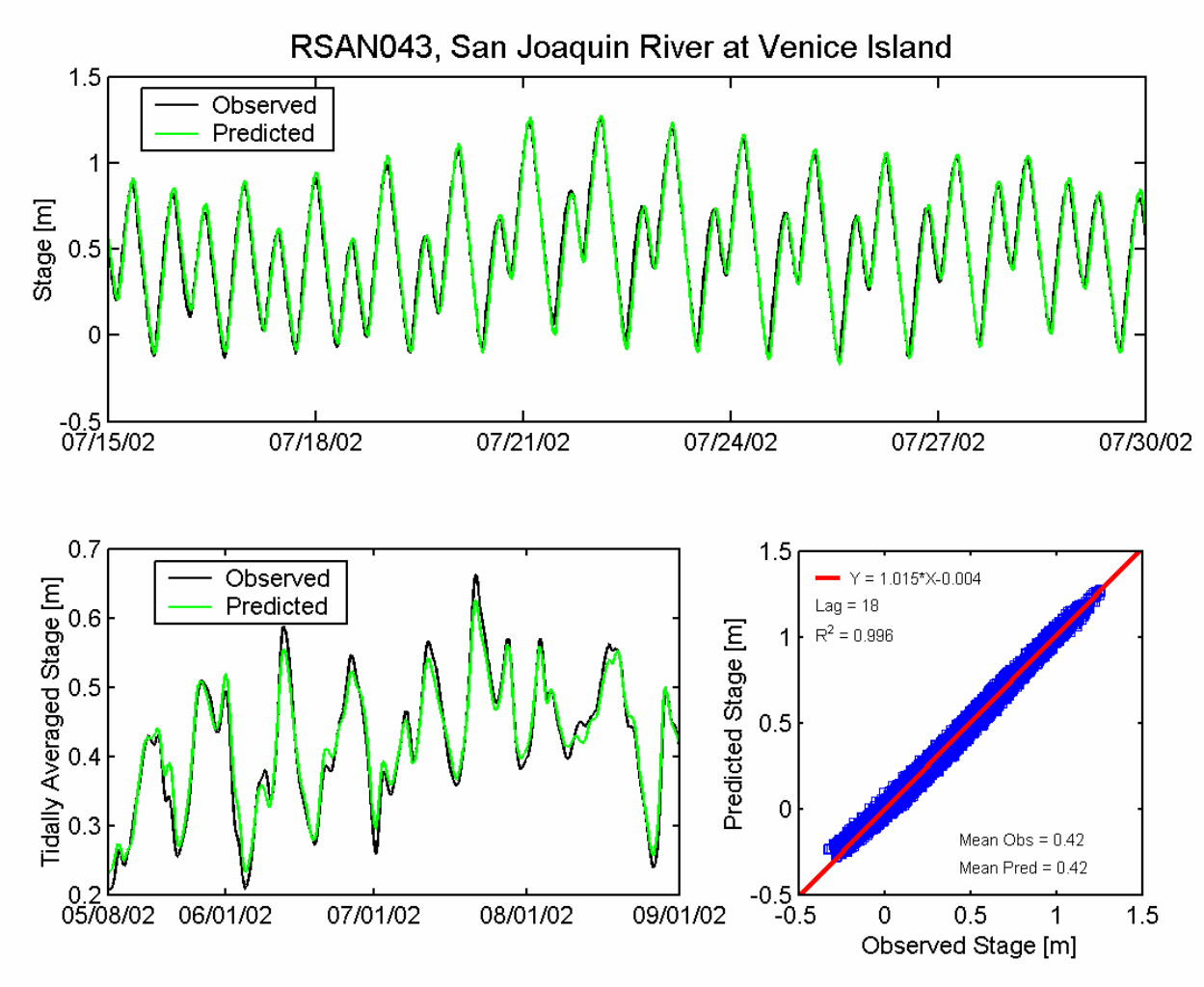

Figure 5.2-33 Observed and predicted stage at San Joaquin River at Venice Island DWR station (RSAN043) during the 2002 simulation period.

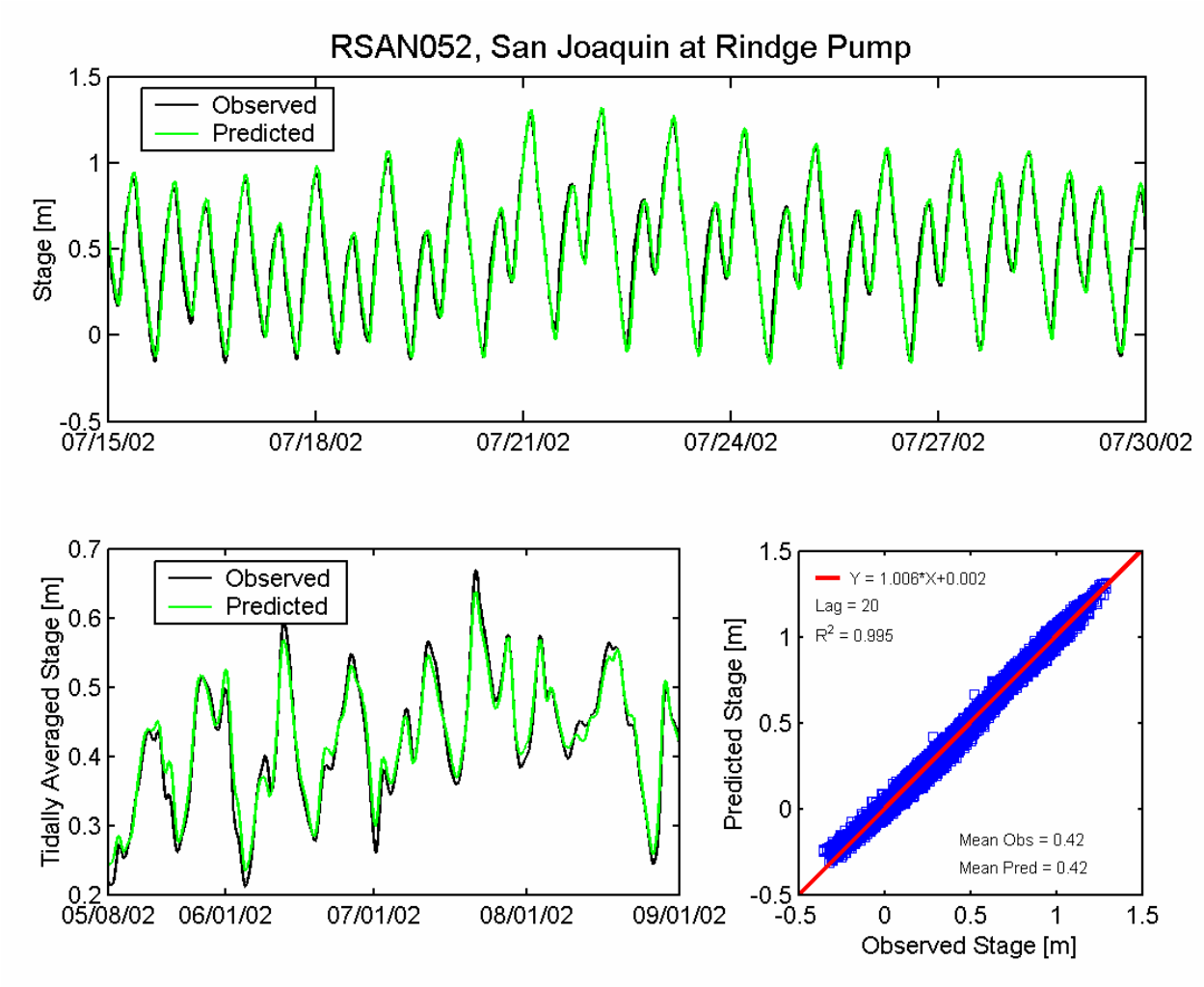

Figure 5.2-34 Observed and predicted stage at San Joaquin River at Rindge Pump DWR station (RSAN052) during the 2002 simulation period.

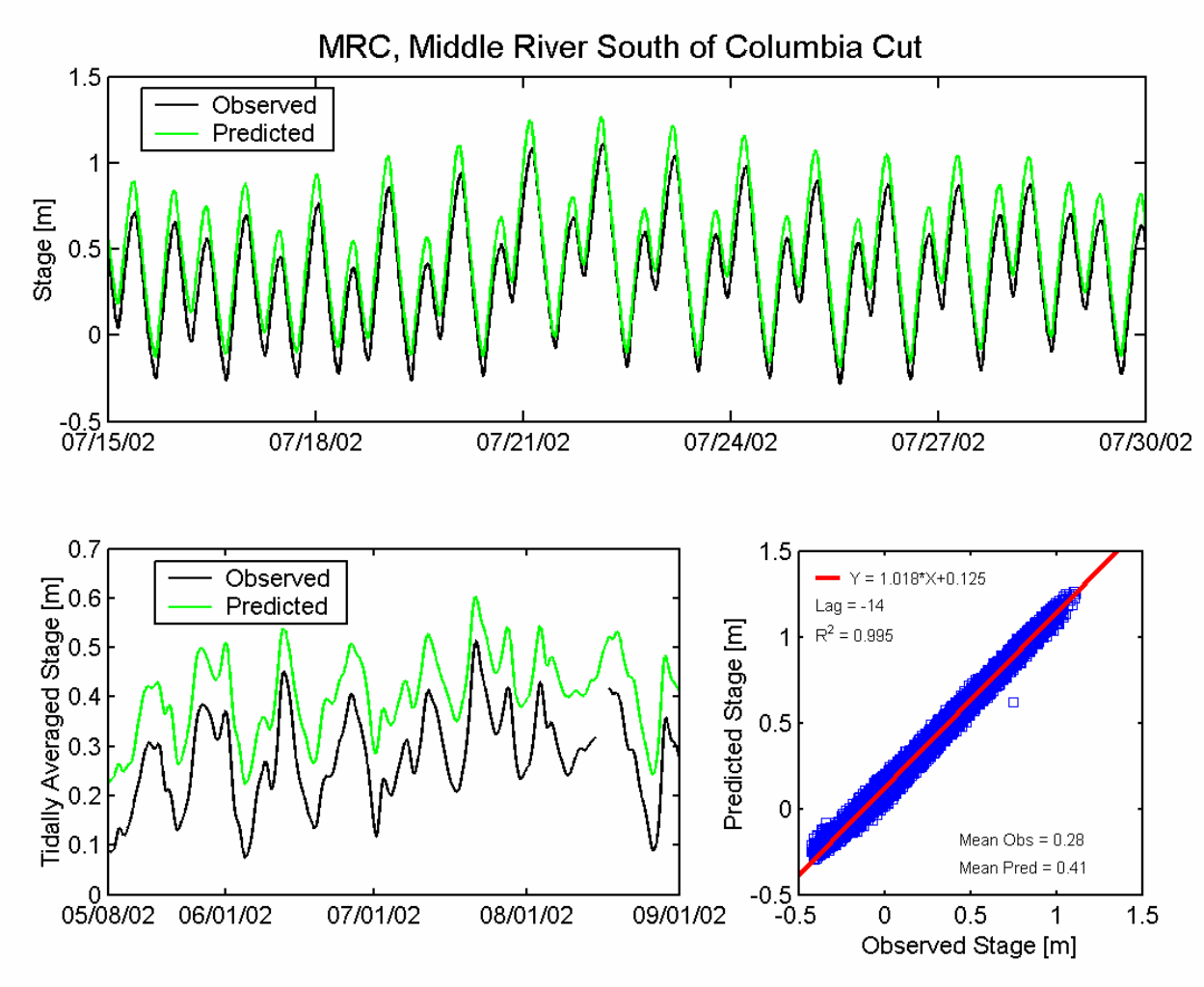

Figure 5.2-35 Observed and predicted stage at Middle River South of Columbia Cut USGS station (MRC) during the 2002 simulation period.

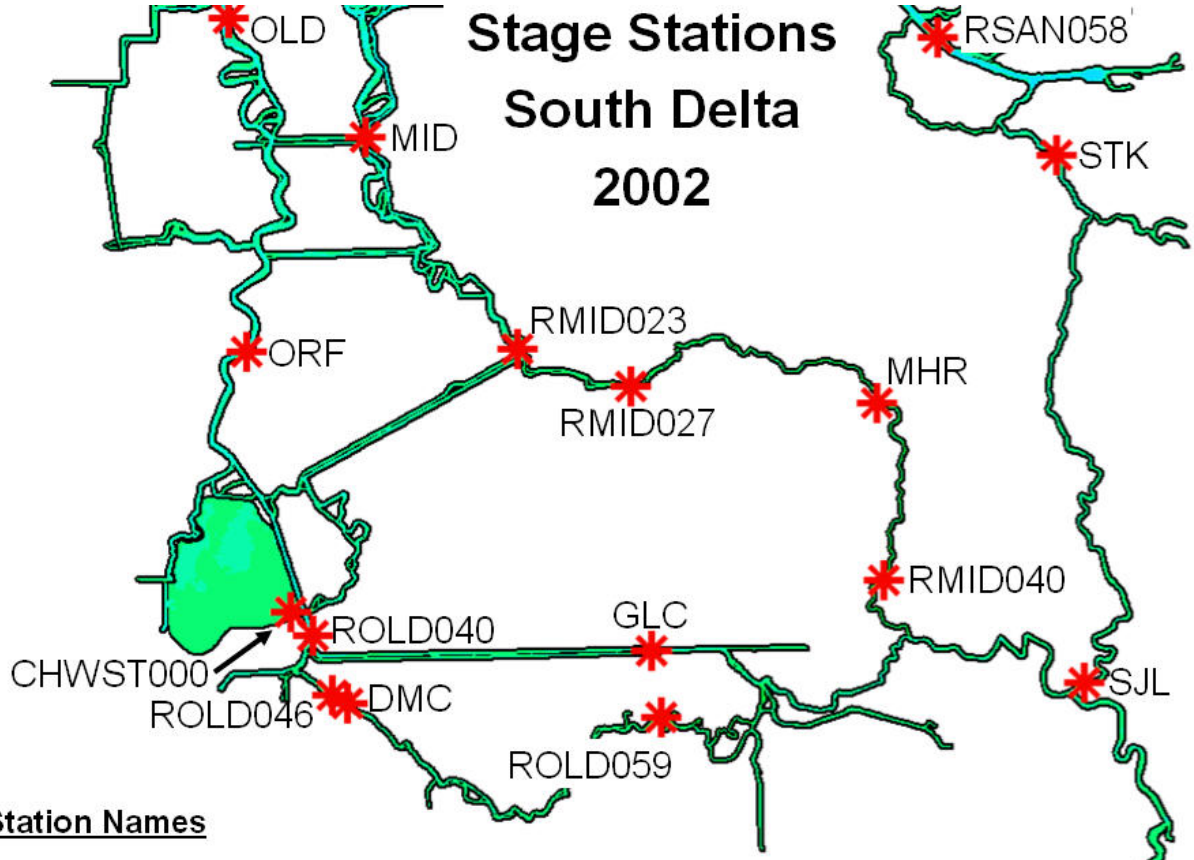

Station Names

MID, Middle River at Middle River

RMID023, Middle River at Borden Hwy

RMID027, Middle River at Tracy Blvd

MHR, Middle River at Howard Road Bridge

RMID040, Middle River at Mowry Bridge

OLD, Old River at Bacon Island

ORF, Old River near Byron

ROLD040, Old River at Clifton Court Ferry

CHWST000, Clifton Court Forebay

GLC, Grant Line Canal at Tracy Blvd

ROLD046, Old River near Delta Mendota Canal (Downstream of Barrier)

DMC, Old River near Delta Mendota Canal (Upstream of Barrier)

ROLD059, Old River at Tracy Blvd

RSAN058, Stockton Ship Channel at Burns Cutoff

STK, San Joaquin River at Stockton

SJL, San Joaquin River below Old River near Lathrop

Figure 5.2-36 Location of water level monitoring stations in the southern portion of the Sacramento-San Joaquin Delta used for 2002 water level calibration.

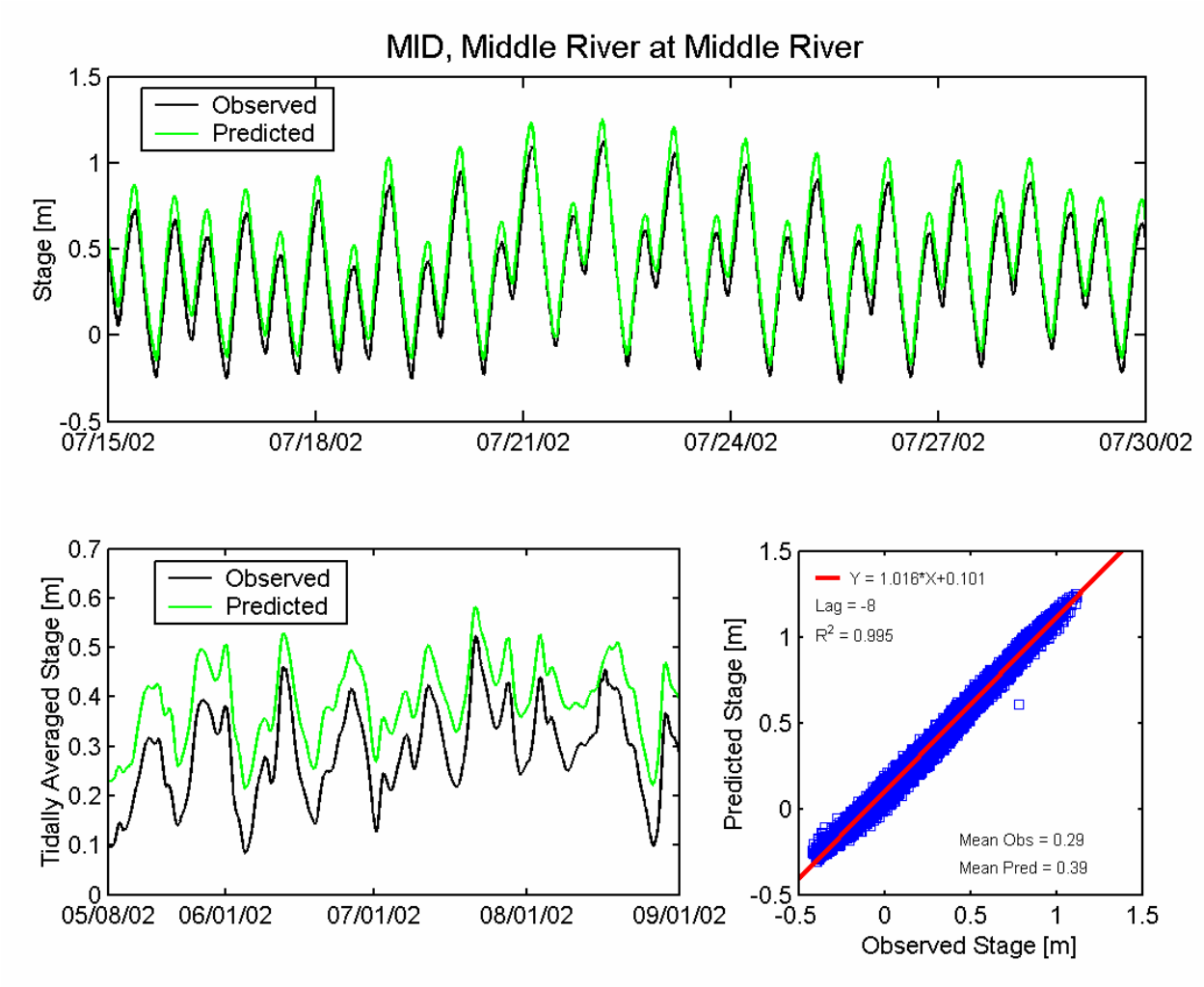

Figure 5.2-37 Observed and predicted stage at Middle River at Middle River USGS station (MID) during the 2002 simulation period.

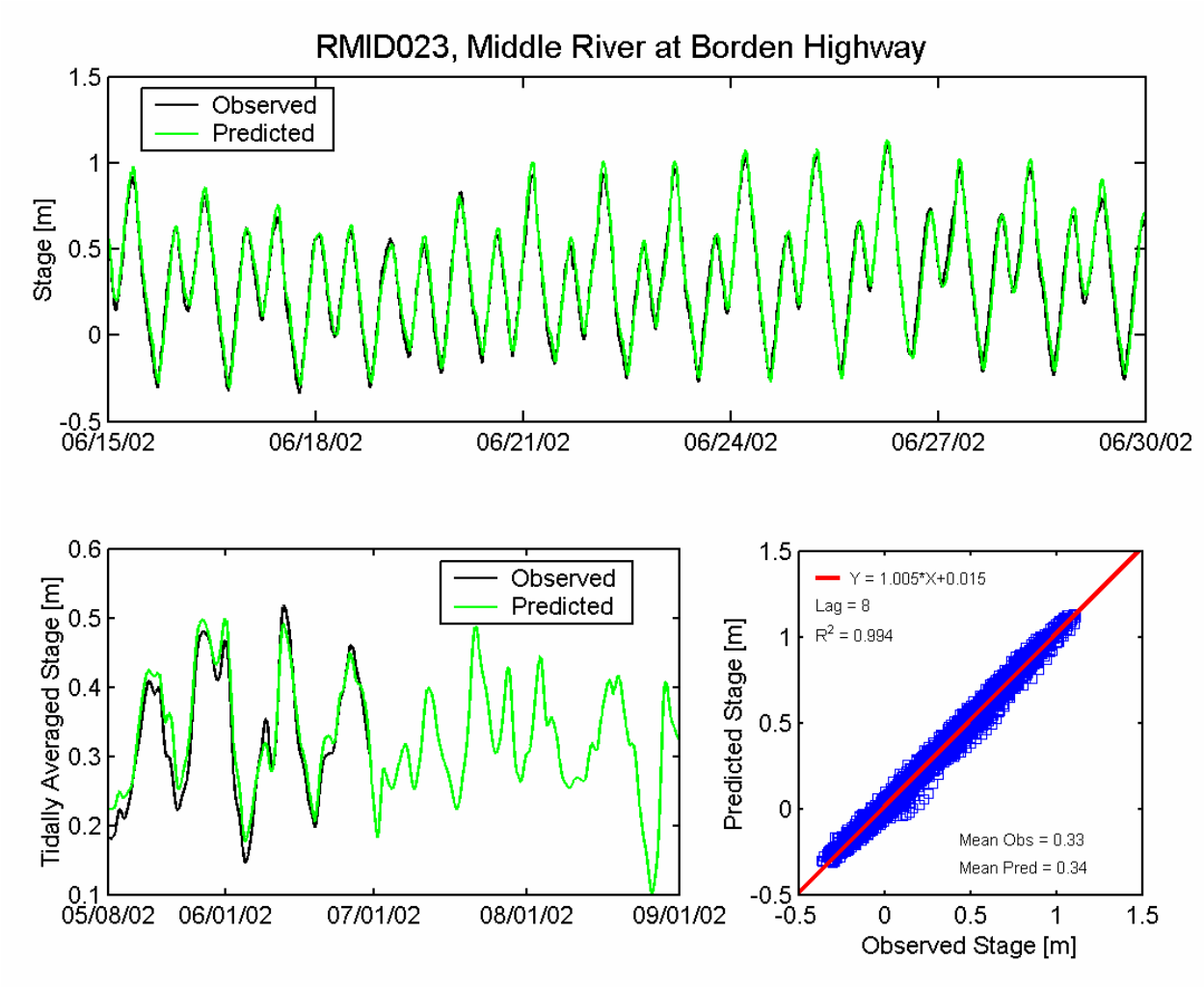

Figure 5.2-38 Observed and predicted stage at Middle River at Borden Highway DWR station (RMID023) during the 2002 simulation period.

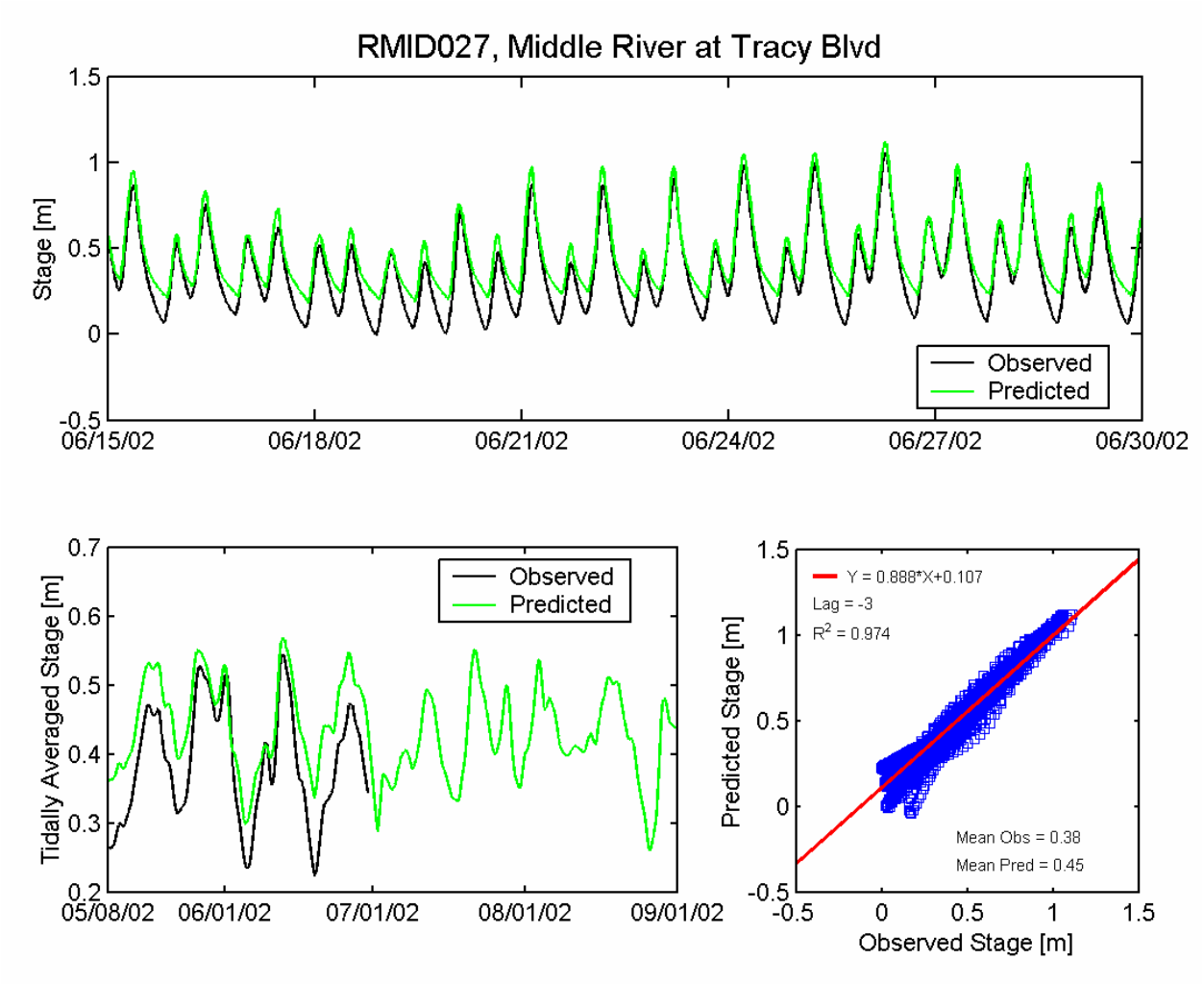

Figure 5.2-39 Observed and predicted stage at Middle River at Tracy Boulevard DWR station (RMID027) during the 2002 simulation period.

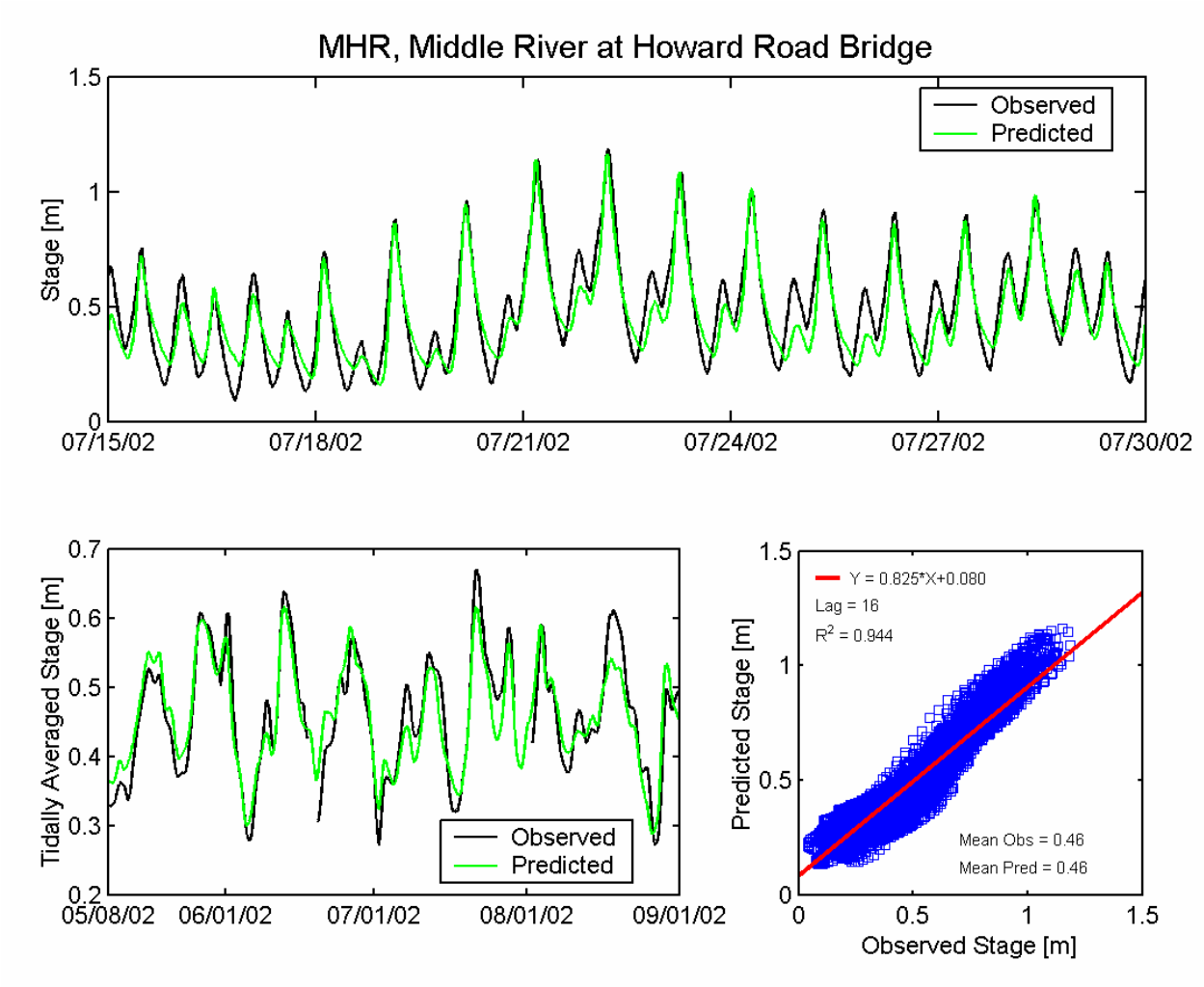

Figure 5.2-40 Observed and predicted stage at Middle River at Howard Road Bridge DWR station (CDEC MHR) during the 2002 simulation period.

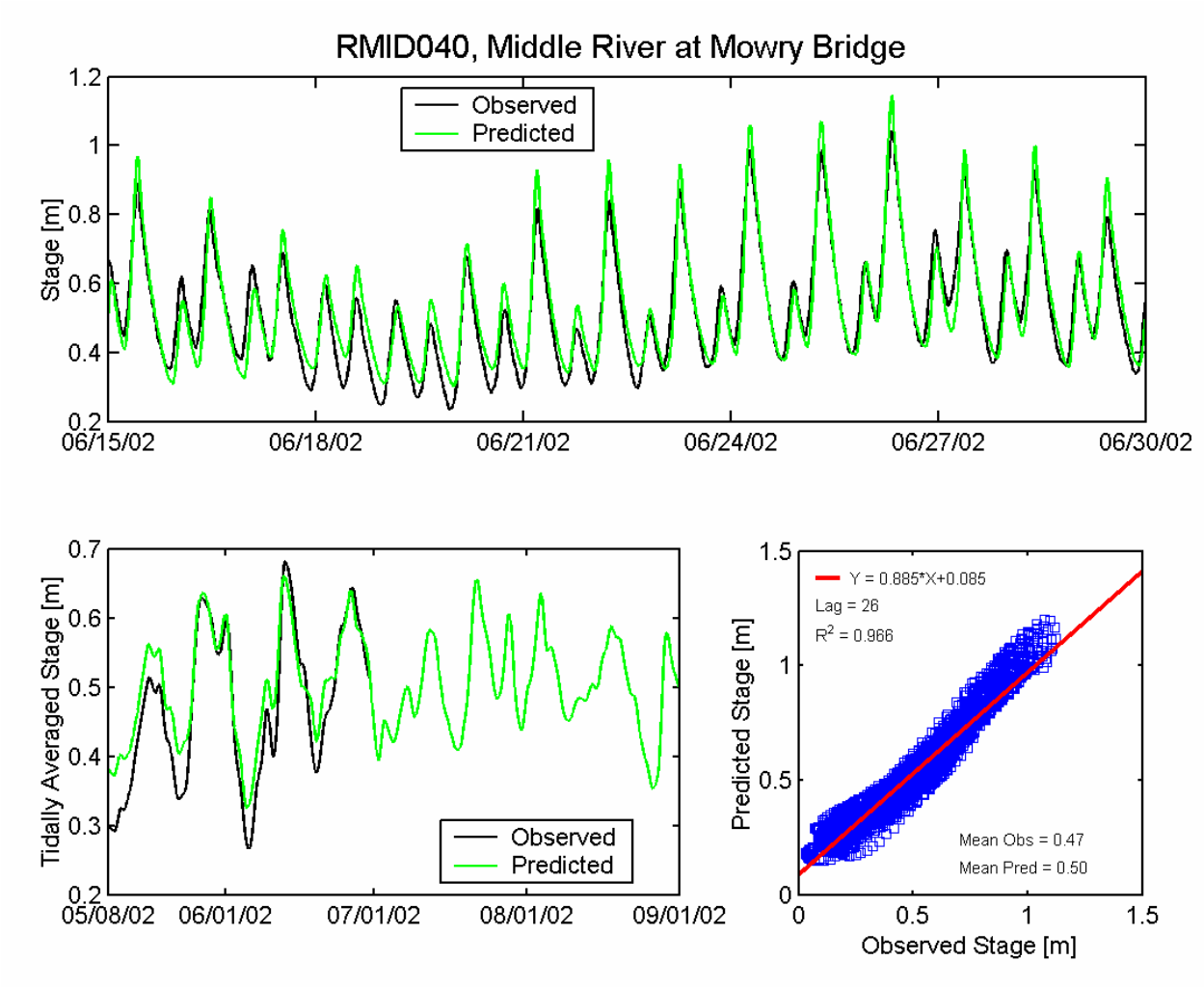

Figure 5.2-41 Observed and predicted stage at Middle River at Mowry Bridge DWR station (RMID040) during the 2002 simulation period.

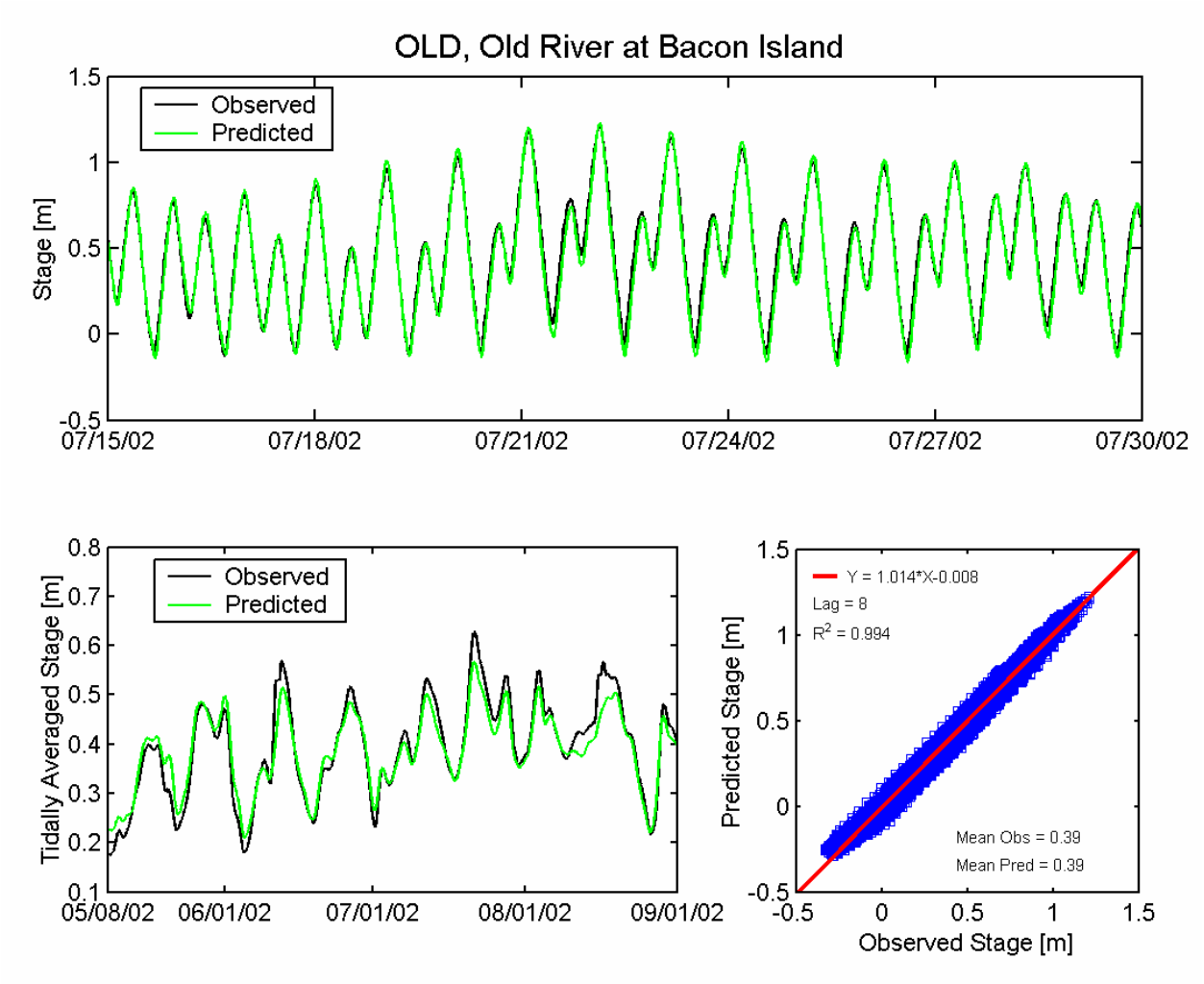

Figure 5.2-42 Observed and predicted stage at Old River at Bacon Island USGS station (OLD) during the 2002 simulation period.

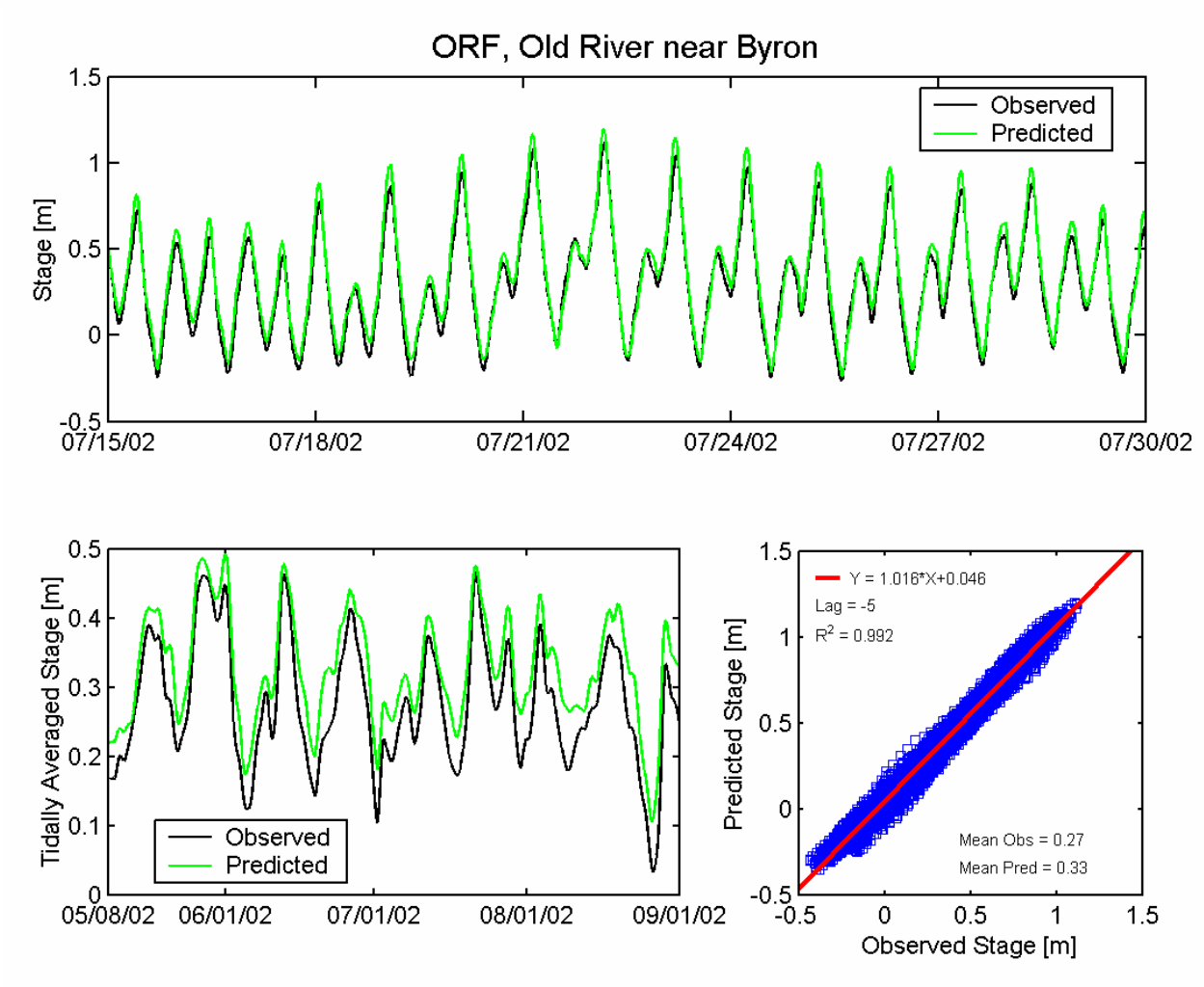

Figure 5.2-43 Observed and predicted stage at Old River near Byron USGS station (ORF) during the 2002 simulation period.

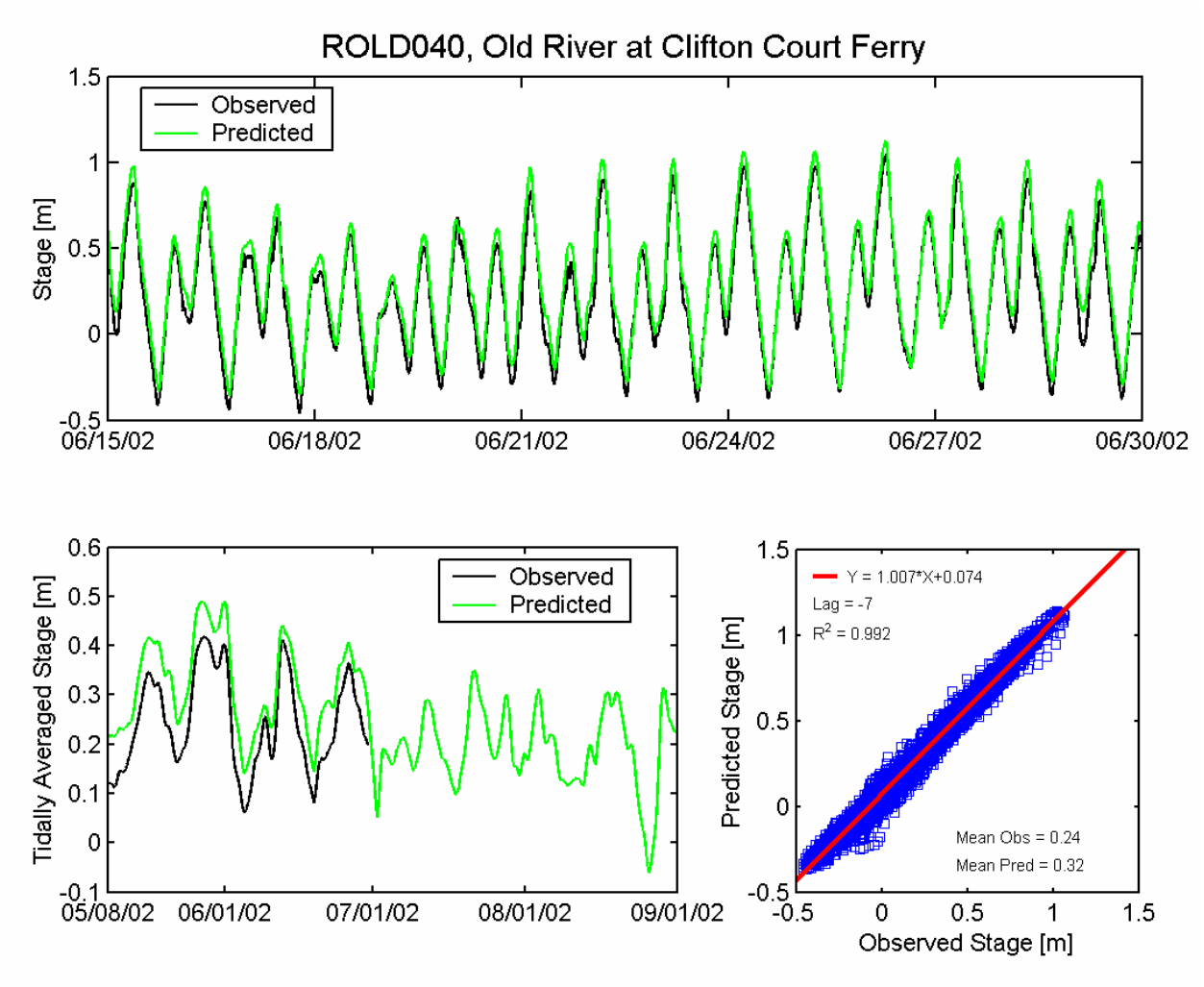

Figure 5.2-44 Observed and predicted stage at Old River at Clifton Court Ferry DWR station (ROLD040) during the 2002 simulation period.

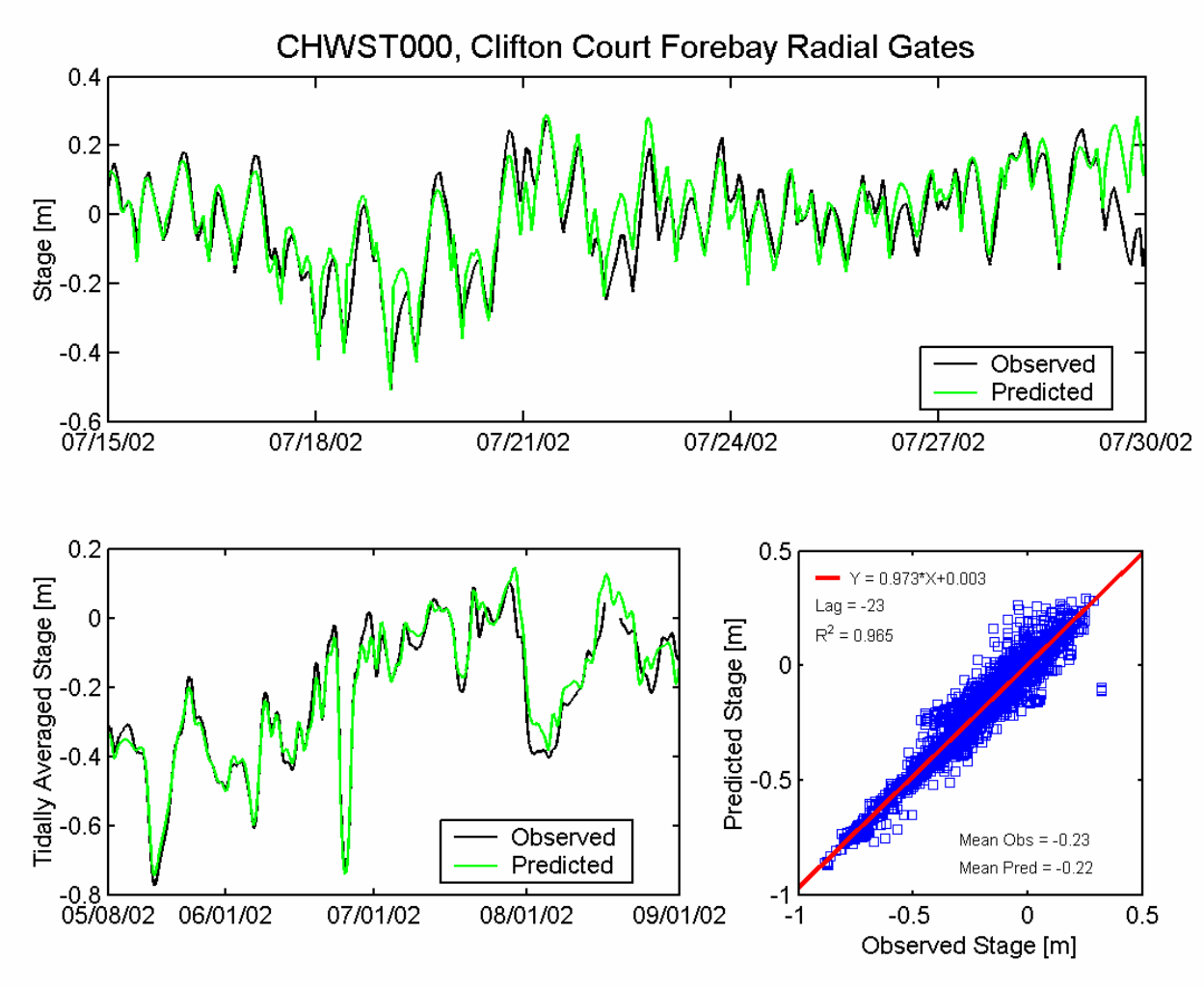

Figure 5.2-45 Observed and predicted stage at Clifton Court Forebay DWR station (CHWST000) during the 2002 simulation period.

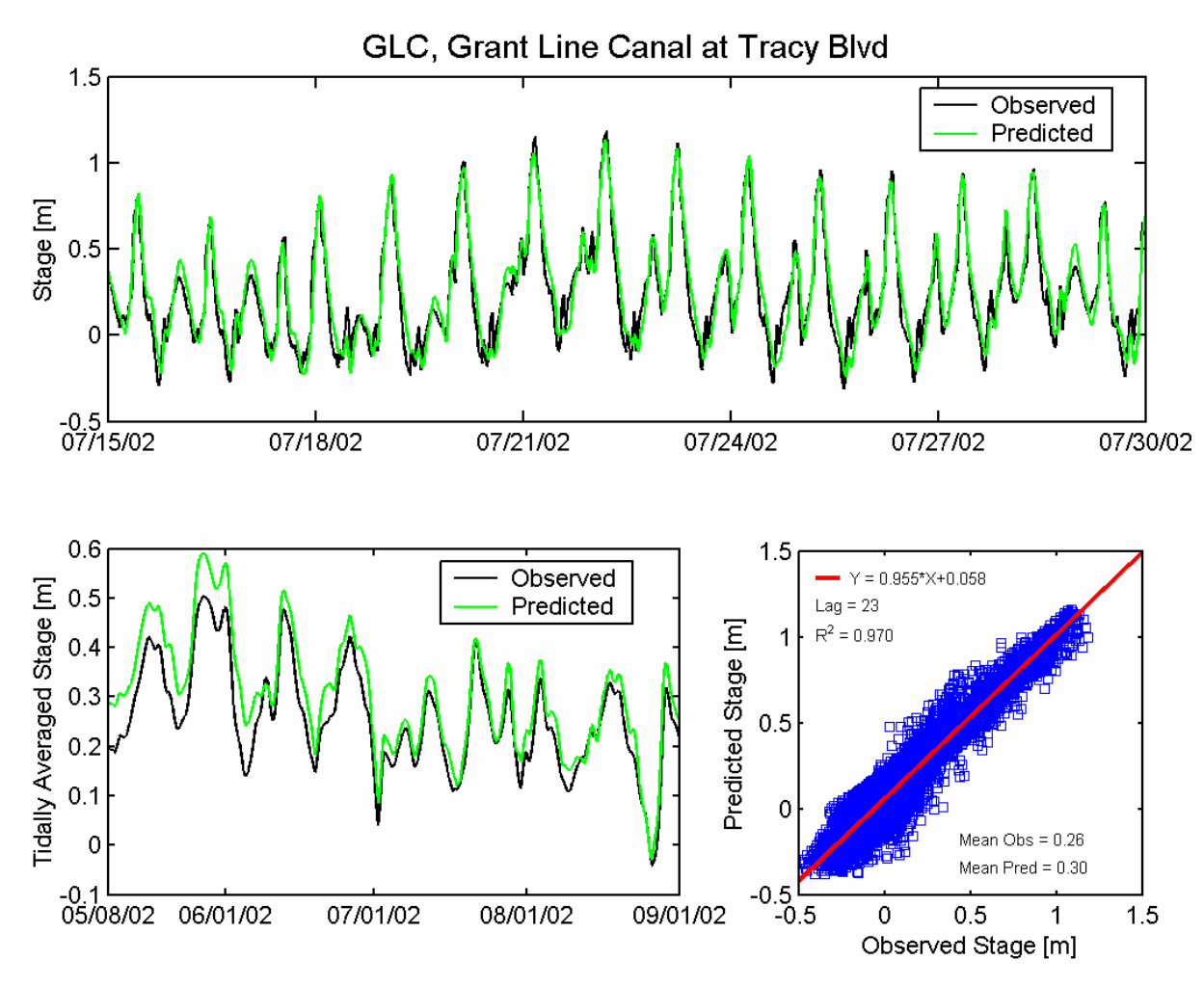

Figure 5.2-46 Observed and predicted stage at Grant Line Canal at Tracy Boulevard USGS station (GLC) during the 2002 simulation period.

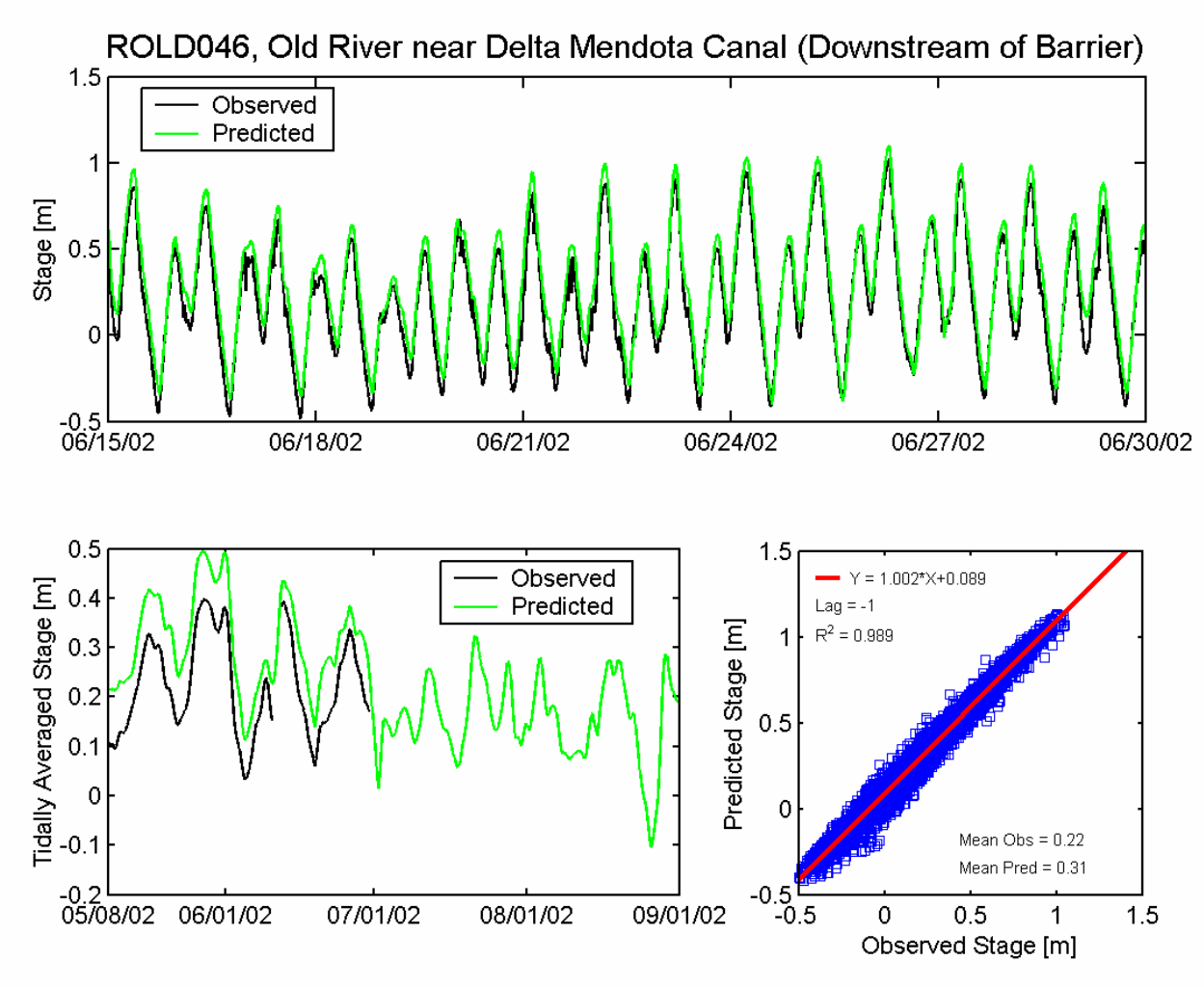

Figure 5.2-47 Observed and predicted stage at Old River near Delta Mendota Canal Downstream of Barrier DWR station (ROLD046) during the 2002 simulation period.

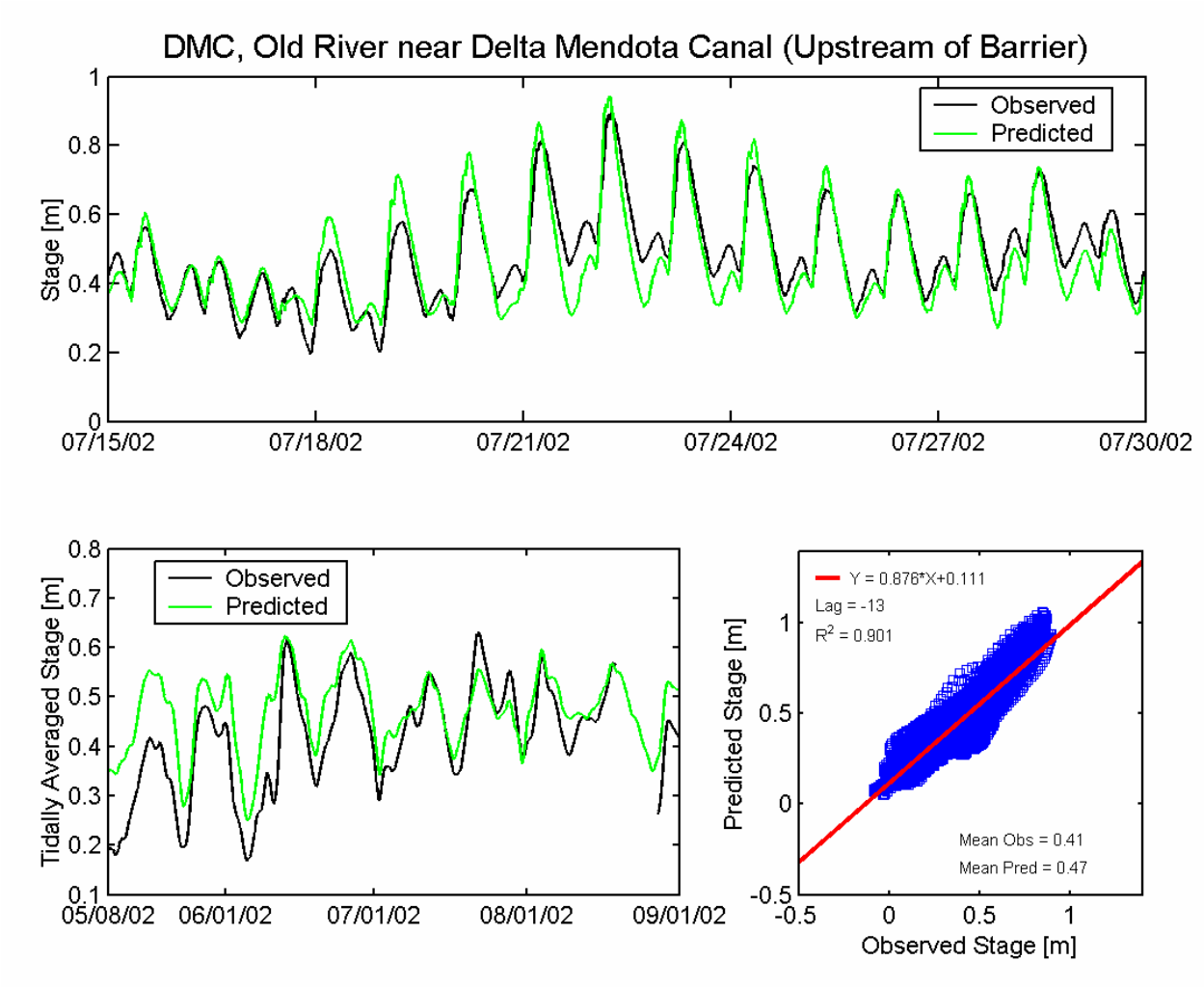

Figure 5.2-48 Observed and predicted stage at Delta Mendota Canal Upstream of Barrier USGS station (DMC) during the 2002 simulation period.

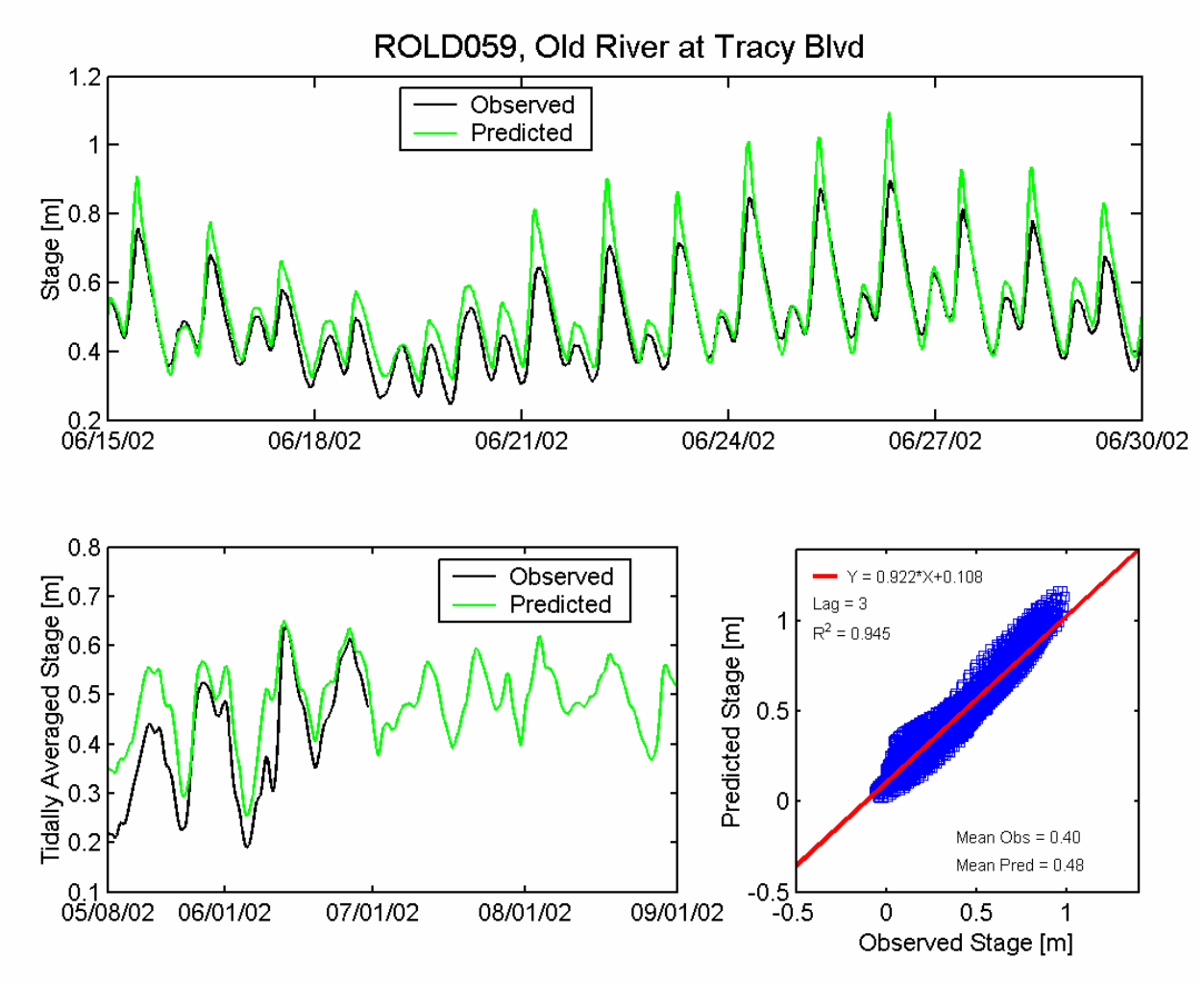

Figure 5.2-49 Observed and predicted stage at Old River at Tracy Boulevard DWR station (ROLD059) during the 2002 simulation period.

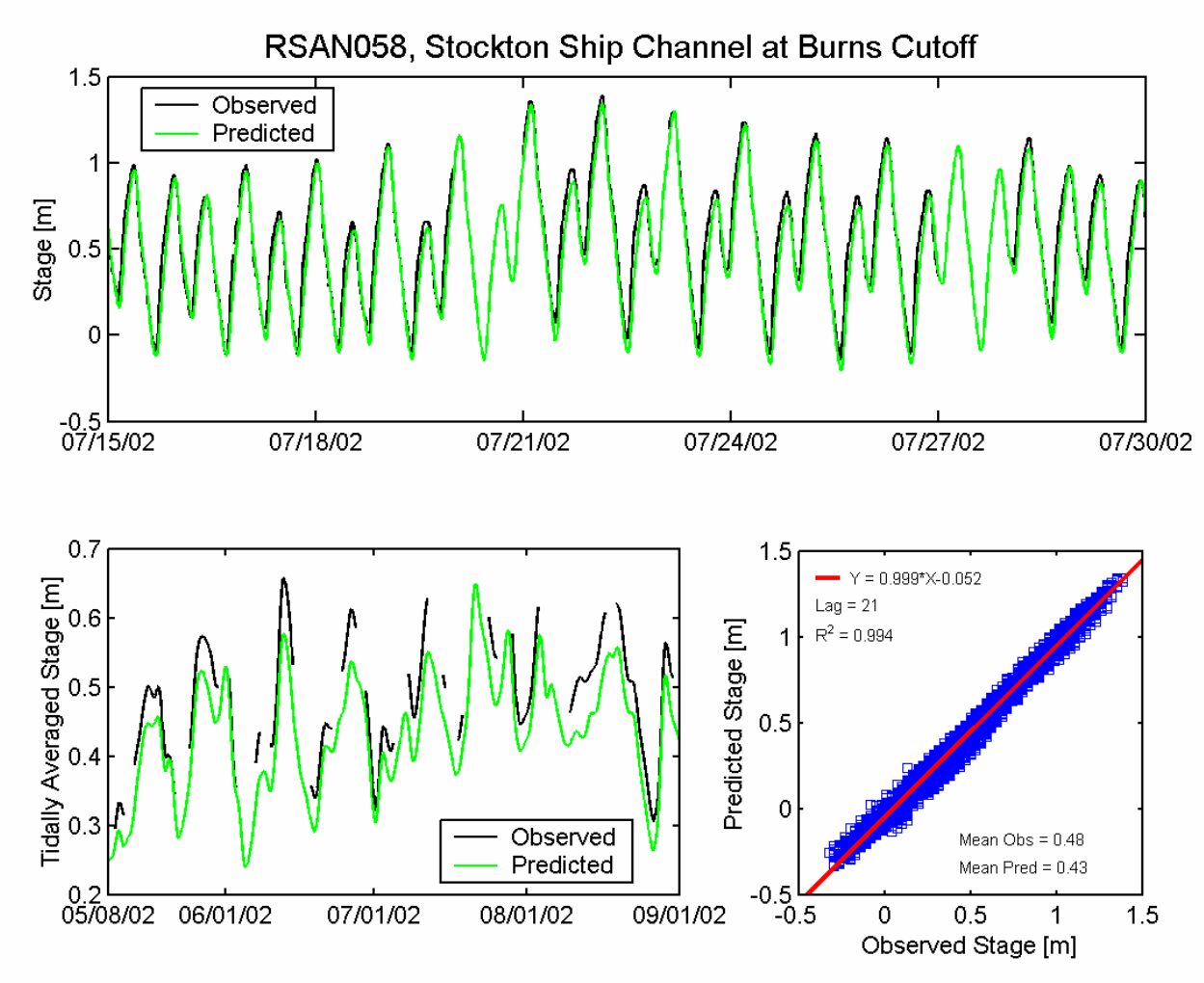

Figure 5.2-50 Observed and predicted stage at Stockton Ship Channel at Burns Cutoff DWR station (RSAN058) during the 2002 simulation period.

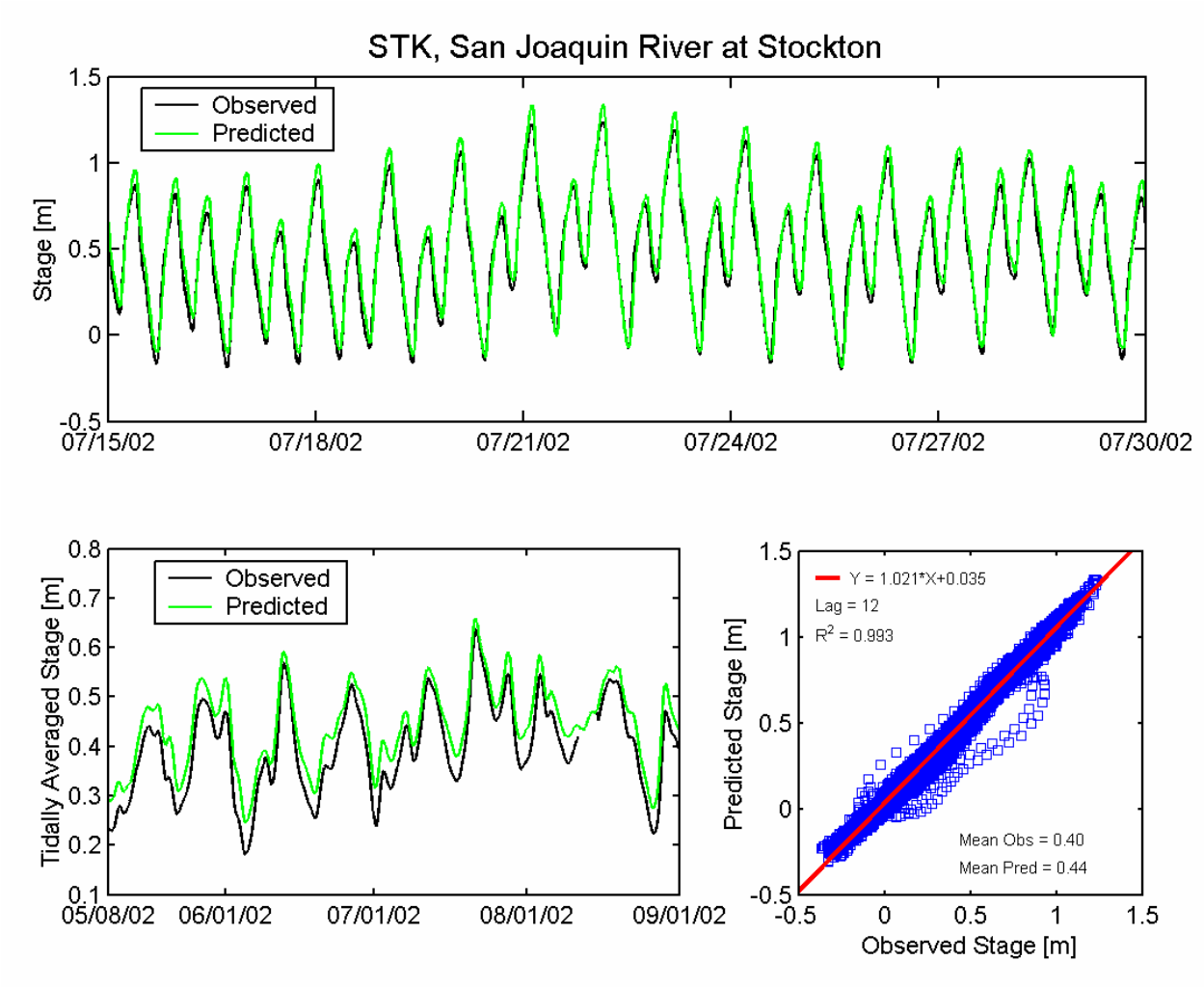

Figure 5.2-51 Observed and predicted stage at San Joaquin River at Stockton USGS station (STK) during the 2002 simulation period.

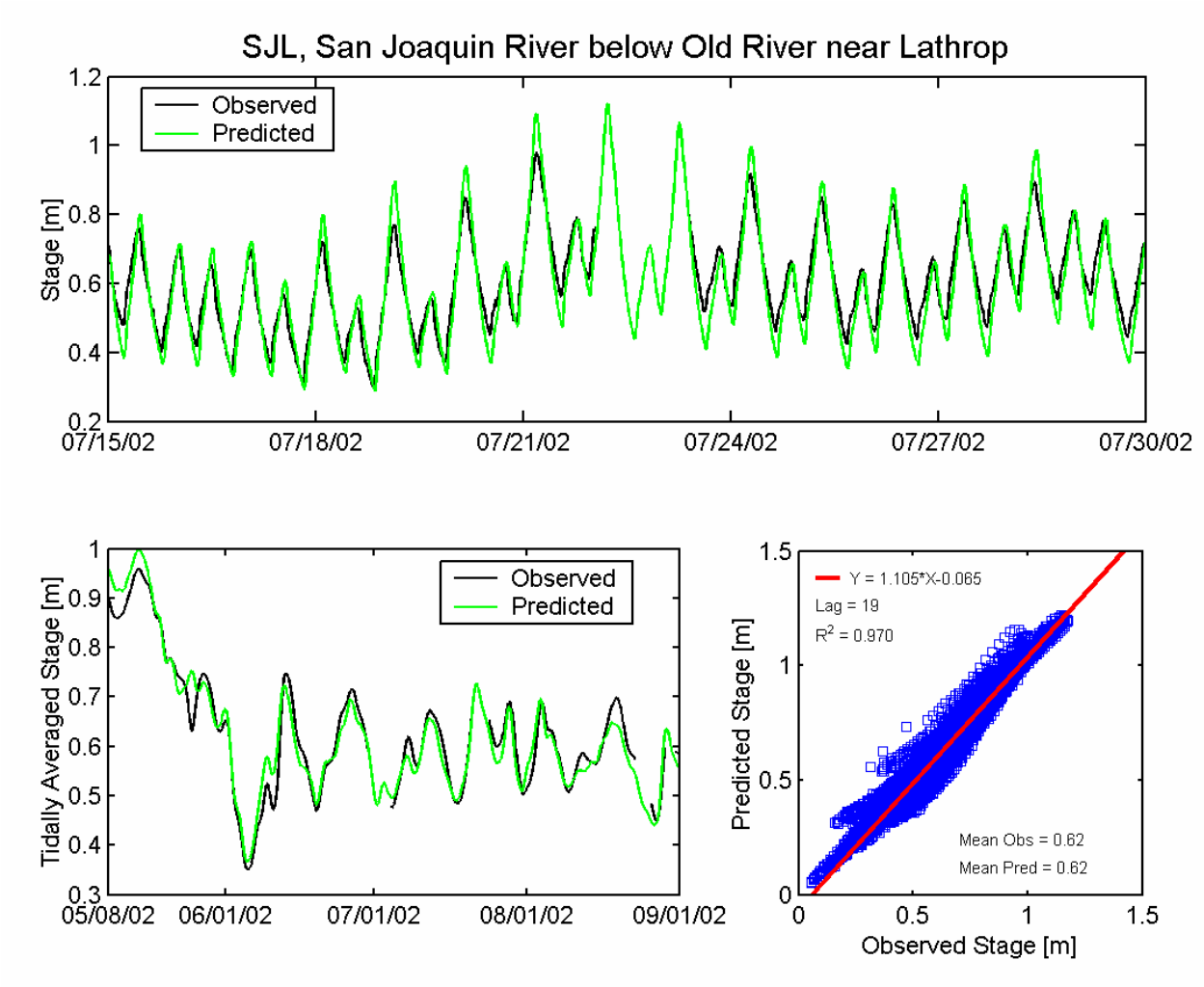

Figure 5.2-52 Observed and predicted stage at San Joaquin River below Old River near Lathrop DWR station (CDEC SJL) during the 2002 simulation period.

5.3 Flow Validation

During the 2002 validation period, flow measurements are available at a total of twenty-three flow monitoring stations in the Sacramento-San Joaquin Delta. Some of these flow data were collected as part of an extensive USGS monitoring program using a large number of temporary stations in the Sacramento-San Joaquin Delta during 2002. Additional data were available at permanent USGS stations and at one DWR station.

For each station, the mean observed and predicted net flow was calculated over the full simulation period, and the same cross-correlation procedure used in the water level analysis was applied to flow. Table 5-2 gives the predicted and observed mean flow at each station as well as the corresponding amplitude ratio, phase lag, and R^2 for each station.

5.3.1 Northern Sacramento-San Joaquin Delta

Flow calibration comparisons were performed at six continuous flow monitoring stations in the northern portion of the Delta, at the locations shown in Figure 5.3-1. Flow comparisons at these stations are shown in Figures 5.3-2 through 5.3-7.

Observed and predicted flows on the Sacramento River south of Georgiana slough (Figure 5.3-2), agree well, both in terms of tidal flow magnitudes with an amplitude ratio of 0.993, and in terms of tidally-averaged flow. Average observed net flow during the simulation period was 111 m^3/s, compared to 109 m^3/s predicted net flow. These results show that the model is accurately predicting flows in the Sacramento River, downstream of the Delta Cross Channel and Georgiana Slough. Predicted tidal and tidally-averaged flows in Georgina Sough (Figure 5.3-3) agree well with observed flows, with observed and predicted net flows of 81.1 m^3/s and 83.9 m^3/s, respectively. In the Delta Cross Channel (Figure 5.3-4), observed and predicted flows agree well during periods when the Delta Cross Channel is open and closed (shown in top panel of Figure 5.3-4; operations schedule shown in Figure 5.1-1), and a similar pattern of tidally-averaged flows is evident. During 2002, experimental operations of the Delta Cross Channel between June 3 and June 14 resulted in an unusually large number of occurrences of gate opening and closing, and the comparisons show that the model is very accurately capturing the effect of these Delta Cross Channel operations. As during the 2007 calibration period, predicted tidally-averaged flows through the Delta Cross Channel are slightly less than observed flows, resulting in observed and predicted average net flows during the simulation period of 123 m^3/s and 110 m^3/s, respectively. In the Sacramento River upstream of the Delta Cross Channel (Figure 5.3-5), observed and predicted flows agree well, both in terms of tidal flow magnitudes with an amplitude ratio of 1.038, and in terms of tidally-averaged flow. Average observed and predicted net flow during the simulation period were nearly identical, with observed and predicted average net flows of 292 m^3/s and 291 m^3/s, respectively. Further upstream on the Sacramento River at Freeport (Figure 5.3-6), predicted tidal flows are somewhat larger than observed tidal flows, with an amplitude ratio of 1.111, but observed and predicted tidally-averaged flows are nearly identical. Observed and predicted average net flow during the simulation period are 453 m^3/s and 446 m^3/s, respectively.

On Steamboat Slough between the Sacramento River and Sutter Slough (Figure 5.3-7), predicted tidal prism is somewhat higher than observed, with an amplitude ratios of 1.175. This result is consistent with the higher predicted than observed range in tidal elevation at this stations (see Figures 5.2-14). However, predicted tidally-averaged and average net flows show better agreement with observed tidally-averaged and observed net flows at this station. Observed and predicted average net flow during the simulation period are 62.1 m^3/s and 62.5 m^3/s, respectively.

5.3.2 Central Sacramento-San Joaquin Delta

Flow calibration comparisons were performed at twelve continuous flow monitoring stations in the central portion of the Delta, at the locations shown in Figure 5.3-8. Flow comparisons at these stations are shown in Figures 5.3-9 through 5.3-20.

At Rio Vista on the Sacramento River (Figure 5.3-9), the observed and predicted flows show good agreement, with typical peak tidal flows of 3000 m^3/s. The cross-correlation analysis yields an amplitude ratio of 0.996, indicating that the model is accurately predicting the flow amplitude, a phase lag of 7 minutes. Overall the model shows similar tidally-averaged net flows over the analysis period, and the observed and predicted mean flows are 294 m^3/s and 265 m3/s, respectively. At Threemile Slough at the San Joaquin River (Figure 5.3-10), observed and predicted peak flows are typically 700 to 1000 m^3/s, with the model predicting slightly larger negative (south) net flows. The predicted flows show a similar amplitude to observed flows, with an amplitude ratio of 1.042 and a phase lag of 16 minutes. Observed and predicted net flows south through Threemile Slough during the simulation period are 25.6 m^3/s and 52.9 m^3/s, respectively, indicating somewhat larger predicted than observed average net flow. The difference between observed and predicted net flow is larger during 2002 than 2007, however the USGS flow station was moved further north in 2005 to avoid some flow rating complications at the previous station (Cathy Ruhl, personal communication). As a result, the 2007 flow comparison should be more representative of model accuracy in Threemile Slough than the 2002 flow comparison. At Jersey Point (Figure 5.3-11), peak flows are typically 4000 m^3/s; predicted flows show a slightly smaller amplitude than observed flows, with an amplitude ratio of 0.901, and a phase lag of 9 minutes. The predicted tidally-averaged flows show good agreement with observed tidally-averaged flows, with a somewhat larger predicted mean observed net flow than mean predicted net flow.

Observed and predicted flows at False River (Figure 5.3-12) show good agreement, with typical peak flows of 1200 m^3/s. Predicted flows show a slightly smaller amplitude than observed flows, with an amplitude ratio of 0.852, and a phase lead of 36 minutes. The predicted tidally-averaged flow shows good agreement with observed tidally-averaged flow, with slightly more negative (east) predicted than observed net flows, of -29.7 m^3/s and -13.0 m^3/s, respectively. An opposite trend is evident in the net flow comparisons for 2007. At Dutch Slough (Figure 5.3-13), with typical peak tidal flows of 250 m^3/s, predicted peak tidal flows tend to be slightly less than observed, both during flood and ebb. Observed and predicted average net flows in Dutch Slough during the simulation period are -3.3 m^3/s (east) and -17.1 m^3/s (east), respectively.

At Taylor Slough (Figure 5.3-14) the observed and predicted flows show similar magnitudes, with typical peak flows around 20 m^3/s. Both the observed and predicted tidal flows show high frequency oscillations. Since flow in Taylor Slough is driven by head differences in False River and Dutch Slough, these oscillations indicate a complex interaction between tidal phase in False River and Dutch Slough. Although the model captures some of this complexity, the cross-correlation yields relatively large phase differences and poor statistical fit at this station. At Fisherman's Cut (Figure 5.3-15), similarly complex patterns in tidal flow are observed. Flow in Fisherman's is driven by head differences in False River and the San Joaquin River, indicating a complex interaction between tidal phase in False River and the San Joaquin River. As with Taylor Slough, significant phase differences are evident and the cross-correlation yields poor statistical fit. However, the model accurately predicts net flow through Fisherman's cut, with observed and predicted net flows of 21.7 m^3/s and 21.3 m^3/s, respectively. Although the magnitude of flows through Fisherman's Cut and Taylor Slough are both relatively small and some differences exist, the accurate prediction of net flows at these stations indicates that the model is providing an accurate representation of head and phase differences between the nearby channels in the central Delta.

At Old River between Franks Tract and the San Joaquin River (Figure 5.3-16), the predicted and observed flows show better agreement with typical peak flows of 400 m^3/s. The predicted tidally-averaged and net flows into Franks Tract through Old River are slightly less negative than observed, resulting in observed and predicted average net flows south during the simulation period of 39.2 m^3/s and 22.6 m^3/s, respectively. At the Mokelumne River near the San Joaquin River (Figure 5.3-17), the predicted and observed flows show relatively good agreement with peak flows typically around 500 m^3/s during ebb and 350 m^3/s during flood tide, and an amplitude ratio of 1.015. Average observed net flow during the simulation period was 89.3 m^3/s, compared to 120 m^3/s predicted net flow, indicating slightly higher predicted net flow through the Mokelumne River than observed.

South of Franks Tract, on Old River at Mandeville Island (Figure 5.3-18) and at Holland Cut (Figure 5.3-19), predicted tidal flows are less than observed tidal flows, indicating a smaller predicted than observed tidal prism south of Franks Tract. This result was also observed for the 2007 calibration period. It is believed that this occurs because some tidal areas south of Franks Tract, such as little Mandeville Island, which is currently flooded, and some additional in-channel islands, which flood near high water, are not included in the available bathymetric data, and are therefore not included in the current model. It is believed that including some of these additional areas will improve the prediction of tidal prism at these stations (see discussion in Section 6.4). Predicted net flows at Old River near Quimby Island are slightly less negative (south) than observed, while they are slightly more negative (south) than observed at Holland Cut. A similar result is also evident in the flow comparisons for the 2007 period.

On Middle River south of Columbia Cut (Figure 5.3-20), the observed and predicted flows show good agreement, with typical peak tidal flows of 500 m^3/s during flood and 200 m^3/s during ebb tide. Peak predicted tidal flows tend to be slightly larger than observed, with an amplitude ratio of 1.133. Overall the model shows similar tidally-averaged net flows over the analysis period, but predicted net flows are consistently less negative (south) than observed, with observed and predicted mean net flows south of 130 m^3/s and 80 m^3/s, respectively.

5.3.3 Southern Sacramento-San Joaquin Delta

Flow calibration comparisons were performed at five continuous flow monitoring stations in the southern portion of the Delta, at the locations shown in Figure 5.3-21. Flow comparisons at these stations are shown in Figures 5.3-22 through 5.3-26.

On Middle River at Middle River (Figure 5.3-22), the predicted tidal flows tend to be somewhat less than the observed tidal flows, particularly during ebb, however the tidally-averaged predicted and observed flows are nearly identical, with observed and predicted mean net flows south of 129 m^3/s and 126 m^3/s, respectively. A similar result is evident at Old River at Bacon Island (Figure 5.3-23), with slightly lower predicted than observed tidal flows, but similar tidally-averaged flows. Observed and predicted average net flows south at Old River at Bacon island during the simulation period are 90.0 m^3/s and 71.9 m^3/s, respectively. The difference between observed and predicted net flows at Old River at Bacon Island is larger during the 2002 period than during the 2007 period.

On Old River near Byron (Figure 5.3-24), the observed and predicted flows show good agreement, with typical peak tidal flows of 50 m^3/s during ebb and 400 to 450 m^3/s during flood tide. The cross-correlation analysis yields an amplitude ratio of 0.967, indicating that the model is accurately predicting the flow amplitude, and no phase difference. The predicted tidally-averaged flows are similar to observed tidally-averaged flows during the simulation period, and the observed and predicted mean net flows south are 133 m^3/s and 144 m^3/s, respectively.

On the San Joaquin River near Stockton (Figure 5.3-25), the observed and predicted flows show good agreement, with typical peak tidal flows of 100 m^3/s. The cross-correlation analysis yields an amplitude ratio of 1.080, indicating that the model is accurately predicting the flow amplitude, a phase lag of 6 minutes. Overall the model shows similar tidally-averaged net flows over the analysis period, and the observed and predicted mean flows are 17.9 m^3/s and 15.5 m^3/s, respectively.

On Old River at Head (Figure 5.3-26), predicted and observed flows show a similar pattern, but predicted flows tend to be somewhat higher than observed flows throughout the tidal cycle. Tidally-averaged observed and predicted flows increase after May 25, when the Head of Old River temporary barrier is removed, but the predicted tidally-averaged-flow is consistently higher than the observed tidally-averaged flow by about 10 m^3/s throughout the simulation. The observed and predicted mean net flows at this station over the simulation period are 10.5 m^3/s and 21.5 m^3/s, respectively.

Table 5-2 Predicted and observed stage and cross-correlation statistics for flow monitoring stations in the Sacramento-San Joaquin Delta during the 2002 simulation period.

Location	Data Source	Figure Number	Mean Flow		Cross Correlation		R^2
			Observed (m^3/s)	Predicted (m^3/s)	Amp Ratio	Lag (min)	
2002 North Delta Flow Stations (Figure 5.3-1)							
Sacramento River South of Georgiana Slough	USGS	5.3-2	111	109	0.993	-6	0.994
Georgiana Slough near Sacramento River	USGS	5.3-3	81.1	83.9	0.991	39	0.929
Delta Cross Channel	USGS	5.3-4	123	110	0.869	-1	0.962
Sacramento River North of Delta Cross Channel	USGS	5.3-5	292	291	1.038	9	0.986
Sacramento River at Freeport	USGS	5.3-6	453	446	1.111	-3	0.989
Steamboat Slough between Sacramento River and Sutter Sl.	USGS	5.3-7	62.1	62.5	1.175	5	0.984
2002 Central Delta Flow Stations (Figure 5.3-8)							
Sacramento River at Rio Vista	USGS	5.3-9	294	265	0.996	7	0.996
Threemile Slough at San Joaquin River	USGS	5.3-10	-25.6	-52.9	1.042	16	0.994
San Joaquin River at Jersey Point	USGS	5.3-11	9.28	37.8	0.901	9	0.994
False River	USGS	5.3-12	-13.0	-28.7	0.852	-36	0.984
Dutch Slough at Jersey Island	USGS	5.3-13	-3.29	-17.1	0.835	8	0.994
Taylor Slough	USGS	5.3-14	-0.36	-5.79	0.447	-58	0.692
Fisherman's Cut	USGS	5.3-15	-21.7	-21.3	0.674	-166	0.751
Old River at San Joaquin River	USGS	5.3-16	-39.2	-22.6	1.009	-70	0.964
Mokelumne River near San Joaquin River	USGS	5.3-17	89.3	120	1.015	-29	0.974
Old River at Mandeville Island	USGS	5.3-18	-54.2	-38.4	0.762	-39	0.981
Holland Cut	USGS	5.3-19	-48.0	-50.3	0.832	-29	0.977
Middle River south of Columbia Cut	USGS	5.3-20	-130	-80.3	1.133	-50	0.976
2002 South Delta Flow Stations (Figure 5.3-21)							
Middle River at Middle River	USGS	5.3-22	-129	-126	0.718	-12	0.972
Old River at Bacon Island	USGS	5.3-23	-90.0	-71.9	0.736	4	0.989
Old River near Byron	USGS	5.3-24	-133	-144	0.967	0	0.985
San Joaquin River at Stockton	USGS	5.3-25	17.9	15.5	1.080	6	0.980
Old River at Head	DWR	5.3-26	10.5	21.5	0.839	11	0.808

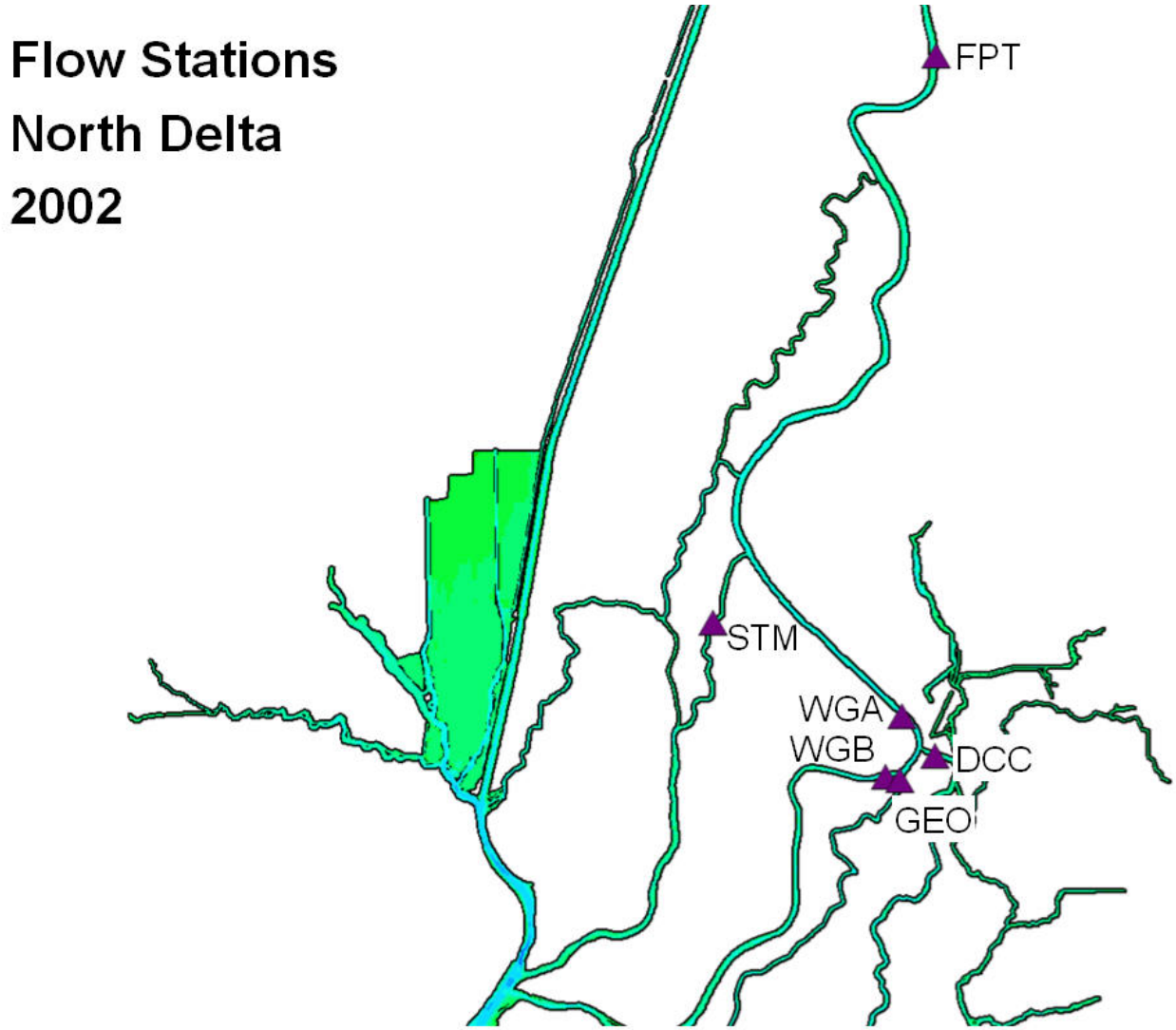

Station Names

WGB, Sacramento River South of Georgiana Slough

GEO, Georgiana Slough near Sacramento River

DCC, Delta Cross Channel

WGA, Sacramento River North of Delta Cross Channel

FPT, Sacramento River at Freeport

CCH, Cache Slough at Ryer Island

MIN, Miner Slough at Hwy 84 Bridge

STM, Steamboat Slough between Sacramento River and Sutter Sl.

SUT, Sutter Slough at Courtland

Figure 5.3-1 Location of flow monitoring stations in the northern portion of the Sacramento-San Joaquin Delta used for 2002 flow calibration.

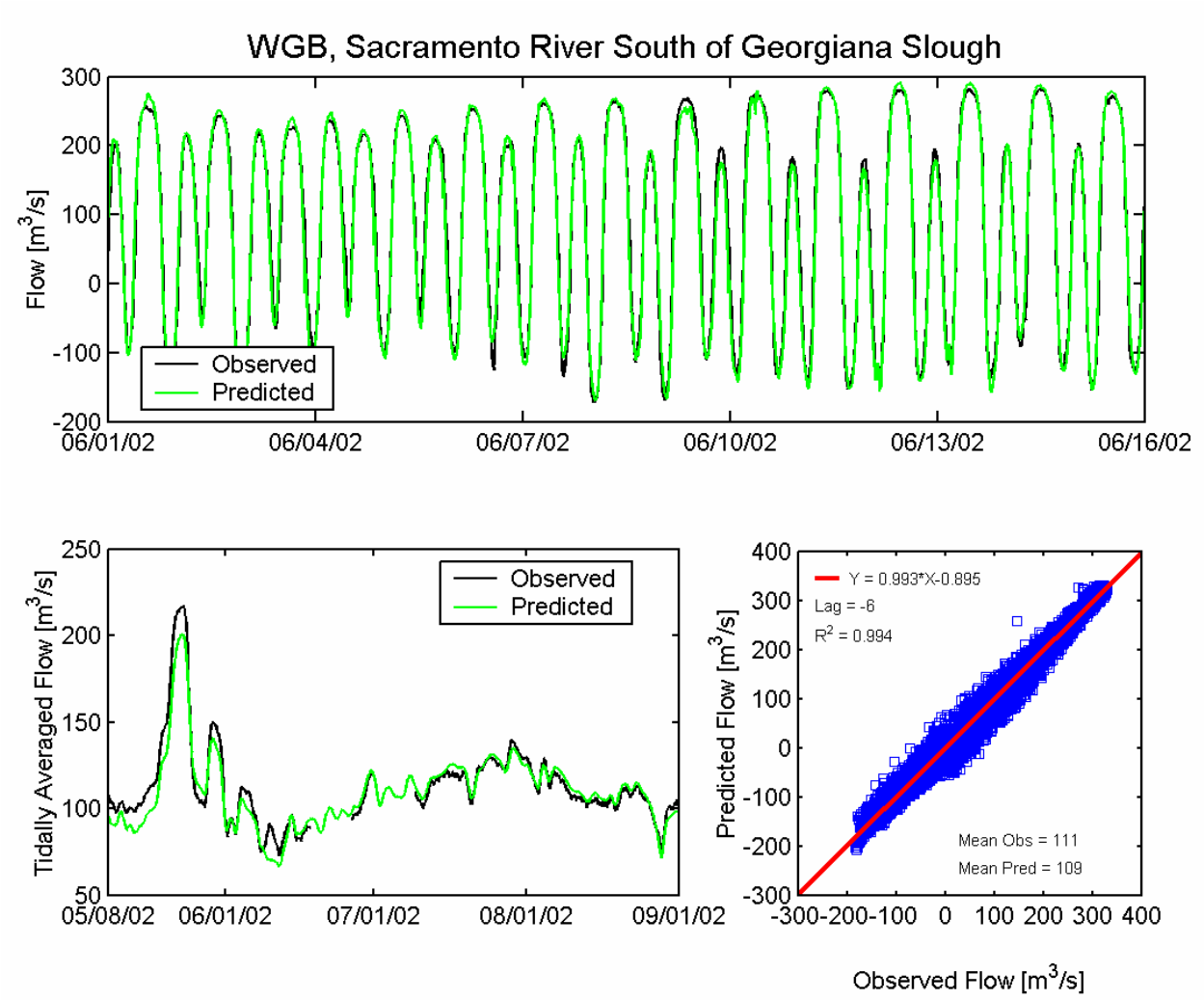

Figure 5.3-2 Observed and predicted flow at Sacramento River South of Georgiana Slough USGS station (WGB) during the 2002 simulation period.

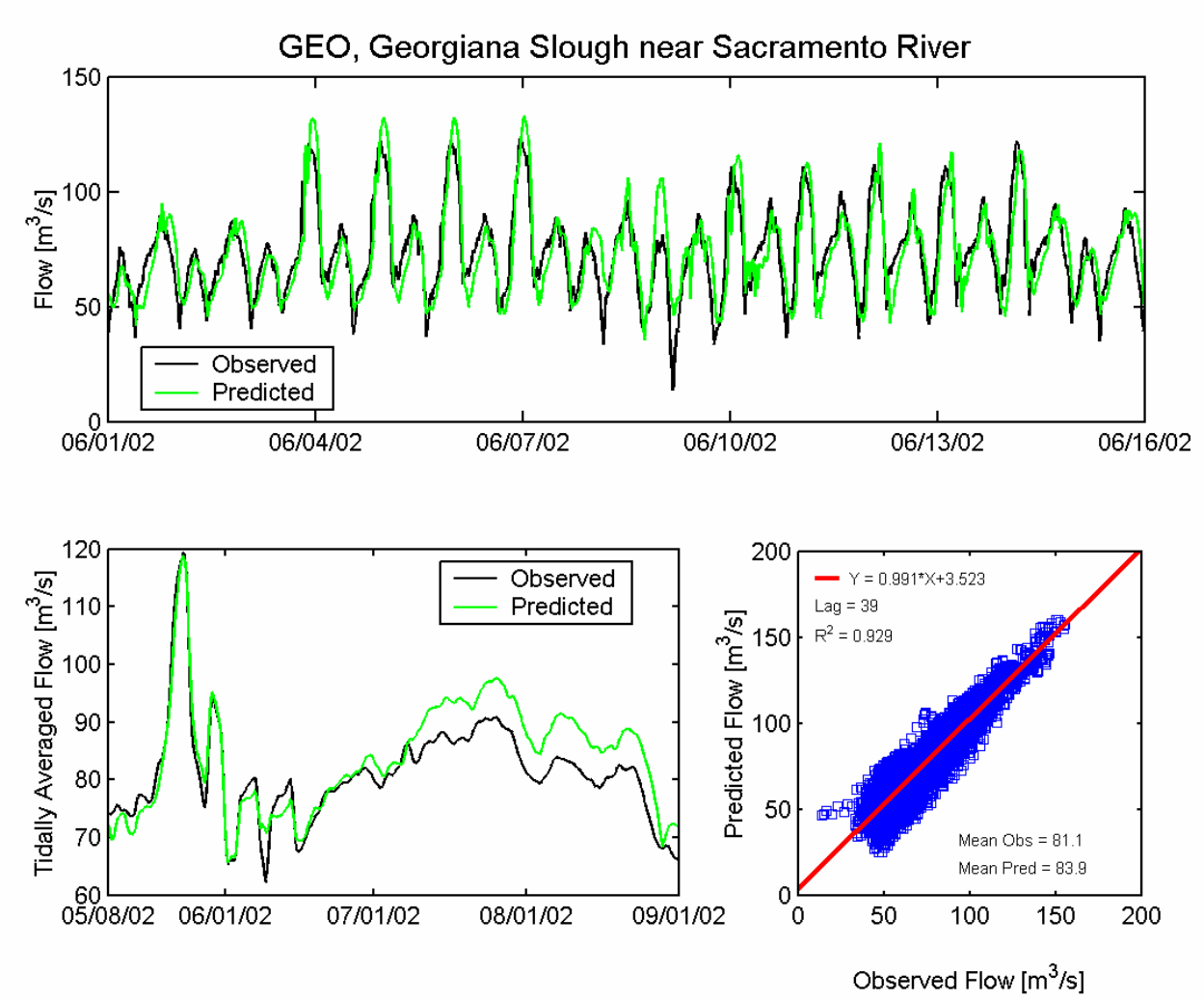

Figure 5.3-3 Observed and predicted flow at Georgiana Slough near Sacramento River USGS station (GEO) during the 2002 simulation period.

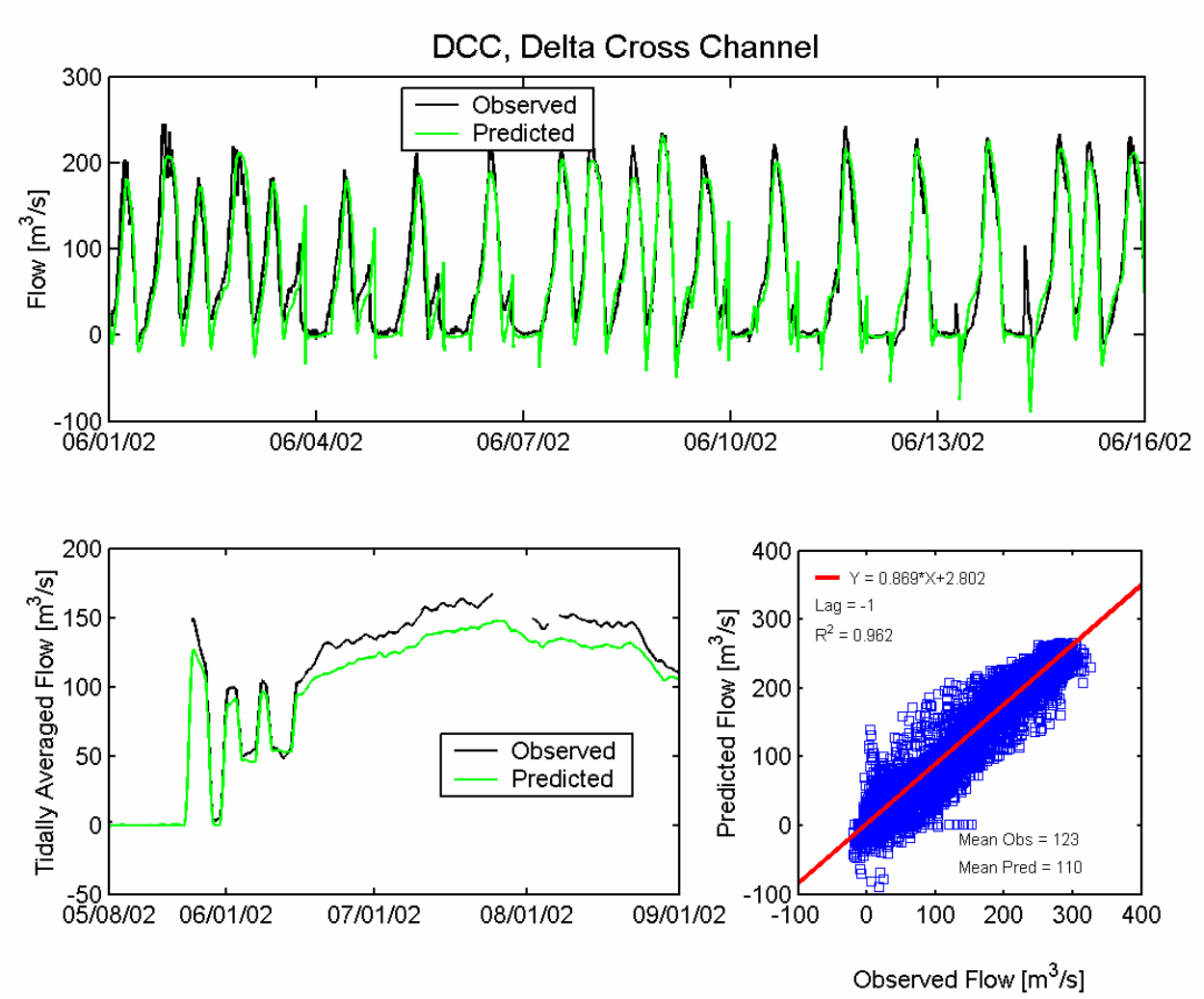

Figure 5.3-4 Observed and predicted flow at Delta Cross Channel USGS station (DCC) during the 2002 simulation period.

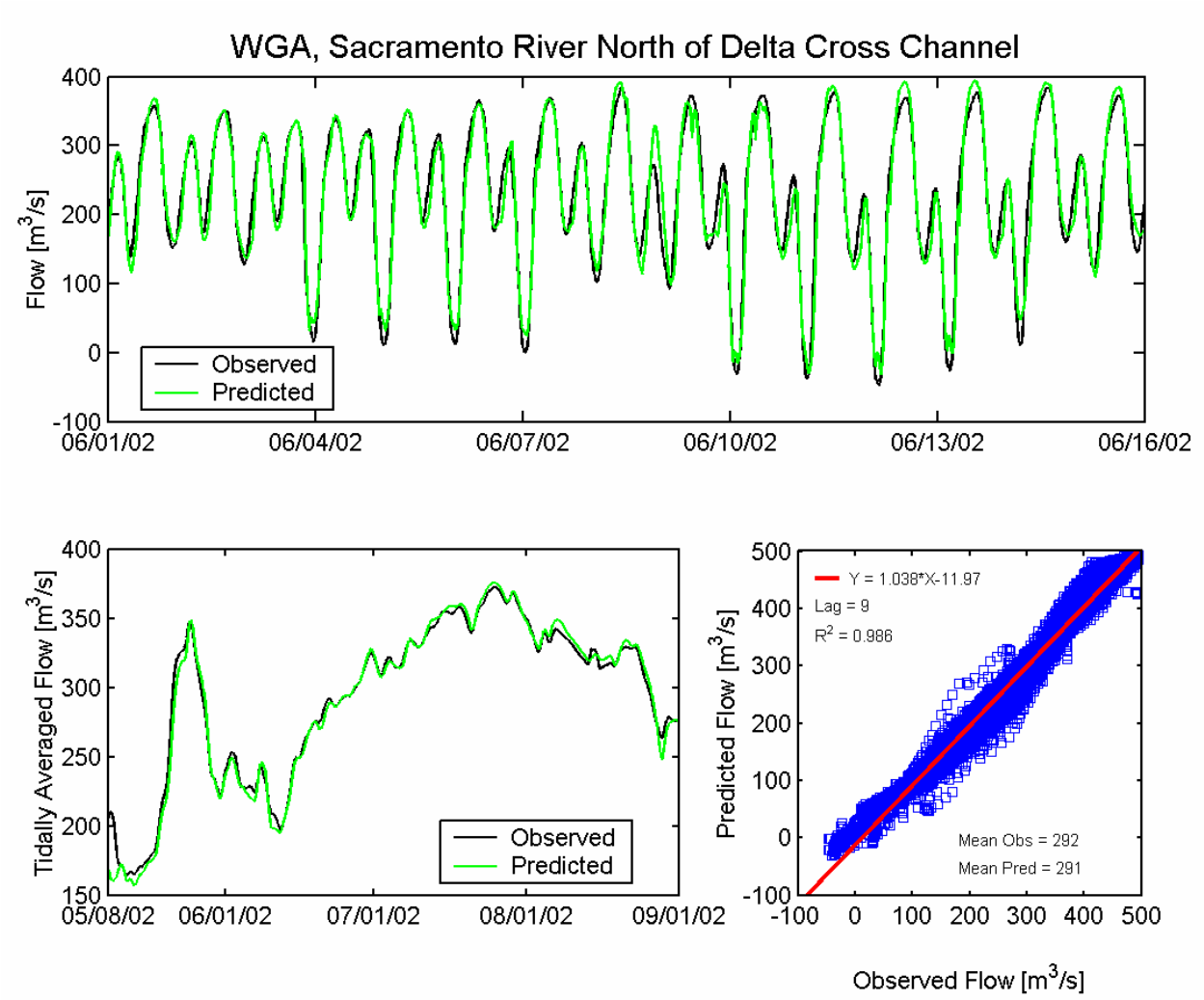

Figure 5.3-5 Observed and predicted flow at Sacramento River North of Delta Cross Channel USGS station (WGA) during the 2002 simulation period.

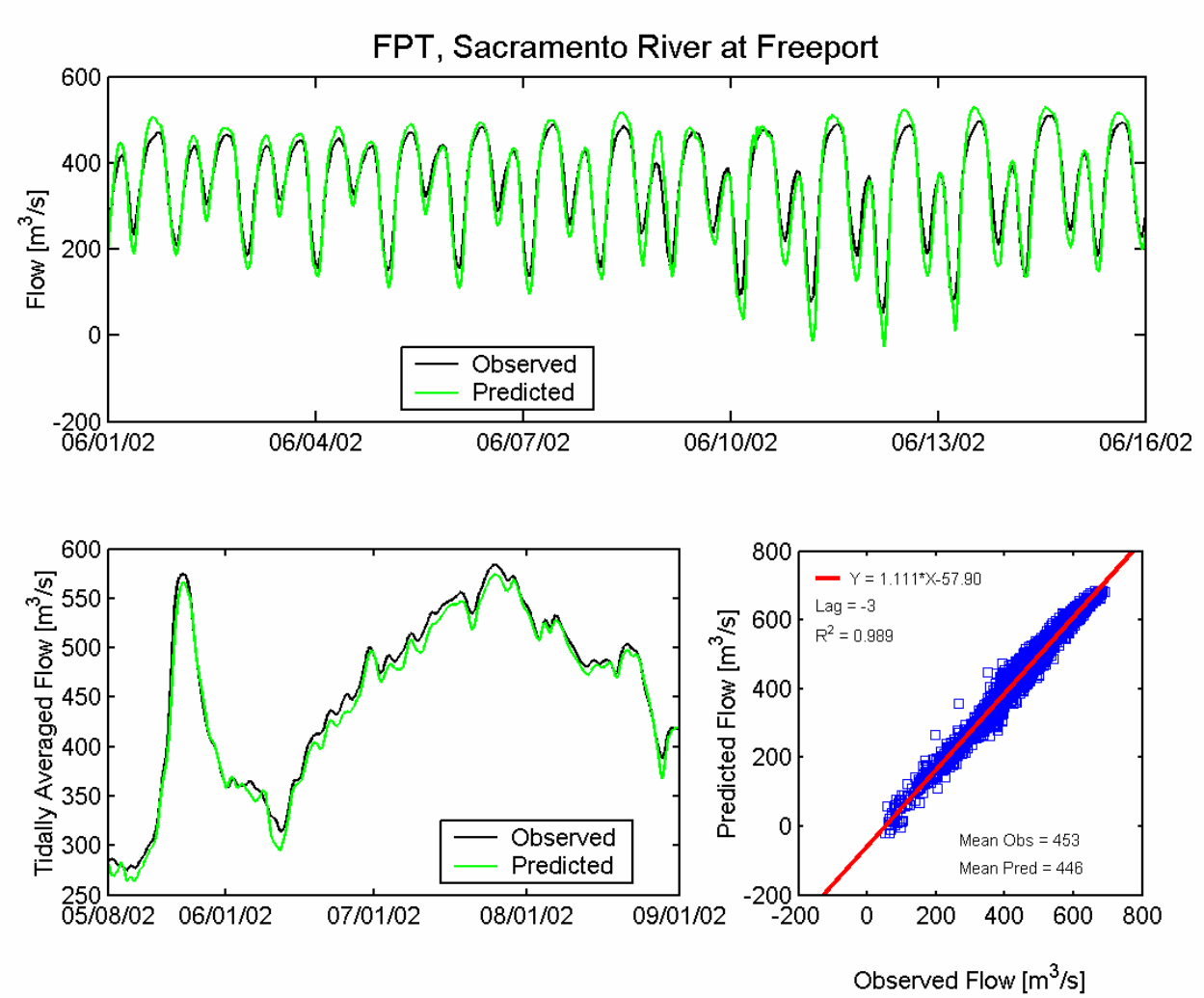

Figure 5.3-6 Observed and predicted flow at Sacramento River at Freeport USGS station (FPT) during the 2002 simulation period.

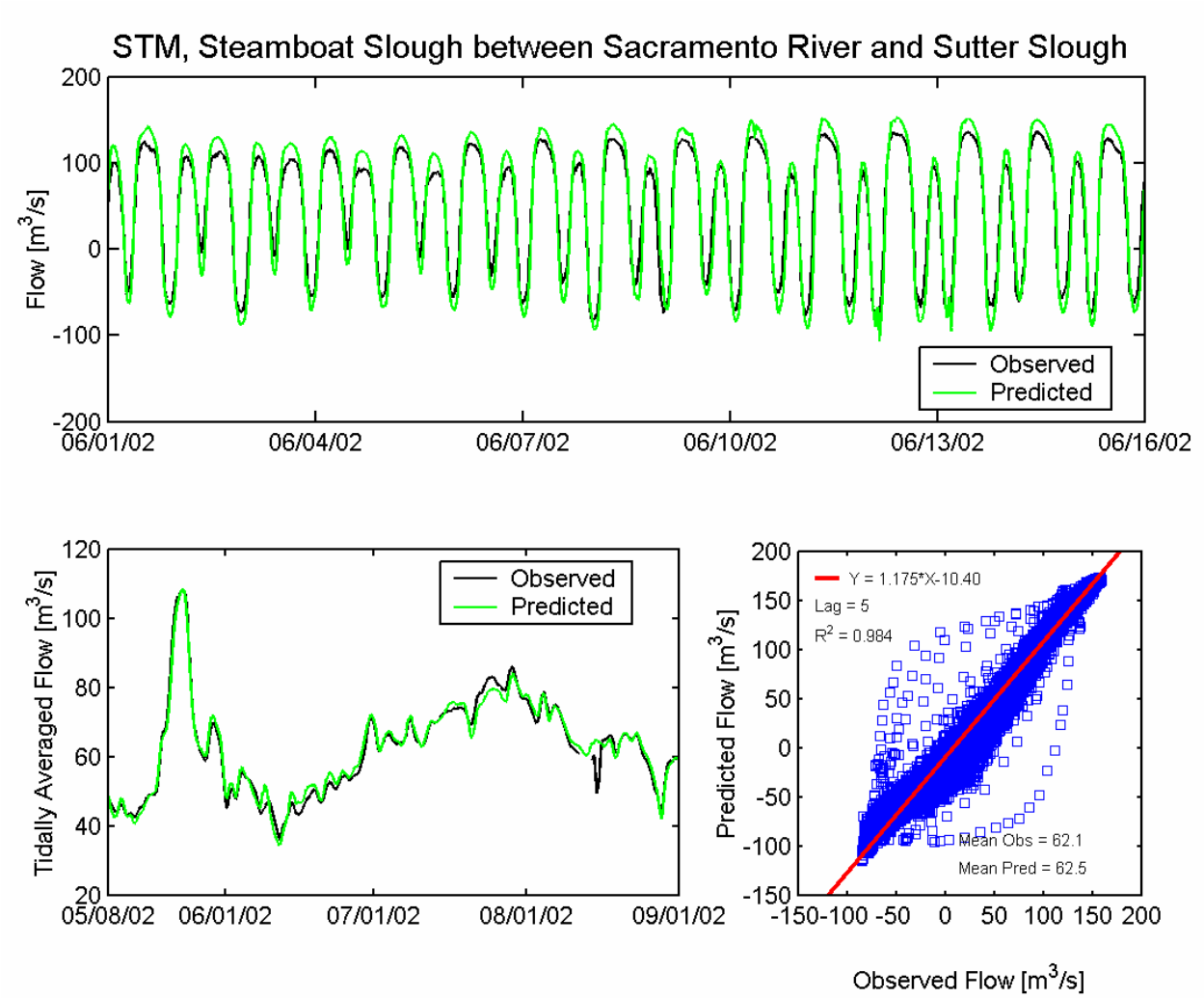

Figure 5.3-7 Observed and predicted flow at Steamboat Slough between Sacramento River and Sutter Slough USGS station (STM) during the 2002 simulation period.

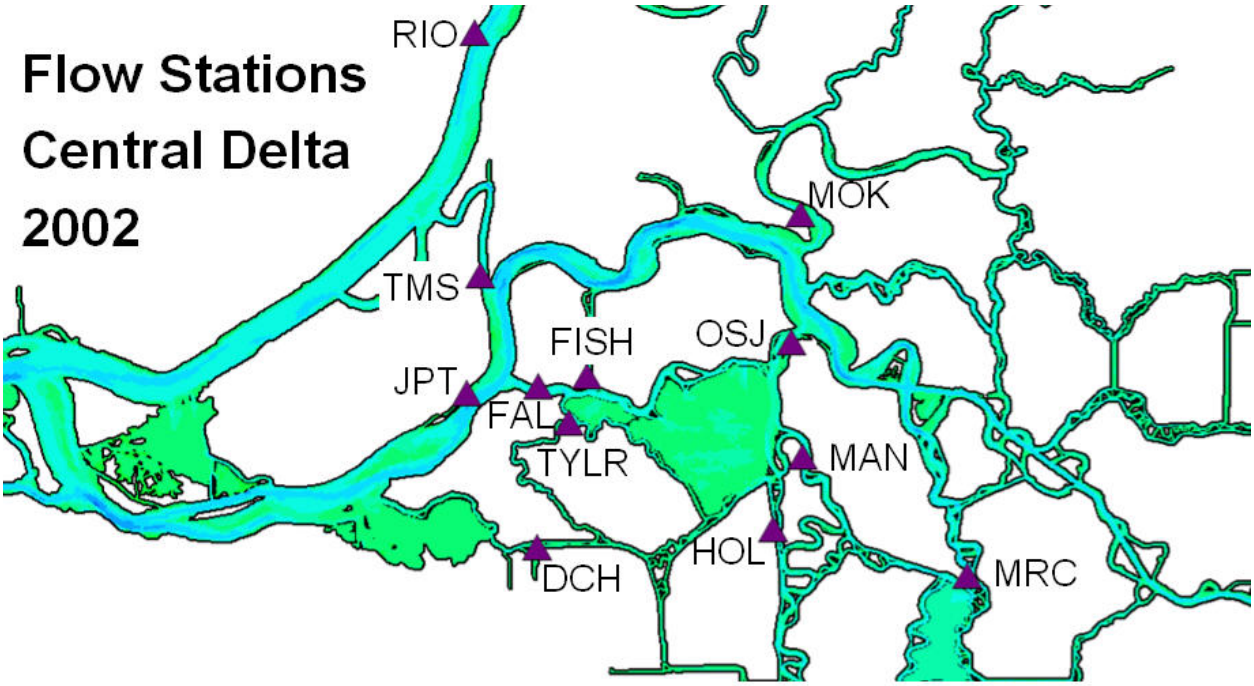

Station Names

RIO, Sacramento River at Rio Vista

TMS, Threemile Slough at San Joaquin River

JPT, San Joaquin River at Jersey Point

FAL, False River

DCH, Dutch Slough at Jersey Island

TYLR, Taylor Slough

FISH, Fisherman's Cut

OSJ, Old River at San Joaquin River

MOK, Mokelumne River near San Joaquin River

MAN, Old River at Mandeville Island

HOL, Holland Cut

MRC, Middle River South of Columbia Cut

Figure 5.3-8 Location of flow monitoring stations in the central portion of the Sacramento-San Joaquin Delta used for 2002 flow calibration.

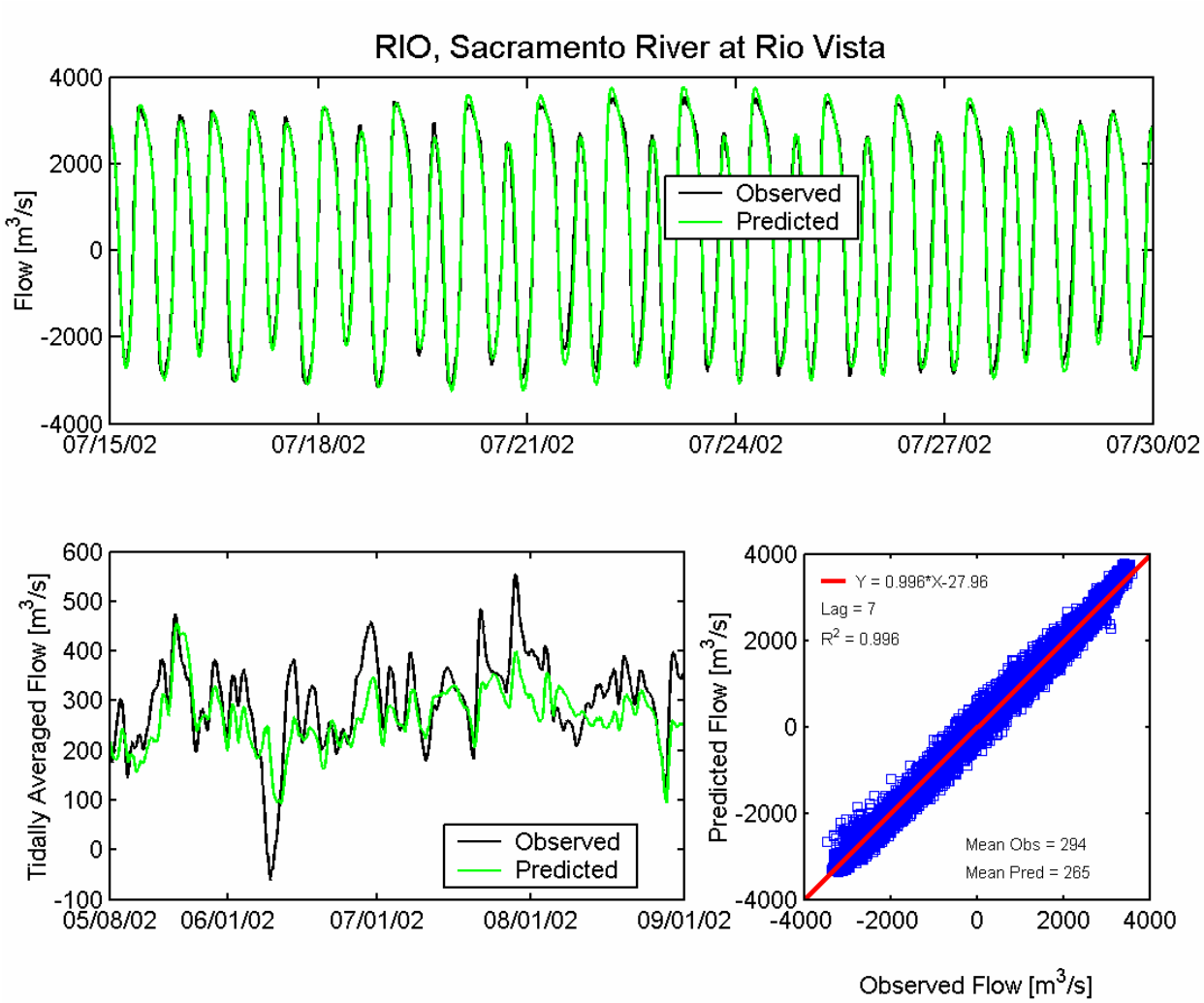

Figure 5.3-9 Observed and predicted flow at Sacramento River at Rio Vista USGS station (RIO) during the 2002 simulation period.

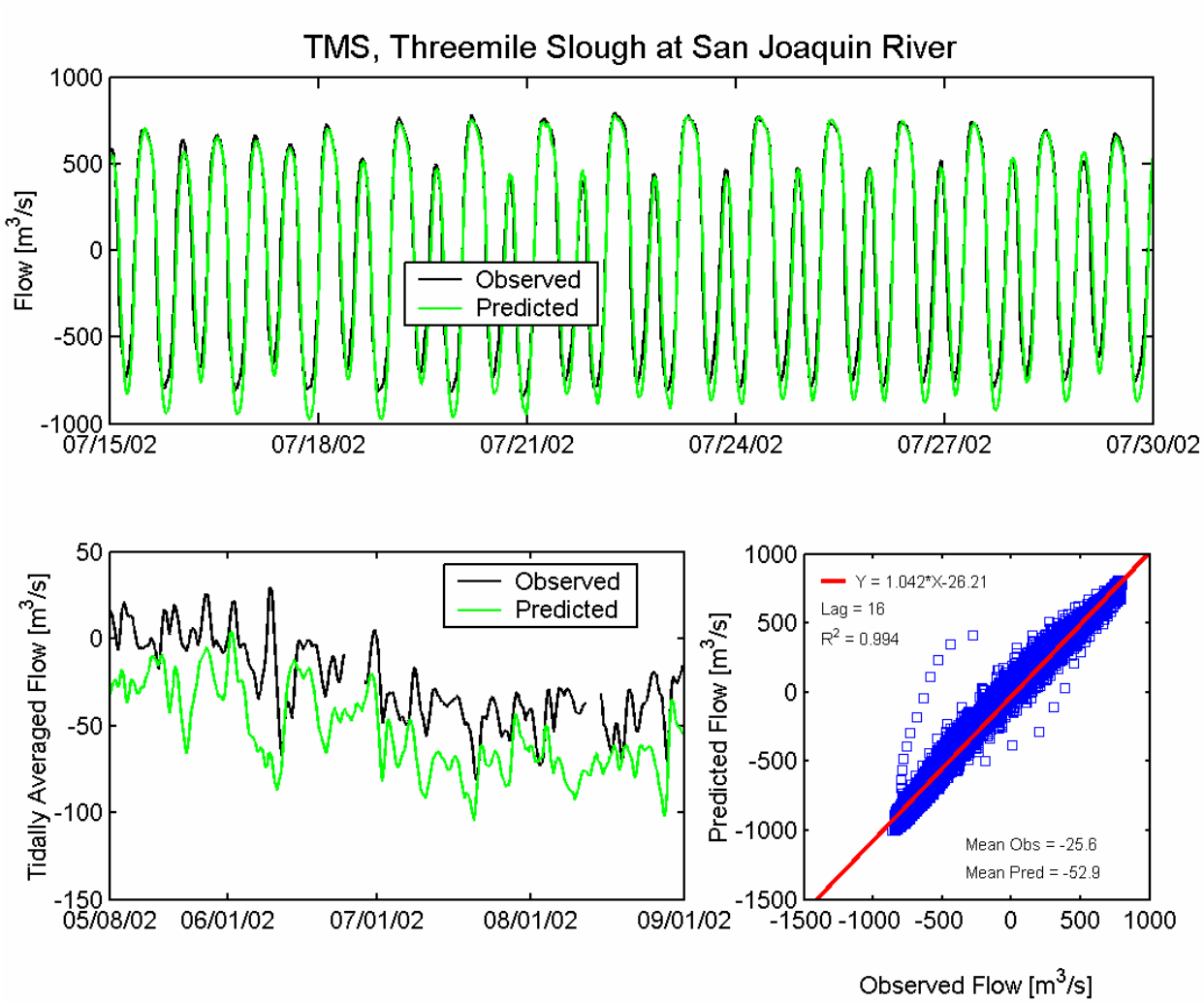

Figure 5.3-10 Observed and predicted flow at Threemile Slough at San Joaquin River USGS station (TMS) during the 2002 simulation period.

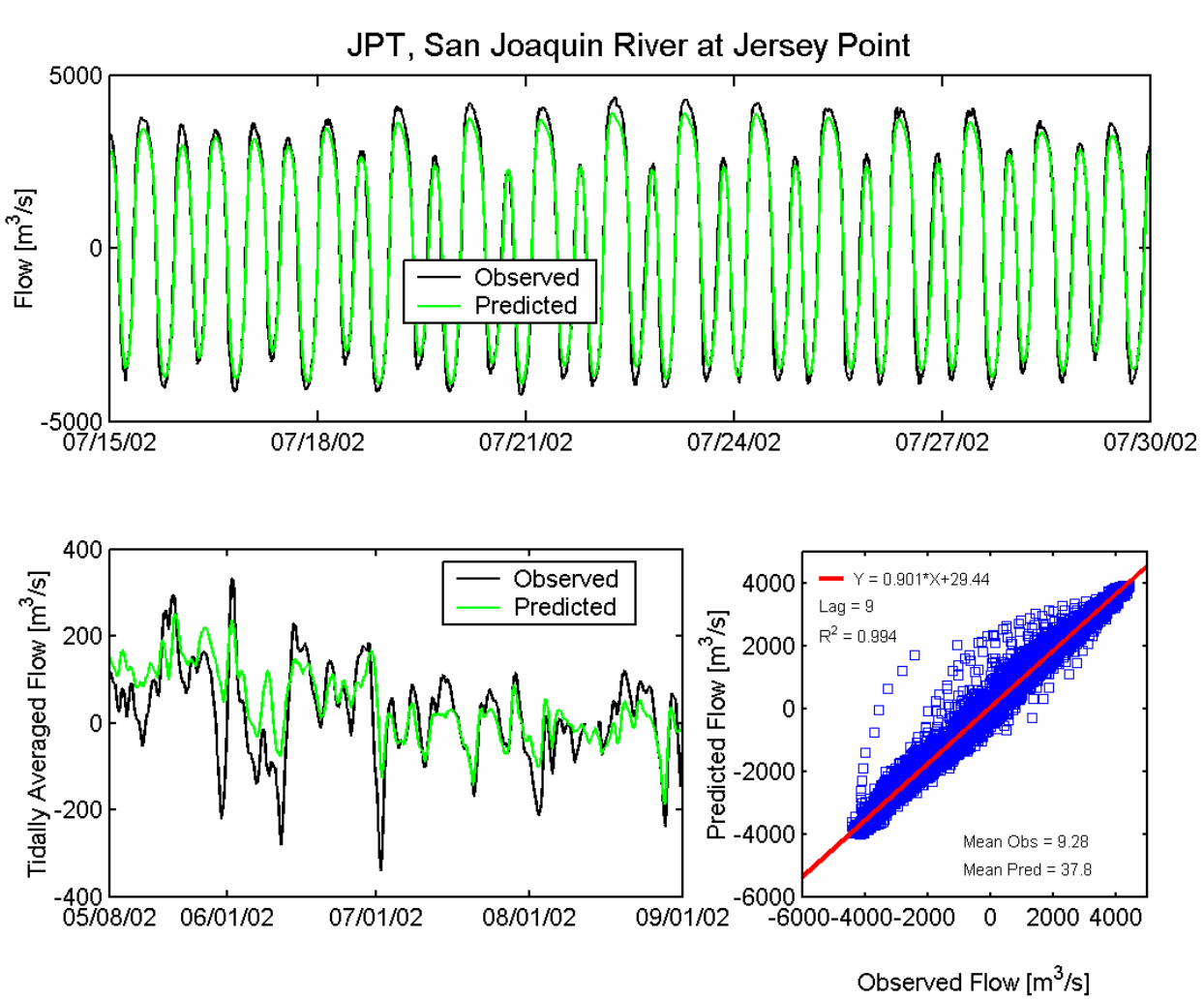

Figure 5.3-11 Observed and predicted flow at San Joaquin River at Jersey Point USGS station (JPT) during the 2002 simulation period.

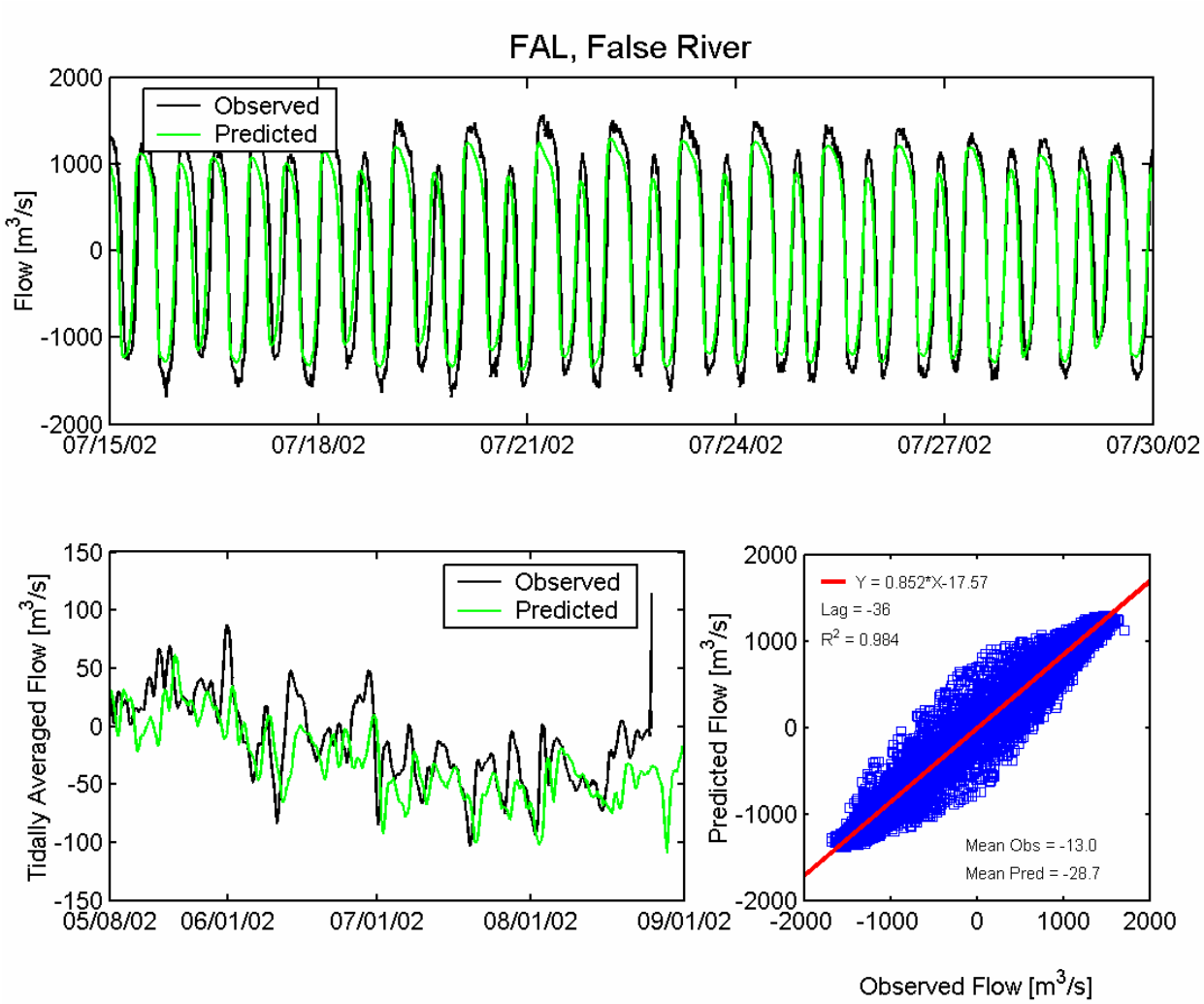

Figure 5.3-12 Observed and predicted flow at False River USGS station (FAL) during the 2002 simulation period.

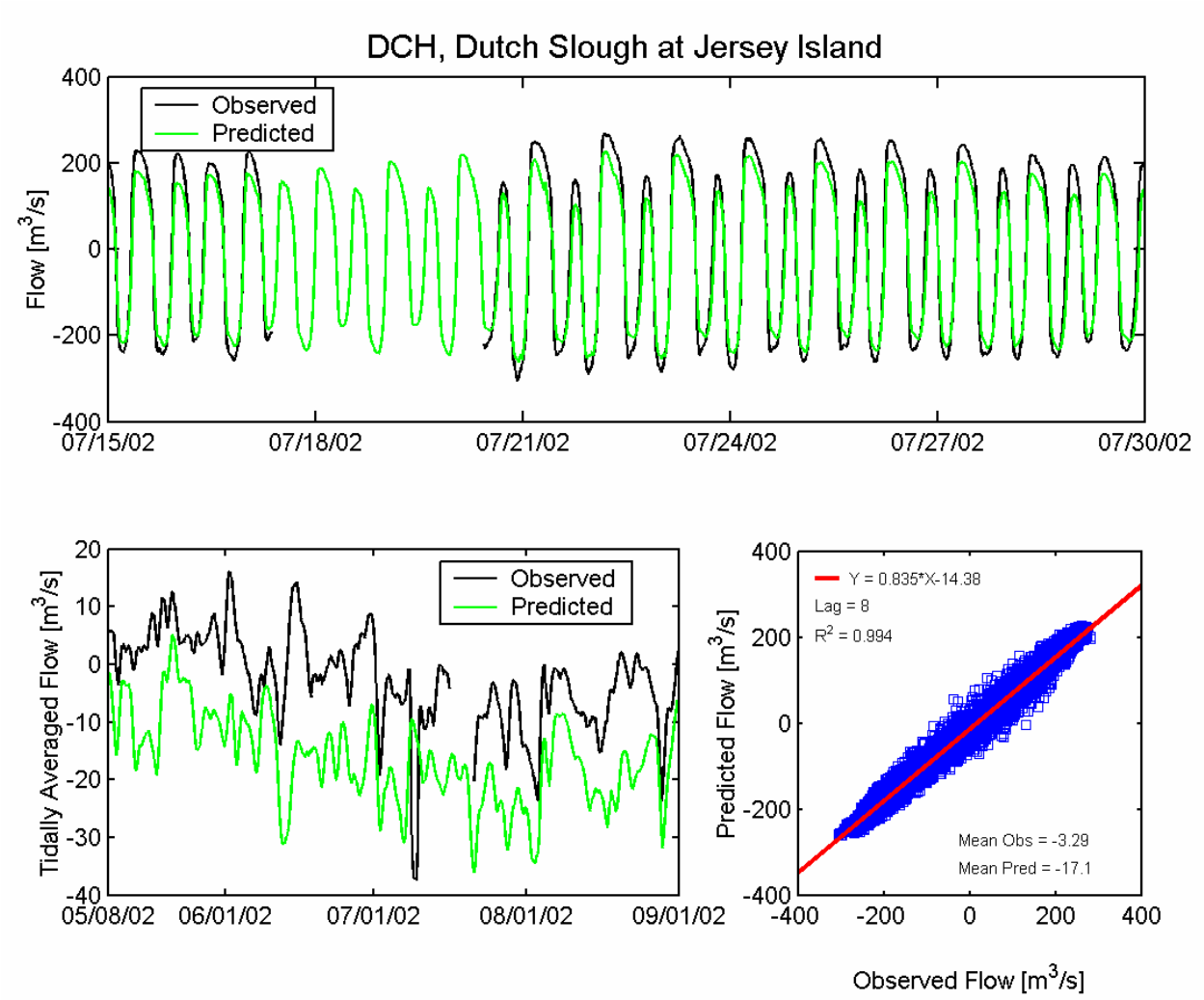

Figure 5.3-13 Observed and predicted flow at Dutch Slough at Jersey Island USGS station (DCH) during the 2002 simulation period.

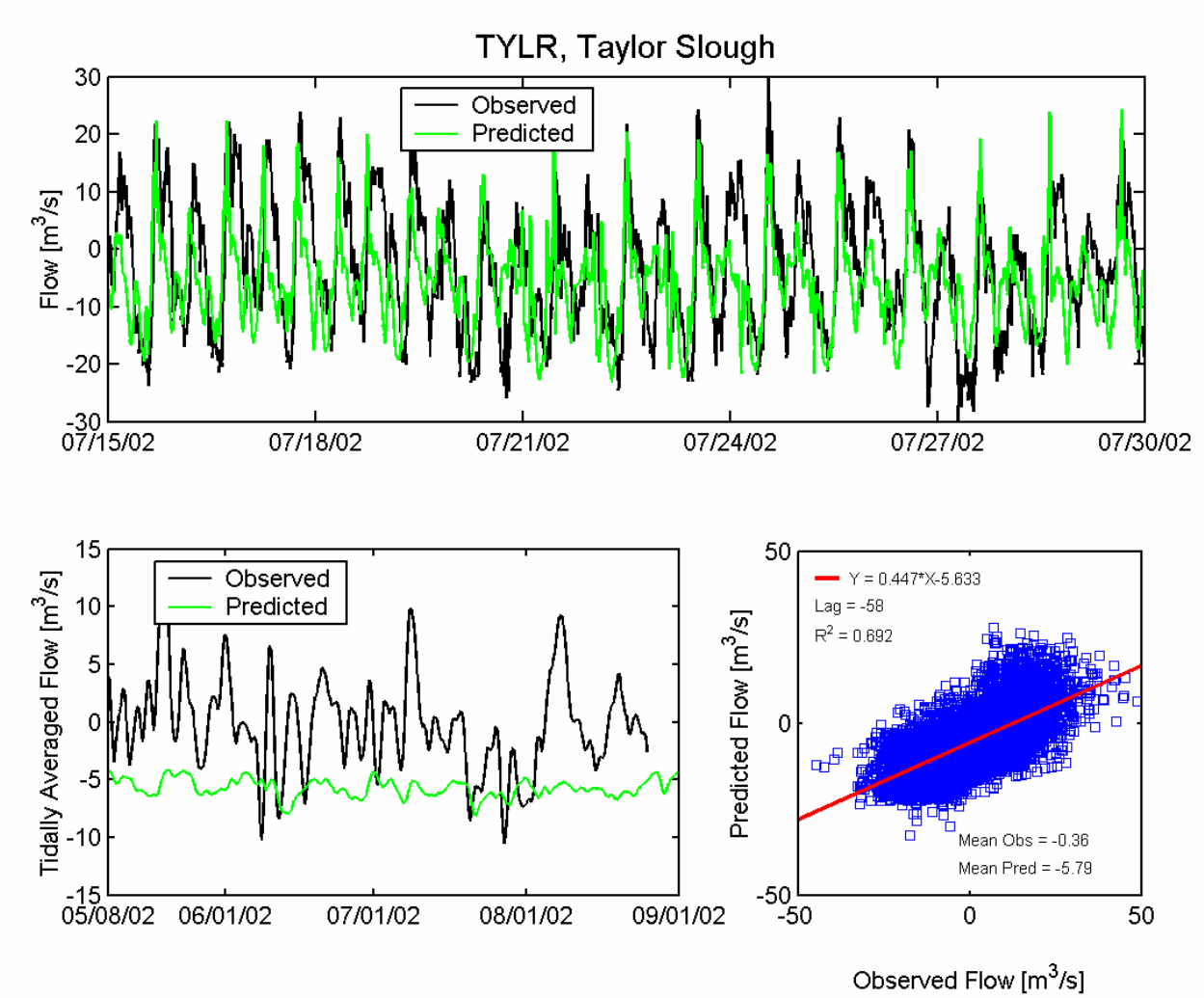

Figure 5.3-14 Observed and predicted flow at Taylor Slough USGS station (TYLR) during the 2002 simulation period.

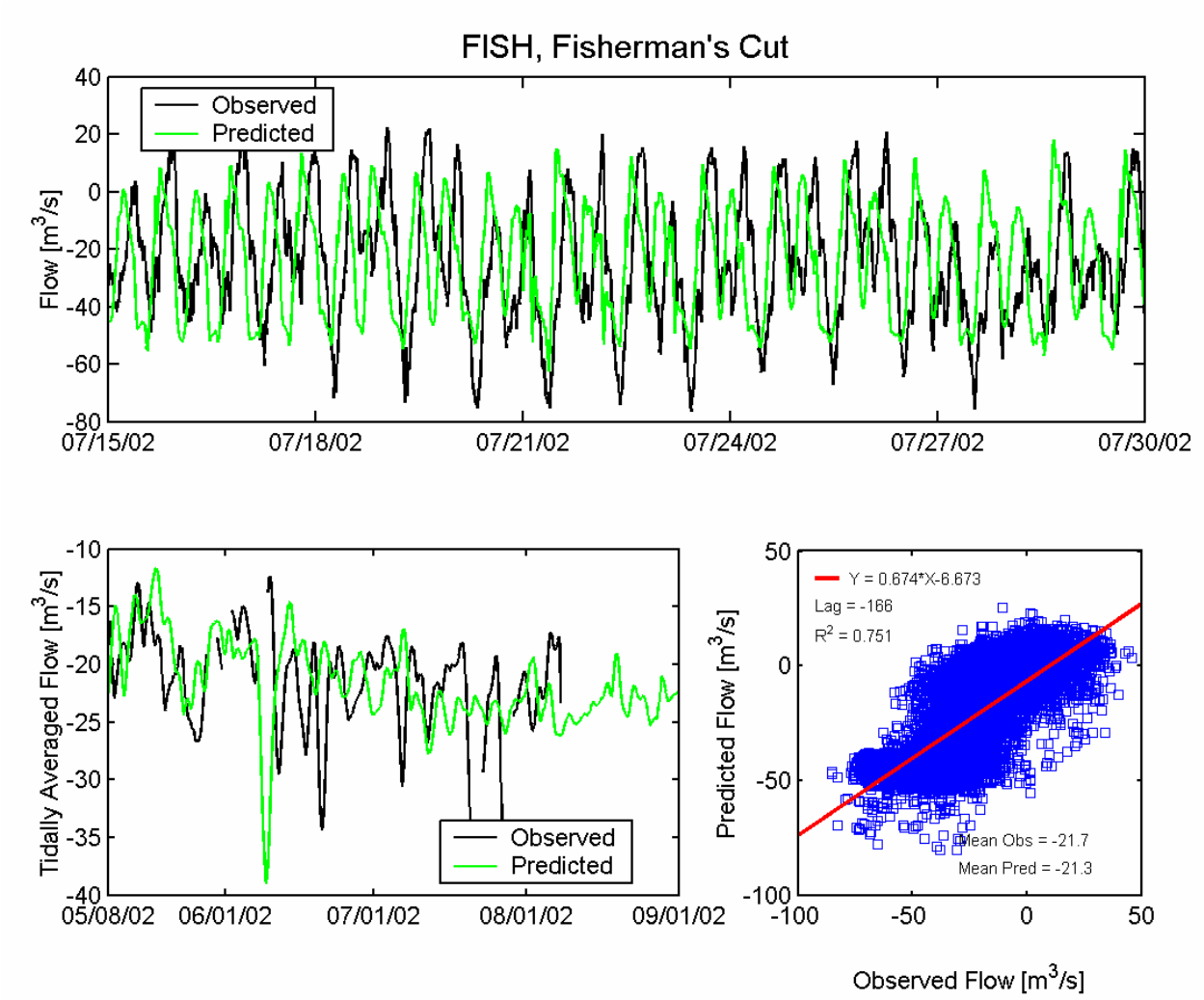

Figure 5.3-15 Observed and predicted flow at Fisherman's Cut USGS station (FISH) during the 2002 simulation period.

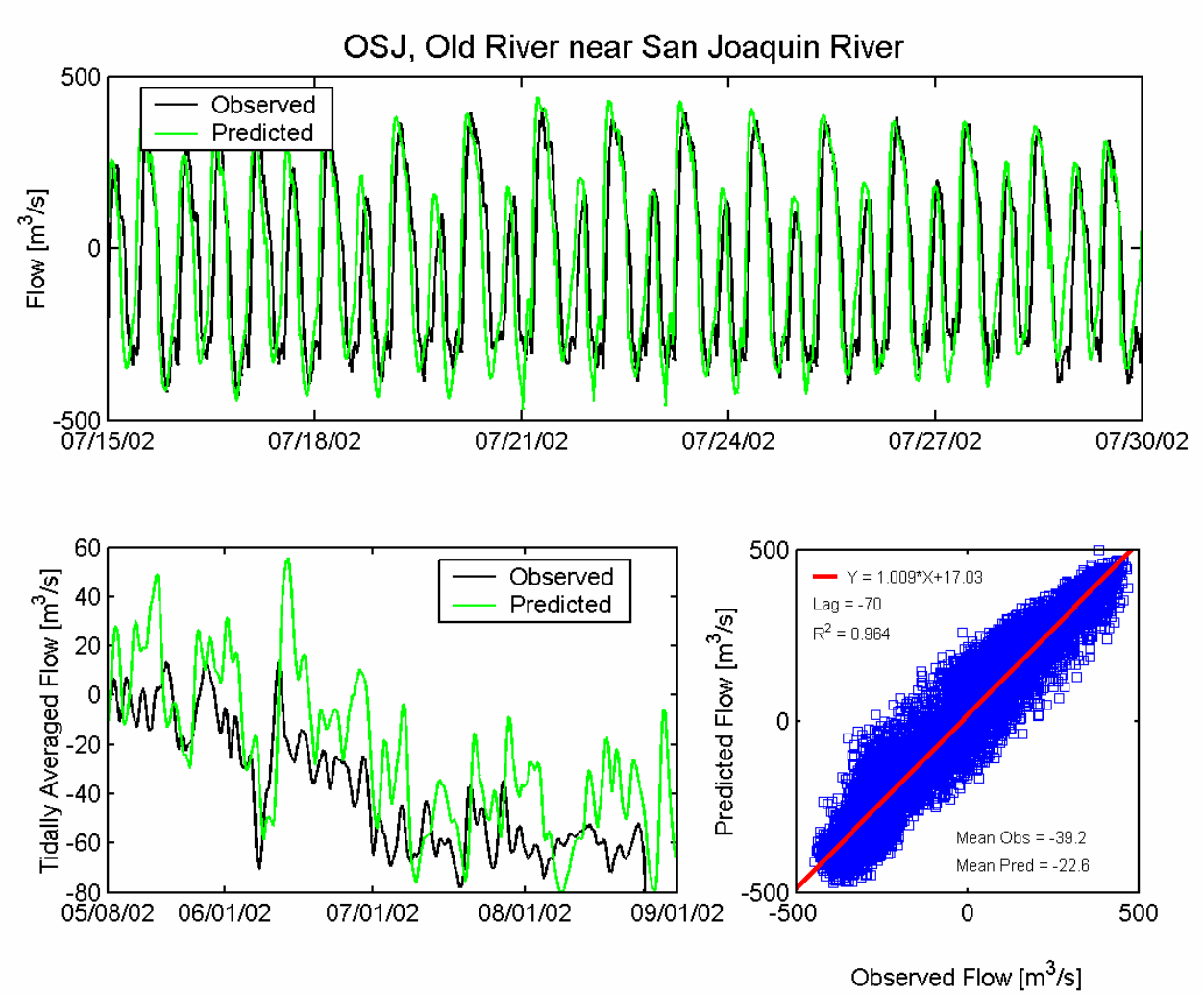

Figure 5.3-16 Observed and predicted flow at Old River at San Joaquin USGS station (OSJ) during the 2002 simulation period.

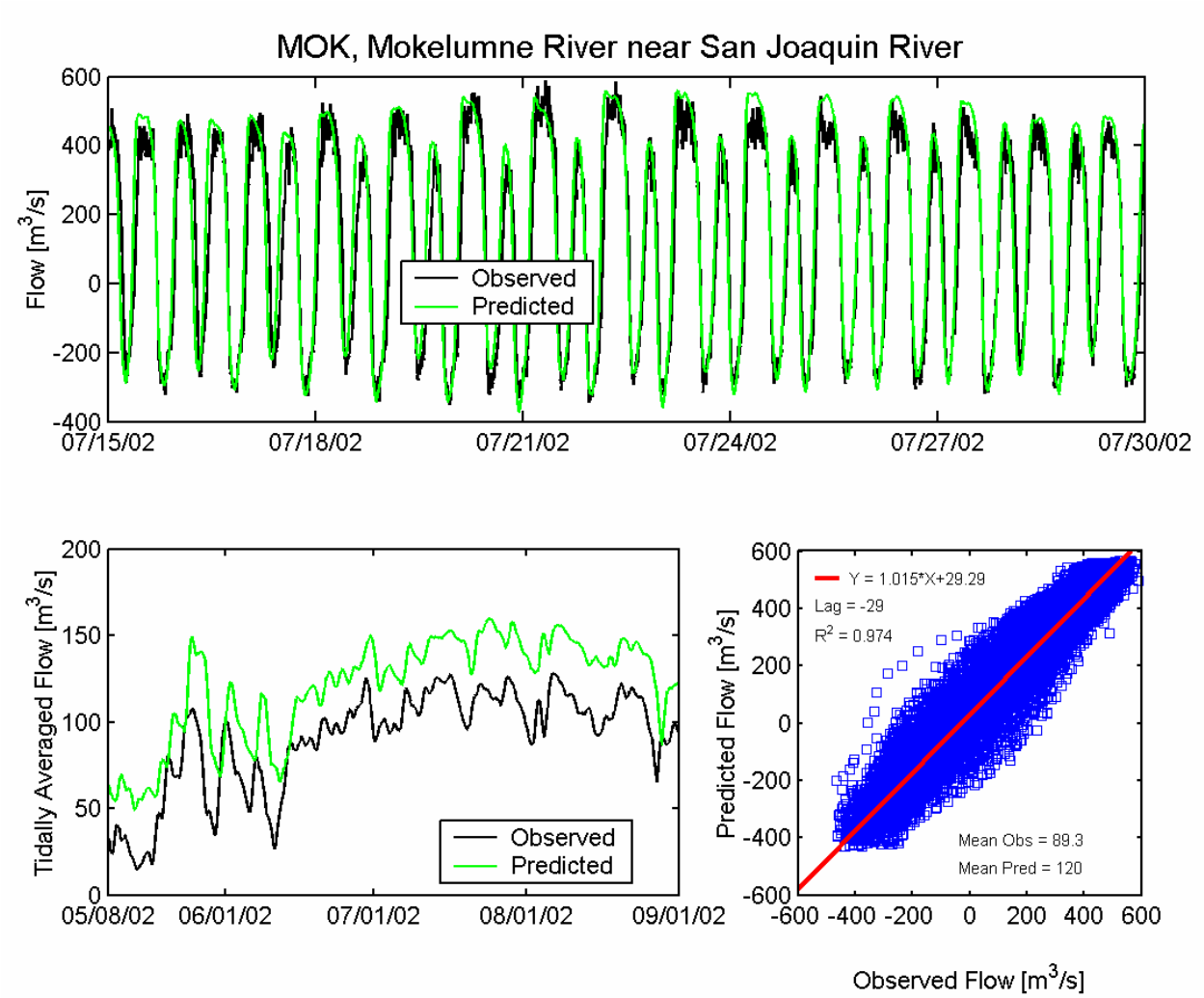

Figure 5.3-17 Observed and predicted flow at Mokelumne River near San Joaquin River USGS station (MOK) during the 2002 simulation period.

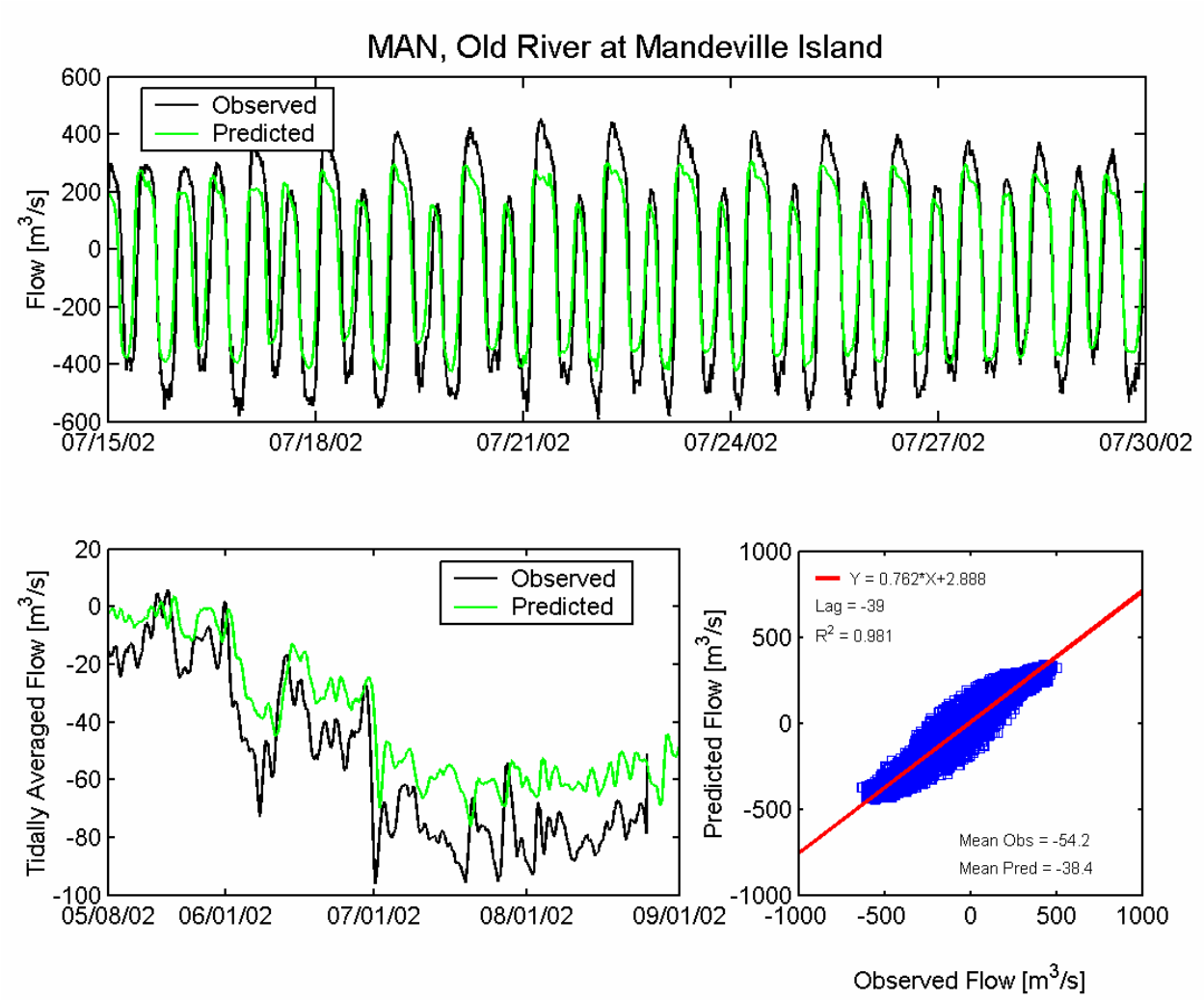

Figure 5.3-18 Observed and predicted flow at Old River at Mandeville Island USGS station (MAN) during the 2002 simulation period.

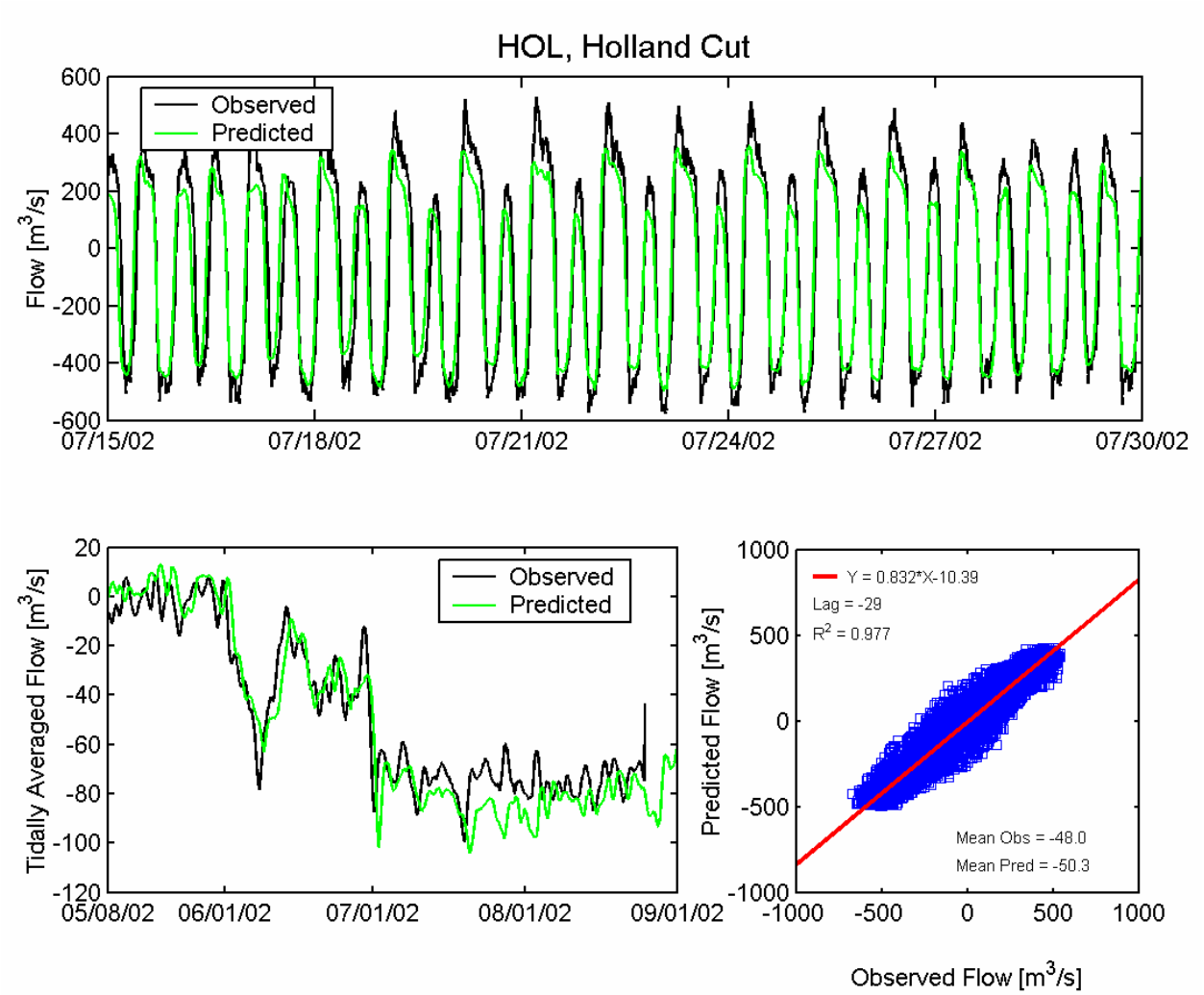

Figure 5.3-19 Observed and predicted flow at Holland Cut USGS station (HOL) during the 2002 simulation period.

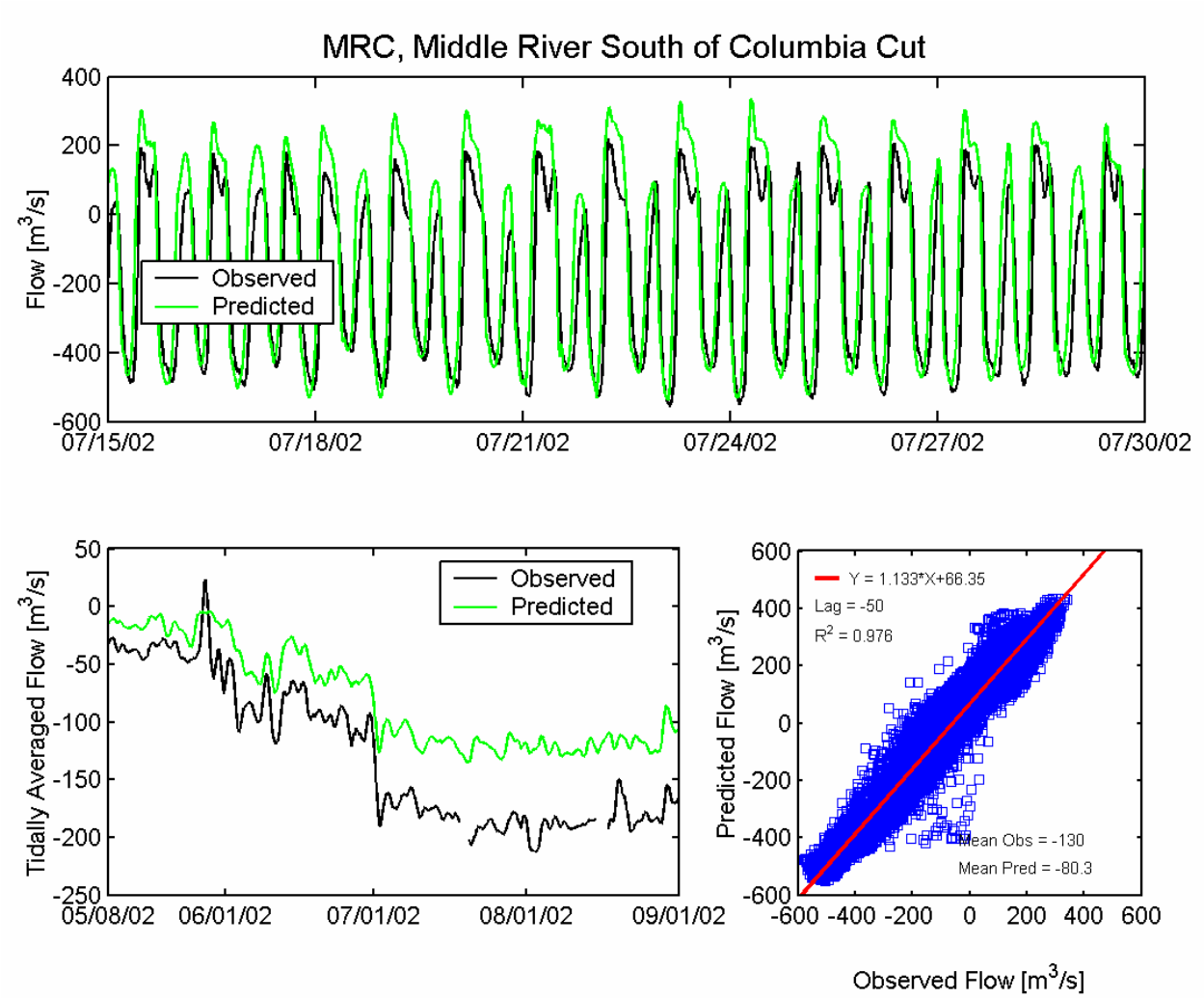

Figure 5.3-20 Observed and predicted flow at Middle River south of Columbia Cut USGS station (MRC) during the 2002 simulation period.

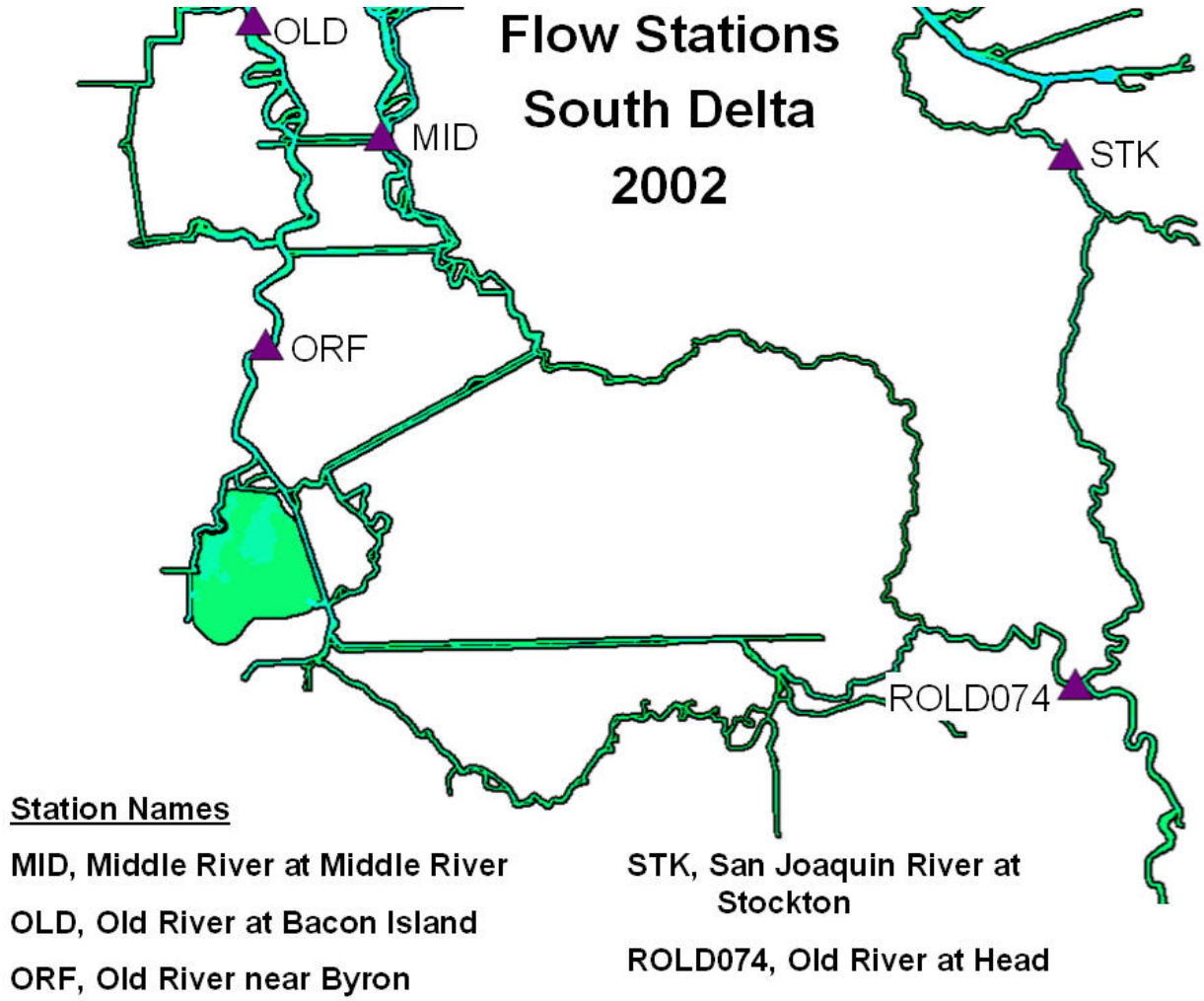

Figure 5.3-21 Location of flow monitoring stations in the southern portion of the Sacramento-San Joaquin Delta used for 2002 flow calibration.

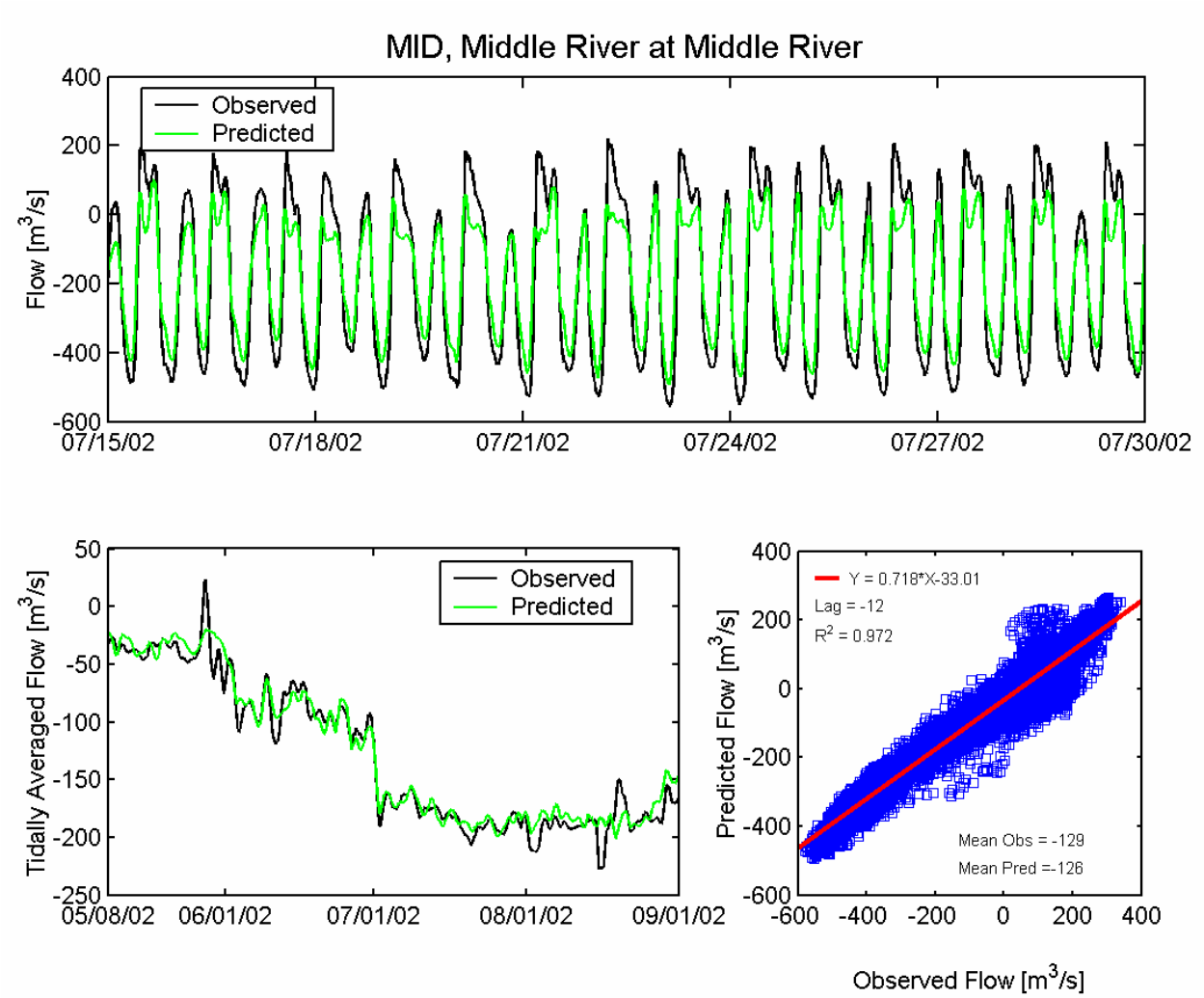

Figure 5.3-22 Observed and predicted flow at Middle River at Middle River USGS station (MID) during the 2002 simulation period.

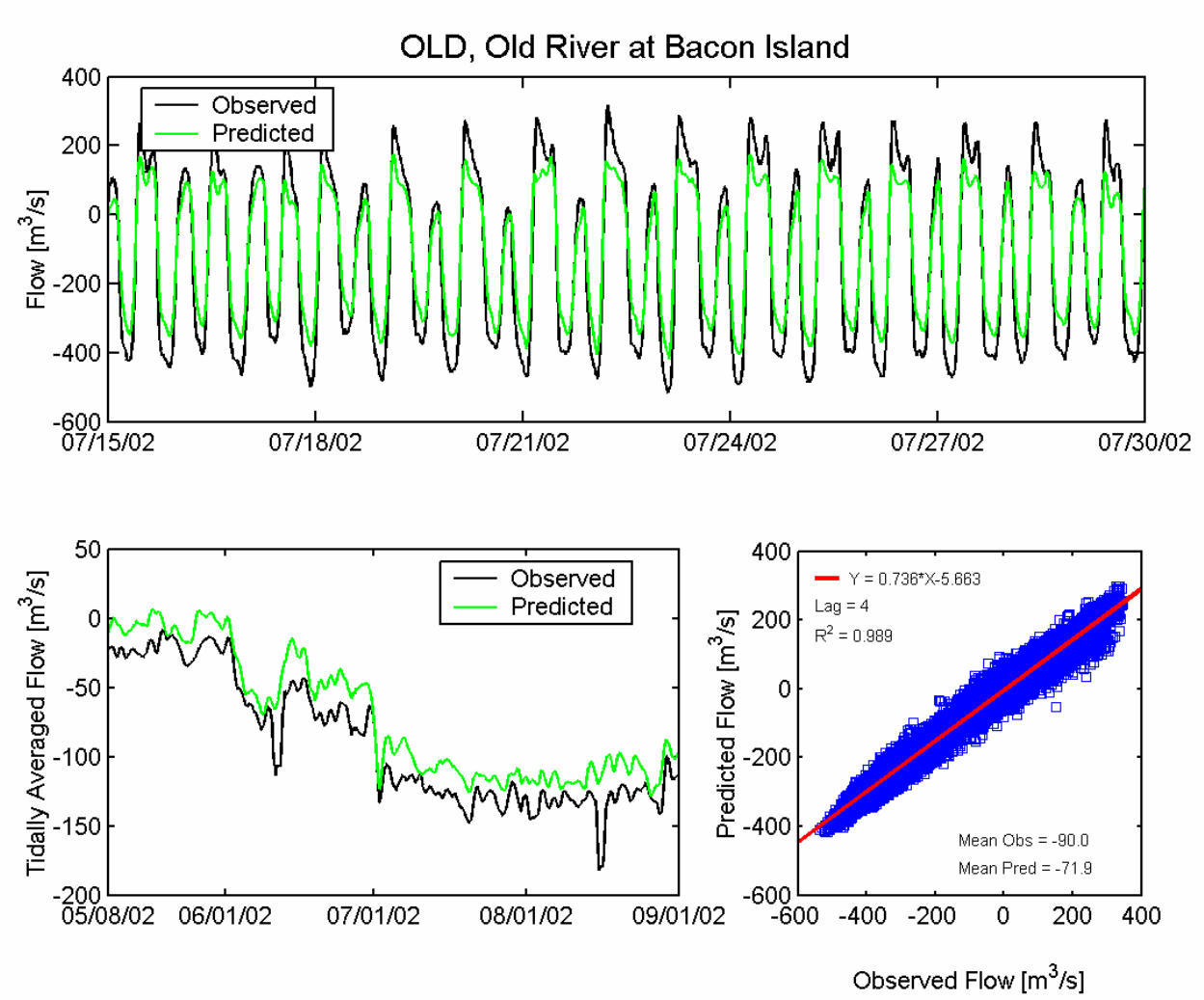

Figure 5.3-23 Observed and predicted flow at Old River at Bacon Island USGS station (OLD) during the 2002 simulation period.

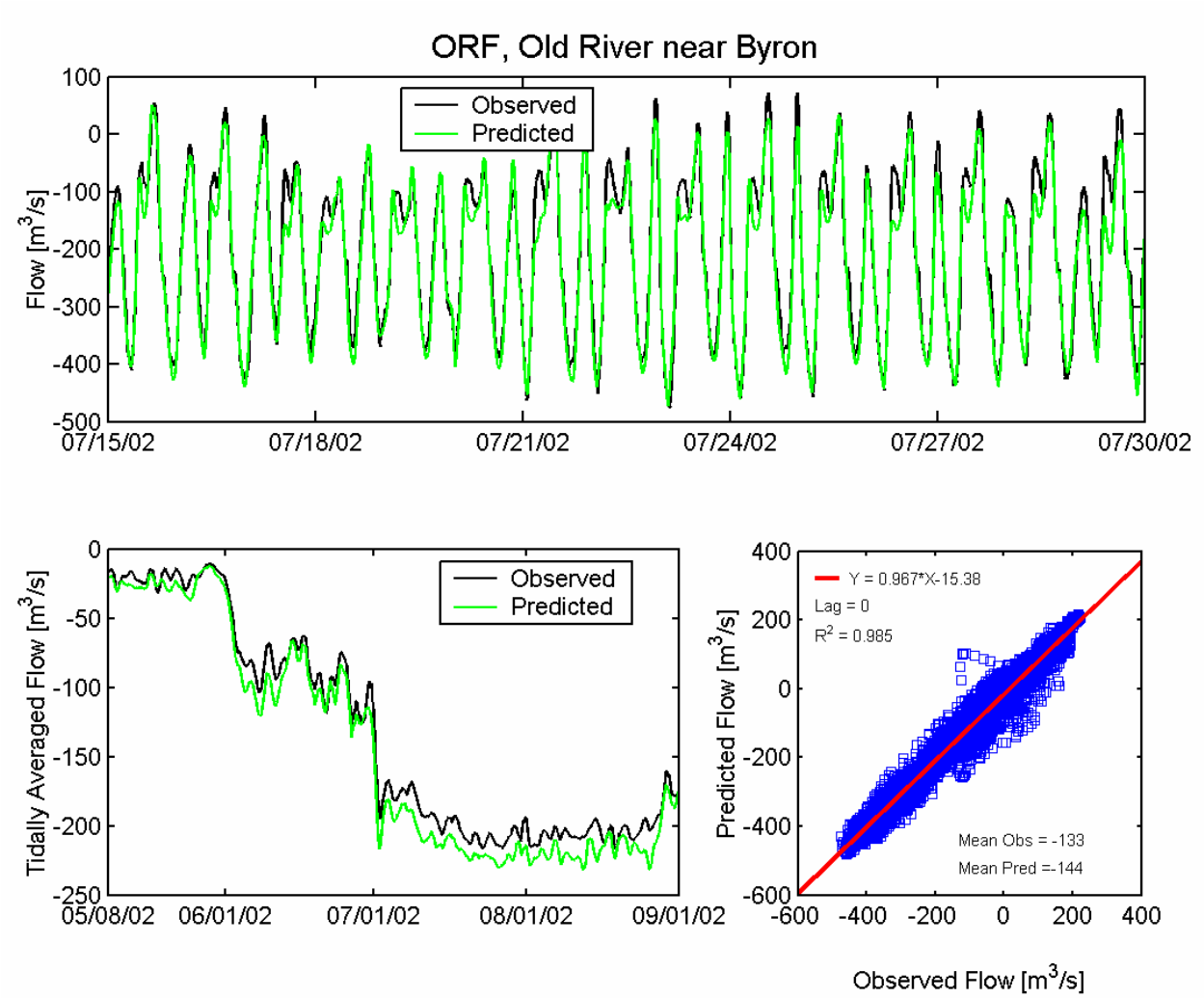

Figure 5.3-24 Observed and predicted flow at Old River near Byron USGS station (ORF) during the 2002 simulation period.

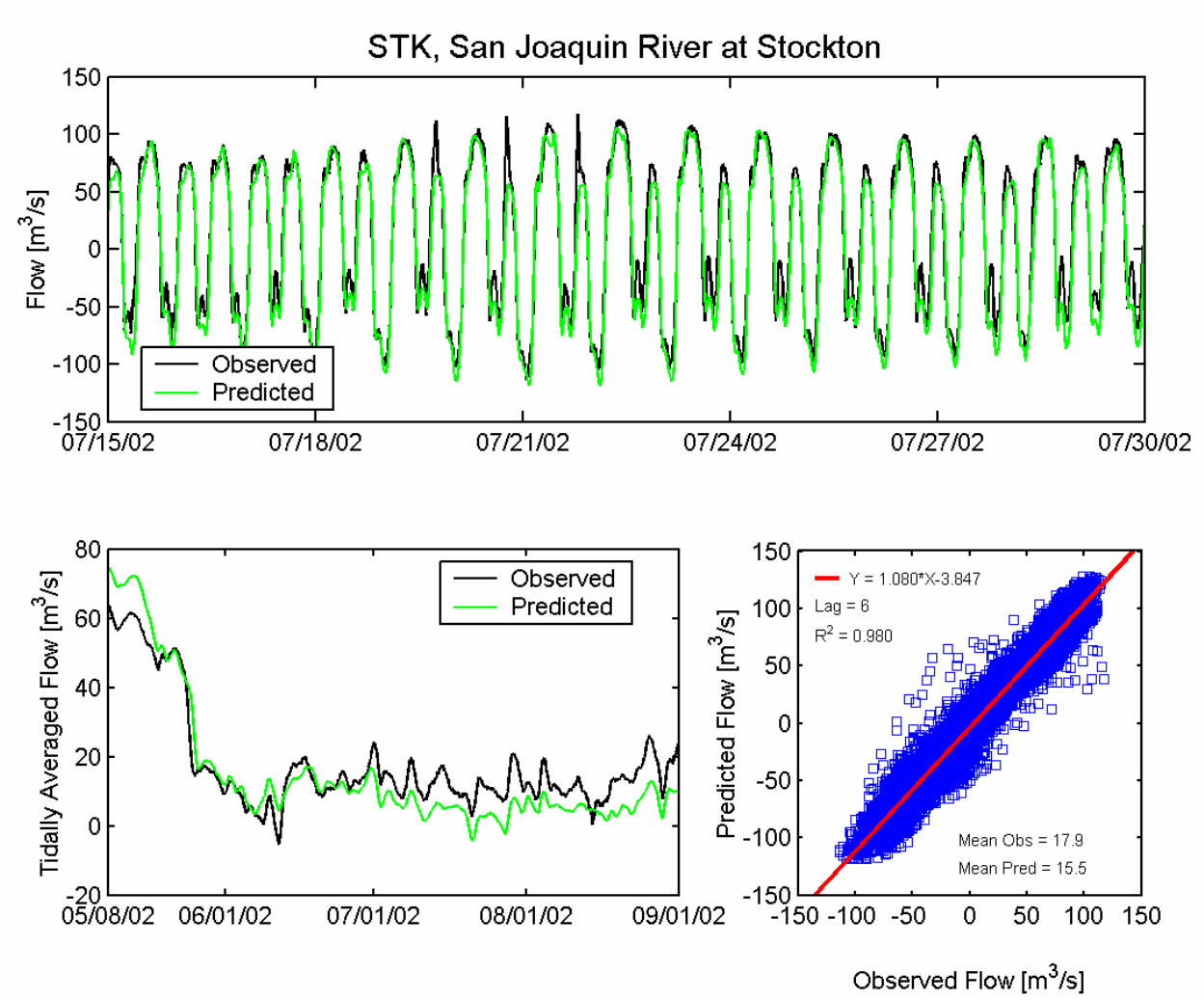

Figure 5.3-25 Observed and predicted flow at San Joaquin River at Stockton USGS station (STK) during the 2002 simulation period.

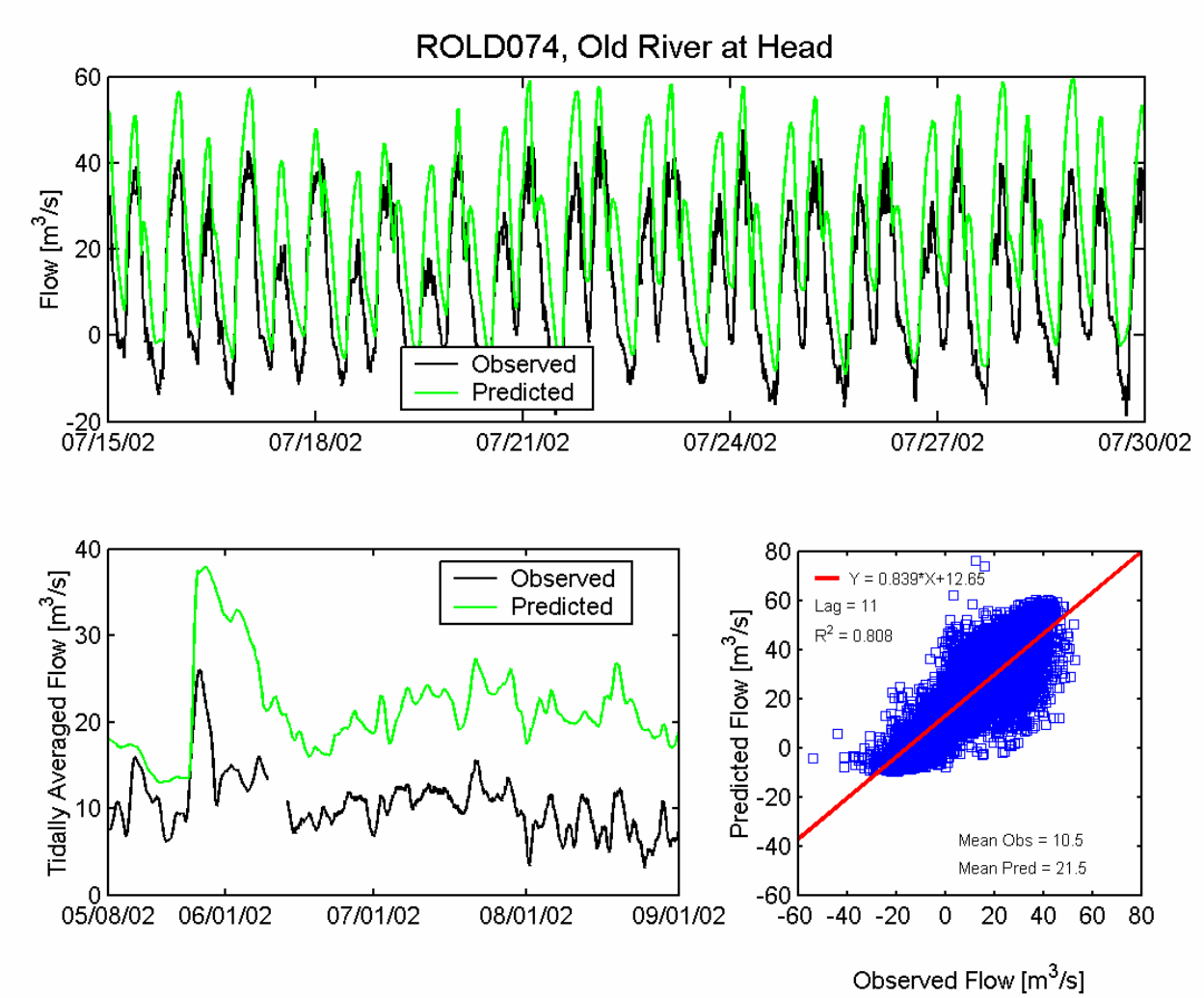

Figure 5.3-26 Observed and predicted flow at Old River at Head DWR station (ROLD074) during the 2002 simulation period.

6. Discussion and Future Improvements

The hydrodynamic calibration and validation demonstrates that the model is accurately predicting water levels from the Golden Gate through the Sacramento-San Joaquin Delta, and accurately predicting both tidal time scale and tidally-averaged (net) flows in the Sacramento San Joaquin Delta. The previous application of UnTRIM in the Sacramento-San Joaquin Delta for the DRMS project (MacWilliams and Gross, 2007) relied on "False Delta" areas to represent the prism of unresolved portions of the Delta; model calibration for that study identified over-predicted tidal range at all stations in the central Delta, resulting from reflection of water levels occurring at the False Delta regions. By fully-resolving the entire Sacramento-San Joaquin Delta, this effect has been removed, and accurate water levels and tidal range are predicted throughout the Sacramento-San Joaquin Delta. As a result, this study constitutes a significant improvement over previous applications (e.g., Gross et al., 2006; MacWilliams and Gross, 2007). This section provides a discussion of future changes which can further improve the current model for future applications.

6.1 UnTRIM Bay-Delta Model Accuracy Relative to RMA2 and DSM2

A full comparison between the UnTRIM Bay-Delta model and previous applications of other 2-D and 1-D models to the Delta is not within the scope of this report. However, some comparisons between predicted flow and stage from these models and observed data provide a valuable context for understanding the relative accuracy of the UnTRIM model and other existing tools.

The "Flooded Islands Pre-Feasibility Study: RMA Delta Model Calibration Report" by RMA (2005) provides a valuable context for comparing the accuracy of the UnTRIM Bay-Delta Model with the RMA2 model, since the calibration period used by RMA (2005) is the identical period used for model validation in this study (see Section 5), and much of the same data were used for model comparisons. The RMA (2005) study made comparisons between observed and predicted stage at a smaller number of stations than the current study, and computed cross-correlation statistics over a slightly different time span. For the period from July 7 to August 4, 2002, cross-correlation statistics at nine stations in the Delta yielded amplitude ratios between 0.96 and 1.09, with phase differences between -17 and 8 minutes (see Table 5-1 in RMA, 2005). At these same nine stations, the UnTRIM Bay Delta model cross-correlation for the period between May 8 and September 1, 2002 yielded amplitude ratios between 0.96 and 1.10 and phase differences between -8 and 23 minutes. Based on this one composite comparison, the overall level of accuracy for stage prediction in the UnTRIM Bay-Delta model is comparable to the accuracy of the stage comparison for the RMA calibration for the same period. A qualitative comparison between the flow comparisons for the RMA and UnTRIM model indicate that each of the models perform better at some stations, and some similarities exist in the differences between observed and predicted values at same stations. For example, at the Delta Cross Channel (see Figure 5.3-4 this report; Figure 6-5 in RMA, 2005) the UnTRIM model more accurately predicts the magnitude of tidal time-scale flow magnitudes, but both models tend to slightly under-predict tidally-averaged flows between June and August. The UnTRIM model results compare more favorably to flow data at Fisherman's Cut than the RMA model results (see Figure 5.3-15 this

report; Figure 6-13 in RMA, 2005), whereas at Dutch Slough (see Figure 5.3-13 this report; Figure 6-14 in RMA, 2005), the RMA model more accurately predicts tidal time-scale flows, but both models show differences between observed and predicted net flows. In the south Delta, on Old River near Byron (see Figure 5.3-24 this report; Figure 6-19 in RMA, 2005), comparisons between observed and predicted flows are similar for both models. Overall, comparison of the results of the RMA model (RMA, 2005) and this study indicate that the level of agreement between observed flows and flows predicted by the RMA and UnTRIM models are similar.

A detailed comparison between observed and predicted stage for the DSM2 model and UnTRIM is not as straight-forward, partly because an equivalent calibration study using the identical flow data is not available. However, a study by Suits and Wilde (2004) included in the "Methodology for Flow and Salinity Estimates in the Sacramento-San Joaquin Delta and Suisun Marsh 25th Annual Progress Report" provides some comparisons between flows predicted by DSM2 and the flow data corrected at locations surrounding Franks Tract in 2002, which is the same data set used for the RMA (2005) and the UnTRIM model validation in this study. The motivation for the Suits and Wilde (2004) comparisons was to explore modified representation of DSM2 geometry around and in Franks Tract. Figure 6.1-1 shows the tidal and tidally-averaged timescale flow comparison for DSM2 on Old River near the San Joaquin River (for comparison see Figure 5.3-16 this report; Figure 6-17 RMA, 2005). Relative to the observations, DSM2 tends to predict much larger tidal flows south on flood and consistently more negative (south) tidally-filtered flows. Figure 6.1-2 shows the tidal and tidally-averaged timescale flow comparison for DSM2 on Fisherman's Cut (for comparison see Figure 5.3-15 this report; Figure 6-13 RMA, 2005). At Fisherman's Cut the flows predicted by DSM2 differ significantly from observed flows in both the tidal and tidally-filtered comparisons.

Although only limited comparisons are available in the Suits and Wilde (2004) report, the "equivalent" comparisons between observed and predicted flows for the UnTRIM and RMA2 models tends to show better agreement between observed and predicted flows than the current DSM2 geometry and calibration. However, some similar trends are evident between the three models. For example, both DSM2 and RMA2 tend to over predict the net flow south on Old River near the San Joaquin River. The UnTRIM model slightly under predicts flow south at this station for 2002, but predicts larger than predicted net flow south for the 2007 period. The UnTRIM model and DSM2 model tend to under predict tidal flow magnitude at Holland Cut, whereas RMA2 somewhat over predicts peak tidal flows. The DSM2 and RMA2 results tend to under predict net flow south at Holland Cut, while the UnTRIM model more accurately predicts net and tidally-averaged flow magnitude at Holland Cut. Because no statistical measure is available to assess the DSM2 comparisons made by Suits and Wilde (2004), a quantitative comparison can not be easily made. However, in general the flow comparisons in the Suits and Wilde (2004) report do not show as good agreement between observed and predicted flows as the RMA (2005) results and the UnTRIM results in the current study. A detailed three-way comparison between the RMA2, UnTRIM, and DSM2 Delta models over the same simulation period would be necessary to provide a more quantitative comparison between the three models, and could also potentially provide insight into how each of the three models could be further improved.

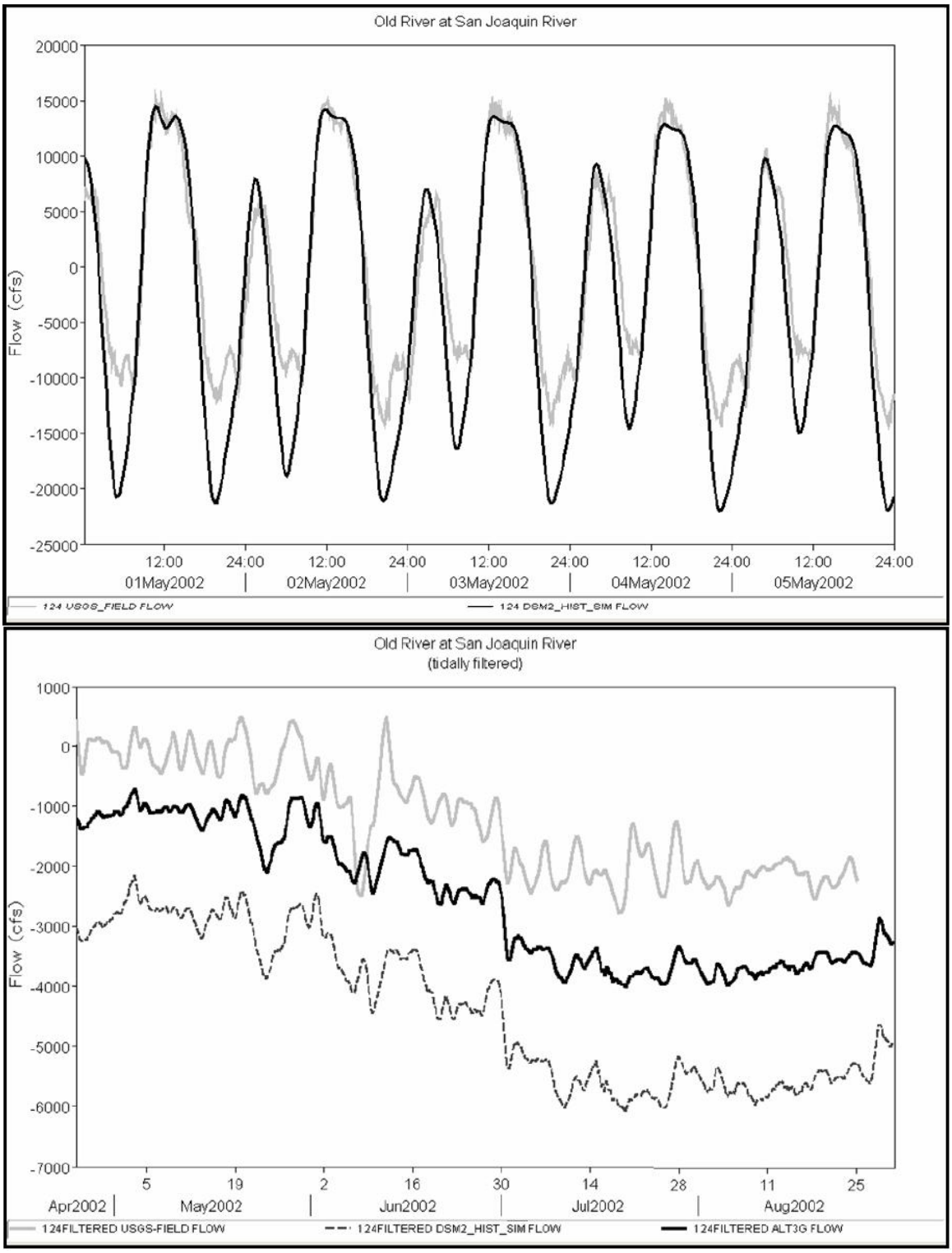

Figure 6.1-1 Comparison between observed flow and flow predicted by DSM2 on Old River at the San Joaquin River. Top figure shows tidal time-scale flow. Bottom figure shows tidally-averaged flow for observed (grey), predicted using current DSM2geometry (dashed grey), and modified DSM2 geometry (black). From Suits and Wilde (2004).

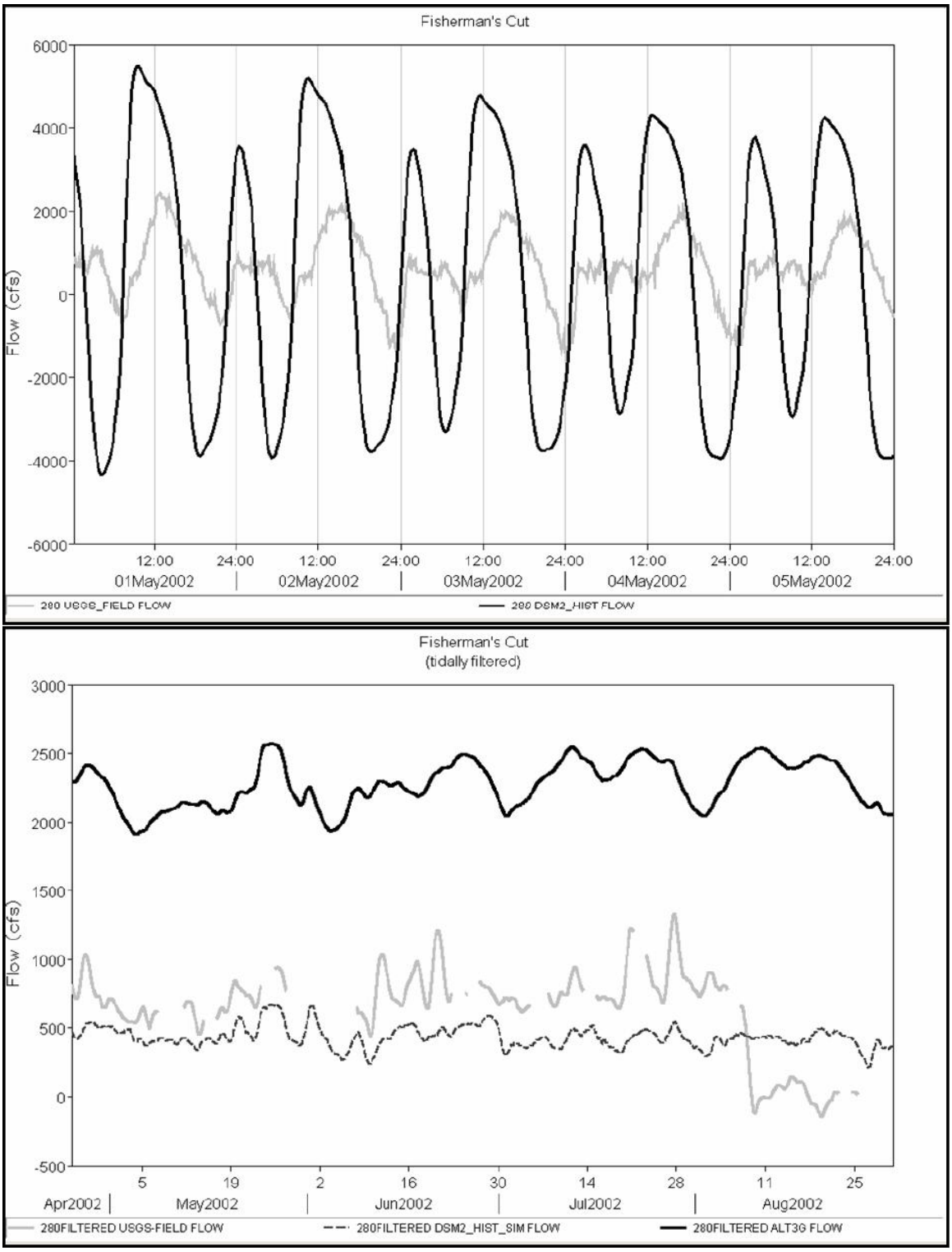

Figure 6.1-2 Comparison between observed flow and flow predicted by DSM2 on Fisherman's Cut. Top figure shows tidal time-scale flow. Bottom figure shows tidally-averaged flow for observed (grey), predicted using current DSM2geometry (dashed grey), and modified DSM2 geometry (black). From Suits and Wilde (2004).

6.2 Vertical Datum and Additional Bathymetry

The current model uses NGVD29 as the vertical datum. The primary reason for using this vertical datum is that the most recent bathymetric DEM for the Sacramento-San Joaquin Delta (Smith et al., 2003) was referenced to NGVD. The implementation of the model assumes that the coordinate system is flat. However, 0 NGVD is not a flat surface, and can vary by about 0.5 feet or more between the Golden Gate and the south Delta. This "datum slope" can create some difficulties in calibrating water levels (since the observation data need to be corrected to account for the datum difference), as well as introducing potential errors in representing heights of weirs on temporary barriers, and elevations of marsh areas that only flood on high tides. The NAVD88 vertical datum is designed to be horizontal and is therefore better suited for use as a vertical datum for the Bay-Delta UnTRIM model. However, converting the processed NGVD29 DEM into NAVD88 is not an ideal solution. Ideally, a new bathymetric data set should be collected for the entire Delta in NAVD88 using vertical controls throughout the Delta. This could then be more easily coupled with recent LiDAR data of Delta islands, marshes, and upland areas.

Additionally, the existing DEM for the Sacramento-San Joaquin Delta (Smith et al., 2003) does not include bathymetry for some islands which are currently flooded, such as Mildred Island and Little Mandeville Island, as well as a large number of "in-channel" islands which, based on aerial photographs, flood on high tides. For example, Figure 6.2-1 shows several islands near Clifton Court Forebay which are not included in the DEM. A large number of in-channel islands which are not included in the bathymetry or model grid are located along the San Joaquin River upstream of Franks Tract (Figure 6.2-2) and also south of Franks Tract (Figure 6.2-3). The absence of these islands from the current model grid results in some under prediction of tidal prism south of Franks Tract. Bathymetry for some of these islands should be available from recent LiDAR data, if the islands are not vegetated and the data were collected when the islands were dry. For other islands, such as Little Mandeville Island and Mildred Island, which are permanently flooded, bathymetric surveys are necessary.

6.3 Spatially-variable Roughness

The current application of the UnTRIM model uses a single uniform roughness value over the entire Sacramento-San Joaquin Delta. As noted in Section 3.11, no channel-specific "tuning" of roughness was used to calibrate net flows. This approach is consistent with field observations by Jon Burau, who has suggested that "the bed is very similar throughout the delta, and except for variations in bed forms, the friction coefficients used in the models should be very similar throughout the Delta" (Jon Burau, personal communication). However, there are some areas where spatially-variable roughness may be justified and could be used to improve model calibration. In particular, regions with seasonal Egeria in Franks Tract could be represented by using a higher roughness locally. Similarly, higher roughness could be applied to vegetated marshes or in-channel islands. However, since improved bathymetry is likely to have a larger effect on model calibration than modified roughness, more recent bathymetry in NAVD88 should be collected before this level of calibration is practical. Otherwise, tuning of roughness could mask areas where better bathymetry is needed.

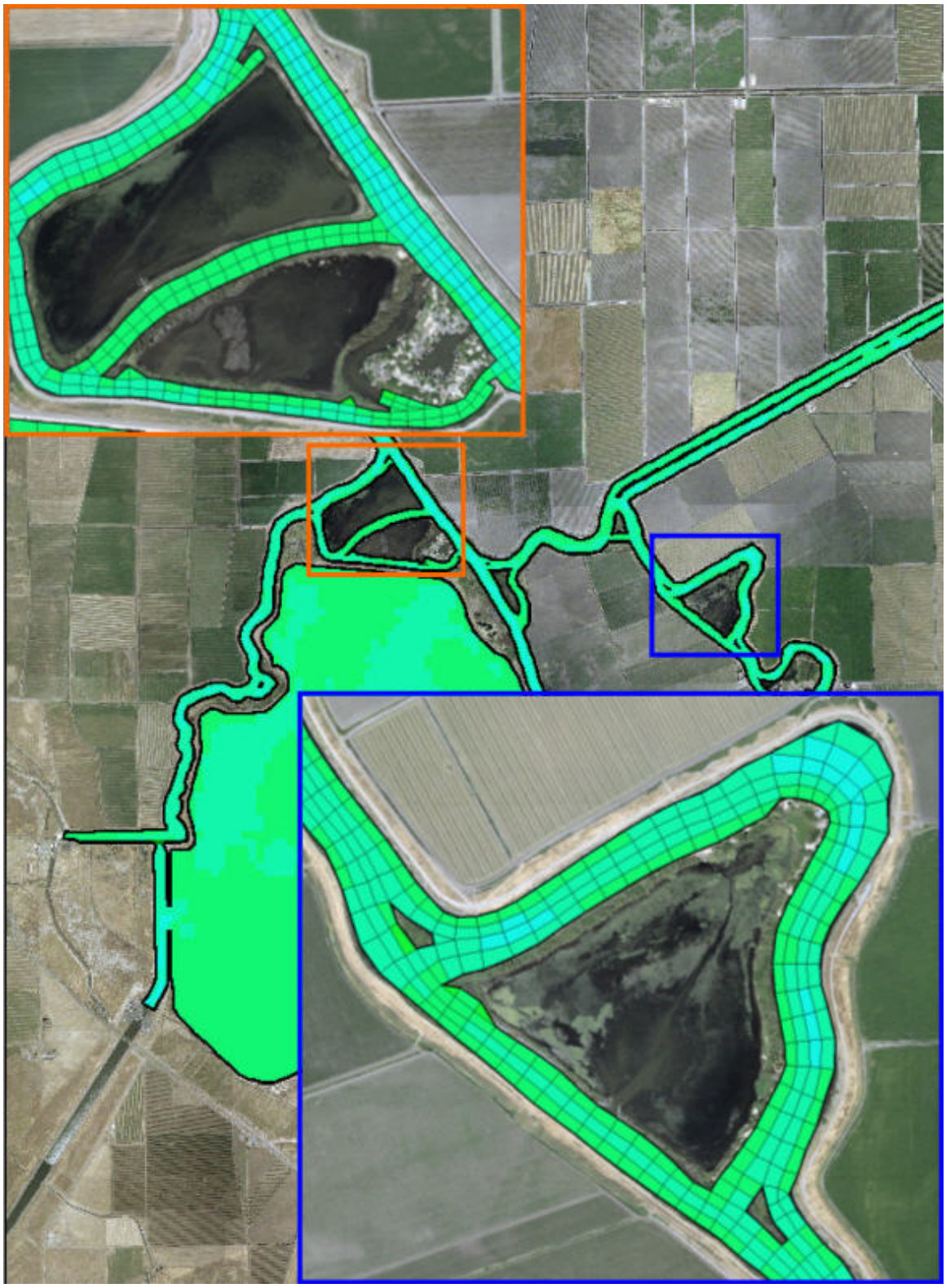

Figure 6.2-1 Location of several islands near Clifton Court Forebay which flood on high tides, but are not included in available Delta bathymetry or the current model grid.

Figure 6.2-2 Location of several islands along the San Joaquin River which flood on high tides or are permanently flooded, but are not included in available Delta bathymetry or the current model grid.

Figure 6.2-3 Location of several islands south of Franks Tract, including Little Mandeville Island (center) and Rhode Island (lower left), which flood on high tides or are permanently flooded, but are not included in available Delta bathymetry or the current model grid.

6.4 Improved Barrier Operations

The current model implementation closely follows the approach used in DSM2 to represent operation of barriers. A detailed discussion of barrier implementation in the Bay-Delta UnTRIM model is presented in Section 3.12. This section evaluates the performance of the barrier implementation of the Delta Cross Channel gates and the Head of Old River temporary barrier.

The extensive flow monitoring data collected by the USGS in the Sacramento-San Joaquin Delta provides a valuable resource for calibrating and evaluating the hydraulic performance of the barrier implementation in Delta models. By evaluating flows over selective "control volumes" this approach can be used to both estimate the accuracy of the observed flows as well as the model performance relative to the observed flows.

6.4.1 Delta Cross Channel Gate Operations

Figure 6.4-1 shows four USGS flow monitoring stations near the Delta Cross Channel. Individual comparisons between observed and predicted flows at each of these stations are shown in Figures 4.4-2 through 4.4-5. Based on the mean observed and predicted flow at each of these stations over the entire simulation period (values found in Table 4-2 and on lower right panel of Figures 4.4-2 through 4.4-5), Figure 6.4-2 shows the observed and predicted average net flows at these four stations during the 2007 simulation period. The observed and predicted average net flow at the upstream Sacramento River North of the Delta Cross Channel (WGB) station, is identical, with observed and predicted average flow rates of 257 m^3/s. Since there is minimal consumptive use in this region, the sum of the three downstream predicted average net flow rates, 69 m^3/s through the Delta Cross Channel (DCC), 81 m^3/s through Georgiana Slough (GEO), and 107 m^3/s on the Sacramento River South of Georgiana Slough (WGB), also totals 257 m^3/s. The sum of the three average observed net flows at these same three stations (76, 80, and 112 m^3/s, respectively) is 268 m^3/s. The difference between the upstream observed flow of 257 m^3/s and downstream observed flow of 268 m^3/s provides a measure of the accuracy of the observed net flow measurements. Based on observed net flows, the UnTRIM model tends to consistently under predict flow through the Delta Cross Channel, as does the RMA2 model (see Figure 5.3-4 this report; Figure 6-5 in RMA, 2005). However, some of this difference could also be due to a bias in the discharge rating for the DCC observations, since the sum of the three observed downstream flows are consistently higher than the upstream flow. The currently available data do not provide sufficient information to definitively determine which station flow ratings are most accurate. Observed and predicted net flows through Georgina Slough (GEO) are nearly identical, while observed flows downstream of Georgiana Slough (WGB) tend to be higher than predicted flows. Overall the comparison between observed and predicted net flows at these four stations indicates that the model predictions are within the uncertainty of the observed flows.

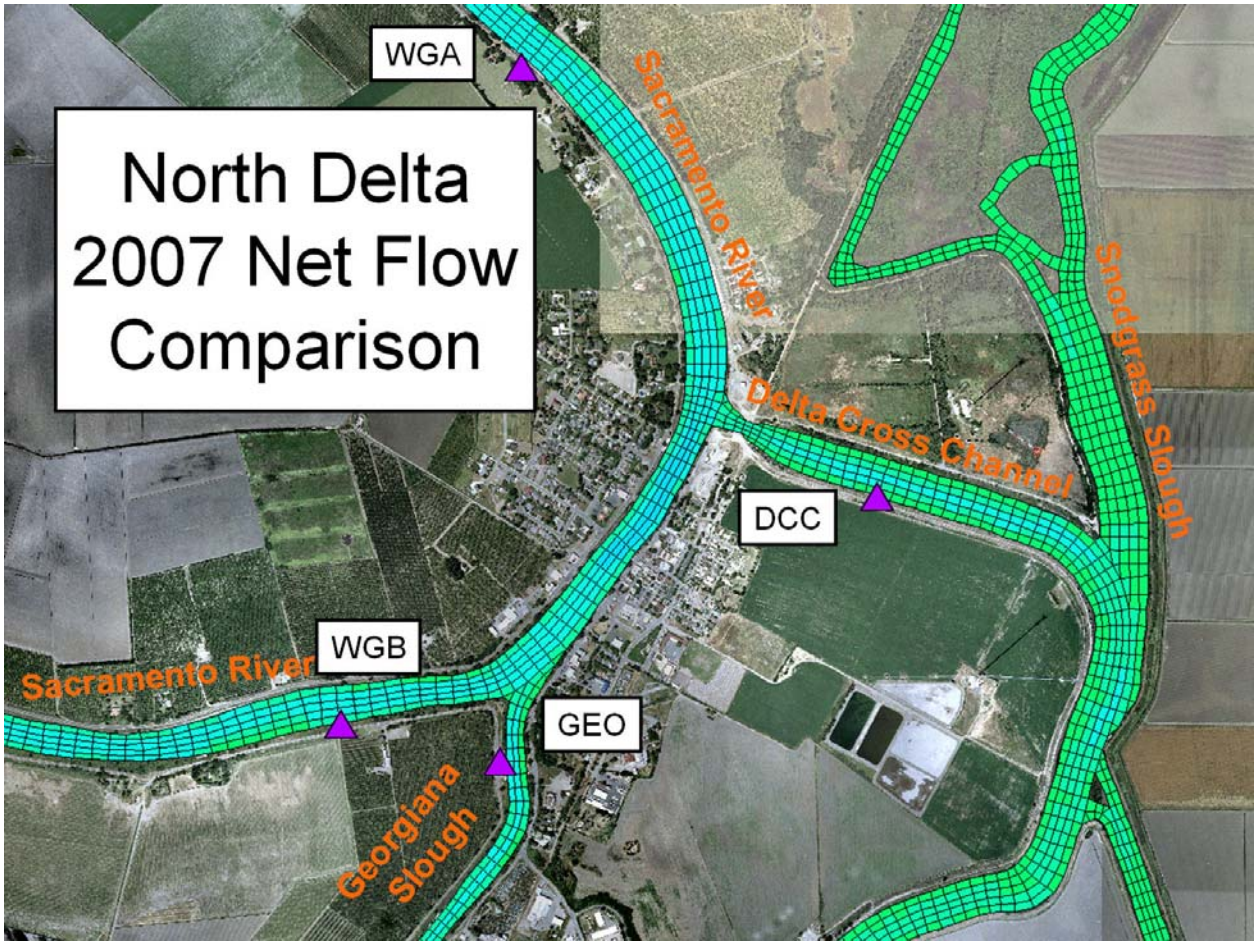

Figure 6.4-1 Location of four USGS flow monitoring stations near the Delta Cross Channel used in net flow comparison for 2007 simulation period.

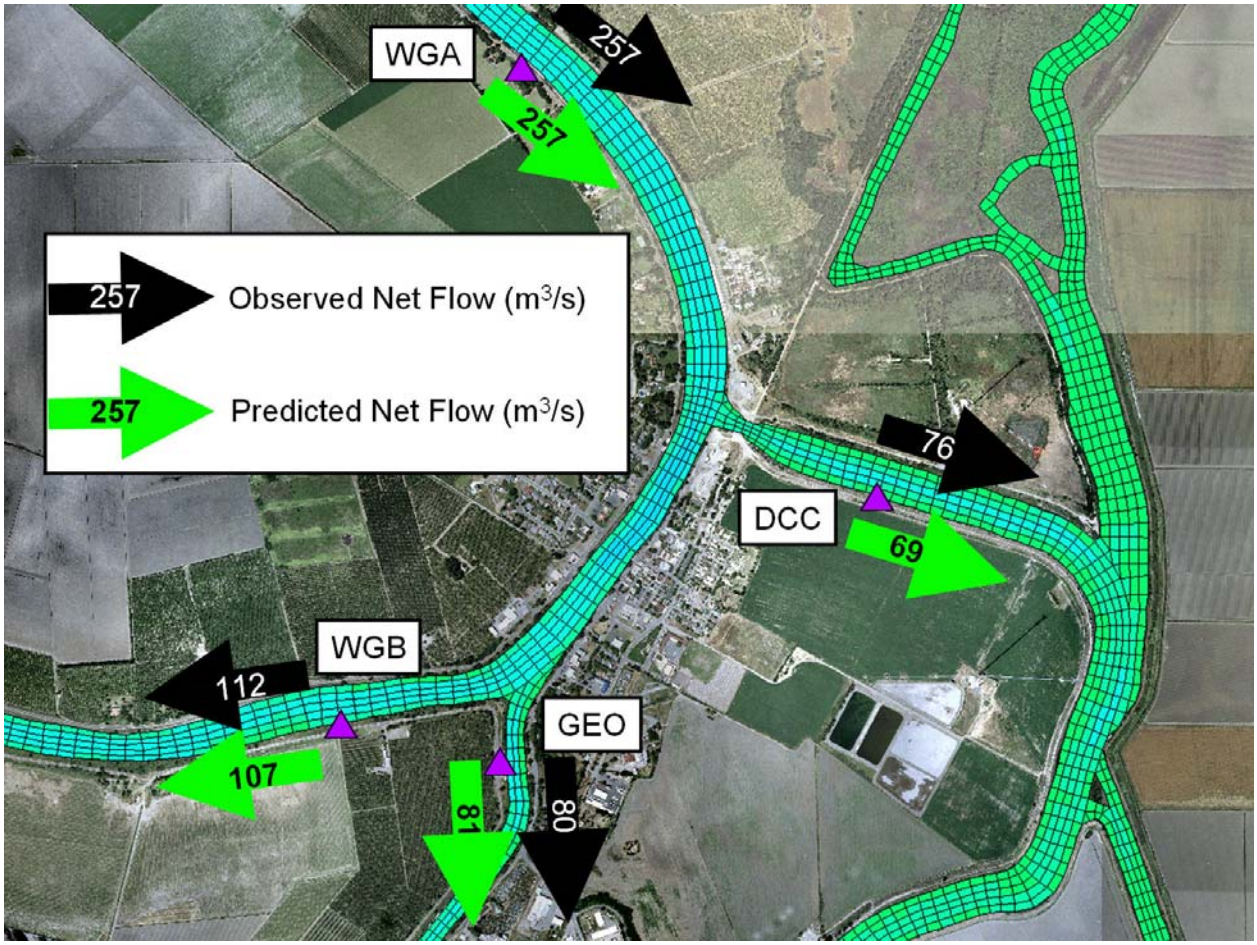

Figure 6.4-2 Observed (black arrows) and Predicted (green arrows) average net flow at four USGS flow monitoring stations near the Delta Cross Channel during 2007 simulation period spanning from April 4, 2007 through September 1, 2007.

6.4.2 Head of Old River Temporary Barrier Operations

In order to evaluate how closely the implementation of the temporary barriers in UnTRIM compares with the implementation of the equivalent barriers in DSM2, observed flows at stations along the San Joaquin River near the Head of Old River Barrier were compared with flows predicted by DSM2 and the Bay-Delta UnTRIM model at the locations shown on Figure 6.4-3. For each comparison, a tidal time-scale and tidally-averaged comparison are shown.

Figure 6.4-4 shows a comparison between observed flows and flows predicted by DSM2 and UnTRIM on the San Joaquin River at Mossdale. In general, the UnTRIM model tends to predict slightly higher than observed peak tidal flows, and the DSM2 model tends to predict somewhat lower than observed peak tidal flows. The tidally-averaged flow comparison shows that the tidally-averaged predicted flows from UnTRIM match the observed flows better than DSM2 for the first half of the simulation, the DSM2 flows match better during July, and the predicted flows from DSM2 and UnTRIM are nearly identical in August, but are both slightly higher than observed. In late-April and early-May, tidally-averaged flows from DSM2 show a peak above the observed flows; otherwise the DSM2, UnTRIM, and observed tidally-averaged flows during the period when the Head of Old River barrier is in place between April 20 and May 22, 2007 are very similar. During the period between April 20 and May 22, the average observed net flow at Mossdale was 83 m^3/s, the average net flow predicted by UnTRIM was 85 m^3/s, and the average net flow predicted by DSM2 was 87 m^3/s. Most of the difference between the net flow from DSM2 and the observed flow can be attributed to the difference observed in late-April and early-May.

Figure 6.4-5 shows a comparison between observed flows and flows predicted by DSM2 and UnTRIM on Old River at Head (ROLD074), just downstream of the temporary barrier. This flow measurement is approximately equivalent to the flow through the barrier when the barrier is in place, and of the flow through Old River during other periods. Both UnTRIM and DSM2 tend to significantly under-predict the tidally-averaged flow, both during the period when the barrier is in place and before and after the barrier is operating. It is not known if this is the result of a bias in the flow rating curves or in the models. During the period when the barrier is in place, between April 20 and May 22, the average observed net flow at ROLD074 was 19 m^3/s, the average net flow predicted by UnTRIM was 11 m^3/s, and the average net flow predicted by DSM2 was 10 m^3/s. On average, UnTRIM tends to under-predict the flow through the barrier by 8 m^3/s and DSM2 under-predicts flow through the barrier by 9 m^3/s.

Figure 6.4-6 shows a comparison between observed flows and flows predicted by UnTRIM on the San Joaquin River near Lathrop (SJL), just downstream of the head of Old River. Predicted DSM2 flows were not available at this station. The observed peak tidal flows and the observed tidally-averaged flows are both consistently less than the flows predicted by UnTRIM. During the period when the Head of Old River barrier is in place, between April 20 and May 22, the average observed net flow at SJL was 46 m^3/s, and the average net flow predicted by UnTRIM was 73 m^3/s. A local volume balance can be used to evaluate whether the observed flows at this station are accurate. For a local mass balance between Mossdale, Head of Old River, and Lathrop, the UnTRIM model predicts 85 m^3/s at Mossdale and a total of 84 m^3/s at the two

downstream stations. The difference between the predicted upstream and downstream net flows is about 1 m^3/s, and corresponds to the specified consumptive use inside the region used to calculate the flow balance. In contrast, the observed flows indicate 83 m^3/s upstream with a total of 65 m^3/s downstream with an effective consumptive use of 18 m^3/s, which is much larger than that specified in the DICU in this region, indicating that there may be some issues with the current flow rating at the Lathrop station.

Figure 6.4-7 shows a comparison between observed flows and flows predicted by DSM2 and UnTRIM on the San Joaquin River at Stockton. On a tidal time-scale, predicted flows from UnTRIM and DSM2 agree well with observed flows. The predicted tidally-averaged flows from DSM2 and UnTRIM agree well with observed tidally-averaged flows during the periods the Head of Old River Barrier is not in place. During the period between April 20 and May 22 when the Head of Old River barrier is operating, the average observed net flow at Stockton was 66 m^3/s, the average net flow predicted by UnTRIM was 72 m^3/s, and the average net flow predicted by DSM2 was 74 m^3/s. The "spike" in tidally-averaged flow predicted by DSM2 in late-April and early-May that was evident at Mossdale is also evident at Stockton. During the period the Head of Old River barrier is in place, UnTRIM tends to over-predict the flow through the San Joaquin River at Stockton by 6 m^3/s and DSM2 over-predicts flow at Stockton by 8 m^3/s. These over-predictions of flow on the San Joaquin are similar in magnitude to the under-predictions of flow through the Head of Old River barrier.

Figure 6.4-8 shows the average net flows for the time period spanning from April 20 to May 22, 2007 when the Head of Old River Barrier was in operation. The poor balance of observed net flows on the San Joaquin River at Mossdale, Lathrop, and Stockton, corroborates the conclusion above that the flow rating at Lathrop is not accurate. The predicted net flow at Stockton of 66 m^3/s is 20 m^3/s greater than at Lathrop, and is more consistent with the flows that would be expected in the San Joaquin based on the net flows at Mossdale and Head of Old River. Similarly, the under prediction of flows through the barrier coupled with over prediction of flows at Stockton suggest that the rating curves used to compute flow through the Head of Old River barrier could be considerably improved.

Since there is significant consumptive use in this area of the Delta, it is not expected that the "volume balance" of the flows will be as precise as it was in the Delta Cross Channel region comparison discussed in Section 6.4.1. However this analysis demonstrates how the extensive flow data collected in the Delta can be used both for quality control (by identifying stations such as Lathrop which have inaccurate flow observations or ratings) as well as providing a tool that could be used to improve barrier operations. Although this comparison emphasized differences between observed and predicted flows, the comparison of predicted flows through the Head of Old River barrier by UnTRIM and DSM2 demonstrate that the implantation of the flow rating curves for the culverts on this barrier in UnTRIM result in very similar flows to the barrier implementation in DSM2. This was the goal of the implementation for the current study. However this result also suggests that the flow rating in both models could be improved to better match observed flows, by reducing the culvert energy loss coefficients in the flow rating.

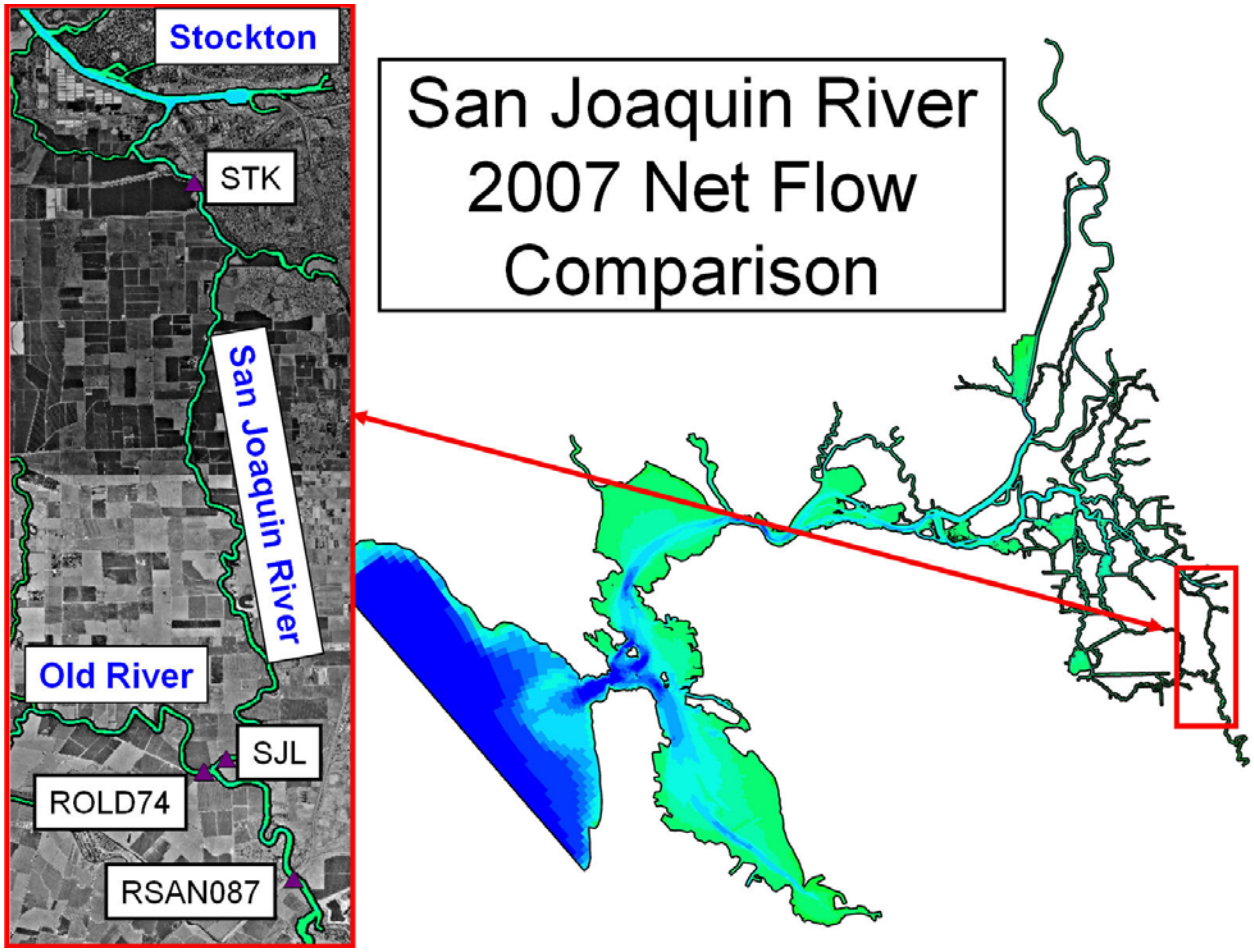

Figure 6.4-3 Location of four USGS and DWR flow monitoring stations near the Head of Old River used in net flow and inter-model comparisons for 2007 simulation period.

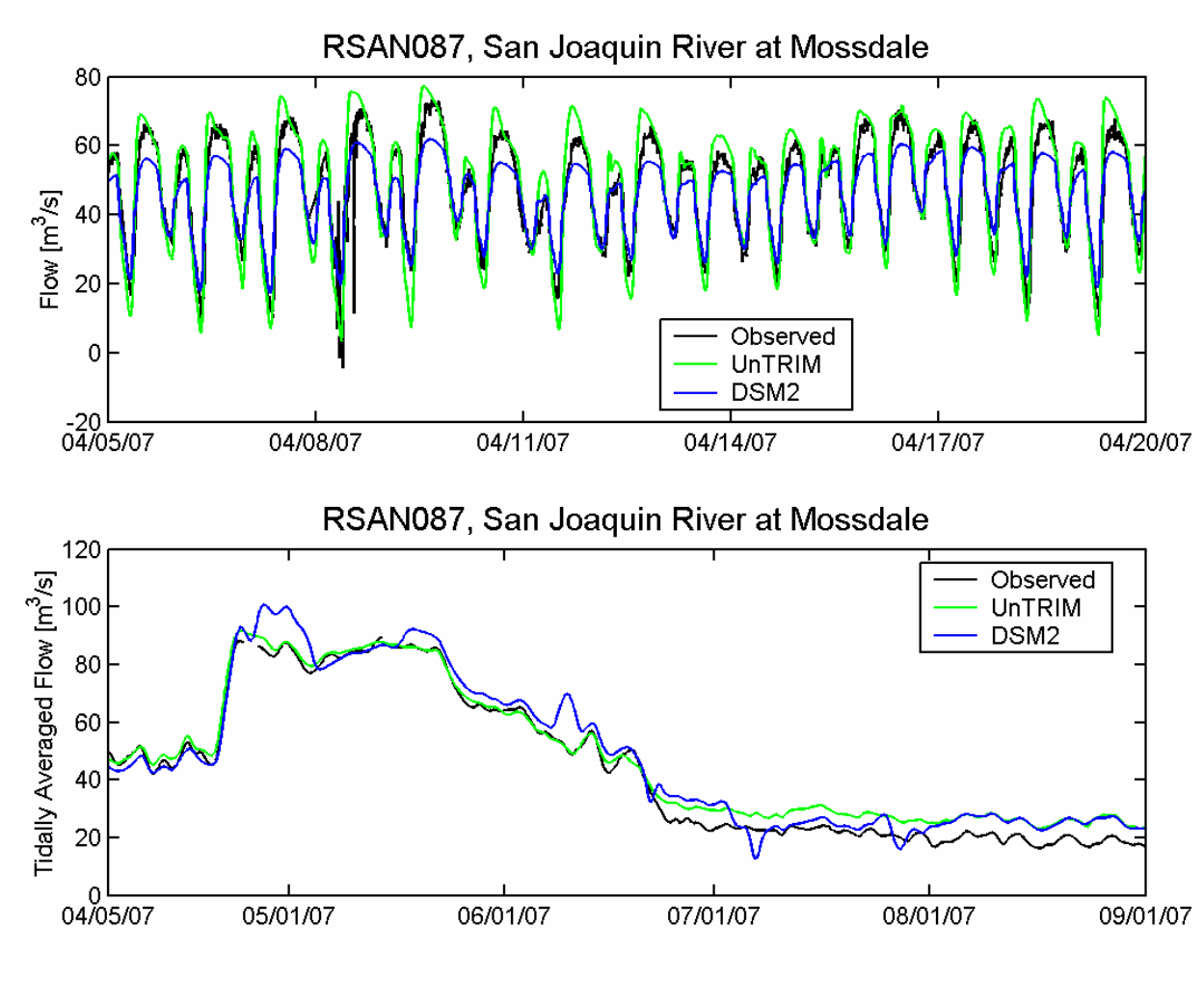

Figure 6.4-4 Comparison between observed flows and flows predicted by DSM2 and UnTRIM on the San Joaquin River at Mossdale (RSAN087). The top figure shows tidal-timescale flows over a 15-day period. The bottom figure shows tidally-averaged flows over the full simulation period between April 5, 2007 and September 1, 2007.

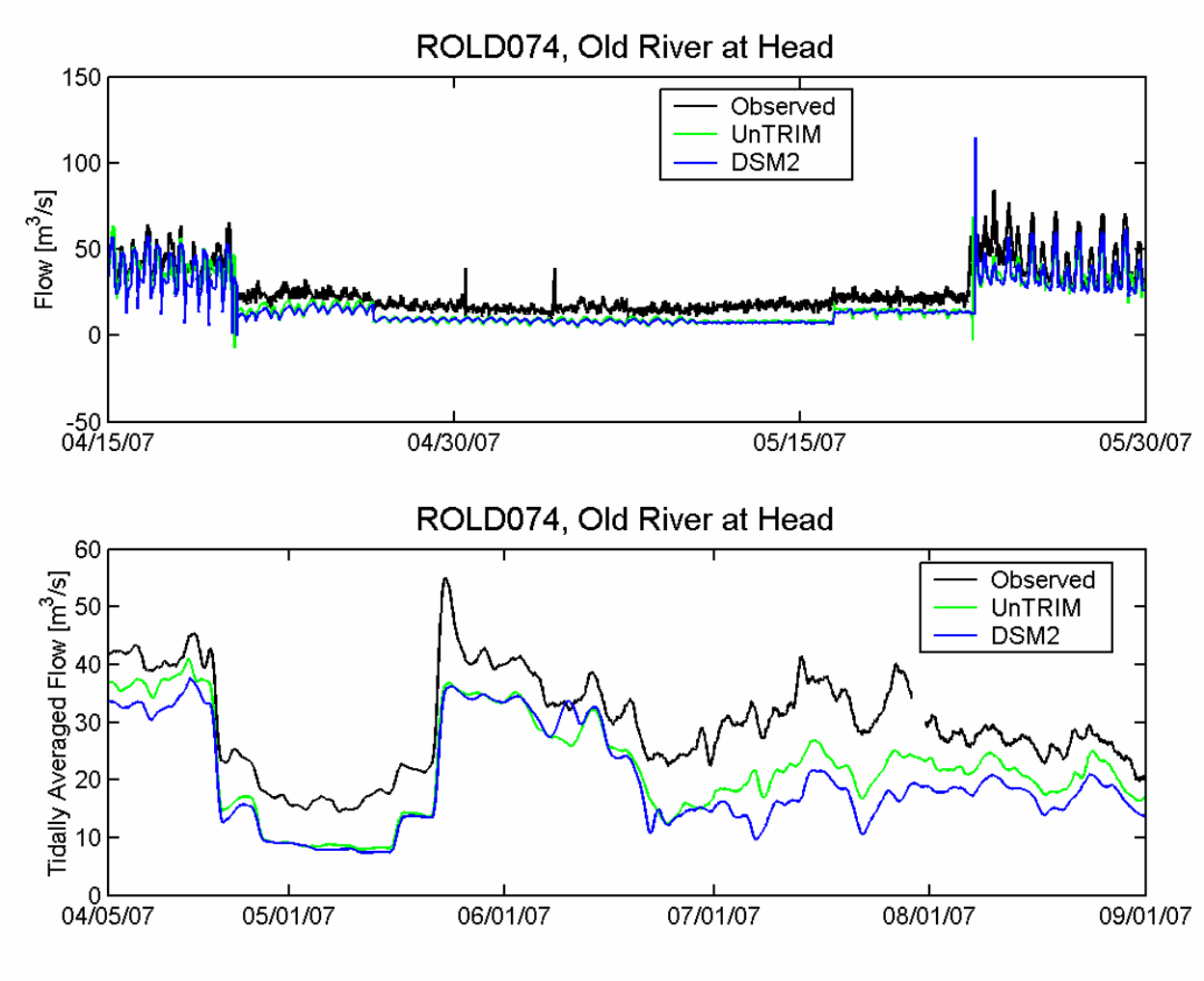

Figure 6.4-5 Comparison between observed flows and flows predicted by DSM2 and UnTRIM on Old River just downstream from the Head of Old River Barrier (ROLD074). The top figure shows tidal-timescale flows over a 55-day period spanning the period between April 20 and May 22 when the Head of Old River barrier was in operation. The bottom figure shows tidally-averaged flows over the full simulation period between April 5, 2007 and September 1, 2007.

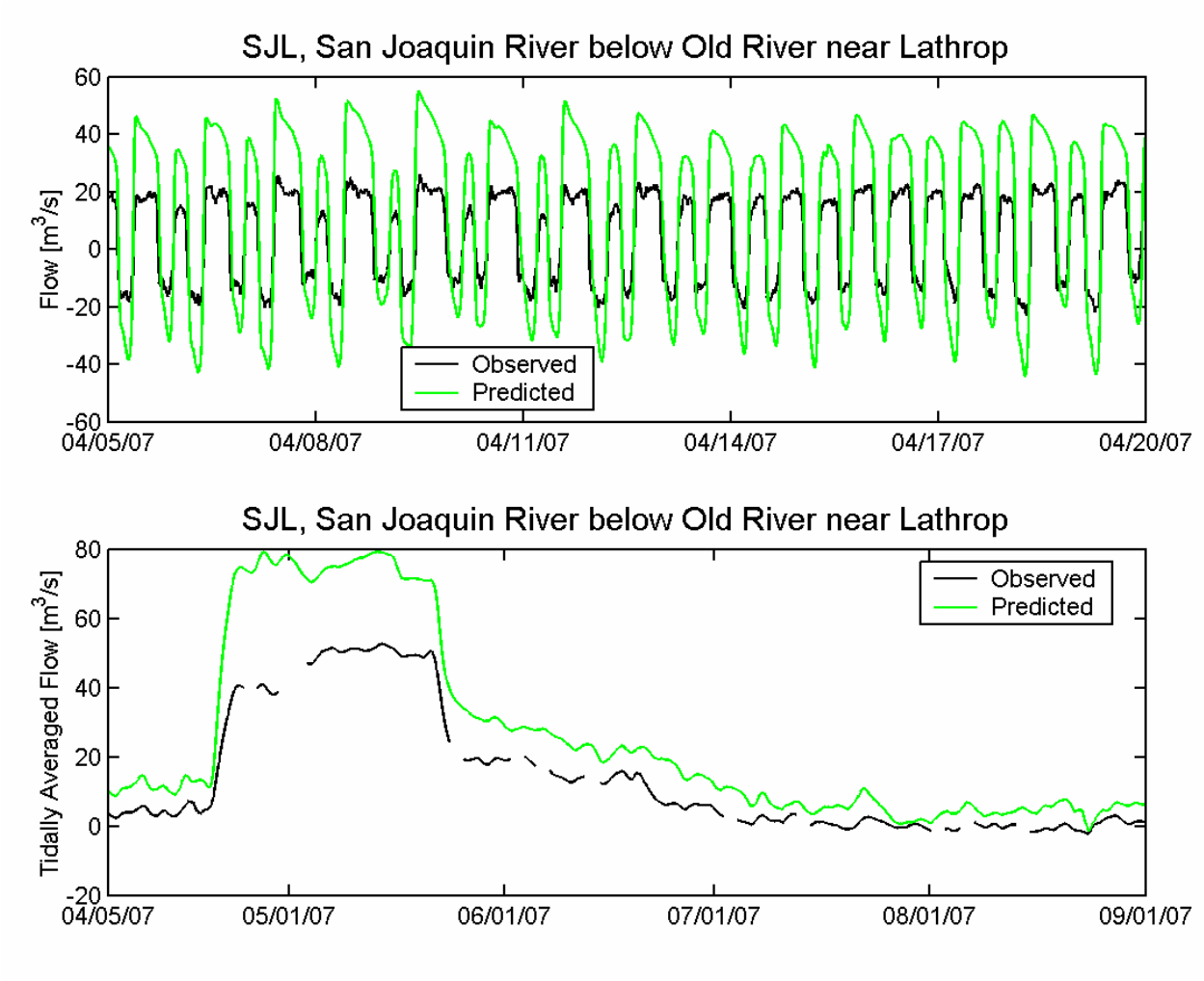

Figure 6.4-6 Comparison between observed flows and flows predicted by UnTRIM on the San Joaquin River below Old River near Lathrop (SJL). Predicted DSM2 flows were not available at this station. The top figure shows tidal-timescale flows over a 15-day period. The bottom figure shows tidally-averaged flows over the full simulation period between April 5, 2007 and September 1, 2007.

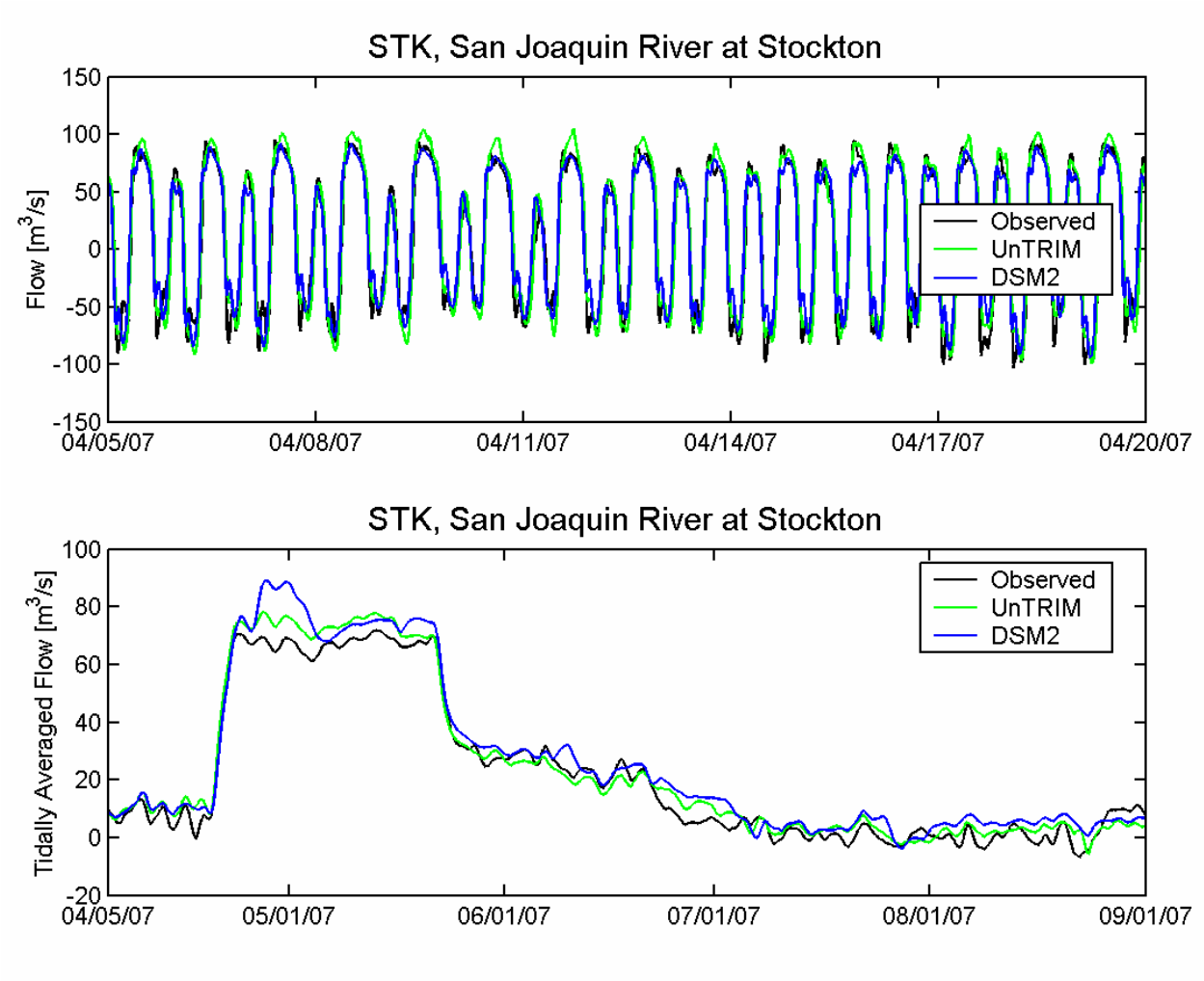

Figure 6.4-7 Comparison between observed flows and flows predicted by DSM2 and UnTRIM on the San Joaquin River at Stockton (STK). The top figure shows tidal-timescale flows over a 15-day period. The bottom figure shows tidally-averaged flows over the full simulation period between April 5, 2007 and September 1, 2007.

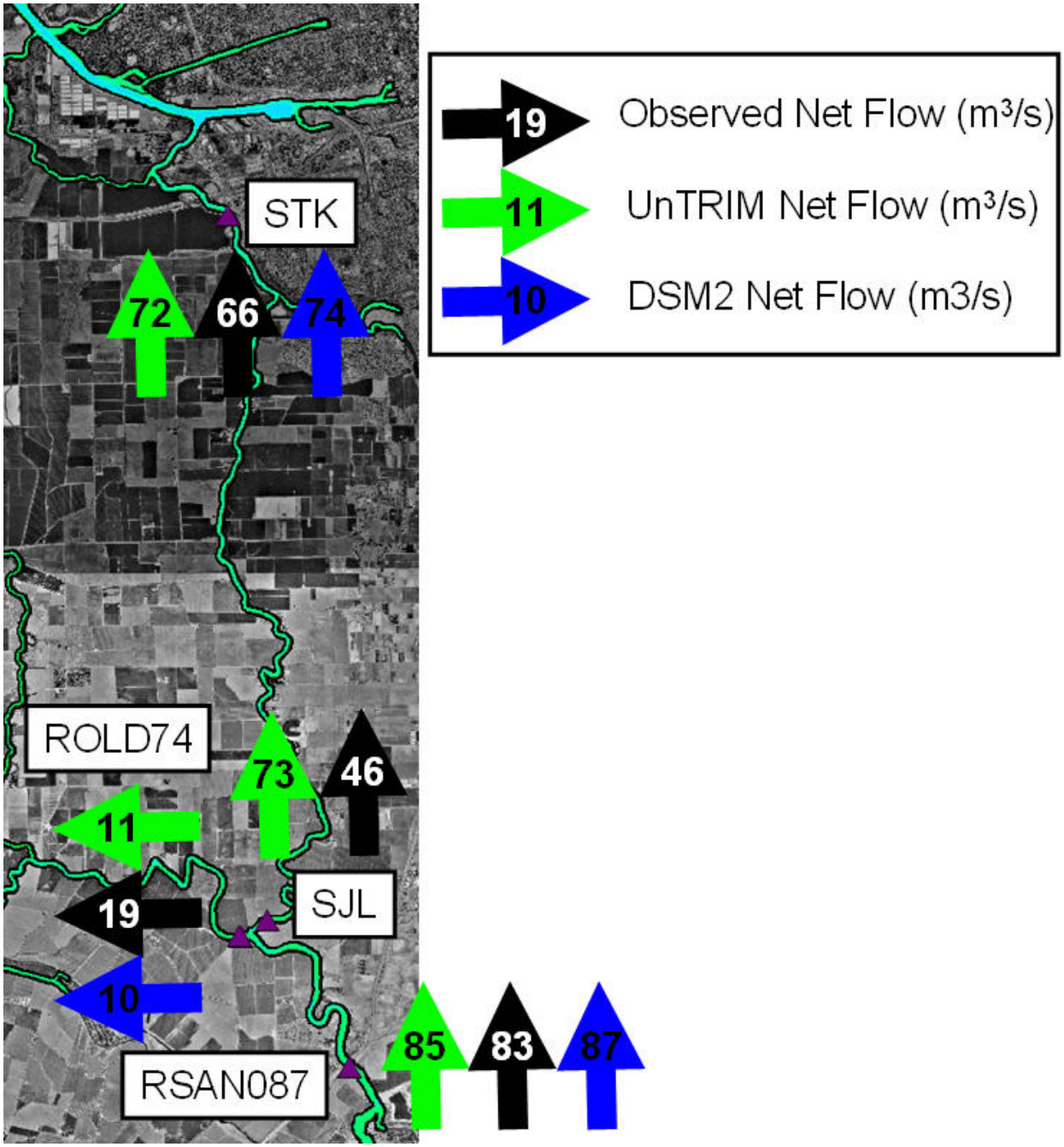

Figure 6.4-8 Observed average net flows (black arrows) and average net flows predicted by UnTRIM (green arrows) and DSM2 (blue arrows) at four USGS and DWR flow monitoring stations on the San Joaquin River and Old River for the time period spanning from April 20 to May 22, 2007 when the spring Head of Old River barrier was in operation during the 2007 simulation period.

6.5 Improved Delta Island Consumptive Use Estimation

The current implementation of DICU follows the approach used by RMA (2005) and makes use of the best available estimates for consumptive use in the Delta. However, DICU estimates are monthly values, which can introduce significant errors when precipitation occurs unevenly over the month. For example, the impact of a late-December storm is averaged over the entire month of December when monthly values are calculated. As a result, the model sees the effect of precipitation in the Delta on December 1, rather than when the storm takes place. Additionally, estimates of flow diversions, return flows, and return salinity are approximate and may introduce significant errors. Since these same estimates are used by DSM2, RMA2, and the Bay-Delta UnTRIM model, these errors affect any model using DICU. Significant improvements to the DICU estimates, as well as implementing daily rather than monthly values provides the potential to significantly improve salinity prediction in the Delta for all models.

6.6 Improved Salinity Calibration

Although salinity was simulated during both the calibration and validation simulations, the primary focus of the calibration effort was focused on stage and flow calibration in the Delta since the accurate prediction of tidal and net flows was the most important process for applying the model to predict delta smelt movements. Comparisons were made between observed and predicted salinity at stations throughout the Delta for all three periods. These comparisons show relatively good agreement with observed salinity at most stations in the Delta, but also show that the model currently tends to under-predict salinity intrusion in the western Delta. The simulation results suggest that the "spin-up" time for salinity in the Delta during summer conditions is fairly long and therefore simulations longer than those used in the current study will be needed to do a detailed salinity calibration for the Bay-Delta UnTRIM model. The salinity calibration conducted for the DRMS project (MacWilliams and Gross, 2007) entailed year-long simulations for salinity calibration. It is expected that a full presentation of salinity calibration results for the Bay-Delta UnTRIM model will be presented as part of a future study and will include longer simulation periods than were used in the current study.

6.7 Future Model Development

The Bay-Delta UnTRIM model is still being refined and improved through significant ongoing development work and additional applications. The lessons learned through the development and calibration effort conducted for this project are already being employed to further improve the model and the calibration for future applications. Additional bathymetry is being incorporated into the model, and some changes and extensions to the model grid are being made to incorporate these changes. In addition, it is expected that some changes to the model will be made in the areas for improvement identified in the previous sections. With these changes, as well as ongoing advancements to the algorithms and numerical methods used in UnTRIM (e.g., Casulli, 2008), it is expected that some changes to the model calibration will occur. These developments will be documented in future model calibration reports.

7. Summary and Conclusions

A three-dimensional hydrodynamic model was applied to simulate hydrodynamics in the Sacramento-San Joaquin Delta, and the hydrodynamic results were used with a particle tracking model to investigate delta smelt distribution and behavior. The model domain extends from the coastal Pacific Ocean west of the Golden Gate through the entire Sacramento-San Joaquin Delta and includes the South Bay, Central Bay, San Pablo Bay, and Suisun Bay embayments. The resulting Bay-Delta UnTRIM model is the first three-dimensional hydrodynamic model extending from the Pacific Ocean through the entire Sacramento-San Joaquin Delta

The Bay-Delta UnTRIM model takes advantage of the grid flexibility allowed in an unstructured mesh by using gradually decreasing grid cell size, beginning with large grid cells in the Pacific Ocean and gradually transitioning to finer grid resolution in the smaller channels of the Sacramento-San Joaquin Delta. This approach takes advantage of the full flexibility of unstructured grids, and offers significant advantages both in terms of numerical efficiency and accuracy.

The model was calibrated using water level and flow data collected in San Francisco Bay and the Sacramento-San Joaquin Delta. Predicted water levels were compared to observed water levels at NOAA stations in San Francisco Bay and DWR and USGS flow and stage monitoring stations in the Sacramento-San Joaquin Delta. The water level and flow calibration for the 2007 simulation period demonstrates that the UnTRIM model is accurately predicting water levels throughout San Francisco Bay, and water levels and tidal and net flows in the Sacramento-San Joaquin Delta. Accurate prediction of water levels in San Francisco Bay demonstrate that tides are accurately propagating from the Pacific Ocean, through the Bay and into the Delta. Comparison of predicted flows to observations in the Delta demonstrate the degree that the model captures the instantaneous, tidally-averaged, and net flows in specific channels within the Delta.

Model validation was conducted for two separate simulation periods in 2002 and 1999. For each of these periods, predicted water levels were compared to observed water levels at NOAA stations in San Francisco Bay and at DWR and USGS stage and flow monitoring stations in the Sacramento-San Joaquin Delta.

The results from the 3-D UnTRIM model of the San Francisco Bay-Delta are being used with a Particle Tracking Model (PTM) developed by Dr. Edward Gross. The results of the particle tracking applications will be presented in a separate report.

Acknowledgments

The authors would like to acknowledge Ted Sommer (DWR) for providing project funding and management through the Pelagic Organism Decline (POD) program. Calibration data were provided by Nick Leach (USGS) and Cathy Ruhl (USGS). Megan Bela assisted in collecting and compiling bathymetric and calibration data. Additional data and information was provided by Tara Smith (DWR), Shawn Mayr (DWR), and Siqing Liu (DWR). The UnTRIM code was developed provided by Professor Vincenzo Casulli (University of Trento, Italy). The authors would especially like to thank Richard Rachiele (RMA) and John DeGeorge (RMA) for sharing their vast experience and knowledge of modeling the Sacramento-San Joaquin Delta and providing guidance on the application of UnTRIM to the Bay-Delta. Additional technical input and expertise was provided by Jon Burau (USGS), Pete Smith (USGS, retired), and Ralph Cheng (USGS, retired).

References

Casulli, V. 1990. Semi-implicit finite difference methods for the two-dimensional shallow water equations. Journal of Computational Physics. 86, 56-74.

Casulli, V. and R. T. Cheng, 1992, Semi-implicit finite difference methods for three-dimensional shallow water flow, Inter. J. for Numer. Methods in Fluids, Vol. 15, p. 629-648.

Casulli, V., and Cattani, E. 1994. Stability, accuracy and efficiency of a semi-implicit method for three-dimensional shallow water flow. Computers and Mathematics with Applications, 27(4), 99-112.

Casulli, V., 1999. A semi-implicit numerical method for non-hydrostatic free-surface flows on unstructured grid, in Numerical Modelling of Hydrodynamic Systems, ESF Workshop, pp. 175-193, Zaragoza, Spain.

Casulli, V. and R.A. Walters, 2000. An unstructured, three-dimensional model based on the shallow water equations, International Journal for Numerical Methods in Fluids 2000, 32: 331 - 348.

Casulli, V. and Zanolli, P., 2002. Semi-Implicit Numerical Modelling of Non-Hydrostatic Free-Surface Flows for Environmental Problems, Mathematical and Computer Modelling, 36: 1131 - 1149.

Casulli, V. and Zanolli, P., 2005. High Resolution Methods for Multidimensional Advection-Diffusion Problems in Free-Surface Hydrodynamics, Ocean Modelling, 2005, v. 10, 1-2, p. 137-151.

Casulli, V., 2008. A high-resolution wetting and drying algorithm for free-surface hydrodynamics, International Journal for Numerical Methods in Fluids, DOI: 10.1002/fld.1896

[CDWR] California Department of Water Resources, 1986. DAYFLOW program documentation and data summary user's guide. California Department of Water Resources, Sacramento.

Cheng, R.T. and Gartner, J.W., 1984, Tides tidal and residual currents in San Francisco Bay, California, results of measurements, 1979-1980. Part IV. Results of measurements in Central Bay Region U. S. Geological Survey, Water-Resources Investigations, Report 84-4339, 398 pp.

Cheng, R.T. and Gartner, J.W., 1985, Harmonic analysis of tides and tidal currents in South San Francisco Bay, California Estuarine, Coastal, and Shelf Science, Vol.21, p.57-74.

Cheng, R.T., Casulli, V., and Gartner, J.W., 1993. Tidal residual intertidal mudflat (TRIM) model and its applications to San Francisco Bay, California. Estuarine, Coastal and Shelf Science, 369, 235-280.

Cheng, R. T. and V. Casulli, 1996. Modeling the Periodic Stratification and Gravitational Circulation in San Francisco Bay, in Proceedings of 4th Inter. Conf. on Estuarine and Coastal Modeling, Spaulding and Cheng (Eds.), ASCE, San Diego, CA, October 1995, p.240-254.

Cheng, R T. and R. E. Smith, 1998, A Nowcast Model for Tides and Tidal Currents in San Francisco Bay, California, Ocean Community Conf. '98, Marine Technology Society, Baltimore, Nov. 15-19, p. 537-543.

Cheng, R. T., and V. Casulli, 2002. Evaluation of the UnTRIM model for 3-D Tidal Circulation, Proceedings of the 7th International Conference on Estuarine and Coastal Modeling, St. Petersburg, FL, November 2001, 628-642.

CSUMB, 2007. California State University Monterey Bay, Seafloor Mapping Lab, Data Library. http://seafloor.csumb.edu/SFMLwebDATA_c.htm

Deleersnijder, E., Beckers, J.M., Campin, J.M., El Mohajir, M., Fichefet, T., and Luyten, P., 1997. Some mathematical problems associated with the development and use of marine models." The Mathematics of Models for Climatology and Environment, Vol. 148., J.I. Diaz, ed., Springer Verlag, Berlin, Heidelberg.

Department of Water Resources, 2003. South Delta Temporary Barriers Project, 2002 South Delta Temporary Barriers Monitoring Report, 204 pp, December 2003.

Department of Water Resources, 2008a. Delta Simulation Model II Documentation, http://modeling.water.ca.gov/delta/models/dsm2/documentation.shtml

Department of Water Resources, 2008b. Historical Geometry Library for WY1987-2008, http://www.iep.water.ca.gov/dsm2pwt/Bay-Delta_barriers_activ.txt

Department of Water Resources Temporary Barrier Project (DWR TBP), 2008. Temporary Barriers Project, http://baydeltaoffice.water.ca.gov/sdb/tbp/web_pg/tempbar.cfm

Dever, E.P., and Lentz, S.J., 1994. Heat and salt balances over the northern California shelf in winter and spring, Journal of Geophysical Research, 99(C8), 16,001-16,017.

Edmunds, J.L., Cole, B.E., Cloern, J.E., Caffrey, J.M., and Jassby, A.D., 1995. Studies of the San Francisco Bay, California, Estuarine Ecosystem. Pilot Regional Monitoring Program Results, 1994: U.S. Geological Survey Open-File Report 95-378, 436p.

Gardner, J.V., Mayer, M.A., and Hughes-Clarke, J., Cruise Report RV Inland Surveyor Cruise IS-98, The Bathymetry of Lake Tahoe, California-Nevada, U.S.G.S. Open-File Report 98-509, 22 pp.

Gross, E.S., Koseff, J.R., and Monismith, S.G., 1999. Three-dimensional salinity simulations of South San Francisco Bay. Journal of Hydraulic Engineering 125 (11), 1199-1209.

Gross, E.S., Schaaf & Wheeler. 2003. South Bay Salt Ponds Initial Stewardship Plan: South San Francisco Bay Hydrodynamic Model Results Report. Prepared for Cargill Salt.

Gross, E.S., M. L. MacWilliams and W. Kimmerer, 2006. Simulating Periodic Stratification in San Francisco Bay, Proceedings of the Estuarine and Coastal Modeling Conference, ASCE.

Harrison, C., 2002. Suisun Marsh Structures Description for updating RMA model, http://iep.water.ca.gov/pub/to_stacie/marsh_structures_for_RMA.doc

Hills, E., 1998. New Flow Equations for Clifton Court Gates, DWR Memo, May 9, 1998.

Huzzey, L.M., Cloern, J.E., and Powell, T.M., 1990. Episodic changes in lateral transport and phytoplankton distribution in South San Francisco Bay: Limnology and Oceanography, 35: 472-478.

Interagency Ecological Program (IEP), 2008. DSS database, http://iep.water.ca.gov/data.html

Interagency Ecological Program (IEP), 2008a. Suisun Marsh Physical Facilities http://www.iep.ca.gov/suisun/facts/physicalFacilities.html

Interagency Ecological Program (IEP), 2008b. Historical SMSCC Schedule for Years 1988-2007, http://iep.water.ca.gov/suisun/dataReports/histsmscgop.pdf

Kantha, L.H., Clayson, C.A., 1994. An improved mixed layer model for geophysical applications, Journal of Geophysical Research, 99, 25235–25266.

Large, W., and Pond, S., 1981. Open ocean momentum flux measurements in moderate to strong winds. *Journal of Physical Oceanography*, 11, 324-336.

Lippert, C. and Sellerhoff, F., 2007. Efficient Generation of Unstructured Orthogonal Grids, The 7th Int. Conf. on Hydroscience and Engineering (ICHE-2006), Sep. 10 – Sep. 13, Philadelphia, USA.

Lower Yolo Bypass Planning Forum, 2008. Meeting #4 10-07-08 DRAFT Final Meeting Summary, http://www.yolobypass.net/

MacWilliams, M.L., and Cheng, R.T., 2007. Three-dimensional hydrodynamic modeling of San Pablo Bay on an unstructured grid, The 7th Int. Conf. on Hydroscience and Engineering (ICHE-2006), Sep. 10 – Sep. 13, Philadelphia, USA.

MacWilliams, M.L., and E.S. Gross, 2007. UnTRIM San Francisco Bay-Delta Model Calibration Report, Delta Risk Management Study, prepared for CA Department of Water Resources, March 2007.

MacWilliams, M.L., E.S. Gross, J.F. DeGeorge, and R.R. Rachiele, 2007. Three-dimensional hydrodynamic modeling of the San Francisco Estuary on an unstructured grid, IAHR, 32nd Congress, Venice Italy, July 1-6, 2007.

Resources Agency, 2007. Pelagic Fish Action Plan, March 2007, prepared by Resources Agency, California Department of Water Resources, California Department of Fish and Game.

[RMA] Resource Management Associates, 2005. Flooded Islands Pre-Feasibility Study: RMA Delta Model Calibration Report, prepared for CA Department of Water Resources for submittal to California Bay-Delta Authority, June 30.

Smith, R.E., Foxgrover, A., and P.E. Smith, 2003. Suisun Bay & Delta Bathymetry: Production of a 10-meter Grid, http://sfbay.wr.usgs.gov/access/Bathy/Delta, Second Biennial CALFED Science Conference: Advances in Science and Restoration in the Bay, Delta and Watershed, Sacramento, California, January 14-16, 2003.

Stacey, M.T., 1996. Turbulent mixing and residual circulation in a partially stratified estuary. Ph.D. thesis, Dept of Civil Engineering, Stanford University, 209 pp.

Suits, B. and J. Wilde, 2004. Methodology for Flow and Salinity Estimates in the Sacramento-San Joaquin Delta and Suisun Marsh, 25th Annual Progress Report , October 2004, Chapter 3: DSM2 Geometry Investigations, http://modeling.water.ca.gov/delta/reports/annrpt/2004/2004Ch3.pdf

Umlauf, L., Burchard, H., 2003. A generic length-scale equation for geophysical turbulence models. *Journal of Marine Research*, 61, 235–265.

USACE, 2008. TEC - Survey Engineering and Mapping Center of Expertise, Corpscon Version 6.0, http://crunch.tec.army.mil/software/corpscon/corpscon.html

USBR, 2008. United States Bureau of Reclamation, Cross Channel Gate Operations Historical Log, http://www.usbr.gov/mp/cvo/vungvari/Ccgates.pdf

USGS, 2007, San Francisco Bay Bathymetry, http://wrgis.wr.usgs.gov/dds/dds55/pacmaps/sf_index.htm

USGS, 2008, USGS Water Quality of SF Bay, http://sfbay.wr.usgs.gov/access/wqdata

Warner J.C., Sherwood C.S., Arango H.G., Signell R.P., 2005. Performance of four turbulence closure models implemented using a generic length scale method. Ocean Modeling 8:81-113.

Appendix A. Model Validation Figures for 1999 Simulation Period

This Appendix provides a full set of water level and flow comparison figures for the 1999 simulation period. This simulation period was selected to provide hydrodynamic output for use with the Particle Tracking Model (PTM) for comparison to observed delta smelt distributions in spring and early summer of 1999. A description of the simulation period is given in Section A.1. Water level validation figures are shown in Section A.2. Comparisons between observed and predicted flows in the Delta are shown in Section A.3.

A.1 Description of 1999 Simulation Period

The 1999 simulation period spans from April 13, 1999 through August 1, 1999. This period was simulated in order to provide hydrodynamic model output for use with the Particle Tracking Model (PTM). Figure A.1-1 shows the historical barrier operations schedule during the 1999 simulation period. During periods when the barriers are closed, no flow is allowed through the barrier. When the barrier is open, no barrier controls are specified and the channel operates normally. During periods when the barrier is operational, the weir and culvert configurations are implemented as discussed in Section 3.12 and described in the historical operations log (DWR, 2008b). Delta operations during the 1999 period differ from the other two periods simulated, primarily in that the spring Head of Old River Barrier was not installed during 1999 due to high flows on the San Joaquin River.

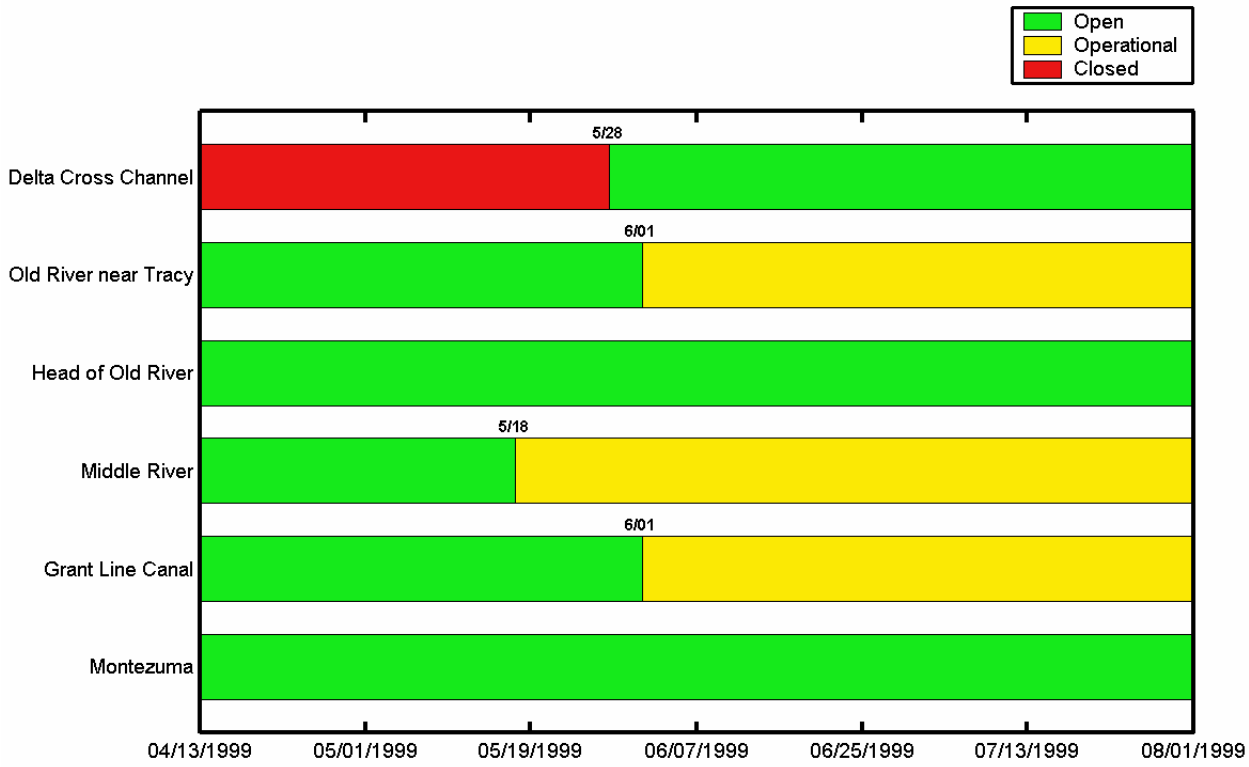

Figure A.1-1 Historical barrier operations schedule during the 1999 simulation period.

A.2 Water Level Comparison Figures

Observed and predicted water levels were compared at five NOAA stations in San Francisco Bay and at twenty-eight stations in the Sacramento-San Joaquin Delta during the 1999 simulation period. At each station, observed and predicted water levels were plotted over a fifteen day period to show the water level agreement over tidal time scales. In addition, the observed and predicted stage are tidally-averaged, to assess the accuracy of the model in predicting water level variability on spring-neap time scales, as well as non-tidal forcing such as storms. Lastly, the cross-correlation (as described in Section 4.1) was used to determine the mean observed and predicted water level, the amplitude ratio, the phase lag, and the correlation coefficient squared (R^2). For each of the water level stations, these values are compiled in Table A-1.

A.2.1 San Francisco Bay

Water level comparisons were made at five NOAA continuous observation stations in the San Francisco Estuary, at the locations shown in Figure A.2-1. Water level comparisons at these stations are shown in Figures A.2-2 through A.2-6.

A.2.2 Northern Sacramento-San Joaquin Delta

Water level comparisons were made at four continuous water level observation stations in the northern portion of the Sacramento-San Joaquin Delta, at the locations shown in Figure A.2-7. Water level comparisons at these stations are shown in Figures A.2-8 through A.2-11.

A.2.3 Central Sacramento-San Joaquin Delta

Water level comparisons were made at ten continuous water level observation stations in the central portion of the Sacramento-San Joaquin Delta, at the locations shown in Figure A.2-12. Water level comparisons at these stations are shown in Figures A.2-13 through A.2-22.

A.2.4 Southern Sacramento-San Joaquin Delta

Water level comparisons were made at fourteen continuous water level observation stations in the southern portion of the Sacramento-San Joaquin Delta, at the locations shown in Figure A.2-23. Water level comparisons at these stations are shown in Figures A.2-24 through A.2-37.

Table A-1 Predicted and observed stage and cross-correlation statistics for stage monitoring stations in San Francisco Bay and the Sacramento-San Joaquin Delta during the 1999 simulation period.

Location	Data Source	Figure Number	Mean Water Level		Cross Correlation		R^2
			Observed (m)	Predicted (m)	Amp Ratio	Lag (min)	
1999 San Francisco Bay Stage Stations (Figure A.2-1)							
San Francisco	NOAA	A.2-2	0.08	0.08	0.996	0	0.999
Alameda	NOAA	A.2-3	0.10	0.12	1.009	9	0.998
Redwood City	NOAA	A.2-4	0.11	0.14	0.987	4	0.998
Richmond	NOAA	A.2-5	0.13	0.12	0.997	0	0.998
Port Chicago	NOAA	A.2-6	0.34	0.311	0.882	7	0.996
1999 North Delta Stage Stations (Figure A.2-7)							
Sacramento River South of Georgiana Slough	USGS	A.2-8	0.65	0.63	0.971	7	0.987
Sacramento River North of Delta Cross Channel	USGS	A.2-9	0.70	0.64	0.983	17	0.985
Mokelumne River near Thornton	DWR	A.2-10	0.50	0.63	0.967	-33	0.908
South Fork Mokelumne River at New Hope Bridge	DWR	A.2-11	0.53	0.50	1.013	-5	0.985
1999 Central Delta Stage Stations (Figure A.2-12)							
San Joaquin River at Antioch	DWR	A.2-13	0.34	0.36	0.843	7	0.995
Sacramento River at Rio Vista	USGS	A.2-14	0.46	0.39	0.854	21	0.994
Threemile Slough at San Joaquin River	USGS	A.2-15	0.48	0.37	0.947	5	0.994
San Joaquin River at Jersey Point	USGS	A.2-16	0.55	0.37	0.910	8	0.987
Dutch Slough at Jersey Island	USGS	A.2-17	0.40	0.37	0.922	9	0.991
San Joaquin River at San Andreas Landing	DWR	A.2-18	0.39	0.39	0.949	11	0.993
North Fork of Mokelumne River at Georgiana Slough	DWR	A.2-19	0.51	0.41	0.958	3	0.992
San Joaquin River at Venice Island	DWR	A.2-20	0.43	0.39	0.948	16	0.993
San Joaquin River at Rindge Pump	DWR	A.2-21	0.41	0.40	0.940	-50	0.993
Middle River south of Columbia Cut	USGS	A.2-22	0.29	0.39	0.956	-32	0.993
1999 South Delta Stage Stations (Figure A.2-23)							
Middle River at Middle River	USGS	A.2-24	0.30	0.38	0.962	-3	0.993
Middle River at Borden Highway	DWR	A.2-25	0.35	0.34	0.969	-3	0.986
Middle River at Tracy Blvd	DWR	A.2-26	0.39	0.39	1.005	-49	0.953
Middle River at Mowry Bridge	DWR	A.2-27	0.63	0.63	0.882	32	0.842
Old River at Bacon Island	USGS	A.2-28	0.29	0.38	0.962	3	0.992
Old River near Byron	DWR	A.2-29	0.32	0.38	0.973	-9	0.990
Old River at Clifton Court Ferry	DWR	A.2-30	0.34	0.41	1.018	-22	0.987

Grant Line Canal at Tracy Blvd	DWR	A.2-31	0.60	0.44	0.867	13	0.955
Grant Line Canal at Head	DWR	A.2-32	0.65	0.59	1.084	-26	0.937
Old River near Delta Mendota Canal (Downstream of Barrier)	DWR	A.2-33	0.22	0.29	1.000	-7	0.967
Old River near Delta Mendota Canal (Upstream of Barrier)	DWR	A.2-34	0.57	0.55	1.093	-63	0.944
Old River at Tracy Blvd	DWR	A.2-35	0.51	0.54	0.786	-6	0.891
San Joaquin River at Stockton	USGS	A.2-36	0.41	0.43	0.964	8	0.993
San Joaquin River at Mossdale	DWR	A.2-37	1.06	0.98	1.072	8	0.992

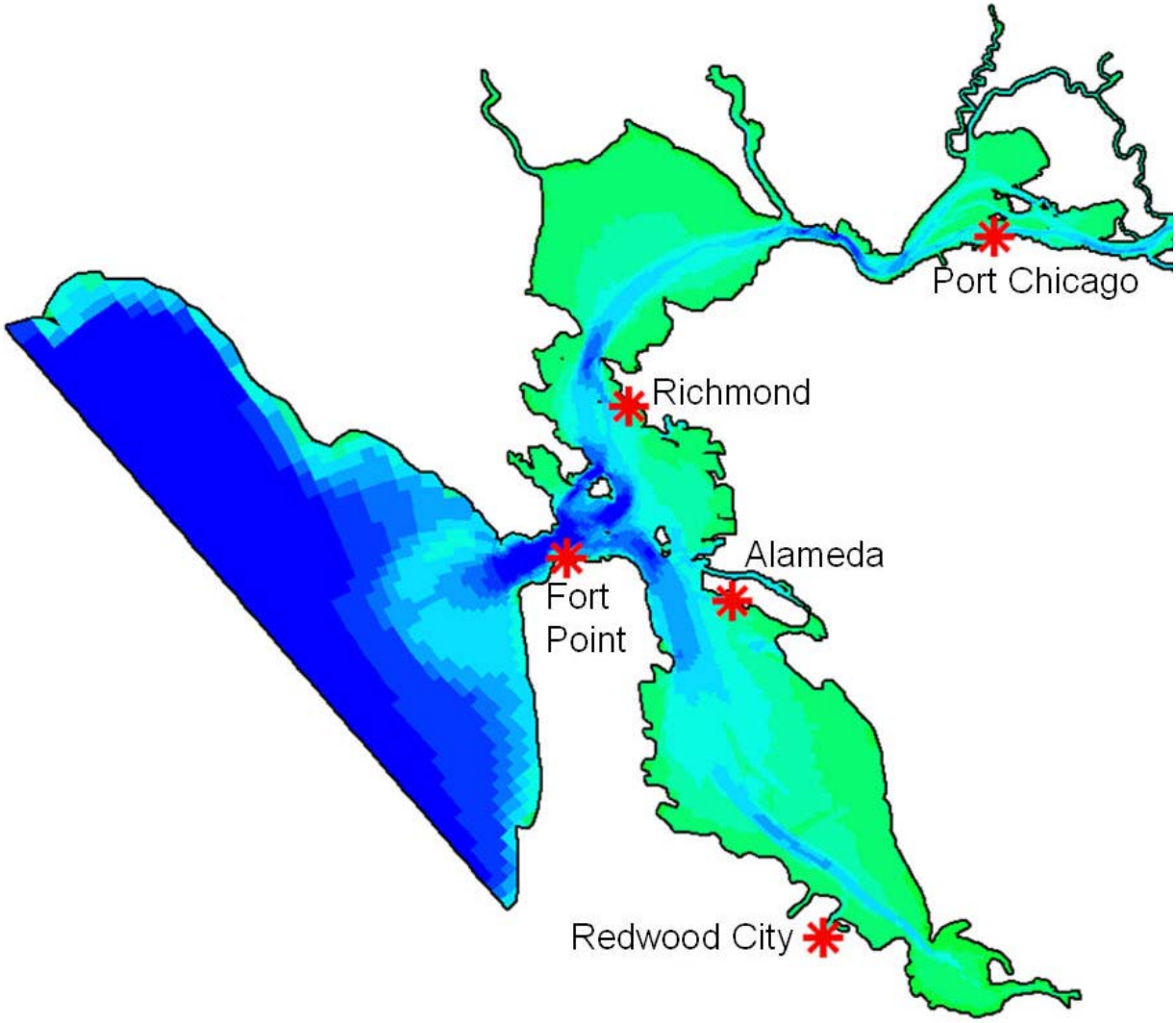

Figure A.2-1 Location of NOAA water level monitoring stations in San Francisco Bay used for 1999 stage calibration.

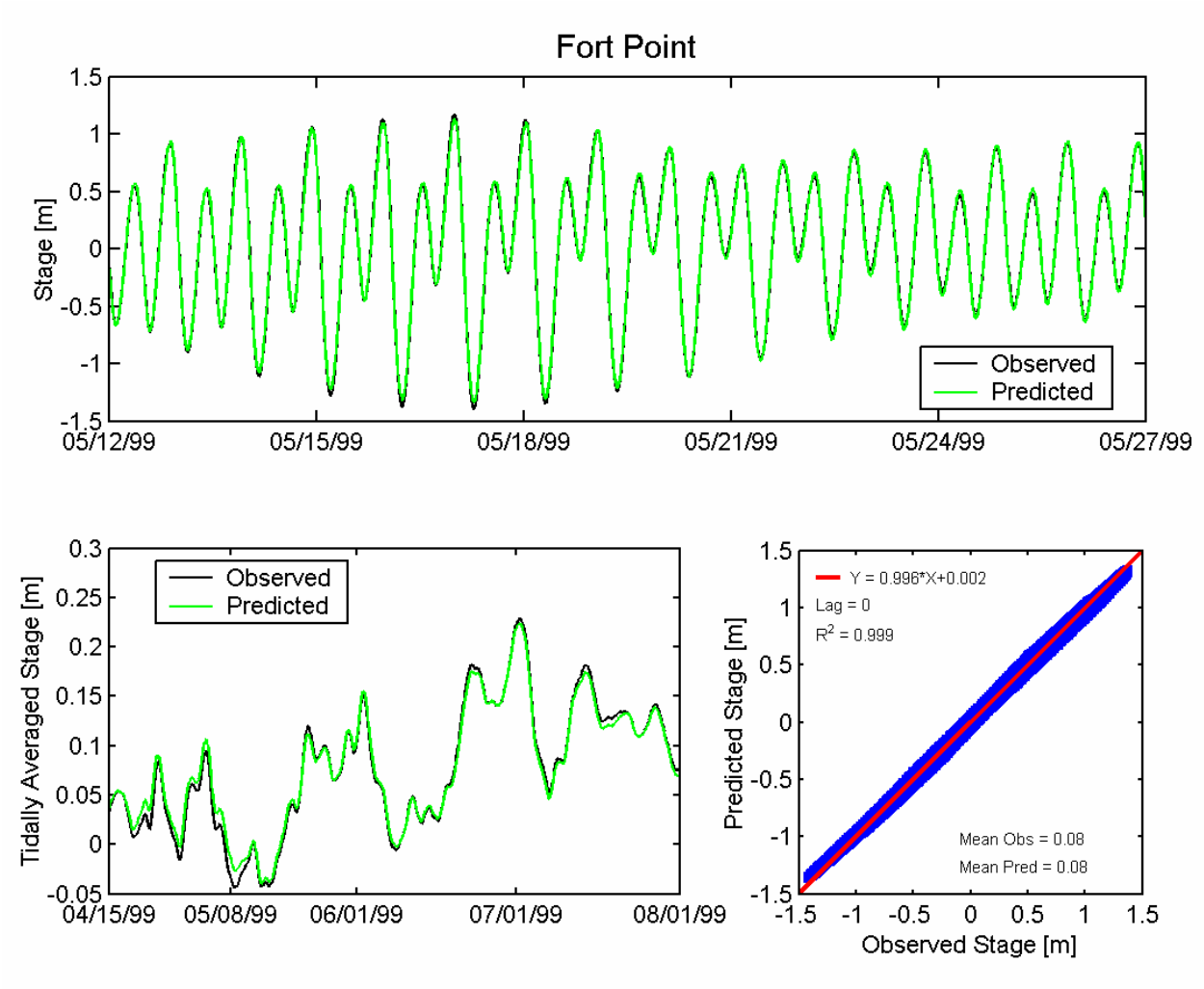

Figure A.2-2 Observed and predicted stage at San Francisco Fort Point NOAA station (9414290) during the 1999 simulation period.

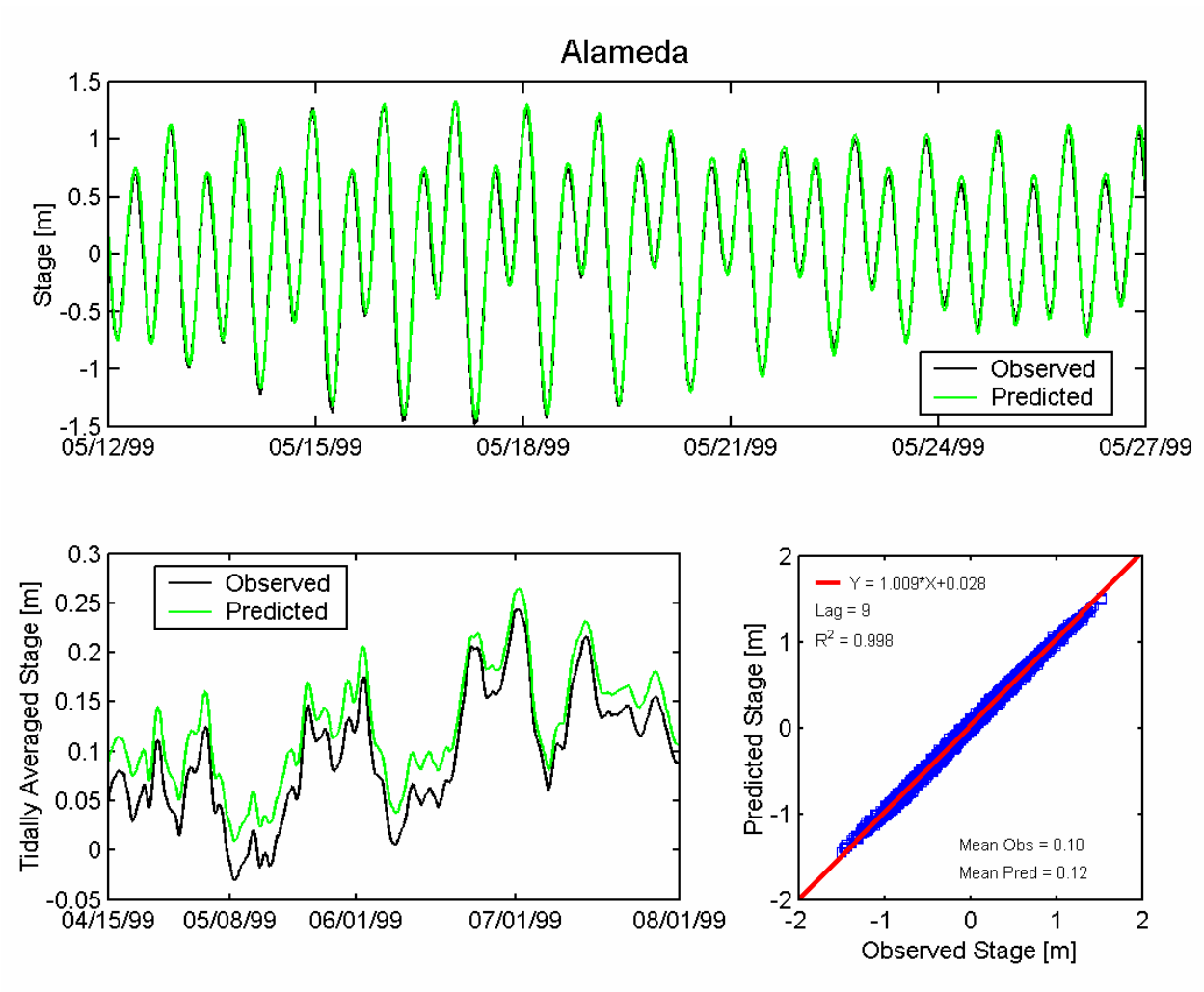

Figure A.2-3 Observed and predicted stage at Alameda NOAA station (9414750) during the 1999 simulation period.

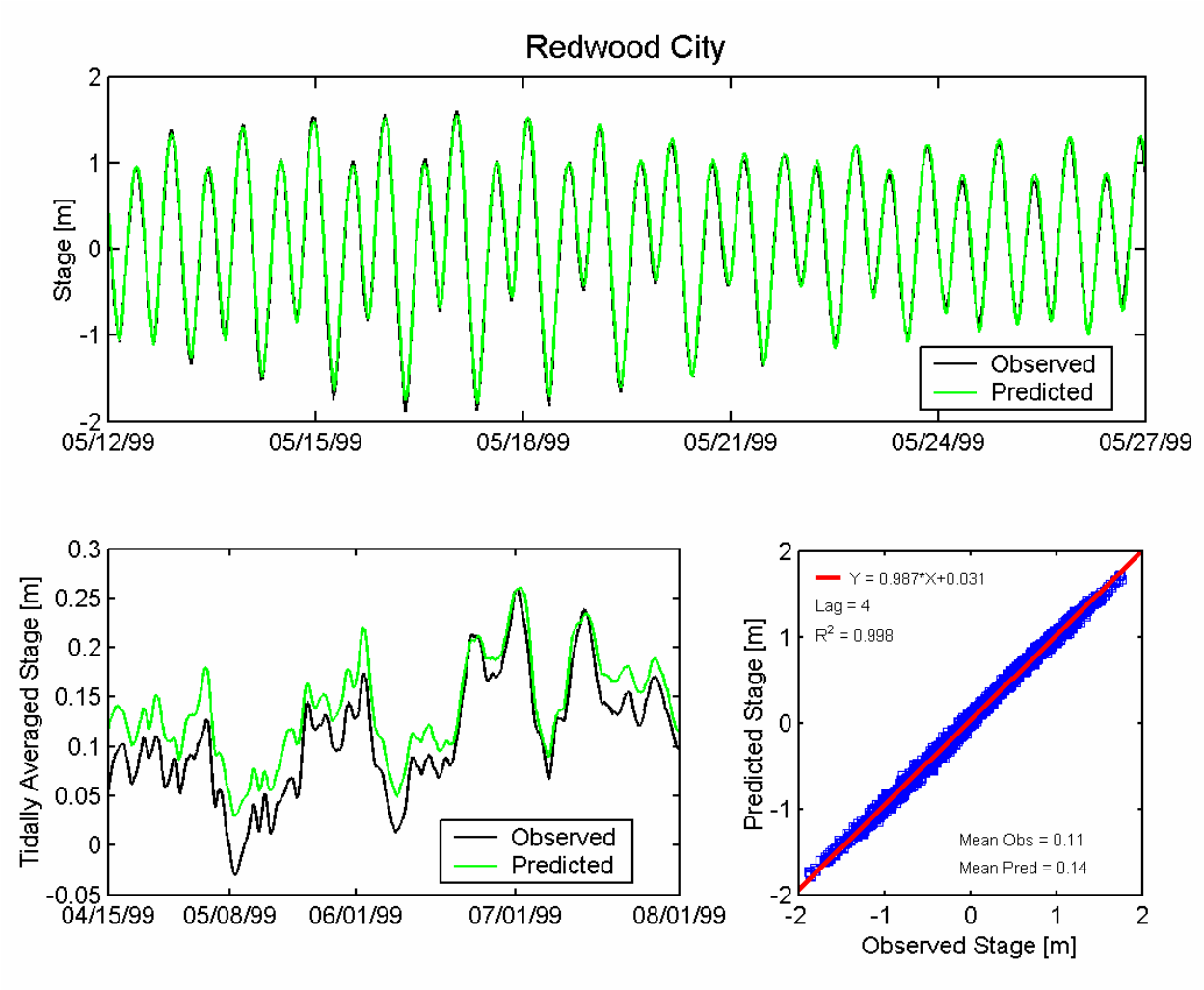

Figure A.2-4 Observed and predicted stage at Redwood City NOAA station (9414523) during the 1999 simulation period.

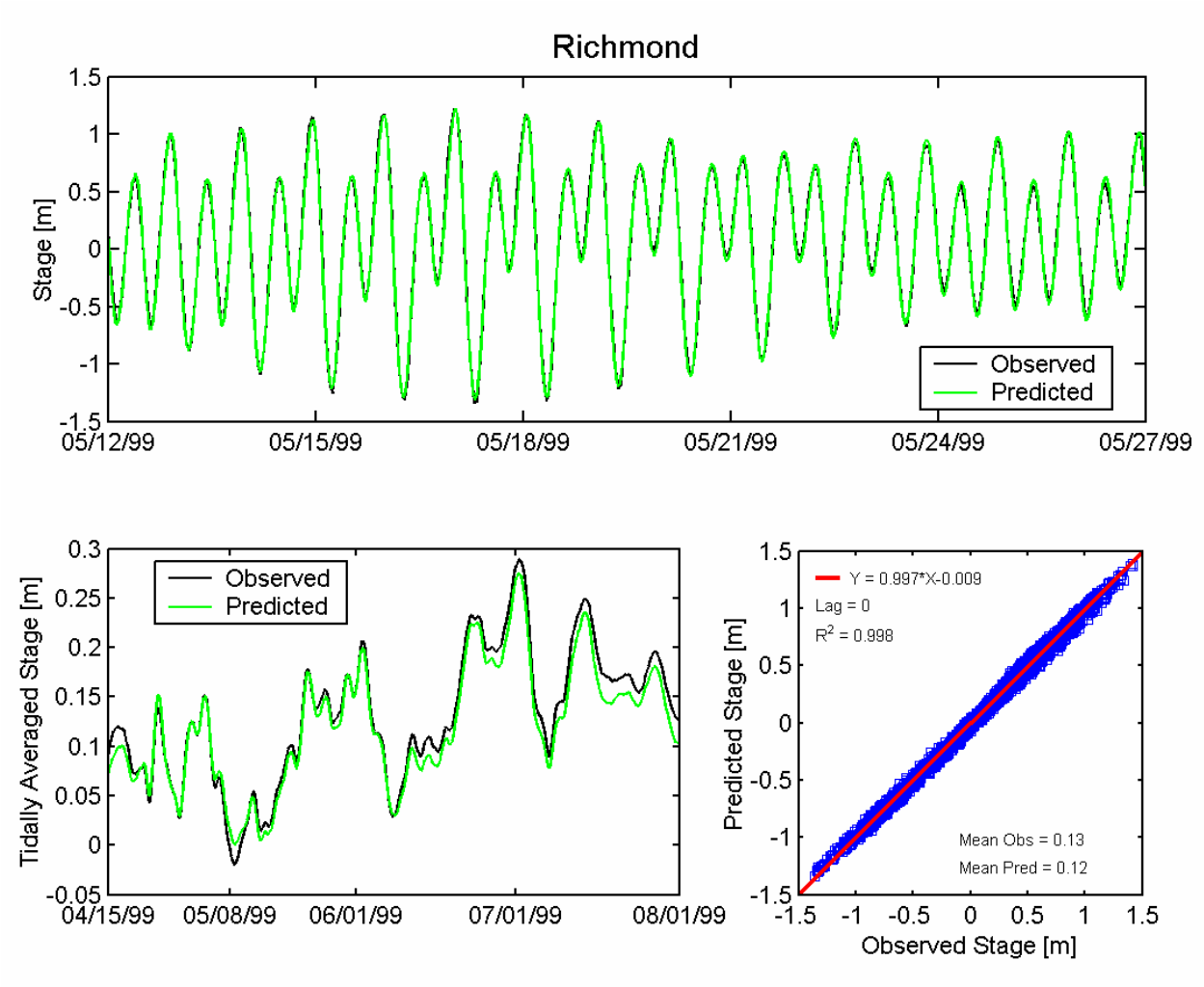

Figure A.2-5 Observed and predicted stage at Richmond NOAA station (9414863) during the 1999 simulation period.

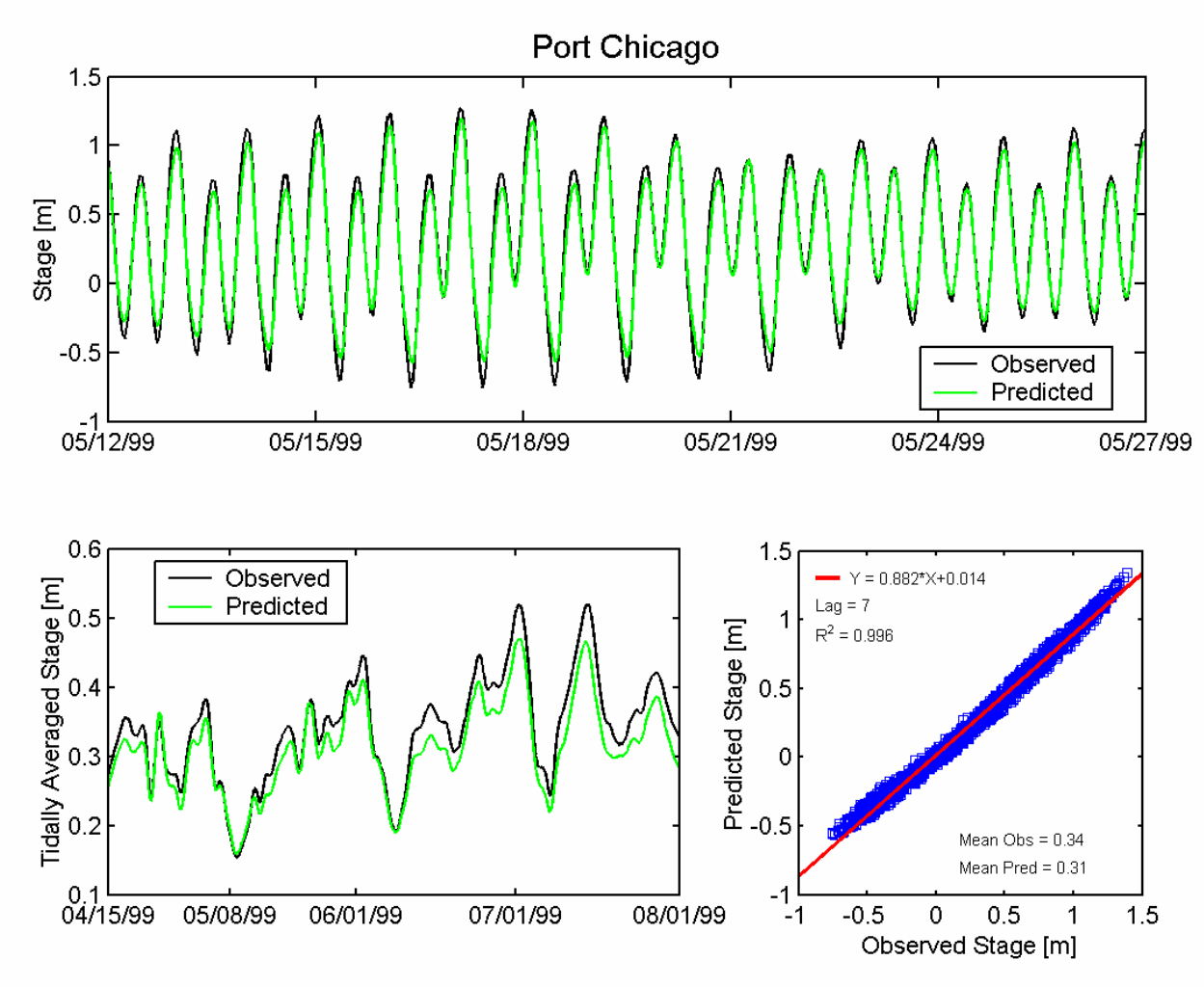

Figure A.2-6 Observed and predicted stage at Port Chicago NOAA station (9415144) during the 1999 simulation period.

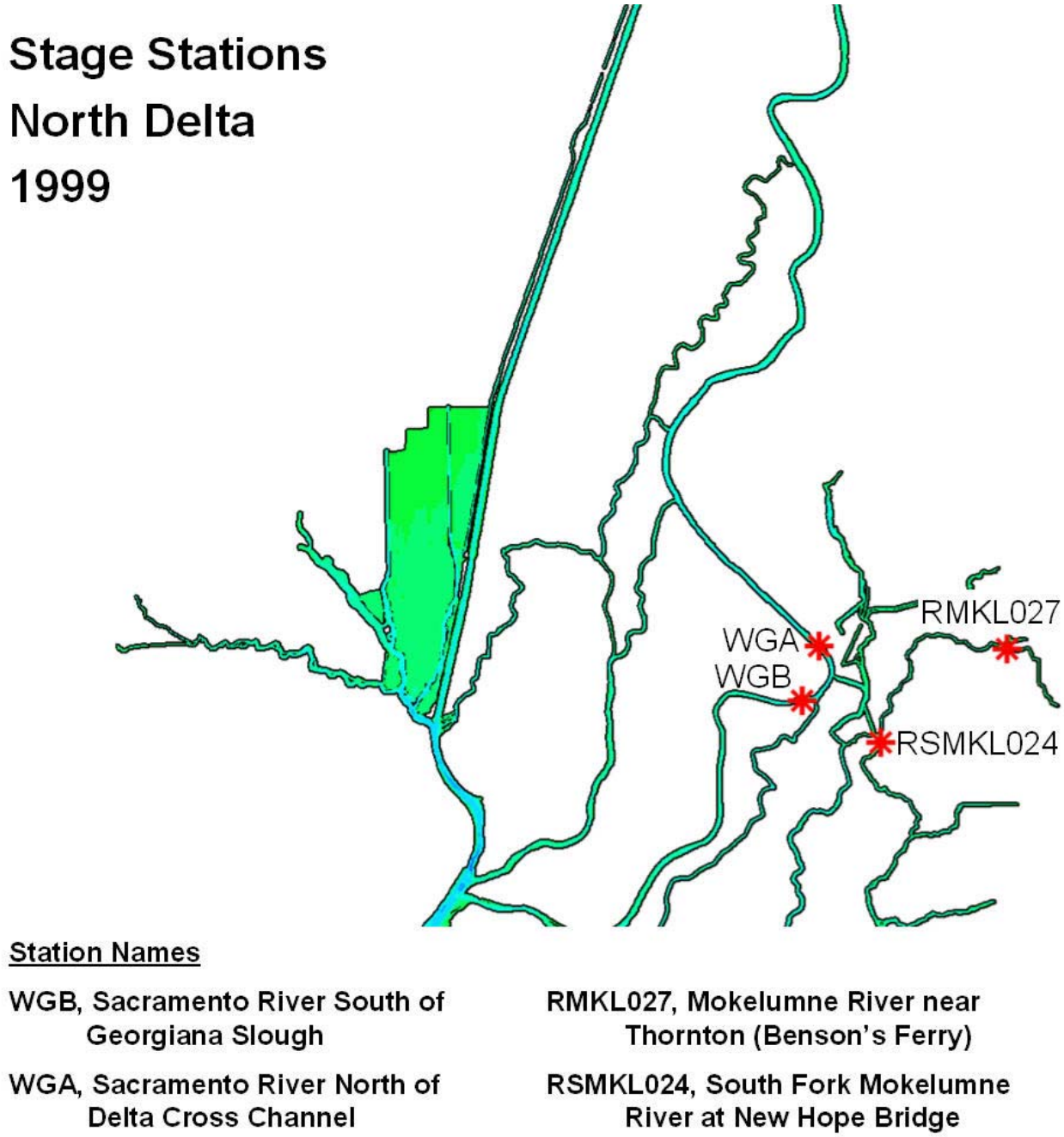

Figure A.2-7 Location of water level monitoring stations in the northern portion of the Sacramento-San Joaquin Delta used for 1999 water level calibration.

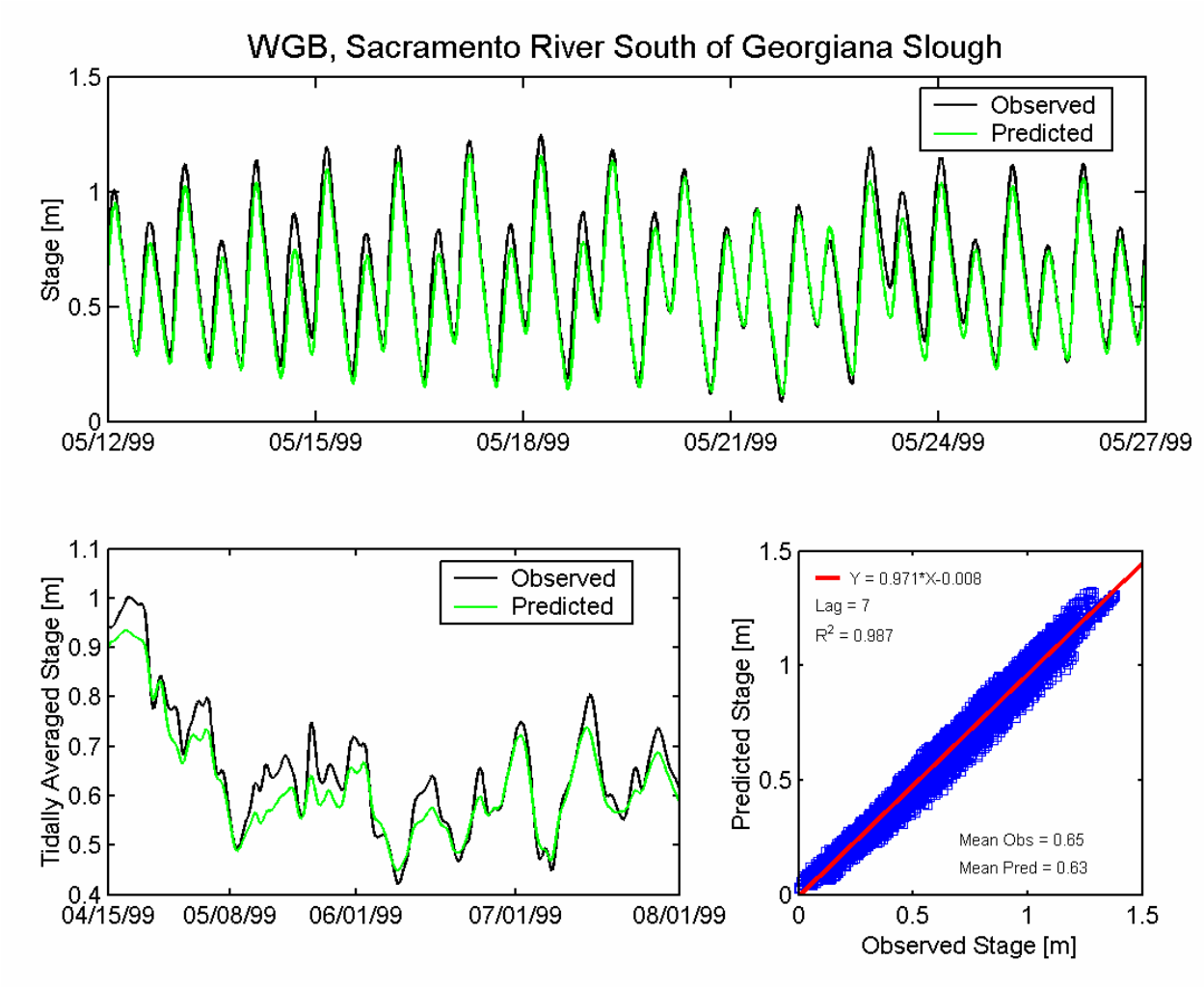

Figure A.2-8 Observed and predicted stage at Sacramento River South of Georgiana Slough USGS station (WGB) during the 1999 simulation period.

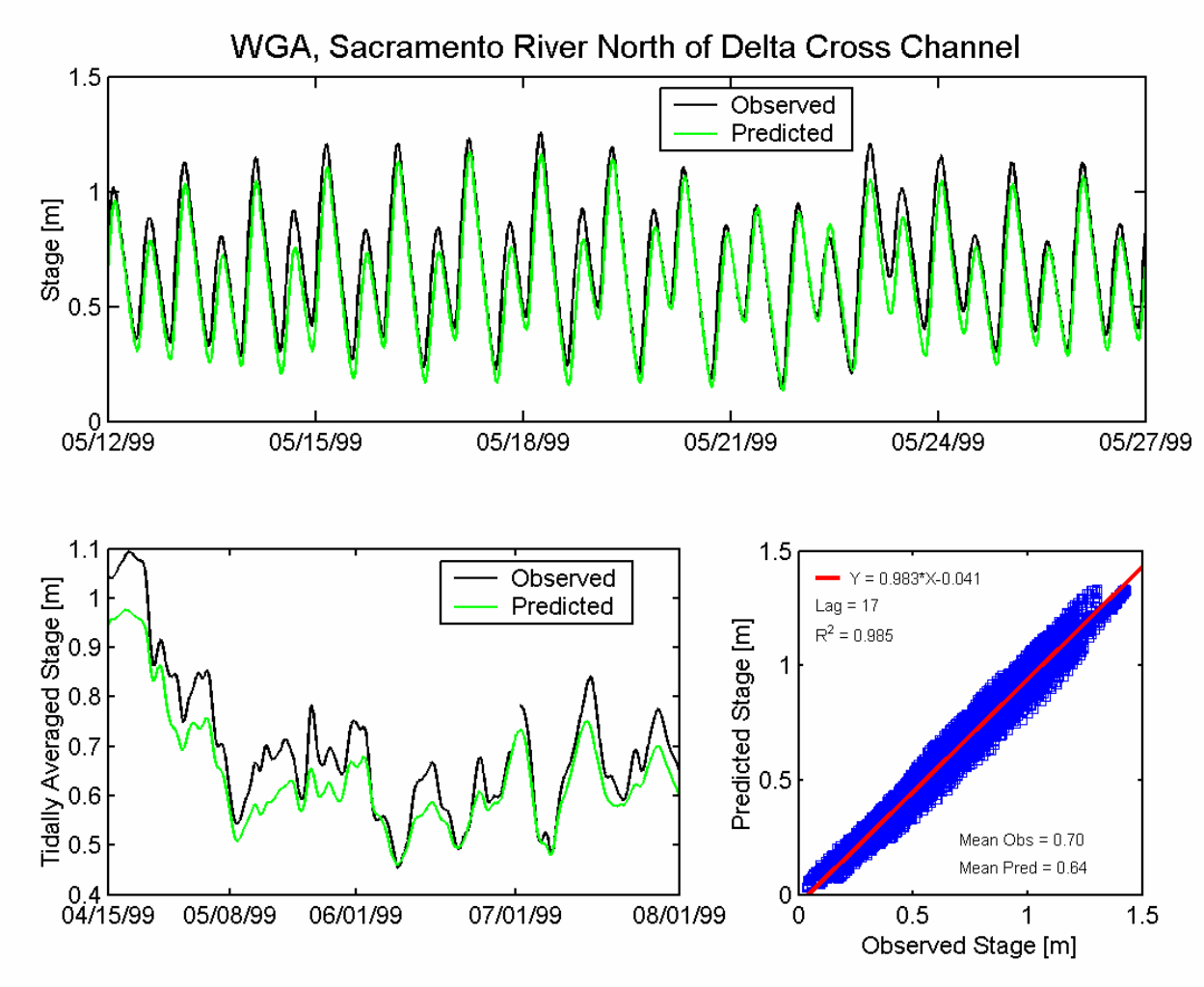

Figure A.2-9 Observed and predicted stage at Sacramento River North of Delta Cross Channel USGS station (WGA) during the 1999 simulation period.

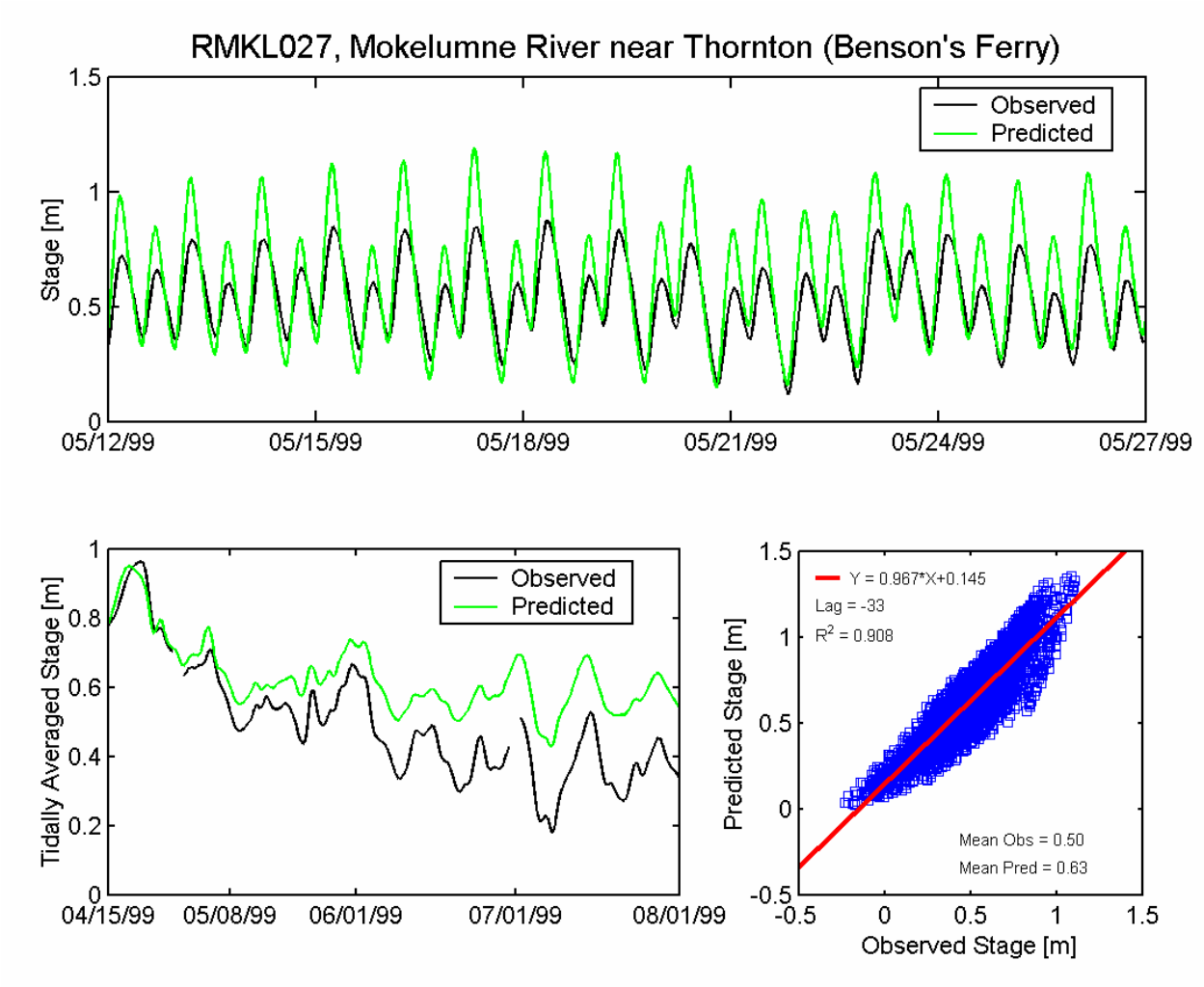

Figure A.2-10 Observed and predicted stage at Mokelumne River near Thornton (Benson's Ferry) DWR station (RMKL027) during the 1999 simulation period.

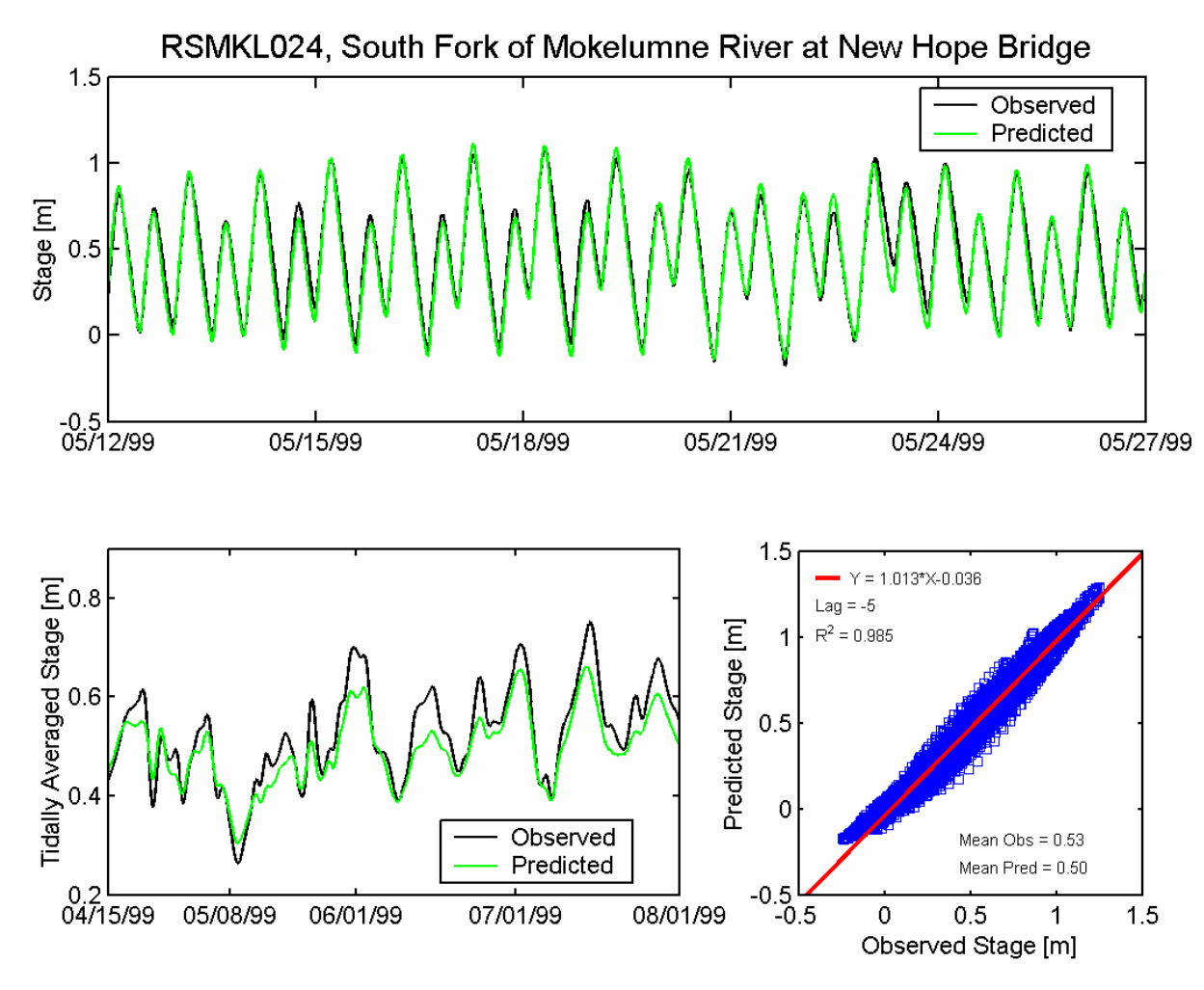

Figure A.2-11 Observed and predicted stage at South Fork Mokelumne River at New Hope Bridge DWR station (RSMKL024) during the 1999 simulation period.

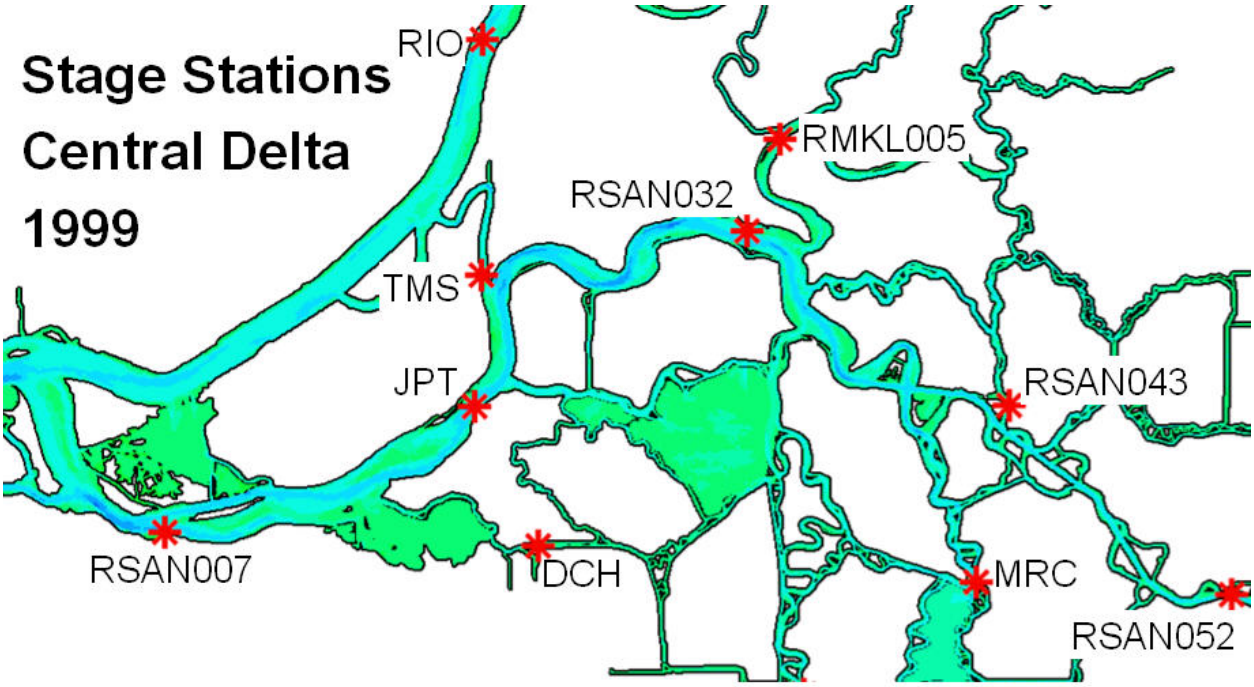

Station Names

RSAN007, San Joaquin River at Antioch

RIO, Sacramento River at Rio Vista

TMS, Threemile Slough at San Joaquin River

JPT, San Joaquin River at Jersey Point

DCH, Dutch Slough at Jersey Island

RSAN032, San Joaquin River at San Andreas Landing

RMKL005, North Fork of Mokelumne River at Georgiana Slough

RSAN043, San Joaquin River at Venice Island

RSAN052, San Joaquin River at Rindge Pump

MRC, Middle River South of Columbia Cut

Figure A.2-12 Location of water level monitoring stations in the central portion of the Sacramento-San Joaquin Delta used for 1999 water level calibration.

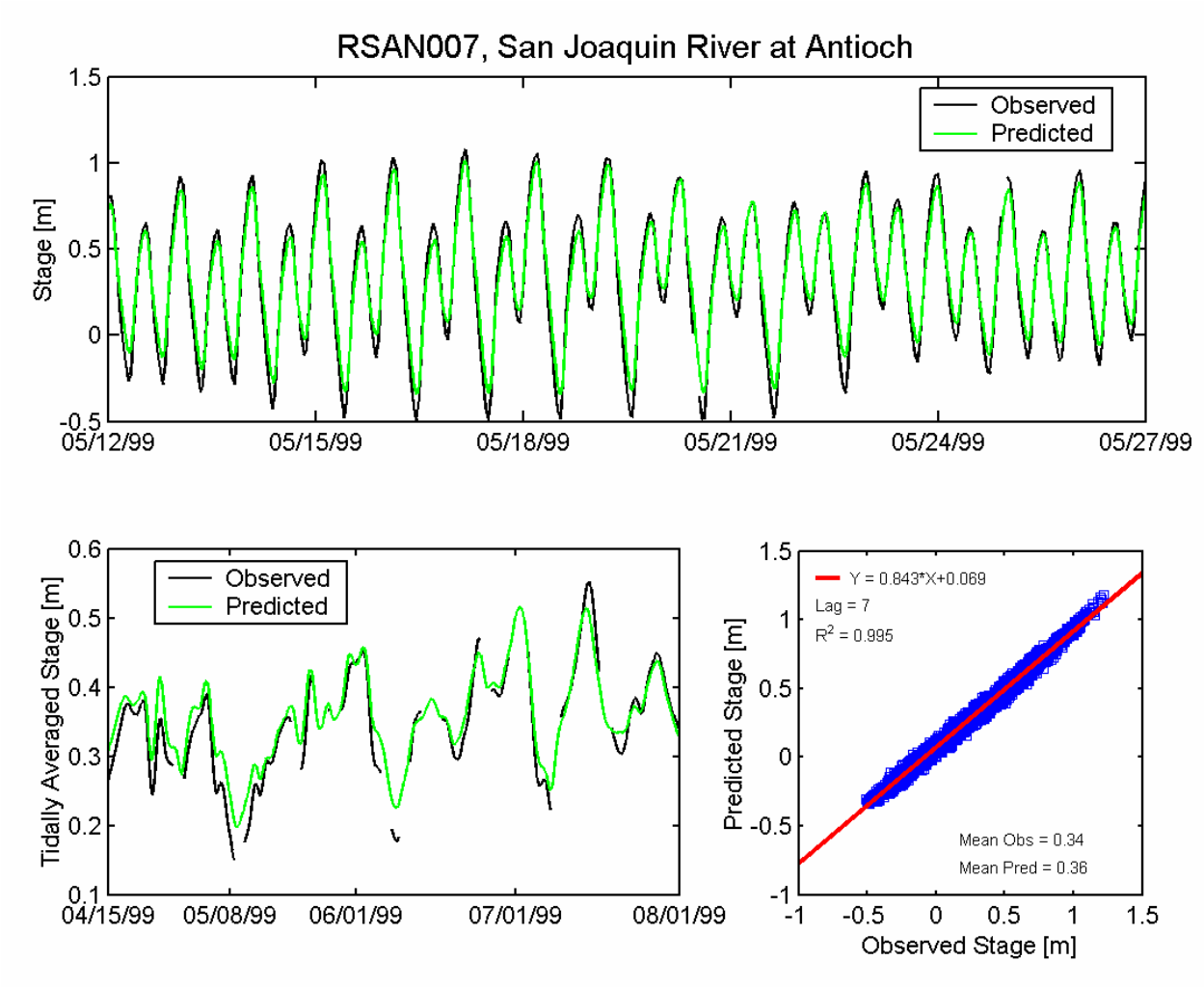

Figure A.2-13 Observed and predicted stage at Antioch DWR station (RSAN007) during the 1999 simulation period.

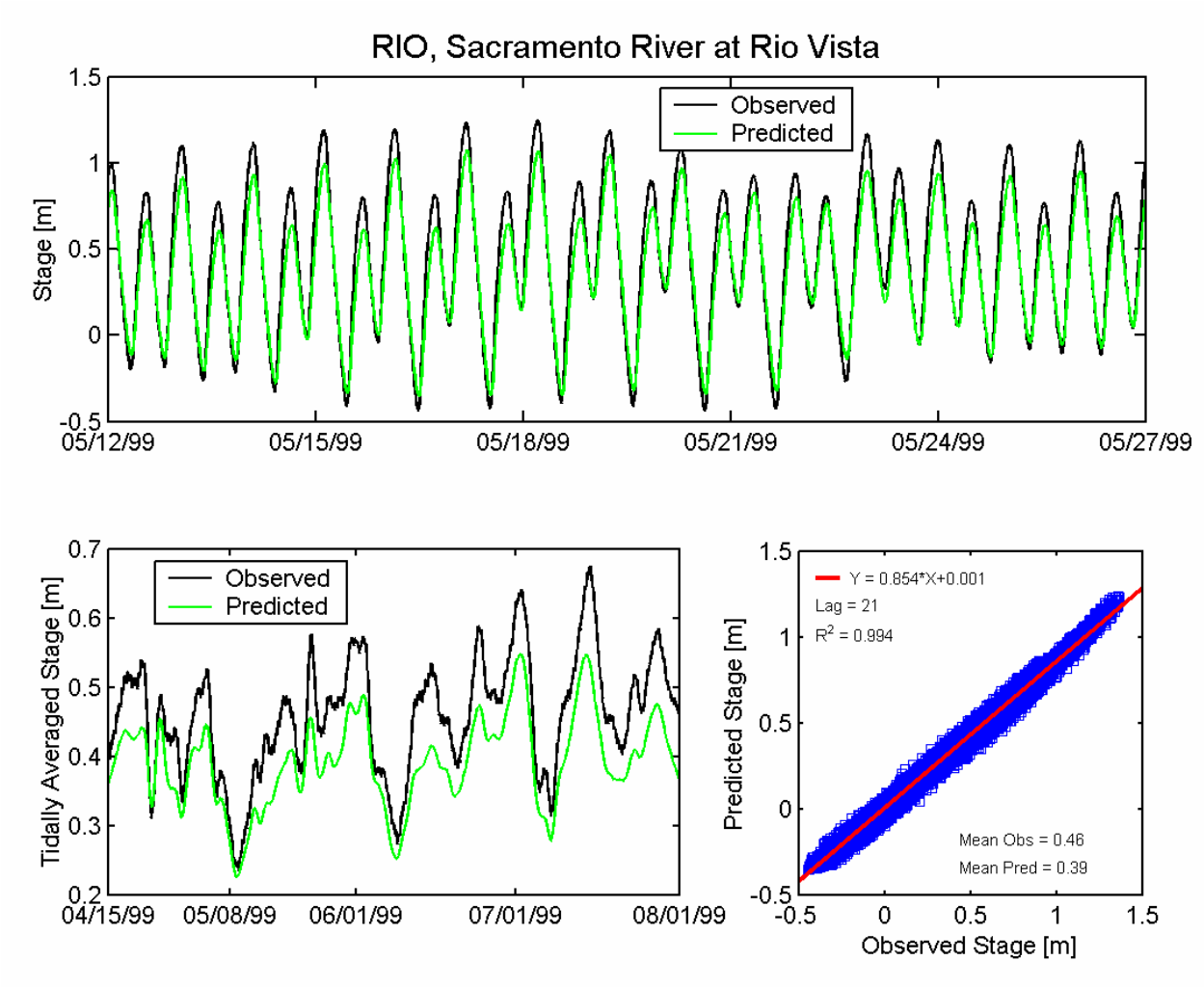

Figure A.2-14 Observed and predicted stage at Sacramento River at Rio Vista USGS station (RIO) during the 1999 simulation period.

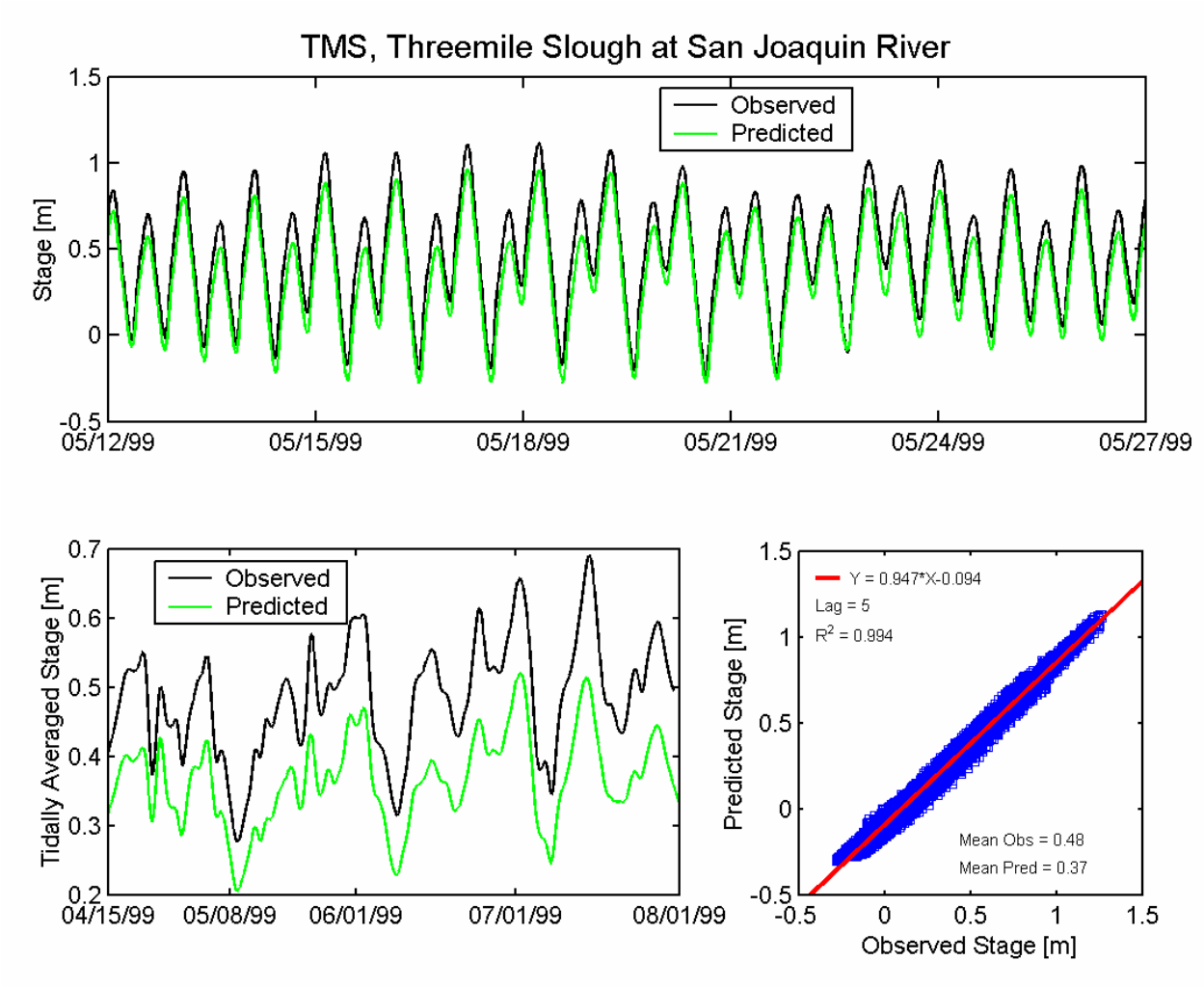

Figure A.2-15 Observed and predicted stage at Threemile Slough at San Joaquin River USGS station (TMS) during the 1999 simulation period.

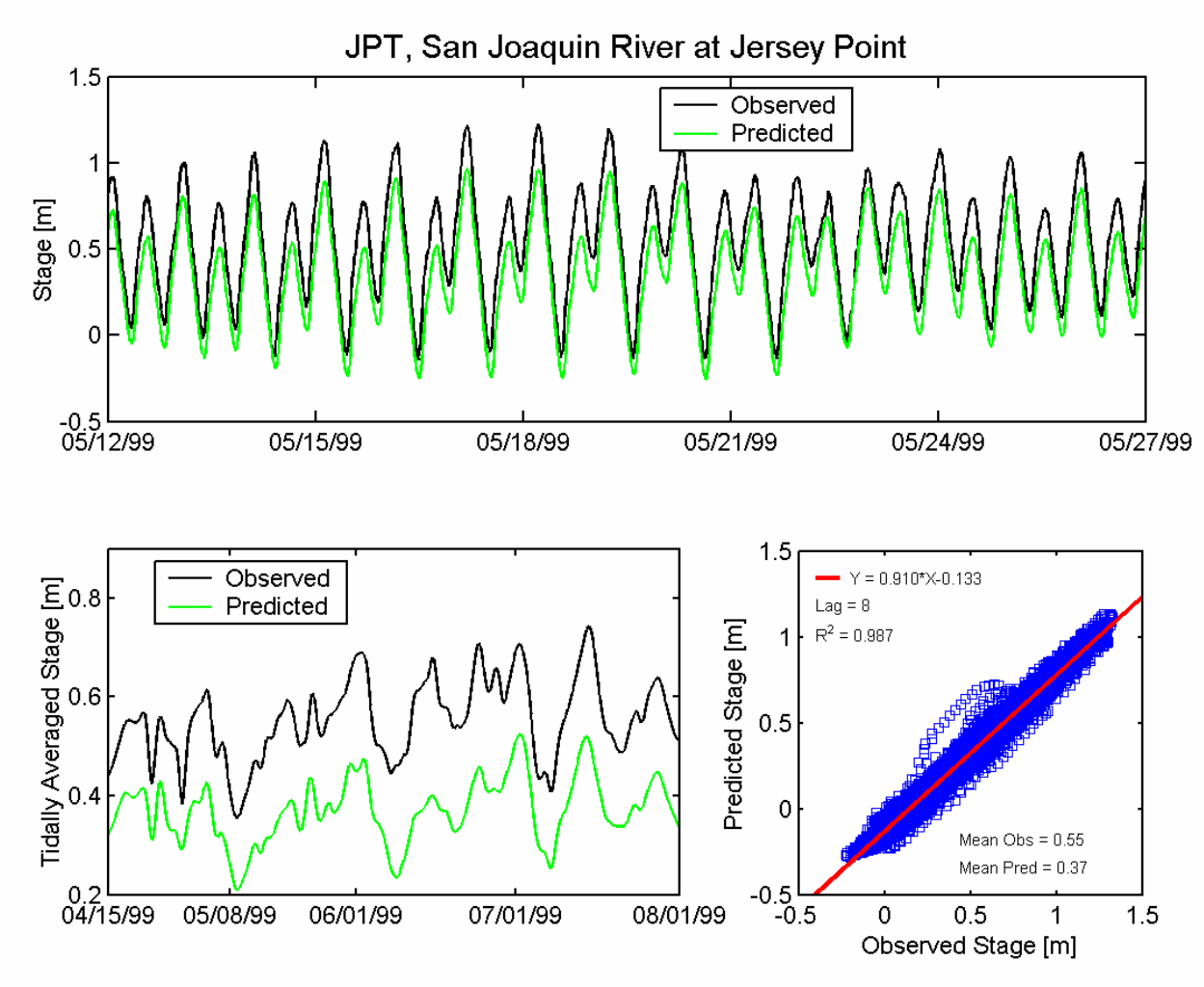

Figure A.2-16 Observed and predicted stage at San Joaquin River at Jersey Point USGS station (JPT) during the 1999 simulation period.

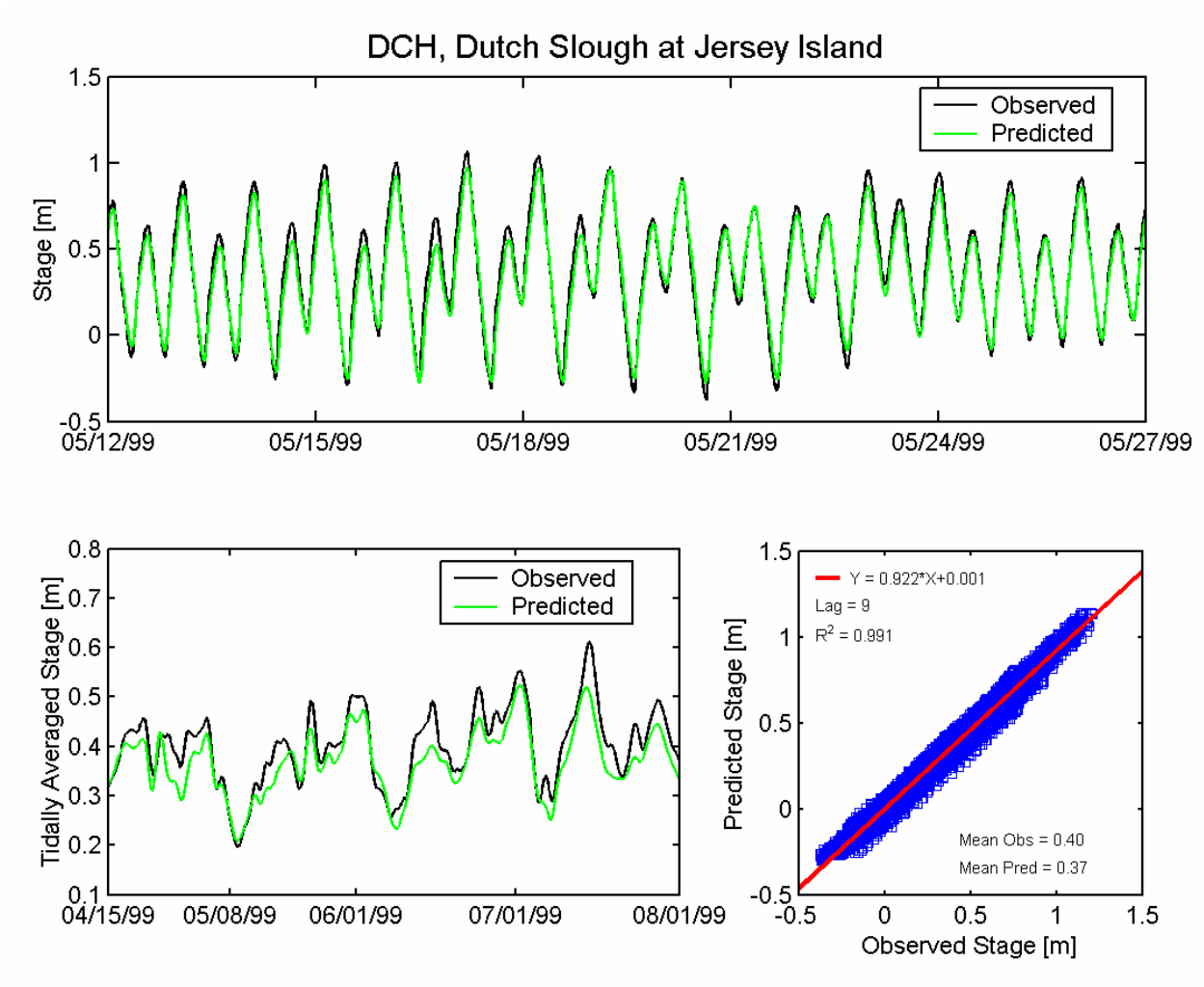

Figure A.2-17 Observed and predicted stage at Dutch Slough at Jersey Island USGS station (DCH) during the 1999 simulation period.

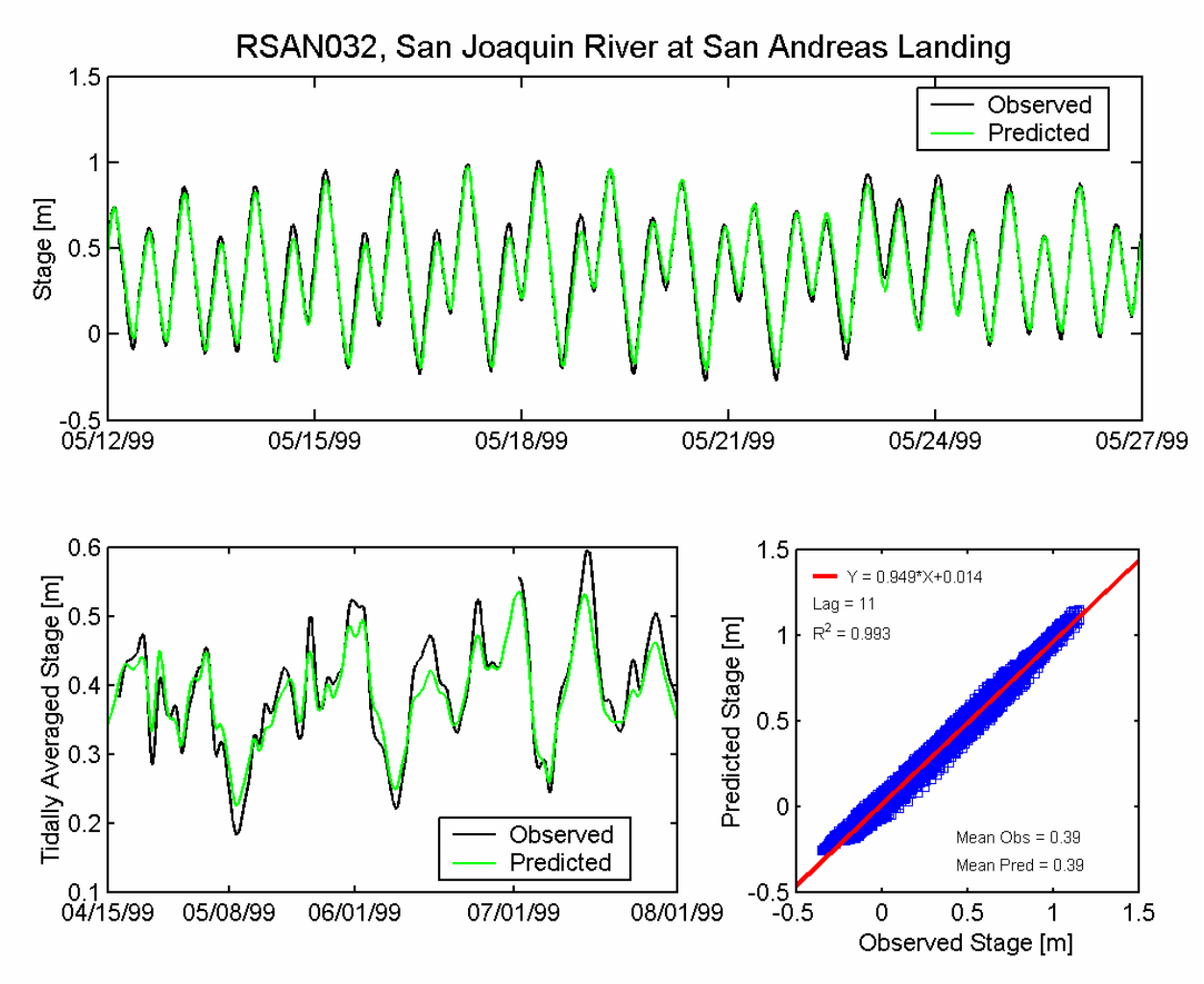

Figure A.2-18 Observed and predicted stage at San Joaquin River at San Andreas Landing DWR station (RSAN032) during the 1999 simulation period.

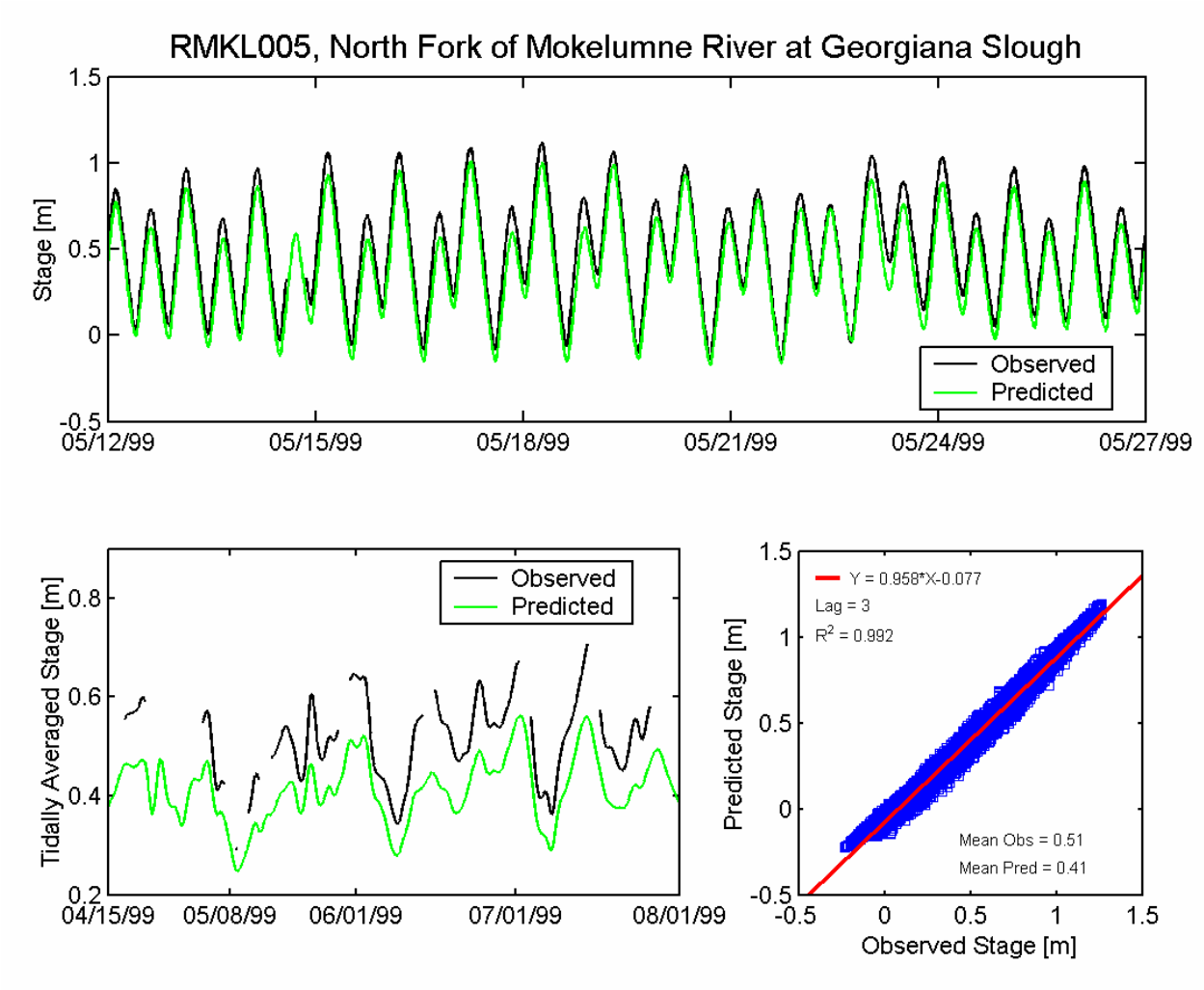

Figure A.2-19 Observed and predicted stage at North Fork Mokelumne River at Georgiana Slough DWR station (RMKL005) during the 1999 simulation period.

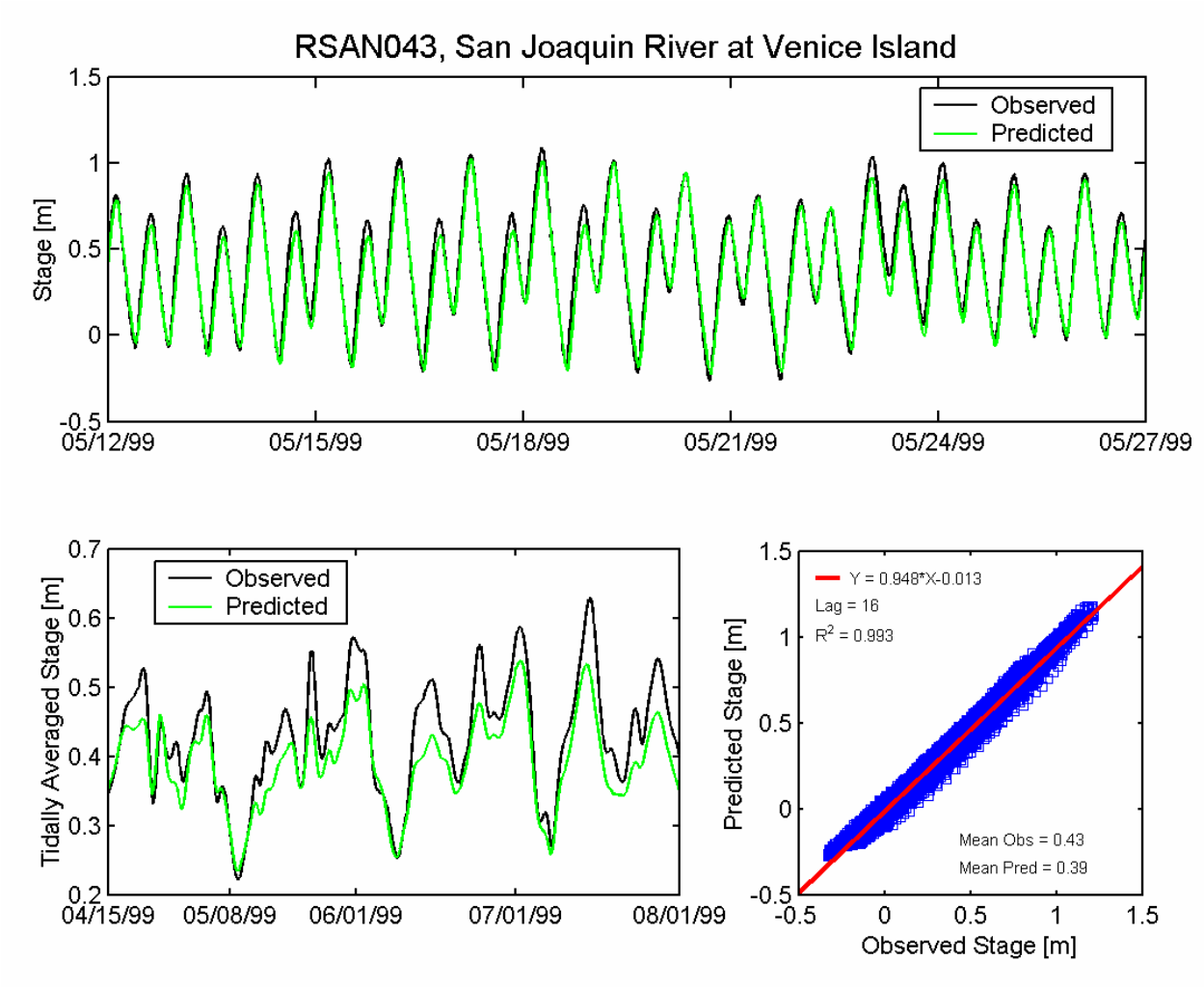

Figure A.2-20 Observed and predicted stage at San Joaquin River at Venice Island DWR station (RSAN043) during the 1999 simulation period.

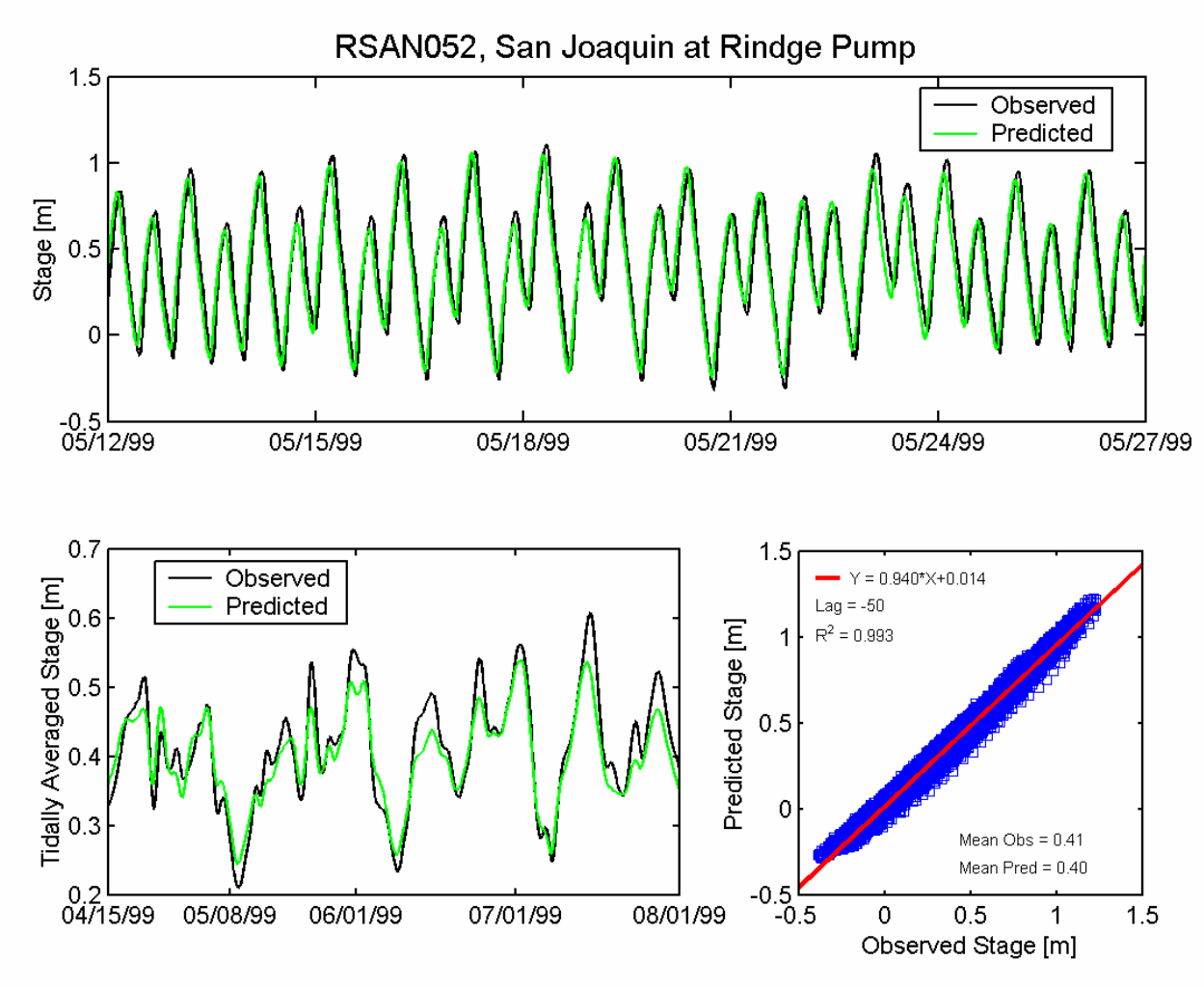

Figure A.2-21 Observed and predicted stage at San Joaquin River at Rindge Pump DWR station (RSAN052) during the 1999 simulation period.

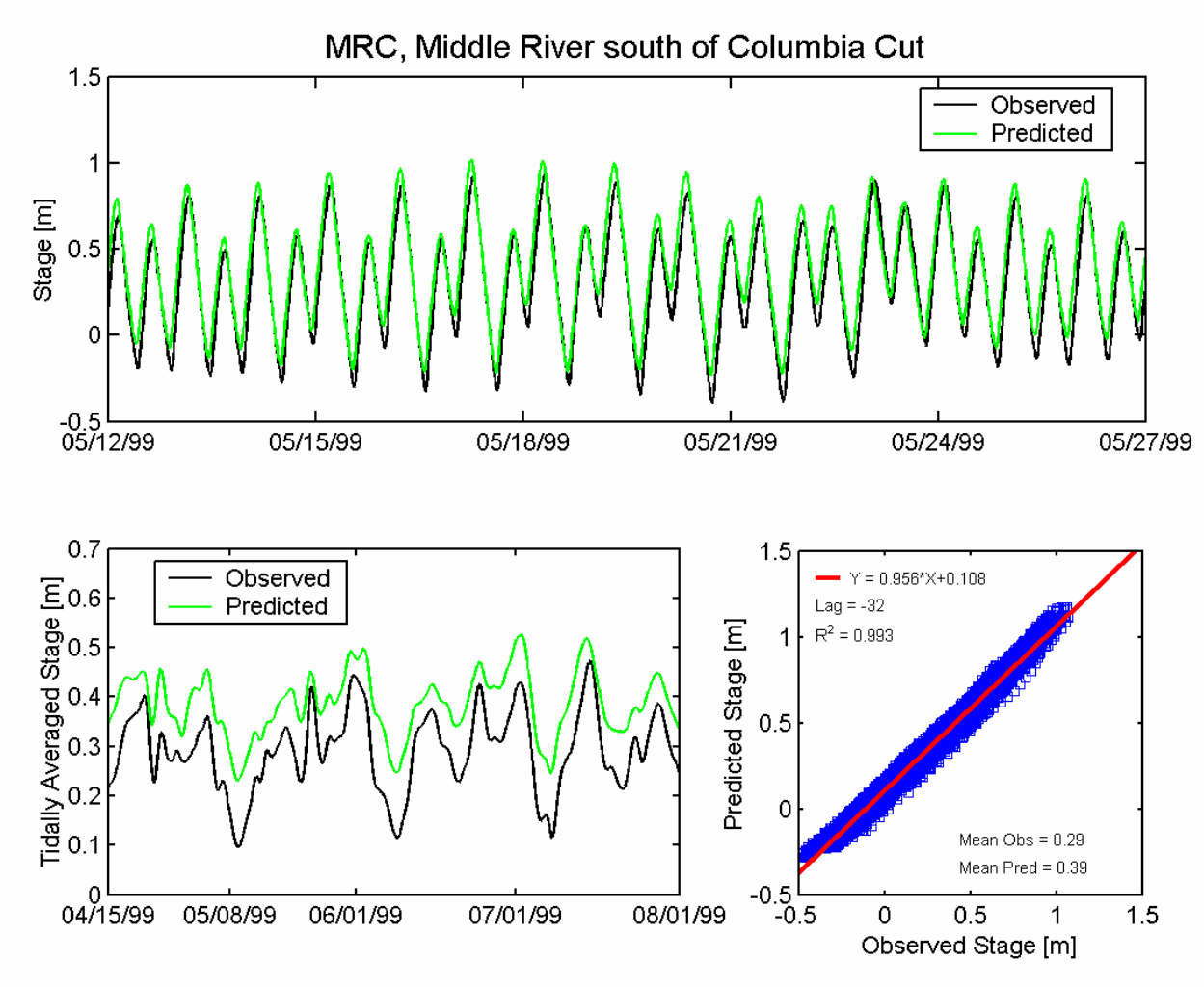

Figure A.2-22 Observed and predicted stage at Middle River south of Columbia Cut USGS station (MRC) during the 1999 simulation period.

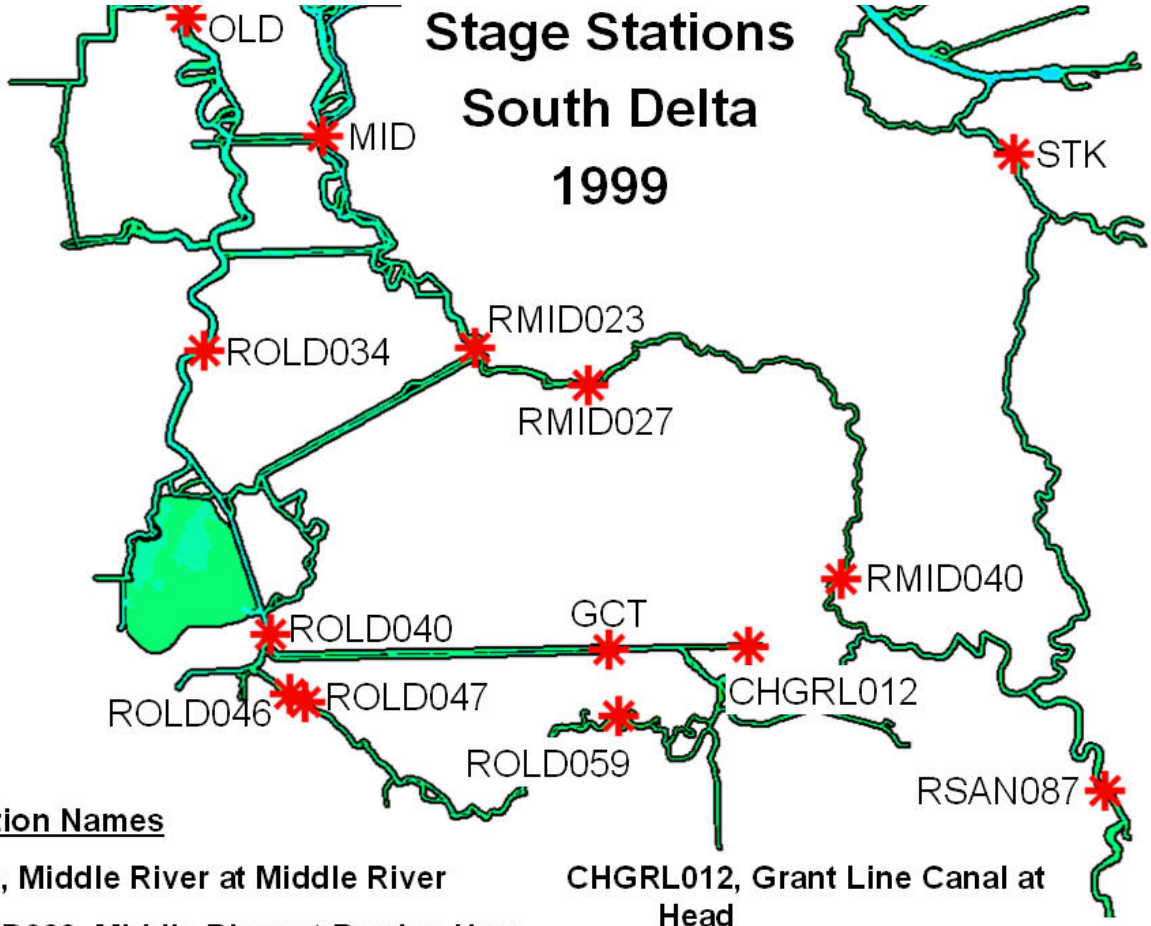

Station Names

MID, Middle River at Middle River

RMID023, Middle River at Borden Hwy

RMID027, Middle River at Tracy Blvd

RMID040, Middle River at Mowry Bridge

OLD, Old River at Bacon Island

ORF, Old River near Byron

ROLD040, Old River at Clifton Court Ferry

GCT, Grant Line Canal at Tracy Blvd

CHGRL012, Grant Line Canal at Head

ROLD046, Old River near Delta Mendota Canal (Downstream of Barrier)

ROLD047, Old River near Delta Mendota Canal (Upstream of Barrier)

ROLD059, Old River at Tracy Blvd

STK, San Joaquin River at Stockton

RSAN087, San Joaquin River at Mossdale

Figure A.2-23 Location of water level monitoring stations in the southern portion of the Sacramento-San Joaquin Delta used for 1999 water level calibration.

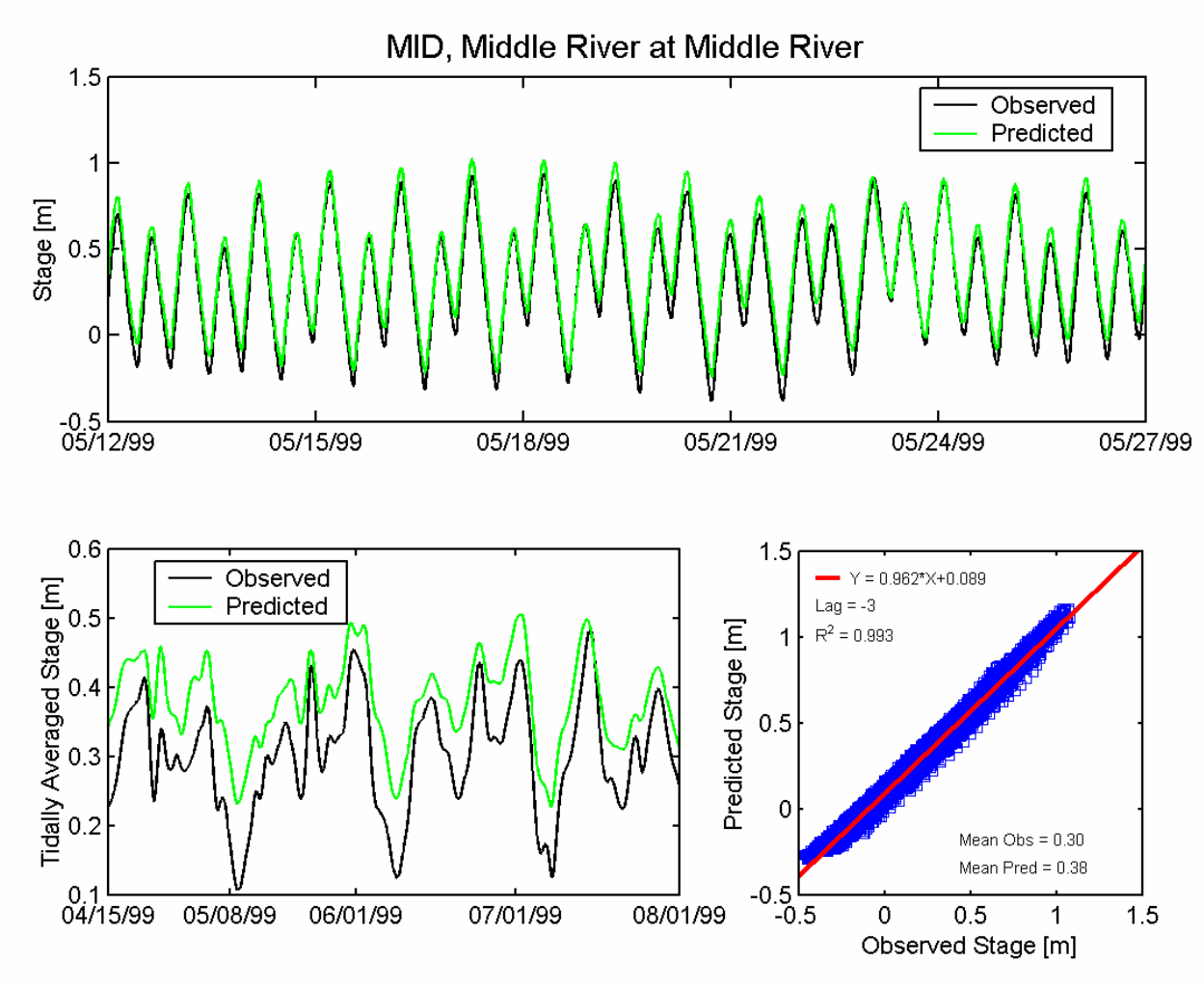

Figure A.2-24 Observed and predicted stage at Middle River at Middle River USGS station (MID) during the 1999 simulation period.

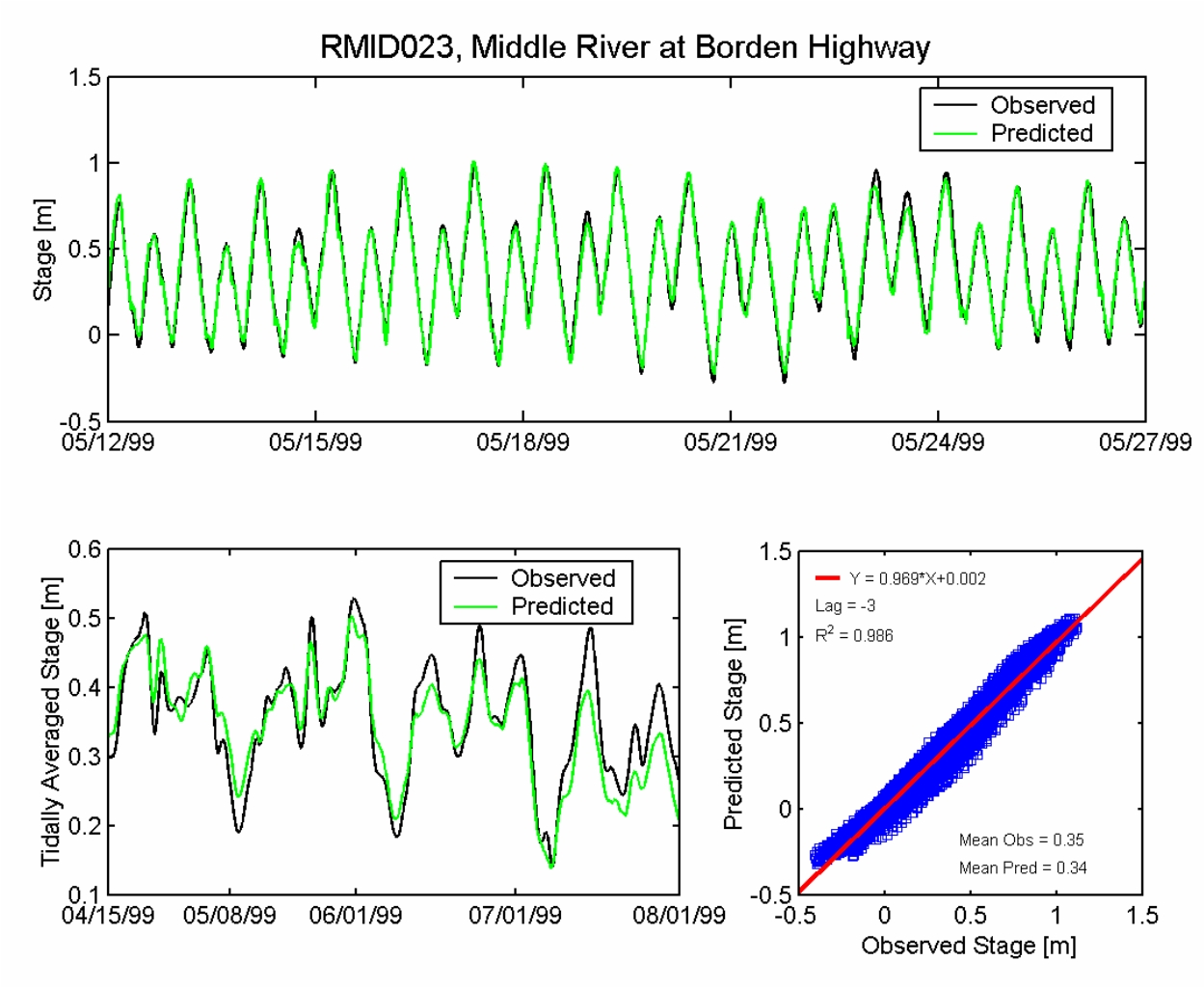

Figure A.2-25 Observed and predicted stage at Middle River at Borden Highway DWR station (RMID023) during the 1999 simulation period.

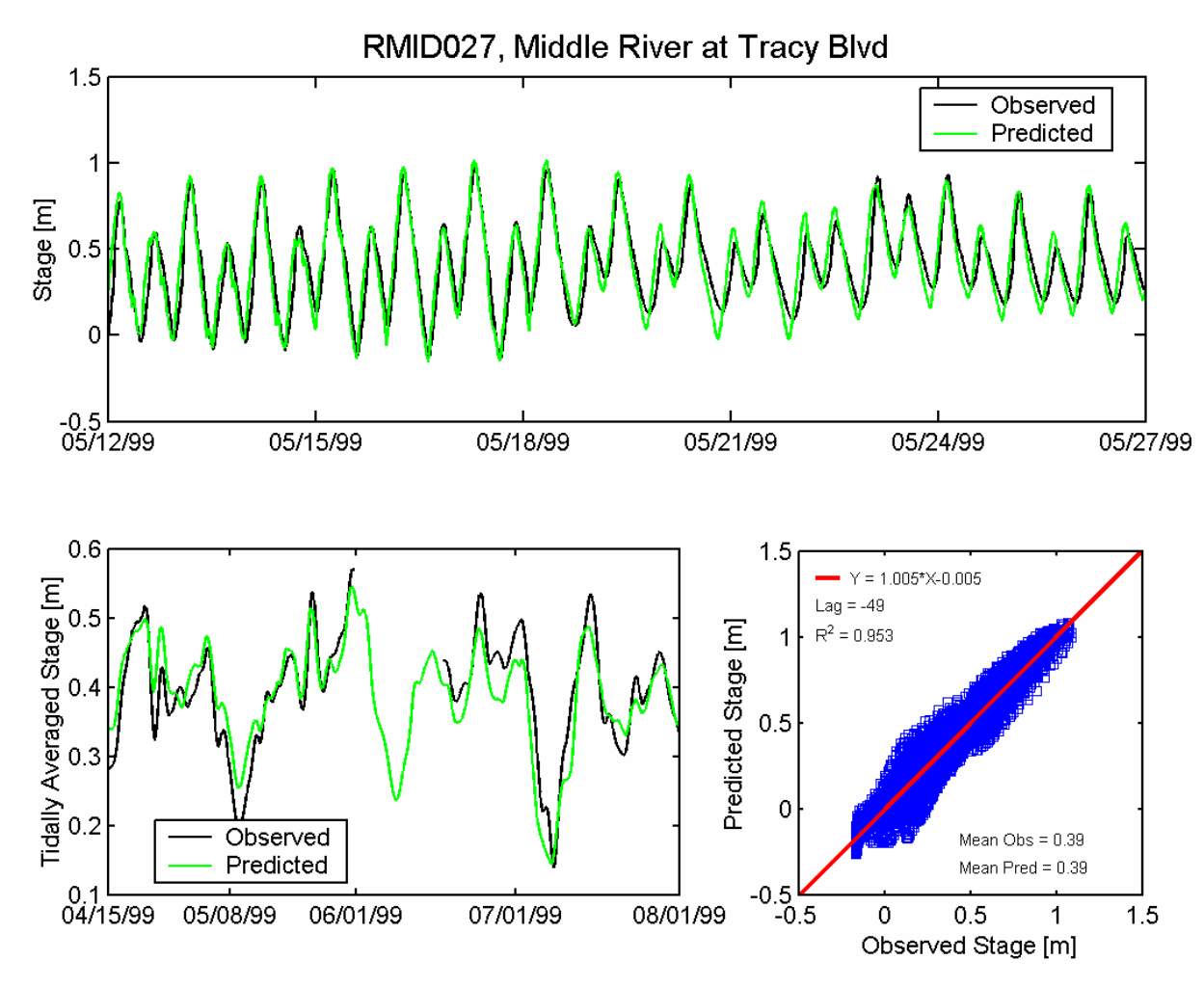

Figure A.2-26 Observed and predicted stage at Middle River at Tracy Boulevard DWR station (RMID027) during the 1999 simulation period.

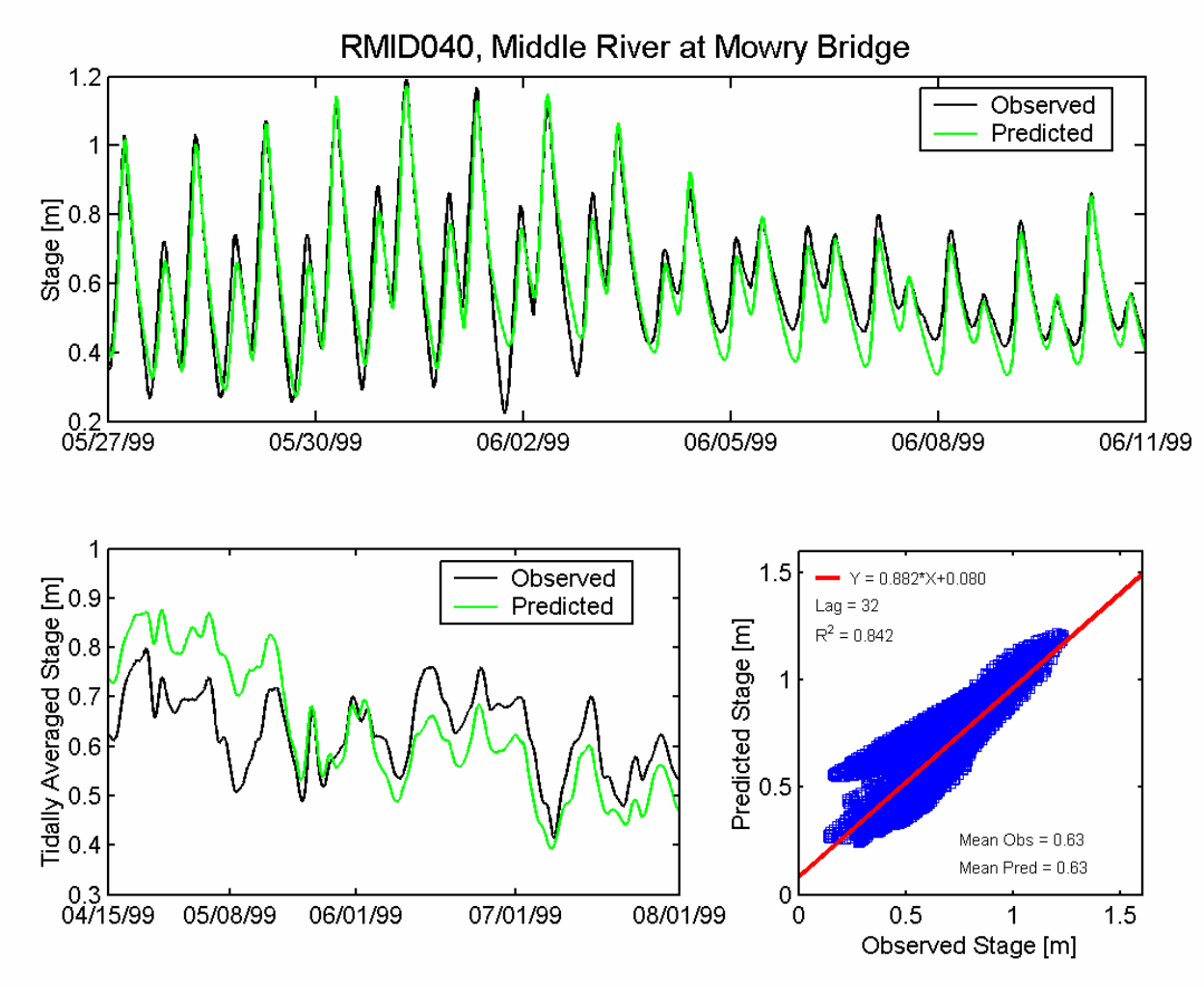

Figure A.2-27 Observed and predicted stage at Middle River at Mowry Bridge DWR station (RMID040) during the 1999 simulation period.

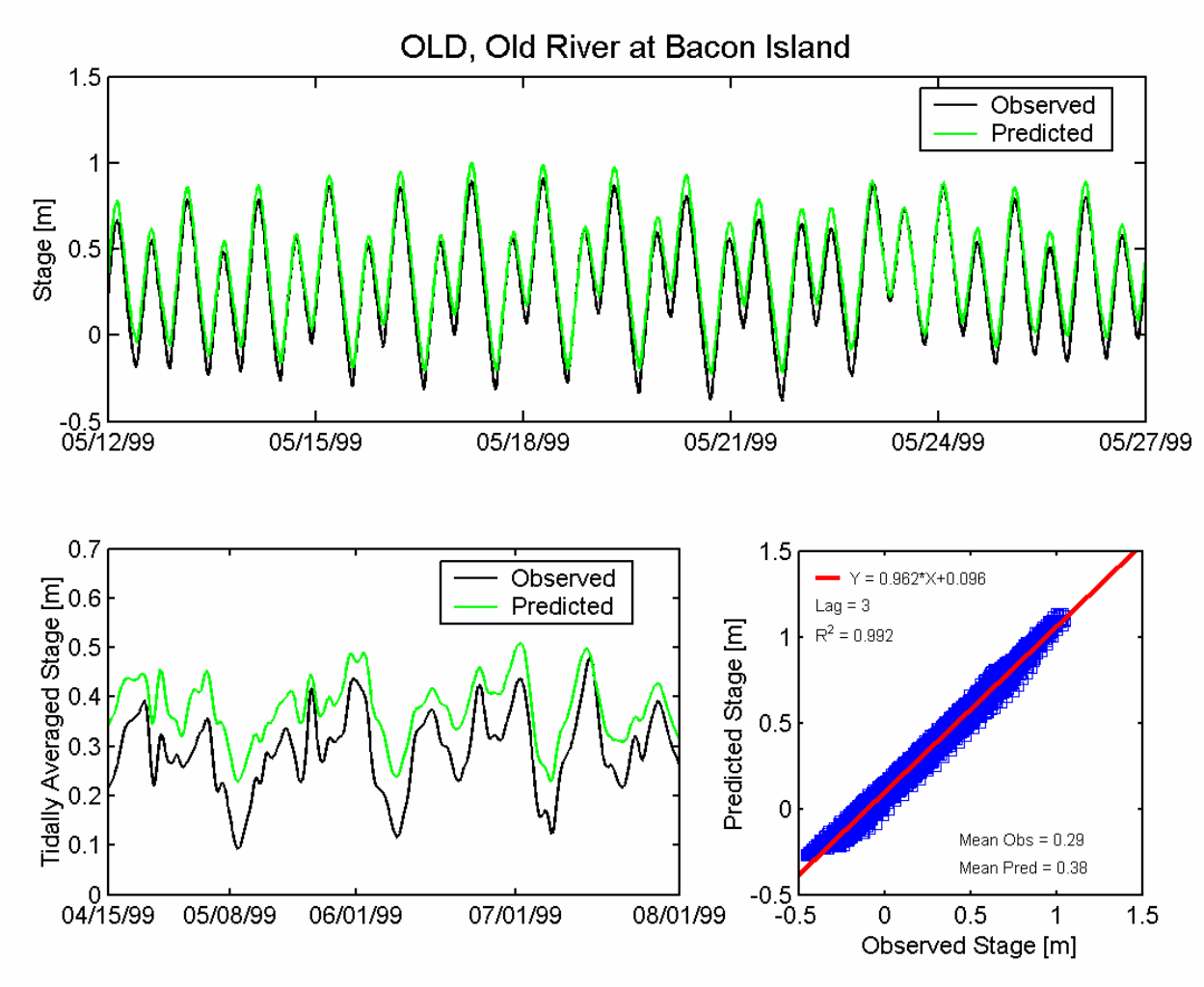

Figure A.2-28 Observed and predicted stage at Old River at Bacon Island USGS station (OLD) during the 1999 simulation period.

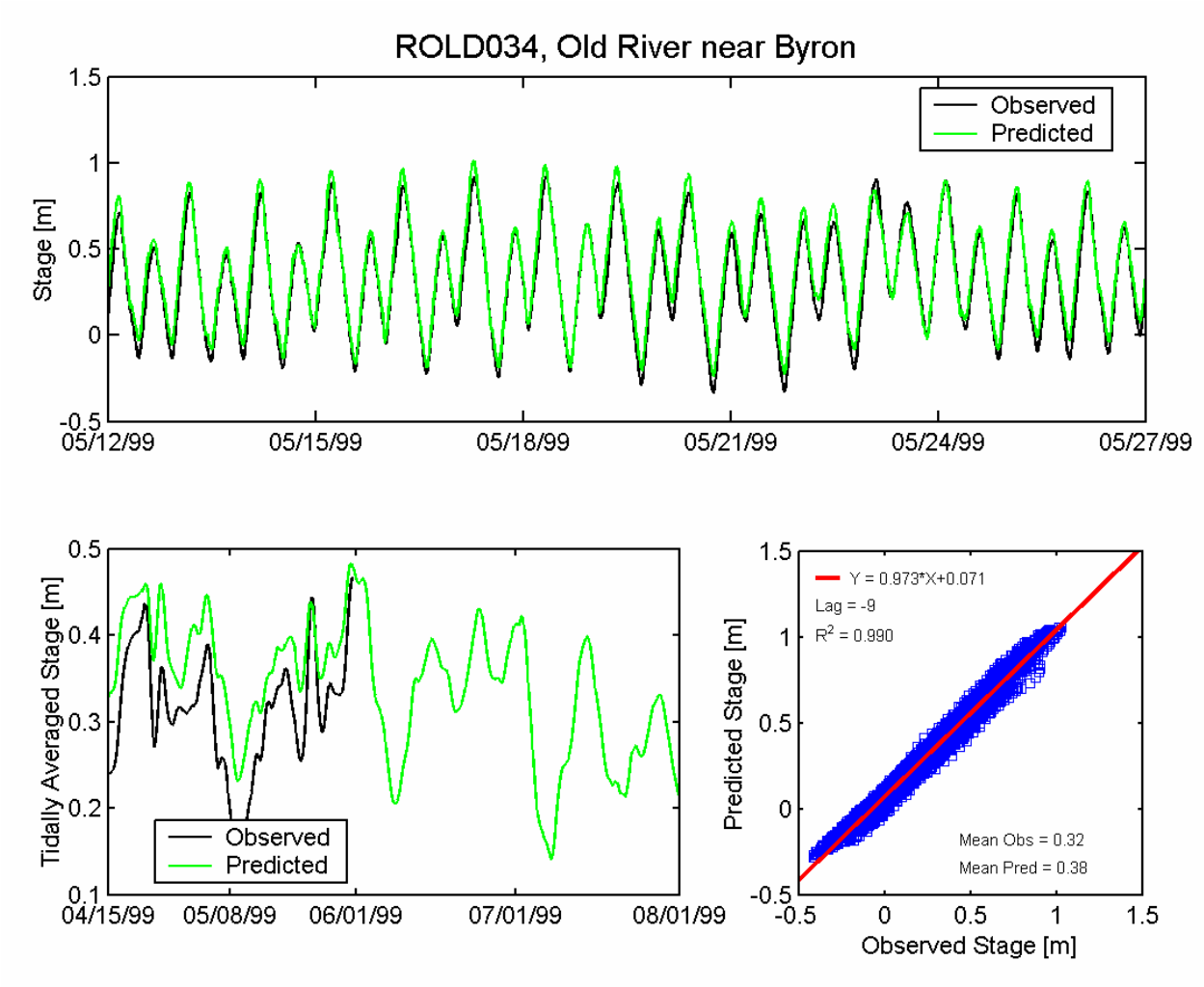

Figure A.2-29 Observed and predicted stage at Old River near Byron DWR station (ROLD034) during the 1999 simulation period.

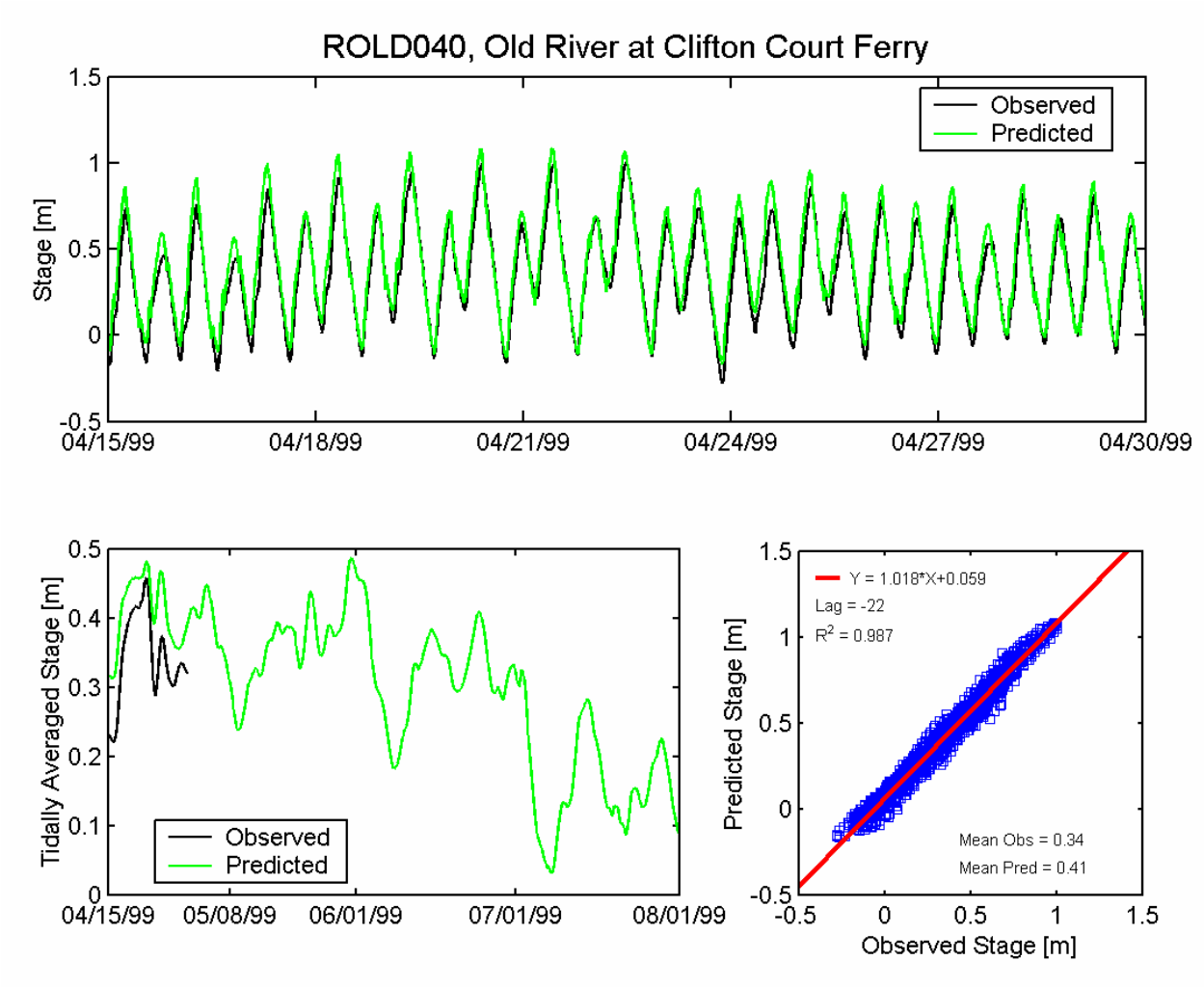

Figure A.2-30 Observed and predicted stage at Old River at Clifton Court Ferry DWR station (ROLD040) during the 1999 simulation period.

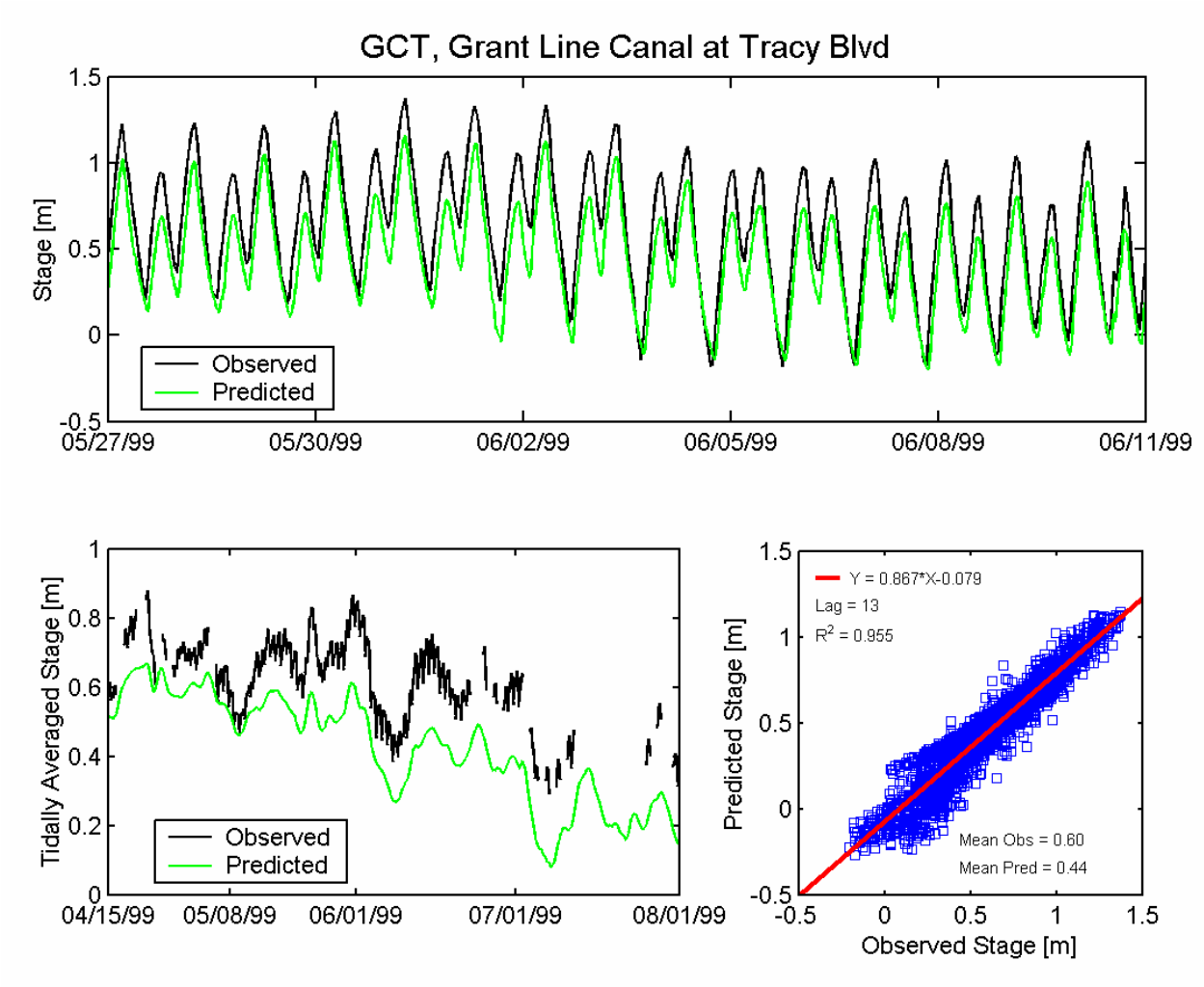

Figure A.2-31 Observed and predicted stage at Grant Line Canal at Tracy Boulevard DWR station (CDEC GCT) during the 1999 simulation period.

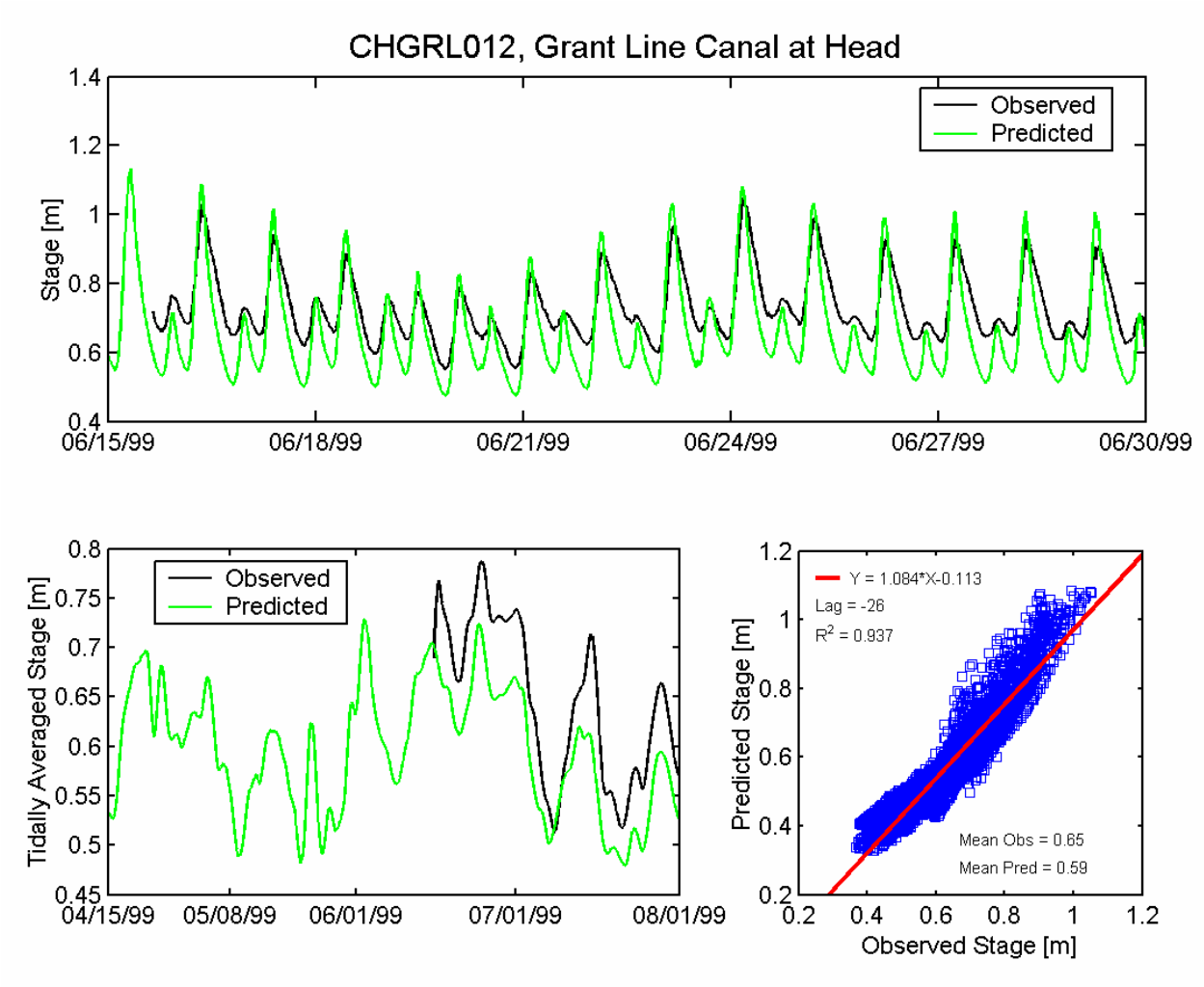

Figure A.2-32 Observed and predicted stage at Grant Line Canal at Head DWR station (CHGRL012) during the 1999 simulation period.

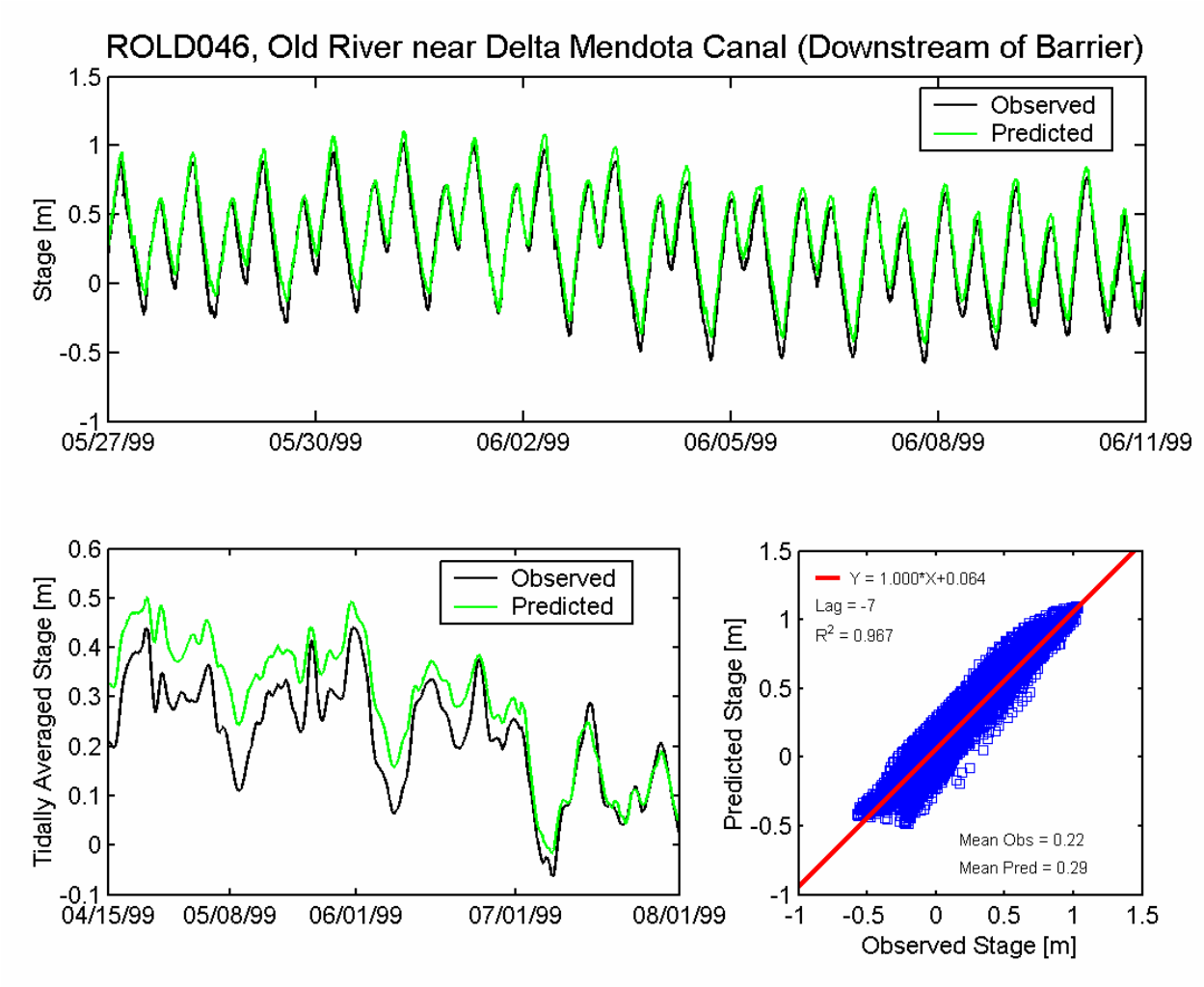

Figure A.2-33 Observed and predicted stage at Old River near Delta Mendota Canal Downstream of Barrier DWR station (ROLD046) during the 1999 simulation period.

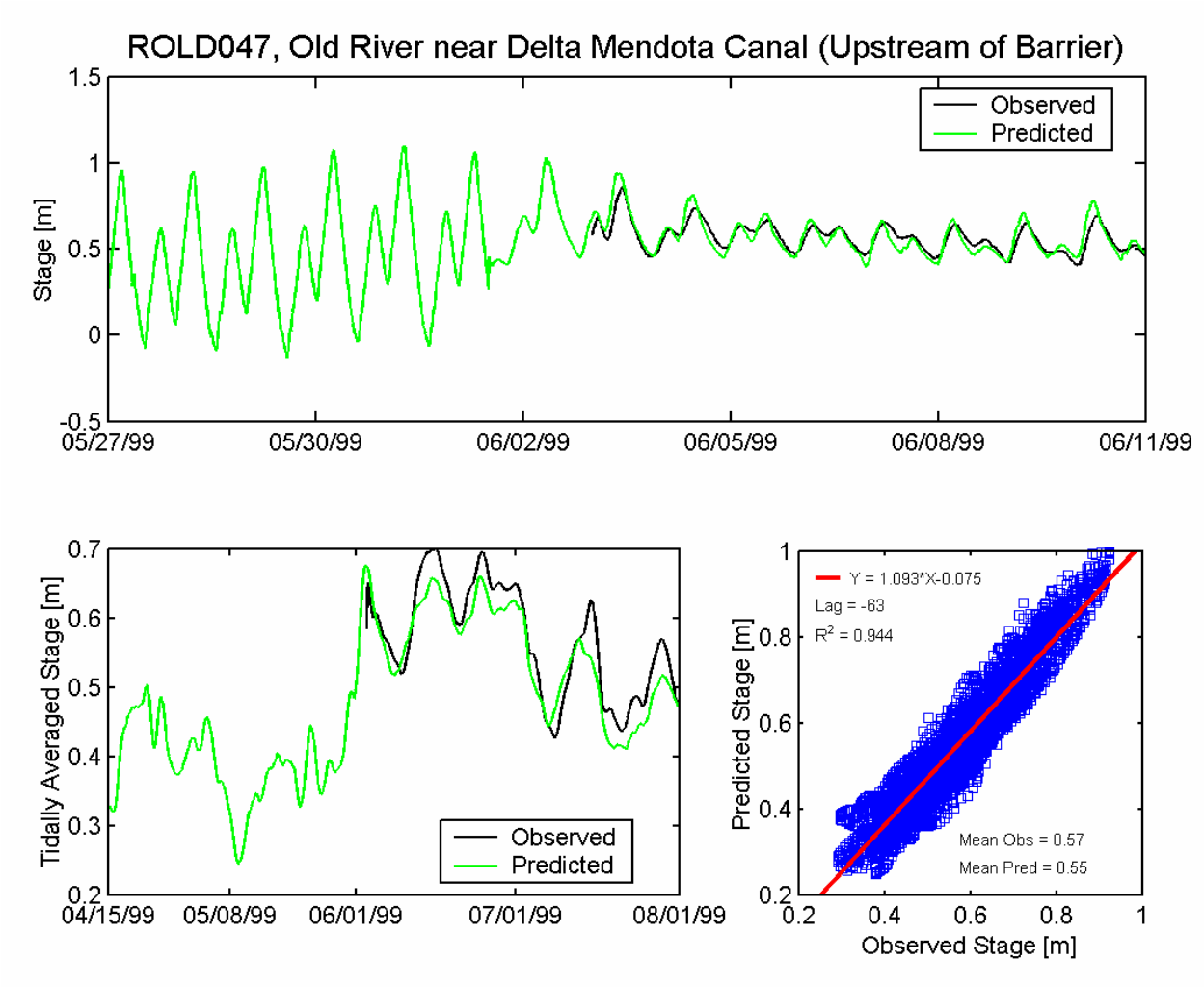

Figure A.2-34 Observed and predicted stage at Old River near Delta Mendota Canal Upstream of Barrier DWR station (ROLD047) during the 1999 simulation period.

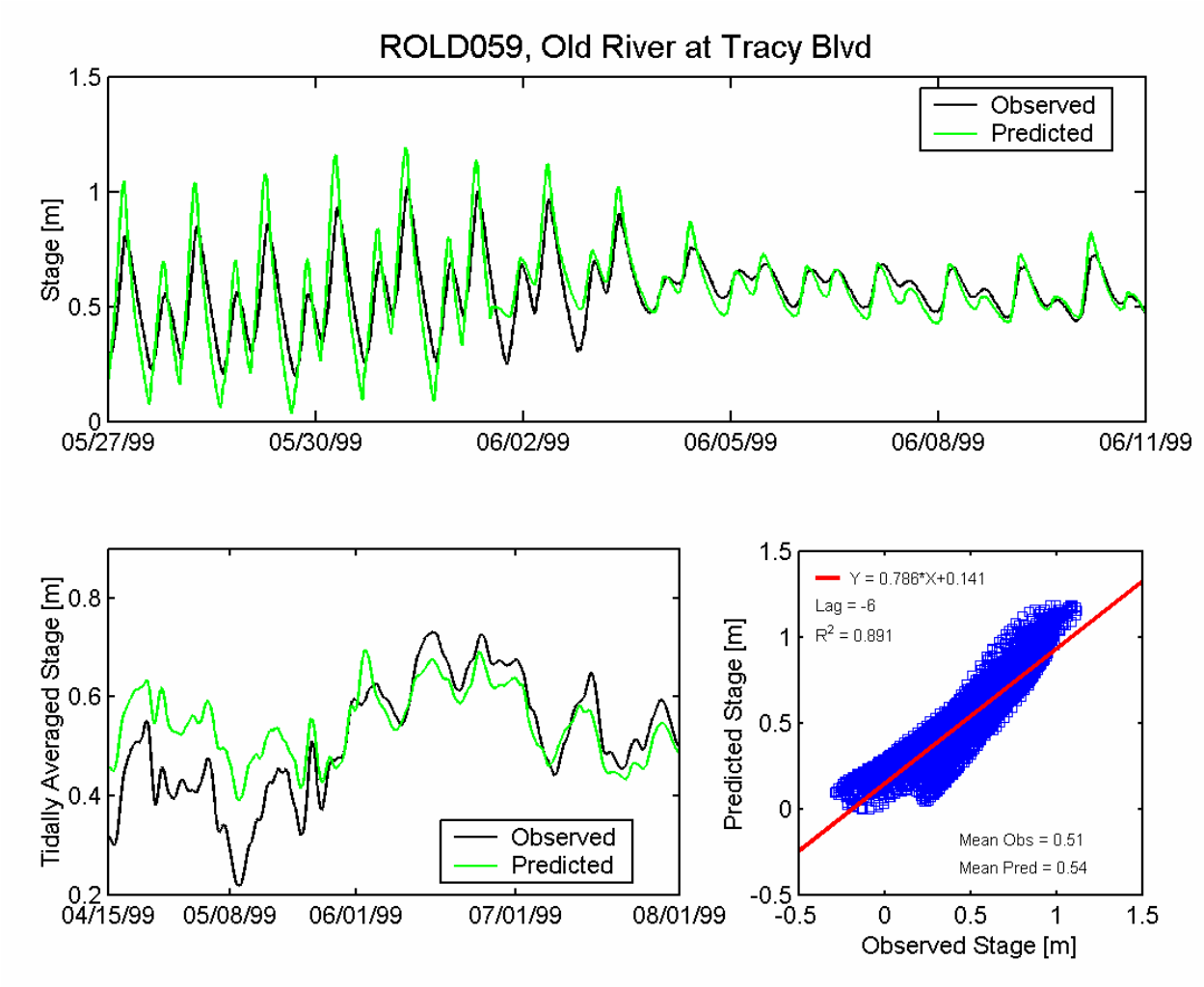

Figure A.2-35 Observed and predicted stage at Old River at Tracy Boulevard DWR station (ROLD059) during the 1999 simulation period.

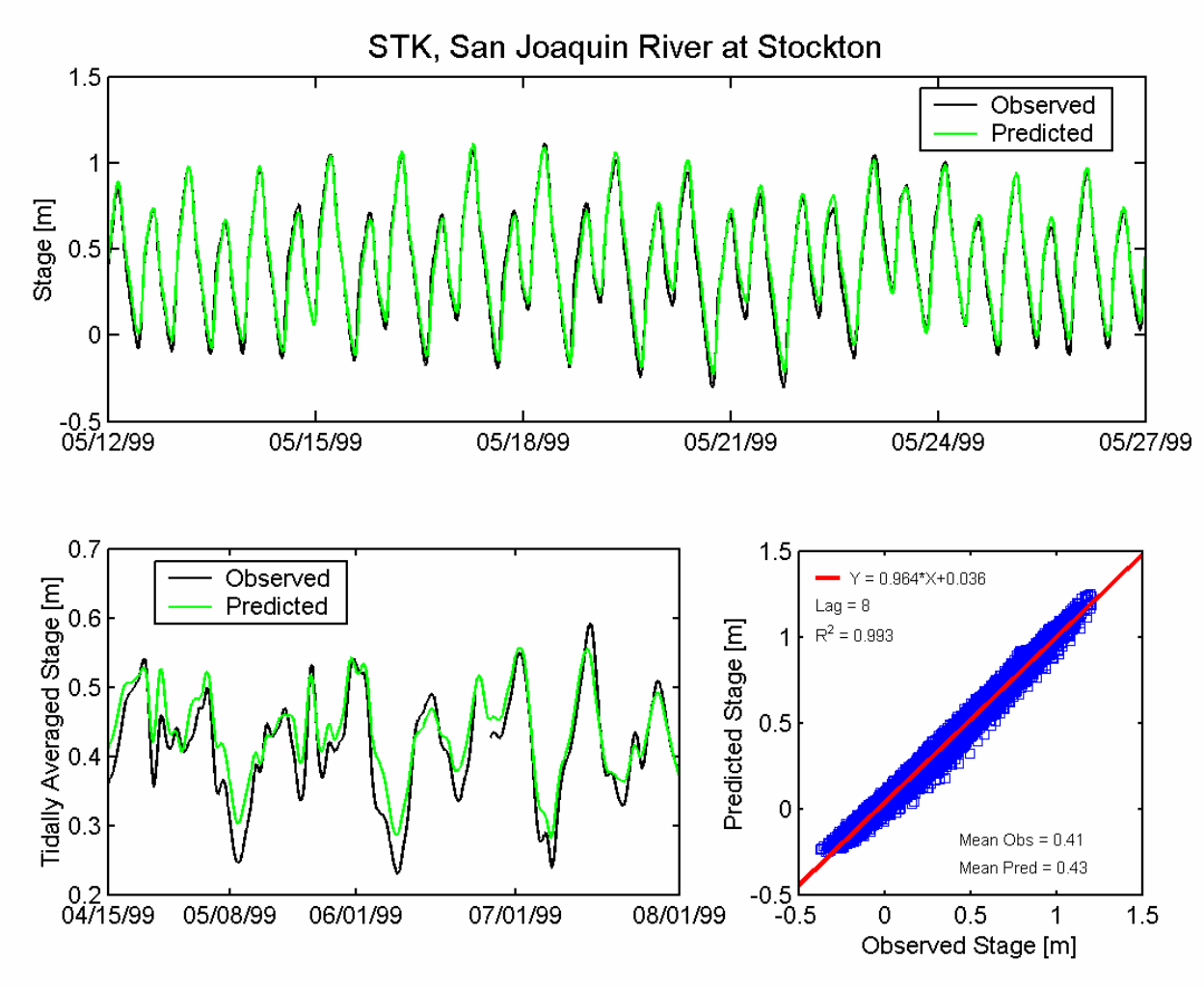

Figure A.2-36 Observed and predicted stage at San Joaquin River at Stockton USGS station (STK) during the 1999 simulation period.

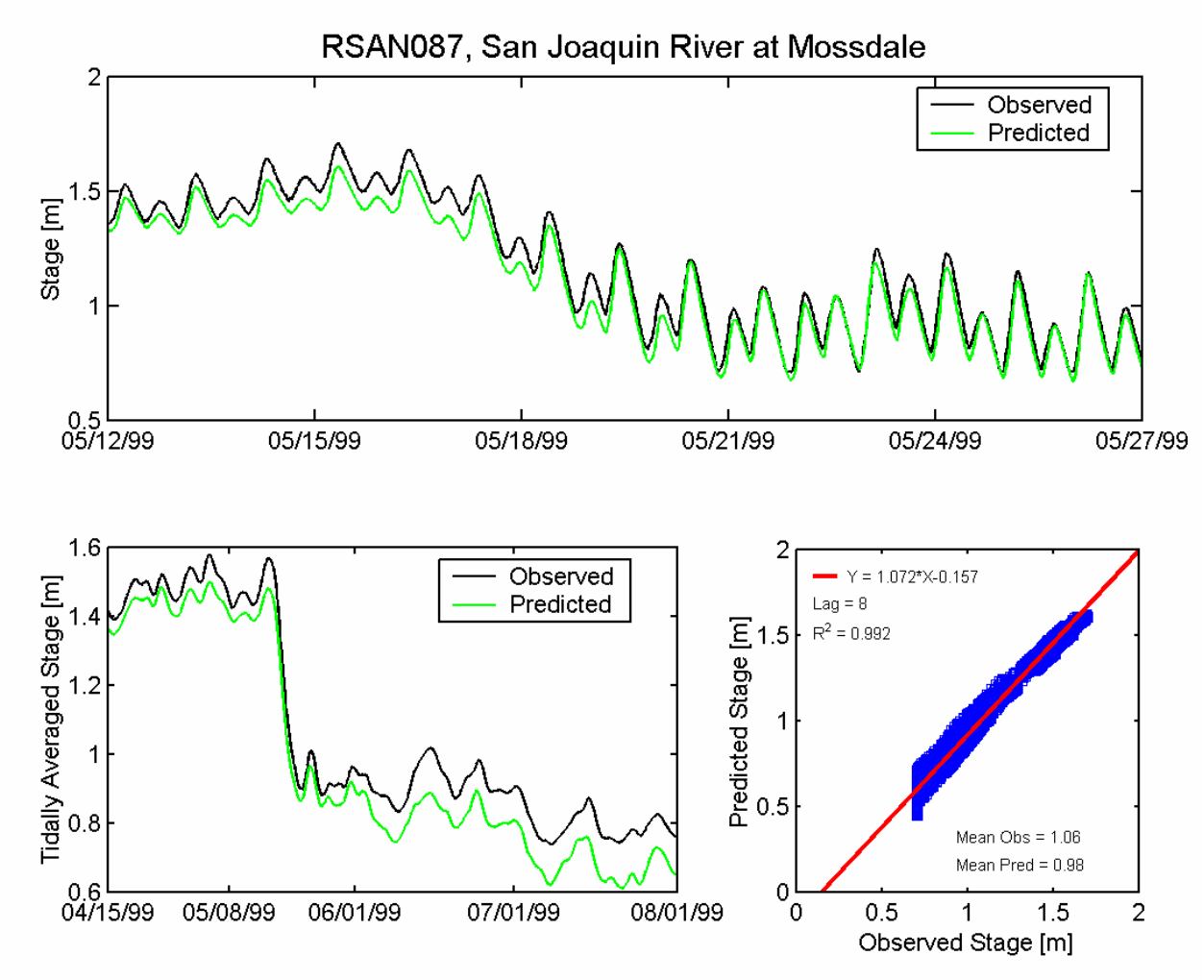

Figure A.2-37 Observed and predicted stage at San Joaquin River at Mossdale DWR station (RSAN087) during the 1999 simulation period.

A.3 Delta Flow Comparison Figures

During the 1999 validation period, flow measurements are available at a total of twelve flow monitoring stations in the Sacramento-San Joaquin Delta. For each station, the mean observed and predicted net flow was calculated over the full simulation period, and the same cross-correlation procedure used in the water level analysis was applied to flow. Table A-2 gives the predicted and observed mean flow at each station as well as the corresponding amplitude ratio, phase lag, and R^2 for each station.

A.3.1 Northern Sacramento-San Joaquin Delta

Flow comparisons were made at three continuous flow monitoring stations in the northern portion of the Sacramento-San Joaquin Delta, at the locations shown in Figure A.3-1. Flow comparisons at these stations are shown in Figures A.3-2 through A.3-4.

A.3.2 Central Sacramento-San Joaquin Delta

Flow comparisons were made at five continuous flow monitoring stations in the central portion of the Sacramento-San Joaquin Delta, at the locations shown in Figure A.3-5. Flow comparisons at these stations are shown in Figures A.3-6 through A.3-10.

A.3.3 Southern Sacramento-San Joaquin Delta

Flow comparisons were made at four continuous flow monitoring stations in the southern portion of the Sacramento-San Joaquin Delta, at the locations shown in Figure A.3-11. Flow comparisons at these stations are shown in Figures A.3-12 through A.3-15.

Table A-2 Predicted and observed stage and cross-correlation statistics for flow monitoring stations in the Sacramento-San Joaquin Delta during the 1999 simulation period.

Location	Data Source	Figure Number	Mean Flow		Cross Correlation		R^2
			Observed (m^3/s)	Predicted (m^3/s)	Amp Ratio	Lag (min)	
1999 North Delta Flow Stations (Figure A.3-1)							
Sacramento River South of Georgiana Slough	USGS	A.3-2	179	184	0.891	-8	0.994
Sacramento River North of Delta Cross Channel	USGS	A.3-3	366	365	1.054	7	0.985
Sacramento River at Freeport	USGS	A.3-4	605	600	1.040	-4	0.995
1999 Central Delta Flow Stations (Figure A.3-5)							
Sacramento River at Rio Vista	USGS	A.3-6	464	431	1.172	20	0.994
Threemile Slough at San Joaquin River	USGS	A.3-7	-43.5	-37.6	0.898	4	0.995
San Joaquin River at Jersey Point	USGS	A.3-8	138	166	0.849	-3	0.996
Dutch Slough at Jersey Island	USGS	A.3-9	-0.62	2.50	0.814	-4	0.995
Middle River south of Columbia Cut	USGS	A.3-10	-64.1	-55.3	1.057	-65	0.988
1999 South Delta Flow Stations (Figure A.3-11)							
Middle River at Middle River	USGS	A.3-12	-63.4	-56.3	0.690	-13	0.981
Old River at Bacon Island	USGS	A.3-13	-46.7	-48.1	0.742	-12	0.989
Grant Line Canal at Tracy Blvd	USGS	A.3-14	83.5	89.4	0.526	-6	0.954
San Joaquin River at Stockton	USGS	A.3-15	49.9	48.0	0.934	-5	0.981

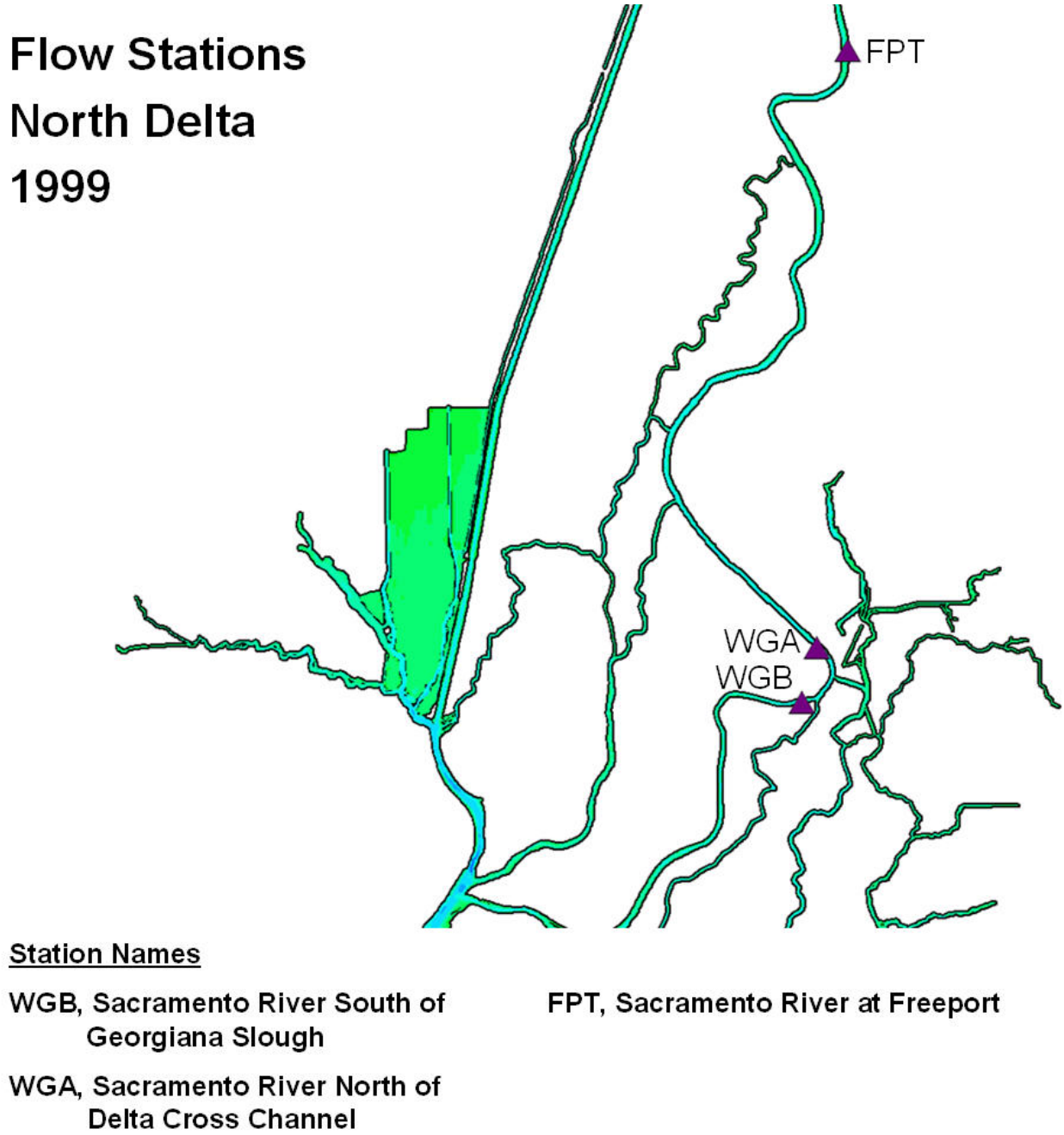

Figure A.3-1 Location of flow monitoring stations in the northern portion of the Sacramento-San Joaquin Delta used for 1999 flow calibration.

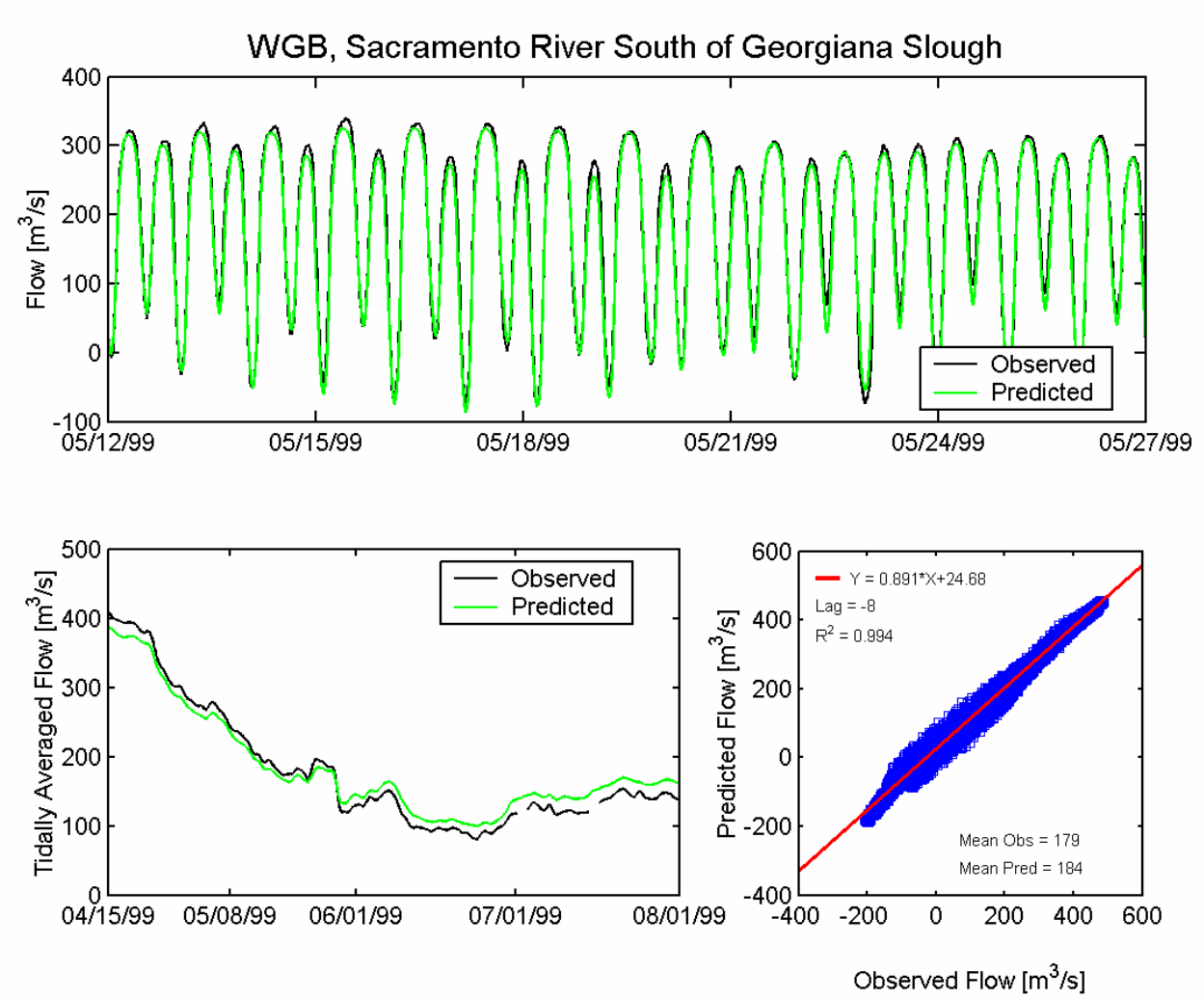

Figure A.3-2 Observed and predicted flow at Sacramento River South of Georgiana Slough USGS station (WGB) during the 1999 simulation period.

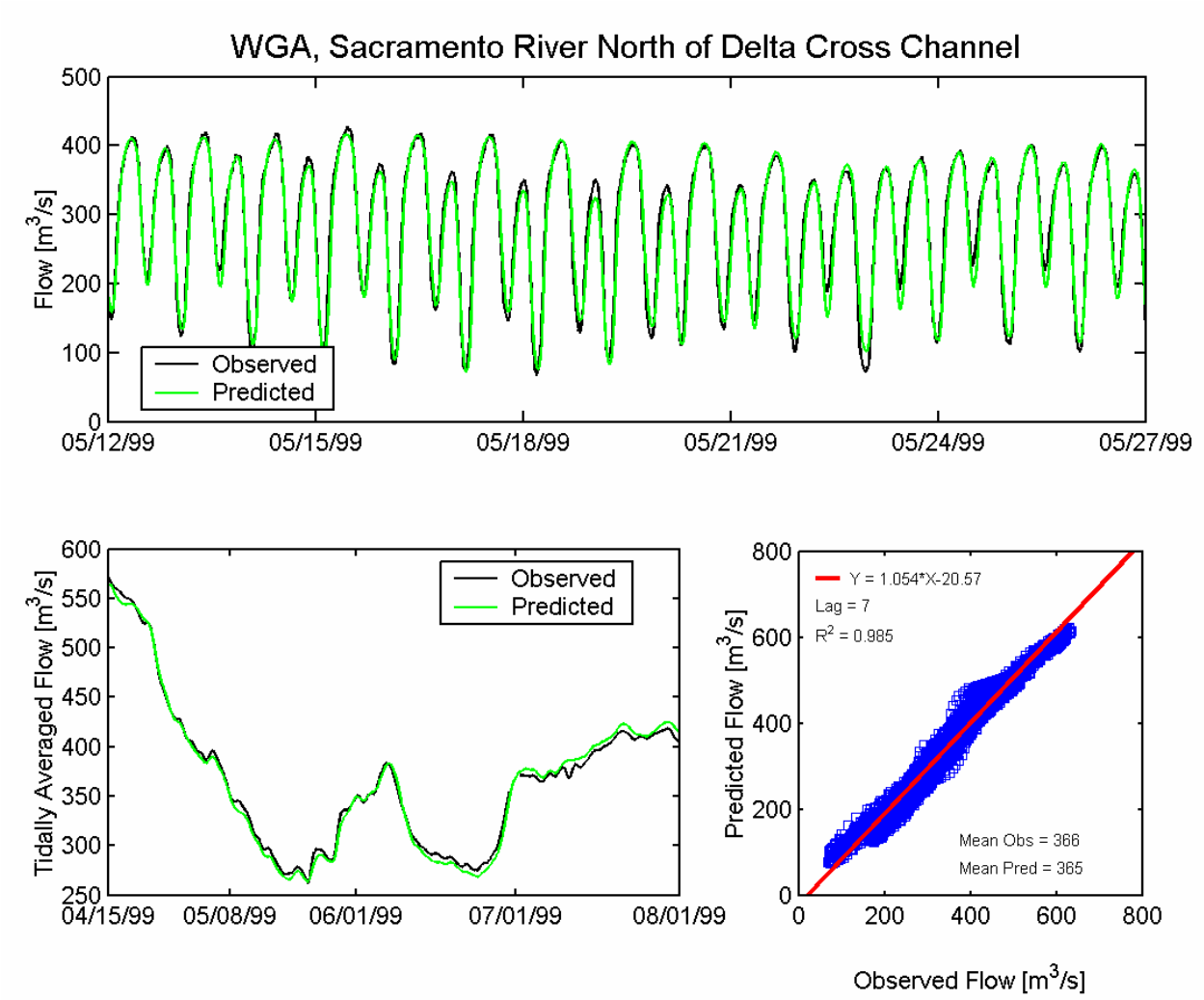

Figure A.3-3 Observed and predicted flow at Sacramento River North of Delta Cross Channel USGS station (WGA) during the 1999 simulation period.

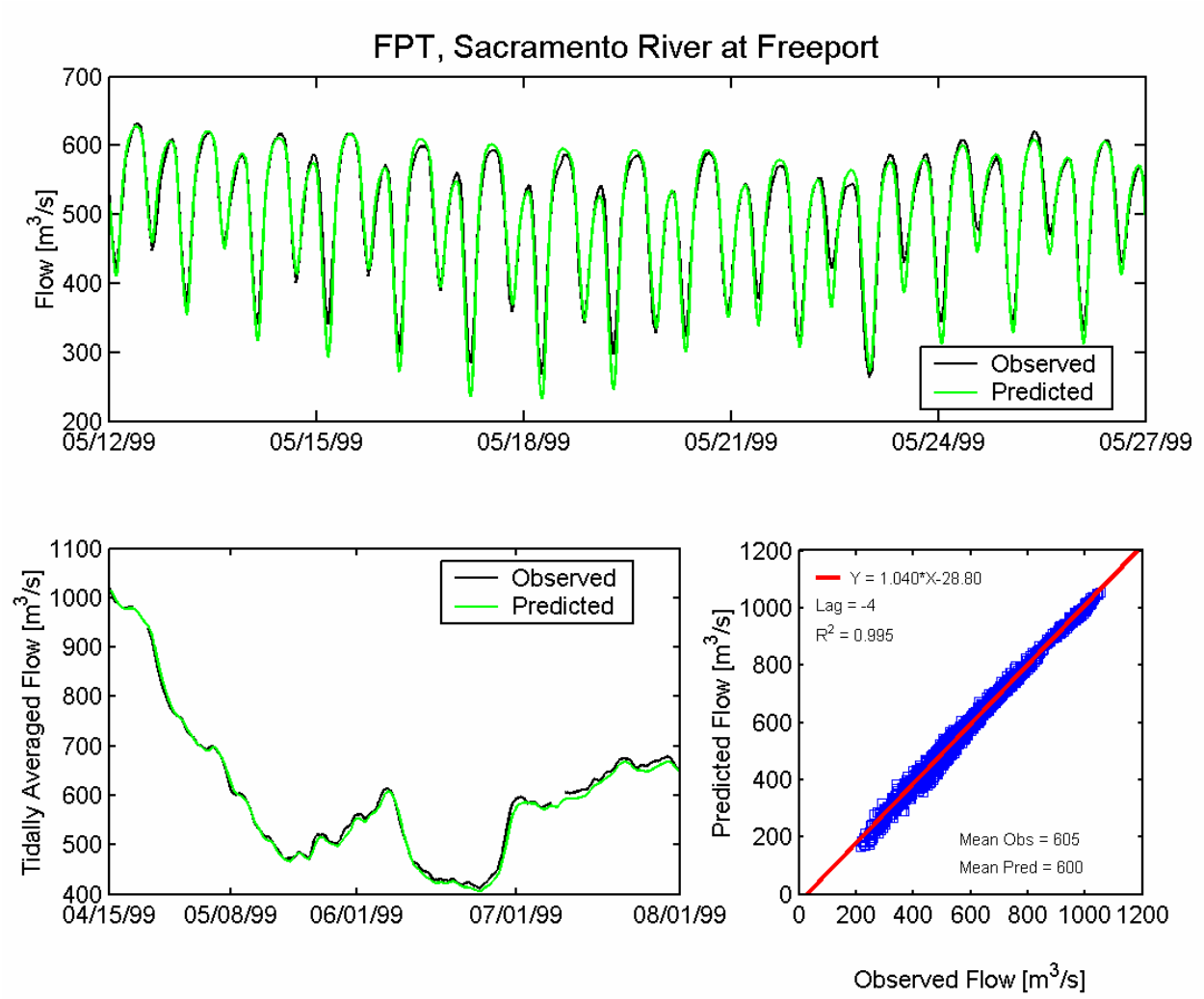

Figure A.3-4 Observed and predicted flow at Sacramento River at Freeport USGS station (FPT) during the 1999 simulation period.

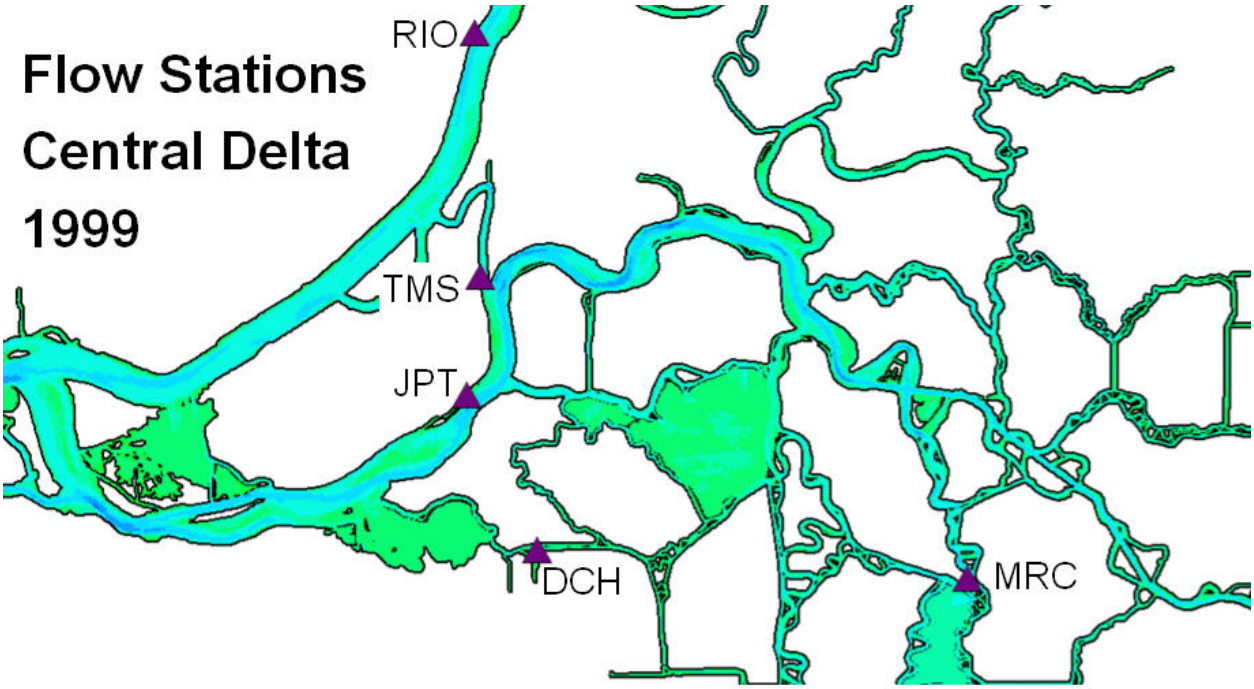

Station Names

RIO, Sacramento River at Rio Vista

TMS, Threemile Slough at San Joaquin River

JPT, San Joaquin River at Jersey Point

DCH, Dutch Slough at Jersey Island

MRC, Middle River South of Columbia Cut

Figure A.3-5 Location of flow monitoring stations in the central portion of the Sacramento-San Joaquin Delta used for 1999 flow calibration.

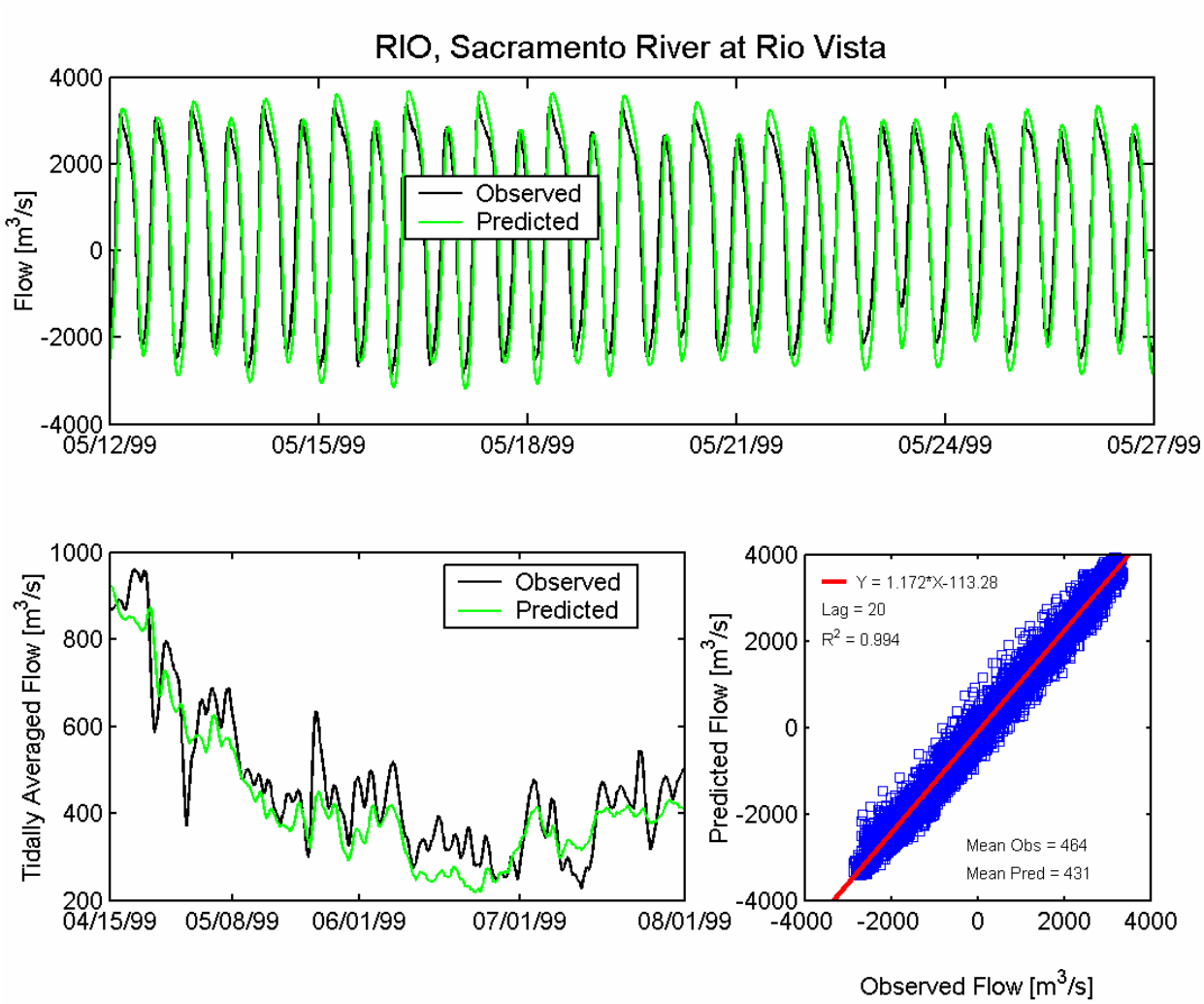

Figure A.3-6 Observed and predicted flow at Sacramento River at Rio Vista USGS station (RIO) during the 1999 simulation period.

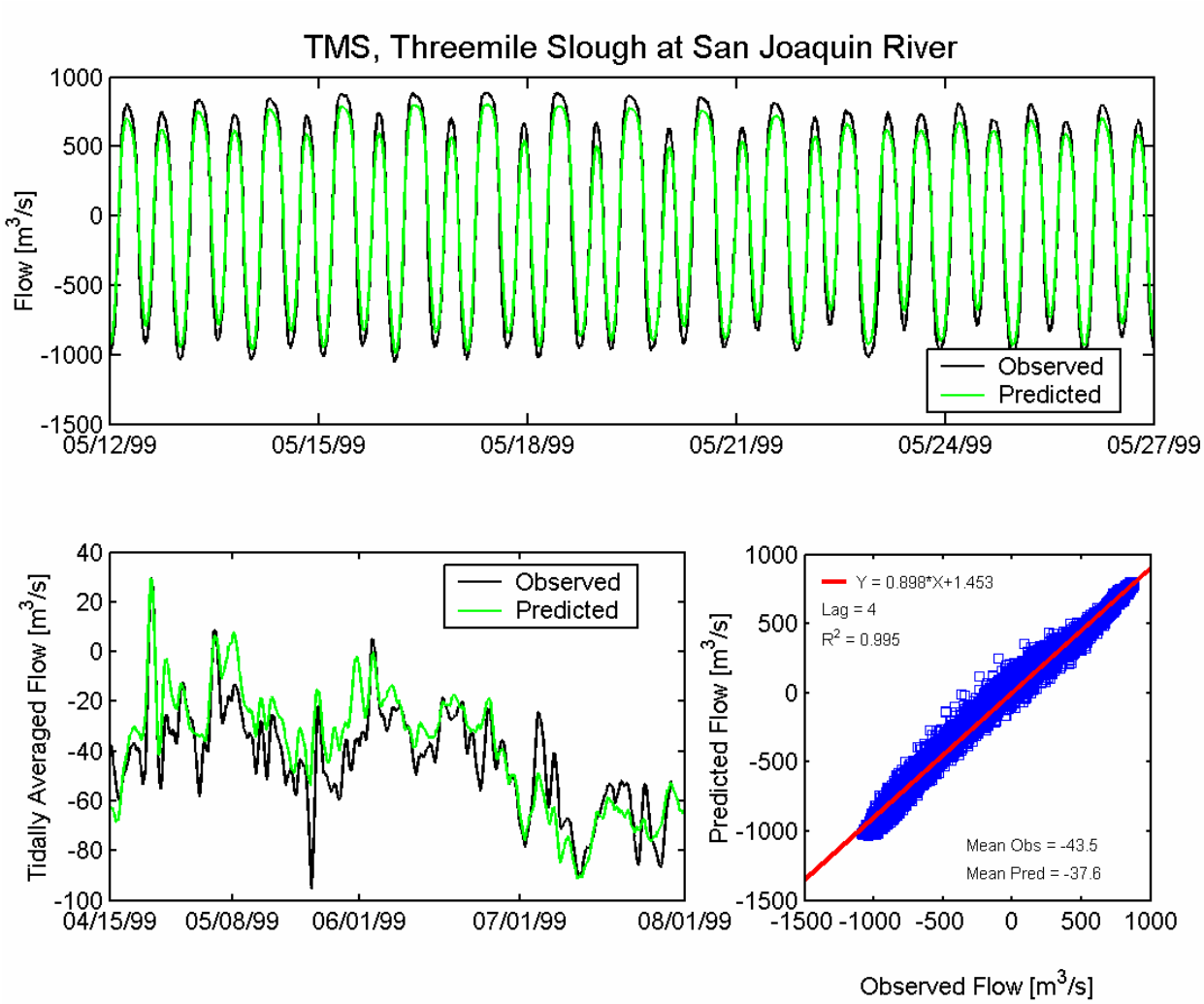

Figure A.3-7 Observed and predicted flow at Threemile Slough at San Joaquin River USGS station (TMS) during the 1999 simulation period.

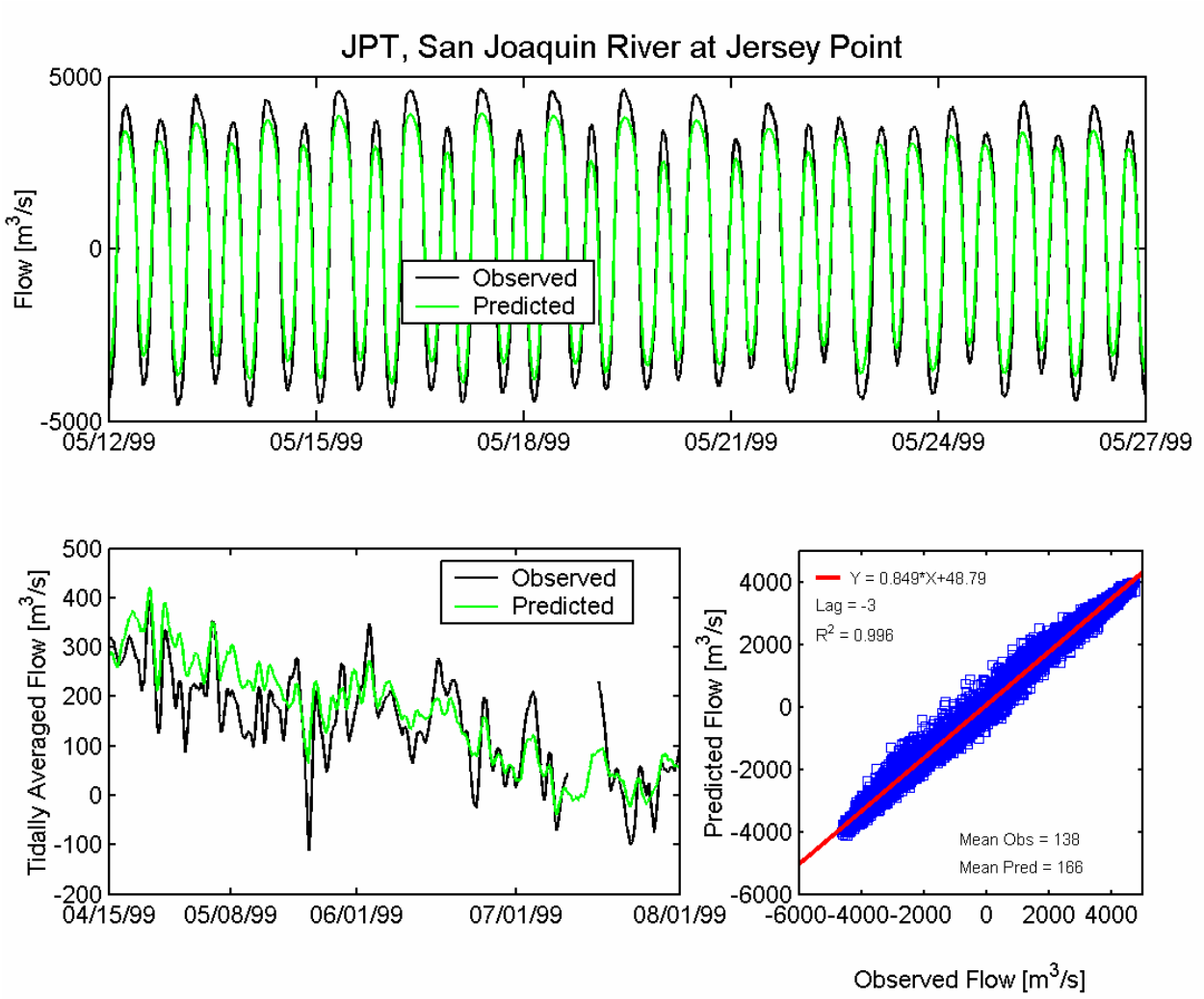

Figure A.3-8 Observed and predicted flow at San Joaquin River at Jersey Point USGS station (JPT) during the 1999 simulation period.

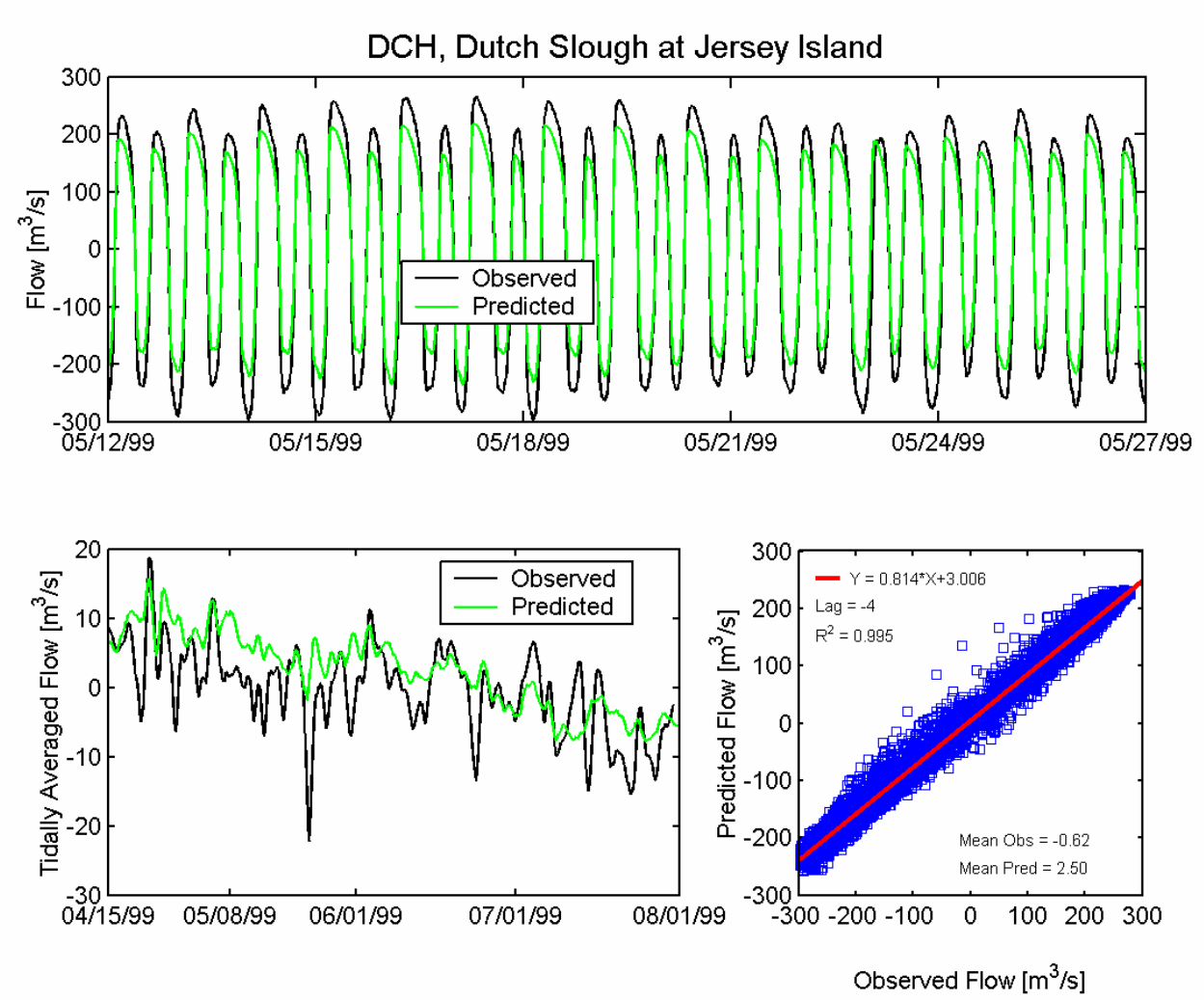

Figure A.3-9 Observed and predicted flow at Dutch Slough at Jersey Island USGS station (DCH) during the 1999 simulation period.

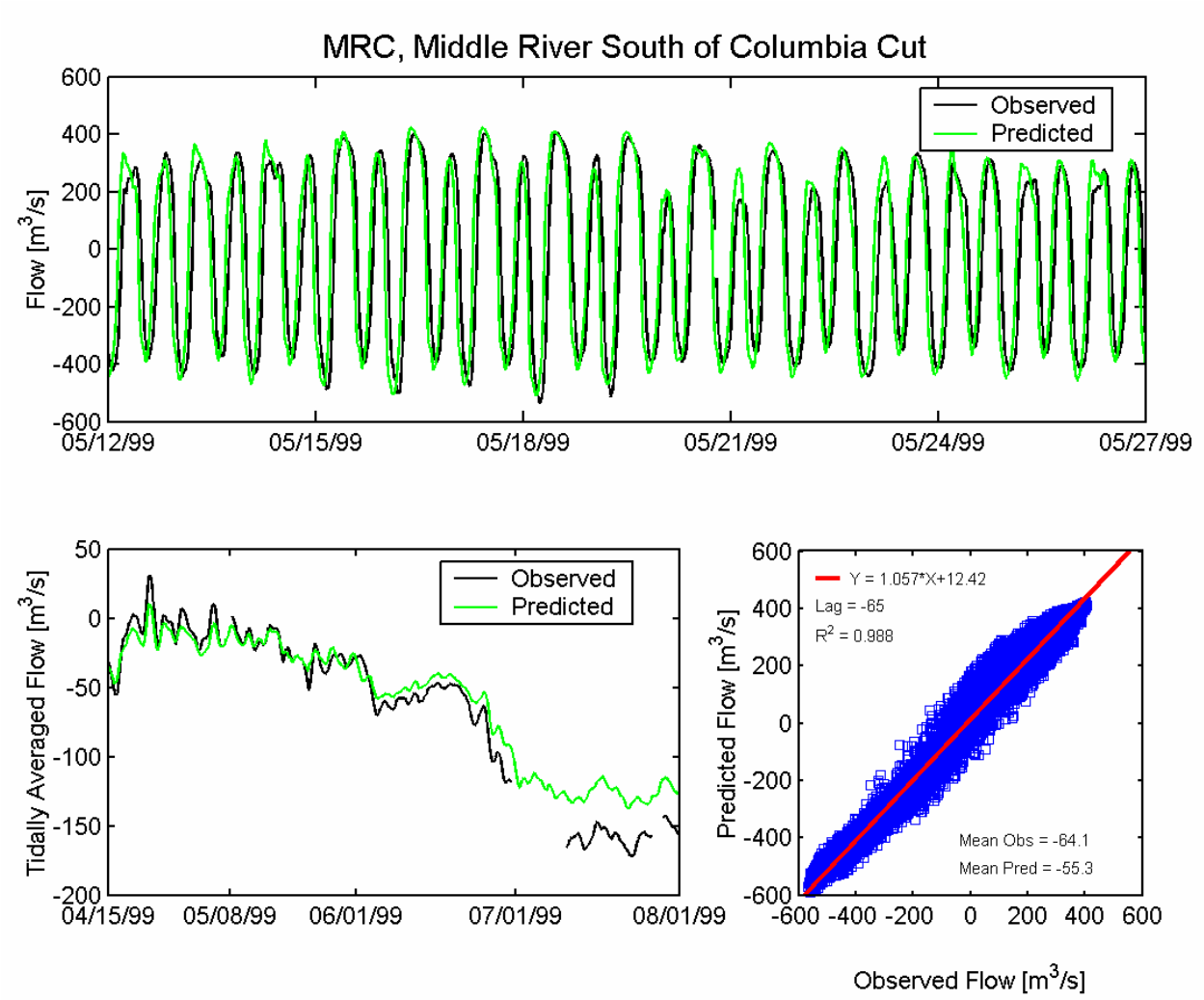

Figure A.3-10 Observed and predicted flow at Middle River south of Columbia Cut USGS station (MRC) during the 1999 simulation period.

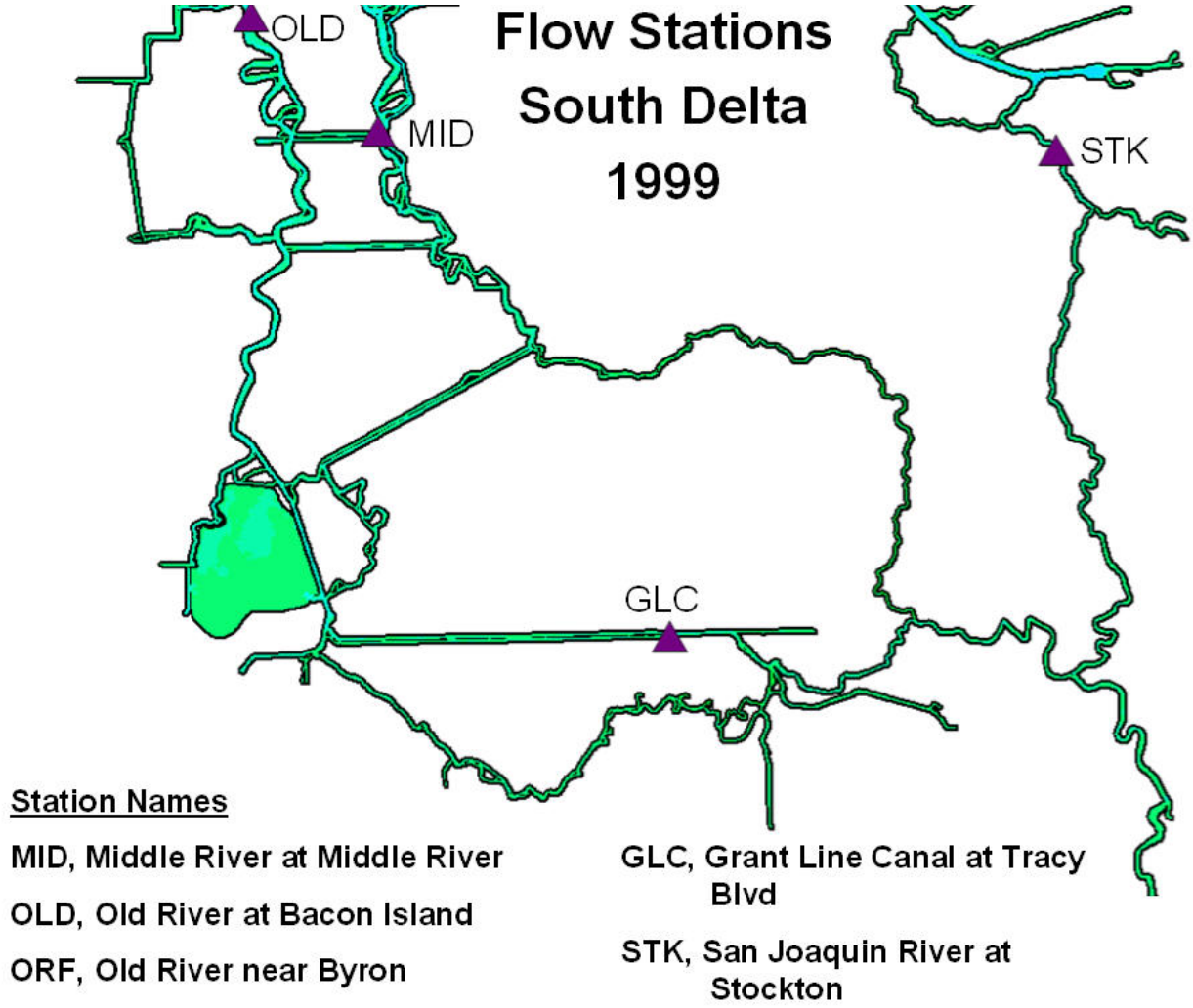

Figure A.3-11 Location of flow monitoring stations in the southern portion of the Sacramento-San Joaquin Delta used for 1999 flow calibration.

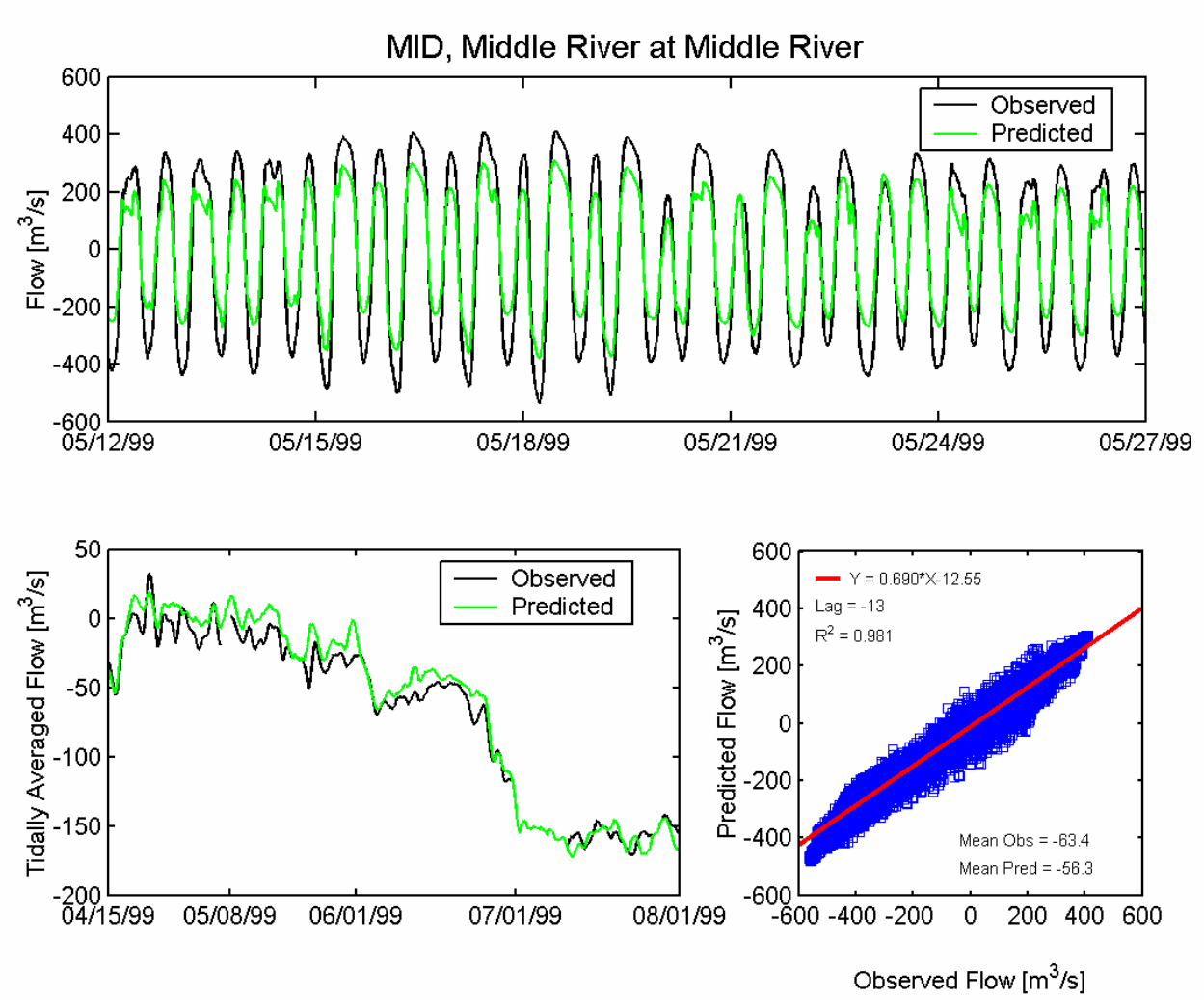

Figure A.3-12 Observed and predicted flow at Middle River at Middle River USGS station (MID) during the 1999 simulation period.

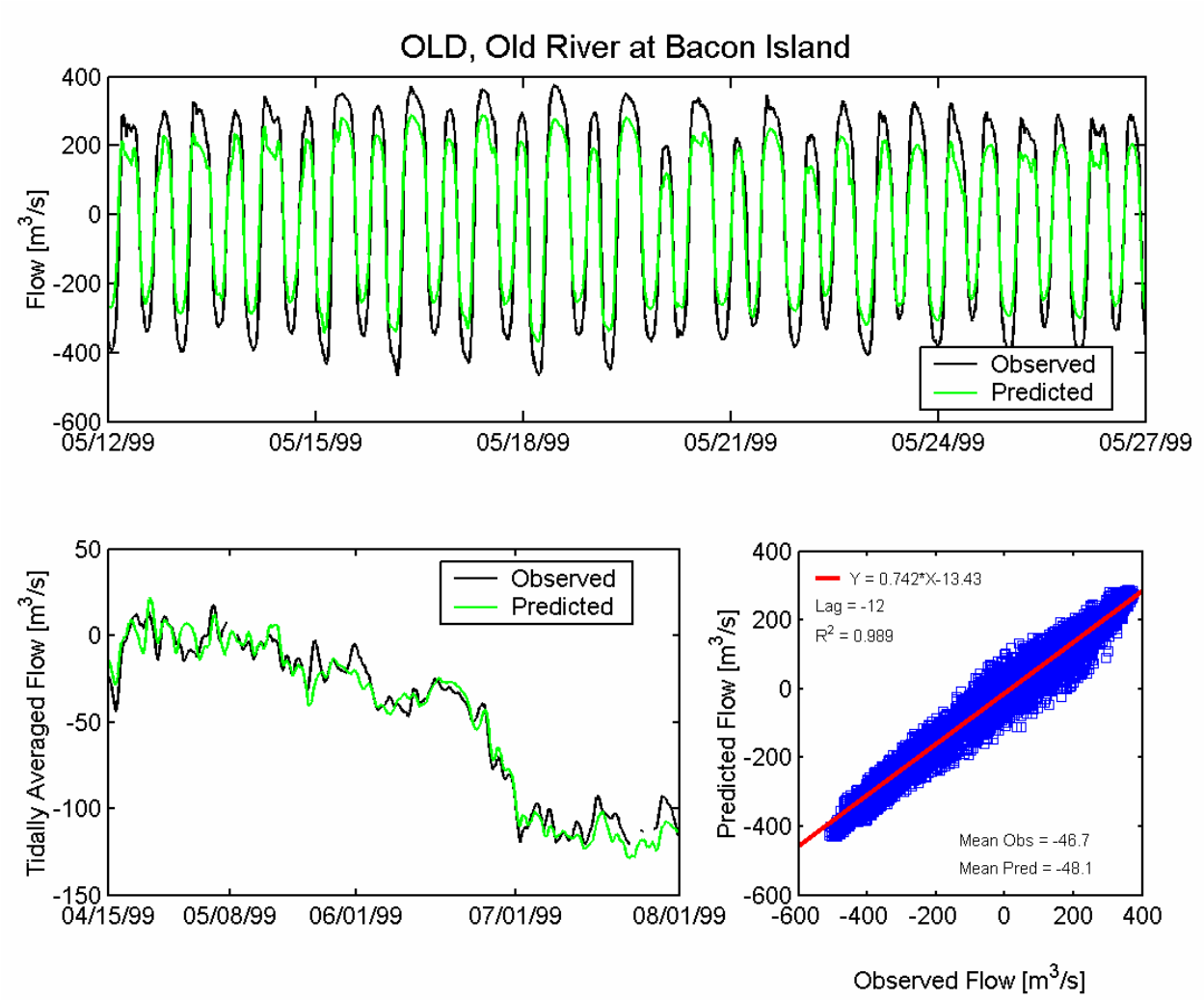

Figure A.3-13 Observed and predicted flow at Old River at Bacon Island USGS station (OLD) during the 1999 simulation period.

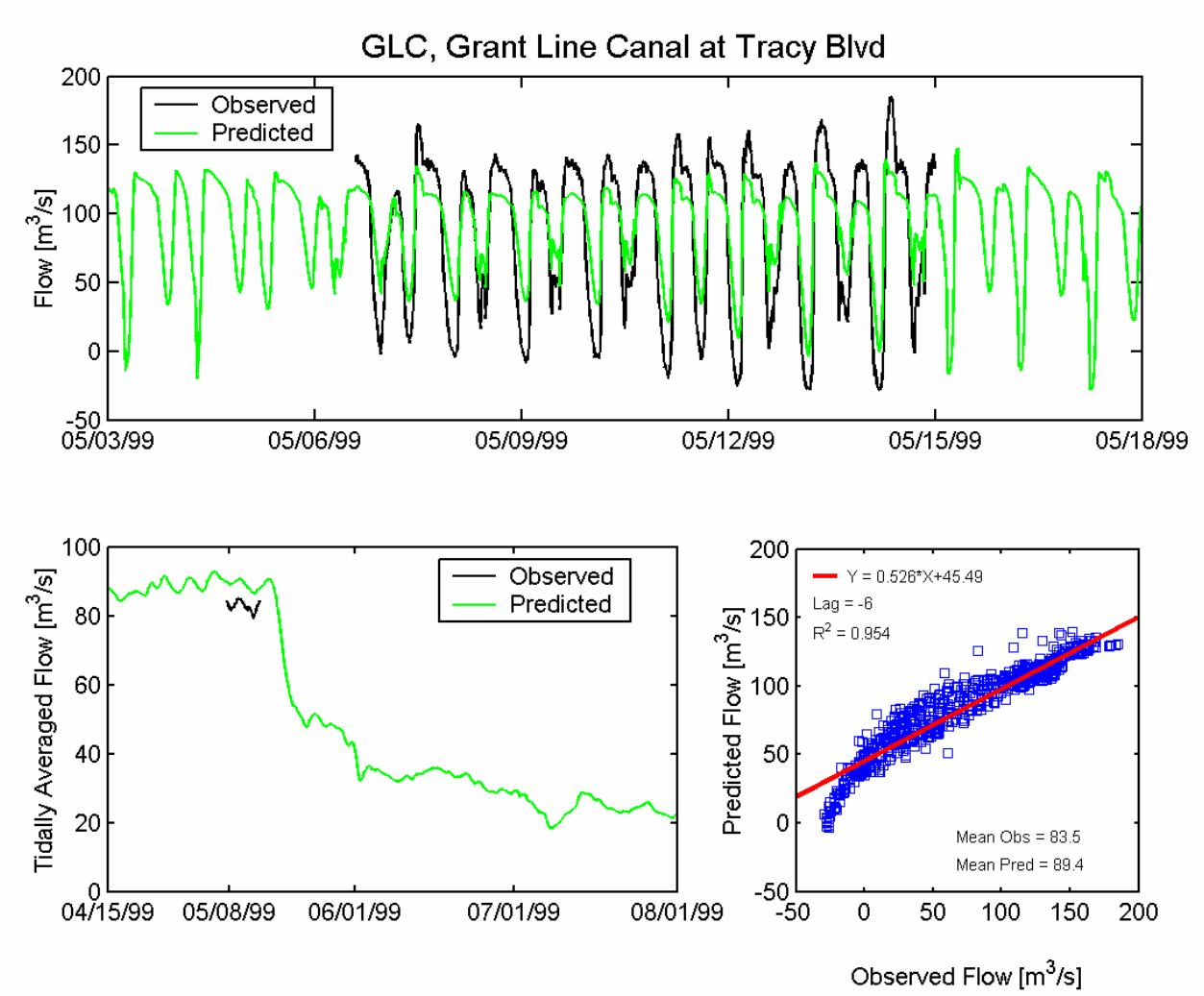

Figure A.3-14 Observed and predicted flow at Grant Line Canal at Tracy Boulevard USGS station (GLC) during the 1999 simulation period.

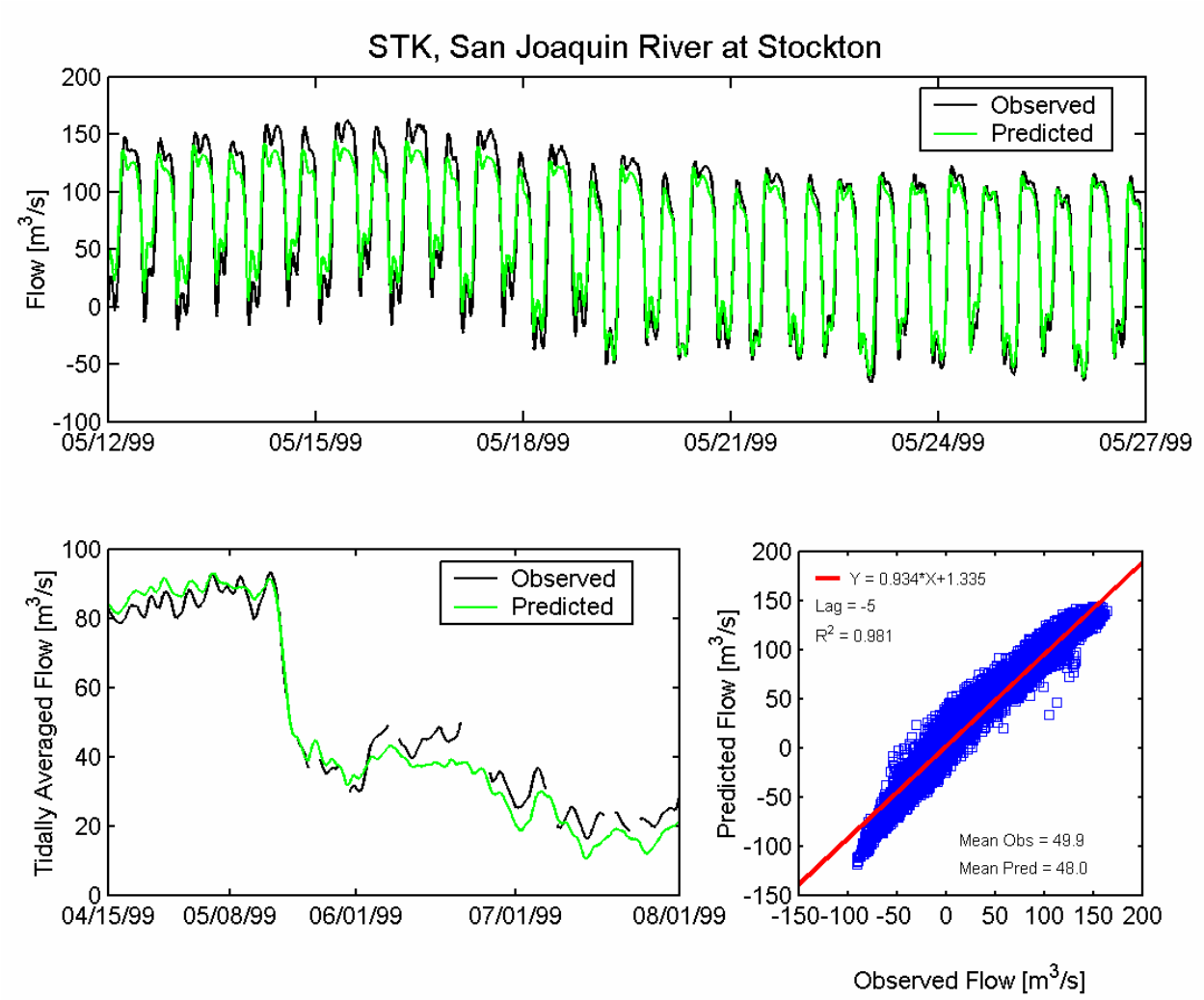

Figure A.3-15 Observed and predicted flow at San Joaquin River at Stockton USGS station (STK) during the 1999 simulation period.